41623R08

Conceptual Design of Optimized Fossil Energy Systems with Capture and Sequestration of Carbon Dioxide

Final Scientific/Technical Report

Reporting Start Date: February 1, 2007

Reporting End Date: December 31, 2010

Principal Authors:

Dr. Nils Johnson

njohnson@ucdavis.edu

Dr. Joan M. Ogden

jmogden@ucdavis.edu

Date Report Issued: July 1, 2012

DOE Award Number: DE-FC26-07NT42929

Address of Submitting Organization:

Institute of Transportation Studies

University of California, Davis

Davis, CA 95616

DISCLAIMER

Conceptual Design of Optimized Fossil Energy Systems with Capture and Sequestration of Carbon Dioxide

Dr. Nils Johnson, Dr. Joan M. Ogden
Institute of Transportation Studies
University of California
Davis, CA 95616

ABSTRACT

In this final report, we describe research results from Phase 2 of a technical/economic study of fossil hydrogen energy systems with carbon dioxide (CO_2) capture and storage (CCS). This work was performed under NETL Award No. DE-FC26-07NT42929 during the period from August 2008 through December 2011. CO_2 capture and storage, or alternatively, CO_2 capture and sequestration, involves capturing CO_2 from large point sources and then injecting it into deep underground reservoirs for long-term storage. By preventing CO_2 emissions into the atmosphere, this technology has significant potential to reduce greenhouse gas (GHG) emissions from fossil-based facilities in the power and industrial sectors. Furthermore, the application of CCS to power plants and hydrogen production facilities can reduce CO_2 emissions associated with electric vehicles (EVs) and hydrogen fuel cell vehicles (HFCVs) and, thus, can also improve GHG emissions in the transportation sector. This research specifically examines strategies for transitioning to large-scale coal-derived energy systems with CCS for both hydrogen fuel production and electricity generation. A particular emphasis is on the development of spatially-explicit modeling tools for examining how these energy systems might develop in real geographic regions.

We employ an integrated modeling approach that addresses all infrastructure components involved in the transition to these energy systems. The overall objective is to better understand the system design issues and economics associated with the widespread deployment of hydrogen and CCS infrastructure in real regions. Specific objectives of this research are to:

- Develop improved techno-economic models for all components required for the deployment of both hydrogen and CCS infrastructure,
- Develop novel modeling methods that combine detailed spatial data with optimization tools to explore spatially-explicit transition strategies,
- Conduct regional case studies to explore how these energy systems might develop in different regions of the United States, and
- Examine how the design and cost of coal-based H_2 and CCS infrastructure depend on geography and location.

TABLE OF CONTENTS

LIST OF FIGURES ..... **VI**

LIST OF TABLES ..... **XIV**

EXECUTIVE SUMMARY ..... **XIX**

1.0 INTRODUCTION **1**

2.0 TASK 4.0: MODELING THE TRANSITION TO A COAL-BASED HYDROGEN TRANSPORTATION SYSTEM WITH CARBON CAPTURE AND STORAGE **4**

2.1 TECHNO-ECONOMIC MODELING 6
2.1.1 Hydrogen Production via Coal Gasification 6
2.1.2 Hydrogen Storage, Pipeline Transport, and Refueling Stations 9
2.1.3 Carbon Dioxide Capture, Transport, and Storage 13
2.1.4 Revenue Requirements Module 22
2.1.5 HFCV Market Penetration Scenarios 24
2.2 DEVELOPMENT OF A REGIONAL HYDROGEN TRANSITION MODEL 26
2.2.1 Hydrogen Demand Module 27
2.2.2 Hydrogen Production and Transmission Model 33
2.2.3 CO_2 Transport and Disposal Model 43
2.2.4 Hydrogen Distribution and Refueling Station Model 53
2.2.5 Post-Processing in Techno-economic and Revenue Requirements Modules 55

3.0 TASK 5.0: ANALYSIS OF EMERGING CO_2 CAPTURE AND STORAGE TECHNOLOGIES IN THE POWER AND INDUSTRIAL SECTORS **60**

3.1 TECHNO-ECONOMIC MODELING OF CO_2 CAPTURE EQUIPMENT 61
3.1.1 Power Sector 61
3.1.2 Industrial Sector 68
3.2 DEVELOPMENT OF A REGIONAL TRANSITION MODEL FOR CARBON CAPTURE AND STORAGE 71
3.2.1 Model Formulation 72
3.2.2 Spatial Inputs 77
3.2.3 Techno-economic Inputs 79
3.3 CASE STUDY OF CCS INFRASTRUCTURE DEPLOYMENT IN THE SOUTHWESTERN UNITED STATES 81
3.3.1 Deployment Scenario 82
3.3.2 Model Inputs 84
3.3.3 Model Results 101
3.3.4 Conclusions 127

4.0 TASK 6.0: CASE STUDIES OF A TRANSITION TO COAL-BASED HYDROGEN INFRASTRUCTURE WITH CCS **129**

4.1 CASE STUDY: WESTERN UNITED STATES 131
4.1.1 Model Inputs 132
4.1.2 Model Results 135
4.1.3 Onsite Production Cases 198
4.1.4 Hydrogen Subsidy Cases 207

4.1.5 Comparison with National Research Council hydrogen transition study 232
4.2 SUB-REGIONAL CASE STUDIES 243
4.2.1 Northwest 245
4.2.2 Plains 256
4.2.3 Pacific 265
4.2.4 Intermountain 275
4.2.5 Midwest 284
4.2.6 Southwest 293
4.2.7 Sub-regional Comparison 301

5.0 CONCLUSIONS 340

5.1 MODEL DEVELOPMENT 340
5.2 CCS CASE STUDY IN THE SOUTHWESTERN UNITED STATES 343
5.3 HYDROGEN CASE STUDY IN THE WESTERN UNITED STATES 344
5.4 SUB-REGIONAL HYDROGEN CASE STUDIES 347
5.5 FINAL COMMENTS 349

REFERENCES 351

LIST OF FIGURES

Figure 1: Model structure for Hydrogen Infrastructure Deployment Model 4

Figure 2: Overnight capital cost estimates for coal-to-H_2 facilities of various sizes 7

Figure 3: Levelized cost for onshore pipeline transport [13] 18

Figure 4: Contribution of each cost component to the total levelized cost of CO_2 injection into a cold/shallow aquifer [13] 22

Figure 5: HFCV market penetration in H_2 Success and H_2 Partial Success scenarios 25

Figure 6: Spatial distribution of demand centers for 2 million HFCVs (~1% market penetration) 30

Figure 7: Spatial distribution of demand centers for 10 million HFCVs 30

Figure 8: Spatial distribution of demand centers for 20 million HFCVs 31

Figure 9: Spatial distribution of demand centers for 50 million HFCVs 31

Figure 10: Spatial distribution of demand centers for 100 million HFCVs 32

Figure 11: Spatial distribution of demand centers for 150 and 220 million HFCVs 32

Figure 12: Total CO_2 storage capacity for each reservoir type 49

Figure 13: Spatial distribution of saline aquifers in the continental U.S. overlaid on top of the other two CO_2 reservoir types 50

Figure 14: Idealized city model [46] 54

Figure 15: Plant capital cost as a function of net electrical output (supercritical pulverized coal without CO_2 capture) 63

Figure 16: Plant capital cost as a function of net electrical output (ultra supercritical pulverized coal without CO_2 capture) 64

Figure 17: Plant capital cost as a function of net electrical output (IGCC coal with CO_2 capture) 66

Figure 18: Plant capital cost as a function of net electrical output (NGCC without CO_2 capture) 67

Figure 19: Case study boundary and candidate sites for CO_2 sources, sinks, and pipelines 83

Figure 20: Percent of total CO_2 emissions emitted by each source type 86

Figure 21: Potential CO_2 storage sinks within the study region 88

Figure 22: Percent of total CO_2 storage capacity by reservoir type 91

Figure 23: Locations and types of candidate injection sites in the study region 92

Figure 24: Histograms of capture costs for a) IGCC plants with CCS and b) NGCC plants with CCS 95

Figure 25: Map legend for CCS infrastructure design figures 102
Figure 26: CCS infrastructure design in Phase 1 – Tranche 1 103
Figure 27: CCS infrastructure design in Phase 1 – Tranche 2 105
Figure 28: CCS infrastructure design in Phase 2 107
Figure 29: CCS infrastructure design in 2030 109
Figure 30: CCS infrastructure design in 2040 111
Figure 31: CCS infrastructure design in 2050 114
Figure 32: Storage capacity utilization of built injection sites in 2050 (Base Capacity scenario) 116
Figure 33: Average avoided cost of CO_2 for each CCS component and each deployment phase (the total average CO_2 abatement cost is labeled and marked with a line) 119
Figure 34: Marginal abatement cost curve for all CCS facilities built through 2050 120
Figure 35: CO_2 price projections from the EPA and the APA [56] 121
Figure 36: Levelized benefit of installing CCS relative to paying the CO_2 price for three price projections 122
Figure 37: Levelized cost of CO_2 transport for each scenario and deployment phase 123
Figure 38: Comparison of 2050 infrastructure design for the a) base capacity and b) low capacity storage scenarios 125
Figure 39: Storage capacity utilization of built injection sites in 2050 (Low Capacity scenario) 126
Figure 40: Total pipeline length in each deployment phase for the Base and Low Capacity scenarios 126
Figure 41: Average total abatement cost (including applicable bonus allowances) in each deployment phase for the Base and Low Capacity scenarios 127
Figure 42: Boundary of the study area (shown in green) 129
Figure 43: Boundary of sub-regions 130
Figure 44: Boundaries of the regional carbon sequestration partnerships [44] 131
Figure 45: Spatial inputs for the *Hydrogen Production and Transmission Model (demand shown for tranche 6)* 134
Figure 46: Spatial inputs for the *CO_2 Transport and Disposal Model* 135
Figure 47: Map legend for optimal infrastructure design figures 136
Figure 48: Optimal infrastructure design in tranche 1 (H_2 Success scenario) 138
Figure 49: Optimal infrastructure design in tranche 2 (H_2 Success scenario) 147
Figure 50: Optimal infrastructure design in tranche 3 (H_2 Success scenario) 149

Figure 51: Optimal infrastructure design in tranche 4 (H_2 Success scenario) 152
Figure 52: Optimal infrastructure design in tranche 5 (H_2 Success scenario) 153
Figure 53: Optimal infrastructure design in tranche 6 (H_2 Success scenario) 155
Figure 54: Optimal infrastructure design in tranche 1 (H_2 Partial Success scenario) 159
Figure 55: New transmission pipeline length by diameter class in each tranche for the H_2 Success and H_2 Partial Success scenarios (new pipeline does not include replacement pipeline) 163
Figure 56: New distribution pipeline length by diameter class in each tranche for the H_2 Success and H_2 Partial Success scenarios 164
Figure 57: New CO_2 pipeline length by diameter class in each tranche for H_2 Success and H_2 Partial Success scenarios 164
Figure 58: Optimal infrastructure design in tranche 2 (H_2 Partial Success scenario) 165
Figure 59: Optimal infrastructure design for tranche 3 (H_2 Partial Success scenario) 166
Figure 60: Optimal infrastructure design in tranche 4 (H_2 Partial Success scenario) 167
Figure 61: Optimal infrastructure design in tranche 5 (H_2 Partial Success scenario) 168
Figure 62: Cumulative capital investment in each tranche for the H_2 Success and H_2 Partial Success scenarios 171
Figure 63: Percentage of total cumulative capital investment associated with each component 172
Figure 64: Breakeven price of hydrogen in each year of the 30-year analysis period for the H_2 Success and H_2 Partial Success scenarios 174
Figure 65: Breakeven price of hydrogen for three 10-year periods for the H_2 Success and H_2 Partial Success scenarios (price in parentheses is the equivalent price for a gallon of gasoline ($/gge) assuming that a HFCV has 63% better fuel economy than a gasoline HEV) 175
Figure 66: Projected equivalent market price for hydrogen based on three EIA AEO oil price cases [70] 177
Figure 67: Relationship between the breakeven price of hydrogen and the projected H_2 market price given the three AEO oil price cases 178
Figure 68: Cumulative cash flow in the H_2 Success scenario given the three AEO oil price cases 179
Figure 69: Cumulative cash flow over the entire study period for the H_2 Success scenario (beyond 2035, hydrogen market price is the price projected in 2035) 180

Figure 70: Cumulative cash flow in the H_2 Partial Success scenario given the three AEO oil price cases 181
Figure 71: Cumulative cash flow over the entire study period for the H_2 Partial Success scenario (beyond 2035, hydrogen market price is the price projected in 2035) 182
Figure 72: Average GHG intensity of the HFCV fleet in the BAU case 186
Figure 73: Average GHG intensity of the HFCV fleet in the H_2-CCS case 187
Figure 74: Average GHG intensity of the HFCV fleet in the GHG case under the H2 Success scenario 188
Figure 75: Projected coal consumption (PJ/yr) to 2050 for the Reference case 192
Figure 76: Projected coal consumption (PJ/yr) to 2050 for the GHG Price Economy-wide case 193
Figure 77: CO_2 storage basins and CCS infrastructure deployment in tranche 6 194
Figure 78: CO_2 storage capacity and percent utilization of developed storage sites 196
Figure 79: Cumulative cash flow in the H_2 Success scenario with centralized infrastructure delayed until tranche 2 199
Figure 80: Cumulative cash flow over the entire study period for the H_2 Success scenario with centralized infrastructure delayed until tranche 2 (beyond 2035, hydrogen market price is the price projected in 2035) 200
Figure 81: Cumulative cash flow in the H_2 Partial Success scenario with centralized infrastructure delayed until tranche 2 200
Figure 82: Cumulative cash flow over the entire study period for the H_2 Partial Success scenario with centralized infrastructure delayed until tranche 2 (beyond 2035, hydrogen market price is the price projected in 2035) 201
Figure 83: Average GHG intensity of the HFCV fleet in the H_2-CCS case when centralized infrastructure is delayed until tranche 2 202
Figure 84: Cumulative cash flow in the H_2 Success scenario with centralized infrastructure delayed until tranche 3 203
Figure 85: Cumulative cash flow over the entire study period for the H_2 Success scenario with centralized infrastructure delayed until tranche 3 (beyond 2035, hydrogen market price is the price projected in 2035) 205
Figure 86: Cumulative cash flow in the H_2 Partial Success scenario with centralized infrastructure delayed until tranche 3 205
Figure 87: Cumulative cash flow over the entire study period for the H_2 Partial Success scenario with centralized infrastructure delayed until tranche 3 (beyond 2035, hydrogen market price is the price projected in 2035) 206

Figure 88: Average GHG intensity of the HFCV fleet in the H_2-CCS case when centralized infrastructure is delayed until tranche 3 207

Figure 89: Cumulative cash flow given the different policy cases in the H_2 Success scenario with centralized infrastructure in tranche 1 (Reference oil price) 212

Figure 90: Cumulative cash flow given the different policy cases in the H_2 Partial Success scenario with centralized infrastructure in tranche 1 (Reference oil price) 213

Figure 91: Cumulative cash flow given the different policy cases in the H_2 Success scenario with centralized infrastructure delayed until tranche 2 (Reference oil price) 216

Figure 92: Cumulative cash flow given the different policy cases in the H_2 Partial Success scenario with centralized infrastructure delayed until tranche 2 (Reference oil price) 217

Figure 93: Cumulative cash flow given the different policy cases in the H_2 Success scenario with centralized infrastructure in tranche 1 (High oil price) 219

Figure 94: Cumulative cash flow given the different policy cases in the H_2 Partial Success scenario with centralized infrastructure in tranche 1 (High oil price) 220

Figure 95: Cumulative cash flow given the different policy cases in the H_2 Success scenario with centralized infrastructure delayed until tranche 2 (High oil price) 221

Figure 96: Cumulative cash flow given the different policy cases in the H_2 Partial Success scenario with centralized infrastructure delayed until tranche 2 (High oil price) 222

Figure 97: Cumulative cash flow given the different policy cases in the H_2 Success scenario with centralized infrastructure in tranche 1 (GHG price) 226

Figure 98: Cumulative cash flow given the different policy cases in the H_2 Partial Success scenario with centralized infrastructure in tranche 1 (GHG price) 227

Figure 99: Cumulative cash flow given the different policy cases in the H_2 Success scenario with centralized infrastructure delayed until tranche 2 (GHG price) 228

Figure 100: Cumulative cash flow given the different policy cases in the H_2 Partial Success scenario with centralized infrastructure delayed until tranche 2 (GHG price) 229

Figure 101: Breakeven price of hydrogen in each analysis period for the HIDM and NRC model (H_2 Success) 240

Figure 102: Boundary of sub-regions 245

Figure 103: Subset of infrastructure required to serve the Northwest sub-region in all tranches 247

Figure 104: Infrastructure requirements within the Northwest sub-region in tranche 6 248

Figure 105: Percentage of total cumulative capital investment associated with each component in the Northwest sub-region 254

Figure 106: Comparison of the breakeven price of hydrogen under the H_2 Success scenario in the Northwest sub-region and western U.S. (number in parentheses is the $/gallon gasoline equivalent) 255

Figure 107: Comparison of the breakeven price of hydrogen under the H_2 Partial Success scenario in the Northwest sub-region and western U.S. (number in parentheses is the $/gallon gasoline equivalent) 256

Figure 108: Subset of infrastructure required to serve the Plains sub-region in all tranches 257

Figure 109: Infrastructure requirements within the Plains sub-region in tranche 6 258

Figure 110: Percentage of total cumulative capital investment associated with each component in the Plains sub-region 263

Figure 111: Comparison of the breakeven price of hydrogen under the H_2 Success scenario in the Plains sub-region and western U.S. (number in parentheses is the $/gallon gasoline equivalent) 264

Figure 112: Comparison of the breakeven price of hydrogen under the H_2 Partial Success scenario in the Plains sub-region and western U.S. (number in parentheses is the $/gallon gasoline equivalent) 265

Figure 113: Subset of infrastructure required to serve the Pacific sub-region in all tranches 267

Figure 114: Infrastructure requirements within the Pacific sub-region in tranche 6 269

Figure 115: Percentage of total cumulative capital investment associated with each component in the Pacific sub-region 273

Figure 116: Comparison of the breakeven price of hydrogen under the H_2 Success scenario in the Pacific sub-region and western U.S. (number in parentheses is the $/gallon gasoline equivalent) 274

Figure 117: Comparison of the breakeven price of hydrogen under the H_2 Partial Success scenario in the Pacific sub-region and western U.S. (number in parentheses is the $/gallon gasoline equivalent) 275

Figure 118: Subset of infrastructure required to serve the Intermountain sub-region in all tranches 276

Figure 119: Infrastructure requirements within the Intermountain sub-region in tranche 6 277

Figure 120: Percentage of total cumulative capital investment associated with each component in the Intermountain sub-region 282

Figure 121: Comparison of the breakeven price of hydrogen under the H_2 Success scenario in the Intermountain sub-region and western U.S. (number in parentheses is the $/gallon gasoline equivalent) 283

Figure 122: Comparison of the breakeven price of hydrogen under the H_2 Partial Success scenario in the Intermountain sub-region and western U.S. (number in parentheses is the $/gallon gasoline equivalent) 283

Figure 123: Subset of infrastructure required to serve the Midwest sub-region in all tranches 285

Figure 124: Infrastructure requirements within the Midwest sub-region in tranche 6 286

Figure 125: Percentage of total cumulative capital investment associated with each component in the Midwest sub-region 290

Figure 126: Comparison of the breakeven price of hydrogen under the H_2 Success scenario in the Midwest sub-region and western U.S. (number in parentheses is the $/gallon gasoline equivalent) 291

Figure 127: Comparison of the breakeven price of hydrogen under the H_2 Partial Success scenario in the Midwest sub-region and western U.S. (number in parentheses is the $/gallon gasoline equivalent) 292

Figure 128: Subset of infrastructure required to serve the Southwest sub-region in all tranches 293

Figure 129: Infrastructure requirements within the Southwest sub-region in tranche 6 295

Figure 130: Percentage of total cumulative capital investment associated with each component in the Southwest sub-region 299

Figure 131: Comparison of the breakeven price of hydrogen under the H_2 Success scenario in the Southwest sub-region and western U.S. (number in parentheses is the $/gallon gasoline equivalent) 300

Figure 132: Comparison of the breakeven price of hydrogen under the H_2 Partial Success scenario in the Southwest sub-region and western U.S. (number in parentheses is the $/gallon gasoline equivalent) 301

Figure 133: Levelized Cost of Production ($/kg) for each sub-region given the H_2 Success scenario 305

Figure 134: Non-fuel levelized cost of production as a function of effective capacity factor 307

Figure 135: Levelized cost of transmission ($/kg) for each sub-region given the H_2 Success scenario 311

Figure 136: Relationship between the mean nearest neighbor distance and the mean pipeline length per demand center 313

Figure 137: Levelized cost of H_2 transmission as a function of effective capacity factor 314

Figure 138: Levelized cost of distribution ($/kg) for each sub-region given the H_2 Success scenario 318

Figure 139: Levelized cost of H_2 distribution as a function of effective capacity factor 319

Figure 140: Levelized cost of refueling stations ($/kg) for each sub-region given the H_2 Success scenario 322

Figure 141: Levelized cost of H_2 refueling stations as a function of effective capacity factor (observations that are influenced by substantial onsite production are circled in red) 323

Figure 142: Levelized cost of H_2 refueling stations as a function of effective capacity factor, including only observations in which less than 15% of hydrogen is supplied by onsite production 324

Figure 143: Levelized cost of CO_2 transport ($/kg) for each sub-region given the H_2 Success scenario 328

Figure 144: Levelized cost of CO_2 transport as a function of the adjusted average pipeline length per production site 329

Figure 145: Annual levelized cost of hydrogen over the 30-year study period for each sub-region given the H_2 Success scenario 331

Figure 146: Levelized cost of hydrogen for each infrastructure component, 10-year analysis period, and sub-region given the H_2 Success scenario 332

Figure 147: Annual levelized cost of hydrogen over the 30-year study period for each sub-region given the H_2 Partial Success scenario 335

Figure 148: Levelized cost of hydrogen for each infrastructure component, 10-year analysis period, and sub-region given the H_2 Partial Success scenario 336

LIST OF TABLES

Table 1: Overnight capital cost for various facility sizes based on Equation 1 8

Table 2: Performance and cost assumptions for coal-to-H_2 facilities 8

Table 3: Delivered coal cost and CO_2 emission rate by state [8, 9] 9

Table 4: Capital cost per km (thousand $) for 100-km hydrogen distribution and transmission pipelines of various nominal pipe diameters 12

Table 5: Common design parameters for pipeline transport [21] 15

Table 6: Comparison between actual and calculated pipeline diameter for existing CO_2 pipelines 15

Table 7: Capacities and base installed costs of pipelines for several nominal pipe sizes in flat, rural terrain 17

Table 8: Common Aquifer and Injection Parameters [28, 29] 19

Table 9: Financial structure and other general economic assumptions [34]............................... 23

Table 10: Number of HFCVs supported by infrastructure built in each tranche and installation year for each market penetration scenario 26

Table 11: Relationship between different metrics for HFCV market penetration in the continental U.S. 29

Table 12: Summary statistics for demand centers in the continental U.S. based on the *Hydrogen Demand Module* 29

Table 13: HyPAT model annotation 35

Table 14: CO_2 model annotation 45

Table 15: Comparison of optimized and alternative planning scenarios 57

Table 16: $/tonne CO_2 avoided for a reference plant (1000 kt CO_2/yr) given different capital recovery factors (CRFs) 69

Table 17: $/tonne CO_2 avoided for a reference plant (1068 kt CO_2/yr) given different capital recovery factors (CRFs) and coal costs.. 70

Table 18: Range of CO_2 capture costs for industrial plants with CCS (Capital Charge = 16.3%) ... 71

Table 19: CCS model annotation.. 73

Table 20: Deployment scenario 83

Table 21: EOR potential by region [59-61].. 89

Table 22: Characteristics of candidate injection sites in the study region 91

Table 23: Range of site-specific CO_2 capture costs for power plants with CCS in the study area (CRF = 7.5%) 95

Table 24: Range of site-specific CO_2 capture costs for industrial plants with CCS in the study area (Capital Charge = 16.3%) 96

Table 25: Learning rates for IGCC and NGCC power plants with CCS (learning stops at 100 GW cumulative capacity) [48] 97

Table 26: Capacities and base installed costs of pipelines for several nominal pipe sizes 97

Table 27: Injection costs for geologic sinks 101

Table 28: Summary of capture and storage facilities built in Phase 1 – Tranche 1 104

Table 29: Summary of capture and storage facilities built in Phase 1 – Tranche 2 106

Table 30: Summary of capture and storage facilities built in Phase 2 108

Table 31: Summary of capture and storage facilities built in 2030 110

Table 32: Summary of capture and storage facilities built in 2040 112

Table 33: Summary of capture and storage facilities built in 2050 113

Table 34: Summary statistics for hydrogen demand at each national HFCV market penetration level 132

Table 35: H_2 production facility requirements for the H_2 Success and H_2 Partial Success scenarios 139

Table 36: H_2 Storage facility requirements for the H_2 Success scenario 140

Table 37: Transmission pipeline requirements for the H_2 Success scenario 141

Table 38: Refueling station requirements for the H_2 Success and H_2 Partial Success scenarios 142

Table 39: Distribution pipeline requirements for the H_2 Success scenario 143

Table 40: CO_2 storage requirements for the H_2 Success and H_2 Partial Success scenarios 143

Table 41: CO_2 pipeline requirements for the H_2 Success scenario 144

Table 42: Number of demand centers served by centralized and onsite supply in each tranche for the H_2 Success and H_2 Partial Success scenarios 144

Table 43 Transmission pipeline requirements for the H_2 Partial Success scenario 160

Table 44 Distribution pipeline requirements for the H_2 Partial Success scenario 161

Table 45: H_2 storage facility requirements for the H_2 Partial Success scenario 161

Table 46: CO_2 pipeline requirements for the H_2 Partial Success scenario 162

Table 47: Cumulative capital investment (Billion $) and capital investment per HFCV ($/HFCV) in each tranche 170

Table 48: Average capacity factors for the five major infrastructure components 175

Table 49: Average GHG intensity of the power sector (kg CO_{2e}/kWh) at the beginning of each infrastructure tranche under the Lieberman-Warner Climate Security Act [72] 184

Table 50: Projected coal consumption and % increase relative to 2010 for the Reference case 190

Table 51: Projected coal consumption and % increase relative to 2010 for the GHG Price Economy-wide case 191

Table 52: Summary statistics for CO_2 storage basins 195

Table 53: Percent of total CO_2 storage capacity utilized at each developed storage site (sites with >90% utilization highlighted in red) 197

Table 54: MACRS-5 depreciation schedule 208

Table 55: Comparison of the impacts of the various policy cases for each HFCV and infrastructure deployment case (Reference oil price) 211

Table 56: Comparison of the impacts of the various policy cases for each HFCV and infrastructure deployment case (High oil price) 215

Table 57: Comparison of the impacts of the various policy cases for each HFCV and infrastructure deployment case (GHG price) 224

Table 58: Comparison of infrastructure requirements in this report and the NRC report (adjusted values reported in brackets for HIDM) 235

Table 59: Comparison of effective capacity factors used in the HIDM and NRC model for major infrastructure components 241

Table 60: H_2 production facility requirements for the H_2 Success and H_2 Partial Success scenarios in the Northwest sub-region 250

Table 61: Number of demand centers served by centralized and onsite supply in the Northwest sub-region 250

Table 62: H_2 and CO_2 pipeline requirements in the Northwest sub-region 251

Table 63: CO_2 storage requirements in the Northwest sub-region 251

Table 64: Cumulative capital investment (Billion $) in the Northwest sub-region for each tranche 253

Table 65: H_2 production facility requirements for the H_2 Success and H_2 Partial Success scenarios in the Plains sub-region 259

Table 66: Number of demand centers served by centralized and onsite supply in the Plains sub-region 259

Table 67: H_2 and CO_2 pipeline requirements in the Plains sub-region 260

Table 68: CO_2 storage requirements in the Plains sub-region....260
Table 69: Cumulative capital investment (Billion $) in the Plains sub-region for each tranche.262
Table 70: H_2 production facility requirements for the H_2 Success and H_2 Partial Success scenarios in the Pacific sub-region....270
Table 71: Number of demand centers served by centralized and onsite supply in the Pacific sub-region....270
Table 72: H_2 and CO_2 pipeline requirements in the Pacific sub-region....271
Table 73: CO_2 storage requirements in the Plains sub-region....271
Table 74: Cumulative capital investment (Billion $) in the Pacific sub-region for each tranche 272
Table 75: H_2 production facility requirements for the H_2 Success and H_2 Partial Success scenarios in the Intermountain sub-region....279
Table 76: Number of demand centers served by centralized and onsite supply in the Intermountain sub-region....279
Table 77: H_2 and CO_2 pipeline requirements in the Intermountain sub-region....280
Table 78: CO_2 storage requirements in the Intermountain sub-region....280
Table 79: Cumulative capital investment (Billion $) in the Intermountain sub-region for each tranche....281
Table 80: H_2 production facility requirements for the H_2 Success and H_2 Partial Success scenarios in the Midwest sub-region....287
Table 81: Number of demand centers served by centralized and onsite supply in the Midwest sub-region....287
Table 82: H_2 and CO_2 pipeline requirements in the Midwest sub-region....288
Table 83: CO_2 storage requirements in the Midwest sub-region....288
Table 84: Cumulative capital investment (Billion $) in the Midwest sub-region for each tranche....289
Table 85: H_2 production facility requirements for the H_2 Success and H_2 Partial Success scenarios in the Southwest sub-region....296
Table 86: Number of demand centers served by centralized and onsite supply in the Southwest sub-region....296
Table 87: H_2 and CO_2 pipeline requirements in the Southwest sub-region....297
Table 88: CO_2 storage requirements in the Southwest sub-region....297
Table 89: Cumulative capital investment (Billion $) in the Southwest sub-region for each tranche....298

Table 90: Comparison of H_2 production metrics for each sub-region given the H_2 Success scenario 304

Table 91: Comparison of H_2 transmission metrics for each sub-region given the H_2 Success scenario 310

Table 92: Comparison of H_2 distribution metrics for each sub-region given the H_2 Success scenario 317

Table 93: Comparison of H_2 refueling station metrics for each sub-region given the H_2 Success scenario 321

Table 94: Comparison of CO_2 transport metrics for each sub-region given the H_2 Success scenario 327

EXECUTIVE SUMMARY

Scope of Research

In this final report, we describe research results from Phase 2 of a technical/economic study of fossil hydrogen energy systems with carbon dioxide (CO_2) capture and storage (CCS). This work was performed under NETL Award No. DE-FC26-07NT42929 during the period from August 2008 through December 2011. CO_2 capture and storage involves capturing CO_2 from large point sources and then injecting it into deep underground reservoirs for long-term storage. By preventing CO_2 emissions into the atmosphere, this technology has significant potential to reduce greenhouse gas (GHG) emissions from fossil-based facilities in the power and industrial sectors. Furthermore, the application of CCS to power plants and hydrogen production facilities can reduce CO_2 emissions associated with electric vehicles (EVs) and hydrogen fuel cell vehicles (HFCVs) and, thus, can also improve GHG emissions in the transportation sector. This research specifically examines strategies for transitioning to large-scale coal-derived energy systems with CCS for both hydrogen fuel production and electricity generation. Two particular emphases of this research are the development of spatially-explicit modeling tools for examining how these energy systems might develop in real geographic regions and the application of these tools to regional case studies.

We employ an integrated modeling approach that addresses all infrastructure components involved in the transition to these energy systems. The overall objective is to better understand the system design issues and economics associated with the widespread deployment of hydrogen and CCS infrastructure in real regions. Specific objectives of this research are to:

- Develop improved techno-economic models for all components required for the deployment of both hydrogen and CCS infrastructure,
- Develop novel modeling methods that combine detailed spatial data with optimization tools to explore spatially-explicit transition strategies,
- Conduct regional case studies to explore how these energy systems might develop in different regions of the United States, and
- Examine how the design and cost of coal-based H_2 and CCS infrastructure depend on geography and location.

Phase 2 of this study includes three research tasks, numbered four to six. The overall objective of Task 4 is the development of a group of models for exploring the transition to a coal-based hydrogen transportation system with CCS. This task is divided into two components: 1) the development of updated techno-economic models for hydrogen infrastructure components and 2) the development of spatially-explicit optimization tools for identifying optimal infrastructure deployment strategies in real geographic regions over time.

In Task 5, the overall objective is to assess the costs and performance of systems for capturing and storing CO_2 from industrial and power sector sources as well as optimal strategies for their deployment. This task includes the development of techno-economic models for CO_2 capture at several types of large point sources in the power and industrial sectors. In addition, a regional transition model is developed to examine optimal CCS deployment strategies in real geographic regions. The model combines detailed spatial and techno-economic data with optimization tools and policy constraints to identify the least-cost CCS infrastructure for meeting a specific CCS target. The techno-economic and optimization models are applied to a case study in the southwestern United States, which explores how a transition from early demonstration projects to widespread adoption of CCS might occur given the subsidies and CO_2 prices proposed in the American Power Act.

In Task 6, we return to the topic of hydrogen infrastructure and present several case studies that examine regional transition strategies for coal-based hydrogen with CCS. The first case study is conducted in the western United States. This study explores system design issues and presents costs, GHG emissions, coal consumption, and CO_2 storage capacity constraints for two HFCV deployment scenarios. The study also explores two alternative scenarios in which centralized production is delayed (i.e., onsite production is utilized during early deployment) and examines the efficacy of various hydrogen subsidies in incentivizing infrastructure investment. The second set of case studies explores the cost and design of hydrogen infrastructure within several sub-regions within the western United States. A comparison is conducted to provide insight into how and why infrastructure design and cost differ between sub-regions.

Task 4.0: Modeling the Transition to a Coal-based Hydrogen Transportation System with Carbon Capture and Storage

The primary objective of task 4 is to develop a spatially-explicit model for simulating a transition to a hydrogen-based transportation sector supplied by coal-derived hydrogen with carbon capture and storage (CCS). The structure of the model that was developed, the *Hydrogen Infrastructure Deployment Model* (HIDM), is illustrated in Figure ES-1 and consists of several sub-models that use detailed spatial and techno-economic data to optimize infrastructure deployment.

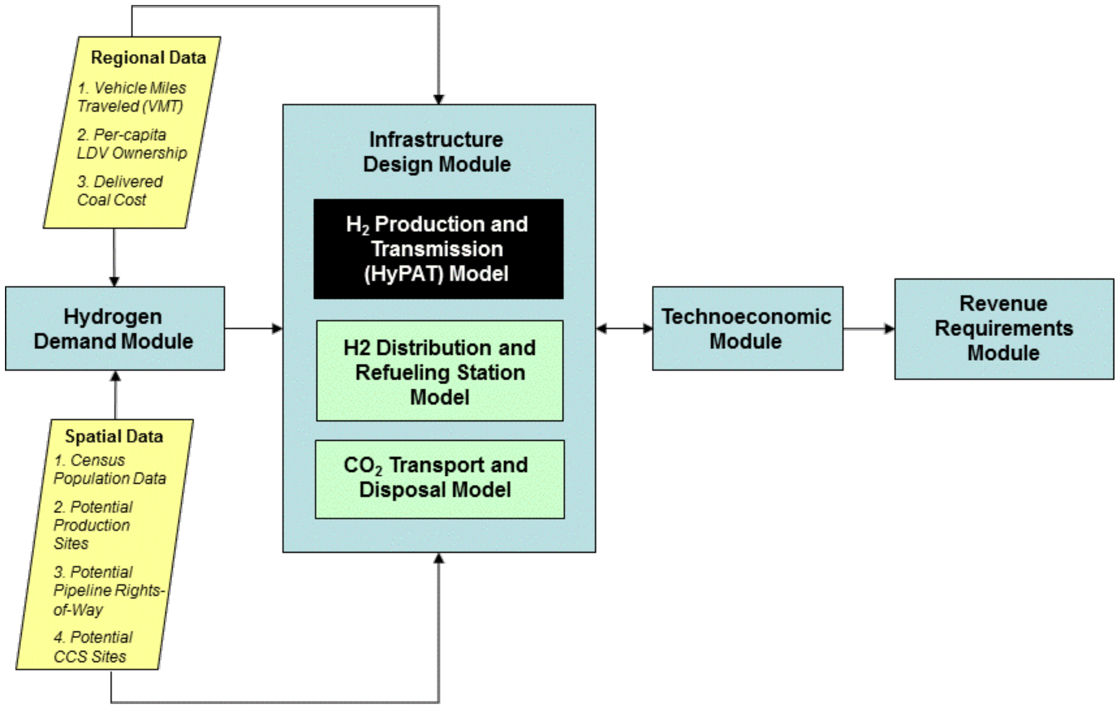

Figure ES-1: Model structure for Hydrogen Infrastructure Deployment Model

In Task 4.1, the *Techno-economic* and *Revenue Requirements Modules* are described. The *Techno-economic Module* includes detailed techno-economic models for each infrastructure component, which are based on a comprehensive survey of the literature. The models encompass the range of processes and equipment necessary for hydrogen production, distribution, and refueling stations, and the capture, transport and storage of carbon dioxide. The models provide detailed and scalable cost estimates for each component. The *Revenue Requirements Module* tracks the timing and annualized cost of infrastructure investments over time. The module can also incorporate different assumptions about the deployment of hydrogen fuel cell vehicles (HFCVs) and the implementation of policies that support hydrogen infrastructure to examine how the timing of HFCV deployment and level of political support impact the cost of hydrogen. Two HFCV market penetration deployment scenarios are considered in this study, which are entitled “Hydrogen Success” and “Hydrogen Partial Success”

(Figure ES-2). These scenarios define the pre-specified market penetration levels at which the optimization tools developed in Task 4.2 are applied (Table ES-1).

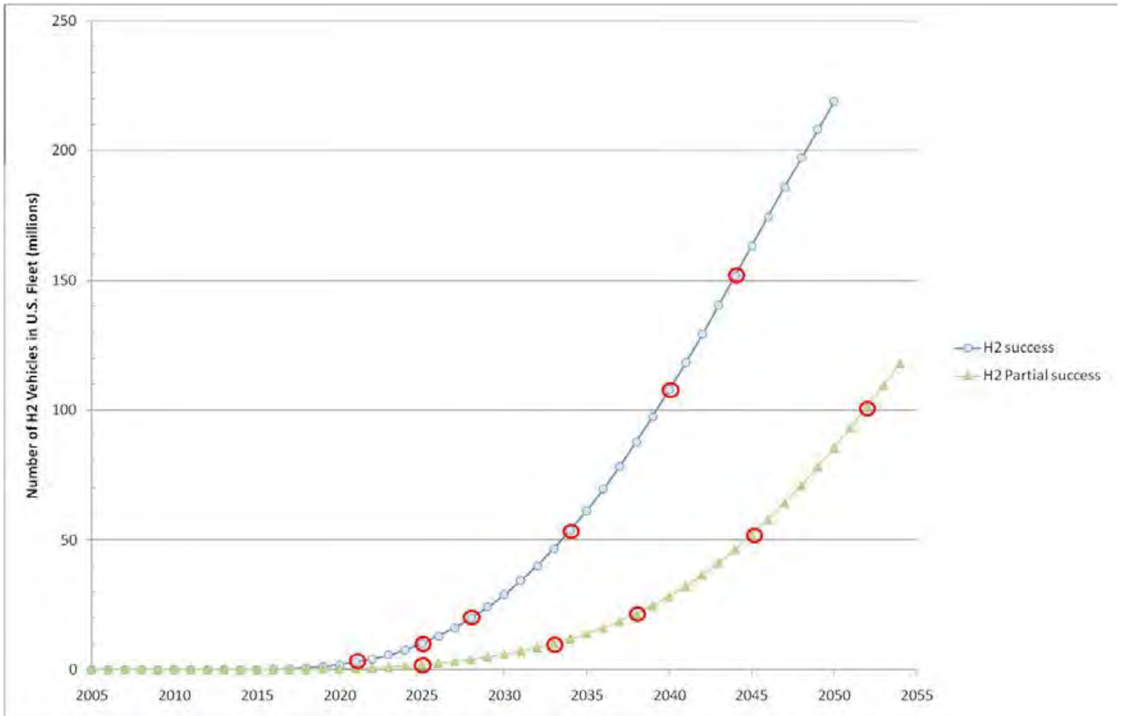

Figure ES-2: HFCV market penetration in H_2 Success and H_2 Partial Success scenarios

Table ES-1: Number of HFCVs supported by infrastructure built in each tranche and installation year for each market penetration scenario

Tranche	# of HFCVs supported by infrastructure (million vehicles in national LDV fleet)	Installation Year (H_2 Success)	Installation Year (H_2 Partial Success)
1	10	2021	2025
2	20	2025	2033
3	50	2028	2038
4	100	2034	2045
5	150	2040	2052
6	220	2044	2057

In Task 4.2, spatially-explicit modeling tools are developed to explore the design and cost of deploying a coal-based hydrogen transportation system with CCS in specific geographic regions. These tools compose the *Hydrogen Demand* and *Infrastructure Design Modules*. The *Hydrogen Demand Module* quantifies the location and magnitude of projected hydrogen demand at the pre-specified HFCV market penetration levels in Table ES-1. These locations represent cities with sufficient demand to warrant centralized infrastructure at the specified market penetration level (e.g., Figure ES-3).

Figure ES-3: Spatial distribution of demand locations for the first 10 million HFCVs in the continental U.S.

The location and magnitude of hydrogen demand at each market penetration level is provided to the *Infrastructure Design Module*, which consists of three sub-models that must be run in a certain sequence. The first model in the sequence is the *H_2 Production and Transmission Model*, which is a network optimization tool that identifies the lowest cost H_2 production and pipeline transmission infrastructure at each HFCV market penetration level. The *H_2 Distribution and Refueling Station Model* is a simple heuristic model that estimates the number of refueling stations and length of distribution pipelines within each of the identified demand centers (i.e., cities). This model is not dependent on the outputs of the other models and can be run independently. The *CO_2 Transport and Disposal Model* is run after the *H_2 Production and Transmission Model* since one input is the optimal locations of production facilities. This model is a network optimization tool that identifies the optimal CO_2 transport and injection infrastructure associated with hydrogen production facilities. It is important to note that the H_2 supply network and CO_2 disposal networks are not co-optimized. If these networks were co-optimized, it is possible that hydrogen production facilities would be located in closer proximity to CO_2 storage sites. However, the cost of CO_2 transport on a dollar per kg H_2 basis is generally 5-10 times smaller than the cost of H_2 transmission. Therefore, priority is given to the optimization of the H_2 transmission pipeline network.

The sub-models in the *Infrastructure Design Module* provide detailed inventories of the H_2 production, transmission, distribution, refueling station, and CCS infrastructure requirements for each HFCV market penetration level in Table ES-1. These inventories are then exported to the *Techno-economic Module*, which calculates detailed cost estimates for the infrastructure required at each market penetration level. These estimates are then provided to the *Revenue Requirements Module*, which calculates the cost of deploying this infrastructure under different market penetration scenarios (i.e., rates of HFCV adoption).

The outputs from the integrated *Hydrogen Infrastructure Deployment Model* include an inventory of infrastructure components and estimates of the total capital requirement, levelized cost of hydrogen ($/kg), cumulative cash flow, and CO_2 captured and emitted during the transition to a coal-based hydrogen transportation system in a specific region. The model also estimates coal use and CO_2 storage requirements. It can be applied to different geographic regions and can incorporate different HFCV market penetration scenarios in order to examine how the timing of infrastructure deployment impacts the cost of hydrogen. Various policy scenarios can also be explored using the model (e.g., accelerated depreciation and production tax credits).

Task 5.0: Analysis of Emerging CO_2 Capture and Storage Technologies in the Power and Industrial Sectors

In Task 5, we assess the costs and performance of systems for capturing and storing CO_2 from industrial and power sector sources as well as optimal strategies for their deployment. This task is divided into two components: 1) the development of technical and economic models of CO_2 capture equipment for large point sources in the industrial and power sectors and 2) the development and application of spatially-explicit optimization tools for examining how CCS might deploy in real geographic regions.

Task 5.1 describes the development of equations for calculating the cost of CO_2 capture ($/t$CO_2$ avoided) at a variety of facility types in the power and industrial sectors. The focus on the power and industrial sectors is important since these sources are likely to dominate CO_2 production in the near-term and, thus, be the best candidates for early CCS adoption. In contrast, it will likely take 10-20 years for hydrogen demand to reach levels where large central plants with CCS might be needed for producing hydrogen transportation fuel. In the power sector, equations for CO_2 capture are described for supercritical and ultra-supercritical pulverized coal steam power plants, integrated gasification combined cycle coal power plants, and natural gas combined cycle power plants. Equations for industrial CO_2 point sources are developed for cement plants, ammonia plants, oil refineries and ethanol plants. These equations can be applied in specific case studies to estimate the cost of CO_2 capture at plants of various sizes (e.g., Tables ES-2 and ES-3).

Table ES-2: Range of site-specific CO_2 capture costs for power plants with CCS in the southwestern U.S. case study (CRF = 7.5%)

Plant type	Size Range ($MtCO_2$ captured/yr)	$\$/tCO_2$ avoided
IGCC Power – new build (75% capacity factor)	1.1 to 19.5	27 to 52
NGCC Power – new build (same capacity factor as replaced)	0.1 to 2.9	29 to 259

Table ES-3: Range of site-specific CO_2 capture costs for industrial plants with CCS in the southwestern U.S. case study (Capital Charge = 16.3%)

Plant type	Size Range ($MtCO_2$ captured/yr)	$\$/tCO_2$ avoided
Refinery	0.1 to 2.5	105 to 223
Cement Plant	0.1 to 2.6	109 to 180
Ethanol Plant	0.02 to 0.5	20 to 82
Ammonia Plant	0.04 to 0.15	49 to 58

Task 5.2 describes the *CCS Deployment Model*, a spatially-explicit network optimization tool for examining the adoption of carbon capture and storage (CCS) technologies in the power and industrial sectors. The model combines detailed spatial and techno-economic data with optimization tools and policy constraints to identify the least-cost CCS infrastructure for meeting a specific CCS target, which can be defined as a CO_2 reduction target (Mt CO_2/year) or as a capacity target (GW installed with CCS). Given the target, the model chooses among several facility types (e.g., cement, ethanol, coal-based power) and sink types (e.g., saline aquifers, depleted oil and gas fields) to identify the least-cost CCS infrastructure for meeting the pre-specified target.

The model inputs include a candidate CO_2 pipeline network, the locations, CO_2 capture potentials, and capture costs of candidate facilities, and the locations, capacities, reservoir types, and injection costs of potential CO_2 injection sites. The model determines the location, length, and diameter of CO_2 pipelines, the number, location, CO_2 captured, and capacity of facilities at which CO_2 capture is installed, and the number, location, reservoir type, and size of injection sites.

The model is applied to a case study in the southwestern United States to examine how a transition from early demonstration projects to widespread adoption of CCS might occur given the subsidies and CO_2 prices proposed in the American Power Act (APA). The APA proposes a cap-and-trade program for greenhouse gas (GHG) emissions and provides specific bonus allowances for early CCS projects (up to 72 GW nationally). Given the proposed incentives, this project examines how CCS infrastructure might develop and whether the bonuses are sufficient to drive investment. It also models whether projected CO_2 prices will support continued CCS deployment after the bonuses expire.

In addition to APA-related results, the model provides valuable insight into the deployment of CCS infrastructure in a real geographic region. Specifically, the model identifies optimal deployment strategies, the levelized cost of CCS, the CO_2 emitted and captured, and constraints on regional CO_2 storage capacity. The model also identifies areas in which interconnected regional pipeline networks are optimal and provides preliminary insight into the conditions that favor networks as opposed to independent dedicated pipelines for each source.

A CCS deployment scenario specifies CO_2 reduction targets for six deployment years from 2016 to 2050 (Table ES-4). The deployment scenario is based on the allotment and timing of APA bonus allowances in Phases 1 and 2 and, beyond the bonus timeframe, it is based on general CO_2 reduction targets. It is assumed that only the power sector is eligible for bonuses during the first three phases. However, the industrial sector is included from 2030 to 2050. For each target/deployment phase, the *CCS Deployment Model* identifies the lowest cost infrastructure for matching CO_2 sources and sinks within the region (Figure ES-4).

Table ES-4: Deployment scenario

	Bonus Allowance ($/t$CO_2$ avoided)*	Bonus Allotment (cumulative GW capacity)**	Reduction Target (%)	Construction Year
Phase 1 – Tranche 1	$106	1.64	N/A	2016
Phase 1 – Tranche 2	$85	3.28	N/A	2020
Phase 2	Reverse Auction	11.8	N/A	2025
2030	N/A	N/A	30%	2030
2040	N/A	N/A	60%	2040
2050	N/A	N/A	80%	2050

*Bonus allowances expire after the first ten years of plant operation

**National bonus allotments are adjusted for the southwestern region (~16.4% of national power capacity)

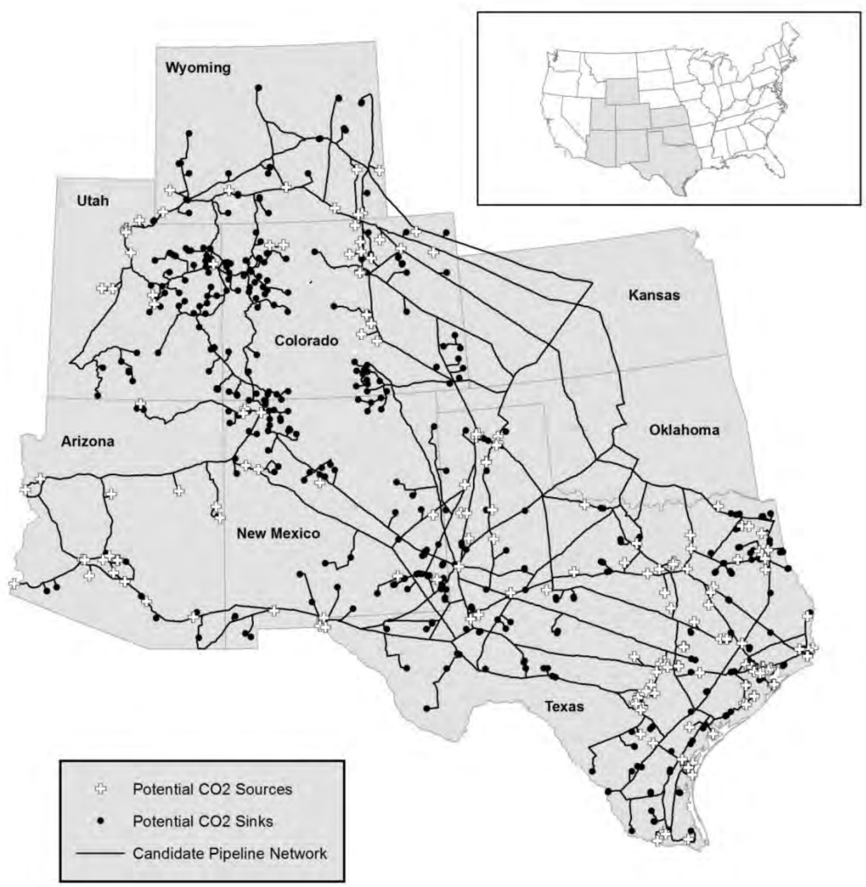

Figure ES-4: Case study boundary and candidate sites for CO_2 sources, sinks, and pipelines

This study also examines two storage capacity scenarios. The "Base Capacity" scenario uses the capacity estimates provided by SWP and SECARB for regional CO_2 sinks and the "Low Capacity" scenario assumes that storage capacity is only 10% of the reported values for saline aquifers. The second scenario examines how smaller storage capacities might affect CCS infrastructure design and cost.

The case study provides several insights into the optimal deployment of CCS in a real geographic region. First, since the cost of capture is generally the largest percentage of the total CCS cost, the capture cost tends to dominate site selection in Phase 1 with sites with low capture costs initially selected even when they require long and expensive pipelines (Figure ES-5; legend in Figure ES-6). However, from Phase 2 to 2040, the difference in capture costs between candidate sites becomes smaller and transport costs tend to dominate site selection, resulting in shorter and more integrated disposal networks (Figure ES-5). However, from 2040 to 2050, capture costs rise substantially as CCS must be applied to higher cost NGCC and industrial plants in order to achieve the stringent reduction target. As a result, capture costs again dominate the site selection process.

a) b)

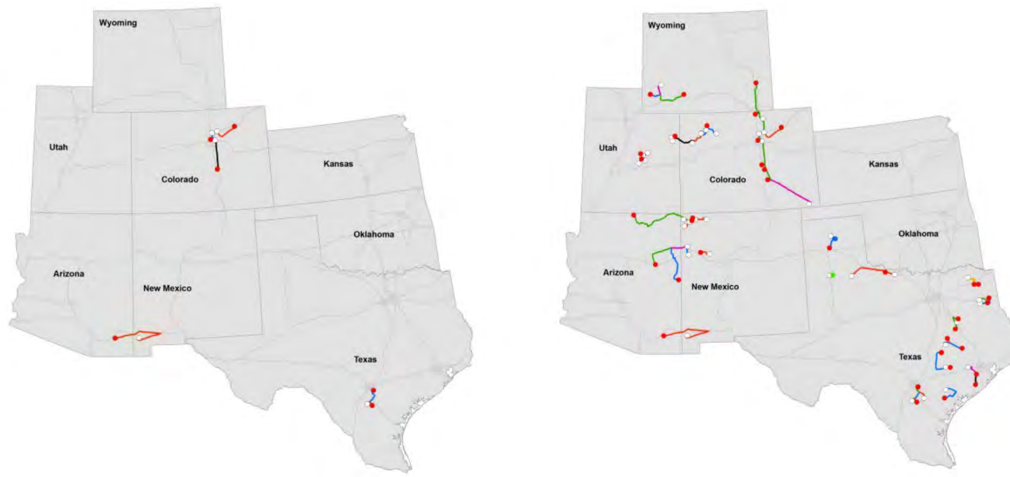

Figure ES-5: CCS infrastructure design in a) Phase 1 (Tranches 1 and 2) and b) 2040

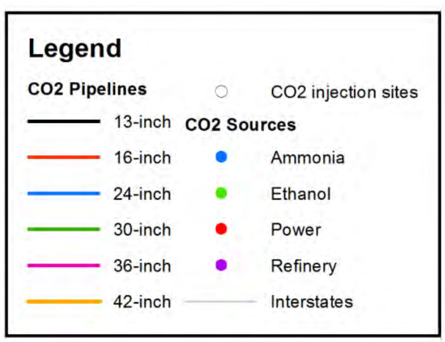

Figure ES-6: Map legend for CCS infrastructure design figures

The second insight concerns the structure of disposal networks in relation to the availability of sufficient local CO_2 storage capacity. In general, more extensive integrated CO_2 disposal networks develop in areas with limited or no availability of local storage capacity. Figure ES-7 illustrates the percent utilization of built injection sites in 2050 in the "Base Capacity" scenario and suggests that more extensive integrated disposal networks develop to access new capacity when either: 1) local capacity has been consumed (e.g., in Colorado and Utah) or 2) local capacity is non-existent (e.g., in Arizona and Utah). This finding is supported by the "Low Capacity" scenario in which disposal networks are even more integrated in response to limited local storage capacity (Figure ES-7). Even though integrated disposal networks take longer to develop in regions with sufficient local storage capacity, the results indicate that sharing of disposal infrastructure is the dominant paradigm in most of the study area by 2050.

a) b)

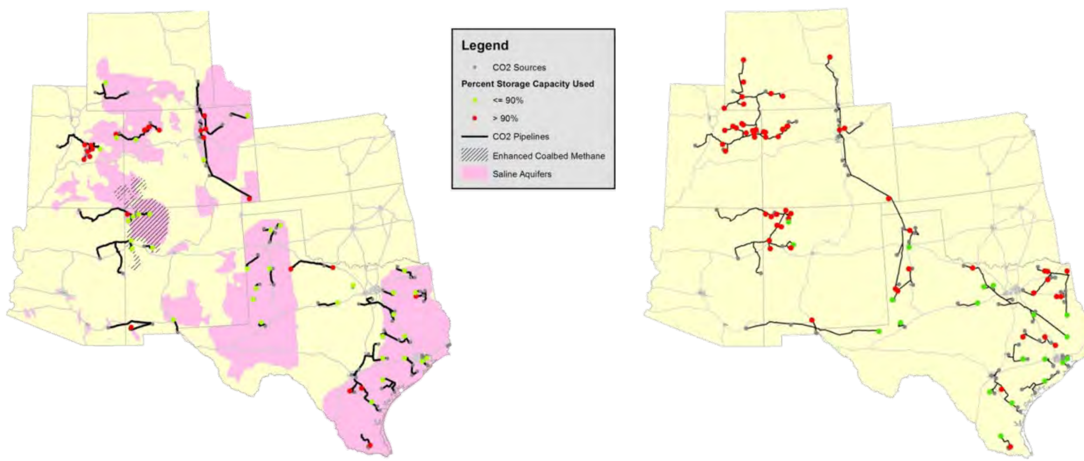

Figure ES-7: Storage capacity utilization of built injection sites in 2050 in the a) Base Capacity and b) Low Capacity scenarios

The third insight is the fact that replacement of pulverized coal plants with IGCC plants with CCS generally yields the lowest capture costs ($/t$CO_2$ avoided). As a result, the majority of emission reductions through 2040 are achieved through the construction of new IGCC plants with CCS, although a few exceptionally low-cost NGCC, ethanol, and ammonia plants do adopt CCS in this time period (Figure ES-8). However, beyond 2040, CCS is adopted extensively at natural gas-fired plants in order to achieve the stringent reduction target by 2050. Figure ES-8 also indicates that about 300 Mt CO_2 per year can be avoided with CCS (~62% of regional emissions from the power and industrial sectors) at a cost below ~$50/t$CO_2$ avoided. Beyond 300 Mt CO_2 per year, the CO_2 abatement cost increases quickly as CCS must be adopted at natural gas-fired power plants and industrial facilities. However, it appears that about 360 Mt CO_2 per year (or ~75% of regional emissions) can be avoided for less than \$114/tCO_2 avoided. Thus, to achieve a full 80% reduction in CO_2 emissions by 2050 with only CCS will require very high CO_2 prices.

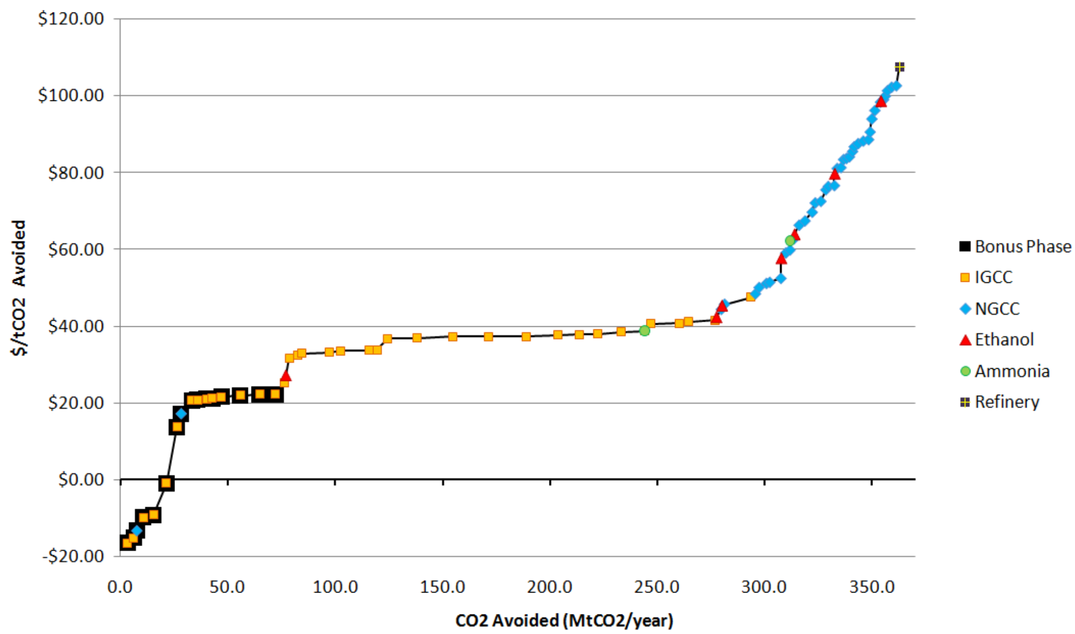

Figure ES-8: Marginal abatement cost curve for all CCS facilities built through 2050

Figure ES-9 illustrates the average avoided cost of CO_2 for each CCS component and each deployment phase. The purple negative values represent the average value of the bonus allowances (i.e., subsidies) for all plants operating in each phase. Over time, this value becomes less negative as the value of bonus allowances declines and fewer plants receive bonus allowances. The average cost of CO_2 capture also declines as a result of learning until 2040. Despite decreasing transport costs, the total average CO_2 abatement cost increases with time as bonus allowances expire and sources with higher capture costs install CCS in 2050.

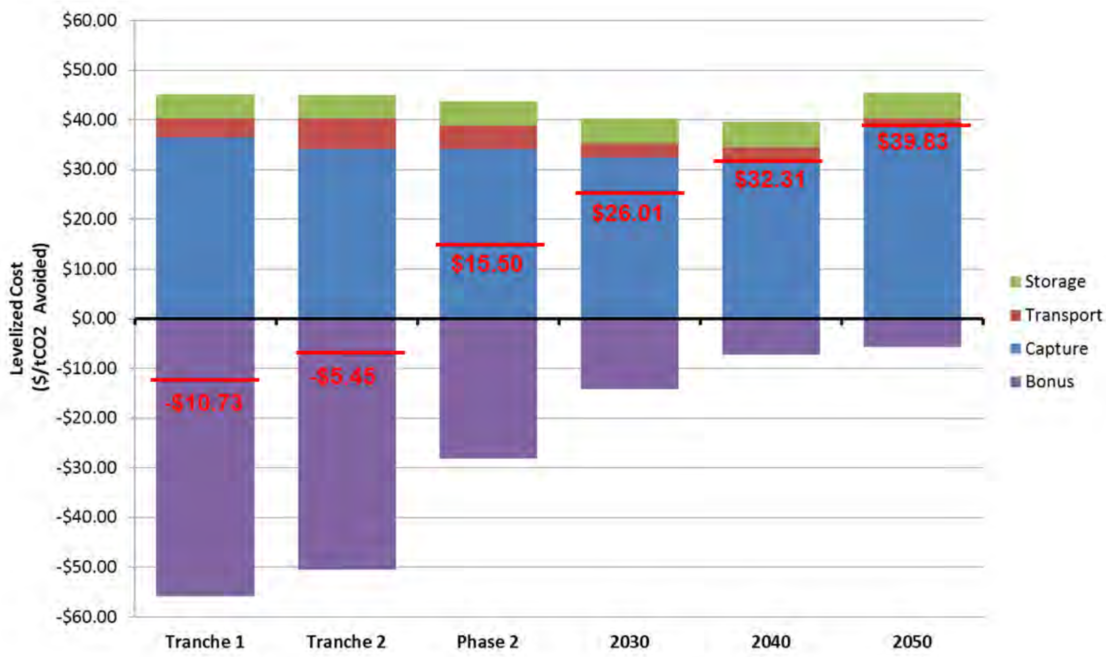

Figure ES-9: Average avoided cost of CO_2 for each CCS component and each deployment phase (the total average CO_2 abatement cost is labeled and marked with a line)

Assuming establishment of a carbon market, it is possible to calculate the levelized benefit derived from installing CCS at each facility relative to the alternative of paying the CO_2 price. The APA promotes the establishment of a carbon market and specifies clearing (i.e., minimum) and maximum CO_2 prices from 2012 to 2050. In addition, the EPA has developed a CO_2 price projection based on an analysis of the APA, which is between the maximum and clearing prices. Figure ES-10 shows the levelized benefit for each plant relative to the three CO_2 price projections. Even at the clearing price, the bonus allowances provided by the APA in the first three deployment phases (i.e., Tranche 1 and 2 and Phase 2) allow early adopters of CCS to derive benefits. This finding confirms that the values of the bonus allowances are sufficient to successfully promote early demonstration projects. However, beyond the incentive period, Figure ES-10 suggests that additional adoption of CCS will only continue if the CO_2 price is above the clearing price. For example, CO_2 prices that follow the maximum or EPA projections should incentivize continued CCS deployment.

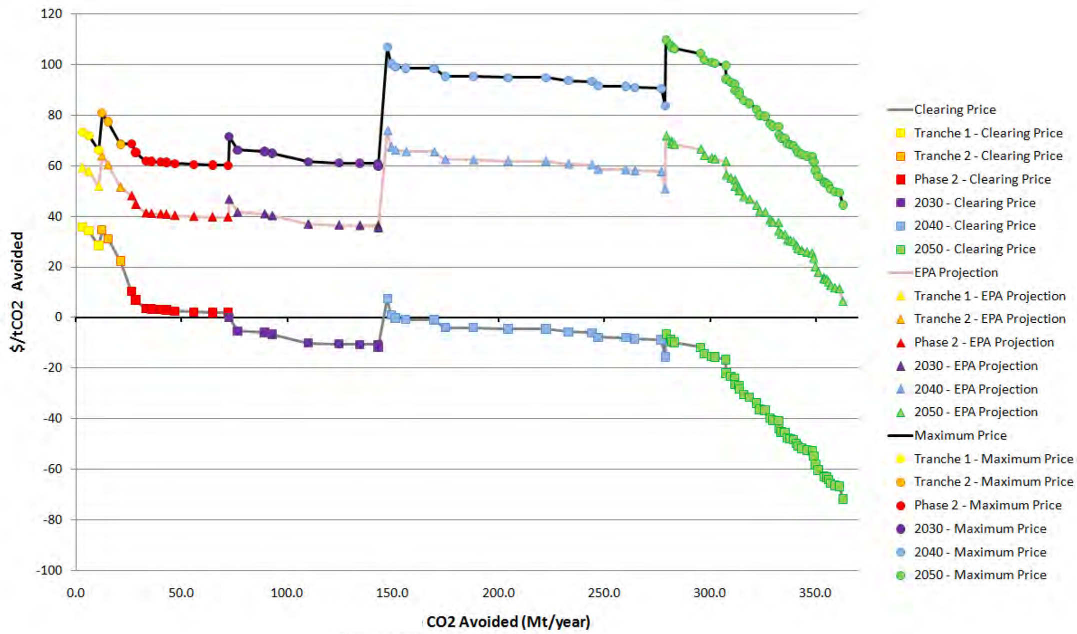

Figure ES-10: Levelized benefit of installing CCS relative to paying the CO_2 price for three price projections

Task 6.0: Case Studies of a Transition to Coal-based Hydrogen Infrastructure with CCS

In Task 6, regional case studies of coal-based hydrogen infrastructure deployment were conducted using the *Hydrogen Infrastructure Deployment Model* described in Task 4. Task 6.1 discusses a case study in the western continental United States and Task 6.2 presents several sub-regional case studies that were conducted to examine the variation in infrastructure design and cost. The boundaries of these sub-regions are defined by the outputs of the infrastructure model for the western United States (i.e., the super-regional case study determines the boundaries of the sub-regional case studies) (Figure ES-11).

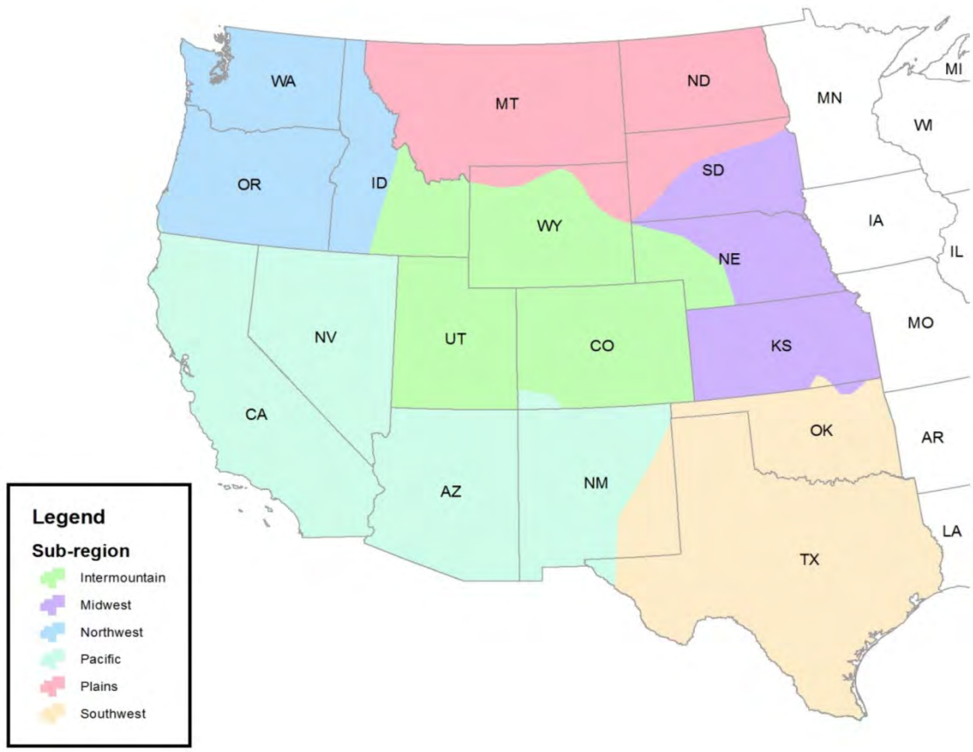

Figure ES-11: Boundaries of western United States case study and sub-regions

The case studies examine optimal infrastructure deployment for supplying regional hydrogen demand with a combination of onsite production via steam methane reformation and centralized production via coal gasification with CCS at six discrete national HFCV market penetration levels (Table ES-1). Each model run results in an optimized infrastructure design and represents a stage in building infrastructure to meet a pre-specified HFCV market penetration level. Together, the six model runs provide a long-term deployment strategy for coal-based hydrogen infrastructure with CCS in a specific region. Two HFCV deployment scenarios are considered, which represent fast and moderate ramp-up of HFCVs (Figure ES-2).

Task 4.1: Western U.S Case Study

Task 4.1 describes the results of the western U.S. case study, including insights into infrastructure design, cost, GHG emissions, coal consumption, and CO_2 storage. In addition, alternative deployment strategies are examined in which the transition from onsite to centralized hydrogen production is delayed. Finally, two policy scenarios for subsidizing early hydrogen infrastructure deployment are evaluated: production tax credits and accelerated depreciation.

Infrastructure Design

Figures ES-13 through ES-16 show the optimal deployment of hydrogen infrastructure for the Hydrogen Success HFCV deployment scenario. A map legend is provided in Figure ES-12. In the first two tranches, the H_2 supply system develops into four independent regional networks. However, as hydrogen demand increases, the supply network becomes increasingly interconnected with large regional trunk pipelines constructed for the purpose of transporting hydrogen westward toward the major regional demand centers in California. As the H_2 transmission pipeline expands, the average length per demand center remains relatively constant between 80 and 100 km.

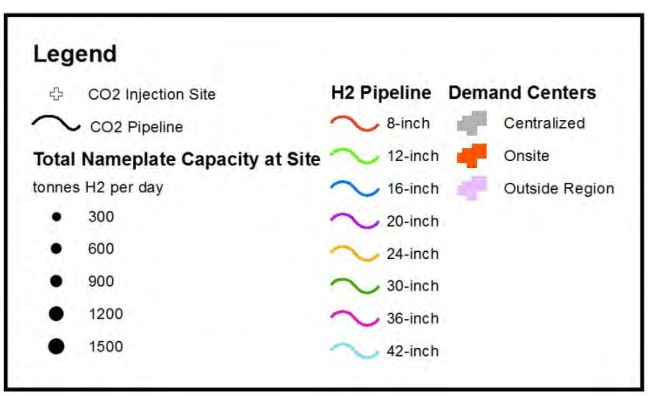

Figure ES-12: Map legend for optimal infrastructure design figures

Figure ES-13: Optimal infrastructure design in tranche 1 (H_2 Success scenario)

Figure ES-14: Optimal infrastructure design in tranche 2 (H_2 Success scenario)

Figure ES-15: Optimal infrastructure design in tranche 4 (H_2 Success scenario)

Figure ES-16: Optimal infrastructure design in tranche 6 (H_2 Success scenario)

The design of the CO_2 disposal network is dependent on the availability of local storage capacity. In locations with adequate capacity, H_2 production facilities tend to have dedicated CO_2 pipelines and injection sites. However, in areas with inadequate local capacity (e.g., Arizona), long CO_2 pipelines are required to access storage aquifers and these pipelines and injection sites are often shared by several H_2 facilities (Figure ES-17). The majority of storage basins do not experience capacity constraints as the CO_2 captured at H_2 production facilities utilizes only 1.4% of the *low estimate* of total aquifer storage capacity in the study region.

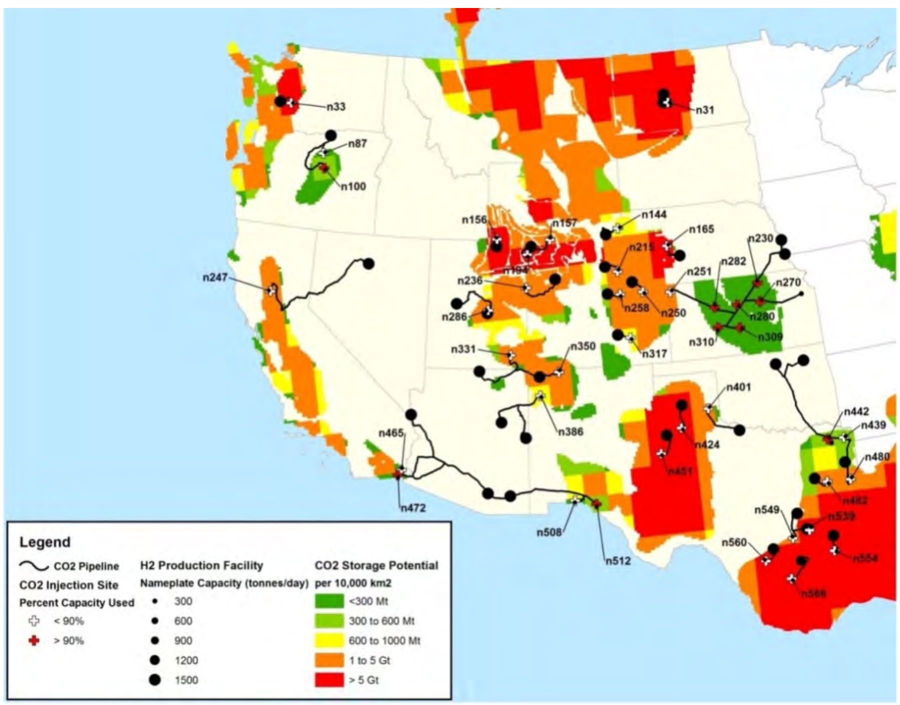

Figure ES-17: CO_2 storage capacity and percent utilization of developed storage sites

Cost

The cumulative capital investment given the H_2 Success scenario is approximately $310 billion for the full HFCV deployment to 2050. This infrastructure serves about 94 million cumulative HFCVs, which translates to a cost of $3,300 per HFCV in 2050. However, this number decreases over time from $7,300 at the end of the first tranche in 2024. In the first tranche, approximately

65% of the cumulative capital investment is associated with H_2 and CO_2 pipeline transport since the pipelines are oversized for the projected flow over their lifetimes. In the sixth tranche, the three largest contributors to the capital cost are pipeline transport (40%), refueling stations (35%), and centralized production (21%). The cost of CO_2 transport and storage infrastructure represents only 4% of the total capital investment.

Figure ES-18 illustrates the annual breakeven price of hydrogen during the 30-year analysis period. In both HFCV deployment scenarios, a price spike occurs in each year in which a new infrastructure tranche is installed. Although the cost of infrastructure is annualized, a spike occurs because new infrastructure capacity is initially underutilized. With time, the infrastructure becomes increasingly utilized and the price declines until the next tranche is installed. Moreover, the price trend is negative over time as a result of both better utilization and economies-of scale.

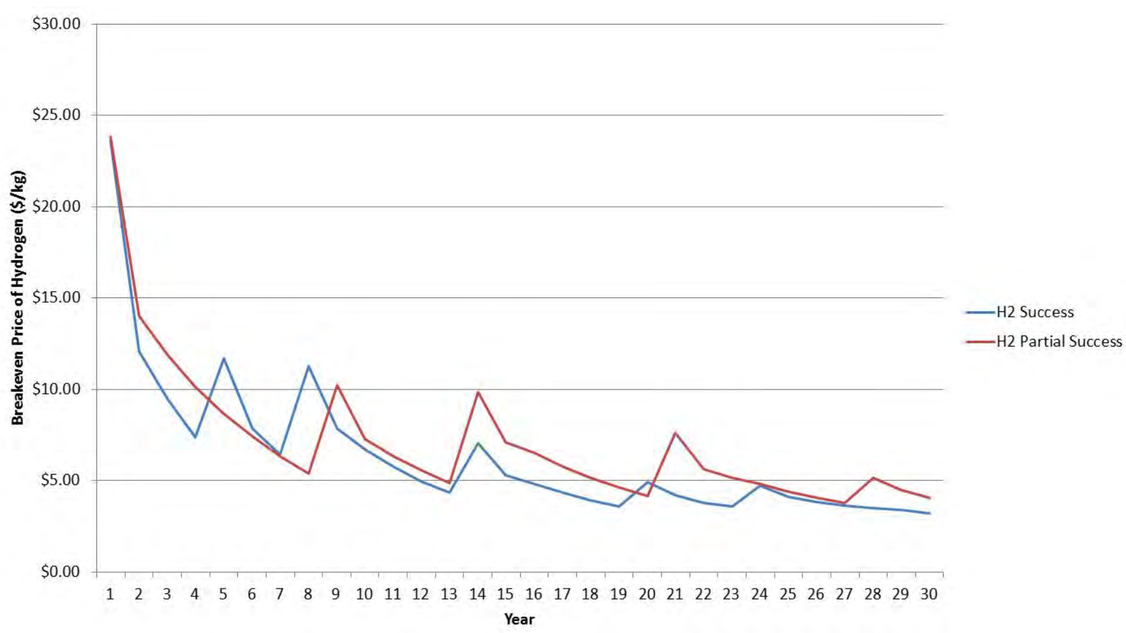

Figure ES-18: Breakeven price of hydrogen in each year of the 30-year analysis period for the H_2 Success and H_2 Partial Success scenarios

Figure ES-19 illustrates the breakdown by infrastructure component of the breakeven price of hydrogen for three 10-year periods. For example, the first period represents the price of hydrogen that would allow the supplier to breakeven over the first ten years of the 30-year analysis period. As a result of the low utilization of capacity in the first period, the breakeven price of hydrogen is approximately \$9/kg in the H_2 Success scenario (~\$6/gallon gasoline equivalent). In the second and third periods, the price declines to ~\$5/kg and ~\$4/kg, respectively, but is still larger than predicted in most steady-state models since this model accounts for underutilization, whereas steady-state models do not. In the H_2 Partial Success scenario when HFCV deployment is slower, the breakeven prices of hydrogen are significantly larger since underutilization is greater and infrastructure components achieve economies-of-scale more slowly. In all periods, the cost of CO_2 transport and storage represents less than 3% of the total breakeven price of hydrogen.

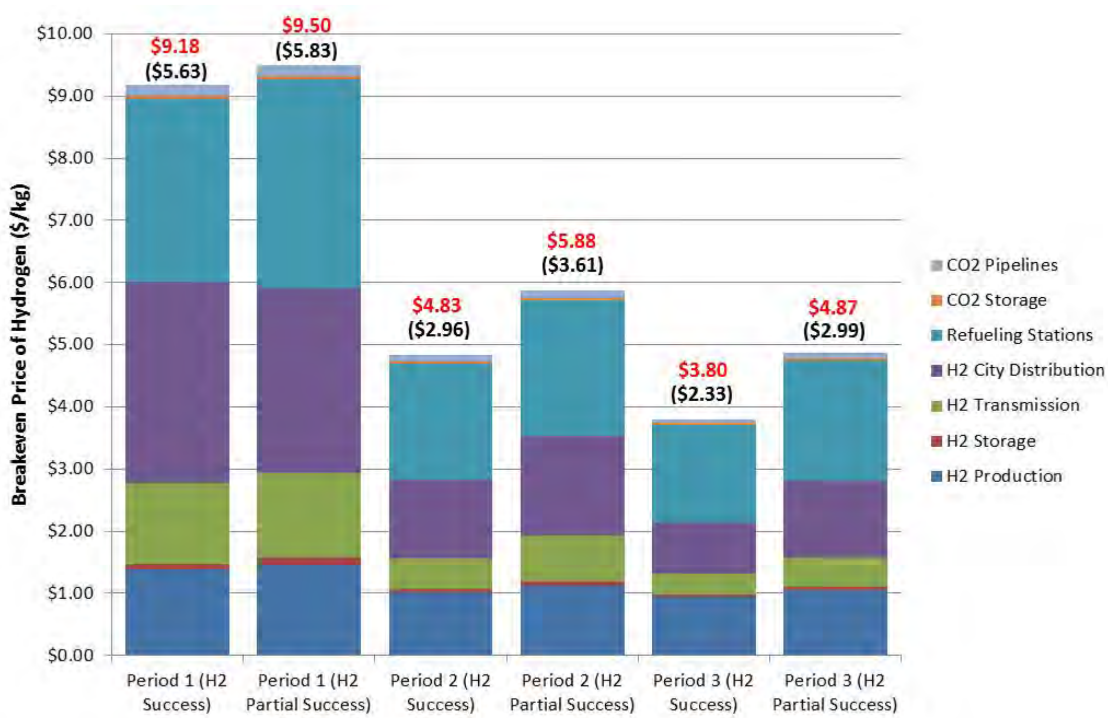

Figure ES-19: Breakeven price of hydrogen for three 10-year periods for the H_2 Success and H_2 Partial Success scenarios (price in parentheses is the equivalent price for a gallon of gasoline ($/gge) assuming that a HFCV has 63% better fuel economy than a gasoline HEV)

Given assumptions about the market price of hydrogen, the analysis of cumulative cash flow suggests that, even in the high price scenario, more than a decade will be required before cumulative cash flow becomes positive. Thus, it is unlikely that private corporations will invest in centralized hydrogen infrastructure without subsidies or other incentives. However, if centralized infrastructure is delayed for one tranche, the buy-down cost is reduced but the year in which cumulative cash flow remains positive does not improve unless the market price of hydrogen is high and HFCV deployment is slow, which further delays centralized infrastructure. Thus, even if early hydrogen demand is supplied by onsite production, subsidies will be required to incentivize early infrastructure deployment.

The best environment for hydrogen infrastructure investment is created when centralized infrastructure is delayed one tranche, the market price for hydrogen is high, and a production tax credit guarantees that suppliers receive $10/kg for all hydrogen supplied in the first ten years of the study period (i.e., subsidy case PTC-10). In this environment, the cumulative cash flow becomes positive within the first two years of infrastructure installation in both HFCV deployment scenarios. However, if the H_2 price is not high, subsidies are only effective if HFCV deployment is relatively fast (i.e., under the H_2 Success scenario). The total net present cost of the production tax credits ranges from $8 billion to $34 billion depending on the market price of hydrogen and the HFCV deployment rate.

GHG Emissions

One of the benefits of producing hydrogen using coal gasification with CCS is the ability to significantly reduce greenhouse gas (GHG) emissions in the transportation sector. In this section, the GHG emissions associated with the following three cases are quantified.

- *Business-as-Usual (BAU):* hydrogen infrastructure is installed as specified in the case study, but CCS is *not* installed at the centralized coal-based production facilities. GHG emissions associated with the power sector remain at 2005 levels.
- *Hydrogen with CCS (H_2-CCS):* coal-based hydrogen infrastructure is installed *with* CCS at the centralized production facilities, but GHG emissions associated with the power sector remain at 2005 levels.
- *Low Greenhouse Gas (GHG):* coal-based hydrogen infrastructure is installed *with* CCS and the power sector decarbonizes according to projections based on enactment of the Lieberman-Warner Climate Security Act of 2007.

In all cases, GHG emissions associated with coal gasification, steam methane reformation, electricity consumption, and fugitive emissions from CO_2 pipelines are included. In the BAU case, the well-to-wheels GHG emissions for H_2 fuel cell vehicles (HFCVs) are about 25% higher relative to gasoline vehicles. However, when CCS is adopted in the H_2-CCS and GHG cases, emissions associated with HFCVs are reduced by 80-90% relative to gasoline vehicles.

Task 4.2: Sub-regional Case Studies

The study area used for the regional case study of the western United States is divided into six sub-regions, which are defined by the optimal rollout strategy defined in the western U.S. case study (Figure ES-11). The purpose of the sub-regional case studies is to compare the infrastructure requirements and costs between sub-regions with the objective of learning how the geographic characteristics of each sub-region and the region as a whole impact hydrogen cost.

The comparison of infrastructure design and cost in the six sub-regions provides several insights into the drivers of infrastructure cost. First, the average percentage of infrastructure capacity utilized over an analysis period is a major determinant of the cost of hydrogen. This metric can be incorporated into infrastructure models as an effective capacity factor for each component and must account for underutilization resulting from the rate of HFCV deployment and oversizing of infrastructure. The effective capacity factor generally increases over time as infrastructure becomes better utilized and tends to be smallest for pipelines since this model oversizes pipelines for the projected flow over their 20-year lifetimes.

Second, the length of pipelines is an important determinant of CO_2 transport and H_2 transmission and distribution costs. Ideally, the length of H_2 transmission and CO_2 transport pipelines will be adjusted in infrastructure models to account for sharing of pipeline capacity between sub-regions. Pipeline supply networks tend to become more interconnected over time and this model suggests that, on average, sharing can be represented as a decrease in the average pipeline length per demand center for transmission pipelines of 1% in the first period and 17% in the third period. Sharing is more significant for CO_2 pipelines, resulting in a 17% decline in the average pipeline length per production site in the first period and a 35% decline in the third period.

Sharing of infrastructure capacity is also an important determinant of cost for other infrastructure components. In examining the total levelized cost in each sub-region, a trend emerges that suggests that more isolated (i.e., less connected) sub-regions tend to have larger levelized costs (Figure ES-20). As sub-regions become more connected over time, the total levelized costs in all sub-regions tend to converge, which suggests that interconnection improves utilization and economies-of-scale.

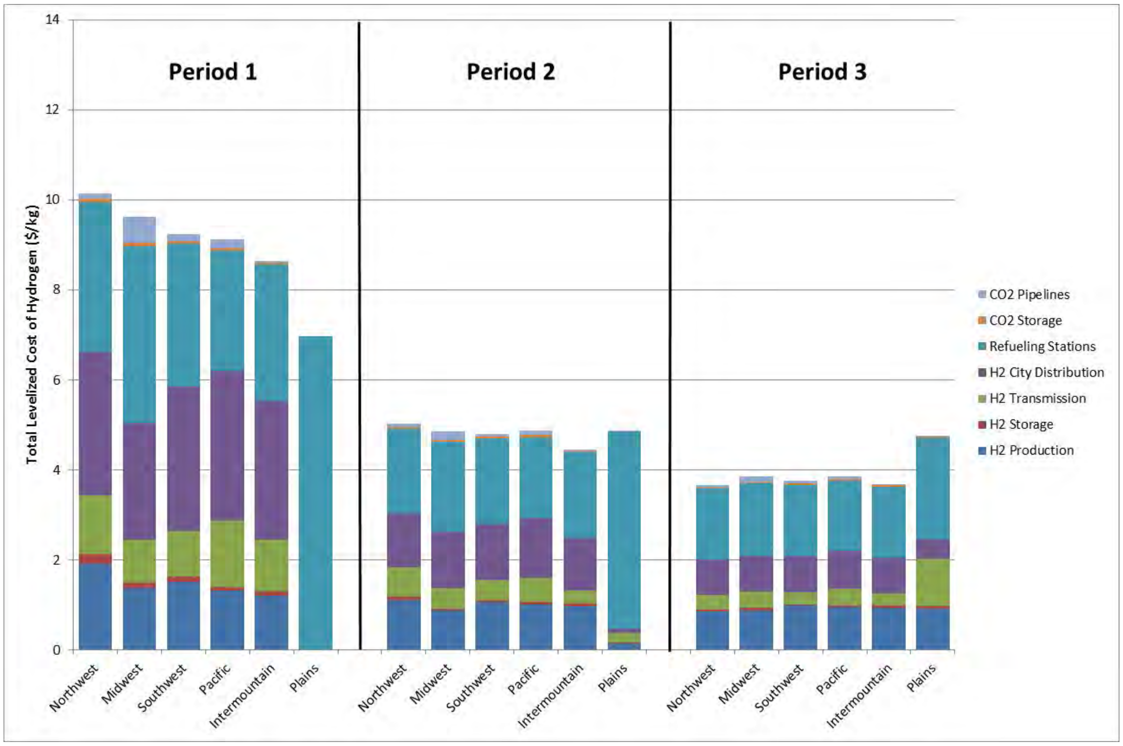

Figure ES-20: Levelized cost of hydrogen for each infrastructure component, 10-year analysis period, and sub-region given the H_2 Success scenario

It is important to note that steady-state infrastructure models generally do not incorporate underutilization, regionally-specific metrics like pipeline length, and regional sharing of infrastructure. Since this study indicates that all of these factors are important determinants of cost, they need to be better incorporated into steady-state models to improve cost estimates.

Final Comments

This document describes models for examining how centralized hydrogen and CCS infrastructure with pipeline distribution might deploy in real geographic regions. They are an improvement over existing hydrogen and CCS infrastructure models since they can incorporate high resolution spatial data, model the development of integrated regional supply networks, and account for the underutilization of infrastructure over time. Although the models examine coal-based hydrogen production in the western United States and CCS deployment in the southwestern United States, they can be modified to examine other feedstocks and geographic regions.

One of the major insights provided by the hydrogen model is the importance of the capacity factor in determining the levelized cost of hydrogen associated with each component. Consequently, any deployment or infrastructure design strategies that can increase infrastructure utilization can lead to substantial reductions in cost. In reality, infrastructure planners will have more flexibility in the timing of investments and the location and sizing of components than is represented in this model. This added flexibility will inevitably lead to improved capacity factors and, thus, it is likely that the results of this model represent a conservative (i.e., high) estimate of hydrogen costs. Consequently, it is suggested that these costs are considered an upper bound with the cost estimates from steady-state models representing the lower bound.

1.0 Introduction

Carbon dioxide capture and storage (CCS) involves capturing CO_2 from large point sources and then injecting it into deep underground reservoirs for long-term storage. By preventing CO_2 emissions into the atmosphere, this technology has significant potential to reduce greenhouse gas (GHG) emissions from fossil-based facilities in the power and industrial sectors. Furthermore, the application of CCS to power plants and hydrogen production facilities can reduce CO_2 emissions associated with electric vehicles (EVs) and hydrogen fuel cell vehicles (HFCVs) and, thus, can improve GHG emissions in the transportation sector as well. This research specifically examines strategies for transitioning to large-scale coal-derived energy systems with CCS for both hydrogen fuel production and electricity generation. Two particular emphases of this research are the development of spatially-explicit modeling tools for examining how these energy systems might develop in real geographic regions and the application of these tools to regional case studies.

We employ an integrated modeling approach that addresses all infrastructure components that are required in the transition to these energy systems. In the case of hydrogen fuels, this infrastructure includes coal-based hydrogen production facilities with CO_2 capture, hydrogen storage, CO_2 and H_2 pipeline distribution networks, hydrogen refueling stations, and CO_2 injection sites. For CCS in the electricity and industrial sectors, CO_2 capture equipment, CO_2 pipeline networks, and CO_2 injection sites are modeled. The overall objective is to better understand the system design issues and economics associated with the widespread deployment of hydrogen and CCS infrastructure in real regions. Specific objectives of this research are to:

- Develop improved techno-economic models for all components required for the deployment of both hydrogen and CCS infrastructure,
- Develop novel modeling methods that combine detailed spatial data with optimization tools to explore spatially-explicit transition strategies,
- Conduct regional case studies to explore how these energy systems might develop in different regions of the United States, and
- Examine how the design and cost of coal-based H_2 and CCS infrastructure depend on geography and location.

In this final report, we describe research results from Phase 2 of a technical/economic study of fossil hydrogen energy systems with CO_2 capture and storage (CCS). This work was performed under NETL Award No. DE-FC26-07NT42929 during the period from August 2008 through December 2011. Phase 2 of this study includes three research tasks, numbered four to six. The overall objective of Task 4 is the development of a group of models for exploring the transition to a coal-based hydrogen transportation system with CCS. The integrated model is called the *Hydrogen Infrastructure Deployment Model* (HIDM) and its various components are described in Section 2. First, the techno-economic models are described and then the details of the various sub-models that optimize the design of each infrastructure component are provided.

In Task 5, we assess the costs and performance of systems for capturing and storing CO_2 from industrial and power sector sources as well as optimal strategies for their deployment. Section 3 begins by presenting technical and economic models for CO_2 capture at a variety of large point sources in the power and industrial sectors. Next, we describe a regional transition model that was developed to examine optimal CCS deployment strategies in real geographic regions. The model combines detailed spatial and techno-economic data with optimization tools and policy constraints to identify the least-cost CCS infrastructure for meeting a specific CCS target. Section 3 concludes with a case study in the southwestern United States, which explores how a transition from early demonstration projects to widespread adoption of CCS might occur given the subsidies and CO_2 prices proposed in the American Power Act.

In Task 6, we return to the topic of hydrogen infrastructure and present several case studies that examine regional transition strategies for coal-based hydrogen with CCS. Section 4 begins with a description of a case study in the western United States. The section explores system design issues and presents costs, GHG emissions, coal consumption, and CO_2 storage capacity constraints for two HFCV deployment scenarios. This section also explores two alternative scenarios in which centralized production is delayed (i.e., onsite production is utilized during early deployment) and examines the efficacy of various hydrogen subsidies in incentivizing infrastructure investment. The second part of Section 4 describes the cost and design of hydrogen infrastructure within several sub-regions within the western United States. A comparison is conducted to provide insight into how and why infrastructure design and cost differ between sub-regions.

2.0 Task 4.0: Modeling the Transition to a Coal-based Hydrogen Transportation System with Carbon Capture and Storage

The primary objective of task 4 is to develop a spatially-explicit model for simulating a transition to a hydrogen-based transportation sector supplied by coal-derived hydrogen with carbon capture and storage (CCS). The structure of the model that was developed, the *Hydrogen Infrastructure Deployment Model* (HIDM), is illustrated in Figure 1 and consists of several sub-models that use detailed spatial and techno-economic data to optimize infrastructure deployment.

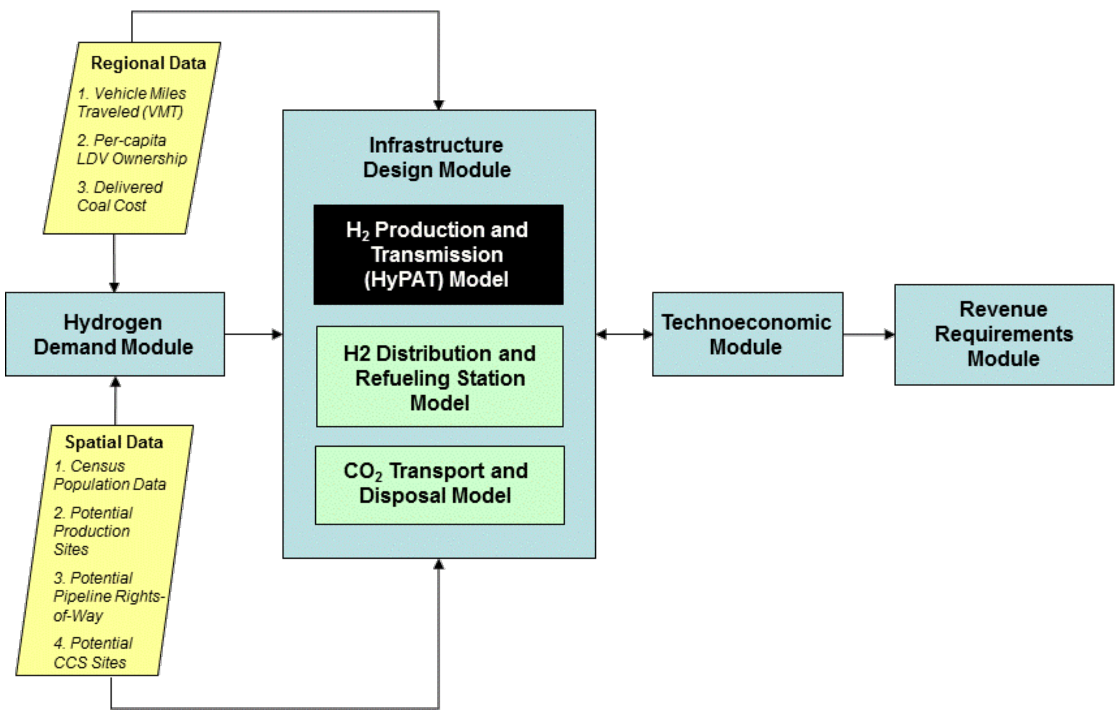

Figure 1: Model structure for Hydrogen Infrastructure Deployment Model

The first module is the *Hydrogen Demand Module*, which identifies the spatial distribution of hydrogen demand at various levels of hydrogen fuel cell vehicle (HFCV) market penetration. The location and magnitude of hydrogen demand at each market penetration level is provided to the *Infrastructure Design Module*, which consists of three sub-models that must be run in a certain sequence. The first model in the sequence is the *H_2 Production and Transmission Model*, which is a network optimization tool that identifies the lowest cost H_2 production and pipeline transmission infrastructure at each HFCV market penetration level. The *H_2 Distribution and Refueling Station Model* is a simple heuristic model that estimates the number of refueling stations and length of distribution pipelines within each of the identified demand centers (i.e., cities). This model is not dependent on the outputs of the other models and can be run independently. The *CO_2 Transport and Disposal Model* is run after the *H_2 Production and Transmission Model* since one input is the optimal locations of production facilities. This model is a network optimization tool that identifies the optimal CO_2 transport and injection infrastructure associated with hydrogen production facilities.

The sub-models in the *Infrastructure Design Module* provide detailed inventories of the H_2 production, transmission, distribution, refueling station, and CCS infrastructure requirements for each HFCV market penetration level. These inventories are then exported to the *Techno-economic Module*, which includes detailed techno-economic models for all infrastructure components. Detailed cost estimates for the infrastructure required at each market penetration level are then provided to the *Revenue Requirements Module*, which calculates the cost of deploying this infrastructure under different market penetration scenarios (i.e., rates of HFCV adoption).

A more detailed description of each sub-model is provided in sections 2.1 and 2.2. Section 2.1 describes the *Techno-economic* and *Revenue Requirements Modules,* which are the fundamental economic models for costing individual infrastructure components and tracking investments over time. Section 2.2 describes the *Hydrogen Demand and Infrastructure Design Modules*, which identify the optimal deployment of coal-derived hydrogen infrastructure in real geographic regions over time.

2.1 Techno-economic Modeling

To model coal-derived hydrogen infrastructure deployment with CCS, detailed techno-economic models are developed for each infrastructure component. The models encompass the range of processes and equipment necessary for hydrogen production, distribution, refueling stations, and transport and storage of carbon dioxide. The models provide detailed and scalable cost estimates for each component. Given these estimates, a revenue requirements model integrates the components and accounts for the timing of infrastructure investments. This section also includes a description of the HFCV market penetration scenarios that are used in this model. All costs are in 2005 U.S. Dollars.

2.1.1 Hydrogen Production via Coal Gasification

Several studies have estimated the cost of H_2 production via coal gasification for a variety of facility sizes [1-7]. However, most individual studies estimate the cost for only one facility size and do not provide an equation for facility cost as a function of size. To derive this equation, facility cost estimates were collected from the literature and normalized to 2005 U.S. Dollars using the Chemical Engineering Plant Cost Index. All cost estimates represent current overnight capital for facilities that maximize H_2 production and include the cost of CO_2 capture, compression and drying (Figure 2). A power function is fit to the cost estimates in Figure 2, resulting in Equation 1, where C_{cap} is the overnight capital cost (million 2005$) and *s* is the facility size (tonnes H_2/day).

1 $$C_{cap} = 6.4362 * (s^{0.7559})$$

Table 1 provides the overnight capital cost for five discrete facility sizes from 300 to 1500 tonnes H_2/day, based on equation 1. The total annual cost for constructing and operating the plant includes the annualized capital cost, O&M cost, feedstock cost, and revenue from electricity co-production. Performance and cost assumptions used to derive plant economics, CO_2 emissions, and energy use are listed in Table 2. It is assumed that the cost for a given plant size remains fixed over time (i.e., costs and efficiencies do not improve with learning and R&D). The delivered coal cost and CO_2 emission rate at each facility is assigned by state [8, 9] and includes embedded CO_2 emissions of 4.38 kg CO_2 per GJ of delivered coal [10] (Table 3). It is assumed that the cost of coal increases by 0.5% per year, excluding inflation. However, the cost of coal could increase more rapidly if significant quantities of coal are used for hydrogen production.

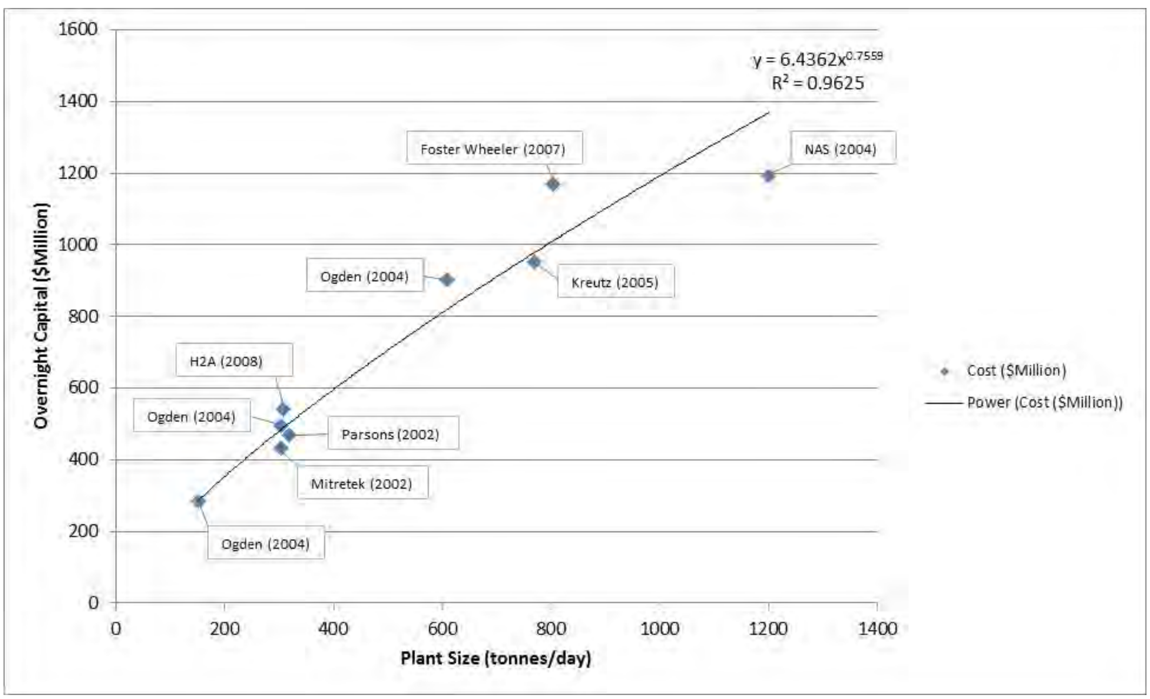

Figure 2: Overnight capital cost estimates for coal-to-H_2 facilities of various sizes

Table 1: Overnight capital cost for various facility sizes based on Equation 1

Facility size (tonnes H_2/day)	Overnight capital cost (million $)
300	479.8
600	810.3
900	1100.9
1200	1368.3
1500	1619.7

Table 2: Performance and cost assumptions for coal-to-H_2 facilities

Parameter	Value	Units	Source
Capacity factor (max)	80	%	[3]
Facility Lifetime	40	years	[7]
Fraction of coal converted to H_2	57.46	% (LHV)	[3]
H_2 output pressure	68	bar	[7]
Fraction of coal converted to electricity	2.09	% (LHV)	[3]
CO_2 capture efficiency	91.28	%	[3]
CO_2 output pressure	150	bar	[7]
Facility O&M cost	4	% of overnight capital, excluding coal feedstock	[3]

Table 3: Delivered coal cost and CO_2 emission rate by state [8, 9]

State	Delivered Coal Cost ($/GJ)	CO_2 Emission Rate (kg/GJ)
Alabama	2.45	92.8
Arkansas	1.70	96.0
Arizona	1.82	93.9
Colorado	1.57	94.8
Connecticut	3.32	92.7
Delaware	3.28	93.5
Florida	3.28	92.4
Georgia	3.52	92.6
Iowa	1.33	95.3
Illinois	1.98	93.2
Indiana	2.23	93.0
Kansas	1.61	95.2
Kentucky	2.16	92.3
Louisiana	2.49	96.1
Massachusetts	3.32	93.5
Maryland	3.28	93.6
Michigan	2.76	94.4
Minnesota	1.84	96.2
Missouri	1.60	93.2
Mississippi	3.77	92.5
Montana	1.67	96.4
North Carolina	3.38	93.0
North Dakota	1.18	98.7
Nebraska	1.38	96.0
New Jersey	4.03	93.4
New Mexico	1.88	93.0
Nevada	2.40	94.2
New York	2.92	93.2
Ohio	2.19	92.4
Oklahoma	1.66	96.0
Oregon	1,71	96.1
Pennsylvania	2.41	93.2
South Carolina	3.60	92.7
Tennessee	2.47	92.3
Texas	1.80	96.1
Utah	1.75	92.4
Virginia	3.28	93.1
Washington	1.69	94.6
Wisconsin	2.27	94.8
West Virginia	2.38	93.6
Wyoming	1.35	95.7

2.1.2 Hydrogen Storage, Pipeline Transport, and Refueling Stations

Techno-economic models for hydrogen storage, pipeline transport, and refueling stations have been developed that are consistent with version 2.2 of the U.S. DOE H2A Delivery Scenario Analysis Model [10].

2.1.2.1 Hydrogen Storage

Hydrogen storage is required at each production facility in order to ensure reliable supply during plant outages and seasonal surges in demand. Consistent with the H2A model, hydrogen is stored in caverns near each production facility. For simplicity, it is assumed that sufficient useable cavern capacity is located adjacent to each potential production location. The cavern associated with each plant is required to store about nine days of demand given the assumption that each plant will experience approximately 120 days each year in which demand will surge a maximum of 10% above the average daily demand, 120 days in which demand will be 10% below the average daily demand, and 10 outage days. Maximum cavern pressure is assumed to be 125 bar with hydrogen released from the cavern at ~68 bar. Detailed technical design and cost parameters are given in the H2A Delivery Scenario Analysis Model [10]. The three largest cost components are associated with the compressors, injection wells, and cushion gas. The capital cost associated with a cavern ranges from about $22 million for a small production facility to about $83 million for a large facility, which is about 5% of the overnight capital of the production facility. The O&M cost, including electricity for the compressors, is about 7% of the total capital cost of the storage cavern.

2.1.2.2 Hydrogen Pipeline Transport

Two types of pipelines are modeled in this study: transmission and distribution. Transmission pipelines are defined as regional pipelines that transport hydrogen from production facilities to distribution hubs in each of the demand centers (i.e., cities). Distribution pipelines are those within cities that transport hydrogen from the distribution hub to the network of refueling stations.

The inlet pressure for transmission pipelines matches the H_2 output pressure from the production facility (~68 bar) so no additional compression is required prior to pipeline transport. Booster compression is not explicitly modeled in this study although it is probable that additional compression will be required for transmission pipelines longer than 200 kilometers. For distribution pipelines, the inlet pressure is 41 bar and the outlet pressure at refueling stations is 20 bar. Both transmission and distribution pipelines are assumed to have a lifetime of 20 years.

Cost and performance equations for both types of pipelines are given in the H2A Delivery Scenario Analysis Model and include installation, materials, right-of-way, operations, and maintenance [10]. For distribution pipeline costs, the equations for downtown installation of service pipelines are used. Table 4 provides the capital cost per kilometer for several nominal pipe diameters for transmission (flat, rural terrain) and distribution (urban terrain) pipelines. It is evident that pipeline costs can be substantially greater in urban environments. For transmission pipelines, it is assumed that the construction cost doubles in urban and/or mountainous terrain, with construction accounting for ~50% of the installed capital cost.

2.1.2.3 Hydrogen Refueling Stations

In each demand center, the *minimum* number of hydrogen refueling stations is set equal to ten percent of the number of conventional gasoline stations in order to ensure consumer convenience. Nicholas et al. [11] has shown that hydrogen provided at 10% of existing gasoline stations could provide adequate coverage for customers. The number of gasoline stations in each demand center is estimated using the U.S. average number of light-duty vehicles per station, which is 1,419 [10]. The average size of H_2 refueling stations in each demand center is then calculated based on the peak hydrogen demand and minimum number of H_2 stations. The peak hydrogen demand accounts for a 10% surge in demand above the average during summer and an additional 8% surge on Fridays [10]. If the average peak station demand is greater than a *maximum* peak dispensing output of 2,400 kg/day, the peak hydrogen demand is divided by an *average* peak dispensing output of 1,800 kg/day to estimate the number of required H_2 stations in each demand center. The size of H_2 refueling stations in each demand center is assumed to be uniform in each build phase. Given the average peak dispensing output and number of H_2 refueling stations in each demand center, the H2A Delivery Scenario Analysis Model is used to design and cost the required station equipment, including compressors, low-pressure storage tanks, dispensers, cascade systems, and associated buildings [10].

Table 4: Capital cost per km (thousand $) for 100-km hydrogen distribution and transmission pipelines of various nominal pipe diameters

Diameter (in)	Transmission (flat, rural terrain)	Distribution (urban terrain)
4	225	364
6	253	662
8	285	1238
10	321	1701
12	361	2140
16	453	2950
20	562	3668
24	687	4292
30	905	5055
36	1160	5609
42	1452	5954

In demand centers where high pipeline transport costs result in prohibitively large hydrogen costs from centralized facilities, it is assumed that all demand is met by onsite production via steam methane reformation at individual refueling stations. The cost and design of these stations is modeled using the H2A Current Forecourt Hydrogen Production from Natural Gas Model [12], which includes the cost of onsite steam methane reformers, process water, electricity, and natural gas. In all stations, gaseous hydrogen is delivered to vehicles at 6,000 psi (~414 bar) and the electricity cost is assumed to be $0.082/kWh, which is the average U.S.

commercial electricity cost in 2005 as specified in the H2A Model [10]. At stations with onsite production, the average U.S. industrial natural gas cost in 2005 is assumed ($0.243/Nm^3$) [10].

2.1.3 Carbon Dioxide Capture, Transport, and Storage

It is assumed that ~91% of the CO_2 produced at hydrogen production facilities is captured and stored in geologic formations [3]. CO_2 is separated from the syngas as part of the hydrogen production process and then compressed and dried in preparation for pipeline transport. The CO_2 is then transported as a supercritical fluid to storage sites where it is injected into onshore deep saline aquifers. The cost of CO_2 capture, compression, and drying is included in the hydrogen production cost described in section 2.1.1. Detailed techno-economic models for CO_2 transport and storage were developed based on an extensive literature review and are described in detail in Ogden and Johnson [13]. Sections 2.1.3.1 and 2.1.3.2 include excerpts relevant to this study.

2.1.3.1 CO2 Transport

Onshore pipeline transport is a proven technology with approximately 2,400 km of large CO_2 pipelines in operation globally [14, 15]. The majority of these pipelines are used to supply enhanced oil recovery operations in the United States. Several studies identify pipeline transport as the most economical method for moving large volumes of CO_2 overland [16, 17].

The cost of pipeline transport is affected by the characteristics of both the pipeline route and the pipeline itself. Elements of the route that can impact cost include both the physical geography (e.g., river and road crossings, parks, terrain) and social geography (e.g. population density, regional labor and land costs, local acceptance) [18]. In addition, pipeline characteristics, such as length, diameter, materials, the number of bends, and the need for booster stations, are important determinants of cost.

Pipeline Design

Fluid flow models that use hydraulic equations for turbulent flow [4, 18-22] are useful in estimating pipe diameter since they include the parameters relevant to pipeline design (i.e., inlet and outlet pressures, pipeline length, CO_2 mass flow rate, pipeline roughness factor, elevation change along the segment, and CO_2 density, viscosity, and average temperature) and are thus flexible in their application. There are practical constraints on pipeline operating conditions. To avoid two-phase flow, CO_2 should be transported in the supercritical phase, which occurs at a pressure greater than 7.38 MPa [23]. It is recommended that it is transported at pressures greater than 8.6 MPa where changes in compressibility can be avoided at a range of temperatures used for pipeline operation. Table 5 lists common design parameters for CO_2 pipeline transport.

Since pipelines are not available in continuous diameters, the pipeline diameter used for a particular project is constrained by the available discrete sizes, or nominal pipe size (NPS). The NPS generally corresponds to the external diameter in inches of commercially available pipelines [20]. In this study, CO_2 pipeline diameter is restricted to six nominal pipe sizes (12.75, 16, 24, 30, 36, and 42 inches).

In some cases, it may be economically advantageous to design the pipeline with booster compressor stations every 150-300 km. If CO_2 is recompressed at intervals, this allows use of smaller diameter, lower cost pipelines. However, there is a trade-off between lower pipe costs and the added costs of compression.

Table 5: Common design parameters for pipeline transport [21]

Parameter	Value	Units
Inlet Pressure	15.2	MPa
Minimum Outlet Pressure	10.3	MPa
Average CO_2 Temperature	25	°C
Average CO_2 Density	884	kg/m^3
Average CO_2 Viscosity	6.06×10^{-5}	$N\text{-}s/m^2$
Pipeline Roughness Factor	4.57×10^{-5}	meters
Pipeline Capacity Factor	100	%
CO_2 Purity in Pipeline	100	%
Change in Elevation	0	meters

The maximum capacity, length, elevation difference, and actual diameter of several existing CO_2 pipelines are known (Table 6) [22]. Using this information, it is possible to compare the actual diameters with those calculated from the pipeline models provided by McCoy and Rubin [20] and Vandeginste and Piessens [22]. Table 6 indicates that both models accurately estimate the diameters of the existing CO_2 pipelines. The model provided by Vandeginste and Piessens [22] is used to identify the maximum capacity of the six nominal pipe sizes used in this study (Table 7).

Table 6: Comparison between actual and calculated pipeline diameter for existing CO_2 pipelines

Pipeline	Maximum Capacity (Mt/year)	Length (km)	Elevation difference (m)*	Actual NPS diameter (in)	McCoy NPS diameter (in)	Vandeginste NPS diameter (in)
Transpetco	3.4	193	1094	12.6	12	14
Sheep Mountain pt. 1	6.4	296	893	20	18	18
Sheep Mountain pt. 2	9.3	360	464	24	24	24
Bravo	7.4	351	955	20	20	20
Weyburn	1.8	330	46	14	14	14

*Elevation difference represents a decrease in the elevation between the start and end points of the pipeline
**For the calculated values, the flow rate (capacity), length, and elevation change given in the table for each specific pipeline are used. The inputs listed in Table 5 are used for the unknown parameters.

Pipeline Cost

For onshore CO_2 pipelines, the costs include capital costs (engineering, installation, and materials) and operations and maintenance (O&M) costs (monitoring, inspection, and repair). If booster stations are required, additional capital and O&M costs are incurred. The energy cost for operating the booster pump or compressor can be a significant annual expense.

Several studies were surveyed that estimate onshore CO_2 pipeline capital costs [18-21, 24]. Based on these studies, average pipeline capital cost functions were developed for six discrete pipeline lengths from 50 to 500 km and several nominal pipe sizes from 4 to 30 inches. These functions were used to derive equation 2 for calculating pipeline capital cost as a function of pipeline NPS and length.

2 $$C^p = 32.086 L^{-0.033} D$$

where C^p is the capital cost (2005$/m), L is the pipeline length (km), and D is the nominal pipe size (in). The capital cost per meter shows very little dependence on overall pipeline length L and is approximately linear in D.

Capital cost estimates given by equation 2 represent *average* CO_2 pipeline construction costs in the United States. Representative capital costs and pipeline capacities for the six nominal pipe sizes are given in Table 7. These values assume a 90% capacity factor and a 250-km pipeline with a design pressure of 150 bar and an available pressure drop of 35 bar. Several project-specific factors can influence the actual cost of construction, including population density, physical terrain, regional location, and river and road crossings. In particular, regional cost variations in the United States can exceed 30% [20] and construction in urban areas or rocky, marshy, or mountainous terrain can significantly increase the installation cost. In this study, it is assumed that the construction cost for CO_2 pipelines doubles in urban and/or mountainous terrain, with construction accounting for ~50% of the installed capital cost.

Table 7: Capacities and base installed costs of pipelines for several nominal pipe sizes in flat, rural terrain

Nominal Pipe Size (inches)	Capacity ($MtCO_2$/year)	Capital Cost ($/km)
12.75	1.5	341,000
16	3	428,000
24	8	642,000
30	17	802,000
36	24	963,000
42	35	1,123,000

The literature provides a range of fixed O&M costs for onshore pipelines between 0.5 and 4% of the total capital cost with an average of 2.2%. The average value is used in this study and is assumed to include the cost of booster compression. The levelized cost of onshore pipeline transport ($/$tCO_2$ transported) is shown in Figure 3 as a function of CO_2 flow rate and pipeline length. For a 100 km pipeline, the levelized cost is between $1 and $2.50/$tCO_2$ for plants producing > 5,000 tCO_2 per day. The levelized cost increases substantially for longer pipelines, but is still between $4 and $10/$tCO_2$ for a 500 km pipeline transporting >5,000 tCO_2/day. Given that, on average, ~0.018 tonnes CO_2 is captured per kg H_2 produced, the cost of CO_2 transport is $0.02-$0.20/kg H_2 if the pipelines are fully utilized. Because the technology associated with onshore pipeline transport is mature, costs are not expected to benefit from technological learning in the future.

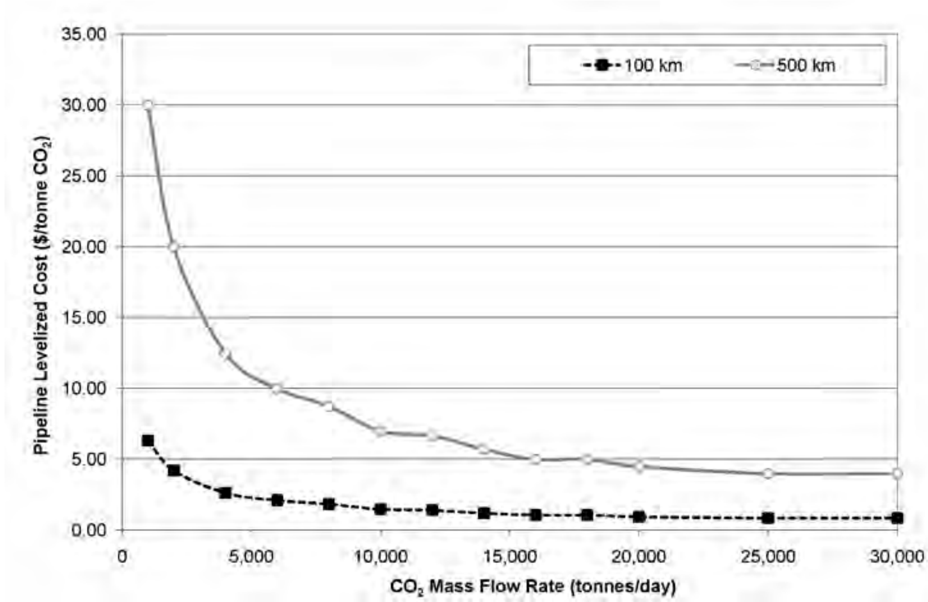

Figure 3: Levelized cost for onshore pipeline transport [13]

2.1.3.2 CO_2 Injection

This section describes the economics of injecting CO_2 into geologic reservoirs for long-term storage. In this study, CO_2 injection is limited to onshore deep saline aquifers since these geologic formations offer much larger long-term storage capacity than other formations (e.g., depleted oil and gas reservoirs). This section begins with an overview of models for injection site infrastructure requirements and then discusses the costs of the various injection components.

Injection Site Design

To estimate the cost of CO_2 injection, it is necessary to calculate the required number of injection wells and the extent of the underground CO_2 plume. The number of injection wells can be derived from the maximum injection rate per well, which is dependent on the specific characteristics of a target reservoir (e.g., permeability, porosity, pressure, and thickness). Ahmed [25] provides a detailed review of the reservoir fluid flow equations that can be used to model CO_2 injection rates. These equations address steady-state, pseudosteady-state, and transient (unsteady-state) flow regimes.

The maximum extent of the underground CO_2 plume over the life of the project is important since it provides the radius of influence (r_e) used in calculating the injection rate and also identifies the area used to identify site characterization costs. Various studies have developed models for calculating plume radius for different reservoir types [21, 26-28]. Table 8 provides parameters for two representative saline aquifers and lists the calculated plume radius and injection rate for each aquifer. The injection rate is highly sensitive to changes in certain reservoir parameters like permeability and thickness and can range from tens to thousands of tonnes CO_2 per day.

Table 8: Common Aquifer and Injection Parameters [28, 29]

Input Parameter	Cold/Shallow	Hot/Deep	Units
Wellhead Injection Pressure	10.3	10.3	MPa
Reservoir Pressure (p_e)	10	30	MPa
Maximum BHIP (p_w)	15	45	MPa
Reservoir Temperature	35	155	°C
Reservoir CO_2 Viscosity (μ)	5.77×10^{-5}	3.95×10^{-5}	Pa-s
Reservoir CO_2 Density (ρ)	714	479	kg/m^3
Reservoir Depth (d)	1000	3000	m
Reservoir Thickness (h)	30	30	m
Porosity (Φ)	0.15	0.15	
Permeability (k)	1.97×10^{-14}	1.97×10^{-14}	m^2
Calculated Parameter			
Plume Radius (r_e) @ 20 years	4.8	5.9	km/well
Max Injection Rate (q_{well})	1850	5300	tonnes/day/well

In the absence of detailed data on the reservoir characteristics of individual aquifers, all aquifers are assumed to have the characteristics of a cold/shallow reservoir (Table 8). The maximum injection rate of 1850 tonnes CO_2 per day per well is used to determine the number of required injection wells at each CO_2 storage site. Given the number of injection wells and a plume radius per well of 4.8 km, the area of the CO_2 plume (or "area of review") can be calculated.

CO_2 Injection Costs

A typical CO_2 injection site includes injection wells and surface equipment (e.g., distribution pipelines and headers). In some cases, compressors or pumps may be required to achieve the required wellhead injection pressure at each well. Costs include site characterization, well drilling, surface equipment, permitting, and monitoring.

Site characterization costs include 3-D seismic imaging of the area of review, drilling of characterization wells, and data processing and modeling services. McCoy [26] estimates these costs as \$38,610/km^2 for 3-D imaging, \$3,000,000 per well for drilling of characterization wells, and 30% of the total cost for data processing, modeling, and other services. One characterization well is required for every 65 km^2 of the area of review. Equation 3 describes the total site characterization cost (corrected to 2005\$) as a function of the area of review.

3 $$C^{site} = 117344A + 2.70x10^{6}$$

where A is the area of review (km^2). In developing an aquifer site for CO_2 injection, permitting studies must be conducted and land, mineral leases, and permits must be purchased. The estimated average cost is approximately \$23,000 per injection well [21, 30].

Well drilling costs include the costs of drilling and completing wells for CO_2 injection. Since limited data is available on the costs of drilling wells specifically for CO_2 injection, most studies assume that the costs will be similar to those for drilling onshore oil wells in the United States

[21, 26, 29, 31]. Based on 2004 Joint Association Survey (JAS) data, equation 4 describes the well drilling cost as a function of well depth [32].

4 $$C^{wd} = (-3.96x10^{-8}d^3 + 4.00x10^{-4}d^2 - 0.84d + 903)d$$

where d is well depth (m) and C^{wd} is the drilling cost (2005$/well). For typical well depths of one to three km, the cost is $0.4 to $2.7 million per well.

Several studies assume that surface equipment costs for CO_2 injection are similar to the costs of equipping water injection wells for secondary oil recovery [21, 26, 31]. These studies use data published by the Energy Information Administration [33] on lease equipment costs for secondary oil recovery in West Texas. Equations 5 and 6 were developed from 2005 EIA data using the approach employed by McCoy [26].

5 $$C^{eq} = 0.0121d^2 - 21.745d + 53818$$

6 $$C_N^{eq} = \left[\begin{array}{c} C_{equip}, N_{wells} > 20 \\ C_{equip}\left(\dfrac{21}{N_{wells}}\right)^{0.5}, N_{wells} \le 20 \end{array} \right.$$

where C^{eq} is the surface equipment cost (2005$/well).

O&M costs include normal daily expenses, surface maintenance, and subsurface maintenance and are derived from EIA data for secondary oil recovery [33].

7 $$C^{OM} = 8.76d + 13267$$

where C^{OM} is the O&M Cost (2005$/well/year). McCoy [26] reports the monitoring cost to be ~$0.02/t$CO_2$ injected.

Figure 4 shows the levelized cost for CO_2 injection into a cold/shallow aquifer for several annual CO_2 flow rates, assuming a project life of 20 years and capital recovery factor (CRF) of 11.75% (corresponding to a discount rate of 10%). The contribution of each cost component to the overall cost is also shown. The most surprising finding is that site characterization contributes ~90% of the total levelized cost while drilling costs contribute less than 7%. The levelized cost of CO_2 injection varies from \$1.70 to \$2.90/tonne CO_2 for the cold/shallow case. Given that, on average, ~0.018 tonnes CO_2 is captured per kg H_2 produced, the cost of CO_2 injection is \$0.03-\$0.05/kg H_2.

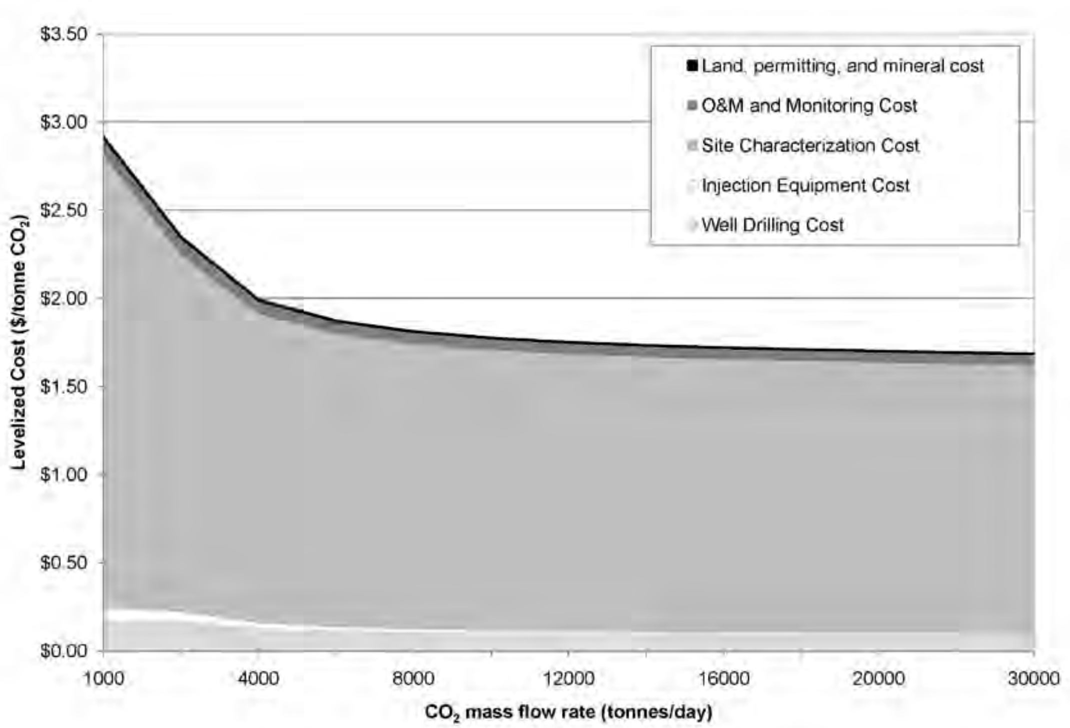

Figure 4: Contribution of each cost component to the total levelized cost of CO_2 injection into a cold/shallow aquifer [13]

2.1.4 Revenue Requirements Module

The *Infrastructure Design* and *Techno-economic Modules* quantify the required infrastructure investments for supplying hydrogen to HFCVs at specific market penetration levels in a particular geographic region (e.g, 20 million HFCVs in the western U.S.). The *Revenue Requirements Module* then tracks the timing and annualized cost of these investments over a 30-year planning period. The capital investments include initial capital costs as well as replacement costs. The timing of the initial infrastructure investments is dictated by projections of HFCV market penetration, as described in Section 2.1.5.

Investment requirements are tracked individually for each major infrastructure component, including H_2 production, H_2 storage, H_2 pipeline transmission, H_2 pipeline distribution, H_2 refueling stations, CO_2 pipeline transport, and CO_2 injection. Specifically, the model tracks the annualized costs and revenues associated with equity, debt, feedstock, non-fuel O&M, depreciation, by-product sales (e.g., electricity), and corporate taxes. The basic economic assumptions used in the model are listed in Table 9 and are consistent with the U.S. DOE Carbon Capture and Sequestration Systems Analysis Guidelines for a high-risk project [34].

Table 9: Financial structure and other general economic assumptions [34]

Parameter	% of Total Investment	Current Dollar Cost (%/yr)
Cost of Capital		10.3
Debt	45	9.0
Equity	55	11.4
Preferred Stock (Equity)	10	8.5
Common Stock (Equity)	45	12.0
Fuel Escalation Rate - above inflation		
Coal		0.5
Natural Gas		0.6
Non-Fuel O&M		0.0
Electricity		0.5
Combined Federal and State Tax Rate		38.0
Inflation Rate		3.0
Depreciation		MACRS (5, 15-yr)

The outputs of the *Revenue Requirements Module* include estimates of the total capital investment requirement, levelized cost of hydrogen ($/kg), cumulative cash flow, and CO_2 captured and emitted during the transition to a coal-based hydrogen transportation system in a specific region. The module can also incorporate different HFCV market penetration scenarios in order to examine how the timing of infrastructure deployment impacts the cost of hydrogen. Various policy scenarios can also be explored using the module (e.g., accelerated depreciation and production tax credits). All values are tracked in current dollars, but outputs from the module are reported in constant 2005 U.S. Dollars.

2.1.5 HFCV Market Penetration Scenarios

The *Infrastructure Design Module* quantifies the design and extent of infrastructure required to support a specific number of HFCVs (Table 10). The infrastructure design is then entered into the *Techno-economic Module*, which quantifies the investments required to build and operate the infrastructure. The timing of these infrastructure investments is dictated by the rate of adoption of HFCVs (i.e., market penetration) and is tracked in the *Revenue Requirements Module*. This study examines two HFCV market penetration scenarios developed by the National Research Council [35].

The first scenario, entitled “Hydrogen Success”, assumes that hydrogen development programs are successful and policies are enacted that support the commercial deployment of hydrogen infrastructure and vehicles. This scenario represents an optimistic case in which there are ~2 million HFCVs nationally by 2021 and ~220 million vehicles by 2050 (Figure 5). The second scenario, entitled “Hydrogen Partial Success”, represents a less optimistic case in which development programs do not achieve cost and performance targets. Thus, market penetration occurs more slowly with the adoption of ~2 million HFCVs postponed until 2025 and less than 100 million HFCVs in 2050 (Figure 5). The red circles in Figure 5 indicate the year in which each new tranche of coal-based hydrogen infrastructure is installed for each market penetration scenario (Table 10). When there are fewer than 2 million HFCVs, it is assumed that hydrogen demand is met entirely by onsite steam methane reformation at individual refueling stations.

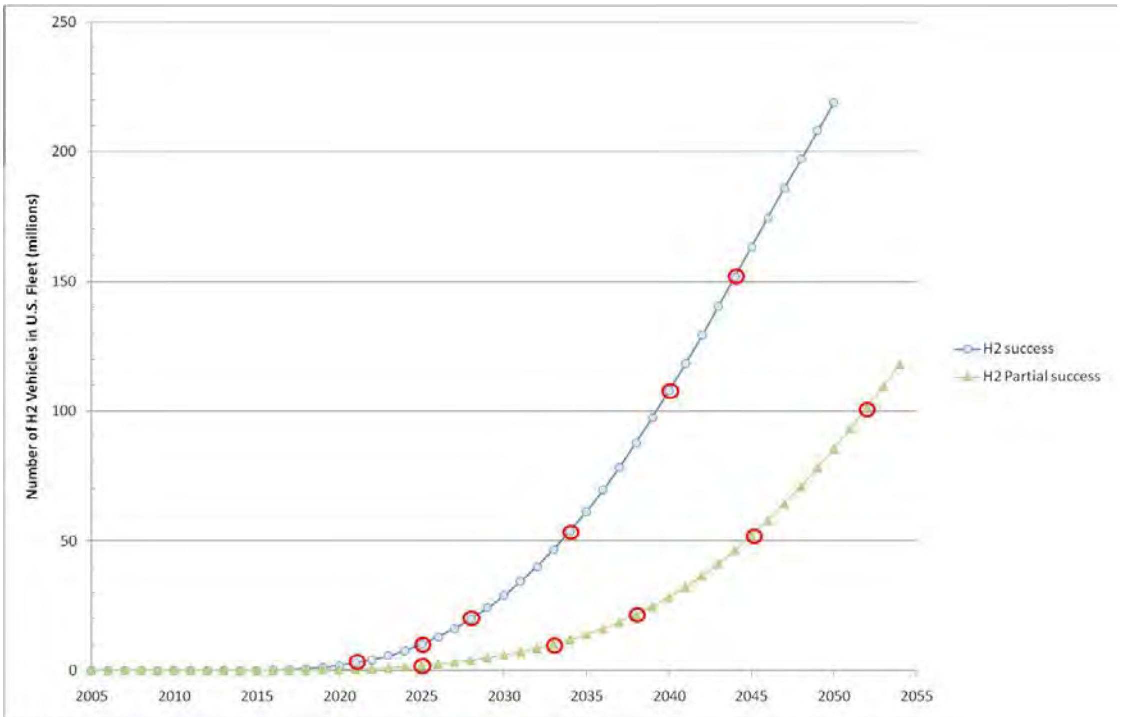

Figure 5: HFCV market penetration in H_2 Success and H_2 Partial Success scenarios

In both scenarios, Tranche 1 is installed when there are ~2 million HFCVs in the national LDV fleet (~ 1% market penetration). This first tranche is designed to support about 10 million HFCVs. Thus, it remains underutilized for several years before it reaches full capacity. The length of time that infrastructure remains underutilized depends on the market penetration rate and is longer in the less optimistic H_2 Partial Success scenario. Once the first tranche becomes fully utilized, the second tranche of infrastructure must be installed to meet growing hydrogen demand. The remaining tranches are built in succession when the hydrogen demand exceeds the capacity of the previously built infrastructure tranche. The *Revenue Requirements Module* accounts for the underutilization of capacity over time.

Table 10: Number of HFCVs supported by infrastructure built in each tranche and installation year for each market penetration scenario

Tranche	# of HFCVs supported by infrastructure (million vehicles in national LDV fleet)	Installation Year (H_2 Success)	Installation Year (H_2 Partial Success)
1	10	2021	2025
2	20	2025	2033
3	50	2028	2038
4	100	2034	2045
5	150	2040	2052
6	220	2044	2057

2.2 Development of a Regional Hydrogen Transition Model

This section describes the development of spatially-explicit modeling tools for examining the transition to a coal-based hydrogen transportation system with CCS in specific geographic regions. To accomplish this task, one must first quantify the location and magnitude of projected hydrogen demand at pre-specified HFCV market penetration levels (Table 10). Given the location of demand centers provided by the *Hydrogen Demand Module*, the *Hydrogen Production and Transmission Model* is then used to identify the least-cost infrastructure design for connecting hydrogen production facilities to demand centers via transmission pipelines. Another optimization tool, the *CO_2 Transport and Disposal Model*, then identifies the least-cost infrastructure for connecting the identified hydrogen production facilities to potential CO_2 injection sites via pipeline. Finally, the *Hydrogen Distribution and Refueling Station Model* estimates the refueling station and distribution pipeline requirements in each demand center. These models are applied at each of the pre-specified HFCV market penetration levels and the combined outputs provide a detailed region-specific inventory of the hydrogen and CCS infrastructure requirements during a transition to a coal-based hydrogen transportation system. The details of the *Hydrogen Demand* and *Hydrogen Infrastructure Design Modules* are explained in this section.

2.2.1 Hydrogen Demand Module

The design of a hydrogen fuel delivery infrastructure depends on the spatial characteristics of the hydrogen demand. In this study, the magnitude and spatial distribution of hydrogen demand in the continental United States is modeled based on exogenously-derived market penetration levels and U.S. Census population data [36]. The Hydrogen Demand Module was developed in a geographic information system (GIS) and utilizes population data, which are mapped at the census block level, to identify areas in which there is sufficient hydrogen demand to warrant investment in centralized hydrogen infrastructure.

Given the population and area of each census block, the population density is derived and Equation 8 is used to calculate the hydrogen demand density within each block.

$$HyDemand = PopDens \times VehOwn \times HyUse \times MarketPen \quad (8)$$

where *HyDemand* is the hydrogen demand density (kg H_2/km^2/day) in each census block, *PopDens* is the population density (people/km^2) given by the US Census Bureau for year 2000, *HyUse* is the projected average daily hydrogen use per vehicle (0.6 kg H_2/HFCV/day), *VehOwn* is the per-capita light duty vehicle ownership (0.7 LDV/person), and *MarketPen* is the percentage of HFCVs in the light duty vehicle fleet (# HFCV/# LDV). *HyUse* is calculated by assuming that the average annual mileage driven by a LDV is 12,000 miles and a HFCV achieves a fuel economy about 2.5 times that of a current gasoline LDV (~57 miles per kg of hydrogen).

In the GIS, buffers of five kilometers width are then applied to census blocks with high demand density (defined as > 150 kg/km^2/day in this study) and neighboring census blocks within these buffers are aggregated into demand clusters. The aggregate hydrogen demand within each cluster is then calculated and a threshold (i.e., filter) is applied to retain only the clusters with sufficient total hydrogen demand to warrant investment in centralized infrastructure (defined as > 3,000 kg H_2/day in this study). These remaining clusters are considered the viable hydrogen "demand centers" to which hydrogen should be supplied at a given percentage of HFCVs in the LDV fleet. This method provides a simple means for identifying potentially viable locations for hydrogen infrastructure investment at static market penetration levels. The spatial distribution of hydrogen demand centers is illustrated for each market penetration level in Figure 6 through Figure 11. As HFCV market penetration increases, the number and size of viable demand centers also increase (Table 12).

It is important to note that *MarketPen* refers to the percentage of HFCVs in relation to the national LDV fleet in year 2000[1]. In other words, at 5% market penetration, it is assumed that 5% of the year 2000 LDV fleet in the continental U.S. are HFCVs. However, the market penetration scenarios described in 2.1.5 are defined by the total number of HFCVs (not the percentage of HFCVs) in the national fleet and reflect population growth over the study period. Fortunately, the hydrogen demand projections from the *Hydrogen* Demand Module can be related to the number of HFCVs by dividing the total hydrogen demand by the average daily hydrogen use per vehicle. Thus, the *Hydrogen Demand Module* effectively identifies the location and magnitude of demand for a given number of HFCVs. Table 11 relates the six market penetration levels considered in this study (Table 10) to the percentage of HFCVs in relation to the year 2000 LDV fleet. As a result of population growth, the number of HFCVs supplied in

[1] Although the analysis is missing Alaska and Hawaii, the term "national" will be used to refer to the continental U.S.

Tranche 6 exceeds the number of LDVs in the year 2000. However, the number of HFCVs in Tranche 6 represents only 60% of the projected LDVs in year 2050 [35].

Table 11: Relationship between different metrics for HFCV market penetration in the continental U.S.

Tranche	National Market Penetration (% of LDVs in Year 2000)	# of HFCVs in National Fleet (million vehicles)
1	5%	10
2	10%	20
3	25%	50
4	50%	100
5	75%	150
6	112%	220

Summary statistics for demand centers at each market penetration level are listed in Table 12. By concentrating hydrogen infrastructure in population centers, service can be provided to a large proportion of the national population in a relatively small fraction of the land area. For example, the first 10 million vehicles are projected to reside in one of 245 cities. Although these cities occupy less than 1% of the land area of the continental U.S., about 42% of the population lives in these initial cities and would have access to refueling infrastructure. The number of demand centers remains constant in the last two market penetration levels because all urban areas are already captured. The remaining 26% of the population resides in rural areas and would likely be supplied by refueling stations with onsite production or by small rural stations along existing hydrogen transmission pipelines. Rural hydrogen supply is not modeled in this study.

Table 12: Summary statistics for demand centers in the continental U.S. based on the *Hydrogen Demand Module*

Market Penetration (million HFCVs)	Number of Demand Centers (i.e., cities)	Population Captured (% of year 2000 population)	Land Area (% of continental U.S.)	Cumulative H_2 Demand (tonnes/day)
10	245	43%	0.9%	6,000
20	450	56%	1.6%	12,000
50	843	66%	2.6%	30,000
100	1281	72%	3.4%	60,000
150	1637	74%	3.9%	90,000
220	1637	74%	3.9%	132,000

Figure 6: Spatial distribution of demand centers for 2 million HFCVs (~1% market penetration)

Figure 7: Spatial distribution of demand centers for 10 million HFCVs

Figure 8: Spatial distribution of demand centers for 20 million HFCVs

Figure 9: Spatial distribution of demand centers for 50 million HFCVs

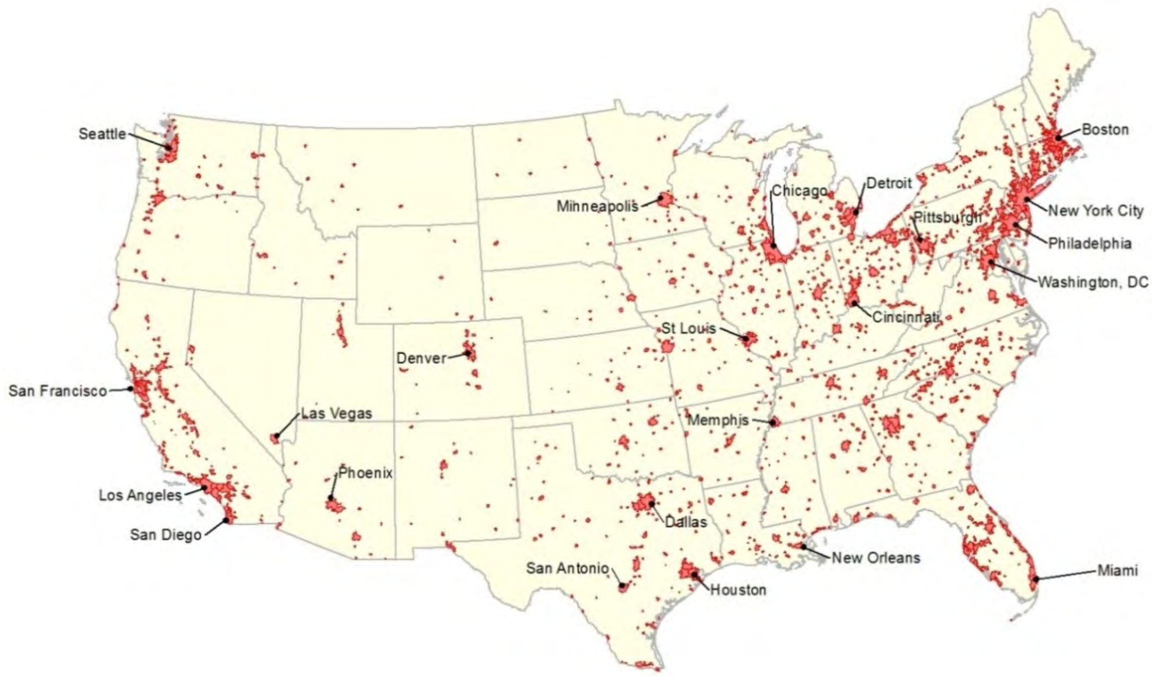

Figure 10: Spatial distribution of demand centers for 100 million HFCVs

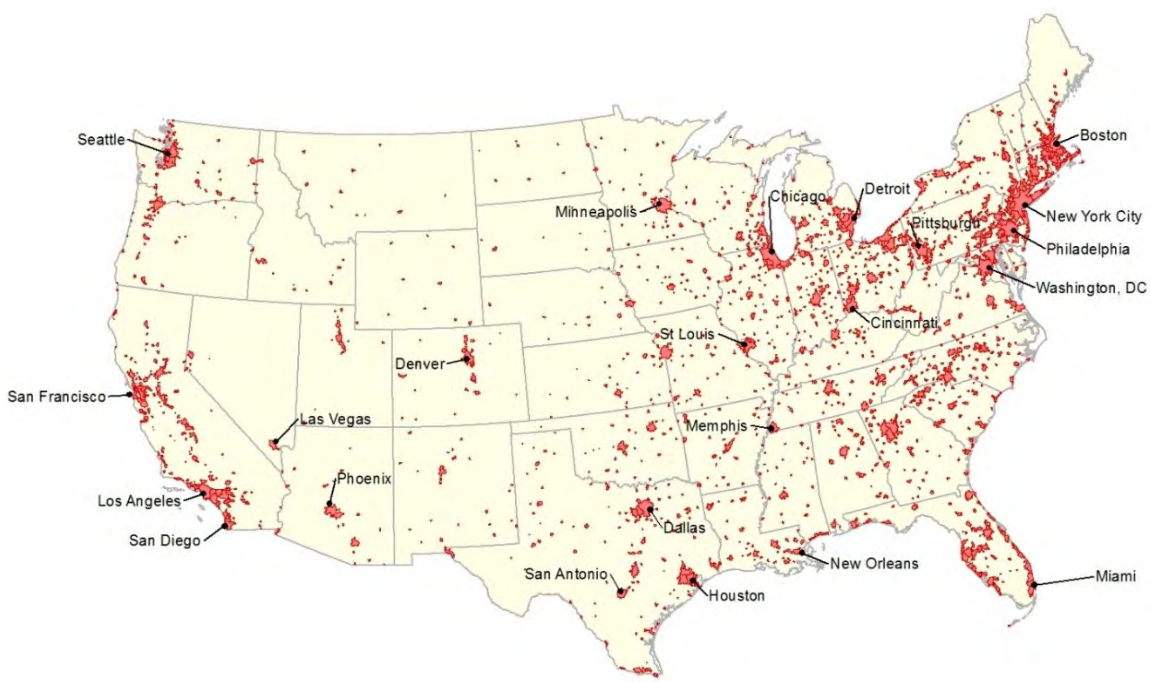

Figure 11: Spatial distribution of demand centers for 150 and 220 million HFCVs

2.2.2 Hydrogen Production and Transmission Model

Given a candidate transmission pipeline network and the locations of H_2 demand and potential centralized production facilities, the Hydrogen Production and Transmission (HyPAT) Model identifies the optimal infrastructure design for producing H_2 and connecting production facilities to distribution hubs in demand centers (i.e., cities). In the process, it develops an interconnected and capacitated regional pipeline network that can link multiple production facilities and demand centers. Specifically, it identifies the optimal number, size, and location of production facilities and the diameter, length, and location of transmission pipeline corridors. The model is not designed to optimize intra-city distribution pipelines, though it could be modified for this purpose. The HyPAT model is described in detail in Johnson and Ogden [37].

The model is run for a series of discrete HFCV market penetration (MP) levels, which define the location and magnitude of hydrogen demand. At each level, the model optimizes the infrastructure design based on current demand, but is constrained by previously built infrastructure. This approach mimics a decision-making process in which infrastructure is built in pre-defined installments (e.g., every 5 to 10 years) in order to meet projected demand in the near term. Unlike dynamic optimization models that often assume perfect foresight over a multi-decade period, this myopic approach may better represent the way in which infrastructure deployment decisions are actually made (i.e., infrastructure is deployed in stages based upon projected near-term demand and future decisions are constrained by previous investments).

2.2.2.1 Model Formulation

The HyPAT model is a mixed integer linear programming (MILP) optimization model that is formulated in the General Algebraic Modeling System (GAMS) and solved using CPLEX [38]. The integer (in this case binary) variables represent decisions regarding whether or not to build a production facility at node i of size s (f_{is}) or construct a pipeline segment between nodes i and j of the candidate pipeline network of diameter d (y_{ijd}). The continuous variables represent decisions regarding the quantity of hydrogen to produce at node i (a_i) and to transport from node i to j (x_{ij}). The subscript d on the pipeline construction decision variable allows the model to identify the optimal pipeline diameter for transporting any amount of hydrogen between two nodes. This is important since the amount of hydrogen flow through any pipeline segment is not known in advance since it depends on the route chosen by the model. It should be noted that the model determines the best route and, thus, the direction of flow between any two nodes. Consequently, the links are assumed bi-directional with the direction of flow determined by the model at each market penetration level. Model annotation is listed in Table 13.

Objective Function

The objective of the model is to identify the infrastructure design that minimizes the total annual cost of production and pipeline transmission (thousand$/year), including both capital and operating costs (Equation 9).

9 Minimize $$\sum_{i \in F} \sum_{s} C_{is}^{f} f_{is} + \sum_{i \in F} V^{f} \left[\frac{a_i}{(1+surge)} \right] (365) + \sum_{i} \sum_{j \in N_i} \sum_{d} C_{ijd}^{p} y_{ijd}$$

The first and third terms of this function are the fixed capital and fixed operating costs for production facilities and pipelines, respectively. The second term represents the variable feedstock cost for hydrogen production. For pipelines, it is assumed that the variable operating cost (e.g., cost of energy for booster compression) is included in the fixed operating cost since booster compression is not explicitly modeled.

Table 13: HyPAT model annotation

Sets:	
N	network nodes
R	demand (city) nodes (subset of N)
F	H_2 production facility nodes (subset of N)
N_i	network nodes that are neighbors of node i (subset of N)
D	pipeline diameters (8, 12, 16, 20, 24, 30, 36, 42-inch)
S	facility sizes (300, 600, 900, 1200, 1500 tonnes/day)
B	previously built facility sizes (actual built sizes)
Decision Variables:	
x_{ij}	units of hydrogen transported from node i to node j (tonnes/day)
a_i	units of hydrogen produced at node i (tonnes/day)
f_{is}	1, if facility is built at node i with size s; 0, otherwise
y_{ijd}	1, if pipeline is constructed from node i to node j with diameter d; 0, otherwise
Input Parameters:	
C^f	fixed annual capital and O&M costs for building a production facility (thousand$/yr)
C^p	fixed annual capital and O&M costs for constructing a pipeline (thousand$/yr)
V^f	variable feedstock cost for producing hydrogen (thousand$/tonne)
Q^f	useable capacity of a facility (tonnes/day)
Q^p	useable capacity of a pipeline (tonnes/day)
R_i	peak demand at node i (tonnes/day)
L_{ij}	adjusted length of pipeline segment from node i to node j (km)
B_{is}	production at previously built facility of size s at node i (tonnes/day)
surge	summer surge in demand (10%) [10]
coal(i)	cost of delivered coal at node i ($/GJ)
s	facility nameplate capacity (tonnes/day)
d	pipeline diameter (inch)
C_{cap}	overnight capital cost for production facility (million$)
OM	annual operating and maintenance cost for a facility or pipeline (4% of fixed capital) [58]
CRF	capital recovery factor (10.2% based on discount rate of 10% and component lifetime of 40 years)
LHV^{H2}	lower heating value of hydrogen (120 GJ/tonne H_2)
eff^f	plant conversion efficiency
CF^f	plant capacity factor

Constraints

The model includes several sets of constraints that must be satisfied by any feasible solution. The first set represents capacity constraints. Equation 10 requires that the maximum flow of H_2 (x_{ij}) through a pipeline is less than or equal to the built pipeline capacity and Equation 11 requires that the maximum H_2 production (a_i) at a plant is less than or equal to the built plant capacity.

10 $$x_{ij} \le \sum_{d} Q_d^p y_{ijd} \qquad \forall i, j \in N_i, d \in D$$

11 $$a_i \le \sum_{s} Q_s^f f_{is} \qquad \forall i \in F, s \in S$$

The second set includes mass balance constraints, which ensure that the flows of hydrogen throughout the network are balanced. Equation 12 dictates that the total H_2 flow out of each node is equal to the total flow into the node where H_2 production (a_i) is considered flow into the node and H_2 demand (R_i) represents flow out of the node. This constraint prevents shortages and excesses of hydrogen at any given node. Equation 13 requires that the total production in the system is equal to the total demand.

12 $$\sum_{j \in N_i} x_{ij} + R_i = \sum_{k \in N_i} x_{ki} + a_i \qquad \forall i, j \in N_i, k \in N_i$$

13 $$\sum_{i \in F} a_i = \sum_{i \in R} R_i$$

The third set contains constraints that define the decision variables. Non-negativity constraints are placed on the two continuous decision variables (Equations 14 and 15) and binary constraints are required for the two binary decision variables (Equations 16 and 17).

14 $$x_{ij} \ge 0 \qquad \forall i, j \in N_i$$

15 $$a_i \ge 0 \qquad \forall i \in F$$

16 $$y_{ijd} \in 0{,}1 \qquad \forall i, j \in N_i, d \in D$$

17 $$f_{is} \in 0{,}1 \qquad \forall i \in F, s \in S$$

The final set represents constraints that can be considered optional. These constraints are included in order to improve the computational efficiency of the model, but can be modified to represent specific beliefs about the infrastructure planning process. The listed constraints represent *one* way to model the planning process, but we do not assert that they are necessarily the best way. Equation 18 dictates that only one production facility can be built at each potential site and Equation 19 stipulates that, once built, a plant will continue to operate at a baseline value, but can be expanded up to the maximum allowable plant size. In essence, the model assumes that, once production capacity is built, this capacity continues to be available. The use of existing capacity is preferable to building new capacity since not using this capacity would result in low utilization of existing capacity and, thus, higher costs. Equation 20 dictates that only one pipeline can be built along any single corridor. This constraint streamlines the network optimization, but does prevent parallel pipelines from being developed.

18 $$\sum_s f_{is} \le 1 \qquad \forall i \in F, s \in S$$

19 $$a_i \ge B_{is} \qquad \forall i \in B, s \in S$$

20 $$\sum_d y_{ijd} \le 1 \qquad \forall i, j \in N_i, d \in D$$

In each model run, the infrastructure built at the previous market penetration level is provided and constrains the outcome. Specifically, the location and diameter of pipelines (y_{ijd}), the location and size of plants (f_{is}), and the actual production capacity of plants (a_i) are passed from the previous model run. Equation 19 constrains the size and location of future plants based upon previously built facilities and cost incentives discussed in section 2.2.2.3 encourage the continued use of pre-existing pipelines. The flow along a pipeline (x_{ij}) is not constrained by previous flows, but must respect the pipeline capacity constraint. However, there is no constraint that prevents an existing pipeline from being removed and replaced by a larger diameter pipeline in the future to meet additional flow requirements. Since links are bi-directional, it is possible for flows to change direction between model runs.

The *Hydrogen Production and Transmission Model* determines the optimal production and transmission infrastructure design for supplying hydrogen at static levels of HFCV market penetration (e.g., 10 million HFCVs). At each level, the model does consider previously built infrastructure, but future infrastructure requirements are not considered. The temporal component of the model is incorporated through post-processing in the *Revenue Requirements Module* (described in Section 2.2.5), which tracks infrastructure investments over time and does allow for oversizing of some infrastructure (e.g., pipelines) in anticipation of future demands. However, the optimization tool itself is myopic and does not explicitly consider future infrastructure requirements.

2.2.2.2 Spatial Inputs

Three spatial inputs are required by this model: 1) the location and magnitude of hydrogen demand, 2) the location of potential hydrogen production facilities, and 3) a candidate pipeline network for connecting supply and demand. These inputs are developed in a geographic information system (GIS).

Hydrogen Demand

The *Hydrogen Demand Module* used for identifying demand centers is described in section 2.2.1. In each demand center, a centroid is used to represent the hydrogen distribution hub, which links to the candidate transmission pipeline network. The input to the optimization model is a list of all demand nodes and their associated peak demand, which includes a 10% summer surge [R_i]. The surge must be included in the model so that pipelines are sized to handle peak summer flow.

Hydrogen Production Facilities

To model the optimal pipeline network connecting production facilities and demand centers, specific locations for potential hydrogen production facilities must be specified. The criteria used for determining these locations depend on the objectives of the particular case study and the availability of data. In this study, we focus on coal-based hydrogen production. In this case, it is assumed that new hydrogen facilities are constrained to the locations of existing coal-fired power plants over 500 MW since these sites presumably have adequate coal delivery and handling capabilities. The U.S. Environmental Protection Agency's eGRID dataset [39] provides the locations of these power plants. In some cases, multiple plants are located in very close proximity (within 16 km). In order to further constrain the plant locations and reduce model solution times, only the plant with the largest capacity is maintained among groups of spatially redundant plants. In the continental U.S., there are approximately 200 candidate production sites that remain after redundant plants are removed. The input to the optimization model is a list of all potential production nodes and the cost of coal at each node [coal(i)]. The cost of coal is assigned to each facility based on the average delivered coal cost by state (Table 3) [8]. The capacity of the hydrogen production facility is not constrained by the capacity of the original power plant.

Candidate Pipeline Network

The candidate pipeline network provides the potential linkages between the locations of production and demand. In this paper, it is assumed that hydrogen pipelines will follow existing pipeline rights-of-way (ROWs) as defined by the National Pipeline Mapping System (NPMS) dataset [40]. However, this dataset includes all pipelines in the United States and is overly complex for modeling purposes. The candidate pipeline network was developed by removing redundancies and manually simplifying the NPMS dataset so that only ROWs that connect the demand and production locations are retained. In cases where existing pipeline ROWs do not connect to the production or demand nodes, a spur was manually added following major roads.

The candidate pipeline network was also modified to reflect the increased cost of pipeline construction in mountainous and urban areas. Assuming that construction costs double in these areas and that construction cost is ~50% of total pipeline installation cost, this additional cost can be included as a 50% increase in pipeline length where a pipeline travels through high cost terrain (Equation 21). Urban terrain is defined by the U.S. Census Bureau's urbanized areas dataset [41] and mountainous terrain is defined as areas with slopes greater than 8% as derived from the U.S. Geological Survey's National Elevation Dataset (NED) [42].

21 $$L_{ij} = l_{ij}^{o} - l_{ij}^{um} + l_{ij}^{um} * 1.5$$

where L_{ij} is the adjusted pipeline length (km), l_{ij}^{o} is the original pipeline length, and l_{ij}^{um} is the pipeline length within urban and mountainous areas.

The candidate pipeline network consists of both nodes and links between the nodes. The network nodes include production and demand locations as well as all intersections along the pipeline network. The input to the optimization model is a list of all potential network links and their associated adjusted lengths along real ROWs [L_{ij}]. In the continental U.S., the candidate transmission pipeline network is approximately 130,000 km in length and contains about 3,600 nodes and 3,900 links.

2.2.2.3 Techno-economic Inputs

The model also requires inputs defining the cost and capacity of production facilities and transmission pipelines. All costs are in constant 2005 dollars and are derived from the techno-economic models described in section 2.1.

Production Facilities

The optimization model allows the user to define a set of discrete facility sizes (set S) from which the model can choose. For each facility size, the cost and capacity are calculated based on equations for a particular facility type. The following equations are applicable to plants producing hydrogen via coal gasification with CO_2 capture and compression. The equation for the overnight capital cost (million$) ($C_{cap}$) was developed by conducting a literature review of coal-based H_2 production with CO_2 capture and fitting a power function to the normalized results of the studies (Equation 22) [1-7]. Equation 23 calculates the annual fixed capital and operating cost (thousand$/yr) ($C^f_{is}$). See Table 13 for a description of the variables.

22 $$C_{cap} = 6.4362 * (s^{0.7559})$$

23 $$C^f_{is} = C_{cap} * 1000 * (OM + CRF)$$

where *s* is the plant nameplate capacity (tonnes/day), *OM* is the annual O&M cost as a percentage of overnight capital, and *CRF* is the capital recovery factor. The variable feedstock cost (thousand$/yr) ($V_f$) is dependent on the cost of delivered coal (*coal(i)*) and can be specified for each plant *i* if data is available (Equation 24). However, in this study, delivered coal costs are only specified by state.

24 $$V^f = \frac{\left(LHV^{H2} / eff^{f} \right) * coal(i)}{1000}$$

In order to equate hydrogen demand (which includes the summer surge in demand) and production, the model includes the surge in the quantity produced by each plant (a_i). However, in reality, the surge will be met by storage and not by increased production. Consequently, the equation for useable plant capacity (Q^f_s) includes the surge term so that plants are sized correctly (Equation 25). The maximum capacity factor (CF^f) and plant efficiency (eff^f) for a coal-to-H_2 plant with CO_2 capture is assumed to be 80% and 57.5%, respectively [43].

25 $$Q_s^f = s*(1+surge)*CF^f$$

Transmission Pipelines

The optimization model allows the user to input a set of discrete pipeline diameters (i.e., nominal pipe sizes). For each diameter, the model calculates the annual capital and operating cost for each pipeline link based on an equation from the U.S. Department of Energy's Hydrogen Analysis (H2A) spreadsheets (Equation 26) [10].

26 $$C_{ijd}^p = \frac{[(L_{ij}*0.621371*(818.64*(d^2)+14288.2*d+284530.3)+431502.5)*(OM+CRF)]}{1000}$$

The model also records the location and diameter of built pipelines (y_{ijd}) and uses this information in subsequent model runs to adjust the costs so that previously built pipelines of a specific diameter are preferred (i.e., less expensive) in later construction periods. Specifically, the annual cost reflects only the operating and maintenance costs and not the annualized capital for existing pipelines (Equation 27). This cost adjustment provides an incentive to maintain previously built pipelines, but does not prevent larger pipelines from being built.

27 $$C_{ijd}^p = \frac{[(L_{ij}*0.621371*(818.64*(d^2)+14288.2*d+284530.3)+431502.5)*(OM)]}{1000}$$

Finally, it is implausible that a pipeline of a particular diameter would be removed and replaced with a pipeline of a smaller diameter[2]. To address this, the model uses the variable y_{ijd} to identify the diameter classes that are smaller than any previously built diameter along each pipeline link and assigns a high cost to these diameter classes (99999). The useable capacity of each pipeline diameter class (Q_d^p) is derived from H2A assuming a pipeline length of 200 km, a pipeline capacity factor of 92%, and a pressure drop of 20 bar [10].

2.2.3 CO_2 Transport and Disposal Model

After the *HyPAT Model* has identified the size and location of hydrogen production facilities, the *CO_2 Transport and Disposal Model* determines the optimal CO_2 pipeline and injection network for disposing of the CO_2 captured by these facilities. Therefore, the H_2 supply network and CO_2 pipeline network are not co-optimized. If these networks were co-optimized, it is possible that hydrogen production facilities would be located in closer proximity to CO_2 storage sites. However, the cost of CO_2 transport on a dollar per kg H_2 basis is generally 5-10 times smaller than the cost of H_2 transmission. Therefore, priority is given to the optimization of the H_2 transmission pipeline network.

The model inputs for the *CO_2 Transport and Disposal Model* include a candidate CO_2 pipeline network, the location of hydrogen production facilities, and the locations and capacities of potential CO_2 injection sites. The model determines the location, length, and diameter of CO_2 pipelines and the number, location, and size of injection sites. Similar to the *HyPAT Model*, it

---

[2] It is possible that the diameter of a pipeline may need to be decreased if the minimum capacity of the pipeline is not met in subsequent model runs. However, the model does not include minimum pipeline capacity.

identifies the infrastructure requirements at static market penetration levels and is constrained by previously built infrastructure.

2.2.3.1 Model Formulation

The *CO_2 Transport and Disposal Model* is a mixed integer linear programming (MILP) optimization model that is formulated in the General Algebraic Modeling System (GAMS) and solved using CPLEX [38]. The integer (in this case binary) variables represent decisions regarding whether or not to build a CO_2 storage facility at reservoir node i (r_i) or construct a pipeline segment between nodes i and j of diameter d (y_{ijd}). The continuous variables represent decisions regarding the quantity of CO_2 to inject at node i (a_i) and to transport from node i to j (x_{ij}). The subscript d on the pipeline construction decision variable allows the model to identify the optimal pipeline diameter for transporting any amount of CO_2 between two nodes. This is important since the amount of CO_2 flow through any pipeline segment is not known in advance since it depends on the route chosen by the model. It should be noted that the model determines the best route and, thus, the direction of flow between any two nodes. Consequently, the links are assumed bi-directional with the direction of flow determined by the model at each market penetration level. Model annotation is listed in Table 14.

Objective Function

The objective of the model is to identify the infrastructure design that minimizes the total cost of CO_2 transport and storage over the project lifetime (thousand$), including both capital and operating costs (Equation 28).

28 Minimize $$\sum_{i \in R}\left[C^{site} r_i + \left(\frac{a_i}{Q^w}\right)(C_i^{wd} + C_i^{eq} + C_i^{om} + V^{site}) + V^{mon} a_i\right] + \sum_i \sum_{j \in N_i} \sum_d C_{ijd}^p y_{ijd}$$

The first term of this function represents the capital and O&M costs associated with CO_2 injection and storage. These costs include site characterization, well drilling, surface equipment, O&M, and monitoring. The second term represents the capital and O&M costs associated with CO_2 pipeline transport.

Table 14: CO_2 model annotation

Sets:	
N	network nodes
R	CO_2 reservoir nodes (subset of N)
F	H_2 production facility nodes (subset of N)
N_i	network nodes that are neighbors of node i (subset of N)
D	pipeline diameters (12.75, 16, 24, 30, 36, 42-inch)
B	previously built storage facility (million tonnes CO_2/project lifetime)
Decision Variables:	
x_{ij}	units of CO_2 transported from node i to node j (million tonnes/year)
a_i	units of CO_2 stored at node i (million tonnes/project lifetime)
r_i	1, if storage facility is built at node i; 0, otherwise
y_{ijd}	1, if pipeline is constructed from node i to node j with diameter d; 0, otherwise
Input Parameters:	
C^{wd}	fixed capital for drilling an injection well (thousand$/well)
C^{eq}	fixed capital for surface equipment (thousand$/well)
C^{om}	fixed O&M cost for CO_2 disposal (thousand$/well over project lifetime)
C^{p}	fixed capital and O&M costs for constructing and operating a pipeline (thousand$/project lifetime)
C^{site}	fixed site characterization cost for CO_2 storage (thousand$/project lifetime)
V^{site}	variable site characterization cost (thousand$/well)
V^{mon}	variable monitoring cost for CO_2 storage (thousand$/million tonnes)
Q^{r}	useable capacity of a storage reservoir (million tonnes/project lifetime)
Q^{p}	useable capacity of a pipeline (million tonnes/year)
Q^{w}	well injection capacity (27 million tonnes/well/project lifetime)
F_i	CO_2 captured at node i (million tonnes/year)
L_{ij}	adjusted length of pipeline segment from node i to node j (km)
B_i	CO_2 stored at previously built facility at node i (million tonnes/project lifetime)
depth (i)	well depth at node i (1000 meters)
d	pipeline diameter (inch)
A	CO_2 plume area (72.4 km^2/well)
OM^{p}	annual operating and maintenance cost for a pipeline (2.2% of fixed capital)
life	project lifetime (40 years)

Constraints

The model includes several sets of constraints that must be satisfied by any feasible solution. The first set represents capacity constraints. Equation 29 requires that the maximum flow of CO_2 (x_{ij}) through a pipeline is less than or equal to the built pipeline capacity and Equation 30 requires that the maximum CO_2 stored (a_i) at a reservoir is less than or equal to the reservoir capacity.

29 $$x_{ij} \leq \sum_{d} Q_d^p y_{ijd} \qquad \forall i, j \in N_i, d \in D$$

30 $$a_i \leq Q^r r_i \qquad \forall i \in R$$

The second set includes mass balance constraints, which ensure that the flows of CO_2 throughout the network are balanced. Equation 31 dictates that the total CO_2 flow into each node is equal to the total flow out of the node where CO_2 captured at a H_2 production facility (F_i) is considered flow into the node and CO_2 stored at a reservoir (a_i) represents flow out of the node. This constraint prevents shortages and excesses of hydrogen at any given node. Equation 32 requires that the total CO_2 stored in the system is equal to the total CO_2 captured.

31 $$\sum_{j \in N_i} x_{ji} life + F_i life = \sum_{k \in N_i} x_{ik} life + a_i \qquad \forall i, j \in N_i, k \in N_i$$

32 $$\sum_{i \in R} \left(\frac{a_i}{life} \right) = \sum_{i \in F} F_i$$

The third set contains constraints that define the decision variables. Non-negativity constraints are placed on the two continuous decision variables (Equations 33 and 34) and binary constraints are required for the two binary decision variables (Equations 35 and 36).

33 $$x_{ij} \geq 0 \qquad \forall i, j \in N_i$$

34 $$a_i \geq 0 \qquad \forall i \in R$$

35 $$y_{ijd} \in 0,1 \qquad \forall i, j \in N_i, d \in D$$

36 $r_i \in 0,1 \qquad \forall i \in R$

The final set represents constraints that can be considered optional. These constraints are included in order to improve the computational efficiency of the model, but can be modified to represent specific beliefs about the infrastructure planning process. Equation 37 stipulates that once CO_2 is allocated to a storage site, the site will continue to store the CO_2 for the project lifetime. However, additional CO_2 can be stored at an existing site until the storage capacity of the site is reached. Equation 38 dictates that only one pipeline can be built along any single corridor. This constraint streamlines the network optimization, but does prevent parallel pipelines from being developed.

37 $a_i \geq B_i \qquad \forall i \in B$

38 $\sum_d y_{ijd} \leq 1 \qquad \forall i, j \in N_i, d \in D$

In each model run, the infrastructure built at the previous market penetration level is provided and constrains the outcome. Specifically, the location and diameter of pipelines (y_{ijd}), the location of storage reservoirs (r_i), and the actual CO_2 stored at reservoirs (a_i) are passed from the previous model run. Equation 37 constrains the location and quantity of CO_2 stored at future storage sites and cost incentives discussed in section 2.2.2.3 encourage the continued use of pre-existing pipelines. The flow along a pipeline (x_{ij}) is not constrained by previous flows, but must respect the pipeline capacity constraint. However, there is no constraint that prevents an existing pipeline from being removed and replaced by a larger diameter pipeline in the future to meet additional flow requirements. Since links are bi-directional, it is possible for flows to change direction between model runs. Similar to the *Hydrogen Production and Transmission Model*, this model employs a myopic approach that does not consider future infrastructure requirements.

2.2.3.2 Spatial Inputs

Three spatial inputs are required by this model: 1) the location and magnitude of CO_2 captured at each hydrogen production facility, 2) the location and capacity of potential CO_2 injection sites, and 3) a candidate pipeline network for connecting CO_2 sources and sinks. These inputs are developed in a geographic information system (GIS).

Hydrogen Production Facilities

At each market penetration level, the hydrogen production facilities selected by the *HyPAT Model* are provided as the CO_2 sources in the *CO_2 Transport and Disposal Model*. Thus, the locations of these sources and the quantity of CO_2 captured at each site are known. The CO_2 emission rate (kg CO_2/GJ coal) is assigned to each facility based on the average CO_2 emission rate by state [9] (Table 3). The total CO_2 captured at each facility is then calculated by multiplying this rate by the required coal input and the CO_2 capture efficiency (91.28%) [3]. The input to the optimization model is a list of all source nodes and the CO_2 captured at each node (F_i).

CO_2 Injection Sites

The National Carbon Sequestration Database (NATCARB) provides information on the location and storage capacity of potential CO_2 reservoirs in the United States [44]. This information is available for saline aquifers, unmineable coal seams, and oil and gas fields. Storage capacity is identified for each 10 km by 10 km (i.e., 100 km^2) grid cell within each reservoir (e.g., ~40,000 cells for saline aquifers alone). To make the model tractable, the number of potential injection sites must be reduced. This was accomplished by changing the resolution of the capacity data to 100 km by 100 km (i.e., 10,000 km^2) grid cells and by limiting potential reservoirs to deep saline aquifers. The centroids of the 10,000 km^2 grid cells represent the potential injection sites and are assigned the aggregated storage capacity of all 100 km^2 grid cells that they contain. The injection sites are limited to saline aquifers because this reservoir type has the largest storage capacity (Figure 12) and is well-distributed through the study area (Figure 13).

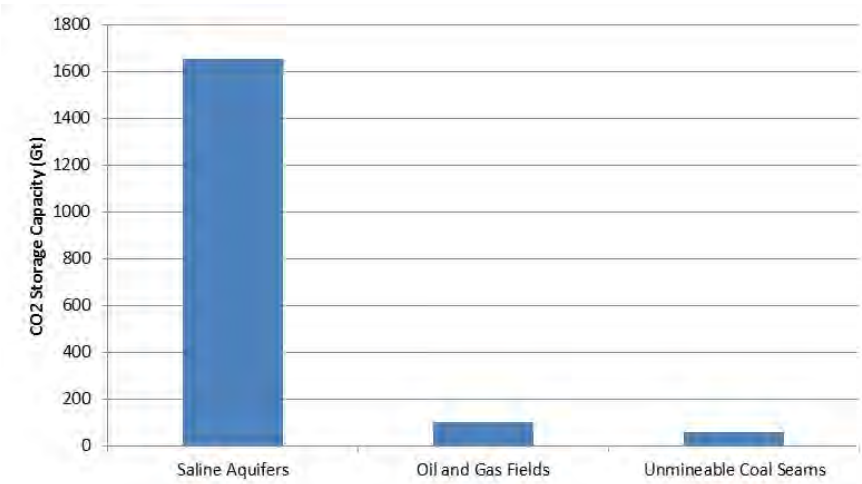

Figure 12: Total CO_2 storage capacity for each reservoir type

The number of potential injection sites is further reduced by deleting all sites that are within 10 km of urban areas, within national park boundaries, and offshore. Offshore CO_2 storage is not considered in this study since there is sufficient onshore storage capacity in the United States. However, local resistance to onshore CO_2 storage may necessitate consideration of offshore storage in the future. Within the continental U.S., the number of potential injection sites in saline aquifers is reduced to 277 sites. The inputs to the optimization model include a list of all potential injection sites and the associated aquifer depth (depth(i)) and storage capacity (Q^r). At present, the depth of individual aquifers is not available. Thus, it is assumed that all aquifers have a depth of 1000 meters, which is consistent with a cold/shallow aquifer [28].

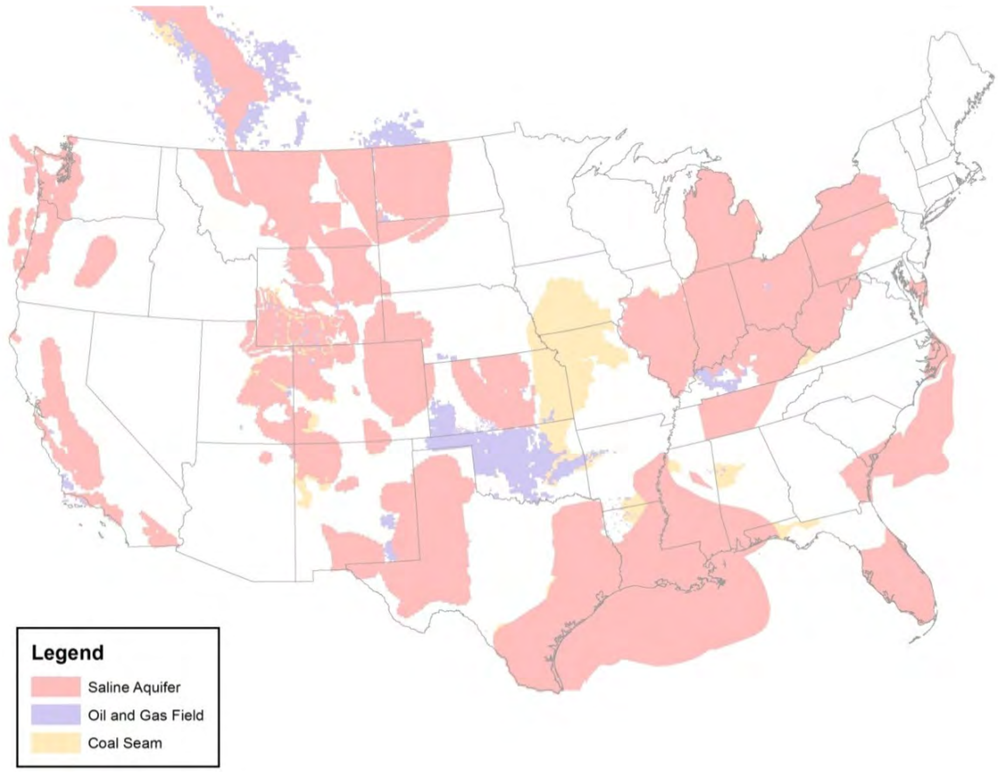

Figure 13: Spatial distribution of saline aquifers in the continental U.S. overlaid on top of the other two CO_2 reservoir types

Candidate Pipeline Network

The candidate pipeline network provides the potential linkages between the locations of CO_2 sources and sinks. In this paper, it is assumed that CO_2 pipelines will follow existing pipeline rights-of-way (ROWs) as defined by the National Pipeline Mapping System (NPMS) dataset [40]. The CO_2 pipeline candidate network was developed by modifying the H_2 candidate pipeline network, which is described in section 2.2.2.2. Specifically, the network was modified by adding pipeline corridors to potential CO_2 injection sites. In cases where existing pipeline ROWs do not connect to the injection nodes, a spur was manually added following major roads.

Similar to the H_2 candidate pipeline network, the CO_2 candidate pipeline network is adjusted to reflect the increased cost of pipeline construction in mountainous and urban areas (as described in section 2.2.2.2). The candidate pipeline network consists of both nodes and links between the nodes. The network nodes include CO_2 source and sink locations as well as all intersections along the pipeline network. The input to the optimization model is a list of all potential network links and their associated adjusted lengths along real ROWs [L_{ij}]. In the continental U.S., the candidate CO_2 pipeline network is about 100,000 km in length and includes approximately 3,200 links.

2.2.3.3 Techno-economic Inputs

The model also requires inputs defining the cost and capacity of injection sites and CO_2 pipelines. All costs are in constant 2005 dollars and are derived from the techno-economic models described in section 2.1.

CO_2 Injection

In calculating the cost of CO_2 injection, it is assumed that all CO_2 is injected into cold/shallow aquifers at a depth of 1000 meters [28]. These wells have a maximum injection capacity of 1850 tonnes/day and a plume radius of 4.8 km per well (Table 8). Based on the daily injection capacity, each well can store about 27 Mt over a 40-year lifetime (Q^w). This value is used to identify the number of required injection wells. The injection cost includes site characterization, well drilling, surface equipment, O&M, and monitoring costs. In the optimization model, the site characterization cost is split into a fixed and variable characterization cost. The fixed site characterization cost (C^{site}) is $2.7 million for each disposal site. The variable cost (V^{site}) is per injection well (thousand$/well) where A is the plume area per well (72.4 km^2) (Equation 39).

39 $$V^{site} = 117.344A + 23$$

The well drilling (C^{wd}), surface equipment (C^{se}), and O&M (C^{om}) costs (thousand$/well) are based on well depth (Equations 40 - 42). The monitoring cost (V^{mon}) is assumed to be $0.02 per tonne CO_2 stored.

40 $$C_i^{wd} = \frac{[-3.9x10^{-8} depth(i)^3 + 4.00x10^{-4} depth(i)^2 - 0.84 depth(i) + 903] * depth(i)}{1000}$$

41 $$C_i^{se} = \frac{\left(0.0121 depth(i)^2 - 21.745 depth(i) + 53818\right)}{1000}$$

42 $$C_i^{om} = \left[\frac{\left(8.76 depth(i) + 13267\right)}{1000}\right] life$$

CO_2 Pipelines

The optimization model allows the user to input a set of discrete pipeline diameters (i.e., nominal pipe sizes). For each diameter, the model calculates the lifetime capital and operating cost for each pipeline link based on an equation from Ogden and Johnson [13] (Equation 43).

43 $$C_{ijd}^{p} = [(32.086(L_{ij})^{-0.033} d) * L_{ij} * (1 + OM^{p} * life)]$$

Similar to the *HyPAT Model*, this model records the location and diameter of built pipelines (y_{ijd}) and uses this information in subsequent model runs to adjust the costs so that previously built pipelines of a specific diameter are preferred (i.e., less expensive) in later construction periods. Specifically, the cost reflects only the operating and maintenance costs and not the capital for existing pipelines (Equation 44). This cost adjustment provides an incentive to maintain previously built pipelines, but does not prevent larger pipelines from being built.

44 $$C_{ijd}^{p} = [(32.086(L_{ij})^{-0.033} d) * L_{ij} * (OM^{p} * life)]$$

Finally, it is implausible that a pipeline of a particular diameter would be removed and replaced with a pipeline of a smaller diameter[3]. To address this, the model uses the variable y_{ijd} to identify the diameter classes that are smaller than any previously built diameter along each pipeline link and assigns a high cost to these diameter classes (99999). The useable capacity of each pipeline diameter class (Q_d^p) is derived from Vandeginste and Piessens [22] assuming a pipeline length of 250 km, a pipeline capacity factor of 90%, and a pressure drop of 35 bar.

2.2.4 Hydrogen Distribution and Refueling Station Model

In the preceding sections, models have been described that identify the location and quantity of demand, the location and size of production facilities, the location and size of CO_2 storage sites, and the location, length, and diameter of hydrogen transmission and CO_2 pipelines. The *Hydrogen Distribution and Refueling Station Model* identifies the infrastructure required for delivering hydrogen to consumers within the demand center boundaries. Specifically, the model determines the number and size of hydrogen refueling stations and the length and diameter of the distribution pipelines needed to transport hydrogen from the demand center centroids (i.e., distribution centers) to the individual refueling stations.

Unlike the other models, this model does not use a spatially explicit optimization tool. Instead, an idealized city model is used to simplify the estimation of the distribution pipeline length and number of refueling stations [45]. This model assumes that each demand center is represented by a circle of equivalent area (Figure 14a). Within this circle, it is assumed that the population distribution is homogeneous and the refueling stations are distributed evenly, uniform in size,

[3] It is possible that the diameter of a pipeline may need to be decreased if the minimum capacity of the pipeline is not met in subsequent model runs. However, the model does not include minimum pipeline capacity.

and connected by pipelines along concentric rings (Figure 14b). As a result of this simplification, the distribution pipeline length can be estimated as a function of the demand center area and the number of refueling stations.

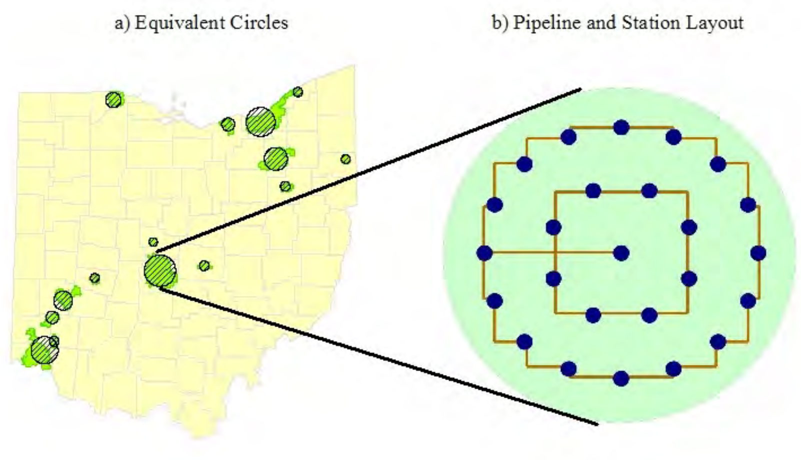

Figure 14: Idealized city model [46]

The method for estimating the number of refueling stations in each demand center is provided in section 2.1.2.3. Given the number of stations and area associated with each demand center, the distribution pipeline length is estimated using Equation 45, which is derived from an equation provided in Yang and Ogden [45].

45 $$L_{pipeline} = \left[\beta \cdot N_{stations}^{\gamma} \cdot r_{city}\right]$$

where $L_{pipeline}$ is the length of distribution pipeline (km), $N_{stations}$ is the number of refueling stations, r_{city} is the demand center radius (km), β is 2.43, and γ is 0.4909.

The average hydrogen flow along distribution pipelines in an individual demand center is calculated by dividing the total hydrogen demand by the number of concentric rings (N_{rings}) where N_{rings} is defined by dividing the city radius by the average distance between rings (4 km).

If the city radius is less than 4 km, the demand center is assigned one ring. It is assumed that the hydrogen flow is uniform throughout all distribution pipelines and defined by the average flow. This flow is used to determine the required pipeline diameter in each demand center based on equations provided in version 2.2 of the U.S. DOE H2A Delivery Scenario Analysis Model [10]. The diameter of distribution pipelines is constrained to nominal pipe sizes ranging from 4 to 20 inches.

2.2.5 Post-Processing in Techno-economic and Revenue Requirements Modules

The *Infrastructure Design Module* provides an inventory of the infrastructure required for both supplying hydrogen and sequestering CO_2. This inventory is input to the *Techno-economic Module* where a more detailed cost analysis of infrastructure components is conducted. However, the optimization models in the *Infrastructure Design Module* employ simplified planning assumptions that improve the tractability of the models, but do not necessarily represent realistic deployment strategies. Thus, the *Techno-Economic and Revenue Requirements Modules* are also used to translate the outputs of the *Infrastructure Design Module* to represent more realistic deployment strategies that are still constrained by the general design and capacities dictated by the *Infrastructure Design Module*. Table 15 compares the planning assumptions in the *Infrastructure Design Module* with alternative scenarios that can be examined via post-processing in the *Techno-economic and Revenue Requirements Modules*.

In this study, the planning assumptions outlined in Scenario 1 are used to represent deployment of infrastructure over time. At each hydrogen production site, expansion is represented by building a new facility to meet additional demand. For example, consider a case in which the *HyPAT Model* indicates that a 300 tonne per day facility is required in the first hydrogen infrastructure tranche and a 1500 tonne per day plant is required in the third tranche. The *Techno-economic Module* represents this expansion by building a 300 tonne per day plant in the first tranche and then building a 1200 tonne per day plant to meet the additional capacity requirement in the third tranche. Thus, where the *HyPAT Model* assumes the replacement of the small facility by a larger facility, the economic model builds a second facility, which is a more realistic strategy. It should be noted that the scenario modeled in the *Techno-economic Module* is not the scenario optimized by the *HyPAT Model*. In fact, if the *HyPAT Model* was required to build a second facility at a site rather than scaling up the existing facility, the economics may favor building a new facility at another site instead. However, incorporating this possibility into the optimization model would be more complex. Thus, we rely on the economic model to translate the results of the *HyPAT Model*, which are based on simple planning assumptions, into more realistic deployment strategies.

Hydrogen storage is not explicitly modeled by the HyPAT Model. However, it is assumed that one cavern is associated with each production site. This assumption is incorporated in the *Techno-economic and Revenue Requirements Modules* by oversizing the storage facility to meet the total storage capacity required over the lifetime of the production site. Therefore, if two production facilities are built at a particular site over the course of 20 years, the storage site built in conjunction with the first plant will be oversized to accommodate the storage requirements of both plants.

Table 15: Comparison of optimized and alternative planning scenarios

Infrastructure Component	Infrastructure Design Module (optimized scenario)	Techno-economic and Revenue Requirements Modules (alternative scenarios)
H_2 Production Facilities	1. Only one plant at each site 2. Plant can be expanded 3. Expansion represented as replacement of existing plant with larger plant 4. Total production capacity at site limited to capacity of one large plant	Scenario 1 1. Expansion represented by building a new plant to meet additional capacity requirement 2. Multiple plants at each site 3. Total production capacity at site limited to capacity of one large plant
		Scenario 2 1. Expansion represented by oversizing original plant if new capacity is required within lifetime of original plant 2. One plant at each site 3. Total production capacity at site limited to capacity of one large plant
H_2 Storage	1. One cavern storage facility associated with each production site	1. Expansion represented by oversizing original cavern to meet maximum storage requirement over lifetime of facility 2. One storage facility for each production site (one plant in Scenario 1 and multiple plants in Scenario 2)
H_2 and CO_2 Pipelines	2. Only one pipeline along each corridor 3. Pipeline diameter can be expanded 4. Pipeline expansion represented as replacement of existing pipeline with larger pipeline 5. Pipeline diameter dictated by current flow	Scenario 1 1. Expansion represented by oversizing pipeline to largest diameter required within lifetime of pipeline 2. Only one pipeline along each corridor 3. Pipeline diameter dictated by largest flow over lifetime of pipeline
		Scenario 2 1. Expansion represented by installing parallel pipeline(s) to meet additional capacity requirements 2. Multiple pipelines along each corridor 3. Pipeline diameter(s) dictated by current flow
H_2 Refueling Stations	1. Multiple refueling stations allowed in each demand center 2. Existing stations cannot be expanded 3. Additional capacity met by building new stations	Same as optimized scenario
CO_2 Injection Sites	1. Only one disposal site at each reservoir 2. Site can be expanded up to reservoir storage capacity 3. Expansion represented by building new injection wells	Same as optimized scenario

In the case of hydrogen and CO_2 pipelines, the *Techno-economic and Revenue Requirements Modules* assume that pipelines are oversized to the maximum diameter required over their lifetime (20 years). Once the lifetime is completed, the pipeline is replaced by another pipeline that meets the diameter requirement for the next 20 years. In this way, the model only requires replacement of pipelines at the end of their lifetime. For example, consider a case in which the *HyPAT Model* indicates that a 12-inch pipeline is required in the first tranche, a 30 inch pipeline is required along the same corridor in the third tranche, and a 36-inch pipeline is required in the fifth tranche. The *HyPAT Model* assumes that the 12-inch pipeline is replaced by a 30-inch pipeline and then replaced by the 36-inch pipeline. However, assuming that the third tranche occurs within 20 years of the first, this transition is represented by the economic models as if a 30-inch pipeline is built in the first tranche and then is replaced at the end of its life with a 36-inch pipeline.

Explicitly incorporating pipeline oversizing into the optimization tools would require a dynamic model with perfect foresight of future flows, which would greatly increase the complexity of the model. In reality, as perfect knowledge of future flows is unlikely, pipeline deployment strategies will likely rely on limited foresight to oversize pipelines based on near-term projections (< 10 years) and then handle additional capacity expansions with parallel pipelines. However, the possibility of parallel pipelines is not modeled in this study.

In the case of hydrogen refueling stations, additional refueling capacity is met by building new stations, not increasing the size of existing stations. In the first tranche, stations are generally small since a minimum number of stations is required. These small stations are maintained throughout the transition, even when their lifetime ends since the model requires that the replacement cost is the same as the original cost. However, stations generally become larger in each tranche with the average station size converging to ~1800 kg per day. At CO_2 injection sites, additional injection wells are added when the maximum injection capacity of existing wells is exceeded. Additional wells can be added until the storage capacity of the site is reached.

The outputs from the *Hydrogen Infrastructure Deployment Model* include an inventory of infrastructure components and estimates of the total capital requirement, levelized cost of hydrogen ($/kg), cumulative cash flow, and CO_2 captured and emitted during the transition to a coal-based hydrogen transportation system in a specific region. The model also estimates coal use and CO_2 storage requirements. It can be applied to different geographic regions and can incorporate different HFCV market penetration scenarios in order to examine how the timing of infrastructure deployment impacts the cost of hydrogen. Various policy scenarios can also be explored using the model (e.g., accelerated depreciation and production tax credits).

3.0 Task 5.0: Analysis of Emerging CO_2 Capture and Storage Technologies in the Power and Industrial Sectors

In Task 5, we assess the costs and performance of systems for capturing and storing CO_2 from industrial and power sector sources as well as optimal strategies for their deployment. In the first section, we present technical and economic models for CO_2 capture options for a variety of large point sources in the power and industrial sectors. The focus on the power and industrial sectors is important since these sources are likely to dominate CO_2 production in the near-term and, thus, be the best candidates for early CCS adoption. In contrast, it will likely take 10-20 years for hydrogen demand to reach levels where large central plants with CCS might be needed for producing hydrogen transportation fuel. In the power sector, capture technologies are described for supercritical and ultra-supercritical pulverized coal steam power plants, integrated gasification combined cycle coal power plants, and natural gas combined cycle power plants. Industrial CO_2 point sources include cement plants, ammonia plants, oil refineries and ethanol plants.

In the second section, we describe a regional transition model that was developed to examine optimal CCS deployment strategies in real geographic regions. The model combines detailed spatial and techno-economic data with optimization tools and policy constraints to identify the least-cost CCS infrastructure for meeting a specific CCS target, which can be defined as a CO_2 reduction target (Mt CO_2/year) or as a capacity target (GW installed with CCS). In the third section, the model is applied to a case study in the southwestern United States to examine how a transition from early demonstration projects to widespread adoption of CCS might occur given the subsidies and CO_2 prices proposed in the American Power Act. This case study provides insights into the design and cost of CCS deployment through the transition.

3.1 Techno-economic Modeling of CO_2 Capture Equipment

An assessment of the regional deployment of CCS in the power and industrial sectors requires equations for calculating the CO_2 capture cost ($/t$CO_2$ avoided) at various types of facilities. In this section, the requisite equations for calculating this cost are provided for several types of facilities in the power and industrial sectors. In the power sector, equations for coal and natural-gas based power plants are provided and, in the industrial sector, large point sources are considered, including refineries and ammonia, ethanol, and cement plants. This section is limited to a discussion of CO_2 capture costs since CO_2 pipeline transport and injection costs are well documented in section 2.1.3. All costs are given in constant 2009 U.S. dollars.

3.1.1 Power Sector

In the power sector, the cost of avoided CO_2 (C_{CO2}^{avoid}) is estimated by equation 46, where COE is the cost of electricity ($/kWh) and CO2 represents the CO_2 emissions (tonnes/kWh) associated with a new plant with CO_2 capture (new) and a reference plant without capture (ref).

46 $$C_{CO2}^{avoid} = \frac{COE_{new} - COE_{ref}}{CO2_{ref} - CO2_{new}}$$

Consequently, equations are needed that provide the cost of electricity for various types of plants with and without CO_2 capture. This section outlines generic equations for calculating the total capital requirement, non-fuel O&M, and fuel input as a function of the net electrical output (MW), or nameplate capacity, of a plant. Given these values, a project-specific COE can be calculated based on the size of the plant, capital recovery factor, fuel cost, and capacity factor.

Equations for all power plants are derived from the Integrated Environmental Control Model (IECM) v. 6.2.4 [47] using a real discount rate of 10% and assuming a capacity factor of 75%. Furthermore, it is assumed that all pulverized coal plants utilize Illinois #6 coal and include Hot-side SCR, Cold-side ESP, and Wet FGD to control NO_x, particulate, and SO_2 emissions, respectively. The IECM provides the cost and design of current power plant technologies and utilizes both existing plant data and ASPEN PLUS modeling for more advanced components like CO_2 capture equipment. Learning rates can be applied exogenously to model how costs decline with deployment [48].

3.1.1.1 Supercritical Pulverized Coal Plants

Supercritical pulverized coal plants with and without CO_2 capture were modeled for eight plant sizes with gross electrical outputs in the range of 100 to 2500 MW. Plants with capture are modeled with a post-combustion amine-based system that captures 90% of CO_2 emissions. Net plant efficiency declines from about 38% without capture to approximately 24% with capture. The IECM provides the net electrical output (MW), coal input (tonnes/hr), capital cost (million$), CO_2 emissions (tonnes/hr), and non-fuel fixed and variable O&M cost (million$/yr). Given these values, regression analysis is used to develop equations for capital cost (C_{cap}), non-fuel O&M cost ($C_{O\&M}$), and coal input (I_{coal}) as a function of net electrical output (MW_{net}) (e.g., Figure 15).

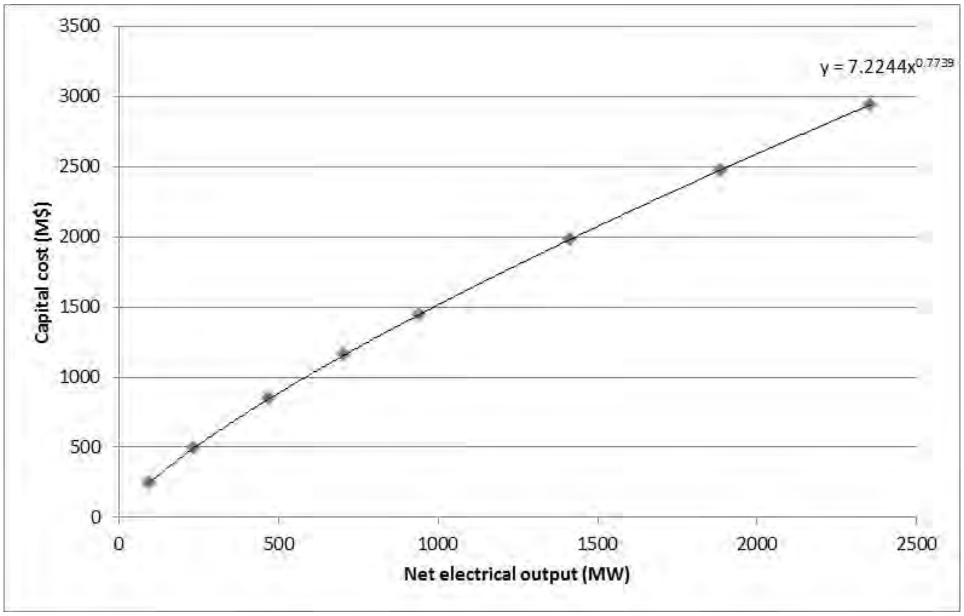

Figure 15: Plant capital cost as a function of net electrical output (supercritical pulverized coal without CO_2 capture)

Equations for supercritical pulverized coal plants without CO_2 capture:

47 $C_{cap} = 7.2244(MW_{net})^{0.7739}$

48 $C_{O\&M} = -3x10^{-6}(MW_{net})^2 + 0.0424(MW_{net}) + 15.594$

49 $I_{coal} = 0.3414(MW_{net}) + 0.3441$

Equations for supercritical pulverized coal plants with CO_2 capture:

50 $C_{cap} = 2.95(MW_{net}) + 263.23$

51 $C_{O\&M} = 0.1696(MW_{net}) + 20.245$

52 $I_{coal} = 0.5513(MW_{net}) + 0.6148$

Using these equations, the cost of electricity (COE) can be estimated for any plant given the nameplate capacity, capacity factor, capital recovery factor, and coal cost. Given a capacity factor of 75%, capital recovery factor of 7.5%, and a coal cost of $1.7/GJ, the COE is $0.04-0.08/kWh for plants without capture and $0.09-0.15/kWh for plants with capture (100 – 2500 MW gross output).

3.1.1.2 Ultra Supercritical Pulverized Coal Plants

Ultra supercritical pulverized coal plants with and without CO_2 capture were modeled for eight plant sizes with gross electrical outputs in the range of 100 to 2500 MW. Plants with capture are modeled with a post-combustion amine-based system that captures 90% of CO_2 emissions. Net plant efficiency declines from about 43% without capture to approximately 28% with capture. The IECM provides the net electrical output (MW), coal input (tonnes/hr), capital cost (million$), CO_2 emissions (tonnes/hr), and non-fuel fixed and variable O&M cost (million$/yr). Given these values, regression analysis is used to develop equations for capital cost (C_{cap}), non-fuel O&M cost ($C_{O\&M}$), and coal input (I_{coal}) as a function of net electrical output (MW_{net}) (e.g., Figure 16).

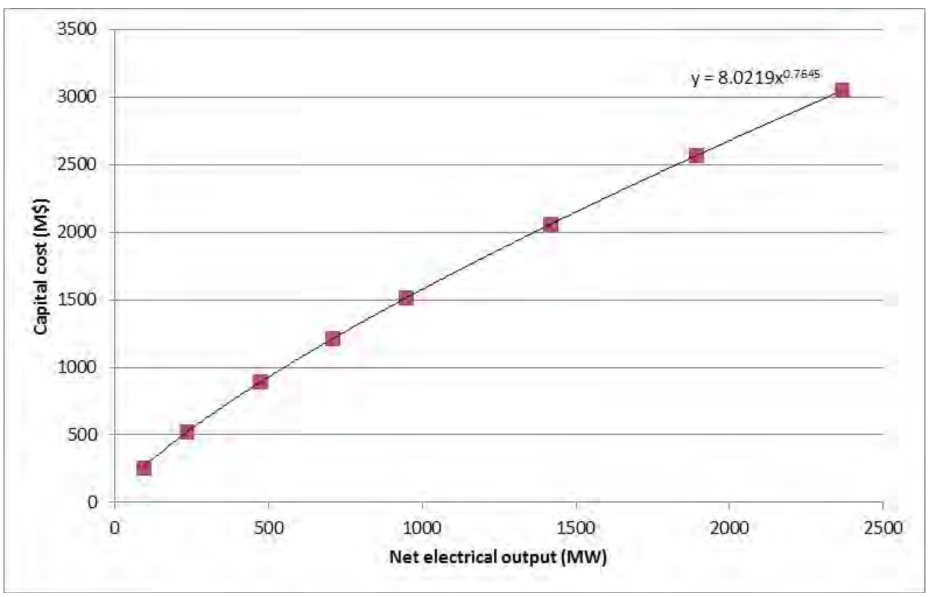

Figure 16: Plant capital cost as a function of net electrical output (ultra supercritical pulverized coal without CO_2 capture)

Equations for ultra supercritical pulverized coal plants without CO_2 capture:

53 $C_{cap} = 8.0219(MW_{net})^{0.7645}$

54 $C_{O\&M} = -3x10^{-6}(MW_{net})^2 + 0.0421(MW_{net}) + 15.546$

55 $I_{coal} = 0.3094(MW_{net}) + 0.3496$

Equations for ultra supercritical pulverized coal plants with CO_2 capture:

56 $C_{cap} = 2.6798(MW_{net}) + 296.45$

57 $C_{O\&M} = 0.1487(MW_{net}) + 20.145$

58 $I_{coal} = 0.4732(MW_{net}) + 0.5454$

Using these equations, the cost of electricity (COE) can be estimated for any plant given the nameplate capacity, capacity factor, capital recovery factor, and coal cost. Given a capacity factor of 75%, capital recovery factor of 7.5%, and a coal cost of $1.7/GJ, the COE is $0.04-0.08/kWh for plants without capture and $0.08-0.14/kWh for plants with capture (100 – 2500 MW gross output).

3.1.1.3 Integrated Gasification Combined Cycle (IGCC) Coal Plants

Only IGCC coal plants *with* CO_2 capture were modeled in this project since it is likely that IGCC plants will not be built without CO_2 capture since the efficiency is low and COE is large relative to pulverized coal plants without CO_2 capture. The IECM models only one gas turbine size (~320 MW gross electrical output) so costs were modeled for plants with between one and five turbines (i.e., 320 to 1600 MW gross output). Plants are modeled assuming Illinois #6 bituminous coal, GE quench gasifiers, GE sour water-gas shift reactors and Selexol CO_2 and H_2S removal systems. The CO_2 removal system is assumed to have a removal efficiency of 95%. Net plant efficiency declines from about 33% in IGCC plants without capture to approximately 28% with capture. The IECM provides the net electrical output (MW), coal input (tonnes/hr), capital cost (million$), CO_2 emissions (tonnes/hr), and non-fuel fixed and variable O&M cost (million$/yr). Given these values, regression analysis is used to develop equations for capital cost (C_{cap}), non-fuel O&M cost ($C_{O\&M}$), and coal input (I_{coal}) as a function of net electrical output (MW_{net}) (e.g.,Figure 17).

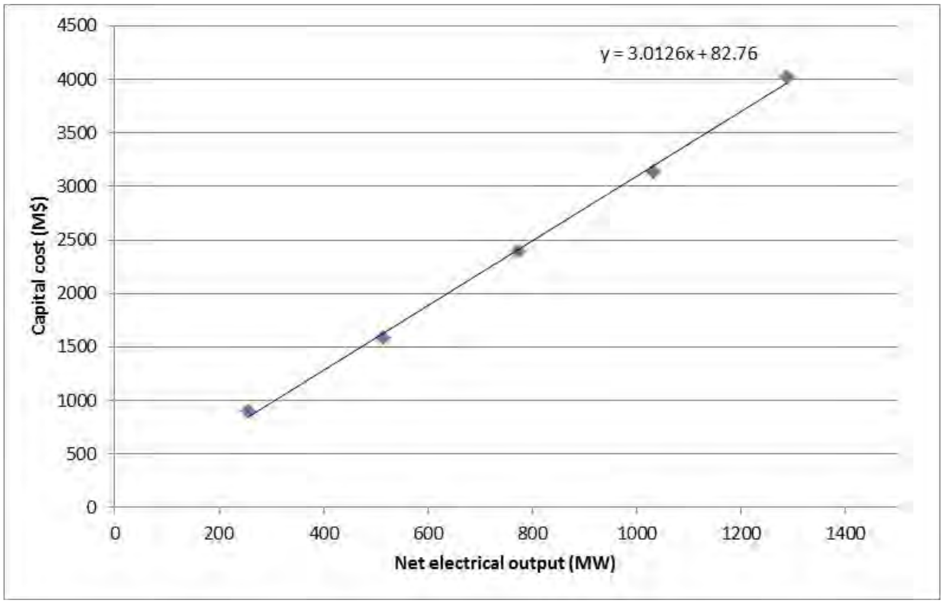

Figure 17: Plant capital cost as a function of net electrical output (IGCC coal with CO_2 capture)

Equations for IGCC coal plants with CO_2 capture:

59 $C_{cap} = 3.0126(MW_{net}) + 82.76$

60 $C_{O\&M} = 0.1367(MW_{net}) + 20.133$

61 $I_{coal} = 0.4715(MW_{net}) + 1.7292$

Using these equations, the cost of electricity (COE) can be estimated for any plant given the nameplate capacity, capacity factor, capital recovery factor, and coal cost. Given a capacity factor of 75%, capital recovery factor of 7.5%, and a coal cost of \$1.7/GJ, the COE is \$0.05-0.06/kWh for plants without capture and \$0.08-0.10/kWh for plants with capture.

3.1.1.4 Natural Gas Combined Cycle (NGCC) Plants

The IECM only models one gas turbine size (GE 7FA) so NGCC plants are modeled with one to five gas turbines. This corresponds to a gross electrical output of 282 to 1412 MW for plants without CO_2 capture and 244 to 1217 MW for plants with capture. All plants are modeled with once-through cooling and plants with CO_2 capture have a post-combustion amine-based system that captures 90% of CO_2 emissions. Net plant efficiency declines from about 50% without capture to approximately 39% with capture. The IECM provides the net electrical output (MW), natural gas input (GJ/hr), capital cost (million$), CO_2 emissions (tonnes/hr), and non-fuel fixed and variable O&M cost (million$/yr). Given these values, regression analysis is used to develop equations for capital cost (C_{cap}), non-fuel O&M cost ($C_{O\&M}$), and natural gas input (I_{gas}) as a function of net electrical output (MW_{net}) (e.g.,Figure 18).

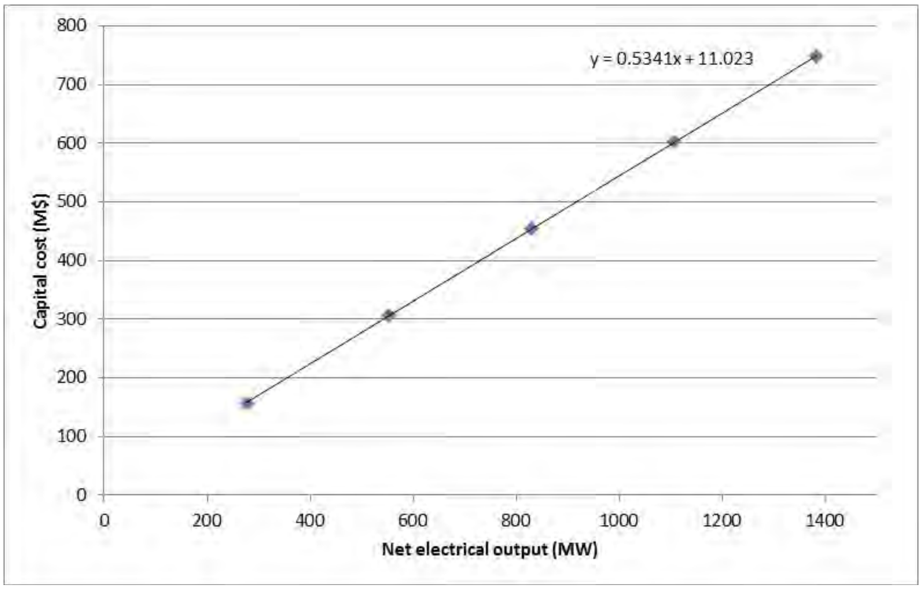

Figure 18: Plant capital cost as a function of net electrical output (NGCC without CO_2 capture)

Equations for NGCC plants without CO_2 capture:

62 $C_{cap} = 0.5341(MW_{net}) + 11.023$

63 $C_{O\&M} = 0.0078(MW_{net}) + 2.9897$

64 $I_{gas} = 7.2709(MW_{net}) - 2.0618$

Equations for NGCC plants with CO_2 capture:

65 $C_{cap} = 1.1803(MW_{net}) + 34.209$

66 $C_{O\&M} = 0.0544(MW_{net}) + 4.4649$

67 $I_{gas} = 9.2261(MW_{net}) - 2.0454$

Using these equations, the cost of electricity (COE) can be estimated for any plant given the nameplate capacity, capacity factor, capital recovery factor, and natural gas cost. Given a capacity factor of 75%, capital recovery factor of 7.5%, and a natural gas cost of \$4.5/GJ, the COE is approximately \$0.05/kWh for plants without capture and \$0.08-0.09/kWh for plants with capture.

The avoided cost of CO_2 capture is highly dependent on the COE and CO_2 emissions of the reference plant (i.e., the plant that is replaced when the new plant is built). Thus, in the context of a case study, the avoided cost of capture can only be calculated on a site-specific basis. A comparison of capture costs in the southwestern United States is provided in Section 3.3.2.2.

3.1.2 Industrial Sector

Capture cost models were developed for several of the largest stationary CO_2 producers in the industrial sector, including refineries and ammonia, cement, and ethanol plants. Although the iron and steel industry is also a large source of anthropogenic CO_2, insufficient data was available to determine capture costs. This section assumes that CO_2 capture equipment is added as a retrofit to existing facilities.

3.1.2.1 Refineries

The refining sector is the third largest stationary source of anthropogenic CO_2 [49]. Refinery capture costs are derived from van Straelen et al. [50] and Simmonds et al. [51], which present capture costs for refineries that employ post-combustion CO_2 capture. van Straelen et al. [50] provides Euro/tCO_2 avoided values for a range of annual CO_2 capture quantities for a flue gas containing 8% CO_2, which corresponds to the CO_2 concentration in flue gas from a large combined stack. Based on this information, a scaling factor for CO_2 avoided costs as a function of CO_2 capture capacity is developed. Simmonds et al. [51] provides a more detailed cost estimate for a post-combustion system that captures one million tonnes CO_2 per year. The data are used to identify reference plant costs for a range of capital recovery factors (Table 16). Equation 68 describes the capture cost (C_{capt}; \$/tCO_2 avoided) as a function of the CO_2 capture capacity ($CO2_{capt}$; kt CO_2/yr), where C_{ref} is the reference cost provided in Table 16.

Table 16: \$/tonne CO_2 avoided for a reference plant (1000 kt CO_2/yr) given different capital recovery factors (CRFs)

CRF	Capture Cost (\$/tCO_2 avoided; C_{ref})
7.5%	79
11%	95
16.27%	120

$$68 \quad C_{capt} = C_{ref}\left(\frac{CO2_{capt}}{1000}\right)^{-0.1434}$$

To calculate the CO_2 capture capacity at each refinery, it is assumed that 50% of total CO_2 emissions are eligible for capture from large flue gas sources. The remaining emissions are assumed to be small, distributed sources with prohibitively high capture costs. Of the eligible emissions, approximately 90% can be captured using an amine-based post-combustion system [50]. The capture equipment is installed as a retrofit on existing refineries and the quantity of CO_2 avoided is about 70% of the captured CO_2 [51].

3.1.2.2 Cement Plants

Cement production is the second largest stationary source of anthropogenic CO_2 [49]. Equations for CO_2 capture costs at cement plants are derived from Barker et al. [52], which is a summary of a technical report on CO_2 capture in the cement industry published by the IEA Greenhouse Gas Programme (IEA GHG) [53]. The IEA GHG report provides a detailed cost model of a new one Mt/yr cement plant in the United Kingdom at which approximately one Mt CO_2/yr are captured. Because the capture cost is modeled for only a single plant size and cement plants and refineries both use amine-based post-combustion capture, the scaling factor for capture costs at refineries is also applied to cement plants [50]. However, the reference plant size and capture costs are derived from data provided in Barker et al. [52] for several capital recovery factors and coal costs (Table 17). Equation 69 describes the capture cost (C_{capt}; \$/tCO_2 avoided) as a function of the CO_2 capture capacity ($CO2_{capt}$; kt CO_2/yr), where C_{ref} is the reference cost provided in Table 17.

Table 17: \$/tonne CO_2 avoided for a reference plant (1068 kt CO_2/yr) given different capital recovery factors (CRFs) and coal costs

CRF	Coal cost (\$/GJ)	Capture Cost (\$/tCO_2 avoided; C_{ref})
7.5%	1.7	80
	1.25	94
11%	1.7	98
	2.5	106
16.27%	1.7	124

$$69 \quad C_{capt} = C_{ref}\left(\frac{CO2_{capt}}{1068}\right)^{-0.1434}$$

To calculate the CO_2 capture capacity, it is assumed that plants are retrofitted with amine-based post-combustion capture with a CO_2 removal efficiency of 85%. According to Barker et al. [52], the quantity of CO_2 avoided is about 56% of the captured CO_2 when the additional power requirements associated with capture are considered.

3.1.2.3 Ethanol and Ammonia Plants

Both ethanol and ammonia plants produce relatively pure streams of CO_2 and require only dehydration and compression of the CO_2 prior to transport. Consequently, CO_2 capture costs are modeled at these plants using equations for dehydration and compression in McCollum and Ogden [54]. It is assumed that CO_2 is compressed from 1 to 150 bar in preparation for pipeline transport.

At an ethanol facility, the annual quantity of CO_2 captured is calculated assuming a CO_2 capture efficiency of 90%. In contrast, 70 to 90% of the CO_2 produced at an ammonia facility is typically used to produce urea [55]. Consequently, this model assumes that only 30% of annual CO_2 emissions at an ammonia facility are compressed and dehydrated for transport. For both types of plants, the compression and dehydration system is installed as a retrofit and is designed assuming a plant capacity factor of 80%. CO_2 capture costs for industrial plants of different sizes are summarized in Table 18.

Table 18: Range of CO_2 capture costs for industrial plants with CCS (Capital Charge = 16.3%)

Plant type	Size Range (MtCO_2 captured/yr)	\$/tCO_2 avoided
Refinery	0.1 to 2.5	105 to 223
Cement Plant	0.1 to 2.6	109 to 180
Ethanol Plant	0.02 to 0.5	20 to 82
Ammonia Plant	0.04 to 0.15	49 to 58

3.2 Development of a Regional Transition Model for Carbon Capture and Storage

This section describes a spatially-explicit modeling tool for examining the adoption of carbon capture and storage (CCS) technologies in the power and industrial sectors. Unlike the *CO_2 Transport and Disposal Model* described in Section 2.2.3, the *CCS Deployment Model* is not designed to determine the least-cost network for connecting pre-determined sources of CO_2 (e.g., built hydrogen production facilities) to potential CO_2 sinks. Rather, the model identifies the least-cost CCS infrastructure for meeting a specific CCS target, which can be defined as a CO_2 reduction target (Mt CO_2/year) or as a capacity target (GW installed with CCS). Given the target, the model chooses among several facility types (e.g., cement, ethanol, coal-based power) and sink types (e.g., saline aquifers, depleted oil and gas fields) to identify the least-cost CCS infrastructure for meeting the pre-specified target.

The model inputs include a candidate CO_2 pipeline network, the locations, CO_2 capture potentials, and capture costs of candidate facilities, and the locations, capacities, reservoir types, and injection costs of potential CO_2 injection sites. The model determines the location, length, and diameter of CO_2 pipelines, the number, location, CO_2 captured, and capacity of facilities at which CO_2 capture is installed, and the number, location, reservoir type, and size of injection sites.

3.2.1 Model Formulation

The *CCS Deployment Model* is a mixed integer linear programming (MILP) optimization model that is formulated in the General Algebraic Modeling System (GAMS) and solved using CPLEX [38]. The integer (in this case binary) variables represent decisions regarding whether or not to build a CO_2 storage facility at a particular type t of reservoir at node i (r_{it}), construct a pipeline segment between nodes i and j of diameter d (y_{ijd}), or install CO_2 capture at a facility at node i (c_i). The continuous variables represent decisions regarding the quantity of CO_2 to inject into a reservoir of type t at node i (a_{it}) and to transport from node i to j (x_{ij}).

The subscript d on the pipeline construction decision variable allows the model to identify the optimal pipeline diameter for transporting any amount of CO_2 between two nodes. This is important since the amount of CO_2 flow through any pipeline segment is not known in advance since it depends on the route chosen by the model. It should be noted that the model determines the best route and, thus, the direction of flow between any two nodes. Consequently, the links are assumed bi-directional with the direction of flow determined by the model at each CCS target. The subscript t on the reservoir decision variables represents the type of reservoir used for CO2 injection. This is important since some injection sites have access to several types of reservoirs with different injection costs and capacities. Model annotation is listed in Table 19.

Table 19: CCS model annotation

Sets:	
N	network nodes
R	CO_2 reservoir nodes (subset of N)
F	CO_2 capture nodes (subset of N)
N_i	network nodes that are neighbors of node i (subset of N)
D	pipeline diameters (12.75, 16, 24, 30, 36, 42-inch)
T	reservoir types (e.g., saline aquifer, depleted oil and gas, ECBM, EOR)
B_r	previously built injection site
Bf	Previously built facility with capture
Decision Variables:	
x_{ij}	units of CO_2 transported from node i to node j (million tonnes/year)
a_{it}	units of CO_2 stored in reservoir type t at node i (million tonnes/project lifetime)
r_{it}	1, if storage facility of type t is built at node i; 0, otherwise
c_i	1, if capture is installed at node i; 0, otherwise
y_{ijd}	1, if pipeline is constructed from node i to node j with diameter d; 0, otherwise
Input Parameters:	
$C^{cap}{}_i$	levelized cost of CO_2 capture (including capital and O&M) at node i (thousand$/Mt CO_2)
$C^{inj}{}_t$	levelized cost of CO_2 injection (including capital and O&M) for reservoir type t (thousand$/Mt CO_2)
$C^p{}_d$	installed cost for pipeline of diameter d (thousand$/km)
$C^p{}_{ijd}$	fixed capital and O&M cost for a pipeline of diameter d from node i to node j (thousand$/project lifetime)
C^{site}	fixed site characterization cost for CO_2 storage (thousand$/site/project lifetime)
$Q^r{}_{it}$	useable capacity of a storage reservoir of type t at node i (million tonnes/project lifetime)
$Q^p{}_d$	useable capacity of a pipeline of diameter d (million tonnes/year)
$Q^f{}_i$	nameplate capacity of facility at node i (GW)
F_i	Potential CO_2 captured at node i (million tonnes/year)
L_{ij}	adjusted length of pipeline segment from node i to node j (km)
$B^r{}_{it}$	CO_2 stored at previously built reservoir of type t at node i (million tonnes/project lifetime)
$B^f{}_i$	CO_2 capture installed at previously built facility at node i (1, if previously built; 0, otherwise)
d	pipeline diameter (inch)
OM^p	annual operating and maintenance cost for a pipeline (2.5% of fixed capital)
life	project lifetime (years)
Tgt_{cap}	Electric capacity target for installation of CCS in power sector (GW)
Tgt_{CO2}	CO_2 reduction target (Mt CO_2/year)

Objective Function

The objective of the model is to identify the infrastructure design that minimizes the total cost of CO_2 capture, transport and storage over the project lifetime (thousand$), including both capital and operating costs (Equation 70).

$$\text{70 Minimize } \sum_{i \in F} c_i F_i C_i^{cap} life + \sum_{i \in R} \sum_{t \in T} \left[r_{it} C^{site} + a_{it} C_t^{inj} \right] + \sum_{i} \sum_{j \in N_i} \sum_{d} C_{ijd}^{p} y_{ijd}$$

The first term of this function represents the capital and O&M costs associated with CO_2 capture while the second term represents the costs associated with CO_2 injection and storage. The final term represents the capital and O&M costs associated with CO_2 pipeline transport.

Constraints

The model includes several sets of constraints that must be satisfied by any feasible solution. The first set represents capacity constraints. Equation 71 requires that the maximum flow of CO_2 (x_{ij}) through a pipeline is less than or equal to the built pipeline capacity and Equation 72 requires that the maximum CO_2 stored (a_{it}) at a reservoir is less than or equal to the reservoir capacity.

$$\text{71} \quad x_{ij} \le \sum_{d} Q_d^p y_{ijd} \qquad \forall i, j \in N_i, d \in D$$

$$\text{72} \quad a_{it} \le Q_{it}^r r_{it} \qquad \forall i \in R, \forall t \in T$$

The second set includes mass balance constraints, which ensure that the flows of CO_2 throughout the network are balanced. Equation 73 dictates that the total CO_2 flow into each node is equal to the total flow out of the node where CO_2 captured at a facility (F_i) is considered flow into the node and CO_2 stored at a reservoir (a_{it}) represents flow out of the node. This constraint prevents shortages and excesses of hydrogen at any given node. Equation 74 requires that the total CO_2 stored in the system is equal to the total CO_2 captured.

73 $$\sum_{j \in N_i} x_{ji} life + c_i F_i life = \sum_{k \in N_i} x_{ik} life + \sum_{t \in T} a_{it} \qquad \forall i, j \in N_i, k \in N_i, t \in T$$

74 $$\sum_{i \in R} \sum_{t \in T} \left(\frac{a_{it}}{life} \right) = \sum_{i \in F} c_i F_i$$

The third set contains the CCS target constraints. These constraints effectively specify how much CCS must be deployed in each model run. Equation 75 represents a CO_2 reduction target (Mt CO_2/year), which specifies the quantity of CO_2 that must be reduced. Specifically, this constraint requires that the total CO_2 stored is greater than or equal to the CO_2 reduction target. One can also specify a capacity target (GW) if one is interested in identifying the least-cost CCS infrastructure for a specific capacity of power plants. Equation 76 requires that the total capacity of power plants that have installed CO_2 capture must be greater than or equal to the capacity target. However, when specifying a capacity target, a reduction target (equation 75) must also be used since the model minimizes the total project cost and not the levelized cost. Without an emissions target, the capacity target will result in the power plants with the lowest emissions being selected since these will have the lowest total cost for CCS. However, the ultimate objective is to discover the CCS system with the lowest levelized cost. Consequently, an iterative process must be used in which the emissions target is varied with a fixed capacity target. After each iteration, the levelized cost of CCS is calculated until the optimal CCS infrastructure is identified that meets the capacity target while achieving the lowest levelized cost.

75 $$\sum_{i \in R} \sum_{t \in T} \left(\frac{a_{it}}{life} \right) \geq Tgt_{CO2}$$

76 $$\sum_{i \in F} c_i Q_i^f \geq Tgt_{cap}$$

The fourth set contains constraints that define the decision variables. Non-negativity constraints are placed on the two continuous decision variables (Equations 77 and 78) and binary constraints are required for the three binary decision variables (Equations 79, 80, and 81).

77 $$x_{ij} \geq 0 \qquad \forall i, j \in N_i$$

78 $$a_{it} \geq 0 \qquad \forall i \in R, \forall t \in T$$

79 $$y_{ijd} \in 0,1 \qquad \forall i, j \in N_i, d \in D$$

80 $$r_{it} \in 0,1 \qquad \forall i \in R, \forall t \in T$$

81 $$c_i \in 0,1 \qquad \forall i \in F$$

The final set represents constraints that can be considered optional. These constraints are included in order to improve the computational efficiency of the model, but can be modified to represent specific beliefs about the infrastructure planning process. Equation 82 stipulates that once CO_2 is allocated to a storage site, the site will continue to store the CO_2 for the project lifetime. However, additional CO_2 can be stored at an existing site until the storage capacity of the site is reached. Equation 83 requires that once CO_2 capture is adopted at a facility, the facility continues to capture CO_2 in the future. Equation 84 dictates that only one pipeline can be built along any single corridor. This constraint streamlines the network optimization, but does prevent parallel pipelines from being developed. Equation 85 states that only one reservoir can be accessed at each potential injection site.

82 $$a_{it} \geq B_{it}^r \qquad \forall i \in B_r$$

83 $$c_i = B_i^f \qquad \forall i \in B_f$$

84 $$\sum_d y_{ijd} \leq 1 \qquad \forall i, j \in N_i, d \in D$$

85 $$\sum_{t \in T} r_{it} \leq 1 \qquad \forall i \in R, t \in T$$

The model can be run for several CCS targets in sequence to examine how CCS is deployed as CO_2 reduction targets become more stringent. In each model run, the infrastructure built at the previous (less stringent) target is provided and constrains the outcome. Specifically, the location and diameter of pipelines (y_{ijd}), the location of storage reservoirs (r_{it}), the actual CO_2 stored at reservoirs (a_{it}), and the location of facilities that adopted capture (c_i) are passed from the previous model run. Equation 82 constrains the location and quantity of CO_2 stored at future storage sites and equation 83 ensures that facilities that previously adopted CO_2 capture continue to contribute to the CCS target. Cost incentives discussed in section 3.2.3.2 encourage the continued use of pre-existing pipelines. The flow along a pipeline (x_{ij}) is not constrained by previous flows, but must respect the pipeline capacity constraint. However, there is no constraint that prevents an existing pipeline from being removed and replaced by a larger diameter pipeline in the future to meet additional flow requirements. Since links are bi-directional, it is possible for flows to change direction between model runs. This model employs a myopic approach that does not consider future infrastructure requirements.

3.2.2 Spatial Inputs

Three spatial inputs are required by this model: 1) the location and type of potential CO_2 sources, 2) the location and type of potential CO_2 sinks, and 3) a candidate pipeline network for connecting CO_2 sources and sinks. These inputs are developed in a geographic information system (GIS).

3.2.2.1 CO_2 Sources

Through the National Carbon Sequestration Database (NATCARB), GIS data is available that provides the locations of several types of CO_2 point sources, including sources in both the power and industrial sectors [44]. These data also provide the annual CO_2 emissions (tonnes CO_2/year) and fuel type associated with each source. The power plant data can be linked to the US EPA Emissions and Generation Resource Integrated Database (eGRID) using the ORIS (Office of the Regulatory Information System) code [39]. The eGRID database provides a wealth of additional information regarding each power plant, including the nameplate capacity (MW), capacity factor (%), annual CO_2 emissions (ton/year), and CO_2 emission rate (lb/MWh). The database also provides information on the year of installation of boilers and generators, which can be used to estimate the age of the power plant. For each source, the location and two other variables are supplied to the optimization model: the CO_2 captured if capture equipment is installed ($C^{cap}{}_{i}$) (Mt CO_2/year) and the CO_2 capture cost (F_i) (thousand$/Mt CO_2). The calculation of these two variables will be discussed in more detail in the context of a case study in section 3.3.2.

3.2.2.2 CO_2 Sinks

The National Carbon Sequestration Database (NATCARB) provides information on the location and storage capacity of potential CO_2 reservoirs in the United States [44]. This information is available for saline aquifers, unmineable coal seams, and oil and gas fields. Storage capacity is identified for each 10 km by 10 km (i.e., 100 km^2) grid cell within each reservoir (e.g., ~40,000 cells for saline aquifers alone). To make the model tractable, the number of potential injection sites must be reduced. This can be accomplished by changing the resolution of the capacity data to 100 km by 100 km (i.e., 10,000 km^2) grid cells. The centroids of the 10,000 km^2 grid cells represent the potential injection sites and are assigned the aggregated storage capacity of all 100 km^2 grid cells that they contain. The number of potential injection sites can be further reduced by deleting all sites that are within 10 km of urban areas, within national park boundaries, and offshore. The inputs to the optimization model include a list of all potential injection sites. For each site, the location, storage capacity ($Q^{r}{}_{it}$) and reservoir type (t) are provided.

3.2.2.3 Candidate Pipeline Network

The candidate pipeline network provides the potential linkages between the locations of CO_2 sources and sinks. There are several possible methods for developing a candidate pipeline network. In this project, it is assumed that CO_2 pipelines will follow existing transportation corridor rights-of-way (ROWs). These corridors could be defined as existing railroad, major road, or pipeline corridors depending on data availability.

The CO_2 candidate pipeline network can also be adjusted to reflect the increased cost of pipeline construction in mountainous and urban areas (as described in section 2.2.2.2). The candidate pipeline network consists of both nodes and links between the nodes. The network nodes include CO_2 source and sink locations as well as all intersections along the pipeline network. The input to the optimization model is a list of all potential network links and their associated adjusted lengths along real ROWs [L_{ij}].

3.2.3 Techno-economic Inputs

The model also requires inputs defining the costs of CO_2 capture, transport and injection. This section discusses how these costs are implemented in a generic application of the model. Specific costs are region-specific and further detail will be provided for a case study in the southwestern U.S. in section 3.3.2.2.

3.2.3.1 CO_2 Capture and Injection

Both CO_2 capture and injection costs are provided to the model exogenously in units of thousand$ per Mt CO_2. Site-specific capture costs (C^{cap}_i) are provided for each node i at which a CO_2 source exists. By incorporating unique capture costs, the model can account for important site-specific factors that influence the cost of capture (e.g., facility type and size). In contrast, the cost of CO_2 injection (C^{inj}_t) is provided for each type t of CO_2 sink (e.g., saline aquifer, EOR, ECBM). The types of sinks are provided by the user and should be limited to types for which there are good capacity and cost data. The model can be modified to incorporate site-specific injection costs if sufficient data is available. However, current characterizations of potential CO_2 sinks are too general to develop accurate cost models for individual injection sites or even reservoirs. A fixed site characterization cost for injection sites (C^{site}) is also required. This cost encourages (though does not require) the model to utilize existing injection sites before building new sites. More detailed examples of how these costs can be estimated in a specific region are provided in section 3.3.2.2.

3.2.3.2 CO_2 Transport

The optimization model allows the user to input a set of discrete pipeline diameters (i.e., nominal pipe sizes). For each diameter d, the fixed capital cost per km of installed pipeline must be provided (C^p_d). The model calculates the lifetime capital and operating cost for each pipeline link based on equation 86 where OM^p is the annual O&M cost, *CRF* is the capital recovery factor, and *life* is the project lifetime.

86 $$\boldsymbol{C^p_{ijd} = (C^p_d L_{ij}) * (OM^p + CRF) * life}$$

The model records the location and diameter of previously built pipelines (y_{ijd}) and uses this information in subsequent model runs to adjust the costs so that previously built pipelines of a specific diameter are preferred (i.e., less expensive) in later construction periods. Specifically, the cost reflects only the operating and maintenance costs and not the capital for existing pipelines (Equation 87). This cost adjustment provides an incentive to maintain previously built pipelines, but does not prevent larger pipelines from being built.

87 $$\boldsymbol{C^p_{ijd} = (C^p_d L_{ij}) * (OM^p) * life}$$

Finally, it is implausible that a pipeline of a particular diameter would be removed and replaced with a pipeline of a smaller diameter[4]. To address this, the model uses the variable y_{ijd} to identify the diameter classes that are smaller than any previously built diameter along each pipeline link and assigns a high cost to these diameter classes (99999). The useable capacity of each pipeline diameter class ($Q^p{}_d$) must also be provided.

3.3 Case Study of CCS Infrastructure Deployment in the Southwestern United States

This case study combines the *CCS Deployment Model*, techno-economic models for CCS components, and regional spatial data to examine how CCS infrastructure might develop in the southwestern United States under the American Power Act (APA). The APA proposes a cap-and-trade program for greenhouse gas (GHG) emissions and provides specific bonus allowances for early CCS projects (up to 72 GW nationally) in the power sector (Table 20) [56]. Given the proposed incentives, this project examines how CCS infrastructure might develop and whether the bonuses are sufficient to drive investment. It also models whether projected CO_2 allowance prices will support continued CCS deployment after the bonuses expire.

In addition to APA-related results, the model provides valuable insight into the deployment of CCS infrastructure in a real geographic region. Specifically, the model identifies optimal deployment strategies, the levelized cost of CCS, the CO_2 emitted and captured, and constraints on regional CO_2 storage capacity. The model also identifies areas in which interconnected

---

[4] It is possible that the diameter of a pipeline may need to be decreased if the minimum capacity of the pipeline is not met in subsequent model runs. However, the model does not include minimum pipeline capacity.

regional pipeline networks are optimal and provides preliminary insight into the conditions that favor networks as opposed to independent dedicated pipelines for each source.

The case study region corresponds with the boundary of the Southwest Regional Carbon Sequestration Partnership (SWP) and includes the states of Colorado, Wyoming, Utah, Arizona, New Mexico, and Texas (Figure 19). Although CO_2 pipeline corridors are modeled in Kansas and Oklahoma, CO_2 sources and sinks within these states were excluded from the model in order to simplify the network. The southeastern portion of Texas is included in this study even though it technically resides within the jurisdiction of the Southeast Regional Carbon Sequestration Partnership (SECARB).

3.3.1 Deployment Scenario

A CCS deployment scenario specifies CO_2 reduction targets for six deployment years from 2016 to 2050 (Table 20). The deployment scenario is based on the allotment and timing of APA bonus allowances in Phases 1 and 2 and, beyond the bonus timeframe, it is based on general CO_2 reduction targets (e.g., 30% reduction by 2030). Only the power sector is eligible for bonus allowances during the first three phases. However, the industrial sector becomes eligible for CCS adoption from 2030 to 2050. For each target/deployment phase, the *CCS Deployment Model* identifies the lowest cost infrastructure for matching CO_2 sources and sinks within the region. Infrastructure in each phase is optimized with knowledge of the infrastructure built in previous phases.

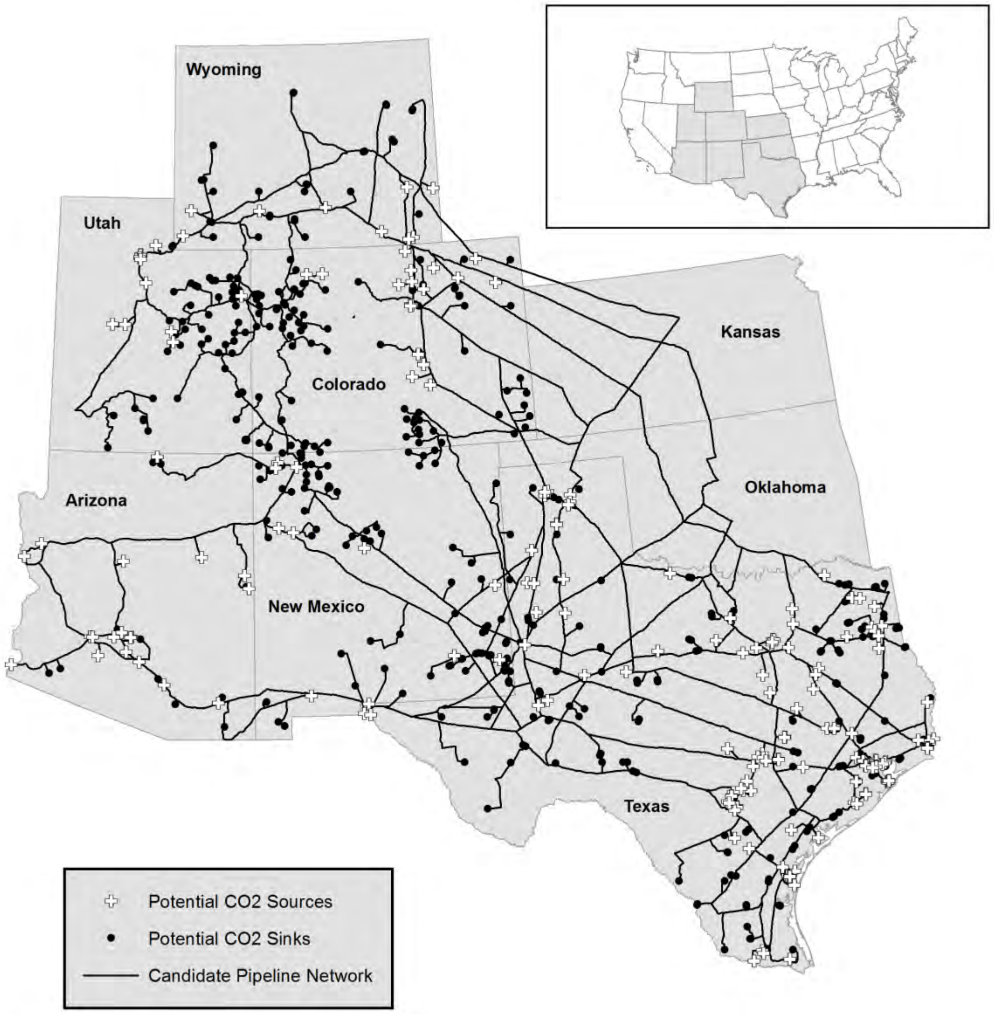

Figure 19: Case study boundary and candidate sites for CO_2 sources, sinks, and pipelines

Table 20: Deployment scenario

	Bonus Allowance ($/t$CO_2$ avoided)*	Bonus Allotment (cumulative GW capacity)**	Reduction Target (%)	Construction Year
Phase 1 – Tranche 1	$106	1.64	N/A	2016
Phase 1 – Tranche 2	$85	3.28	N/A	2020
Phase 2	Reverse Auction	11.8	N/A	2025
2030	N/A	N/A	30%	2030
2040	N/A	N/A	60%	2040
2050	N/A	N/A	80%	2050

*Bonus allowances expire after the first ten years of plant operation

**National bonus allotments are adjusted for the southwestern region (~16.4% of national power capacity)

This study also examines two storage capacity scenarios. The first scenario uses the capacity estimates provided by SWP and SECARB for regional CO_2 sinks and the second scenario assumes that storage capacity is only 10% of the reported values for saline aquifers. Storage capacities for depleted oil and gas fields and unmineable coal seams are held constant in the "Low Capacity" scenario. The second scenario is pursued because there is significant uncertainty regarding current capacity estimates, which are rough estimates based on generic assumptions about storage efficiencies for entire basins. Consequently, it is possible that these values are grossly overestimated [57] and the second scenario examines how smaller storage capacities might affect CCS infrastructure design and cost.

3.3.2 Model Inputs

The model requires detailed spatial data regarding the costs and characteristics of potential CO_2 sources, sinks, and pipeline corridors. This section provides a detailed description of these inputs in the context of the case study and builds upon the generic descriptions in sections 3.2.2 and 3.2.3.

3.3.2.1 Spatial Inputs

The spatial inputs to the model include the locations of facilities with the potential for CO_2 capture, the potential locations and capacities of CO_2 injection sites, and a candidate CO_2 pipeline network (Figure 19). These GIS datasets are derived primarily from data provided by SWP with data on CO_2 sources and sinks in southeastern Texas provided by SECARB. The following sections describe how the original datasets were modified for the purposes of this study.

CO_2 Sources

GIS data is available that details the locations of existing CO_2 sources in the power and industrial sectors. In this case study, sources within the power sector are restricted to coal and natural gas-fired power plants and sources in the industrial sector are restricted to refineries and cement, ethanol, and ammonia plants. In the power sector, each plant includes the ORIS code, which allows the plant to be linked to the eGRID database [39]. This database provides the nameplate capacity, capacity factor, and CO_2 emissions for each existing plant. Only power plants with nameplate capacities > 250 MW and capacity factors > 10% are included as potential capture sites. Since the model assumes replacement of power plants, the model also restricts the list of potential candidate sites in each deployment phase to those that are greater than 30 years old. This constraint prevents relatively new plants from being replaced in early deployment phases. The age of each plant is estimated based on the earliest reported year in which a generator or boiler was installed at the plant [39].

In the industrial sector, CO_2 emissions are provided in the GIS database for both ethanol and cement plants. However, for ammonia plants and refineries, CO_2 emissions are not reported by SWP. As a result, conversion factors had to be developed for estimating CO_2 emissions from plant output. For ammonia facilities, a CO_2 intensity of 1.27 tonnes CO_2 per tonne NH_3 produced is used to convert annual ammonia output to annual CO_2 emissions [49]. For refineries, CO_2 emissions are provided by SECARB and atmospheric crude distillation capacity (barrels per calendar day) is provided by SWP. The distillation capacities for refineries included in the SECARB dataset were determined from a list of U.S. refinery operable capacities provided by the Energy Information Administration (EIA) [58]. Using these values, a CO_2 intensity of 0.027 tonnes CO_2 per barrel was derived and this value was used to calculate CO_2 emissions for the refineries included in the SWP dataset. Given the CO_2 emissions associated with each industrial facility, only those facilities with emissions greater than 25,000 tonnes CO_2 per year are considered candidates for capture retrofits. There are 196 individual CO_2 sources considered for CO_2 capture within the study area, including 127 power plants, 35 refineries, 20 cement plants, 11 ethanol plants, and three ammonia plants. These sources emit approximately 486.6 $MtCO_2$/year of which over 65% is emitted by coal-fired power plants (Figure 20).

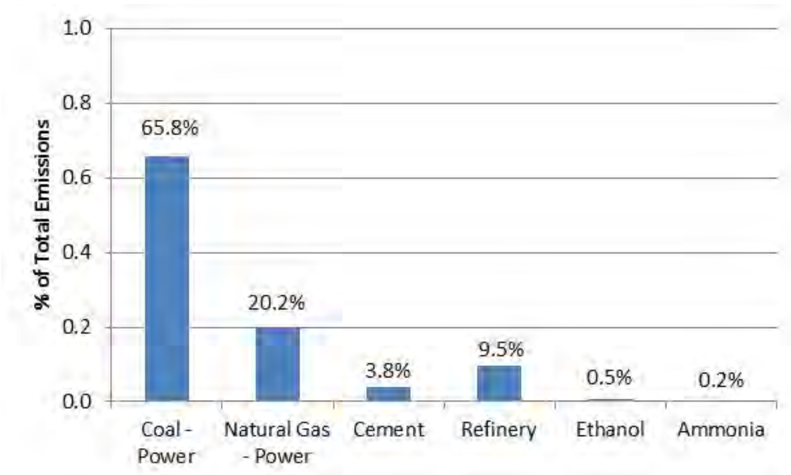

Figure 20: Percent of total CO_2 emissions emitted by each source type

Candidate Pipeline Network

The candidate pipeline network provides the potential linkages between the locations of CO_2 sources and sinks. In this paper, it is assumed that CO_2 pipelines will follow existing pipeline rights-of-way (ROWs) as defined by the National Pipeline Mapping System (NPMS) dataset [40]. In cases where existing pipeline ROWs do not connect to the injection nodes, a spur was manually added following major roads.

Similar to the H_2 candidate pipeline network, the CO_2 candidate pipeline network is adjusted to reflect the increased cost of pipeline construction in mountainous and urban areas (as described in section 2.2.2.2). The candidate pipeline network consists of both nodes and links between the nodes. The network nodes include CO_2 source and sink locations as well as all intersections along the pipeline network. The input to the optimization model is a list of all potential network links and their associated adjusted lengths along real ROWs [L_{ij}]. In the southwestern U.S., the candidate CO_2 pipeline network is about 38,000 km in length and includes approximately 1,150 nodes and 1,200 links.

CO2 Sinks

GIS datasets describing the locations and storage capacities of potential CO_2 reservoirs in the study region are provided by SWP and SECARB (Figure 21). This information is available for saline aquifers, unmineable coal seams, and oil and gas fields. In the case of saline aquifers and unmineable coal seams, the storage capacity is provided only at the level of the geologic formation, which is a coarse spatial resolution. In contrast, Figure 21 indicates that oil and gas field data are provided at a much finer resolution. In both cases, further processing is required to refine the locations and capacities of candidate injection sites.

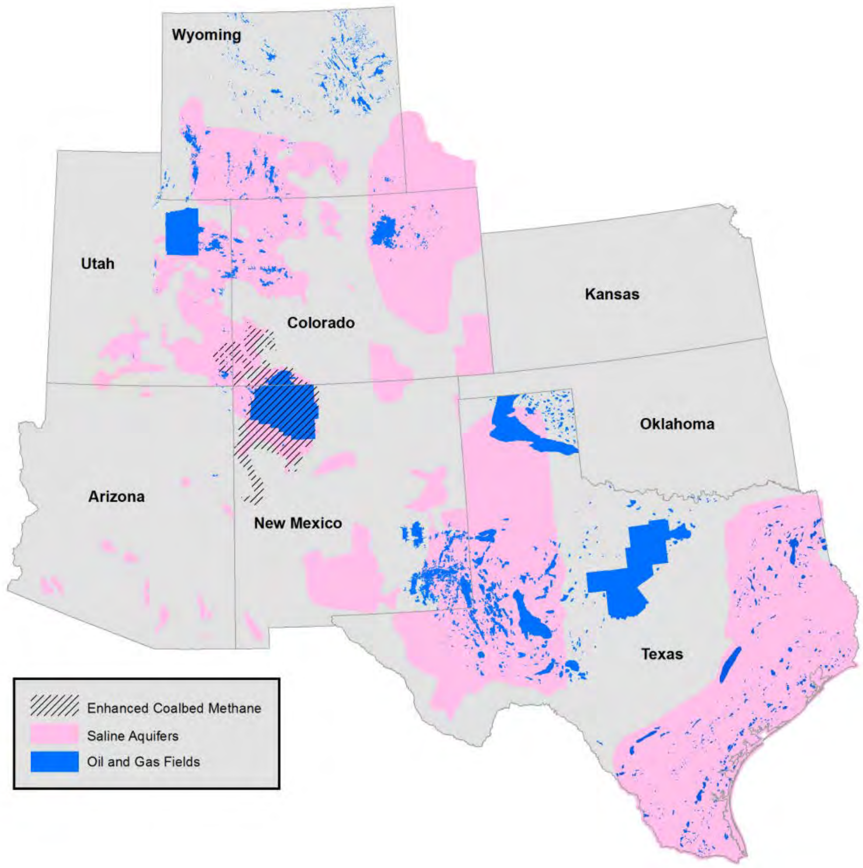

Figure 21: Potential CO_2 storage sinks within the study region

For both saline aquifers and unmineable coal seams, a method was developed to identify individual candidate injection sites within each formation and disaggregate the capacity estimates to these sites. First, a grid consisting of 100 km by 100 km (i.e., 10,000 km^2) grid cells was superimposed on the formations and the centroids of these grid cells were designated as the locations of potential injection sites. In the case of spatially overlapping formations (i.e., those at different depths), at least one injection site was added to access each formation. As a result, clusters of injection sites are evident in locations with several overlapping formations. For each injection site, the storage capacity is estimated by dividing the total formation capacity by the number of sites that access it. For example, four injection sites that access a formation with a capacity of 20 Mt CO_2 would each be assigned a capacity of 5 Mt CO_2. This method provides the locations and capacities of candidate injection sites for both unmineable coal seams and saline aquifers. ECBM injection sites are limited to unmineable coal seams within the San Juan Basin.

In the case of oil and gas fields, the datasets from SECARB and SWP provide the locations of thousands of fields within the study area. Since including all of these fields would yield an intractable optimization problem, a method was developed to simplify the representation of injection sites at oil and gas fields. In addition, capacity data were not available for oil and gas fields in Wyoming and Central and West Texas so proxies were developed for these regions using CO_2 enhanced oil recovery (EOR) potentials developed by Advanced Resources International, Inc. (ARI) [59-61]. Specifically, ARI assesses the number of candidate reservoirs, market for purchased CO_2 and total storage capacity of reservoirs within the storage basins in the case study (Table 21).

Table 21: EOR potential by region [59-61]

Region	Number of EOR Candidate Reservoirs (n)	Market for Purchased CO_2 (Mt CO_2)	Market for Recycled CO2 (Mt CO_2)	Total CO2 Stored (Mt CO_2)
Colorado	8	116.3	238.7	355.0
Utah	10	191.4	466.8	658.2
Wyoming	53	252.1	556.4	808.5
New Mexico	19	257.2	580.8	838.1
West Texas	75	2468.1	5241.3	7709.4
Central Texas	24	294.9	608.7	903.6
East Texas	13	605.4	1317.6	1923.0
Gulf Coast Texas	91	819.1	1794.5	2613.5

For regions in which capacity data were available (i.e., Colorado, Utah, New Mexico, East Texas, and Gulf Coast Texas), an injection site was placed in the *n*-largest (by storage capacity) oil reservoirs within the region, where *n* is the number of EOR candidate reservoirs determined by ARI (Table 21). For example, in Colorado, candidate injection sites were placed in the eight oil reservoirs with the largest storage capacities. In addition, in regions that distinguish gas from oil reservoirs (Colorado and New Mexico), all gas reservoirs within the same range of storage capacities were selected. In Gulf Coast Texas, the number of EOR candidate reservoirs is still very large so the number of candidate injection sites was further reduced by aggregating the 91 sites into 23 spatially distributed sites. For regions in which capacity data were not available (i.e., Wyoming and West and Central Texas), candidate injection sites were placed in the ten largest (by area) reservoirs and capacities were assigned by uniformly distributing the total storage capacities identified by ARI (Table 21) over the ten sites. For example, in Wyoming, each candidate site was assigned a value of 81 Mt CO_2.

The effective storage capacity associated with CO_2 EOR was also estimated by region based on the market for purchased CO_2 provided by ARI (Table 21). Figure 22 indicates that greater than 90% of potential CO_2 storage capacity within the study region is contained in saline aquifers. Storage associated with EOR was not modeled in this study since it occupies less than one percent of regional storage capacity and presents several modeling issues (e.g., accounting for the diminishing demand for fresh CO_2 and increasing reliance on recycled CO_2).

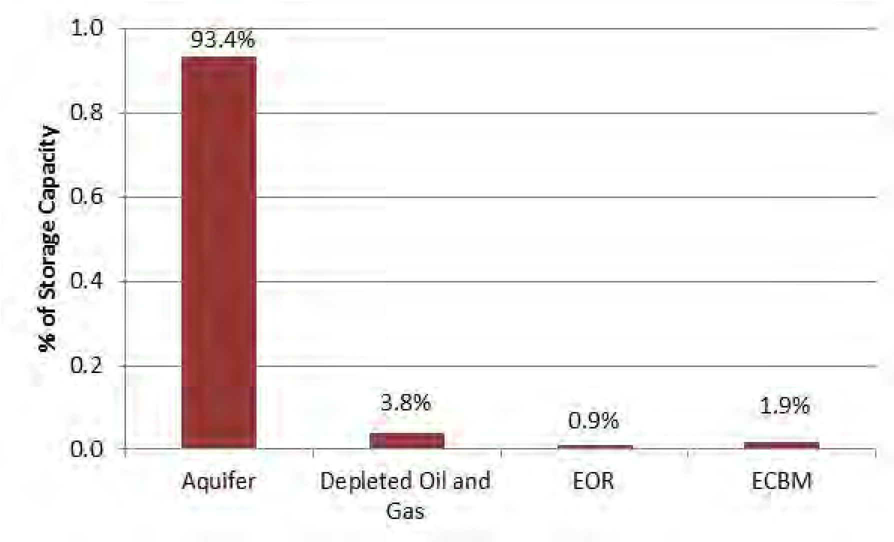

Figure 22: Percent of total CO_2 storage capacity by reservoir type

It should also be noted that offshore CO_2 storage is not considered in this study since there is sufficient onshore storage capacity within the southwestern U.S. In addition, in each deployment phase, the model must develop sufficient storage capacity to store fifty years of CO_2 emissions from the selected CO_2 sources. The inputs to the optimization model include a list of all potential injection sites, their types, and their associated storage capacities (Q^r). The characteristics and locations of candidate injection sites used in this case study are summarized in Table 22 and Figure 23, respectively.

Table 22: Characteristics of candidate injection sites in the study region

Reservoir Type	Number of Candidate Injection Sites	Size Range (Mt CO_2 storage capacity per site)	Total Storage Capacity (Gt CO_2)
Saline Aquifer	208	0.4 – 35373	496.6
Depleted Oil and Gas	112	10.8 - 867	19.9
Unmineable Coal Seams	7	1486	10.4
Total	327	0.4 – 35373	526.9

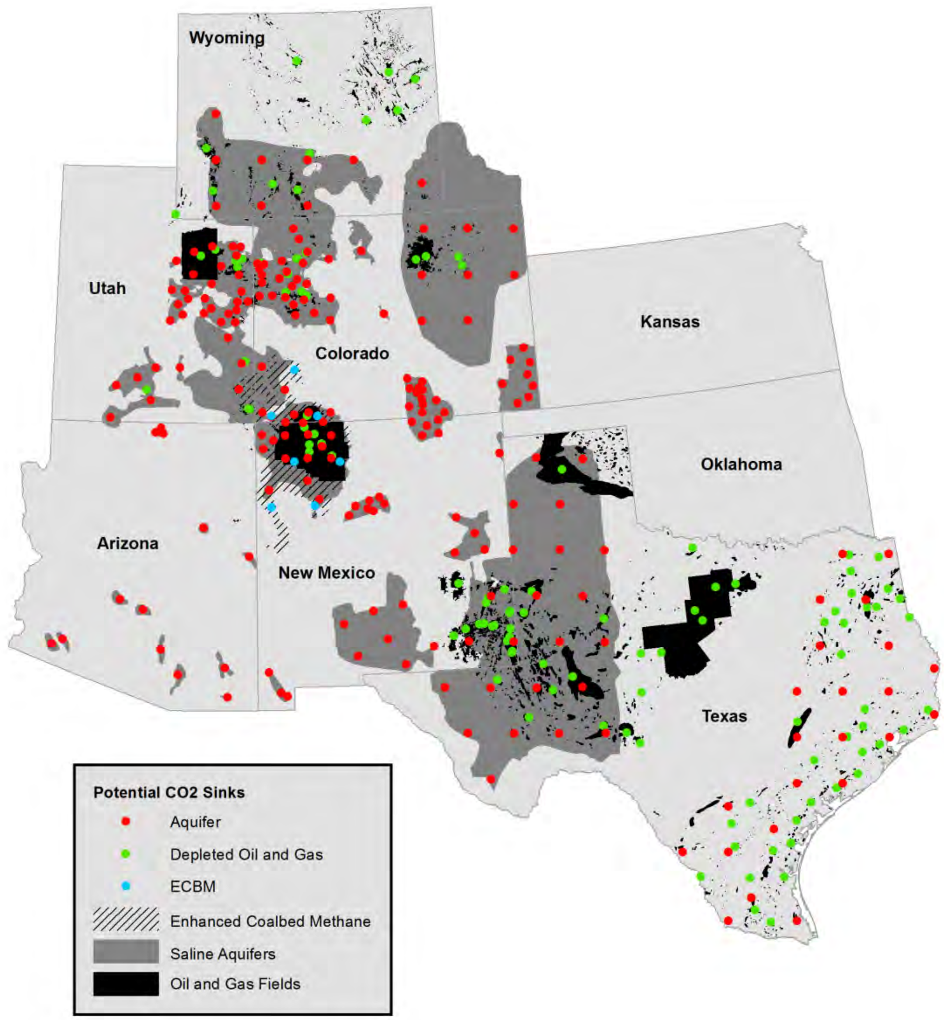

Figure 23: Locations and types of candidate injection sites in the study region

3.3.2.2 Economic Inputs

In addition to spatial inputs, the model also requires economic inputs regarding the costs associated with CO_2 capture, transport, and storage. This section describes how these inputs were developed for the candidate infrastructure within the southwestern U.S.

CO_2 Capture

CO_2 capture costs must be calculated for each individual point source within the study area. Even though the CO_2 flows in the model are based on the quantity of CO_2 captured, we chose to use \$/tCO_2 avoided (rather than \$/tCO_2 captured) to represent the costs of capture at each source since emitters will receive credits for the quantity of CO_2 avoided, not captured. Thus, the avoided cost better represents the trade-offs between plants[5].

In the case of power plants, it is assumed that existing coal-fired power plants are replaced with new Integrated Gasification Combined Cycle (IGCC) plants with CCS while existing natural gas-fired power plants are replaced with new Natural Gas Combined Cycle (NGCC) plants with CCS[6]. In both cases, each new plant is modeled with the same net annual generation (MWh/year) as the replaced plant. The costs of new IGCC plants with CCS are modeled using the equations provided in section 3.1.1.3 and assuming a capacity factor of 75% and coal cost of \$1.7/GJ.

The costs of new NGCC plants with CCS are modeled using the equations in section 3.1.1.4 given the assumption that the capacity factor of the new plant matches the capacity factor of the original plant. Since many NGCC plants are used to manage peak loads, this assumption ensures that new plants continue to provide the same service as the replaced plant (e.g., peaking or baseload). Peaking plants with low capacity factors will generally have higher capture costs and,

---

[5] Since the \$/tCO_2 avoided value is multiplied by the total CO_2 captured, the lifetime cost of CCS deployment calculated by the model will be incorrect. However, to select the best sites for capture, it is more important that the cost trade-offs between plants are accurately represented in the model using the avoided cost of capture. The real cost of CCS deployment can be calculated in techno-economic models after the optimization is complete.

[6] The conversion of existing coal-fired power plants to natural gas-fired power plants is not considered in this study. However, it should be noted that such a conversion could achieve low capture costs as a result of lower CO_2 emissions associated with the use of natural gas.

thus, will not be selected for replacement before plants with more cost-effective CO_2 capture. The cost of natural gas is assumed to be \$4.5/GJ. For both coal- and natural gas-fired power plants, a low capital recovery factor of 7.5% is used since it is assumed that new power plants will be built by public or regulated utilities with a discount rate of 7% and 40 year project life.

The replaced plant acts as the reference plant in the calculation of the avoided cost of CO_2 capture (equation 46). Since the eGRID database does not provide the cost of electricity associated with each existing facility, the costs of replaced coal plants are calculated using the equations for supercritical pulverized coal plants without CCS (section 3.1.1.1) and the costs of replaced natural gas plants are estimated using the equations for NGCC plants without CCS (section 3.1.1.4). The costs of electricity for replaced plants are calculated with the capacity factor reported for each plant in eGRID [39]. CO_2 emissions for existing (reference) plants are provided by eGRID while emissions for new plants with CCS are calculated using the Integrated Environmental Control Model (IECM) [47] and assuming a CO_2 capture efficiency of 90%. For IGCC plants with CCS, the CO_2 emissions rate is estimated to be 0.091 tCO_2/MWh with 0.990 tCO_2/MWh captured. For NGCC plants, the rate is estimated to be 0.047 tCO_2/MWh with 0.430 tCO_2/MWh captured.

By using the existing plant as the reference plant in equation 46, a site-specific CO_2 capture cost (\$/tCO_2 avoided) can be calculated that accounts for not only the reduction in CO_2 emissions attributed to capture equipment, but also reductions resulting from improved plant efficiency and/or capacity factor. For example, a relatively low capture cost can be achieved when an old coal plant with low efficiency (i.e., high tCO_2/MWh) and a low capacity factor (i.e., high COE) is replaced with a modern plant with CCS and a higher capacity factor[7]. By using this method, a broad range of capture costs are identified within the study area (Table 23). However, the histograms in Figure 24 indicate that most plants fall within a narrower range (\$30-50/tCO_2 avoided for IGCC and \$40-120/tCO_2 avoided for NGCC). Low capacity factors are responsible for the high end of the capture cost range for NGCC power plants.

Table 23: Range of site-specific CO_2 capture costs for power plants with CCS in the study area (CRF = 7.5%)

Plant type	Size Range (MtCO_2 captured/yr)	\$/tCO_2 avoided
IGCC Power – new build (75% capacity factor)	1.1 to 19.5	27 to 52
NGCC Power – new build (same capacity factor as replaced)	0.1 to 2.9	29 to 259

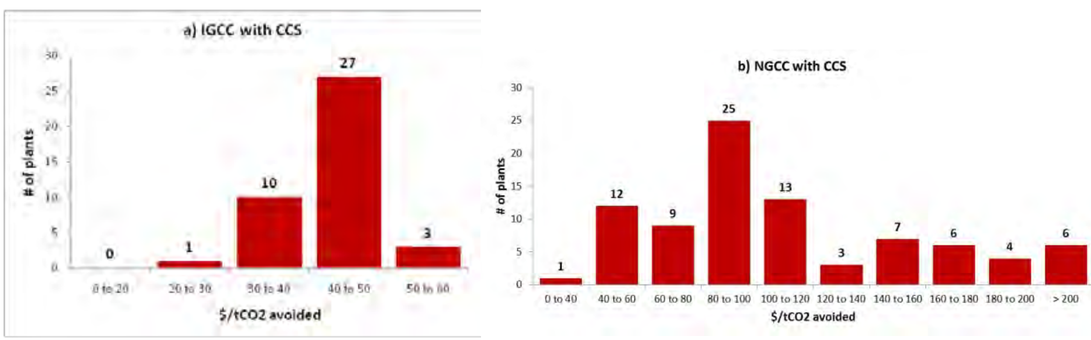

Figure 24: Histograms of capture costs for a) IGCC plants with CCS and b) NGCC plants with CCS

The avoided cost of capture for industrial facilities is calculated based on the size of the capture unit (tonnes CO_2 captured) using the equations provided in section 3.1.2. It is assumed that capture equipment is installed as a retrofit to existing facilities. For each refinery, the total CO_2 captured is calculated by assuming that approximately 50% of total CO_2 emissions can be captured from large flue gas sources with a CO_2 removal efficiency of 90% [50]. For cement

---

[7] Since this model estimates COE for old plants based on equations for new supercritical pulverized coal plants, it may overestimate the COE for older plants for which the COE is determined by only O&M costs. Ideally, the real COE of candidate sites would be known, which would allow for a more accurate calculation of the avoided cost of CO_2 at each site.

plants, it is assumed that approximately 85% of total CO_2 emissions are captured [52]. For ethanol and ammonia plants, capture costs are much smaller since the CO_2 only has to be compressed and dehydrated prior to pipeline transport. It is assumed that approximately 90% of ethanol plant emissions can be captured while only 30% of ammonia plant emissions are captured with the remainder being used to produce urea [49]. In estimating the capture cost, it is assumed that industrial facilities are operated by private corporations with a relatively high capital recovery factor of 16.3% (i.e., discount rate of 10% and project lifetime of 10 years).

The ranges of industrial plant sizes and capture costs are provide in Table 24. Note that the quantity of CO_2 captured is typically smaller for industrial plants than power plants, which results in poor economies-of scale. This is especially evident in ethanol and ammonia plants, which do not require expensive capture equipment, but still have moderate capture costs since the quantity of CO_2 captured is small.

Table 24: Range of site-specific CO_2 capture costs for industrial plants with CCS in the study area (Capital Charge = 16.3%)

Plant type	Size Range ($MtCO_2$ captured/yr)	$/t$CO_2$ avoided
Refinery	0.1 to 2.5	105 to 223
Cement Plant	0.1 to 2.6	109 to 180
Ethanol Plant	0.02 to 0.5	20 to 82
Ammonia Plant	0.04 to 0.15	49 to 58

Learning rates are used to account for decreasing capture costs over time. The learning rate is the percentage cost reduction for each doubling of the cumulative installed capacity. The learning rates for power plants are based on Rubin et al. [48] and listed in Table 25. Since refineries and cement plants both use post-combustion capture, the learning rates for NGCC with CCS are used to model learning for these industrial plants. For ammonia and ethanol plants, it is assumed that there is no learning since compression and dehydration technologies are well-established.

Table 25: Learning rates for IGCC and NGCC power plants with CCS (learning stops at 100 GW cumulative capacity) [48]

Plant type	Cumulative capacity after which learning applies (GW)	CAPEX learning rate	OPEX learning rate	COE learning rate
IGCC Power with CCS	7	0.05	0.048	0.049
NGCC Power with CCS	3	0.022	0.039	0.033

CO_2 Transport

The *CCS Deployment Model* considers only onshore CO_2 pipelines and uses as inputs the capacities ($Q^p{}_d$) and capital costs ($C^p{}_d$) of several pipeline diameter classes (d), or nominal pipe sizes. In this case study, the capital costs and pipeline capacities are provided by the Interstate Natural Gas Association of America (INGAA) [62] (Table 26). The reported pipeline capacity assumes a 90% capacity factor and a 250-km pipeline with a design pressure of 150 bar and an available pressure drop of 35 bar.

Table 26: Capacities and base installed costs of pipelines for several nominal pipe sizes

Nominal pipe size (inches)	Capacity ($MtCO_2$/year)	Capital Cost (thousand$/km)	$/t$CO_2$ (250-km, level, onshore, 90% capacity)
12.75	1.5	594	18.6
16	3	777	12.2
24	8	1,255	7.4
30	17	1,611	4.5
36	24	1,984	3.9
42	35	2,374	3.2

It is assumed that CO_2 pipelines will be built by private corporations and, thus, a high capital recovery factor of 16.3% is used. Booster compressors are not explicitly modeled in this study, but the cost of booster compression is included in the annual O&M cost, which is assumed to be

2.5% of capital expenditure. The levelized cost of CO_2 for a 250-km onshore pipeline on level terrain that is operating at 90% capacity is also given in Table 26.

The base pipeline costs in Table 26 are for pipelines in rural areas with level terrain. In mountainous and populated areas, it is assumed that construction costs are doubled with construction being 50% of the total installed pipeline cost (i.e., total installed cost is 1.5 times larger). Since CO_2 transport is an established technology, learning is not expected to result in cost reductions over time (i.e., no learning rate is applied).

CO_2 Injection

The *CCS Deployment Model* requires representative injection costs (C^{inj}_t) for the three types (t) of geologic sinks considered in this study: saline aquifers, depleted oil and gas fields, and enhanced coalbed methane (ECBM) recovery. The injection costs ($/t$CO_2$ injected) are derived from models developed at the University of California at Davis and are summarized in Ogden and Johnson [13]. As CO_2 injection sites are assumed to be owned and operated by private corporations, a capital recovery factor of 16.3% is used in these calculations. In addition, a learning rate is not applied to CO_2 injection costs since most technologies associated with CO_2 injection (e.g., well drilling) are well-established.

Given the \$/tCO_2 injected values, a CO_2 loss rate (as a percentage of CO_2 injected) is estimated for each sink type to estimate the \$/tCO_2 avoided. This rate accounts for any CO_2 emissions associated with the energy requirements for injection, fossil fuel production, and/or CO_2 recycling as well as any CO_2 leakage at the injection site. The CO_2 emitted in association with injection is important because it also impacts the avoided cost of CO_2 for all upstream components since credits will only be given for CO_2 permanently sequestered. For example, if 10% of the CO_2 injected is "lost", the avoided cost of capturing, transporting, and storing that CO_2 increases by ~11%, which should discourage the use of sinks with large CO_2 loss rates. By incorporating these upstream impacts into the injection cost, the trade-offs between different sink types are better represented. Equation 88 estimates the \$/tCO_2 avoided for each sink type *t*, given the \$/tCO_2 injected ($C^{inj}{}_{t,stored}$) for each sink type, representative capture and transport costs (C^{capt}; \$/tCO_2 captured and C^{tran}; \$/tCO_2 transported), and the CO_2 loss rate ($CO2^{loss}{}_t$) for each sink type.

88 $$C_t^{inj} = C_{t,stored}^{inj} + (C_{t,stored}^{inj} + C^{capt} + C^{tran})\left[\frac{1}{CO2_t^{loss}} - 1\right]$$

Using this equation, the avoided cost of injection is dependent on the magnitudes of the capture and injection costs, which suggests that the injection cost depends on the facility to which the sink is connected. However, since the model requires a single injection cost for each source type, representative capture and transport costs were estimated for C^{capt} and C^{tran}. Specifically, we used the average capture and transport costs for a model run in which CO_2 emissions in the power and industrial sectors are reduced by 30%. In this scenario, the average capture cost of selected facilities (C^{capt}) is \$35/tCO_2 and the average transport cost (C^{tran}) is \$4/tCO_2.

There is very little information in the literature on the life cycle CO_2 emissions associated with CO_2 injection. Consequently, it is difficult to quantify the CO_2 loss rate associated with different sink types. In the case of saline aquifers and depleted oil and gas fields, we assume that CO_2 leakage is negligible, but that additional energy is required to compress CO_2 for storage, which represents a CO_2 loss rate of ~2%. For ECBM sites, we assume that the CO_2 loss rate is the same as the value reported by Jaramillo et al. [63] for crude oil production at enhanced oil recovery (EOR) sites. This paper estimates that CO_2-equivalent emissions from the production of crude oil and management of CO_2 (i.e., injection and recycling) at EOR sites represents about 25% of the CO_2 purchased. Consequently, the CO_2 loss rate for ECBM and EOR sites is substantially larger than that for injection into saline aquifers or depleted oil and gas fields. The CO_2 loss rates used in this project are very rough estimates and more research is needed to quantify the life cycle CO_2 emissions associated with CO_2 injection. However, this preliminary analysis indicates the potentially large cost penalties associated with CO_2 losses at injection sites.

It is assumed that the costs for saline aquifers and depleted oil and gas fields are identical. The model for injection into these sink types includes costs for well drilling, injection equipment, site characterization, O&M, monitoring, land, mineral rights, and permitting. The model indicates that the cost varies from \$3-4/tCO_2 injected. A CO_2 loss rate of 2% applied to all upstream components according to equation 88 increases the cost by ~\$1/tCO_2. Thus, the avoided cost of CO_2 injection for saline aquifers and depleted oil and gas fields is set at \$5/tCO_2 avoided. However, it should be noted that at very low CO_2 injection rates (<500 tCO_2/day), the costs can be significantly higher.

The model for ECBM includes costs for well drilling, injection and production equipment, O&M, water disposal, gas processing, monitoring, land, mineral rights, and permitting. Since ECBM sites within the study area are limited to the San Juan Basin, reservoir characteristics from this basin are used in the analysis [64]. The model also includes revenue from the sale of produced gas and, consequently, the injection cost is highly sensitive to the wellhead gas price. Assuming a wellhead gas price of \$4/GJ, the cost of injection is about -\$10/tCO_2 injected (i.e., ECBM operators would be willing to pay about \$10/tCO_2). However, the large CO_2 loss rate of 25% adds about \$13/tCO_2 to the cost. Consequently, the ECBM injection cost is set at \$3/tCO_2

avoided, which represents a slight cost advantage over injection into aquifers or depleted oil and gas fields. Injection costs for the three sink types are summarized in Table 27.

Table 27: Injection costs for geologic sinks

Sink type	$/t$CO_2$ avoided
Saline Aquifer	5
Depleted Oil and Gas Field	5
Enhanced Coalbed Methane (ECBM)	3

3.3.3 Model Results

Given the spatial and techno-economic inputs, the *CCS Deployment Model* is employed at each deployment phase in succession from Tranche 1 to 2050 (Table 20). Each model run results in an optimized infrastructure design for either meeting an installed capacity target (Phases 1 and 2) or CO_2 reduction target (2030 – 2050). Together, the six model runs provide a long-term deployment strategy for CCS deployment in the southwestern United States under the American Power Act (APA). This section highlights the results of the case study, including infrastructure design, costs, and CO_2 storage requirements under the two storage capacity scenarios described in section. Full results are presented for the “Base Capacity” scenario and then the main insights provided by the “Low Capacity” scenario are discussed.

3.3.3.1 Infrastructure Design

In the “Base Capacity” scenario, the CO_2 sinks are assumed to have the full storage capacities reported by SWP and SECARB and described in section 3.3.2.1. The *CCS Deployment Model* provides a detailed inventory of infrastructure requirements for each deployment phase. In this section, these inventories are combined with maps to describe the optimal CCS deployment strategy under the APA. A legend for the maps in this section is given in Figure 25.

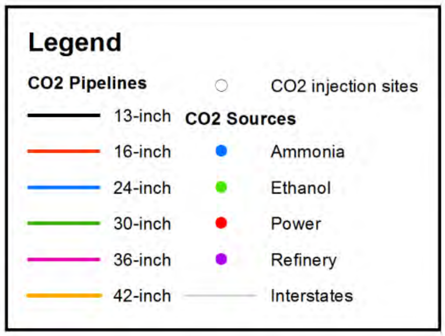

Figure 25: Map legend for CCS infrastructure design figures

Phase 1 – Tranche 1

In the first tranche of Phase 1, the APA proposes a bonus allowance (i.e., subsidy) of \$106/tCO_2 avoided for the first 10 GW of power plant capacity built in the United States with CCS. Assuming that the bonuses are allocated to the southwestern U.S. according to the fraction of total national power capacity contained within the region (~16.4%), the first tranche of bonuses would apply to the first 1.64 GW of power plant capacity built in the southwestern U.S. Essentially, very large subsidies are offered for early CCS demonstration projects in the power sector.

Given that tranche 1 applies to only 1.64 GW of power capacity, only three power plants with CCS are built in 2016 (Figure 26). One of the plants is an independent IGCC power plant with a dedicated pipeline and injection site in Texas. However, the other two IGCC power plants share an integrated disposal network, which accesses three separate injection sites (Table 28). The CO_2 injection site in Texas accesses a saline aquifer while the injection sites in Colorado access two depleted oil and gas reservoirs and one saline aquifer. This design suggests that limited storage capacity in Colorado provides incentive to share disposal among multiple sources.

About 240 km of pipeline are built in the entire region, or ~80 km per capture facility. The CCS equipment installed during the first tranche avoids approximately 11 Mt CO_2 per year, which is a reduction of ~2.2% from the total current emissions of the candidate sources in the region.

Figure 26: CCS infrastructure design in Phase 1 – Tranche 1

Table 28: Summary of capture and storage facilities built in Phase 1 – Tranche 1

CO_2 Sources	Number of Facilities	Net Generating Capacity (GW)	Total CO_2 Avoided (Mt CO_2/year)
IGCC with CCS	3	1.64	10.9
NGCC with CCS	0	0	0
Refinery	0	N/A	0
Cement	0	N/A	0
Ammonia	0	N/A	0
Ethanol	0	N/A	0
Total	3	1.64	10.9
CO_2 Sinks	Number of Injection Sites	Total CO_2 Storage Capacity (Mt CO_2)	
Saline Aquifers	2	591	
Depleted Oil and Gas	2	416	
ECBM	0	0	
Total	4	1007	

Phase 1 – Tranche 2

In the second tranche, a bonus allowance of $85/t$CO_2$ avoided is provided for another 10 GW of installed power plant capacity with CCS in the U.S. This translates to another 1.64 GW of capacity in the southwestern U.S., which is installed at two new IGCC plants and one new NGCC plant (Table 29). The NGCC plant and one of the new IGCC plants connect to the existing disposal networks in Texas and Colorado (Figure 27). Although relatively long pipelines are required to make these connections, no new injections sites are required on pre-existing networks. However, a new disposal network also develops in Arizona and New Mexico to connect a new IGCC plant to an injection site in New Mexico via a dedicated and relatively long pipeline.

The construction of long pipelines in this phase results from the model having access to candidate sites with low avoided costs of capture. These “low hanging fruit” have sufficiently low capture costs that they are still selected despite transport costs as high as $17/t$CO_2$. The total pipeline length increases to ~780 km and the average length per capture facility is about 130 km. The CCS equipment installed during the first two tranches avoids approximately 21 Mt

CO_2 per year, which is a reduction of ~4.3% from the total current emissions of the candidate sources in the region.

Figure 27: CCS infrastructure design in Phase 1 – Tranche 2

Table 29: Summary of capture and storage facilities built in Phase 1 – Tranche 2

CO_2 Sources	Number of Facilities	Net Generating Capacity (GW)	Total CO_2 Avoided (Mt CO_2/year)
IGCC with CCS	5	2.98	19.6
NGCC with CCS	1	0.28	1.5
Refinery	0	N/A	0
Cement	0	N/A	0
Ammonia	0	N/A	0
Ethanol	0	N/A	0
Total	6	3.26	21.1
CO_2 Sinks	Number of Injection Sites	Total CO_2 Storage Capacity (Mt CO_2)	
Saline Aquifers	3	789	
Depleted Oil and Gas	2	416	
ECBM	0	0	
Total	5	1205	

Phase 2

In Phase 2, bonus allowances are provided based on a reverse auction for an additional 52 GW of power plant capacity with CCS nationally (8.5 GW in the study region). A reverse auction means that the lowest cost CCS projects receive subsidies. The definition of this bonus allowance in the APA is unclear so we have assumed that the bonus allowance would cover the difference between the total avoided cost of CO_2 and the clearing (i.e., minimum) price of CO_2 on the proposed carbon market. In essence, the subsidy would ensure that these plants would breakeven at the defined clearing price and derive economic benefits if the CO_2 price is larger. A more detailed explanation of this calculation will be provided in the section on the costs of CCS deployment.

In Phase 2, the total installed capacity of power plants with CCS approximately triples from 3.28 GW to 11.8 GW. As a result, ten additional power plants are built, including nine new IGCC plants and one new NGCC plant (Table 30). As the remaining candidate power plants have larger capture costs, most plants in this phase are built close to CO_2 sinks and have dedicated disposal networks (Figure 28). However, the regional disposal network in Colorado does expand to serve an additional CO_2 source. The total pipeline length increases to ~1700 km, but the average length per capture facility declines to 107 km as more plants are built in close proximity to sinks. The CCS installations supported by subsidies under the APA avoid approximately 72 Mt CO_2 per year, which is a reduction of ~15% from the total current emissions of the candidate sources in the region.

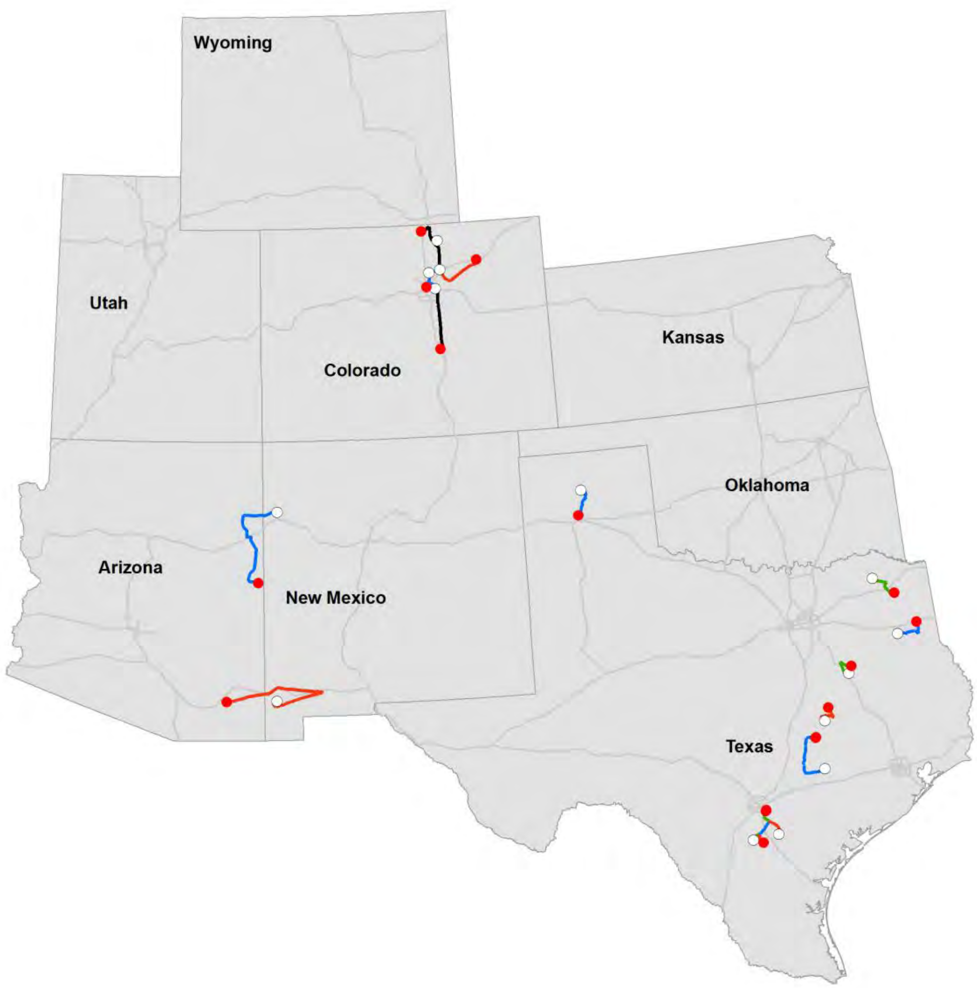

Figure 28: CCS infrastructure design in Phase 2

Table 30: Summary of capture and storage facilities built in Phase 2

CO_2 Sources	Number of Facilities	Net Generating Capacity (GW)	Total CO_2 Avoided (Mt CO_2/year)
IGCC with CCS	14	10.5	68.5
NGCC with CCS	2	1.3	3.4
Refinery	0	N/A	0
Cement	0	N/A	0
Ammonia	0	N/A	0
Ethanol	0	N/A	0
Total	16	11.8	71.9
CO_2 Sinks	Number of Injection Sites	Total CO_2 Storage Capacity (Mt CO_2)	
Saline Aquifers	9	31127	
Depleted Oil and Gas	5	1829	
ECBM	0	0	
Total	14	32956	

30% reduction by 2030

In this phase, it is assumed that the sources included in this study must reduce their total CO_2 emissions by 30% by 2030. Unlike in the previous deployment phases, the model now considers the potential for retrofitting CO_2 sources in the industrial sector. However, only two industrial plants are retrofit in this phase, including one ethanol plant and one ammonia plant (Table 31). Although these plants have very low capture costs since they only require dehydration and compression of CO_2, they also tend to have high transport and disposal costs since they produce small quantities of CO_2. Figure 29 suggests that these plants are selected because they are either located very close to a sink (e.g., the ethanol plant) or piggyback off existing infrastructure for nearby power plants (e.g., the ammonia plant).

Aside from these two industrial retrofits, the remaining CO_2 reduction is achieved by replacing old coal-fired power plants with new IGCC plants with capture. Several integrated disposal networks serving multiple sources are built, but the majority of these networks are small and localized. In addition, this phase highlights the impacts of limited local storage capacity in the development of a long distance network in Arizona and the connection of single sources in Utah to multiple injection sites. As more sources share disposal infrastructure, the average pipeline length per capture site declines to 94 km. The CCS installations avoid approximately 143 Mt CO_2 per year, which achieves the target reduction of 30% stipulated in this phase.

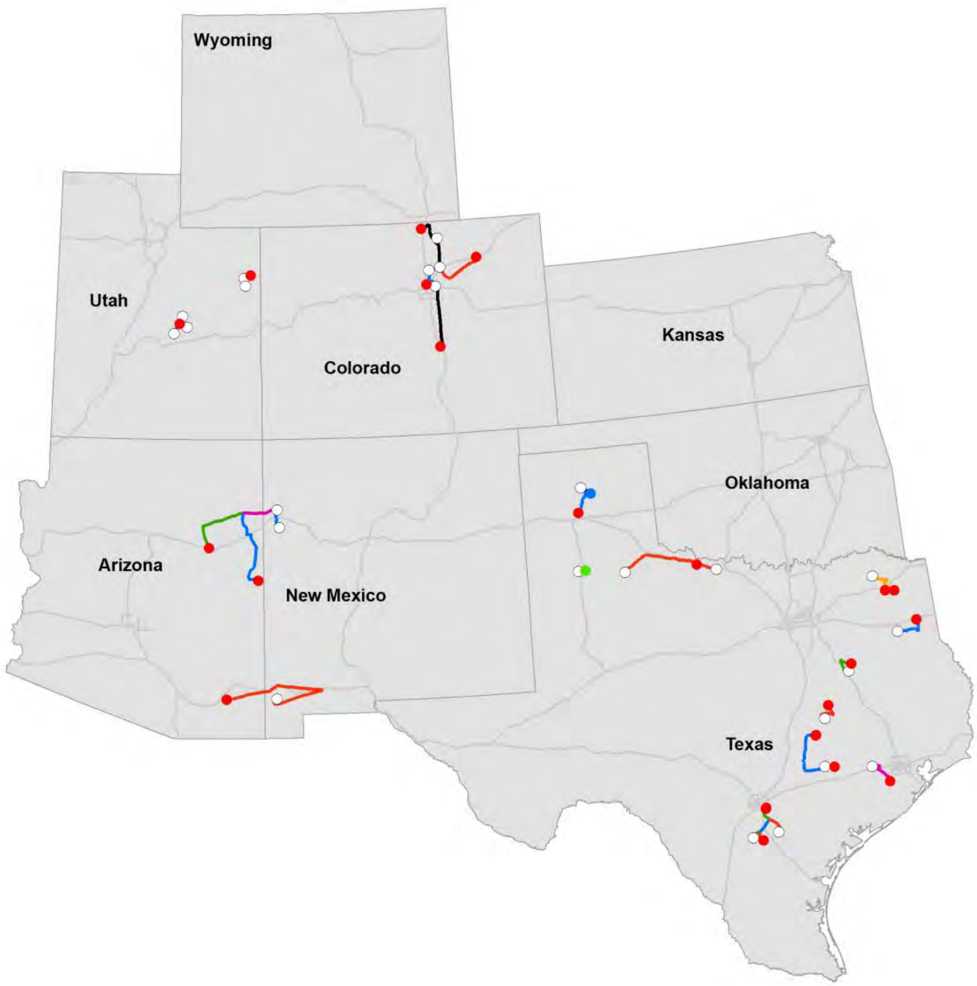

Figure 29: CCS infrastructure design in 2030

Table 31: Summary of capture and storage facilities built in 2030

CO_2 Sources	Number of Facilities	Net Generating Capacity (GW)	Total CO_2 Avoided (Mt CO_2/year)
IGCC with CCS	21	22.3	138.9
NGCC with CCS	2	1.3	3.4
Refinery	0	N/A	0
Cement	0	N/A	0
Ammonia	1	N/A	0.1
Ethanol	1	N/A	0.4
Total	25	23.6	142.9
CO_2 Sinks	Number of Injection Sites	Total CO_2 Storage Capacity (Mt CO_2)	
Saline Aquifers	16	56657	
Depleted Oil and Gas	7	1964	
ECBM	1	1485	
Total	24	60107	

60% reduction by 2040

In this phase, the *CCS Deployment Model* estimates the lowest-cost CCS infrastructure for meeting a 60% reduction in CO_2 emissions by 2040. Replacement of pulverized coal plants with IGCC plants with CCS continue to provide the most cost effective option for reducing CO_2 emissions, with approximately 45 GW of capacity at 36 plants built by 2040 (Table 32). In contrast, only about 2 GW of NGCC capacity is built and only two industrial plants are retrofitted.

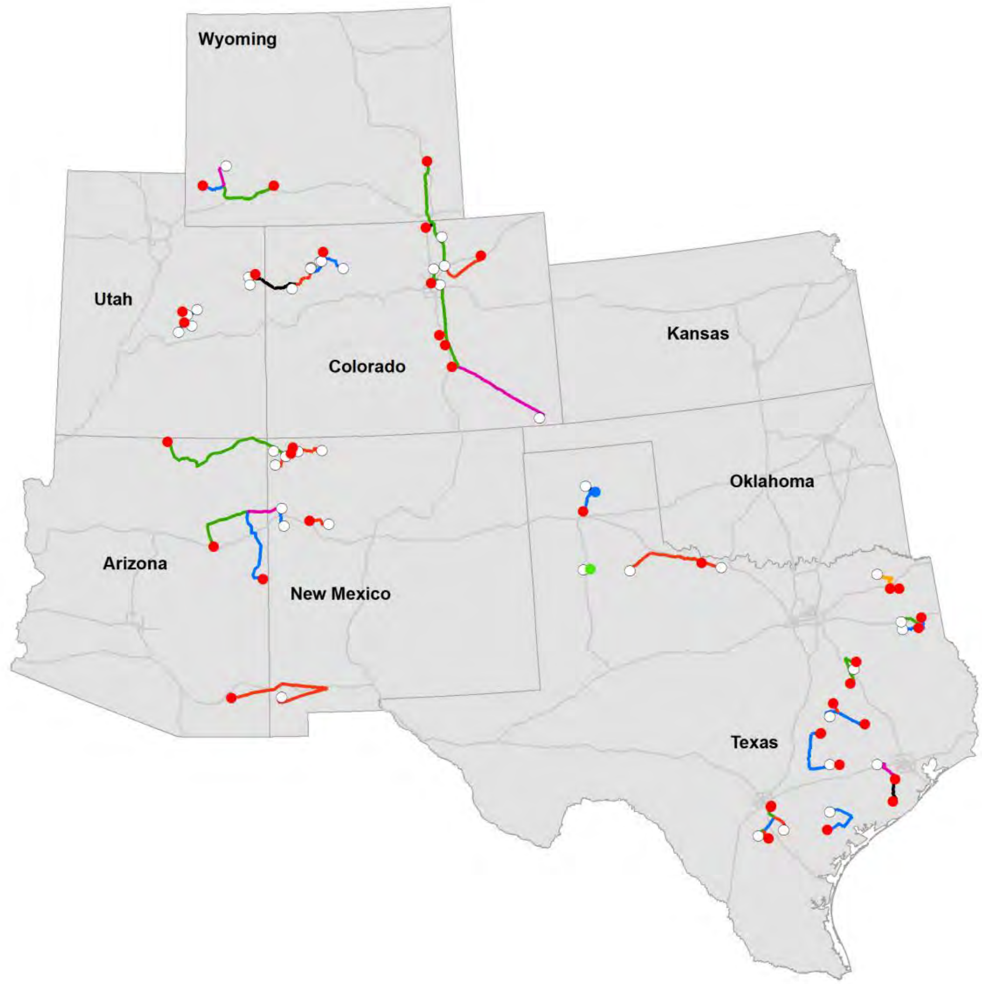

Figure 30: CCS infrastructure design in 2040

In the northern and western portions of the study area where CO_2 storage capacity is more limited, several integrated regional disposal networks develop (Figure 30). However, in Texas, which has abundant storage capacity, integrated disposal networks do develop, but they tend to be smaller. The majority of storage capacity is provided by saline aquifers with ECBM sites providing more installed capacity than depleted oil and gas fields (Table 32). About 4300 km of CO_2 pipeline are built and the average length per capture site remains around 100 km. The CCS installations avoid approximately 279 Mt CO_2 per year, or about 57% of the total current emissions of the plants considered in this study.

Table 32: Summary of capture and storage facilities built in 2040

CO_2 Sources	Number of Facilities	Net Generating Capacity (GW)	Total CO_2 Avoided (Mt CO_2/year)
IGCC with CCS	36	44.6	272.8
NGCC with CCS	3	1.9	5.4
Refinery	0	N/A	0
Cement	0	N/A	0
Ammonia	1	N/A	0.1
Ethanol	1	N/A	0.4
Total	41	46.5	278.7
CO_2 Sinks	**Number of Injection Sites**	**Total CO_2 Storage Capacity (Mt CO_2)**	
Saline Aquifers	29	94618	
Depleted Oil and Gas	10	2045	
ECBM	2	2971	
Total	41	99698	

80% reduction by 2050

In this phase, the *CCS Deployment Model* estimates the lowest-cost CCS infrastructure for meeting an 80% reduction in CO_2 emissions by 2050. Only one remaining pulverized coal plant can be cost-effectively converted to an IGCC plant with CCS so the model must rely on replacements of natural gas-fired power plants with NGCC plants with CCS in order to achieve the required CO_2 reduction (Table 33). In fact, almost all of the natural gas-fired power plants in the study area are converted to NGCC plants with CCS in this phase. This represents construction of about 42 GW of NGCC capacity in the span of ten years. In addition, several industrial facilities are retrofitted, including one ammonia plant, six ethanol plants, and one refinery. This finding suggests that, if CCS is the only option for reducing power and industrial CO_2 emissions, the majority of the power sector and part of the industrial sector would need to adopt CCS to achieve an 80% reduction in CO_2[8].

[8] This study assumes that all CO_2 emission reductions are achieved by CCS. In fact, other mitigation options would likely contribute to this effort (e.g., low-carbon renewable energy and efficiency improvements).

Table 33: Summary of capture and storage facilities built in 2050

CO_2 Sources	Number of Facilities	Net Generating Capacity (GW)	Total CO_2 Avoided (Mt CO_2/year)
IGCC with CCS	37	46.7	285.5
NGCC with CCS	39	43.8	73.7
Refinery	1	N/A	1.7
Cement	0	N/A	0
Ammonia	2	N/A	0.2
Ethanol	7	N/A	1.7
Total	86	90.5	362.8
CO_2 Sinks	Number of Injection Sites	Total CO_2 Storage Capacity (Mt CO_2)	
Saline Aquifers	43	219874	
Depleted Oil and Gas	17	4818	
ECBM	2	2971	
Total	62	227663	

Throughout the study area, the majority of disposal networks are now shared by multiple CO_2 sources (Figure 31). However, the networks in Texas remain compact while those in the other states are much more extensive as a result of limited storage capacity. In particular, the network that began near Denver, Colorado now extends the length of the state and into Wyoming. Because the networks are shared among multiple sources, the average pipeline length per capture site declines to 76 km. Given a maximum cost of \$110/tCO_2 avoided, the model was only able to reduce emissions by about 75% by 2050. Thus, achieving the final 5% reduction through CCS will require extremely expensive projects in the industrial sector. As a result, other mitigation options (e.g., renewable energy) will likely be needed to achieve an 80% reduction.

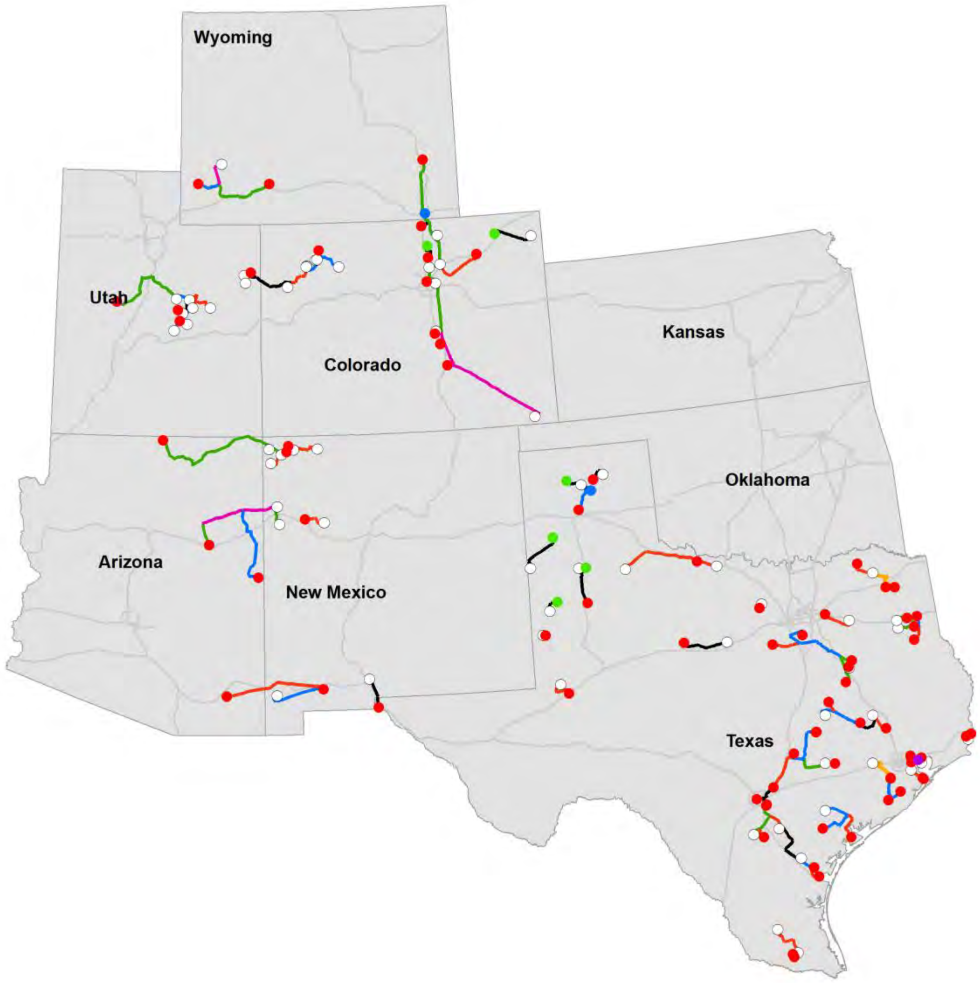

Figure 31: CCS infrastructure design in 2050

General Insights

This analysis provides several insights into the optimal deployment of CCS in a real geographic region. First, since the cost of capture is generally the largest percentage of the total CCS cost, the capture cost tends to dominate site selection in Phase 1 with sites with low capture costs initially selected even when they require long and expensive pipelines. However, from Phase 2 to 2040, the difference in capture costs between candidate sites becomes smaller and transport costs tend to dominate site selection, resulting in shorter and more integrated disposal networks. However, from 2040 to 2050, capture costs rise substantially as CCS must be applied to higher cost NGCC and industrial plants in order to achieve the stringent reduction target. As a result, capture costs again dominate the site selection process.

The second insight is the fact that replacement of pulverized coal plants with IGCC plants with CCS generally yields the lowest capture costs ($/tCO$_2$ avoided). As a result, the majority of emissions reductions through 2040 are achieved through the construction of new IGCC plants, although a few exceptionally low-cost NGCC, ethanol, and ammonia plants do adopt CCS in this time period. However, beyond 2040, CCS is adopted extensively at natural gas-fired plants in order to achieve the stringent reduction target by 2050. At carbon prices below $110/tCO$_2$ avoided, very few industrial plants and no cement plants are retrofitted.

The third insight concerns the structure of disposal networks in relation to the availability of sufficient local CO_2 storage capacity. In general, more extensive integrated CO_2 disposal networks develop in areas with limited or no availability of local storage capacity. Figure 32 illustrates the percent utilization of built injection sites in 2050 and suggests that more extensive integrated disposal networks develop to access new capacity when either: 1) local capacity has been consumed (e.g., in Colorado and Utah) or 2) local capacity is non-existent (e.g., in Arizona and Utah). Even though integrated disposal networks take longer to develop in regions with sufficient local storage capacity, the results indicate that sharing of disposal infrastructure is the dominant paradigm in most of the study area by 2050. Although plants must transport their CO_2 further to reach available storage capacity in 2050, the average pipeline length per source is small since disposal networks are shared by many plants.

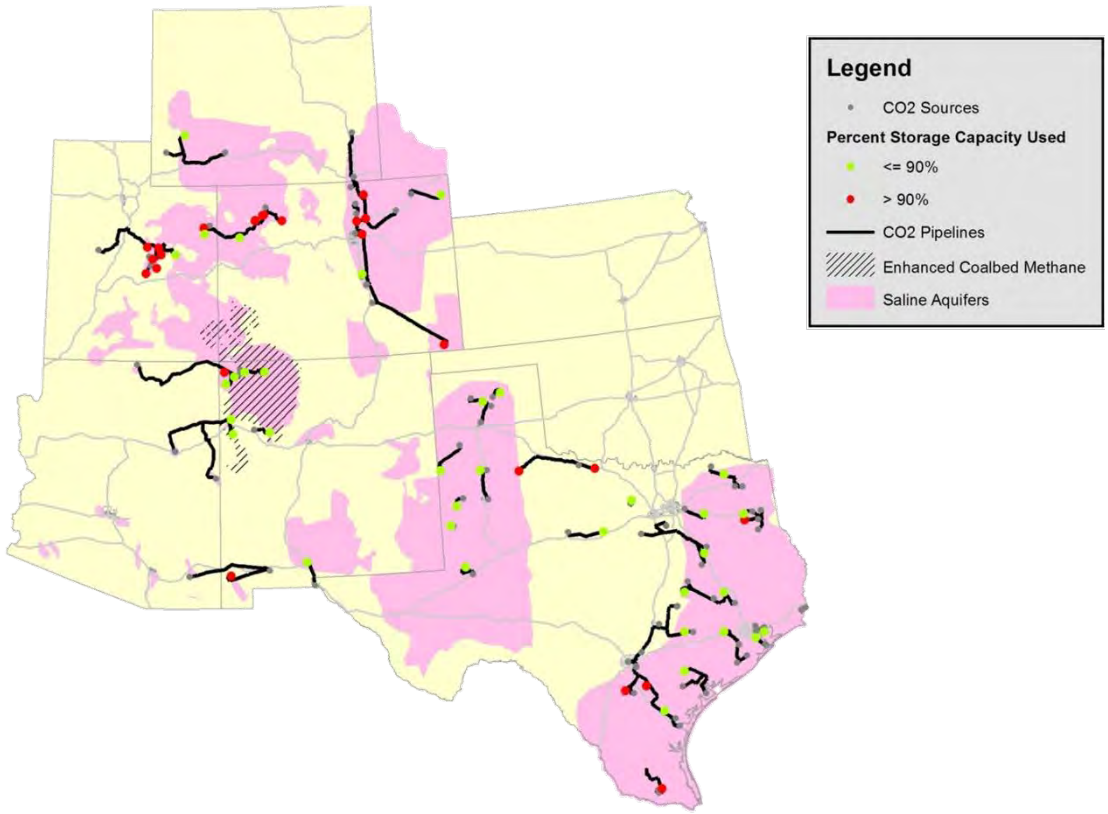

Figure 32: Storage capacity utilization of built injection sites in 2050 (Base Capacity scenario)

Finally, the results suggest that achieving an 80% reduction in CO_2 emissions by 2050 with only CCS is not possible at a carbon price below \$110/tCO_2 avoided. Reducing emissions by more than 75% would require installing CCS at sites with prohibitively large capture costs and, thus, other CO_2 mitigation options will be needed to achieve the 80% target.

3.3.3.2 System Costs

Given the optimal infrastructure design from the *CCS Deployment Model*, the inventories of CO_2 capture, transport, and storage equipment are imported to a spreadsheet model for calculating system costs. Although the model considers previously-built infrastructure in the optimization, pipelines are optimized for the flows required in each phase (i.e., pipelines are sized to meet current demands). As a result, the model assumes that pipeline diameters are increased as needed. In reality, pipelines would either need to be oversized in anticipation of future flows or parallel pipelines would be required to meet additional flow requirements. Although the *CCS Deployment Model* does not optimize the pipeline network under these conditions, they can be explored in the spreadsheet model.

The first scenario assumes that pipelines are always oversized for 2050 flow requirements. In this "Oversize 2050" scenario, results from the 2050 phase are used to size all pipelines in previous phases (e.g., pipelines built in Phase 1 – Tranche 1 are oversized for the flows modeled in the 2050 phase). The second scenario assumes that pipelines develop organically with pipelines sized for only current flows. As additional pipeline capacity is required in this "Organic Growth" scenario, parallel pipelines are built to meet this capacity. Although the routing of the pipeline networks may change if the model optimized for these scenarios, long solution times with the current model discouraged the development of a more complex model. Full results are provided for the "Organic Growth" scenario while only the main insights are provided for the "Oversize 2050" scenario.

Organic Growth Scenario

To calculate the total CO_2 abatement cost for each plant in the first three phases, it is necessary to account for the net present value (NPV) of the bonus allowance, which is received for the first ten years of plant operation. It is assumed that the bonus allowances are provided to power plant operators, which are modeled with a real discount rate of 7% and CRF of 7.5%. In the first two tranches of Phase 1, the avoided cost of CO_2 capture, including the bonus allowance, is simply the annualized NPV of bonus allowances subtracted from the avoided cost of CO_2 capture without the bonus allowance.

In Phase 2, the calculation is more complex since the bonus allowances are provided in a reverse auction. In this case, it is assumed that the bonus allowance will provide the difference between the total avoided cost of CO_2 capture, transport, and storage and the annualized NPV of paying the clearing (i.e., minimum) price of CO_2 in a carbon market for the lifetime of the plant (40 years). The APA specifies clearing and maximum CO_2 prices in 2012 as well as an annual escalation rate for these prices [56]. Thus, the avoided capture cost, including the bonus allowance, for each plant built in Phase 2 is the avoided cost of CO_2 capture, transport, and storage subtracted from the sum of the avoided cost of CO_2 capture without the bonus allowance and the total annualized NPV of paying the clearing price for the lifetime of the plant. The total CO2 abatement cost is then the sum of the avoided cost of CO_2 capture with the bonus allowance and the avoided costs of CO_2 transport and storage.

Figure 33 illustrates the average avoided cost of CO_2 for each CCS component and each deployment phase. The purple negative values represent the average value of the bonus allowances for all plants operating in each phase. Over time, this value becomes less negative as the value of bonus allowances declines and fewer plants receive bonus allowances. The average cost of CO_2 capture also declines as a result of learning until 2040. However, beyond 2040, the average capture cost increases since CCS must be installed on plants with high capture costs (e.g., natural gas power plants and industrial facilities) in order to achieve the 80% CO_2 reduction target in 2050. While the cost of CO_2 transport declines over time as the development of regional pipeline networks provides economies of scale, the injection cost remains constant as it does not benefit from economies of scale or learning in this study. Despite decreasing transport costs, the total average CO_2 abatement cost increases with time as bonus allowances expire and sources with higher capture costs install CCS in 2050. However, the negative values in Tranches 1 and 2 and the low value in Phase 2 suggest that the values of the bonus allowances are sufficient to incentivize CCS deployment.

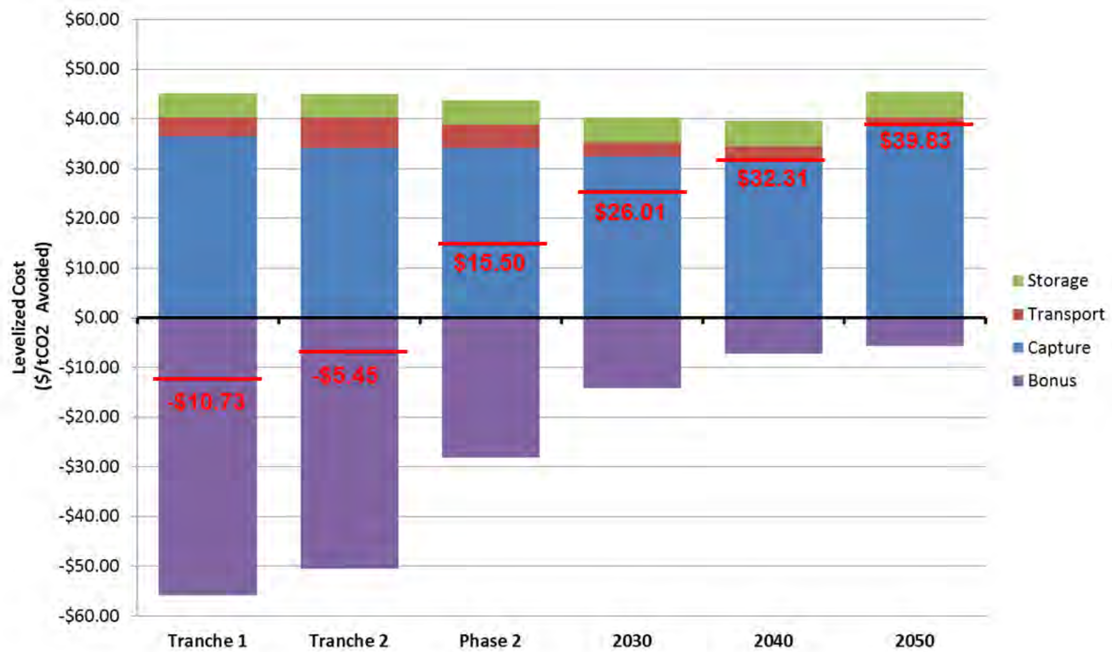

Figure 33: Average avoided cost of CO_2 for each CCS component and each deployment phase (the total average CO_2 abatement cost is labeled and marked with a line)

Given the CO_2 abatement cost for each facility, it is possible to develop a marginal abatement cost curve, which illustrates how the abatement cost increases as CO_2 emissions are reduced through CCS (Figure 34). In the study region, the analysis indicates that about 300 Mt CO_2 per year can be avoided with CCS (~62% of regional emissions from the power and industrial sectors) at a cost below ~$50/t$CO_2$ avoided. The majority of the avoided CO_2 is achieved by replacing old coal-fired power plants with new IGCC plants with CCS. Beyond 300 Mt CO_2 per year, the CO_2 abatement cost increases quickly as CCS must be adopted at natural gas-fired power plants and industrial facilities. However, it appears that about 360 Mt CO_2 per year (or ~75% of regional emissions) can be avoided for less than $114/t$CO_2$ avoided.

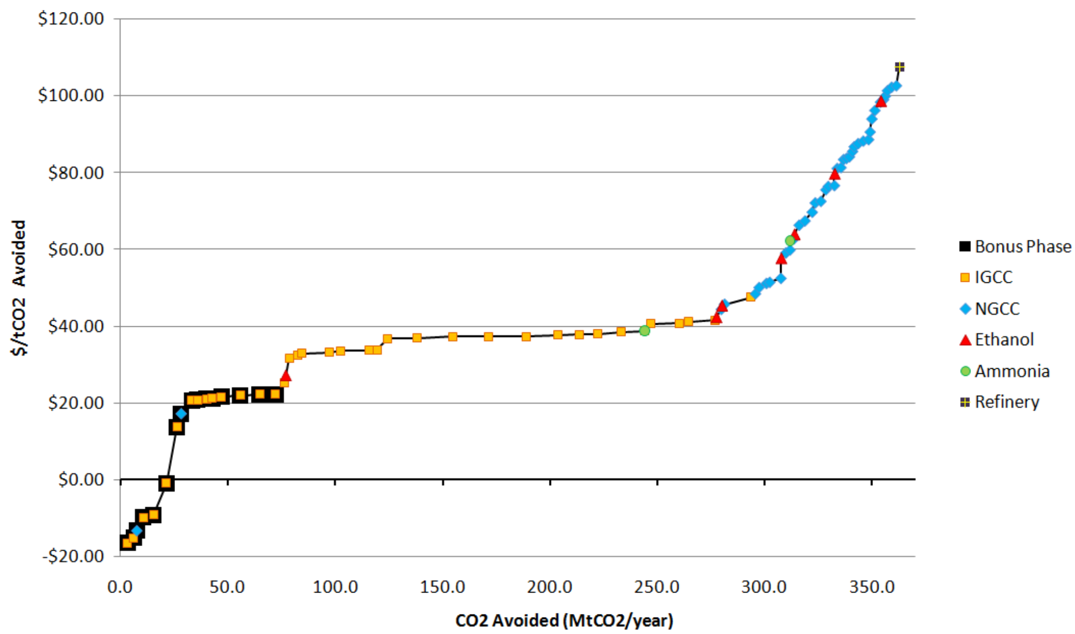

Figure 34: Marginal abatement cost curve for all CCS facilities built through 2050

Assuming establishment of a carbon market, it is possible to calculate the levelized benefit derived from installing CCS at each facility relative to the alternative of paying the CO_2 price. The APA promotes the establishment of a carbon market and specifies clearing (i.e., minimum) and maximum CO_2 prices from 2012 to 2050. In addition, the EPA has developed their own CO_2 price projection based on an analysis of the APA (Figure 35) [56]. Given these CO_2 prices, it is possible to calculate the levelized benefit of installing CCS at each facility, which is defined as the difference between the CO_2 abatement cost (including the bonus allowance if applicable) and the annualized NPV of paying the CO_2 price for the lifetime of the plant.

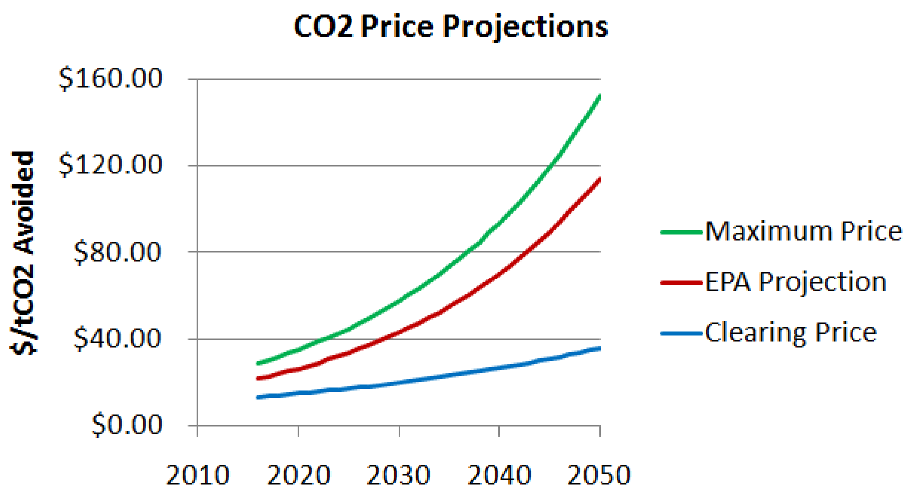

Figure 35: CO_2 price projections from the EPA and the APA [56]

Figure 36 shows the levelized benefit for each plant relative to the three CO_2 price projections. The smallest benefits are obviously derived when the clearing price is assumed, since the cost associated with emitting CO_2 is the lowest. However, even at the clearing price, the bonus allowances provided by the APA in the first three deployment phases (i.e., Tranche 1 and 2 and Phase 2) allow early adopters of CCS to derive benefits. This finding confirms that the values of the bonus allowances are sufficient to successfully promote early demonstration projects. However, beyond the incentive period, Figure 36 suggests that additional adoption of CCS will only continue if the CO_2 price is above the clearing price. For example, CO_2 prices that follow the maximum or EPA projections should incentivize continued CCS deployment. An upward jump occurs in each new deployment phase because we assume that all plants are built in the beginning of each phase and each phase occurs at a later date when the projected CO_2 price is projected to be higher. Thus, as the CO_2 price increases, the higher cost of paying for emitted CO_2 in later phases allows plants with high capture costs to become viable candidates for CCS. In fact, this analysis confirms that approximately 360 Mt CO_2 per year can be avoided with CCS by 2050 at an abatement cost less than or equal to the EPA projected CO_2 price in 2050 (~\$114/tCO_2 avoided).

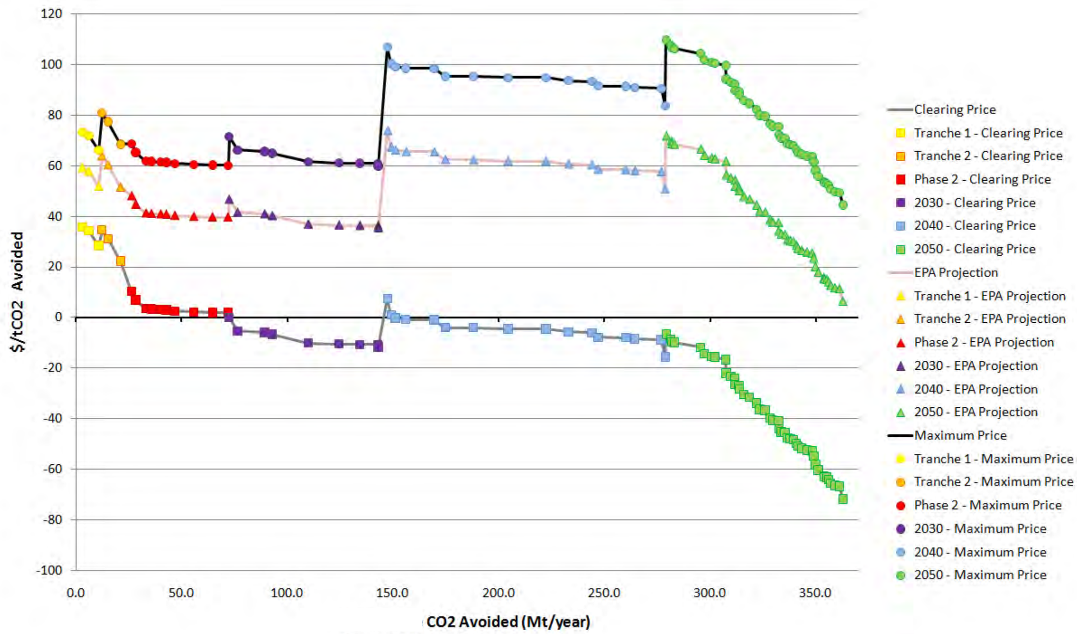

Figure 36: Levelized benefit of installing CCS relative to paying the CO_2 price for three price projections

Oversize 2050 Scenario

In the “Oversize 2050” scenario, it is assumed that pipelines are always oversized for projected flows in 2050. As a result, large investments in underutilized pipeline capacity are required in early phases. However, in later phases, the capacity of pre-existing pipelines does not need to be expanded to meet additional flow requirements, which results in lower investment costs in the long-term. This scenario is modeled to examine whether it is cheaper to oversize pipelines for future flows or to build the pipeline network for current flows and then expand it as needed like in the “Organic Growth” scenario.

In the “Oversize 2050” scenario, larger diameter pipelines are built in early phases, but ultimately less pipeline length is required than the “Organic Growth” scenario, which builds parallel pipelines to meet additional capacity requirements. The larger diameter pipelines also achieve better economies-of-scale when fully utilized, leading to lower investment costs in later phases. However, Figure 37 suggests that the cost benefits in the long-term are small relative to the additional investments required in the near-term. Comparing the NPV of the total pipeline cost in each scenario using a real discount rate of 10% provides confirmation that the “Oversize 2050” scenario does require more pipeline investment[9]. Specifically, the total cost of pipelines in the “Oversize 2050” scenario is about 12% (~$230 million) greater than the cost of pipelines in the “Organic Growth” scenario. The analysis indicates that a discount rate of 2% would be required to make oversizing the preferred deployment strategy.

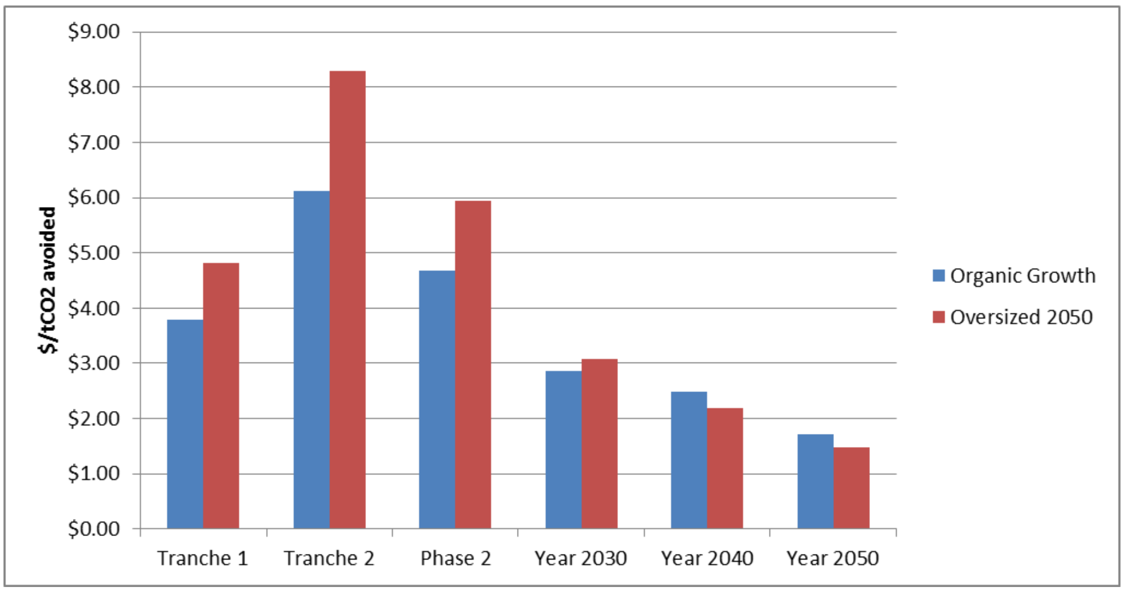

Figure 37: Levelized cost of CO_2 transport for each scenario and deployment phase

[9] This analysis compares only two pipeline strategies. It is possible that other strategies that were not examined may provide the lowest cost (e.g., pipelines that are oversized for near-term projected flows (e.g., 10 years))

3.3.3.3 Low Capacity Scenario

In the “Low Capacity” scenario, it is assumed that CO_2 storage capacity in saline aquifers is only 10% of the reported value. This scenario provides insight into how CCS infrastructure design and cost are impacted when regional storage capacity is more limited. Figure 38 compares the design of CCS infrastructure in 2050 for both the “Low Capacity” and “Base Capacity” scenarios. Given lower storage capacities, more extensive CO_2 pipeline networks are required to access additional injection sites. In addition, the need to transport CO_2 longer distances incentivizes the development of more integrated regional disposal networks. In the “Low Capacity” scenario, nearly all facilities are members of large regional disposal networks serving multiple CO_2 sources and sinks.

Figure 39 illustrates storage capacity utilization at built injection sites and suggests that large integrated regional disposal networks develop in areas with poor local storage availability, which is indicated by high utilization of local capacity. These areas require extensive networks to access new storage capacity. An example is the pipeline through Colorado that extends almost the extent of the study area from north to south. The CO_2 sources built in Wyoming and Colorado exhaust their local storage capacity and are forced to transport their CO_2 further and further south to access new capacity. As expected, the total length of CO_2 pipelines in the “Low Capacity” scenario is 30-50% larger in later deployment phases as local storage capacity becomes exhausted (Figure 40). In comparison to the “Base Capacity” scenario, the additional length of pipeline translates to a 30-75% increase in the average transport cost and a 3-10% increase in the average total abatement cost (Figure 41).

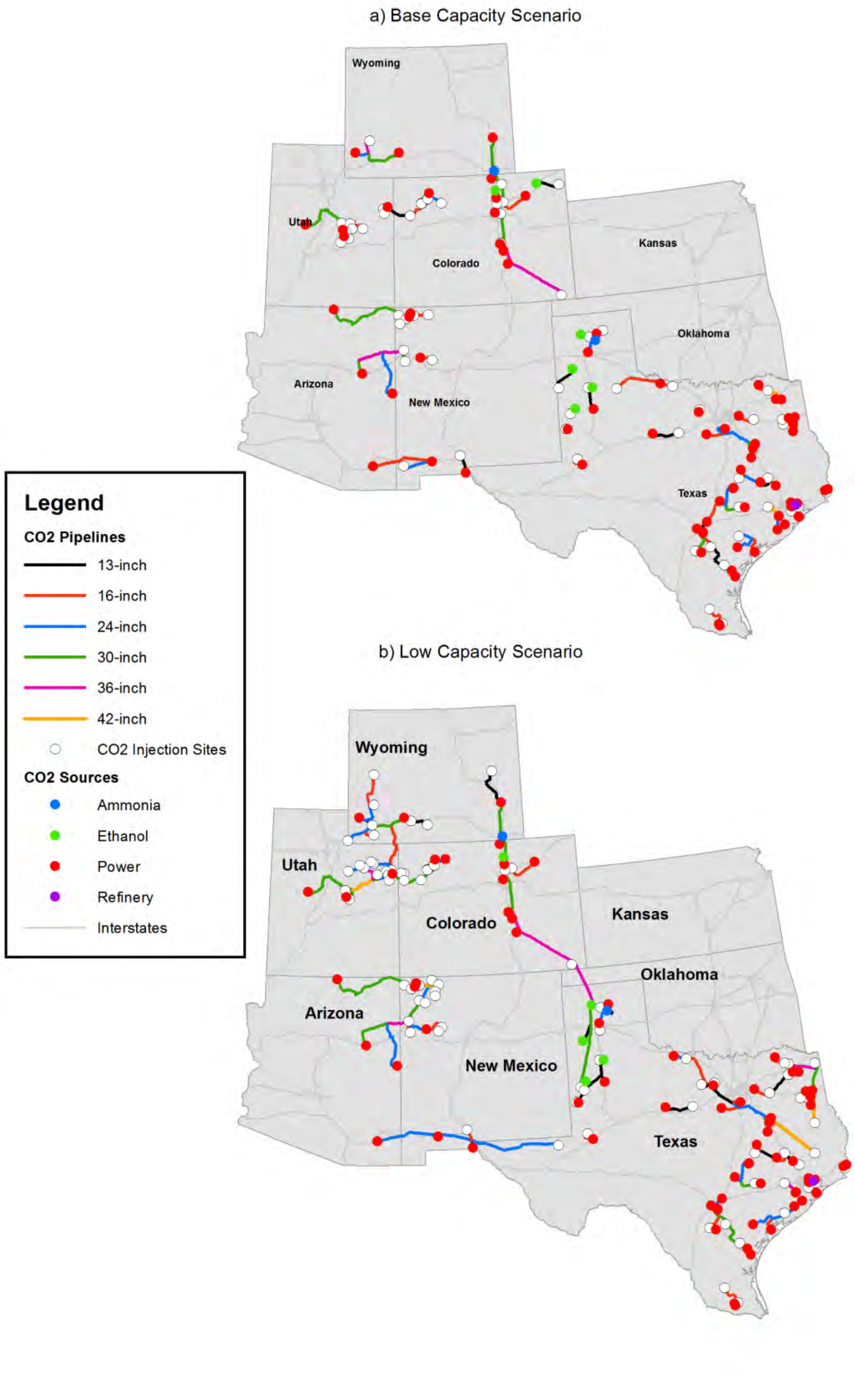

Figure 38: Comparison of 2050 infrastructure design for the a) base capacity and b) low capacity storage scenarios

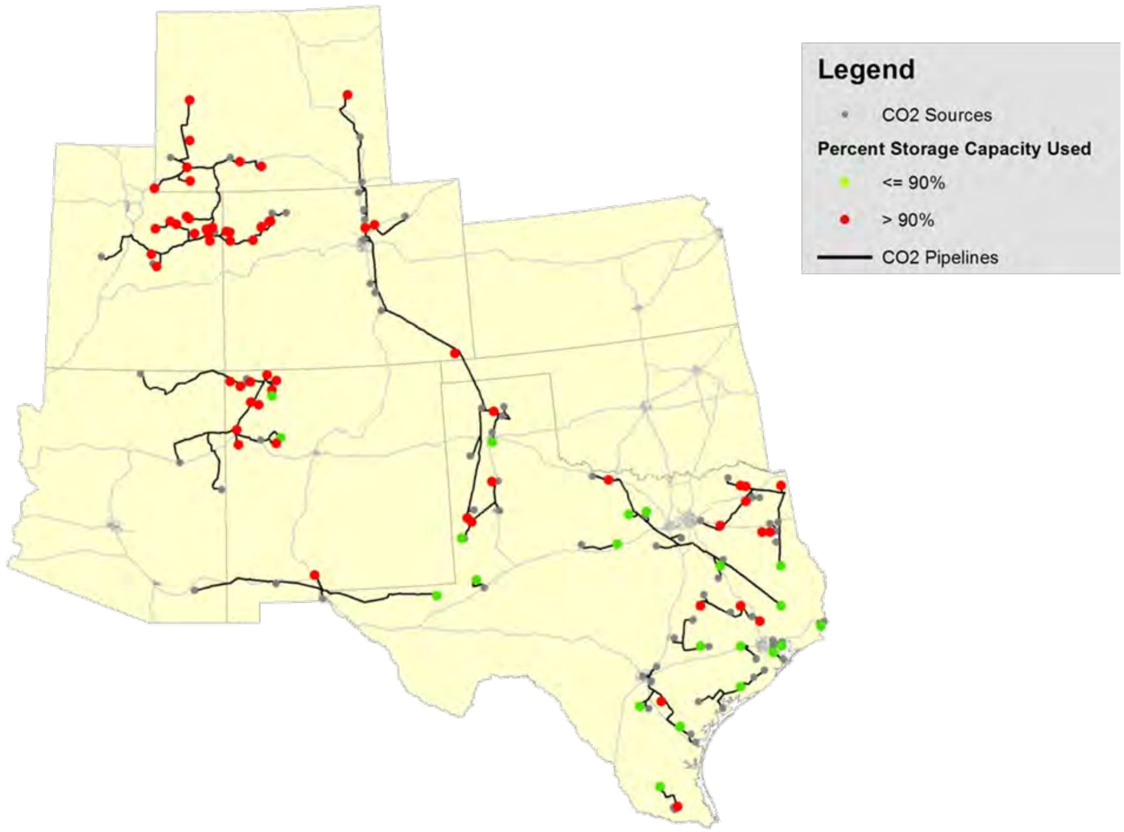

Figure 39: Storage capacity utilization of built injection sites in 2050 (Low Capacity scenario)

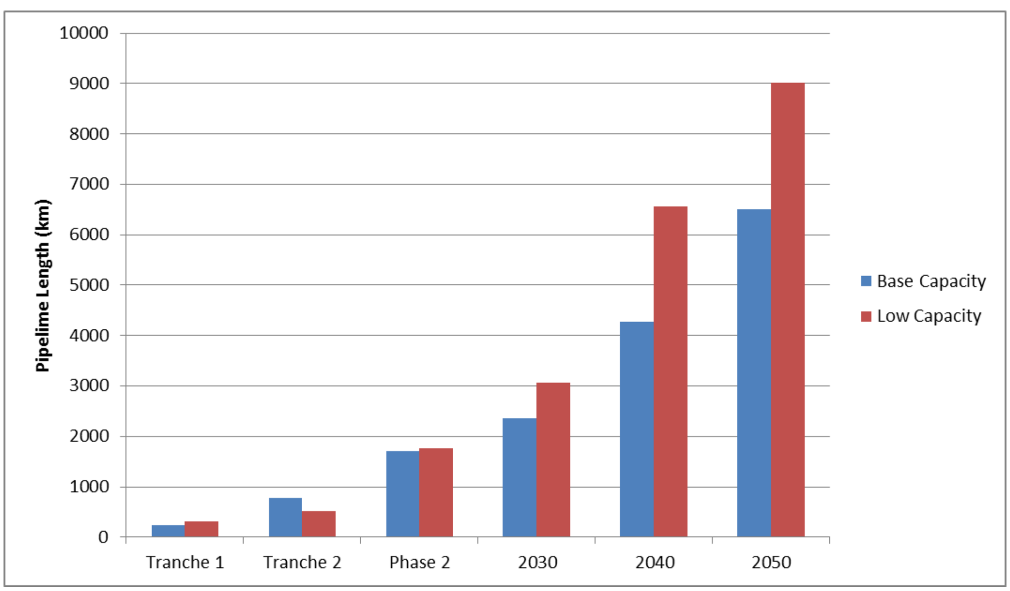

Figure 40: Total pipeline length in each deployment phase for the Base and Low Capacity scenarios

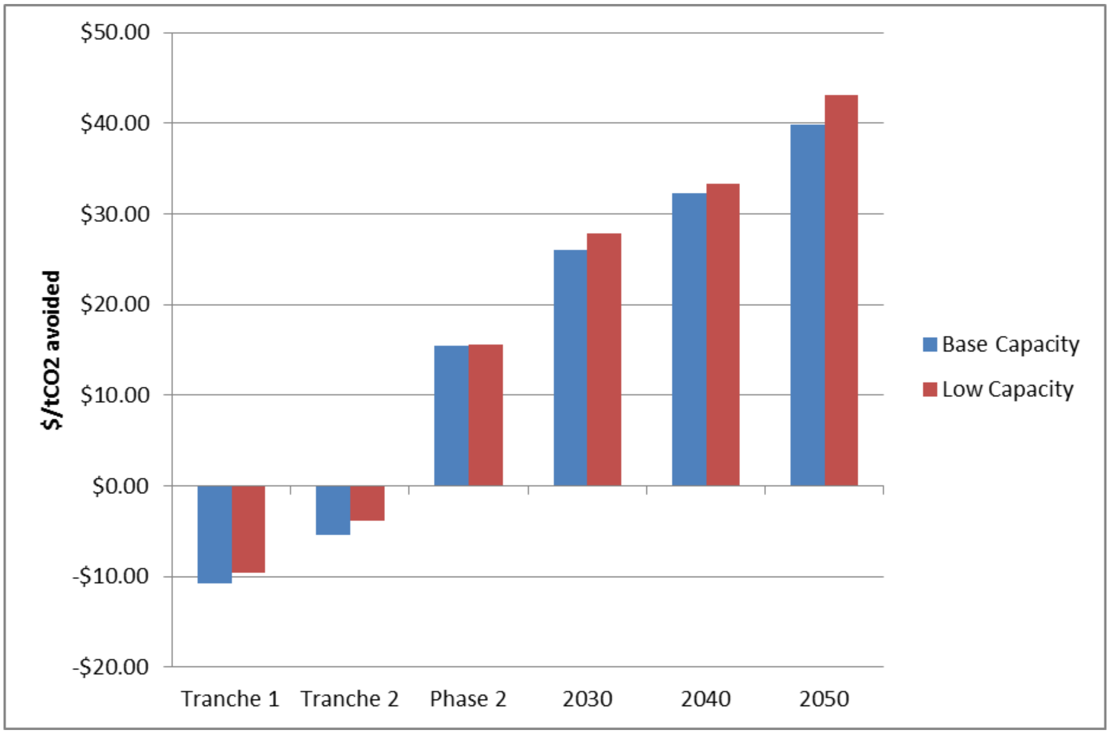

Figure 41: Average total abatement cost (including applicable bonus allowances) in each deployment phase for the Base and Low Capacity scenarios

3.3.4 Conclusions

With widely distributed potential CO_2 injection sites in the southwestern U.S., large regional networks are not common in early stages of CCS deployment. However, as CCS adoption increases and local storage capacity is consumed, integrated regional disposal networks develop in some areas to access additional storage capacity. In the "Low Capacity" scenario, in which CO_2 storage capacity is considered more limited, longer and more integrated networks develop throughout the study area. The deployment strategies identified by this model suggest that storage capacity constraints are the primary cause for the development of integrated regional disposal networks.

CCS abatement costs for individual CO_2 sources indicate that ~300 Mt CO_2 per year can be avoided via CCS for a cost below ~$50/t$CO_2$ avoided. In order to achieve a 360 Mt CO_2 per year reduction (~75% of regional emissions) via CCS, the cost increases to $105/t$CO_2$ avoided since CCS must be installed on industrial and power plants with higher capture costs. However, this value still falls below the EPA projected CO_2 price in 2050, which is $114/t$CO_2$ avoided. In exploring the levelized benefit of installing CCS rather than paying a CO_2 price for emissions, it appears that the CCS bonus allowances proposed by the American Power Act are sufficient to drive investment in Phases 1 and 2 even if the CO_2 price remains at the clearing price. However, after these subsidies expire, CCS investment will only continue if the CO_2 price remains above the clearing price.

The "Low Capacity" scenario suggests that longer and more integrated disposal networks develop when capacity is more limited. As a result, the total average abatement cost increases by 3-10%. However, since capture costs constitute the majority of the abatement cost, this will likely have little impact on the viability of CCS deployment. In exploring the trade-offs between oversizing pipelines for 2050 flow requirements versus organically expanding pipelines to meet incremental flow increases, it appears that the latter (i.e., organic) approach is more cost-effective.

4.0 Task 6.0: Case Studies of a Transition to Coal-based Hydrogen Infrastructure with CCS

Using the *Hydrogen Infrastructure Deployment Model* described in Section 2, regional case studies of coal-based hydrogen infrastructure deployment in the western United States were conducted. The detailed spatial resolution of this model made it infeasible for application to a national case study within a reasonable timeframe. A national case study using this model would require simplification of the spatial representation of demand and production and/or computing resources beyond those available to this research group. Another approach is to run the model in small regions and use the outputs of these models to develop a more simplified candidate network as an input to a national model. Though feasible, this approach would be very time consuming. For this reason, the study is limited to the western continental United States and is defined by the boundary of the Western Governors' Association (Figure 42).

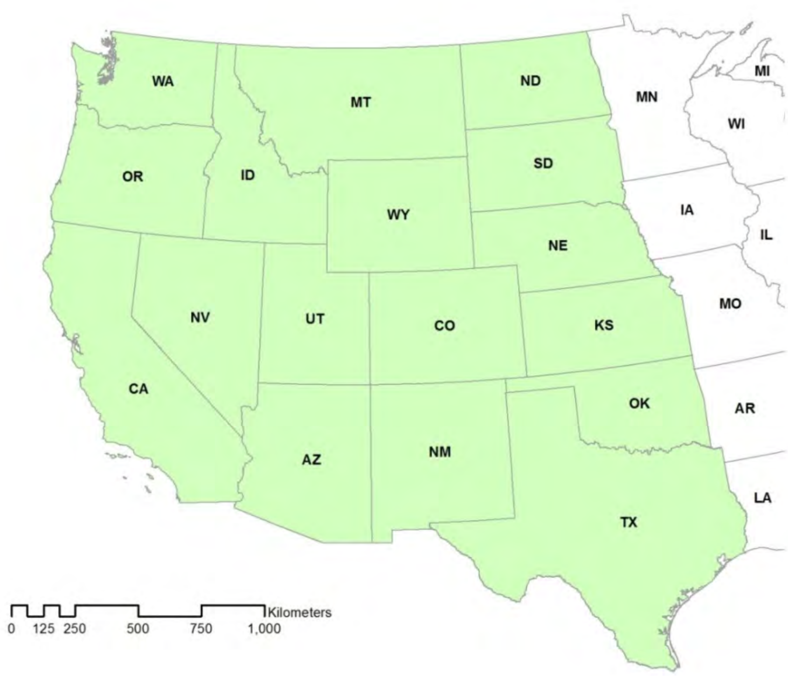

Figure 42: Boundary of the study area (shown in green)

Within the western United States, sub-regional case studies were conducted to examine the variation in infrastructure design and cost. The boundaries of these sub-regions are defined by the outputs of the infrastructure model for the entire western United States (i.e., the super-regional case study determines the boundaries of the sub-regional case studies) (Figure 43).

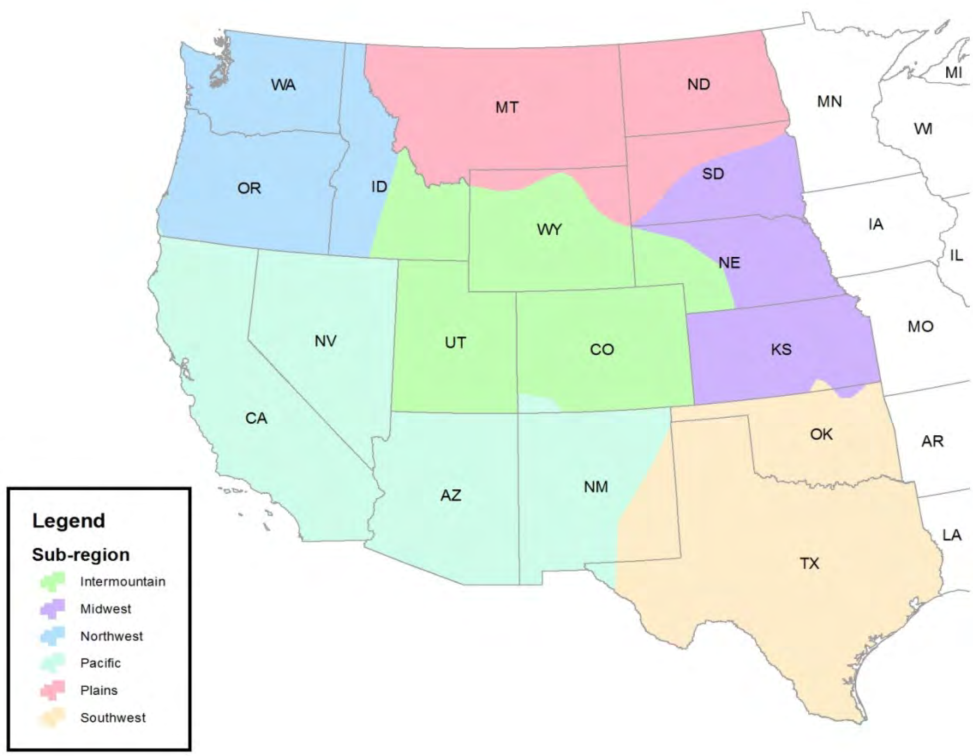

Figure 43: Boundary of sub-regions

Although there was an attempt to match the sub-regions to the regional carbon sequestration partnerships, it was determined that the partnership boundaries do not capture the natural breaks in hydrogen supply networks as modeled by the super-regional case study. As a result, the six sub-regions do not correspond closely to the four regional carbon sequestration partnerships within the western United States (Figure 44). The Northwest sub-region shares much of the territory of the Big Sky Carbon Sequestration Partnership and the Plains and Midwest sub-regions reside completely within the Plains CO_2 Reduction Partnership. However, the other three sub-regions (Pacific, Intermountain, and Southwest) span multiple partnerships, including the Western, Southwest, Plains, and Southeast carbon sequestration partnerships.

Figure 44: Boundaries of the regional carbon sequestration partnerships [44]

4.1 Case Study: Western United States

The case study of the western United States encompasses seventeen states, including Washington, Oregon, California, Idaho, Nevada, Utah, Arizona, Montana, Wyoming, Colorado, New Mexico, North Dakota, South Dakota, Nebraska, Kansas, Oklahoma, and Texas (Figure 42). The case study examines optimal infrastructure deployment for supplying regional hydrogen demand with a combination of onsite production via steam methane reformation and centralized production via coal gasification with CCS at six discrete national HFCV market penetration levels (Table 34).

This section begins by describing the regional inputs to the *Hydrogen Infrastructure Deployment Model* and the results of the case study, including insights into infrastructure design, cost, GHG emissions, coal consumption, and CO_2 storage. Next, alternative deployment strategies are examined in which the transition from onsite to centralized hydrogen production is delayed. The next section evaluates two policy scenarios for subsidizing early hydrogen infrastructure deployment: production tax credits and accelerated depreciation. Finally, the results of this study are compared with those reported in the hydrogen transition study conducted by the National Research Council (2008) [35].

Table 34: Summary statistics for hydrogen demand at each national HFCV market penetration level

Tranche	*National* HFCV Market Penetration (million vehicles)	*Western* HFCV Market Penetration (million vehicles)	*Western* Hydrogen Demand (tonne H_2/day)	# of Demand Centers	*Western* Market Penetration (% of LDVs in year 2000)
1	10	3.9	2,373	99	6%
2	20	7.9	4,732	162	12%
3	50	18.4	11,096	289	28%
4	100	35.5	21,370	422	54%
5	150	52.0	31,300	542	80%
6	220	74.0	44,516	542	114%

4.1.1 Model Inputs

The spatial inputs to the model include the locations and magnitudes of hydrogen demand, the potential locations of production facilities, the potential locations and capacities of CO_2 injection sites, and candidate pipeline networks for both hydrogen and CO_2. The development of the spatial inputs is described in section 2.2.2.2 and section 2.2.3.2. Section 2.2 also provides a detailed description of the economic inputs used in the case studies. The spatial distribution of hydrogen demand at each market penetration level is illustrated in Figure 7 to Figure 11[10]. Summary statistics for hydrogen demand are given in Table 34.

Figure 45 shows the spatial inputs to the *Hydrogen Production and Transmission Model*, including the locations of potential H_2 production facilities, the candidate hydrogen pipeline network, and demand centers. Note that there are no potential large scale coal to H_2 production sites in California since there are no existing large coal-fired power plants in the state[11]. The candidate H_2 transmission pipeline network is approximately 58,000 km in length and contains 1,300 links and 1,200 nodes. There are 50 potential hydrogen production sites.

Figure 46 shows the spatial inputs to the *CO_2 Transport and Disposal Model*, including the locations of potential H_2 production facilities (i.e., CO_2 sources), the locations and capacities of potential CO_2 injection sites, and the candidate CO_2 pipeline network. The capacities of the CO_2 storage sites are illustrated for each 10,000 km^2 grid cell. Given that approximately 8 million tonnes CO_2 would be captured from a large (1500 t/day) fully utilized H_2 production facility each year, a single storage site would need to store about 320 million tonnes CO_2 over a facility's 40-year lifetime. Therefore, basins that can store less than 300 Mt/year per storage site will require multiple storage sites for each large facility (e.g., the large green basin in Kansas). Figure 46 also indicates that there is extremely limited CO_2 storage capacity in close proximity to potential production sites in Nevada and Arizona. The CO_2 candidate pipeline network is

[10] These figures show the spatial distribution of hydrogen demand for the continental United States. For this case study, only the demand centers within the study boundary are considered.

[11] The focus of this study is on coal-based hydrogen production with CCS. Large scale centralized hydrogen production using other feedstocks (e.g., natural gas or biomass) are outside the scope of this study.

approximately 42,000 km in length and contains 627 links and 575 nodes. There are 197 potential injection sites identified in saline aquifers within the western United States.

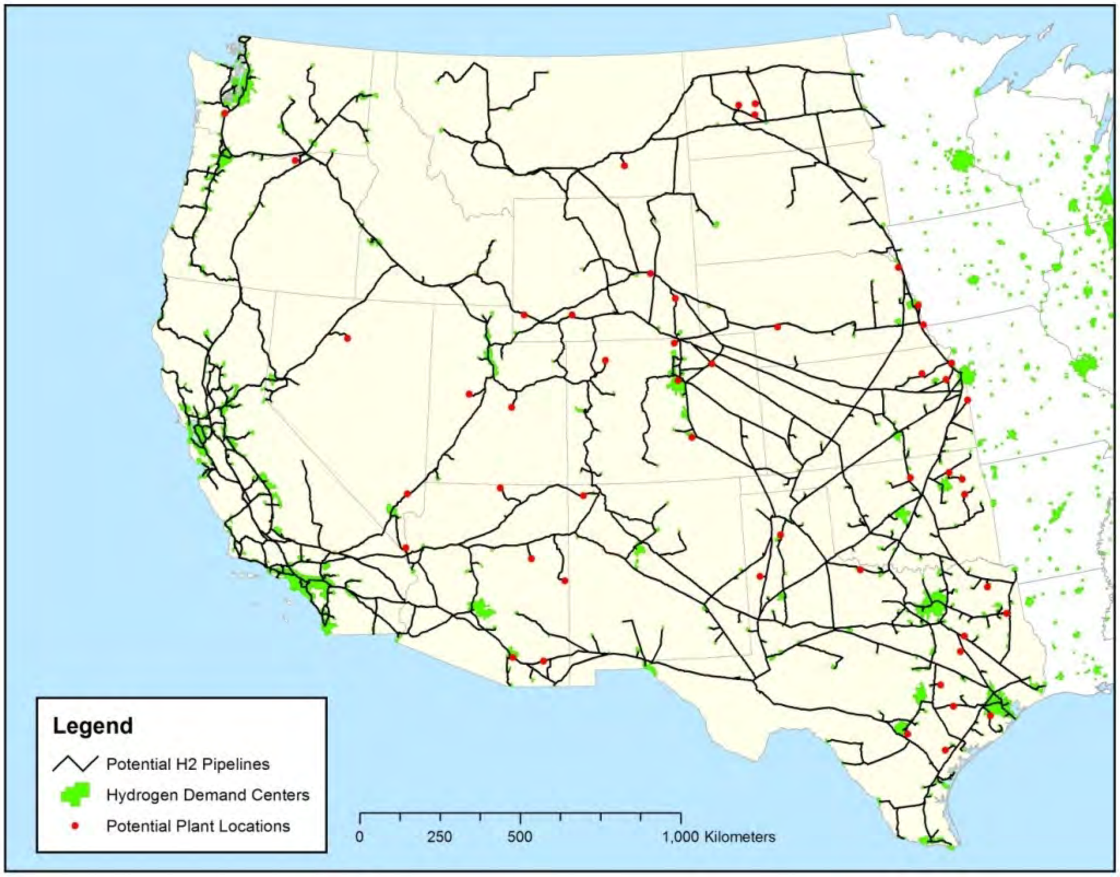

Figure 45: Spatial inputs for the *Hydrogen Production and Transmission Model (demand shown for tranche 6)*

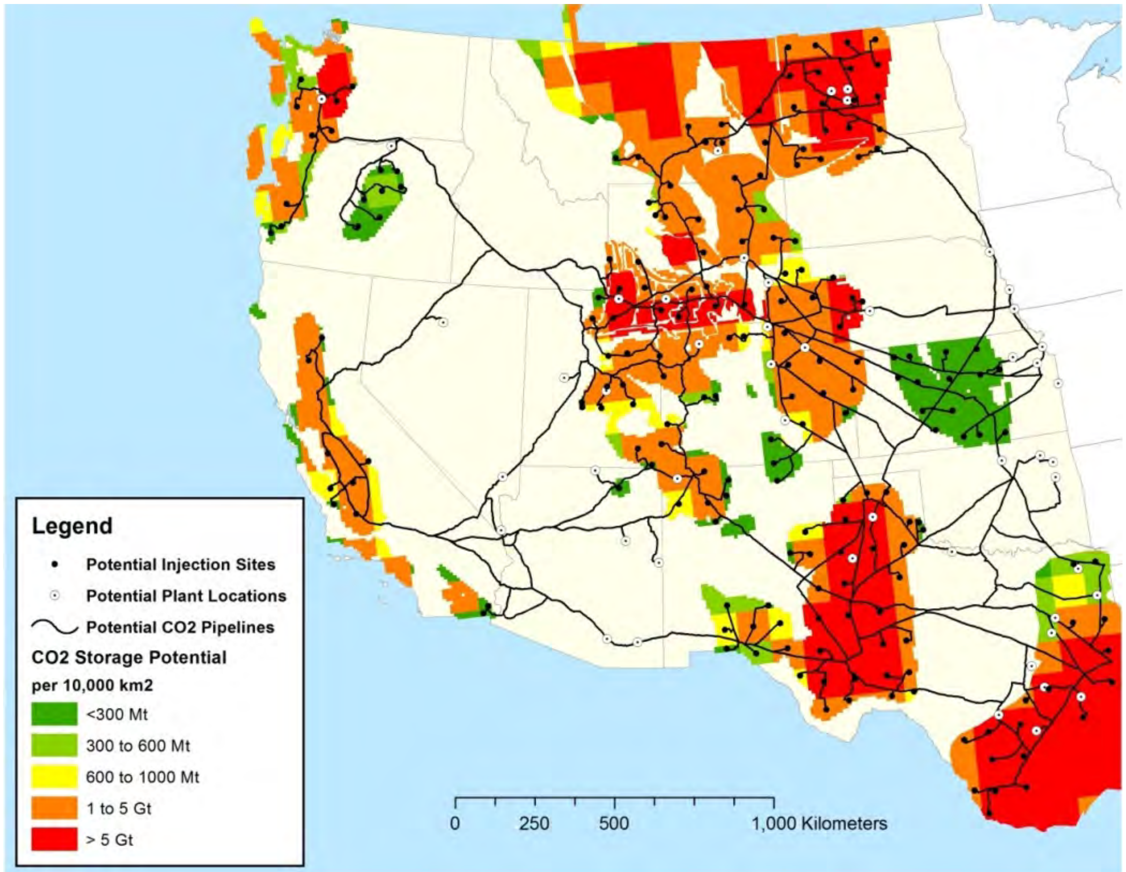

Figure 46: Spatial inputs for the *CO_2 Transport and Disposal Model*

4.1.2 Model Results

Given the spatial and techno-economic inputs, the *Hydrogen Infrastructure Deployment Model* is employed at each HFCV market penetration level in succession from Tranche 1 to Tranche 6. Each model run results in an optimized infrastructure design and represents a stage in building infrastructure to meet a pre-specified HFCV market penetration level. Together, the six model runs provide a long-term deployment strategy for coal-based hydrogen infrastructure with CCS in the western United States. This section highlights the results of the case study, including infrastructure design, costs, GHG emissions, coal consumption, and CO_2 storage requirements under the two HFCV deployment scenarios described in section 2.1.5.

4.1.2.1 Infrastructure Design – H_2 Success Scenario

The *Hydrogen Infrastructure Deployment Model* provides a detailed inventory of infrastructure requirements for each installation tranche. In this section, these inventories are combined with maps to describe the optimal hydrogen infrastructure rollout strategy for the H_2 Success HFCV deployment scenario. Detailed inventories of the infrastructure requirements for each individual component are provided in Table 35 to Table 41 and a map legend is given in Figure 47.

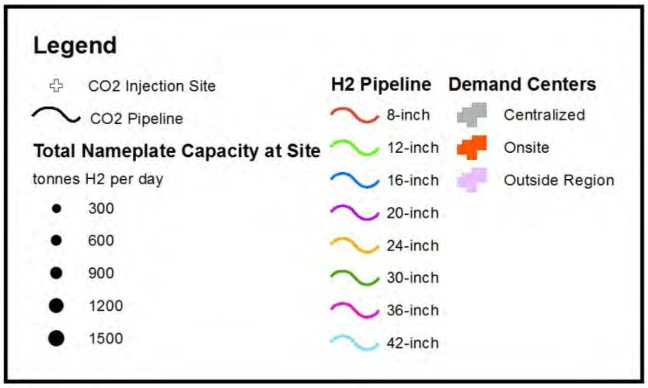

Figure 47: Map legend for optimal infrastructure design figures

Tranche 1

In the first tranche, infrastructure is installed in the year 2021 to serve approximately 4 million HFCVs in 99 demand centers. One-third of the demand centers have insufficient demand and/or are too remote to warrant investment in a centralized supply infrastructure (Table 42). These demand centers are supplied via onsite steam methane reformation at individual stations and represent about 12% of the total hydrogen demand. The remaining demand centers are supplied via pipeline from large centralized coal-based hydrogen production facilities with CCS.

In the first tranche, three independent regional supply networks develop (Figure 48). One network is installed in the Pacific Northwest and serves primarily the Seattle and Portland metropolitan areas. This region is supplied by a single small (300 t/day) hydrogen facility located at node n256 that is connected to a single CO_2 storage facility by a 70-km pipeline.

A large interstate supply network develops in the southwestern U.S. to supply the large projected H_2 demand in California. Because California does not have any potential coal-based production sites, large interstate H_2 transmission pipelines are built to connect California demand to low cost production facilities in Arizona and Wyoming. The majority of supply is delivered via a large trunk pipeline from a 1,500 t/day H_2 facility in Wyoming (n1543), which is selected as a result of the low delivered coal cost in this state. This plant also serves the Denver and Salt Lake City metropolitan areas. Another medium size H_2 facility is built in Arizona (n3329), which serves the Phoenix metropolitan area and connects to California via another large trunk pipeline. Since the model oversizes each pipeline for the projected flow over its 20-year lifetime, some very large pipelines (up to 42-inch diameter) are built in the first tranche despite the relatively small flows during this period. The Wyoming facility is located in close proximity to a CO_2 storage facility while low CO_2 storage availability in Arizona requires the construction of a 476-km CO_2 pipeline to connect the Arizona H_2 facility to a storage site in California.

Figure 48: Optimal infrastructure design in tranche 1 (H_2 Success scenario)

The final H_2 supply network develops in Texas and connects a single medium size production facility (n3438) to the Dallas, Houston, Austin, and San Antonio metropolitan areas. This facility is connected to a single CO_2 storage facility via a 146-km CO_2 pipeline. The metropolitan areas in the Midwest have insufficient demand to warrant centralized infrastructure investment and thus are served by onsite hydrogen production.

Table 35: H_2 production facility requirements for the H_2 Success and H_2 Partial Success scenarios

	Tranche 1	Tranche 2		Tranche 3		Tranche 4		Tranche 5		Tranche 6	
Plant Nameplate Capacity (tonnes/day)	# of H_2 Plants	# of New H_2 Plants	Cumulative # of H_2 Plants	# of New H_2 Plants	Cumulative # of H_2 Plants	# of New H_2 Plants	Cumulative # of H_2 Plants	# of New H_2 Plants	Cumulative # of H_2 Plants	# of New H_2 Plants	Cumulative # of H_2 Plants
300	1	3	4	2	6	1	7	1	8	3	11
600	2	1	3	3	6	0	6	2	8	2	10
900	0	0	0	1	1	1	2	3	5	2	7
1200	0	0	0	1	1	2	3	2	5	1	6
1500	1	1	2	2	4	6	10	4	14	8	22
Total	4	5	9	9	18	10	28	12	40	16	56
Average Nameplate Capacity (tonnes/day)	750	667		750		932		968		996	
Total Nameplate Capacity (tonnes/day)	3,000	6,000		13,500		26,100		38,700		55,800	
Hydrogen Demand (tonnes/day)	2,373	4,732		11,096		21,370		31,300		44,516	
Cumulative Capital Investment (Billion$)*	3.7	7.6		16.7		30.7		45.3		64.9	

* Cumulative capital investment includes the cost of infrastructure replacement as necessary

Table 36: H_2 Storage facility requirements for the H_2 Success scenario

	Tranche 1	Tranche 2		Tranche 3		Tranche 4		Tranche 5		Tranche 6	
Corresponding Plant Size (tonnes/day)	# of Storage Caverns	# of New Caverns	Cumulative # of Caverns	# of New Caverns	Cumulative # of Caverns	# of New Caverns	Cumulative # of Caverns	# of New Caverns	Cumulative # of Caverns	# of New Caverns	Cumulative # of Caverns
300	0	0	0	0	0	0	0	0	0	2	2
600	0	0	0	0	0	0	0	0	0	0	0
900	0	0	0	0	0	0	0	0	0	0	0
1200	0	0	0	0	0	0	0	0	0	1	1
1500	4	2	6	5	11	8	19	9	28	8	36
Total	4	2	6	5	11	8	19	9	28	11	39
Total Nameplate Capacity (tonnes/day)	6,000	9,000		16,500		28,500		42,000		55,800	
Cumulative Capital Investment (Billion$)*	0.3	0.5		0.9		1.6		2.3		3.3	

* Cumulative capital investment includes the cost of infrastructure replacement as necessary

Table 37: Transmission pipeline requirements for the H_2 Success scenario

	Tranche 1	Tranche 2		Tranche 3		Tranche 4		Tranche 5		Tranche 6	
Diameter	New Pipeline (km)	New Pipeline (km)	Cumulative Pipeline (km)	New Pipeline (km)	Cumulative Pipeline (km)	New Pipeline (km)	Cumulative Pipeline (km)	New Pipeline (km)	Cumulative Pipeline (km)	New Pipeline (km)	Cumulative Pipeline (km)
8-inch	371	731	1102	3100	4202	3303	7505	5210	12715	8080	20794
12-inch	1534	654	2188	955	3143	939	4082	1556	5638	860	6498
16-inch	910	1107	2017	592	2609	601	3209	408	3617	264	3881
20-inch	778	801	1580	866	2445	102	2547	1034	3580	27	3607
24-inch	732	726	1458	332	1790	1035	2825	1066	3892	492	4383
30-inch	549	523	1072	1034	2107	690	2797	894	3690	0	3690
36-inch	104	917	1021	296	1317	702	2019	92	2111	73	2184
42-inch	772	260	1032	111	1143	19	1162	574	1736	0	1736
Total (km)	5750	5720	11469	7286	18755	7390	26145	10834	36979	9795	46774
Cumulative Capital Investment (Billion$)*	4.3	8.3		12.3		16.3		21.9		30.6	
# of demand centers (centralized supply)	66	116		222		336		470		542	
Average pipeline length per demand center (km)	87	99		84		78		79		86	

* Cumulative capital investment includes the cost of infrastructure replacement as necessary

Table 38: Refueling station requirements for the H_2 Success and H_2 Partial Success scenarios

	Tranche 1	Tranche 2		Tranche 3		Tranche 4		Tranche 5		Tranche 6	
Station Type	# of Stations	# of New Stations	Cumulative # of Stations	# of New Stations	Cumulative # of Stations	# of New Stations	Cumulative # of Stations	# of New Stations	Cumulative # of Stations	# of New Stations	Cumulative # of Stations
Centralized	2260	1426	3911	4061	8162	6675	15005	6616	21979	8905	31193
Onsite	315	189	279	253	342	317	491	176	309	0	0
Total	2575	1615	4190	4314	8504	6992	15496	6792	22288	8905	31193
Avg Daily Dispensing Capacity (kg/day)	921	1461	1129	1475	1305	1469	1379	1462	1404	1484	1427
Cumulative Capital Investment - H2 Success(Billion$)*	6.0	10.8		23.5		43.9		74.2		112.5	
Cumulative Capital Investment - H2 Partial Success(Billion$)*	6.0	10.8		23.5		49.9		74.2		N/A	

* Cumulative capital investment includes the cost of infrastructure replacement as necessary

Table 39: Distribution pipeline requirements for the H_2 Success scenario

	Tranche 1	Tranche 2		Tranche 3		Tranche 4		Tranche 5		Tranche 6	
Diameter	New Pipeline (km)	New Pipeline (km)	Cumulative Pipeline (km)	New Pipeline (km)	Cumulative Pipeline (km)	New Pipeline (km)	Cumulative Pipeline (km)	New Pipeline (km)	Cumulative Pipeline (km)	New Pipeline (km)	Cumulative Pipeline (km)
4-inch	572	869	1441	3091	4532	4241	8773	4744	13517	3750	17267
6-inch	2231	1844	4075	3116	7191	2926	10117	2467	12584	2174	14758
8-inch	4689	2581	7269	3124	10394	3394	13788	2729	16517	2712	19228
10-inch	1638	1127	2765	2040	4804	2450	7254	1886	9140	1950	11091
12-inch	0	98	98	207	305	242	547	183	729	217	946
16-inch	1170	235	1405	512	1917	698	2615	484	3099	550	3649
Total (km)	10300	6754	17054	12088	29142	13952	43094	12492	55586	11353	66940
Cumulative Capital Investment (Billion$)*	13.7	21.3		33.7		48.1		59.9		87.1	
# of demand centers (centralized supply)	66	116		222		336		470		542	
Average pipeline length per demand center (km)	156	147		131		128		118		124	

* Cumulative capital investment includes the cost of infrastructure replacement as necessary

Table 40: CO_2 storage requirements for the H_2 Success and H_2 Partial Success scenarios

	Tranche 1	Tranche 2		Tranche 3		Tranche 4		Tranche 5		Tranche 6	
	New	New	Cumulative	New	Cumulative	New	Cumulative	New	Cumulative	New	Cumulative
# of storage sites	4	4	8	10	18	6	24	9	33	9	42
# of injection wells	22	25	47	65	112	100	212	104	316	137	453
Avg well injection capacity (tonnes/day)	1738	1703		1721		1779		1784		1795	
Cumulative Capital Investment - H2 Success(Billion$)*	0.2	0.5		1.1		2.0		3.0		4.5	
Cumulative Capital Investment - H2 Partial Success(Billion$)*	0.2	0.5		1.1		2.2		3.2		N/A	

* Cumulative capital investment includes the cost of infrastructure replacement as necessary

Table 41: CO_2 pipeline requirements for the H_2 Success scenario

	Tranche 1	Tranche 2		Tranche 3		Tranche 4		Tranche 5		Tranche 6	
Diameter	New Pipeline (km)	New Pipeline (km)	Cumulative Pipeline (km)	New Pipeline (km)	Cumulative Pipeline (km)	New Pipeline (km)	Cumulative Pipeline (km)	New Pipeline (km)	Cumulative Pipeline (km)	New Pipeline (km)	Cumulative Pipeline (km)
12.75-inch	0	136	136	48	184	0	184	48	232	294	526
16-inch	419	63	483	209	691	58	749	0	749	218	967
24-inch	216	246	462	1026	1488	1007	2496	670	3165	528	3694
30-inch	151	819	970	281	1251	827	2079	444	2523	611	3133
36-inch	0	0	0	0	0	0	0	0	0	0	0
42-inch	0	0	0	0	0	0	0	0	0	0	0
Total (km)	786	1265	2051	1564	3615	1892	5507	1162	6669	1651	8320
Cumulative Capital Investment (Billion$)*	0.5	1.4		2.5		3.9		4.8		6.3	
# of H_2 production sites	4	6		11		19		28		39	
Average pipeline length per production site (km)	197	342		329		290		238		213	

* Cumulative capital investment includes the cost of infrastructure replacement as necessary

Table 42: Number of demand centers served by centralized and onsite supply in each tranche for the H_2 Success and H_2 Partial Success scenarios

	Tranche 1	Tranche 2	Tranche 3	Tranche 4	Tranche 5	Tranche 6
	# of demand centers	# of demand centers	# of demand centers	# of demand centers	# of demand centers	# of demand centers
Centralized Supply	66	116	222	336	470	542
Onsite Supply	33	46	67	86	72	0
Total	99	162	289	422	542	542
% Onsite Demand Centers	33%	28%	23%	20%	13%	0%
% Hydrogen Supplied Onsite	12%	7%	4%	3%	1%	0%

Throughout the western U.S., hydrogen is delivered via 5,750 km of transmission pipeline that connect four production facilities to the demand centers. On average, there is 87 km of H_2 transmission pipeline associated with each demand center. Each production facility has an onsite H_2 storage facility and is associated with a single CO_2 storage site. The onsite H_2 storage sites are much larger than the production facilities since it is assumed that only one cavern exists at each site. Consequently, the storage caverns must be oversized to meet the total production at the site over its lifetime. For example, if a 300 t/day plant is built in tranche 1 and a 900 t/day plant is built in tranche 2, the storage cavern will be sized for a 1200 t/day plant in the first tranche.

The CO_2 captured at the production facilities is transported via 786 km of CO_2 pipeline, which is an average of ~200 km of CO_2 pipeline per unique H_2 production site. There are a total of 2,575 H_2 refueling stations with an average daily dispensing output of ~900 kg/day per station. Approximately 12% of total hydrogen demand is supplied at refueling stations via onsite H_2 production in cities that are either too small or too remote for centralized hydrogen supply. As a reminder, hydrogen is supplied via onsite production in cities in which the fully utilized steady-state cost of centralized hydrogen is greater than $5/kg. The remaining hydrogen is supplied at refueling stations by 10,300 km of distribution pipeline within the demand centers. The total capital investment in the first tranche is approximately $29 billion, which is about $7,300 per HFCV. The capital investment per HFCV is based on the cumulative number of HFCVs sold from the beginning of sales until the end of the tranche as derived from the 2008 National Research Council study, which uses a simple vehicle turnover model [35].

Tranche 2

In the second tranche, additional hydrogen infrastructure is installed in the year 2025 to serve approximately 8 million HFCVs operating in 162 demand centers of which 63 are new. Approximately 28% of the demand centers are served by onsite production (~7% of total hydrogen demand) with the remaining stations supplied via pipeline from centralized production facilities with CCS. The cumulative number of refueling stations with onsite production declines in this tranche since the number of stations that are converted to centralized supply is greater than the number of new onsite stations (Table 38).

The three regional supply networks installed in tranche 1 remain independent and an additional supply network is developed in the Midwest, which serves the Omaha and Kansas City metropolitan areas (Figure 49). The midwestern cities are supplied by a single small production facility (300 t/day) (n1491). As a result of inadequate local CO_2 storage capacity, a 335-km CO_2 pipeline is required for connecting the production facility to a storage aquifer.

In the Northwest region, a second small production facility is built at the same location as the original facility (n256) in order to meet the additional hydrogen demand. The production site continues to use the same CO_2 storage site, which is expanded to meet the increased CO_2 injection requirements. The transmission pipeline network is also extended to serve new demand centers.

In the southwestern region, two additional production facilities are constructed in Arizona. The first is a new 1,500 t/day facility built in the northern part of the state (n2892) and the second is a 300 t/day facility built in the same location as the previous facility near Phoenix (n3329). Large trunk pipelines are built to transport the hydrogen from these facilities to the major demand centers in California, Arizona, and New Mexico. The new facilities both require long CO_2 pipelines to access distant CO_2 storage sites.

In the Texas region, the transmission pipeline network expands to serve additional demand centers in Oklahoma and Texas. One additional 600 t/day production facility is built at the site of the original facility (n3438) and continues to use the same CO_2 storage site.

Figure 49: Optimal infrastructure design in tranche 2 (H_2 Success scenario)

In tranche 2, a total of nine production facilities operate at six independent sites. Each production site has a single H_2 storage facility that is shared by the production facilities at each site. Eight CO_2 storage sites with 47 injection wells are connected to the production facilities by ~2,000 km of CO_2 pipeline. There are ~11,500 km of H_2 transmission pipeline and ~17,000 km of H_2 distribution pipeline within the entire study region. There are a total of 4,190 refueling stations with an average daily dispensing output of ~1,100 kg/day per station. The cumulative capital investment in tranche 2 is approximately $50 billion, which translates to about $6,400 per HFCV, based on the cumulative number of HFCVs sold from the beginning of sales until the end of the tranche.

Tranche 3

In the third tranche, additional hydrogen infrastructure is built in the year 2028 to meet the hydrogen demand of approximately 18 million HFCVs in 289 demand centers. About 23% of the demand centers are served by onsite hydrogen production at individual refueling stations (~4% of total demand) with the remaining demand centers supplied via pipeline from centralized coal-based production facilities with CCS.

In tranche 3, the four independent supply networks developed in tranche 2 coalesce into two large regional networks (Figure 50). The Northwest and Southwest networks are connected into a single large hydrogen distribution network via a trunk pipeline through Idaho. A new 900 t/day plant is built at the existing site near Seattle (n256), which serves the Northwestern region, while several new plants are built in Utah, Nevada, and Arizona to serve the growing hydrogen demand in the southwestern U.S. and California. For example, a new 600 t/day plant is built in Nevada (n1670) to supply hydrogen to Northern California. With no CO_2 storage capacity in Nevada, a 191-km CO_2 pipeline is required for connecting the plant to a CO_2 storage site in California. In Utah and Arizona, the entire production from two new 1500 t/day plants (n2046 and n3343) is dedicated to the California market. An additional 600 t/day plant is also built at site n3329 in Arizona. Finally, a small 300 t/day plant is built in Colorado (n1956) to supplement hydrogen supply to the Denver metropolitan area.

Figure 50: Optimal infrastructure design in tranche 3 (H_2 Success scenario)

The two regional supply networks in Texas and the Midwest are also combined into a single large distribution network. A new large 1,200 t/day facility at the existing production site near Omaha (n1491) is built with much of the output exported into Oklahoma and Texas. Six CO_2 injection sites are required to store the CO_2 from this plant since the aquifer in this vicinity has a low storage capacity. In the Texas region, a 300 t/day H_2 facility is built at the existing production site (n3438) and a 600 t/day facility is built at a new site near Houston (n3501). Both sites are located in close proximity to CO_2 storage sites.

Throughout the entire study area, a total of 18 production facilities at 11 independent sites are constructed over the three tranches. At eight of the eleven sites, the combined nameplate production capacity of all facilities is at the maximum allowed for an individual site (1500 t/day). As a result, additional production capacity in future tranches cannot be installed at these sites. The eighteen production facilities are connected to the 222 demand centers supplied by centralized production via ~19,000 km of H_2 transmission pipeline. These facilities are also connected to the eighteen CO_2 storage sites by ~3,600 km of CO_2 pipeline. Within the demand centers, ~29,000 km of distribution pipelines connect 8,162 refueling stations to local hydrogen terminals. The remaining 67 demand centers are supplied by onsite production at 342 refueling stations. The average daily dispensing output of all stations increases to ~1,300 kg/day per station. The cumulative capital investment in tranche 3 is approximately $91 billion, which translates to about $4,500 per HFCV.

Tranche 4

In the fourth tranche, additional infrastructure is built in the year 2034 to meet the hydrogen demand of approximately 36 million HFCVs in 422 demand centers. About 20% of the demand centers are supplied by onsite hydrogen production (~3% of total demand) with the remaining demand centers supplied by pipeline from centralized production facilities with CCS. It is notable that centralized infrastructure is still not viable in the northern states of Montana, North Dakota, and South Dakota where demand centers with relatively low demand are widely dispersed.

In this tranche, a single pipeline through New Mexico links the eastern and western supply networks into one interconnected hydrogen distribution network. This pipeline is built to connect hydrogen produced in the eastern network to the expanding hydrogen demand in California. Specifically, a portion of the hydrogen produced at the new plant in Oklahoma (n2464) is transported over 2,000 km to demand centers in California. Ten additional production facilities are built throughout the study area. The majority of these new plants are large 1500 t/day facilities and eight facilities are built at new sites. Six new CO_2 storage sites are constructed and the total length of CO_2 pipeline increases to 5,507 km.

Within the demand centers, the total number of refueling stations increases to 15,496 of which only 491 are supplied by onsite production. As a result of the oversizing of pipelines in early tranches, only about 20% of new transmission pipelines have a diameter greater than 24 inches and about 45% are 8-inch pipelines that connect to small demand centers. The cumulative capital investment in tranche 4 is approximately $147 billion, which translates to about $3,800 per HFCV.

Figure 51: Optimal infrastructure design in tranche 4 (H_2 Success scenario)

Tranche 5

In the fifth tranche, additional infrastructure is built in the year 2040 to meet the hydrogen demand of 52 million HFCVs in 542 demand centers. The quantity of hydrogen supplied via onsite production decreases to 1% of the total demand as centralized infrastructure becomes viable in the states of Montana, North Dakota, and South Dakota. It is notable that two production facilities are built in North Dakota (n228 and n265), which has the lowest delivered coal cost in the study area.

The H_2 transmission pipeline network also becomes more interconnected and begins to resemble the existing natural gas pipeline network (Figure 52). The interconnectivity of the network is driven primarily by the massive hydrogen demand in California and the unavailability of coal-based H_2 production within the state. Five large trunk pipelines along the state's border transport large quantities of imported hydrogen to California. In addition, the trunk pipelines connecting Texas and New Mexico are also developed in order to transport hydrogen to California from more distant facilities. Twelve new H_2 production facilities are installed of which nine are developed on new sites. Hydrogen must be moved to California from more distant production sites since the production capacities of all of the potential H_2 production sites near California are maximized.

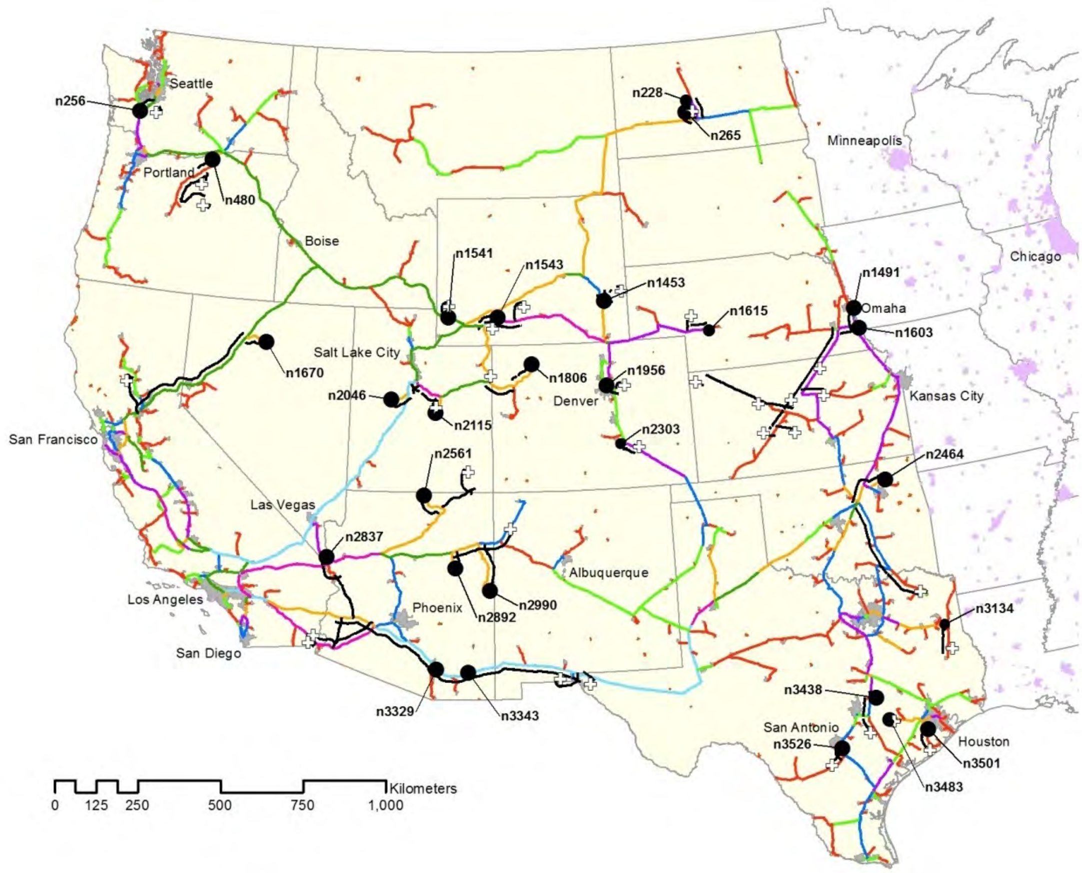

Figure 52: Optimal infrastructure design in tranche 5 (H_2 Success scenario)

A few interconnected CO_2 disposal networks also begin to develop in Arizona in order to link multiple production facilities to more distant storage sites. In southern Arizona, three H_2

facilities share a connected CO_2 disposal network and, in northern Arizona, two facilities share the same pipeline network and disposal site. Over 22,000 H_2 refueling stations are required in this tranche of which only 309 are supplied via onsite production. The cumulative capital investment in tranche 5 is approximately $211 billion and the cost per HFCV declines to about $3,600.

Tranche 6

In the sixth tranche, additional infrastructure is built in year 2044 to meet the hydrogen demand of approximately 74 million HFCVs in 542 demand centers. It is assumed that all demand centers are served via pipeline by centralized coal-based hydrogen production with CCS (i.e., no demand centers are served by onsite production).

In this tranche, the H_2 transmission pipeline network becomes even more interconnected and most demand nodes can be served by several different pipeline routes (Figure 53). Although redundancy was not specified as an objective of the model, the pipeline network has developed so that a pipeline disruption could be managed by redirecting flows along alternative routes. As in previous tranches, the general direction of hydrogen flow is west towards the largest demand centers in California. California demand is served by production facilities in states as distant as North Dakota and Oklahoma. However, if the eastern U.S. were included in this study, much of the hydrogen production in the Midwest may be redirected towards the large demand centers in Chicago and Minneapolis.

Figure 53: Optimal infrastructure design in tranche 6 (H_2 Success scenario)

Sixteen new production facilities are required in tranche 6 of which eleven are at new sites. There are a total of 56 H_2 production facilities at 39 unique sites built over the 30-year study period and these facilities have an average nameplate capacity of ~1,000 tonnes H_2 per day. The production facilities are connected to the demand centers via approximately 47,000 km of transmission pipeline. Within the demand centers, over 31,000 refueling stations are supplied by ~ 67,000 km of distribution pipeline. The average daily dispensing output of the refueling stations is 1,427 kg per day.

In areas with inadequate CO_2 storage capacity (i.e., Nevada, Arizona, Kansas, and Nebraska), multiple H_2 production facilities share a common CO_2 disposal network. However, in much of the study area, local CO_2 storage capacity is adequate and individual H_2 production facilities have a dedicated independent CO_2 pipeline and storage site. If other CO_2 sources (e.g., power and industrial plants) were included in this study, it is possible that interconnected regional CO_2 disposal networks would be more common than indicated in this study. During the study period, 42 CO_2 storage sites are connected to 39 unique H_2 production sites, which include 56 H_2 production facilities, by 8,320 km of CO_2 pipeline, which equates to ~ 200 km of CO_2 pipeline per unique production site. The cumulative capital investment in tranche 6 is approximately $309 billion and the cost per HFCV declines to about $3,300.

General Insights

In the first two tranches, four independent hydrogen supply territories develop. As hydrogen demand increases, the supply network becomes increasingly interconnected with large regional trunk pipelines constructed for the purpose of transporting hydrogen westward toward the major regional demand centers in California. As the H_2 transmission pipeline expands, the average length per demand center remains relatively constant between 80 and 100 km.

The design of the CO_2 disposal network is dependent on the availability of local storage capacity. In locations with adequate capacity, H_2 production facilities tend to have dedicated CO_2 pipelines and injection sites. However, in areas with inadequate local capacity (e.g., Arizona), long CO_2 pipelines are required to access storage aquifers and these pipelines and injection sites are often shared by several H_2 facilities.

As a result of the relatively large distances between cities in the arid western U.S., the total length of hydrogen transmission pipelines is only about 30% smaller than the total length of hydrogen distribution pipelines. However, this finding may not apply in the eastern U.S. where population density is much higher. The total length of CO_2 pipelines amounts to only about 7% of the total length of hydrogen pipelines (i.e., transmission plus distribution).

In this model, it is assumed that demand centers that will be supplied via centralized coal-based production if the fully utilized steady-state cost of delivered hydrogen is less than $5 per kg. Otherwise, the demand centers are served by onsite production. Given this assumption, the model indicates that the source of hydrogen is predominantly from centralized coal plants, with the supply via onsite production approaching zero by 2050. Unlike earlier hydrogen infrastructure models, this model allows regional aggregation of demand and the development of interconnected transmission and production networks. Therefore, it predicts more centralized production than earlier steady-state studies that considered each city separately [35]. However, a more detailed economic analysis is conducted in section 4.1.3, which evaluates whether centralized production should be delayed given the underutilization of infrastructure that will occur during real deployment.

4.1.2.2 Infrastructure Design - H_2 Partial Success Scenario

In the H_2 Partial Success scenario, HFCVs penetrate the light-duty vehicle market more slowly. As a result, the construction of each infrastructure tranche is delayed. Since the model oversizes pipelines and H_2 storage facilities based on projected size requirements over the lifetime of the component, the slower market penetration means that the size of these infrastructure components will not need to be as oversized in the first two tranches. Thus, the difference in infrastructure design between the H_2 Success and H_2 Partial Success scenarios is limited to the sizing of pipelines and H_2 storage facilities. Furthermore, in the H_2 Partial Success scenario, HFCV market penetration is not sufficient at the end of the 30-year study period to require the construction of tranche 6. Detailed inventories for the affected components (i.e., H_2 storage sites and transmission, distribution, and CO_2 pipelines) are listed in Table 43 to Table 46.

Tranche 1

In the H_2 Partial Success scenario, the construction of the first tranche is delayed until the year 2025. The spatial layout of the infrastructure (i.e., length and location) is identical to the design in the H_2 Success scenario, but smaller diameter hydrogen and CO_2 pipelines are built since the flows along these corridors are not projected to be as large over the equipment lifetime (Figure 54 to Figure 57). The size and location of remaining infrastructure (i.e., CO_2 storage, H_2 production and storage, and refueling stations) is identical to the H_2 Success scenario. However, because the pipelines are not as oversized in the first tranche, the capital investment in the H_2 Partial Success scenario is ~25% smaller than in the H_2 Success scenario. The capital investment is $21.5 billion, or about $5,400 per HFCV.

Figure 54: Optimal infrastructure design in tranche 1 (H_2 Partial Success scenario)

Table 43 Transmission pipeline requirements for the H_2 Partial Success scenario

	Tranche 1	Tranche 2		Tranche 3		Tranche 4		Tranche 5		Tranche 6	
Diameter	New Pipeline (km)	New Pipeline (km)	Cumulative Pipeline (km)	New Pipeline (km)	Cumulative Pipeline (km)	New Pipeline (km)	Cumulative Pipeline (km)	New Pipeline (km)	Cumulative Pipeline (km)	New Pipeline (km)	Cumulative Pipeline (km)
8-inch	804	1025	1830	3100	4930	3303	8233	5210	13443	N/A	N/A
12-inch	1890	1138	3028	955	3982	939	4921	1556	6478	N/A	N/A
16-inch	1276	878	2155	592	2746	601	3347	408	3755	N/A	N/A
20-inch	592	1029	1620	866	2486	102	2588	1034	3621	N/A	N/A
24-inch	321	817	1138	332	1471	1035	2506	1066	3572	N/A	N/A
30-inch	866	498	1364	1034	2398	690	3088	894	3982	N/A	N/A
36-inch	0	329	329	296	625	702	1328	92	1419	N/A	N/A
42-inch	0	5	5	111	116	19	135	574	709	N/A	N/A
Total (km)	5750	5720	11469	7286	18755	7390	26145	10834	36979	N/A	N/A
Cumulative Capital Investment (Billion$)*	3.2	6.6		10.6		20.0		25.5		N/A	
# of demand centers (centralized supply)	66	116		222		336		470		N/A	
Average pipeline length per demand center (km)	87	99		84		78		79		N/A	

* Cumulative capital investment includes the cost of infrastructure replacement as necessary

Table 44 Distribution pipeline requirements for the H_2 Partial Success scenario

	Tranche 1	Tranche 2		Tranche 3		Tranche 4		Tranche 5		Tranche 6	
Diameter	New Pipeline (km)	New Pipeline (km)	Cumulative Pipeline (km)	New Pipeline (km)	Cumulative Pipeline (km)	New Pipeline (km)	Cumulative Pipeline (km)	New Pipeline (km)	Cumulative Pipeline (km)	New Pipeline (km)	Cumulative Pipeline (km)
4-inch	2528	1448	3976	3091	7066	4241	11307	4744	16051	N/A	N/A
6-inch	6110	2500	8610	3116	11726	2926	14652	2467	17119	N/A	N/A
8-inch	493	1991	2484	3124	5608	3394	9002	2729	11731	N/A	N/A
10-inch	1170	579	1749	2040	3789	2450	6239	1886	8125	N/A	N/A
12-inch	0	0	0	207	207	242	448	183	631	N/A	N/A
16-inch	0	235	235	512	747	698	1445	484	1929	N/A	N/A
Total (km)	10300	6754	17054	12088	29142	13952	43094	12492	55586	N/A	N/A
Cumulative Capital Investment (Billion$)*	7.6	13.9		26.3		56.3		68.1		N/A	
# of demand centers (centralized supply)	66	116		222		336		470		N/A	
Average pipeline length per demand center (km)	156	147		131		128		118		N/A	

* Cumulative capital investment includes the cost of infrastructure replacement as necessary

Table 45: H_2 storage facility requirements for the H_2 Partial Success scenario

	Tranche 1	Tranche 2		Tranche 3		Tranche 4		Tranche 5		Tranche 6	
Corresponding Plant Size (tonnes/day)	# of Storage Caverns	# of New Caverns	Cumulative # of Caverns	# of New Caverns	Cumulative # of Caverns	# of New Caverns	Cumulative # of Caverns	# of New Caverns	Cumulative # of Caverns	# of New Caverns	Cumulative # of Caverns
300	0	0	0	0	0	0	0	0	0	N/A	N/A
600	0	0	0	0	0	0	0	0	0	N/A	N/A
900	0	0	0	0	0	0	0	0	0	N/A	N/A
1200	0	0	0	0	0	0	0	0	0	N/A	N/A
1500	4	2	6	5	11	8	19	9	28	N/A	N/A
Total	4	2	6	5	11	8	19	9	28	N/A	N/A
Cumulative Capital Investment (Billion$)*	0.3	0.5		0.9		1.9		2.7		N/A	

* Cumulative capital investment includes the cost of infrastructure replacement as necessary

Table 46: CO_2 pipeline requirements for the H_2 Partial Success scenario

	Tranche 1	Tranche 2		Tranche 3		Tranche 4		Tranche 5		Tranche 6	
Diameter	New Pipeline (km)	New Pipeline (km)	Cumulative Pipeline (km)	New Pipeline (km)	Cumulative Pipeline (km)	New Pipeline (km)	Cumulative Pipeline (km)	New Pipeline (km)	Cumulative Pipeline (km)	New Pipeline (km)	Cumulative Pipeline (km)
12.75-inch	0	136	136	48	184	0	184	48	232	N/A	N/A
16-inch	476	63	540	209	748	58	806	0	806	N/A	N/A
24-inch	305	246	552	1026	1578	1007	2585	670	3255	N/A	N/A
30-inch	4	819	824	281	1105	827	1932	444	2376	N/A	N/A
36-inch	0	0	0	0	0	0	0	0	0	N/A	N/A
42-inch	0	0	0	0	0	0	0	0	0	N/A	N/A
Total (km)	786	1265	2051	1564	3615	1892	5507	1162	6669	N/A	N/A
Cumulative Capital Investment (Billion$)*	0.4	1.3		2.4		4.3		5.2		N/A	
# of H_2 production sites	4	6		11		19		28		N/A	
Average pipeline length per production site (km)	197	342		329		290		238		N/A	

* Cumulative capital investment includes the cost of infrastructure replacement as necessary

Tranche 2

In the H_2 Partial Success scenario, the construction of the second tranche does not occur until the year 2033. Again, the only difference in the infrastructure design between deployment scenarios is the fact that smaller hydrogen and CO_2 pipelines are generally required in the H_2 Partial Success scenario (Figure 55 to Figure 58). As a result, the cumulative capital investment in this tranche is ~18% smaller at \$41.2 billion, which translates to about \$5,100 per HFCV.

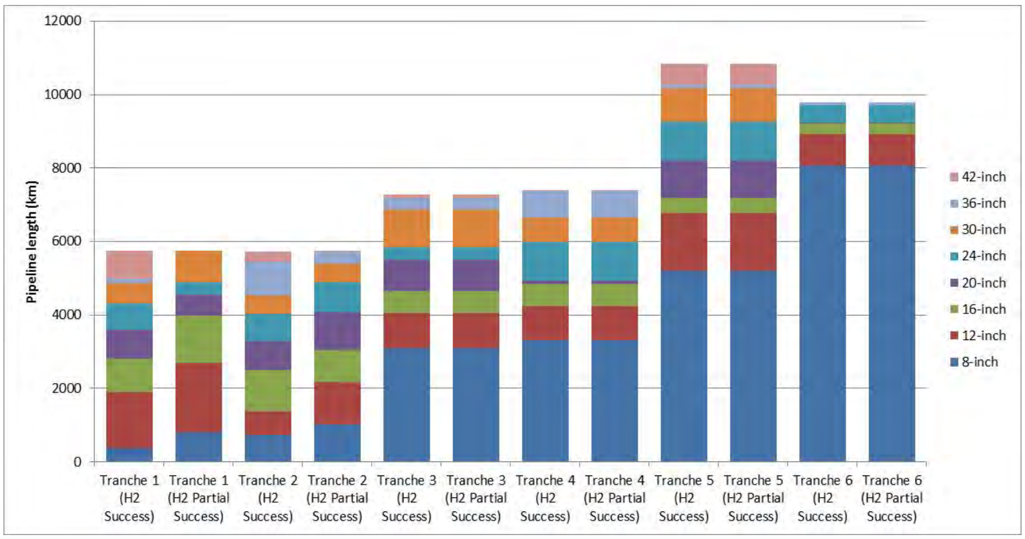

Figure 55: New transmission pipeline length by diameter class in each tranche for the H_2 Success and H_2 Partial Success scenarios (new pipeline does not include replacement pipeline)

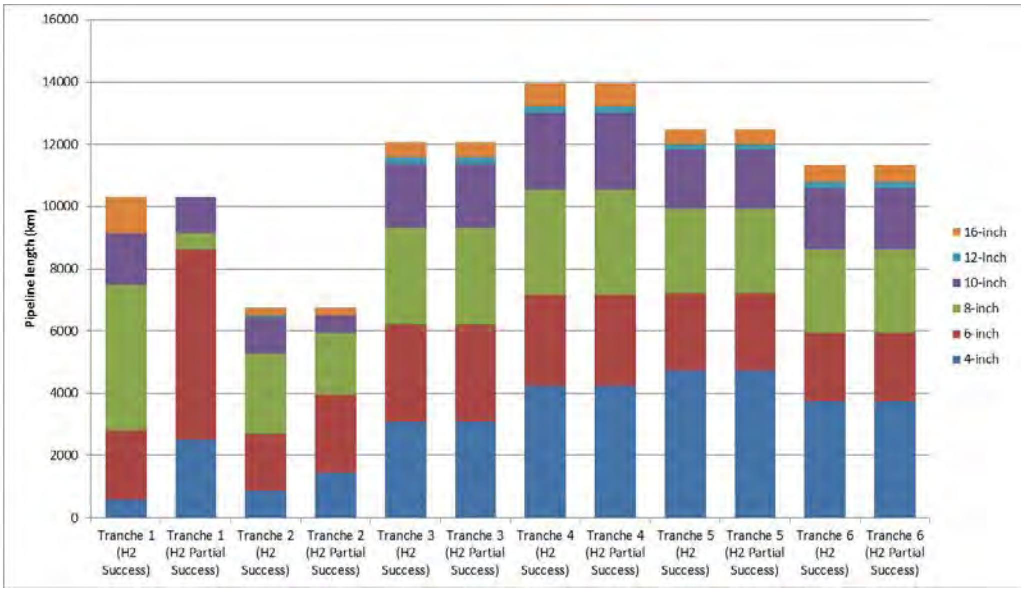

Figure 56: New distribution pipeline length by diameter class in each tranche for the H_2 Success and H_2 Partial Success scenarios

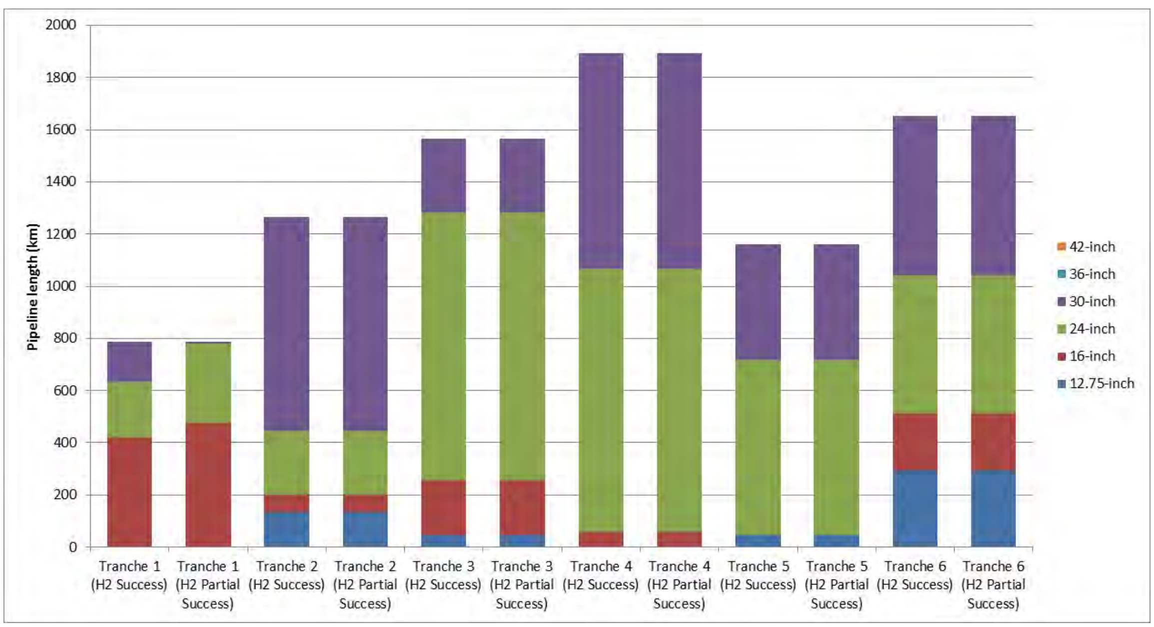

Figure 57: New CO_2 pipeline length by diameter class in each tranche for H_2 Success and H_2 Partial Success scenarios

Figure 58: Optimal infrastructure design in tranche 2 (H_2 Partial Success scenario)

Tranche 3

The construction of the third tranche occurs in the year 2038. In this tranche, the new infrastructure built is identical to that constructed in the H_2 Success scenario since the new pipelines are oversized for the maximum flows projected in the study. However, the smaller pipelines built in the first two tranches remain (Figure 59) and, thus, the cumulative capital investment is still about 10% smaller than the investment in the H_2 Success scenario. The cost per HFCV is about $4,100.

Figure 59: Optimal infrastructure design for tranche 3 (H_2 Partial Success scenario)

Tranche 4

The construction of the fourth tranche occurs in the year 2045 and again the new infrastructure is identical to the infrastructure installed in the H_2 Success scenario. However, all of the infrastructure installed in the first tranche, except the H_2 production facilities, must be replaced in 2045 since the maximum lifetime of these components is reached. When these infrastructure components are replaced, they are oversized for the projected capacity requirements over their new lifetimes. In the year 2045, these components are oversized for the maximum required capacities projected in this study (Figure 60). Since the cumulative capital investment includes the cost of both new and replacement infrastructure, the cumulative capital investment in the H_2 Partial Success scenario is now 13% *larger* than the cost in the H_2 Success scenario.

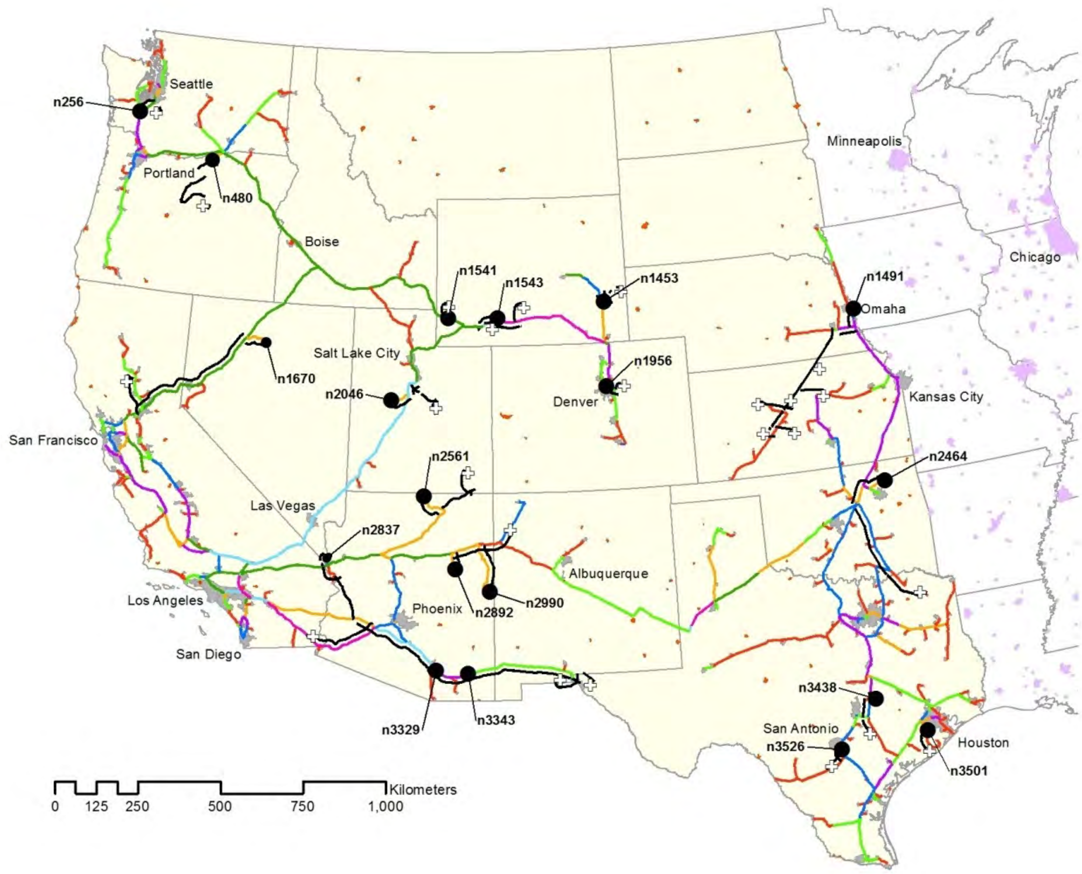

Figure 60: Optimal infrastructure design in tranche 4 (H_2 Partial Success scenario)

Tranche 5

The construction of the fifth tranche occurs in the year 2052 and the infrastructure designs in each deployment scenario are now identical. The cumulative capital cost remains 6% larger than the cost in the H_2 Success scenario since more infrastructure requires replacement in the H_2 Partial Success scenario (Figure 61). Tranche 6 is not built in the H_2 Partial Success scenario since it is not required within the 30-year analysis period.

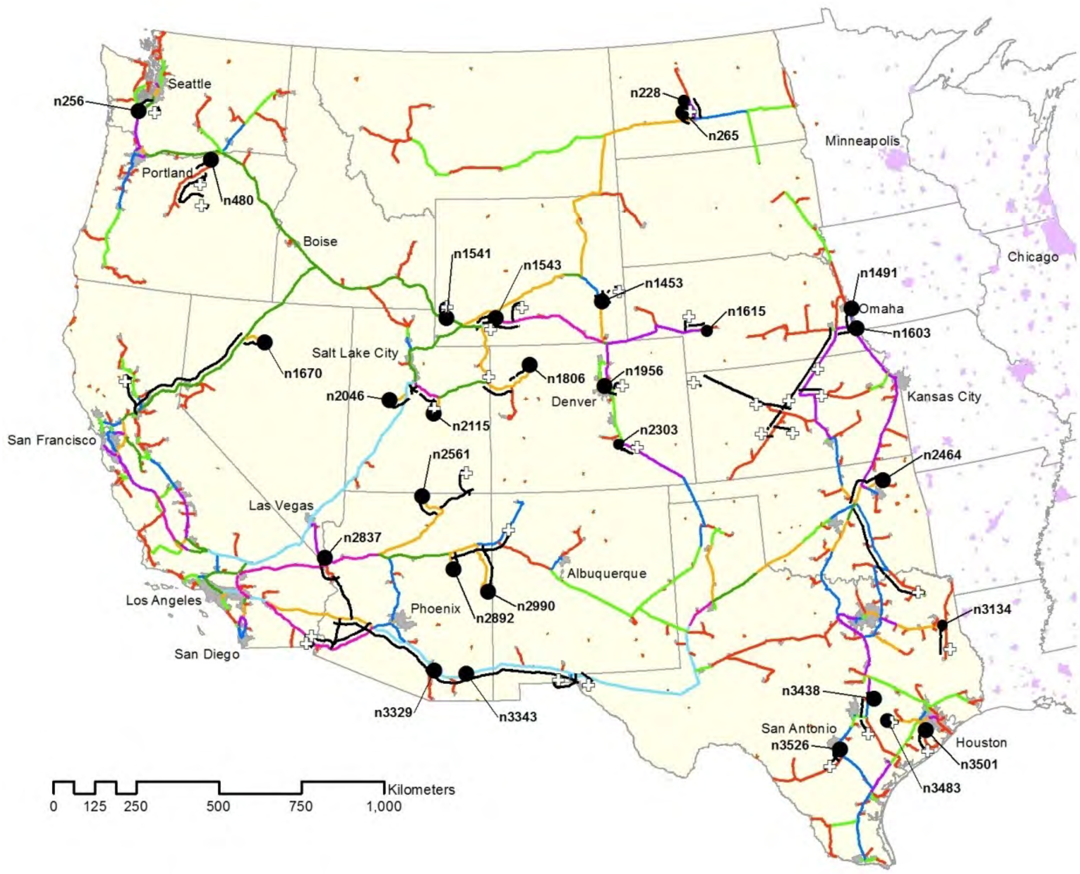

Figure 61: Optimal infrastructure design in tranche 5 (H_2 Partial Success scenario)

General Insights

In the H_2 Partial Success scenario, the market penetration of HFCVs occurs more gradually. For example, the first infrastructure tranche is not installed until 2025 and the fourth tranche is not built for another 20 years in 2045. As a result, the pipelines in the first two tranches do not have to be as oversized as required in the H_2 Success scenario. For this reason, the required capital investment is initially smaller in the first three tranches of the H_2 Partial Success scenario.

However, in the fourth tranche, most of the infrastructure built in the first tranche must be replaced with much larger capacity infrastructure. In contrast, no infrastructure is replaced in the fourth tranche of the H_2 Success scenario since tranche 4 occurs in 2034, which is less than

20 years after the first tranche is installed in 2021. Consequently, in tranches 4 and 5, the cumulative capital investment is larger in the H_2 Partial Success scenario than in the H_2 Success scenario.

Essentially, the slower HFCV market penetration reduces the oversizing required in the H_2 Partial Success scenario, but also requires that early infrastructure is replaced in earlier tranches since it is not built with sufficient capacity for the demands in tranches 4 and 5. As a result, the cumulative capital investment is ultimately larger in tranches 4 and 5 in the H_2 Partial Success scenario.

4.1.2.3 Cost

In this section, the cost of building and operating the infrastructure outlined in sections 4.1.2.1 and 4.1.2.2 is reported. Specifically, we summarize the cumulative capital investment in each tranche, the breakeven price of hydrogen, and the cumulative cash flow given different scenarios of the future price of hydrogen.

Cumulative Capital Investment

In each tranche, hydrogen supply and CCS infrastructure is built that can meet the H_2 demand of a specific number of HFCVs. As infrastructure components reach the end of their lifetimes, these components are replaced and the cost of the replacement components is included in the cumulative capital investment. Table 47 lists the cumulative capital investment for each infrastructure component in each tranche for the H_2 Success and H_2 Partial Success deployment scenarios. As explained in section 4.1.2.2, smaller diameter CO_2 and hydrogen pipelines are built in the H_2 Partial Success scenario, resulting in smaller initial capital costs. However, because the initial pipelines are built with less capacity, they are replaced in an earlier tranche, resulting in higher cumulative capital costs in tranches 4 and 5 (Figure 62).

Table 47: Cumulative capital investment (Billion $) and capital investment per HFCV ($/HFCV) in each tranche

	Tranche 1	Tranche 2	Tranche 3	Tranche 4	Tranche 5	Tranche 6
H2 Success						
H_2 Production	3.7	7.6	16.7	30.7	45.3	64.9
H_2 Storage	0.3	0.5	0.9	1.6	2.3	3.3
H_2 Transmission	4.3	8.3	12.3	16.3	21.9	30.6
H_2 Distribution	13.7	21.3	33.7	48.1	59.9	87.1
Refueling Stations	6.0	10.8	23.5	43.9	74.2	112.5
CO_2 Transport	0.5	1.4	2.5	3.9	4.8	6.3
CO_2 Injection	0.2	0.5	1.1	2.0	3.0	4.5
Total Capital Investment (Billion 2005$)	28.7	50.3	90.7	146.6	211.4	309.3
Capital per HFCV ($)	7,300	6,400	4,500	3,800	3,600	3,300
H_2 Partial Success						
H_2 Production	3.7	7.6	16.7	30.7	45.3	N/A
H_2 Storage	0.3	0.5	0.9	1.9	2.7	N/A
H_2 Transmission	3.2	6.6	10.6	20.0	25.5	N/A
H_2 Distribution	7.6	13.9	26.3	56.3	68.1	N/A
Refueling Stations	6.0	10.8	23.5	49.9	74.2	N/A
CO_2 Transport	0.4	1.3	2.4	4.3	5.2	N/A
CO_2 Injection	0.2	0.5	1.1	2.2	3.2	N/A
Total Capital Investment (Billion 2005$)	21.5	41.2	81.5	165.4	224.2	N/A
Capital per HFCV ($)	5,400	5,100	4,100	4,000	3,400	N/A

At the end of the 30-year study period, six infrastructure tranches are built in the H_2 Success scenario. These tranches require a cumulative capital investment of approximately $310 billion and serve about 94 million cumulative HFCVs over the study period [35]. The capital investment per HFCV ranges from ~$7,300 in tranche 1 to ~$3,300 in tranche 6. In the H_2 Partial Success scenario, only five tranches are constructed and these tranches require a cumulative capital investment of about $224 billion and serve about 65 million cumulative HFCVs over the study period [35]. The capital investment per HFCV ranges from ~$5,400 in tranche 1 to ~$3,400 in tranche 5.

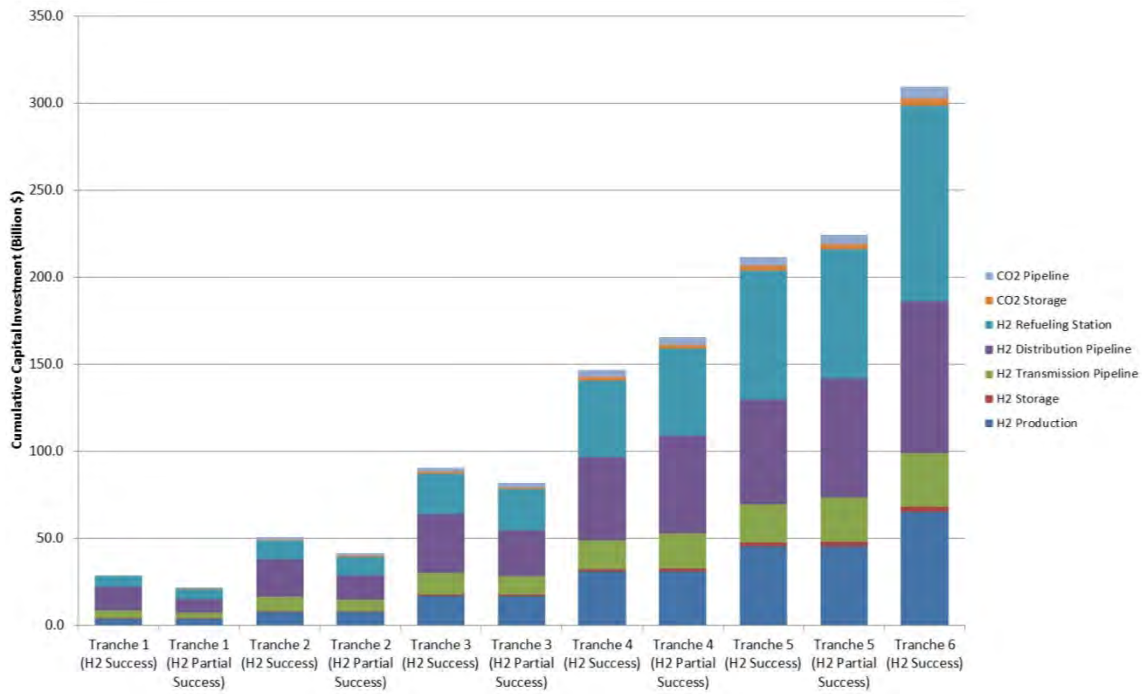

Figure 62: Cumulative capital investment in each tranche for the H_2 Success and H_2 Partial Success scenarios

Figure 63 indicates the percentage of the total cumulative capital investment associated with each component in each infrastructure tranche. In both deployment scenarios, H_2 and CO_2 pipelines are oversized to meet the projected capacity requirements over their lifetimes. As a result, pipeline capital accounts for over half of the cumulative capital investment in tranche 1. This value is higher in the H_2 Success scenario since pipelines are more oversized in the first two tranches. However, as HFCV deployment continues, pipeline diameter is better matched to current capacity requirements and the pipeline cost as a percentage of total cumulative capital investment declines relative to other components.

In tranche 6, about 40% of the capital is associated with pipeline transport, 35% is related to refueling stations and 21% is associated with H_2 production. The percentage of capital associated with H_2 production and refueling stations increases over time since the benefits from economies of scale and better capacity utilization are not as great as those achieved by pipeline transport. The cost of CO_2 transport and storage represents less than 4% of the cumulative capital required and H_2 Storage also represents a tiny fraction of the cumulative capital investment.

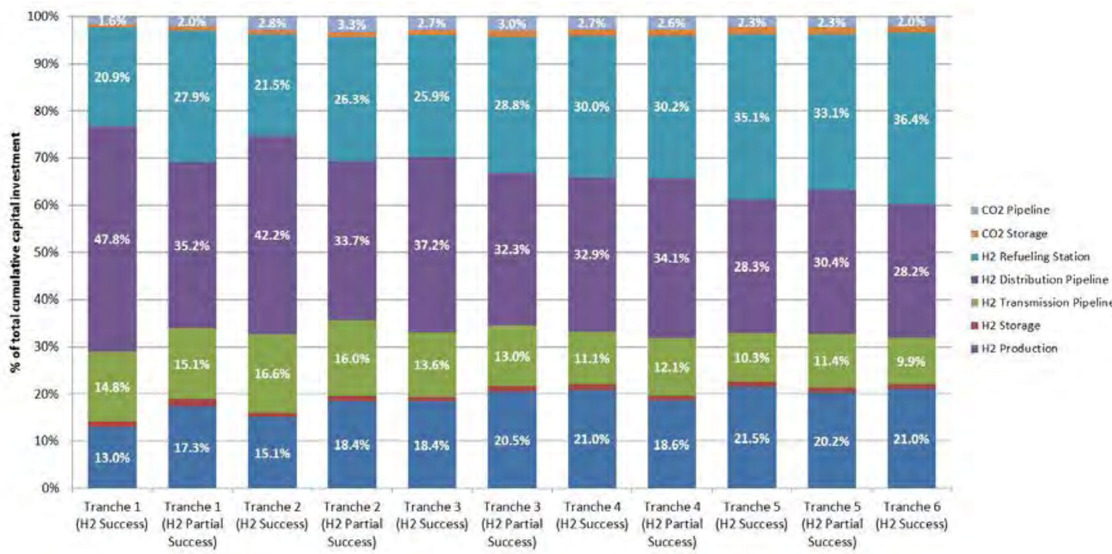

Figure 63: Percentage of total cumulative capital investment associated with each component

Breakeven Price of Hydrogen

The breakeven price of hydrogen is the price without excise taxes at which the revenue generated from the sale of hydrogen is equal to the cost of supplying the hydrogen over a specific time period (equation 89).

$$P_{H2} = \frac{C_{supply}}{Q_{H2}} \quad (89)$$

where P_{H2} is the breakeven price of hydrogen ($/kg), C_{supply} is the total annual cost of delivering hydrogen ($/year), and Q_{H2} is the annual quantity of hydrogen sold (kg/year). Figure 64 illustrates the annual breakeven price of hydrogen during the 30-year analysis period. In both HFCV deployment scenarios, a price spike occurs in each year in which a new infrastructure tranche is installed. Although the cost of infrastructure is annualized, a spike occurs because new infrastructure capacity is initially underutilized. With time, the infrastructure becomes increasingly utilized and the price declines until the next tranche is installed. Moreover, the price trend is negative over time as a result of both better utilization and economies-of scale.

The more rapid deployment of hydrogen infrastructure in the H_2 Success scenario is evident in Figure 64 from the number of price spikes (i.e., tranche installations) in the first decade. The breakeven price of hydrogen initially declines rapidly as the first infrastructure tranche quickly becomes fully utilized. Then, in year 5, the second tranche is installed resulting in a price spike. The rapid deployment of HFCVs means that this tranche also quickly achieves full utilization and the third tranche is installed in year 8, resulting in another price spike. As a result of the large capital investment required in the first decade, the breakeven price of hydrogen is higher in the H_2 Success scenario than the H_2 Partial Success scenario from years 5 to 8. However, the breakeven price of hydrogen is lower in the H_2 Success scenario in all other years as a result of better average utilization and faster achievement of economies of scale.

In the H_2 Partial Success scenario, HFCV market penetration occurs more slowly and thus each infrastructure tranche remains underutilized for a longer period of time. As a result, the breakeven cost of hydrogen is larger than it is in the H_2 Success scenario in most years of the analysis period. In both deployment scenarios, the breakeven cost of hydrogen is approximately $24/kg in year 1 since the infrastructure is highly underutilized, but ranges from $4/kg to $12/kg for most of the analysis period. Given that one kilogram of hydrogen has about the same energy content as one gallon of gasoline and assuming that a HFCV is anticipated to have about 63%

better fuel economy than a gasoline hybrid electric vehicle (HEV) [35, 65-69][12], \$4-12/kg is equivalent to about \$2.50-7.50/gallon of gasoline.

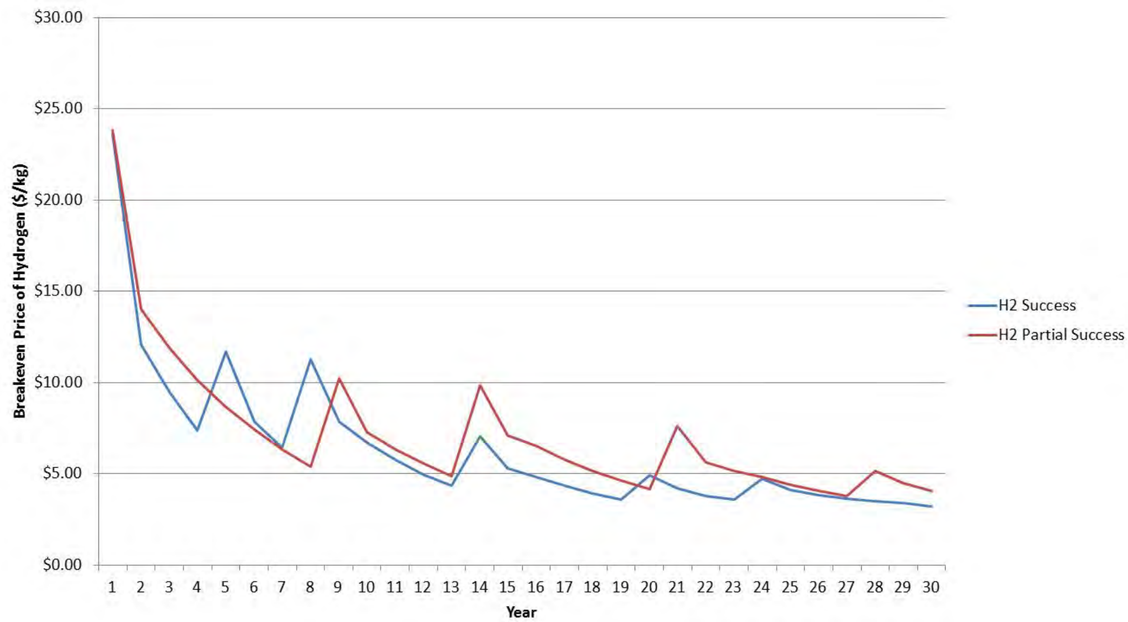

Figure 64: Breakeven price of hydrogen in each year of the 30-year analysis period for the H_2 Success and H_2 Partial Success scenarios

Figure 65 illustrates the breakdown by infrastructure component of the breakeven price of hydrogen for three 10-year periods. For example, the first period represents the price of hydrogen that would allow the supplier to breakeven over the first ten years of the 30-year analysis period. In the first period, the breakeven price of hydrogen is over \$9/kg in both deployment scenarios, which is equivalent to a gasoline price of approximately \$5.50/gallon in 2005 dollars. The price is dominated by the cost of refueling stations and H_2 transmission and distribution pipelines, which are very oversized in early tranches. The breakeven price is slightly larger in the H_2 Partial Success scenario since slower deployment leads to less economies-of-scale. In addition, a higher proportion of hydrogen is supplied by small onsite stations, which

[12] The relative fuel economy of 1.63 for HFCVs relative to gasoline HEVs is the average of the values reported in the listed references.

results in higher station costs. Table 48 lists the average capacity factor in each time period for the five infrastructure components that contribute most to cost. This metric indicates the average utilization of the components and helps to explain the large breakeven prices of hydrogen in the first two periods.

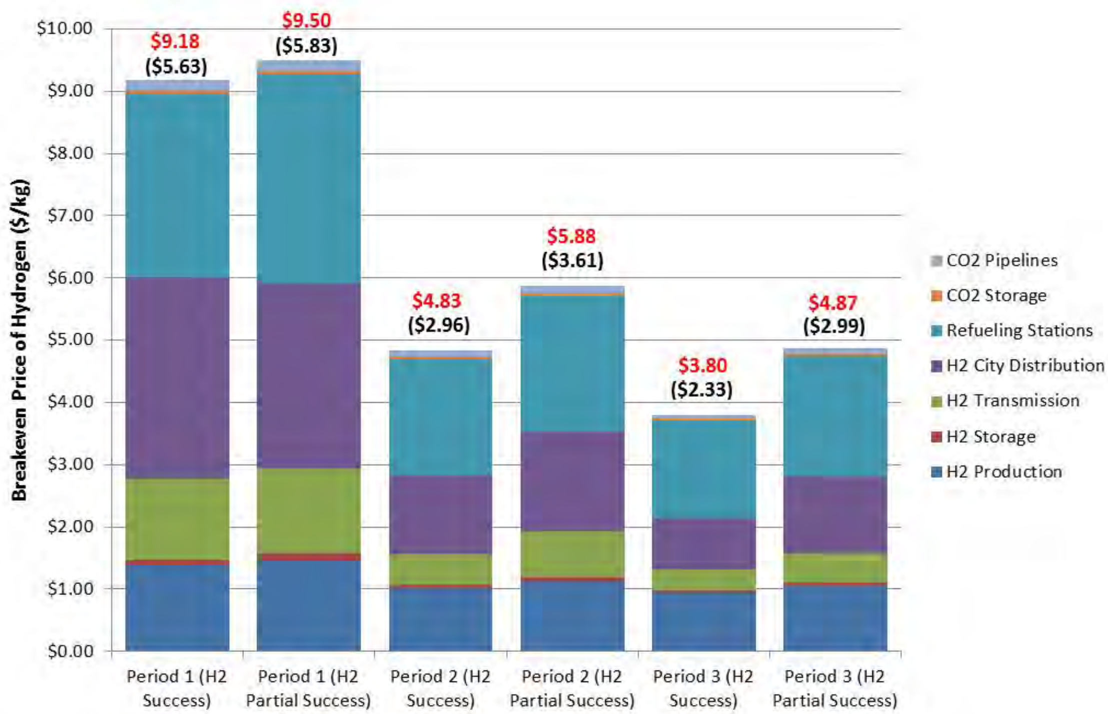

Figure 65: Breakeven price of hydrogen for three 10-year periods for the H_2 Success and H_2 Partial Success scenarios (price in parentheses is the equivalent price for a gallon of gasoline ($/gge) assuming that a HFCV has 63% better fuel economy than a gasoline HEV)

Table 48: Average capacity factors for the five major infrastructure components

	Period 1		Period 2		Period 3	
	H2 Success	H2 Partial Success	H2 Success	H2 Partial Success	H2 Success	H2 Partial Success
H_2 production	0.44	0.43	0.64	0.58	0.70	0.62
H_2 transmission	0.12	0.21	0.30	0.27	0.60	0.31
H_2 distribution	0.13	0.15	0.37	0.35	0.60	0.36
H_2 refueling stations	0.49	0.50	0.67	0.62	0.74	0.65
CO_2 pipelines	0.26	0.27	0.47	0.41	0.60	0.47

In the second period, better average utilization of capacity and economies-of-scale greatly reduce the breakeven price of hydrogen in both deployment scenarios. In the H_2 Success scenario, the cost of H_2 pipelines declines by about 60% as oversized pipelines begin to be better utilized. Overall, the breakeven price of hydrogen declines by 47% in the H_2 Success scenario and by 38% in the H_2 Partial Success scenario. In the second period, the discrepancy between the prices of hydrogen in the two deployment scenarios becomes more distinct as the more rapid HFCV deployment in the H_2 Success scenario results in a much lower breakeven price.

In the third period, economies of scale and greater utilization of oversized pipelines are responsible for an additional ~20% decline in the breakeven price of hydrogen in both deployment scenarios. These benefits are particularly evident in the costs of CO_2 and H_2 pipelines which decline an additional ~35% in period 3. The cost of refueling stations declines by about 15% as the average refueling station size increases and stations with onsite production are phased out. The cost of H_2 production declines only 7% since the average size of production facilities does not change significantly between periods (Table 35). In all periods, the cost of CO_2 transport and storage represents less than 3% of the total breakeven price of hydrogen.

Cumulative Cash Flow

The cumulative cash flow is calculated to identify when and if a supplier is projected to breakeven under different hydrogen price scenarios. In order to calculate the cumulative cash flow, an assumption must be made regarding the price of hydrogen that the supplier is projected to receive in the market during the analysis period. Assuming that hydrogen will continue to compete with gasoline, this study calculates equivalent hydrogen prices[13] in 2005 dollars based on three oil price projections provided by the EIA in the 2011 Annual Energy Outlook (AEO) (Figure 66) [70]. Specifically, the analysis uses the oil price projections provided by the Reference, High Oil Price, and GHG Price Economy-wide cases[14]. The GHG Price Economy-wide case represents a scenario in which the oil price reflects an economy-wide CO_2 price of $25/tonne starting in 2013 that increases to $75/tonne by 2035.

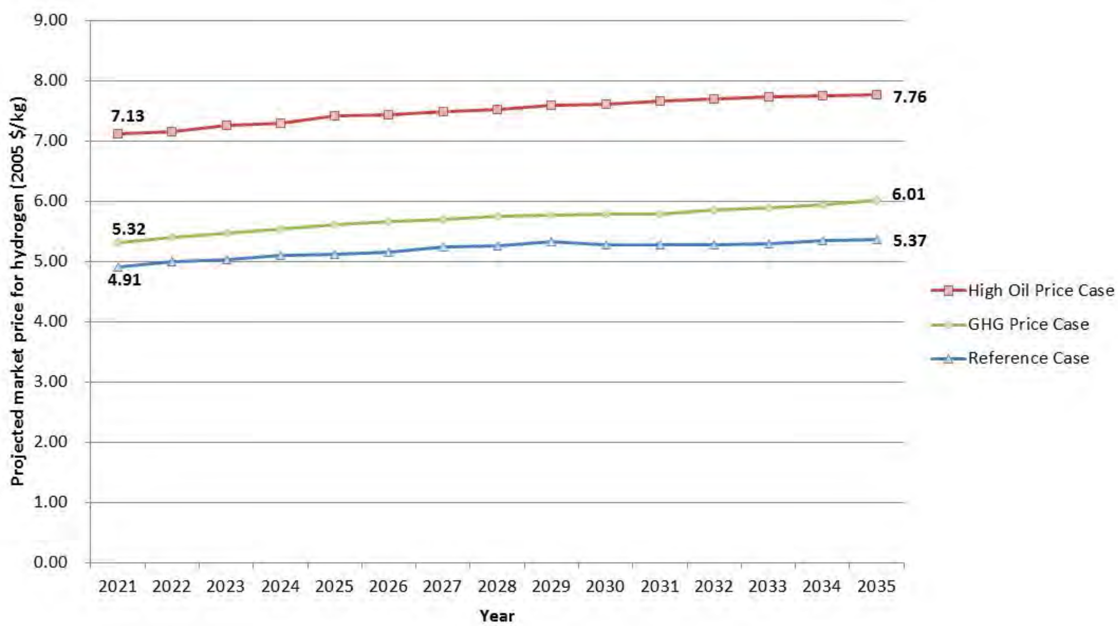

Figure 66: Projected equivalent market price for hydrogen based on three EIA AEO oil price cases [70]

Since the AEO does not project prices beyond 2035, the cumulative cash flow analysis is limited to the period up to 2035. This period represents the first fifteen years of the H_2 Success scenario (2021 to 2035) and the first eleven years of the H_2 Partial Success scenario (2025 to

---

[13] The AEO oil prices are converted from 2009 to 2005 dollars and then the oil prices are converted to equivalent hydrogen prices by assuming that HFCVs are projected to have 63% better fuel economy than gasoline HEVs.

[14] From 2021 to 2035, oil prices in 2009 dollars range from $3.39 to $3.71 in the AEO Reference case, from $4.92 to $5.36 in the High Oil Price case, and from $3.67 to $4.15 in the GHG Price Economy-wide case.

2035). This period is sufficient since a private company would expect to breakeven within the first ten years of its initial investment.

Figure 67 shows the relationship between the breakeven prices of hydrogen for the two HFCV deployment scenarios and the projected market prices for hydrogen given the three AEO oil price scenarios. Essentially, this figure indicates that the cost of supplying hydrogen remains larger than the projected market prices for several years. In the H_2 Success scenario, the breakeven price is not consistently below the market price projected in the High Oil Price scenario for nine years and does not remain below the Reference and GHG Price scenarios for 15 years. In the H_2 Partial Success scenario, the breakeven price is not consistently below the High Oil Price scenario for ten years and does not fall below the Reference scenario during the period of the cash flow analysis. Consequently, the prospects for positive cumulative cash flows in the first ten to fifteen years are not optimistic in either deployment scenario.

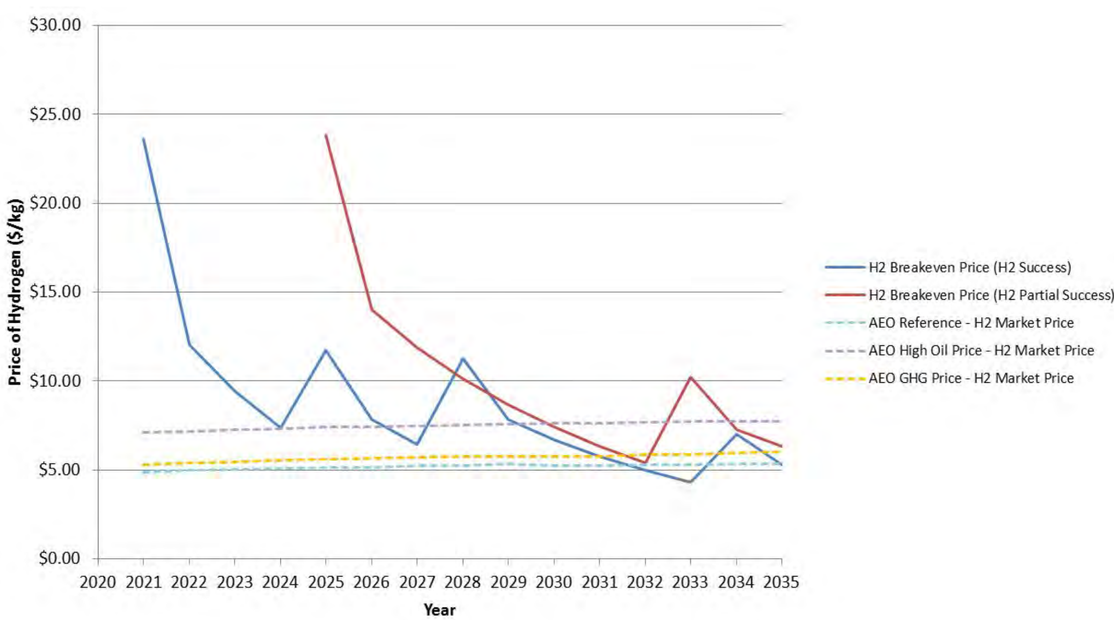

Figure 67: Relationship between the breakeven price of hydrogen and the projected H_2 market price given the three AEO oil price cases

In the H_2 Success HFCV deployment scenario, the only case in which the cumulative cash flow becomes positive by 2035 is the High Oil Price case (Figure 68). In this case, the losses continue to grow for the first nine years as the cost of producing hydrogen exceeds the market price. The cumulative cash flow reaches its lowest point in 2029 at about $18 billion. At this point, the cumulative cash flow begins an upward trajectory as annual cash flow becomes positive. However, cumulative cash flow only becomes positive in 2033 (i.e., 13 years after the first tranche is installed).

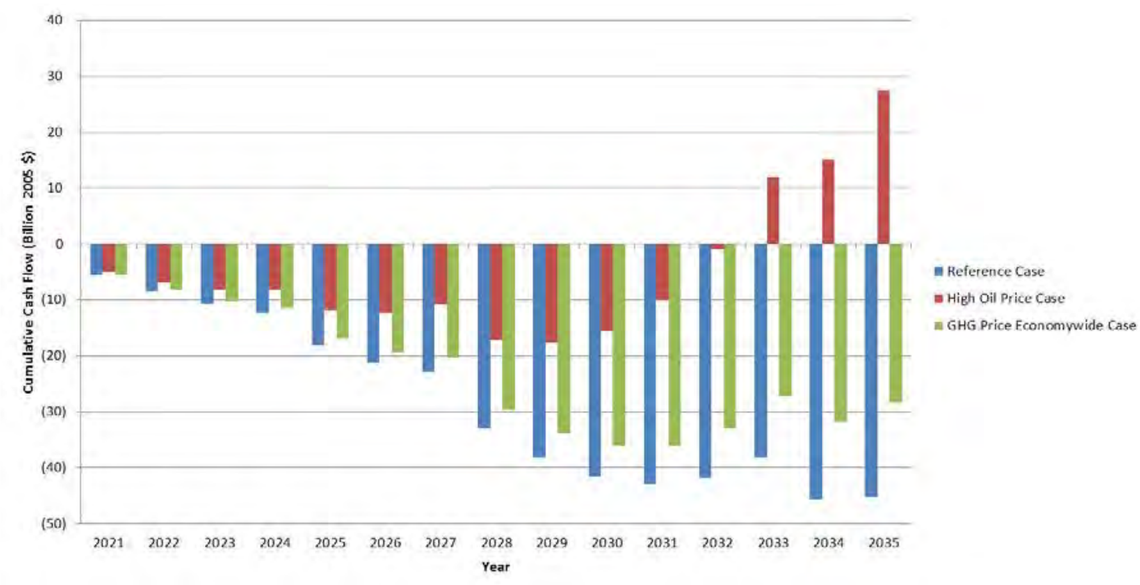

Figure 68: Cumulative cash flow in the H_2 Success scenario given the three AEO oil price cases

In the Reference case, which projects the lowest market prices for hydrogen, the cumulative cash flow reaches its lowest point with a loss of $46 billion in the year 2034 and remains strongly negative through 2035. The outlook in the GHG Price Economy-wide case is only slightly improved with the low in the cumulative cash flow occurring in the year 2030 with a loss of $36 billion. The cumulative cash flow slowly improves but the loss remains close to $30 billion in 2035. Assuming that the market price of hydrogen remains constant at the 2035 price after 2035, cumulative cash flow would expect to become positive in 2038 and 2041 for the GHG Price Economy-wide and Reference case, respectively (Figure 69).

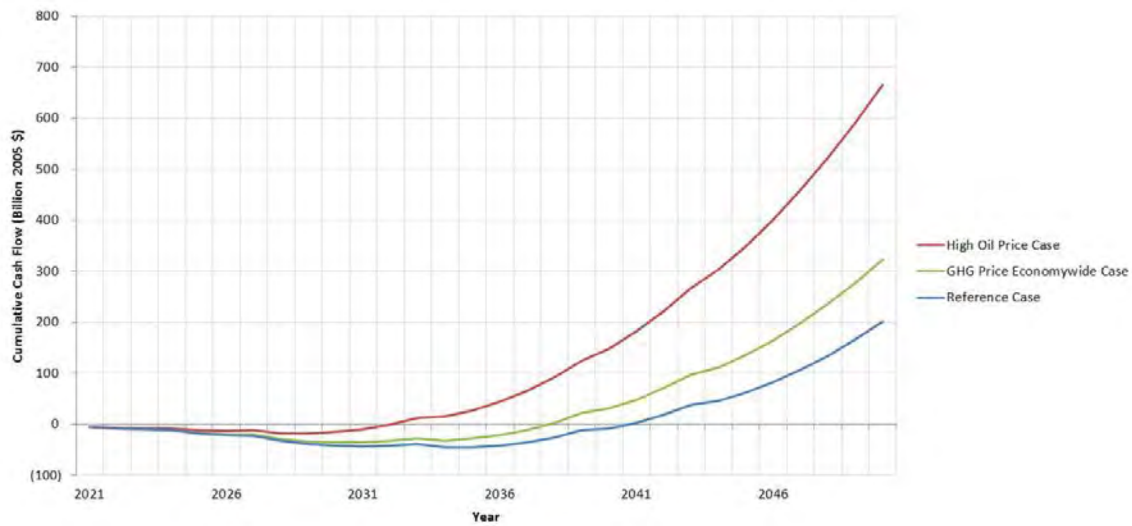

Figure 69: Cumulative cash flow over the entire study period for the H_2 Success scenario (beyond 2035, hydrogen market price is the price projected in 2035)

In the H_2 Partial Success scenario, the cumulative cash flow remains negative through 2035 in all of the AEO oil price cases (Figure 70). As expected, losses are minimized in the High Oil Price case with the cumulative cash flow reaching its low in 2029 at a loss of $8.5 billion. In both the Reference and GHG Price Economy-wide cases, the cumulative cash flow continues on a negative trajectory through 2035.

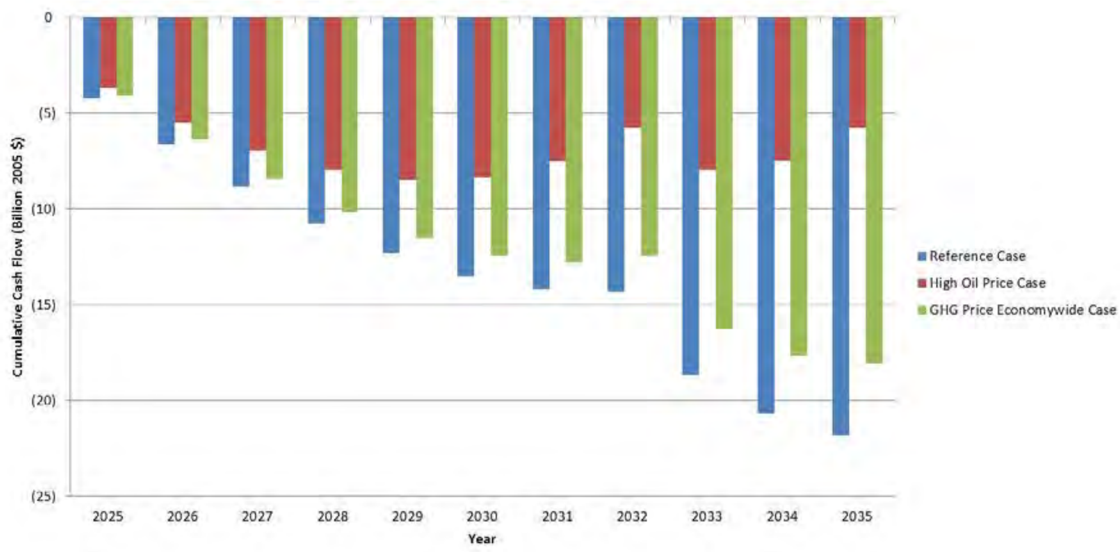

Figure 70: Cumulative cash flow in the H_2 Partial Success scenario given the three AEO oil price cases

Assuming that the hydrogen market price remains constant at the 2035 price after 2035, the cumulative cash flow is projected to become and remain positive in the High Oil Price Case in 2040 (i.e., 16 years after the first tranche installment) (Figure 71). In the Reference and GHG Price Economy-wide cases, positive cumulative cash flows are not realized for over 20 years. The cumulative cash flow analysis indicates that, without subsidies, early installment of centralized coal-based hydrogen infrastructure with CCS is not financially viable (i.e., supporting four million regional HFCVs). In the best case scenario (fast HFCV deployment and high oil prices), the cumulative cash flow does not become positive until thirteen years after the first tranche installment. Sections 4.1.3 and 4.1.4 examine whether hydrogen infrastructure can become viable with subsidies and/or if early supply is met exclusively by onsite production (i.e., centralized infrastructure is delayed).

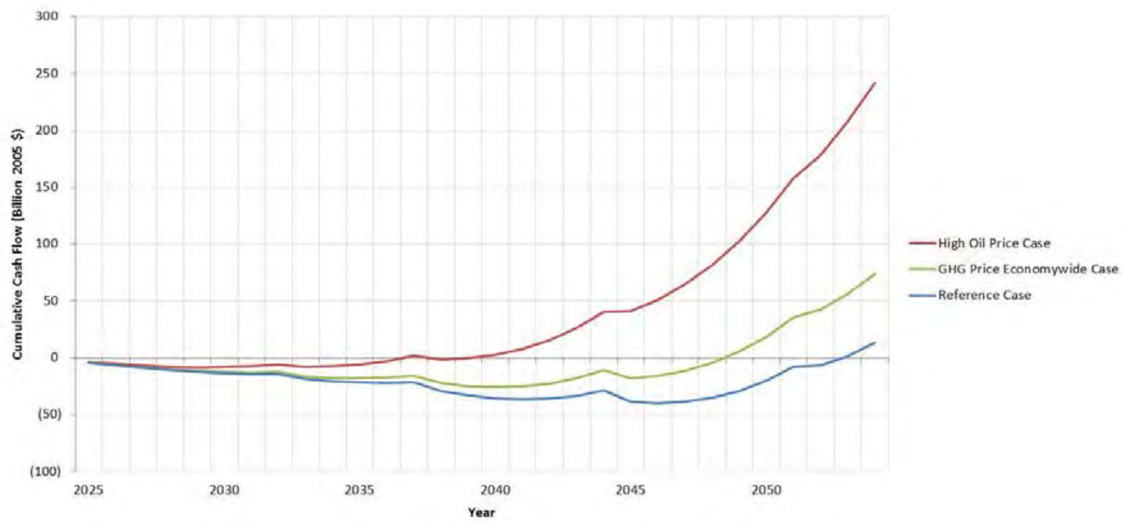

Figure 71: Cumulative cash flow over the entire study period for the H_2 Partial Success scenario (beyond 2035, hydrogen market price is the price projected in 2035)

4.1.2.4 GHG Emissions

One of the benefits of producing hydrogen using coal gasification with CCS is the ability to significantly reduce greenhouse gas (GHG) emissions in the transportation sector. In this section, the GHG emissions associated with the following three cases are quantified.

- *Business-as-Usual (BAU):* hydrogen infrastructure is installed as specified in the case study, but CCS is *not* installed at the centralized coal-based production facilities. GHG emissions associated with the power sector remain at 2005 levels.

- *Hydrogen with CCS (H_2-CCS):* coal-based hydrogen infrastructure is installed *with* CCS at the centralized production facilities, but GHG emissions associated with the power sector remain at 2005 levels.

- *Low Greenhouse Gas (GHG):* coal-based hydrogen infrastructure is installed *with* CCS and the power sector decarbonizes according to projections based on enactment of the Lieberman-Warner Climate Security Act of 2007.

In all cases, GHG emissions associated with coal gasification, steam methane reformation, electricity consumption, and fugitive emissions from CO_2 pipelines are included. GHG emissions associated with booster compression for CO_2 and H_2 pipeline transport are not included since booster compression is not explicitly modeled in this study. GHG emissions associated with coal-based hydrogen production are limited to CO_2 emissions and are calculated based on the CO_2 emission factors (kg CO_2/GJ coal) described in section 2.1.1 for each state (Table 3). In the H_2-CCS and GHG scenarios, it is assumed that 91% of the CO_2 produced is captured and stored [3]. At refueling stations with onsite hydrogen production via steam methane reformation, natural gas usage is assumed to be 4.5 Nm^3 per kg of hydrogen and the GHG emissions factor including upstream emissions is 64.1 kg CO_{2e} per GJ natural gas [10]. The fugitive emission from CO_2 pipelines is assumed to be 2.32 tonnes CO_2 per km of CO_2 pipeline per year [71].

In the BAU and H_2-CCS cases, it is assumed that GHG emissions associated with electricity production remain at 2005 levels as defined by US EPA EGrid data [39]. These data provide annual GHG emissions in the power sector (tonnes CO_{2e}) and net generation (MWh) by state, which are used to calculate a GHG emission factor (kg CO_{2e}/kWh) for each state. These emission factors range from 0.13 kg CO_{2e}/kWh in Washington, which has significant hydropower, to 1.13 kg CO_{2e}/kWh in Wyoming, which is dominated by coal-based power production.

The GHG case examines a scenario in which HFCV deployment occurs concurrently with policy that reduces GHG emissions in the power sector. The rate at which the GHG intensity of the power sector declines is modeled based on an analysis of the energy market impacts of S.2191, the Lieberman-Warner Climate Security Act of 2007, by the Energy Information Agency [72]. This study projects the impacts of S.2191 on the net availability of electricity to the grid (kWh) and total GHG emissions from the power sector (tCO_{2e}) in the United States from 2005 to 2030[15]. Based on these statistics, an average GHG intensity (tCO_{2e}/kWh) is calculated for each year in which an infrastructure tranche is built (Table 49). The GHG intensity is assumed to remain constant after 2030.

Table 49: Average GHG intensity of the power sector (kg CO_{2e}/kWh) at the beginning of each infrastructure tranche under the Lieberman-Warner Climate Security Act [72]

	Tranche 1	Tranche 2	Tranche 3	Tranche 4	Tranche 5	Tranche 6
H2 Success	0.42	0.28	0.14	0.08	0.08	0.08
H2 Partial Success	0.28	0.08	0.08	0.08	0.08	N/A

[15] The projections of the S.2191 Core Case are used in this analysis. The Core Case “represents an environment where key low-emissions technologies, including nuclear, fossil with carbon capture and sequestration (CCS), and various renewables, are developed and deployed in a timeframe consistent with the emissions reduction requirements without encountering any major obstacles, even with rapidly growing use on a very large scale, and the use of offsets, both domestic and international, is not significantly limited by cost or regulation.”

The GHG emissions associated with supplying hydrogen in each infrastructure tranche are reported in units of gCO_{2e}/mile assuming that an average HFCV has a fuel economy of 68 miles per kg H_2. These values are compared with the emissions associated with a gasoline HEV with an average fuel economy of 42 miles per gallon. The GHG emission factor associated with gasoline supplied at a refueling station is assumed to be 11 $kgCO_{2e}$ per gallon, which includes upstream emissions [10].

Business-as-Usual

In the BAU case, coal-based hydrogen production *without* CCS results in a significant increase in the average GHG intensity of a HFCV relative to a gasoline HEV (Figure 72). In each tranche, the proportion of HFCVs served by refueling stations with onsite production declines. As a result, the average GHG emissions associated with refueling stations also declines since the emissions related to steam methane reformation are eliminated. However, the shift to centralized production also means that, over time, more vehicles are served by coal-based facilities without CCS, which results in an increase in the average GHG intensity of the HFCV fleet. Between 85 to 92% of the GHG emissions in this scenario are associated with hydrogen production. In tranche 6, when all hydrogen is supplied by centralized facilities, the GHG intensity of an average HFCV is approximately 25% greater than that of an average gasoline HEV.

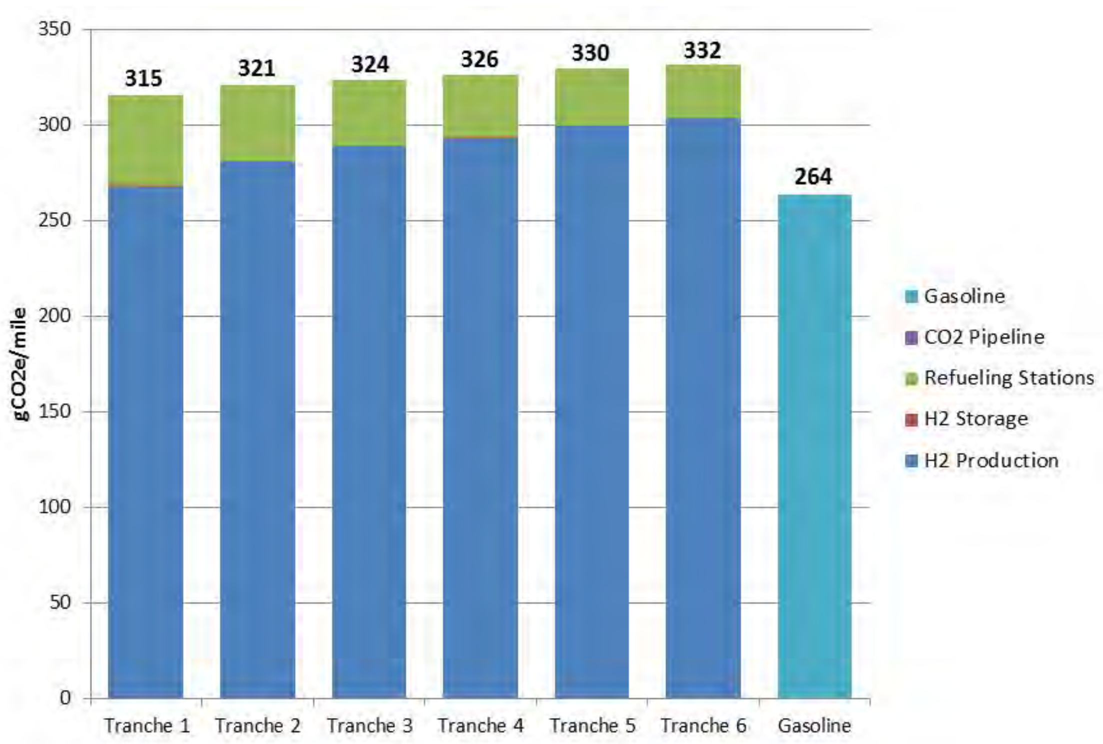

Figure 72: Average GHG intensity of the HFCV fleet in the BAU case

Hydrogen with CCS

In the H_2-CCS case, centralized coal-based hydrogen production includes CCS, which allows a significant decrease in GHG emissions to be achieved (Figure 73). Since the average GHG intensity associated with centralized production with CCS is lower than that associated with onsite production, the transition to centralized production results in a decline in the average GHG intensity of the HFCV fleet over time. This is evident in the reduction in the average GHG intensity associated with refueling stations as onsite production is phased out. However, refueling station emissions associated with electricity consumption remain significant in this case since the GHG intensity of the power sector remains at 2005 levels.

In tranche 6, when all hydrogen is supplied by centralized facilities, the GHG intensity of an average HFCV is approximately 80% lower than that of an average gasoline HEV. The BAU and

H_2-CCS cases illustrate the importance of CCS in achieving a reduction in GHG emissions associated with coal-based hydrogen. The GHG emissions associated with fugitive emissions from CO_2 pipelines and compression at H_2 storage facilities are negligible.

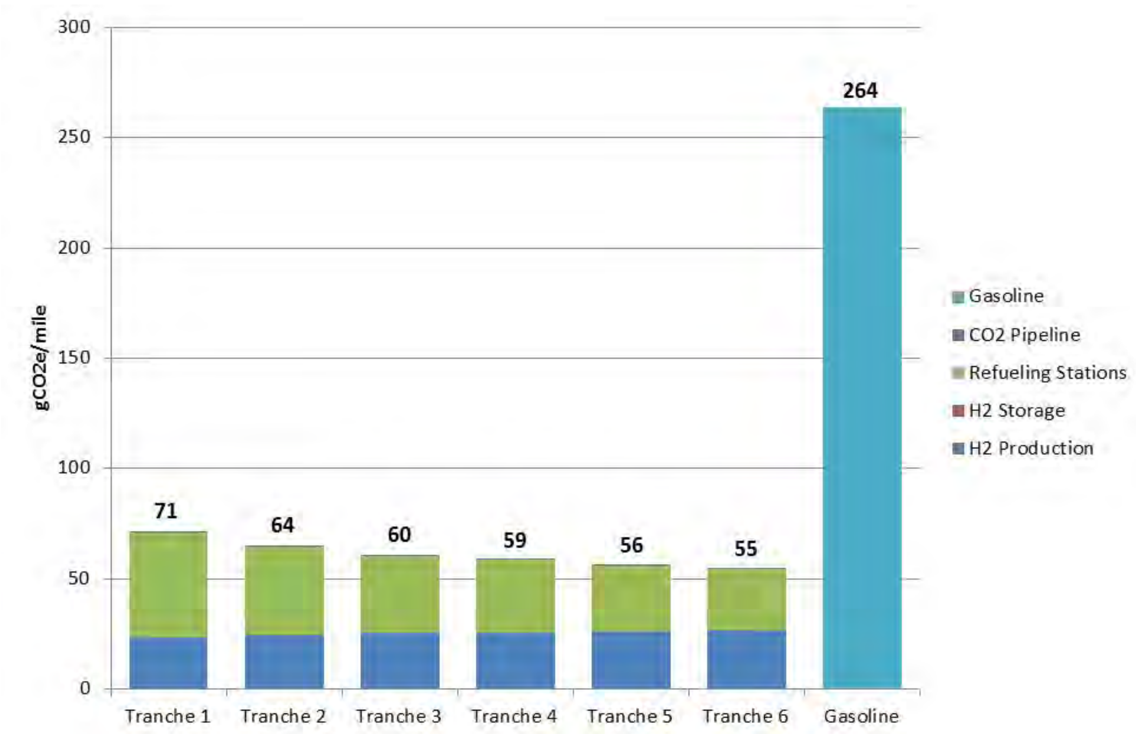

Figure 73: Average GHG intensity of the HFCV fleet in the H_2-CCS case

Low Greenhouse Gas

In the GHG case, it is assumed that the Lieberman-Warner Climate Security Act (S.2191) has been enacted, which incentivizes a reduction in GHG emissions throughout the economy. As a result, not only is CCS installed on the centralized hydrogen production facilities, but reductions in the GHG intensity of the power sector are also achieved. Based on modeling conducted by the EIA, S.2191 would reduce the average GHG intensity of the power sector by 32% in 2021 (relative to 2005) when the first tranche is installed in the H_2 Success scenario. In 2030 and beyond, the reduction would be 88% relative to the 2005 value.

As a result of the significant reduction in power sector GHG intensity, a large decrease in the emissions associated with electricity consumption for H_2 storage and refueling stations is achieved (Figure 74). This reduction is particularly evident for refueling stations where the average GHG intensity is reduced to ~1 gCO_{2e}/mile in tranche 6 once onsite production is completely phased out. In the H_2 Success scenario[16], the GHG intensity of an average HFCV is approximately 77% lower than that of an average gasoline HEV in tranche 1 and 90% lower in tranche 6.

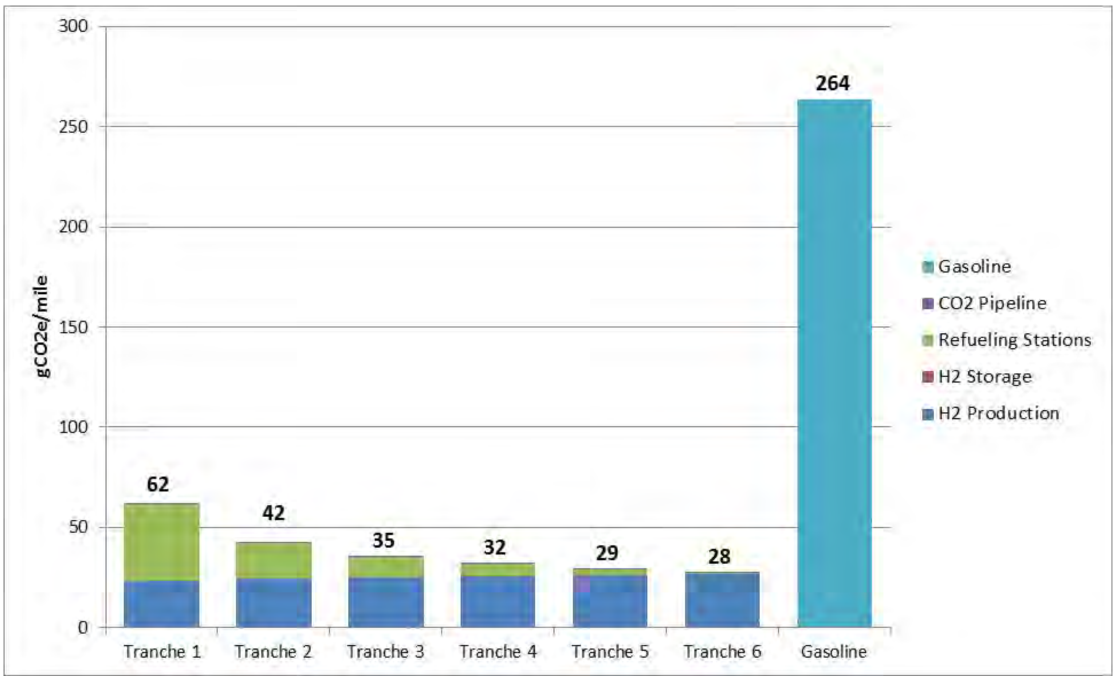

Figure 74: Average GHG intensity of the HFCV fleet in the GHG case under the H2 Success scenario

4.1.2.5 Coal Consumption

In the two HFCV market penetration scenarios, hydrogen is supplied primarily by coal-based production facilities. This section quantifies the coal consumption attributed to H_2 production

[16] Average GHG intensity is 1-2% lower in the first three tranches of the H_2 Partial Success scenario since the installation of these tranches is delayed, which results in slightly lower power sector GHG intensities associated with the year of installation.

and compares it with two projections of future coal consumption in the study region. Specifically, the coal consumption projections of the Reference and GHG Price Economy-wide cases in the EIA Annual Energy Outlook are examined [70]. The national projections provided in this report are converted to regional projections assuming that 30% of national coal consumption occurs in the study region [73]. The projections in the AEO are provided to the year 2035. Beyond this year, the projections are extended based on the average annual growth rate from 2009 to 2035 (0.8% for the Reference case and -2.7% for the GHG Price Economy-wide case) [70].

Reference Case

In the Reference case, economy-wide coal consumption (not including H_2 production) is projected to increase 30% between 2010 and 2050. In the H_2 Success scenario, hydrogen production in the first ten years (i.e., 2021 to 2030) increases coal consumption by about 7% relative to the base consumption in 2010 (Table 50). However, by 2050, hydrogen production increases consumption by approximately 50%. In total, coal consumption is projected to increase by 80% relative to the 2010 level, of which almost two-thirds of the increase is attributable to hydrogen production (Figure 75).

In the H_2 Partial Success scenario, slower HFCV market penetration translates to less hydrogen demand and, thus, less hydrogen produced. As a result, there is less coal consumption associated with H_2 production in this scenario (Figure 75). By 2030, H_2 production increases coal consumption by less than 3% relative to the base consumption in 2010. In 2050, total coal consumption is projected to increase by 50% with less than half of the increase attributed to hydrogen production.

Table 50: Projected coal consumption and % increase relative to 2010 for the Reference case

Year	2010	2025	2030	2040	2050
H_2 Success					
Coal Consumption (PJ/yr)					
Base (Existing Sectors)	6745	7245	7495	8103	8775
H_2 Production	0	174	489	1773	3428
Total Consumption	6745	7419	7984	9877	12204
Percent increase from 2010 consumption (%)					
Base (Existing Sectors)	N/A	7.4%	11.1%	20.1%	30.1%
H_2 Production	N/A	2.6%	7.2%	26.3%	50.8%
Total Consumption	N/A	10.0%	18.4%	46.4%	80.9%
H_2 Partial Success					
Coal Consumption (PJ/yr)					
Base (Existing Sectors)	6745	7245	7495	8103	8775
H_2 Production	0	42	103	478	1401
Total Consumption	6745	7287	7598	8582	10177
Percent increase from 2010 consumption (%)					
Base (Existing Sectors)	N/A	7.4%	11.1%	20.1%	30.1%
H_2 Production	N/A	0.6%	1.5%	7.1%	20.8%
Total Consumption	N/A	8.0%	12.6%	27.2%	50.9%

GHG Price Economy-wide Case

In this case, it is assumed that a CO_2 price will shift the power sector to cleaner feedstocks and, thus, the consumption of coal (not including H_2 production) is projected to decrease by 70% from 2010 to 2050 (Figure 76). With rapid HFCV deployment in the H_2 Success scenario, coal consumption associated with H_2 production increases and accounts for over half of the coal consumed in 2050. However, total coal consumption in 2050 is projected to decline by about 19% relative to the 2010 level in this scenario (Table 51).

In the H_2 Partial Success scenario, less coal is consumed for H_2 production and, thus, a nearly 50% decline in total coal consumption is projected in 2050 (Table 51). Of the total coal consumed in 2050, about 40% is attributed to H_2 production.

Table 51: Projected coal consumption and % increase relative to 2010 for the GHG Price Economy-wide case

Year	2010	2025	2030	2040	2050
H_2 Success					
Coal Consumption (PJ/yr)					
Base (Existing Sectors)	6858	4288	3906	2719	2068
H_2 Production	0	174	489	1773	3428
Total Consumption	6858	4461	4395	4493	5496
Percent increase from 2010 consumption (%)					
Base (Existing Sectors)	N/A	(36.4%)	(42.1%)	(59.7%)	(69.3%)
H_2 Production	N/A	2.6%	7.2%	26.3%	50.8%
Total Consumption	N/A	(33.9%)	(34.8%)	(33.4%)	(18.5%)
H_2 Partial Success					
Coal Consumption (PJ/yr)					
Base (Existing Sectors)	6858	4288	3906	2719	2068
H_2 Production	0	42	103	478	1401
Total Consumption	6858	4330	4009	3197	3469
Percent increase from 2010 consumption (%)					
Base (Existing Sectors)	N/A	(36.4%)	(42.1%)	(59.7%)	(69.3%)
H_2 Production	N/A	0.6%	1.5%	7.1%	20.8%
Total Consumption	N/A	(35.8%)	(40.6%)	(52.6%)	(48.6%)

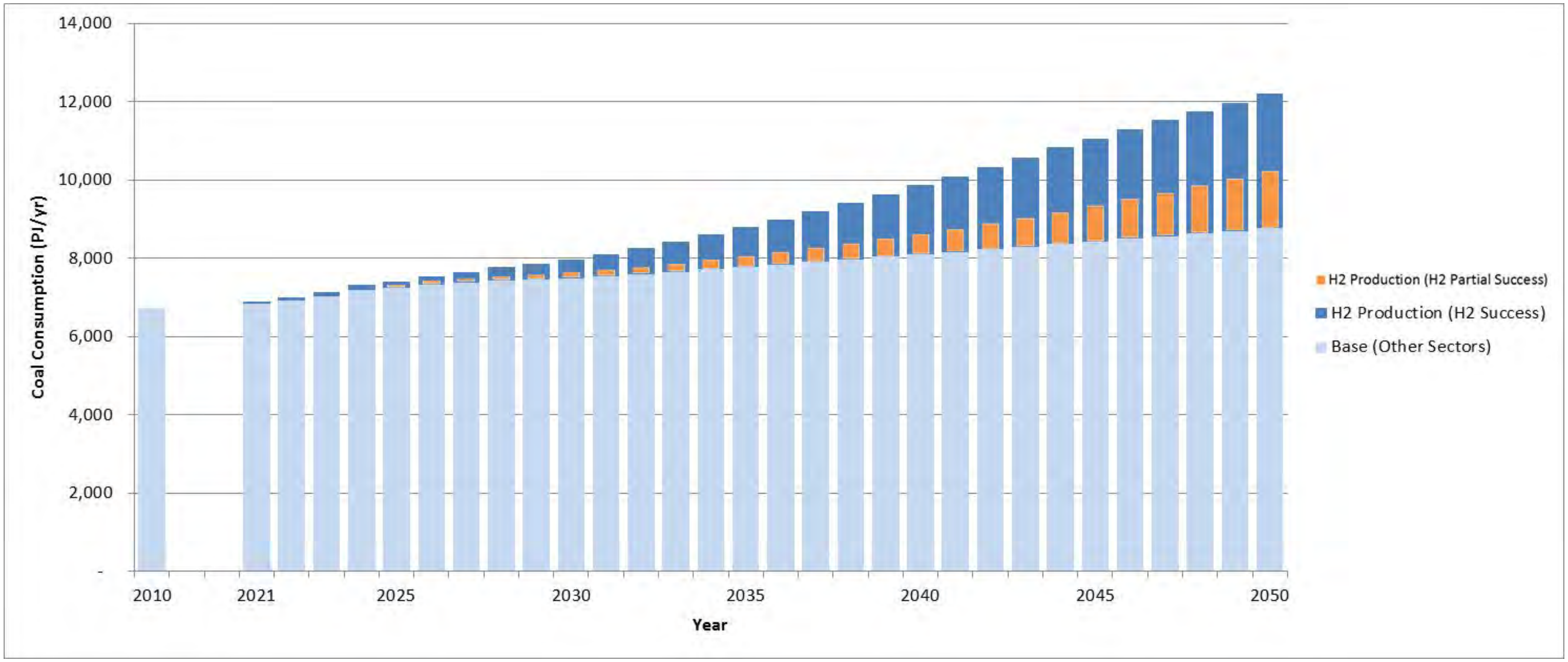

Figure 75: Projected coal consumption (PJ/yr) to 2050 for the Reference case

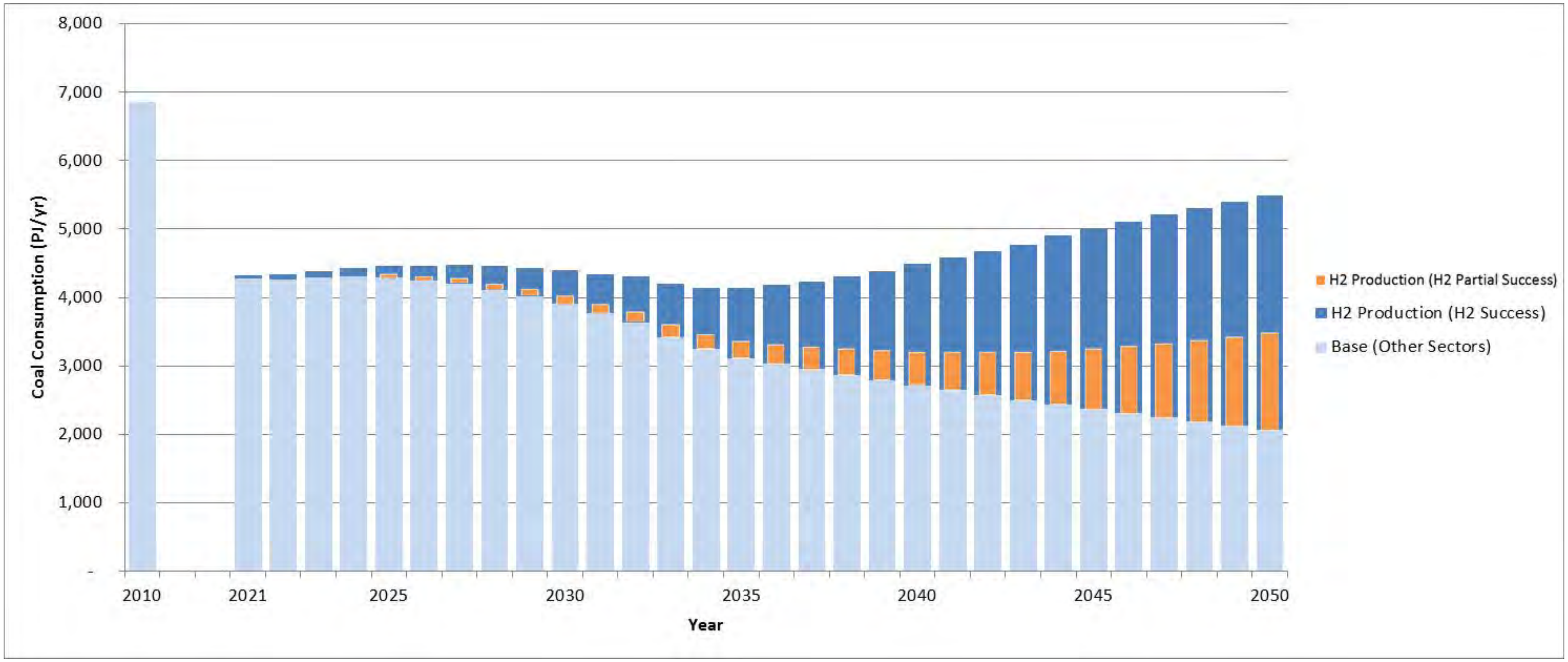

Figure 76: Projected coal consumption (PJ/yr) to 2050 for the GHG Price Economy-wide case

4.1.2.6 CO_2 Storage Capacity

The National Carbon Sequestration Database (NATCARB) provides data on the CO_2 storage capacities of saline aquifers within the study region [44]. In this section, the CO_2 storage requirements of H_2 production facilities are compared with the total storage capacity within the region in order to identify any CO_2 storage limitations. The saline aquifers provided by NATCARB are grouped into twelve storage basins (Figure 77). Table 52 compares the high and low estimates of CO_2 storage capacity for each basin with the CO_2 storage requirements identified by the *Hydrogen Infrastructure Deployment Model*.

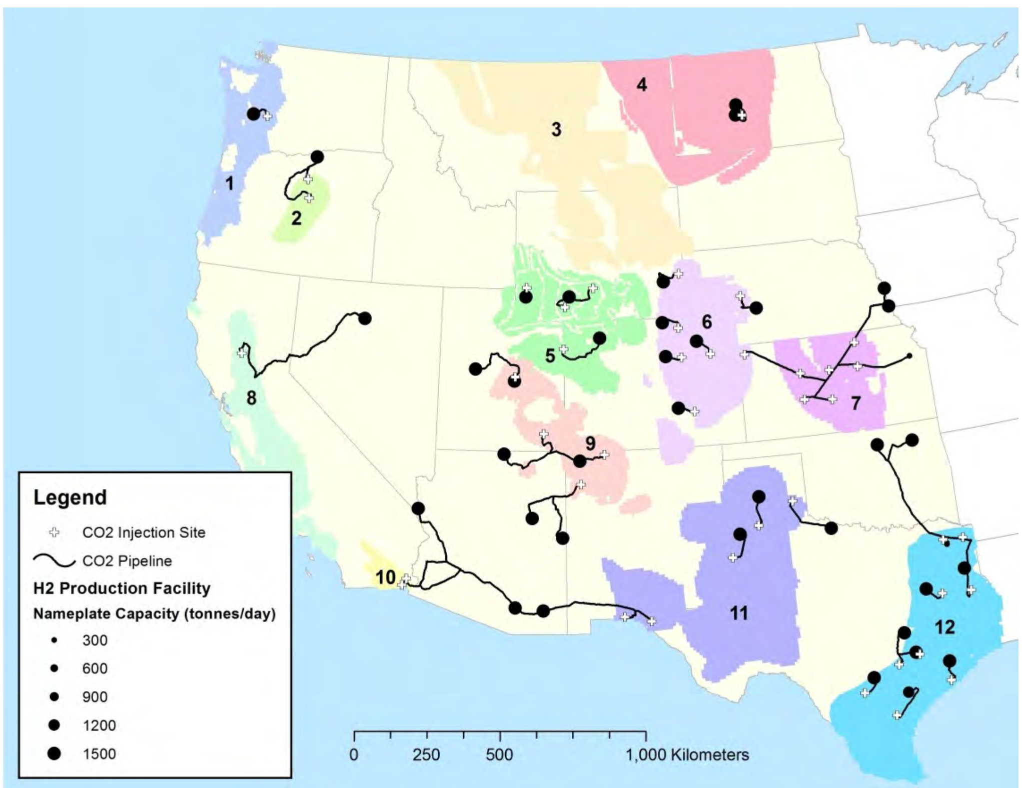

Figure 77: CO_2 storage basins and CCS infrastructure deployment in tranche 6

The CO_2 storage requirement associated with the lifetime operation of the coal-based H_2 production facilities installed in all tranches is less than 10% of the *low estimate* of storage capacity within all but three basins (2, 7, and 10). Of these basins, only basin 7 exhibits any limitations associated with storing the CO_2 associated with H_2 production. In particular, low CO_2 storage capacity results in the development of seven disposal sites for three production facilities and the final disposal site is located in basin 6. Thus, if CCS technology was also installed in the power and industrial sectors, the region surrounding basin 7 would likely experience CO_2 storage capacity constraints and any additional sources might require long CO_2 pipelines to other basins. Basins 2 and 10 might also experience some limitations if CCS were adopted in the power and industrial sectors. The remaining basins appear to have sufficient storage capacity and the CO_2 captured at H_2 production facilities utilizes only 1.4% of the *low estimate* of total aquifer storage capacity in the study region. If the *high* capacity estimate is considered, no basins experience capacity constraints and the CO_2 captured at H_2 production facilities utilizes only 0.1% of total aquifer storage capacity over the lifetime of all facilities.

Table 52: Summary statistics for CO_2 storage basins

Basin	CO_2 Storage Capacity – Low Estimate (Gt)	CO_2 Storage Capacity – High Estimate (Gt)	# of potential storage sites	# of developed storage sites	Total CO_2 Stored* (Gt)	% of Low Estimate	% of High Estimate
1	42	571	9	1	0.3	0.8%	0.1%
2	0.8	12	7	2	0.3	38.6%	2.8%
3	111	1523	19	0	0.0	0.0%	0.0%
4	169	914	22	1	0.6	0.4%	0.1%
5	69	953	21	4	1.0	1.4%	0.1%
6	43	357	20	7	2.3	5.3%	0.6%
7	0.4	6	15	6	0.3	73.8%	5.4%
8	28	380	8	1	0.3	1.1%	0.1%
9	20	281	17	4	1.9	9.2%	0.7%
10	3	37	2	2	0.3	11.6%	0.8%
11	156	2150	39	5	1.6	1.0%	0.1%
12	210	2886	18	9	2.9	1.4%	0.1%
Total	852	10069	197	42	11.9	1.4%	0.1%

* Total CO_2 stored is the cumulative CO_2 stored over the 40-year lifetime of all production facilities

In examining the capacity utilization at individual storage sites, the same pattern emerges with high utilization (i.e., greater than 90%) occurring in the basins with the lowest CO_2 storage density (Gt CO_2/10,000 km^2 grid cell) (Figure 78). Basin 7 has particularly low CO_2 storage density and, consequently, the disposal sites can handle only small quantities of CO_2. These sites quickly reach full capacity and multiple sites are required to meet local CO_2 storage requirements (Table 53). However, most individual storage sites use only a small fraction of their potential CO_2 capacity.

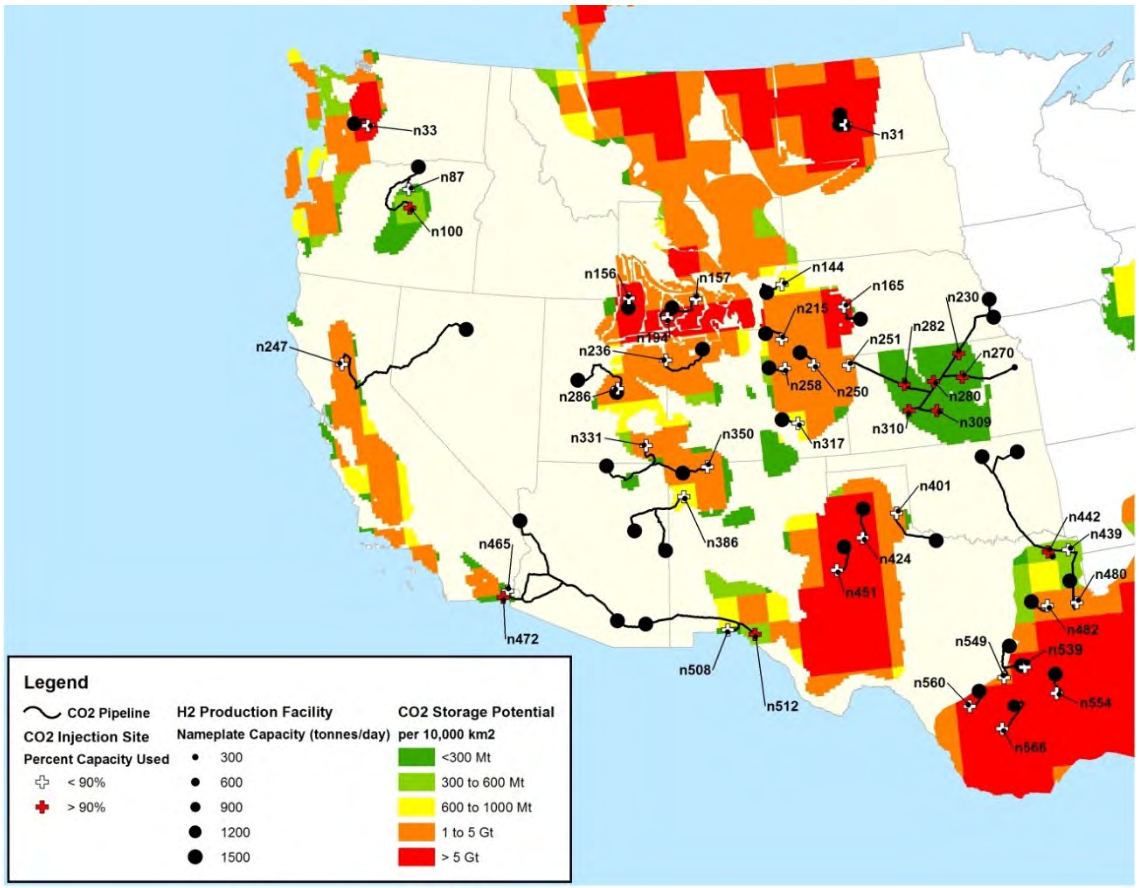

Figure 78: CO_2 storage capacity and percent utilization of developed storage sites

Table 53: Percent of total CO_2 storage capacity utilized at each developed storage site (sites with >90% utilization highlighted in red)

			Tranche 1		Tranche 2		Tranche 3		Tranche 4		Tranche 5		Tranche 6	
Basin	Storage Site ID	Total CO_2 Storage Capacity – Low Estimate (Gt)	CO_2 Stored (Gt)	% of Total Capacity	CO_2 Stored (Gt)	% of Total Capacity	CO_2 Stored (Gt)	% of Total Capacity	CO_2 Stored (Gt)	% of Total Capacity	CO_2 Stored (Gt)	% of Total Capacity	CO_2 Stored (Gt)	% of Total Capacity
1	N33	10.4	0.04	0.4%	0.09	0.9%	0.29	2.8%	0.32	3.1%	0.32	3.1%	0.32	3.1%
2	N100	0.4							0.24	66.9%	0.32	90.1%	0.32	90.1%
	N87	0.1									<0.01	5.4%	<0.01	5.4%
4	N31	19.3									0.53	2.7%	0.63	3.3%
5	N194	5.6	0.31	5.6%	0.31	5.6%	0.31	5.6%	0.31	5.6%	0.31	5.6%	0.31	5.6%
	N157	4.1			0.01	0.2%	0.01	0.2%	0.01	0.2%	0.01	0.2%	0.01	0.2%
	N156	5.6							0.32	5.8%	0.32	5.8%	0.32	5.8%
	N236	2.5									0.32	12.6%	0.32	12.6%
6	N258	1.6					0.06	3.9%	0.32	19.4%	0.32	19.4%	0.32	19.4%
	N144	0.9							0.32	34.0%	0.32	34.0%	0.32	34.0%
	N317	0.6									0.13	21.0%	0.32	52.6%
	N165	12.6									0.19	1.5%	0.32	2.6%
	N251	1.4									0.32	22.0%	0.38	26.5%
	N215	1.7											0.32	18.6%
	N250	2.0											0.32	16.0%
7	N280	0.05			0.05	90.6%	0.05	100%	0.05	100%	0.05	100%	0.05	100%
	N310	0.04					0.04	100%	0.04	100%	0.04	100%	0.04	100%
	N230	0.04					0.04	100%	0.04	100%	0.04	100%	0.04	100%
	N282	0.05					0.05	100%	0.05	100%	0.05	100%	0.05	100%
	N270	0.07					0.06	90.1%	0.06	90.1%	0.07	100%	0.07	100%
	N309	0.07					0.07	100%	0.07	100%	0.07	100%	0.07	100%
8	N247	2.4					0.12	4.8%	0.12	4.8%	0.31	13.0%	0.32	13.1%
9	N386	0.8			0.30	35.3%	0.31	37.3%	0.63	74.9%	0.63	74.9%	0.63	74.9%
	N286	4.0					0.31	7.8%	0.31	7.8%	0.62	15.6%	0.62	15.6%
	N331	1.7							0.32	19.0%	0.32	19.0%	0.32	19.2%
	N350	2.0											0.31	15.6%
10	N465	0.2	0.10	41.5%	0.12	48.4%	0.12	48.4%	0.12	48.4%	0.12	48.4%	0.12	48.4%
	N472	0.2									0.20	92.3%	0.20	92.3%
11	N508	0.1			0.05	36.7%	0.05	36.7%	0.05	36.7%	0.10	81.4%	0.10	81.4%
	N512	0.6					0.46	83.1%	0.53	94.5%	0.53	94.5%	0.53	94.5%
	N401	4.3											0.32	7.5%
	N424	8.5											0.32	3.8%
	N451	7.2											0.32	4.5%
12	N549	2.0	0.10	5.1%	0.24	12.4%	0.32	16.0%	0.32	16.3%	0.32	16.3%	0.33	16.5%
	N554	17.1					0.13	0.8%	0.32	1.9%	0.32	1.9%	0.32	1.9%
	N560	5.0							0.31	6.2%	0.32	6.4%	0.32	6.4%
	N442	0.4							0.32	71.9%	0.32	71.9%	0.45	100%
	N539	9.1									0.26	2.8%	0.32	3.5%
	N480	4.6									0.12	2.6%	0.32	6.9%
	N566	12.8											0.26	2.0%
	N439	0.4											0.26	64.4%
	N482	3.1											0.32	10.5%

4.1.3 Onsite Production Cases

Given the poor economics associated with early installation of centralized hydrogen infrastructure, this section examines two alternative cases in which centralized infrastructure is delayed until the second and third tranches. These cases examine whether the economics associated with hydrogen supply can be improved if centralized infrastructure is delayed.

4.1.3.1 Centralized Infrastructure Delayed to Tranche 2

In this case, the development of centralized coal-based hydrogen production is delayed until tranche 2. Thus, all hydrogen is supplied in the first tranche by onsite production using steam methane reformation at individual refueling stations. In the second tranche, the infrastructure reverts to the designs described in sections 4.1.2.1 and 4.1.2.2 (i.e., a mix of centralized and onsite production).

Cost

In the H_2 Success scenario, centralized infrastructure is delayed four years until the year 2025. The delay substantially improves the cumulative cash flow during the first tranche with positive cash flow realized within the first three years in the High Oil Price case and very small losses in the other AEO oil price cases (Figure 79). However, the large investment in centralized infrastructure in the second tranche pushes the cumulative cash flow back into negative territory in the year 2025. Although delaying centralized infrastructure does reduce the maximum cumulative loss and, thus, the total subsidy that might be required in the High Oil Price case, it does not change the year in which supplying hydrogen becomes profitable in any of the AEO oil price cases (Figure 80).

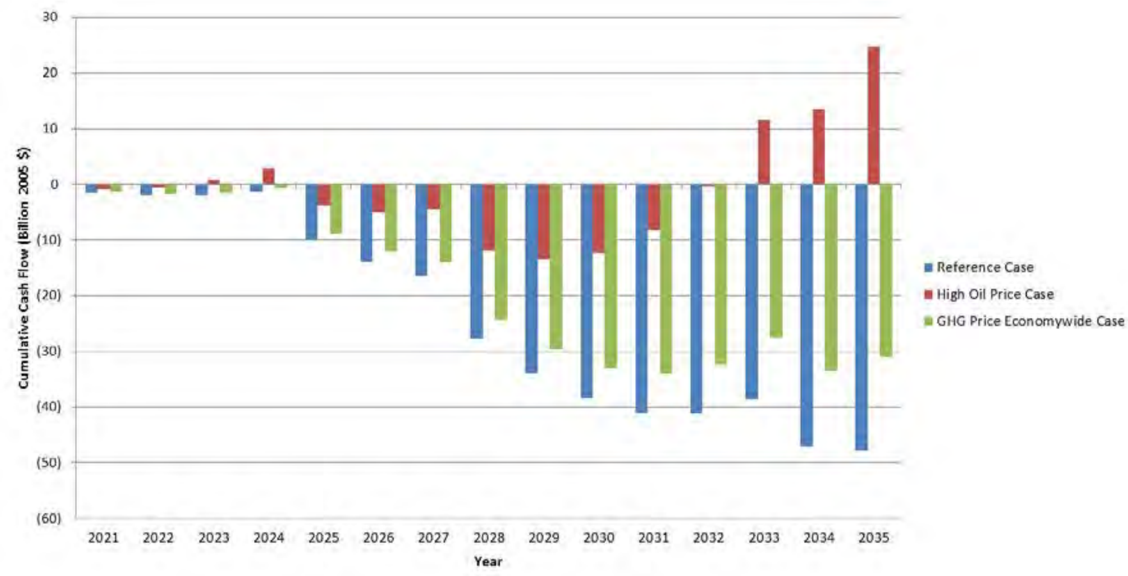

Figure 79: Cumulative cash flow in the H_2 Success scenario with centralized infrastructure delayed until tranche 2

In the H_2 Partial Success scenario, centralized infrastructure is delayed for eight years until the year 2033. Although the refueling stations with onsite production are underutilized initially, positive cumulative cash flow is achieved within the first five years in the High Oil Price case (Figure 81). The profits accumulated before centralized infrastructure is introduced in the second tranche are sufficient to maintain positive cumulative cash flow throughout the remainder of the analysis period. In the Reference and GHG Price Economy-wide cases, cumulative cash flow is improved during the first tranche, but losses grow once centralized infrastructure is introduced. Ultimately, delaying the introduction of centralized infrastructure does not change the year in which supplying hydrogen becomes profitable in the Reference and GHG Price Economy-wide cases (Figure 82).

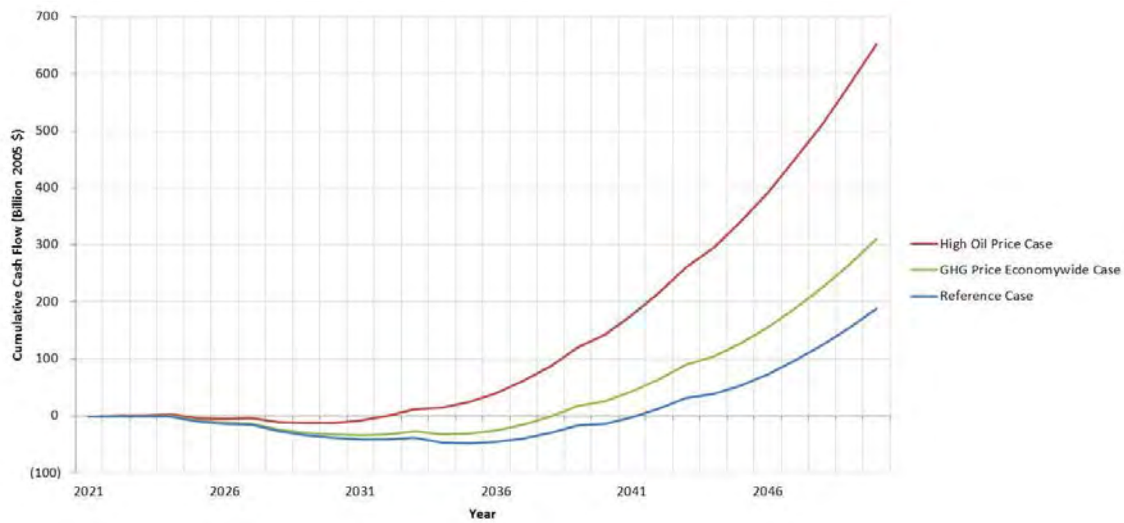

Figure 80: Cumulative cash flow over the entire study period for the H_2 Success scenario with centralized infrastructure delayed until tranche 2 (beyond 2035, hydrogen market price is the price projected in 2035)

Figure 81: Cumulative cash flow in the H_2 Partial Success scenario with centralized infrastructure delayed until tranche 2

Although delaying the introduction of centralized infrastructure improves the economics of hydrogen supply in the near-term, it does not alter the long-term economics except in the case with high oil prices and slow deployment of HFCVs (i.e., H_2 Partial Success scenario). In this case, utilizing onsite production in the first tranche does accelerate profitability since deployment of this infrastructure is more flexible and the economics rely less on economies-of-scale than large regional centralized infrastructure.

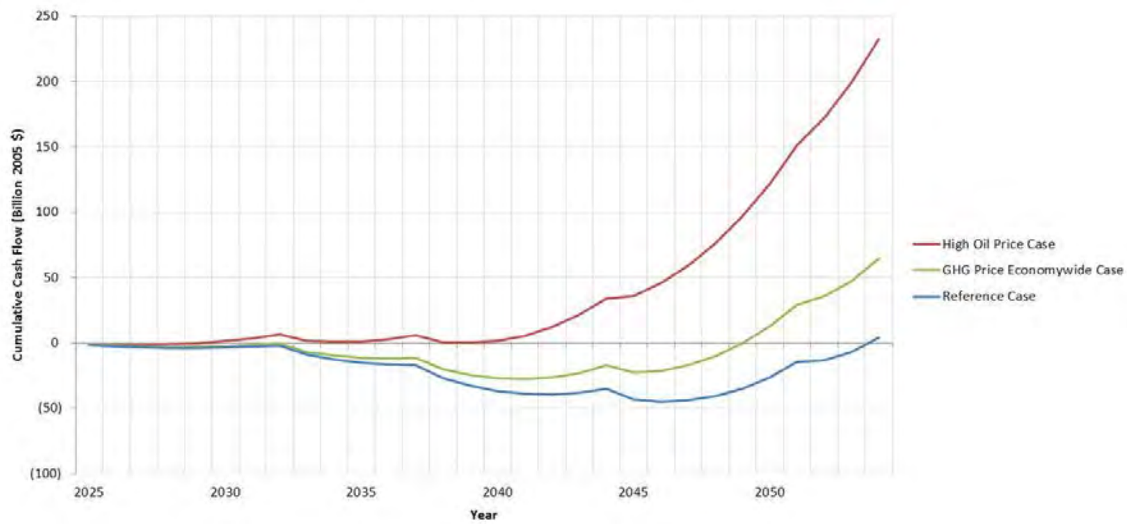

Figure 82: Cumulative cash flow over the entire study period for the H_2 Partial Success scenario with centralized infrastructure delayed until tranche 2 (beyond 2035, hydrogen market price is the price projected in 2035)

GHG Emissions

Although delaying centralized infrastructure does reduce near-term infrastructure costs, onsite production using steam methane reformation is also expected to increase GHG emissions relative to centralized coal-based production with CCS. In this section, the difference in GHG emissions is quantified to determine whether the higher cost of centralized infrastructure could be justified by lower GHG emissions. Figure 83 indicates that HFCVs supplied by onsite production can achieve a 27% reduction in GHG emissions relative to a gasoline HEV. In comparison, HFCVs supplied by centralized coal-based production with CCS can achieve an almost 80% reduction.

Despite the three-fold reduction achieved by centralized infrastructure with CCS, HFCVs constitute a very small percentage of the total LDV fleet during the period that centralized infrastructure is delayed. In addition, even when centralized infrastructure is installed, some demand centers are still supplied by onsite production and, thus, the HFCV fleet does not achieve the full 80% reduction. Consequently, the difference in the reduction of fleet-wide GHG emissions during this period is projected to be small.

Assuming that all gasoline vehicles are HEVs with an average GHG intensity of 264 gCO_{2e}/mile, the deployment of HFCVs under the H_2 Success scenario would reduce the annual GHG emissions of the national LDV fleet by an average of 0.5% from 2021 to 2024 if centralized infrastructure is delayed. In contrast, if centralized infrastructure with CCS is not delayed, the reduction would be 1.3%, a difference of less than 1% in fleet-wide emissions. This analysis indicates that the increase in GHG emissions associated with a delay in centralized infrastructure is not sufficient to justify installing centralized infrastructure at a higher cost.

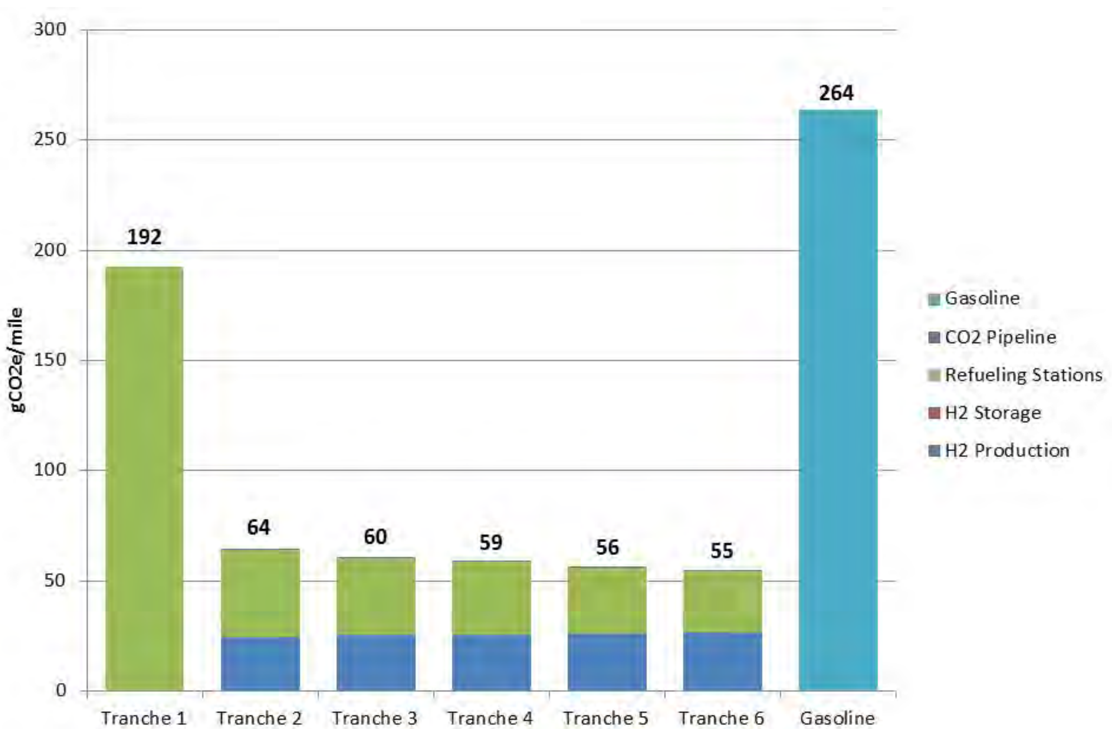

Figure 83: Average GHG intensity of the HFCV fleet in the H_2-CCS case when centralized infrastructure is delayed until tranche 2

4.1.3.2 Centralized Infrastructure Delayed to Tranche 3

In this case, centralized infrastructure is delayed until the third tranche. In the first two tranches, hydrogen is supplied exclusively by onsite production at each refueling station. In tranche 3, the infrastructure reverts to the designs described in sections 4.1.2.1 and 4.1.2.2.

Cost

In the H_2 Success scenario, centralized infrastructure is delayed for seven years until the year 2028. Utilizing onsite production improves the cash flow with cumulative cash flow becoming positive within the first three years in the High Oil Price case and within seven years in the GHG Price Economy-wide case (Figure 84). However, when centralized infrastructure is installed in 2029, the cumulative cash flow becomes negative in all AEO price cases. The maximum loss is significantly reduced to $1.6 billion in the High Oil Price case and the point at which cumulative cash flow remains positive occurs two years earlier than in the case in which centralized infrastructure is built in tranche 1.

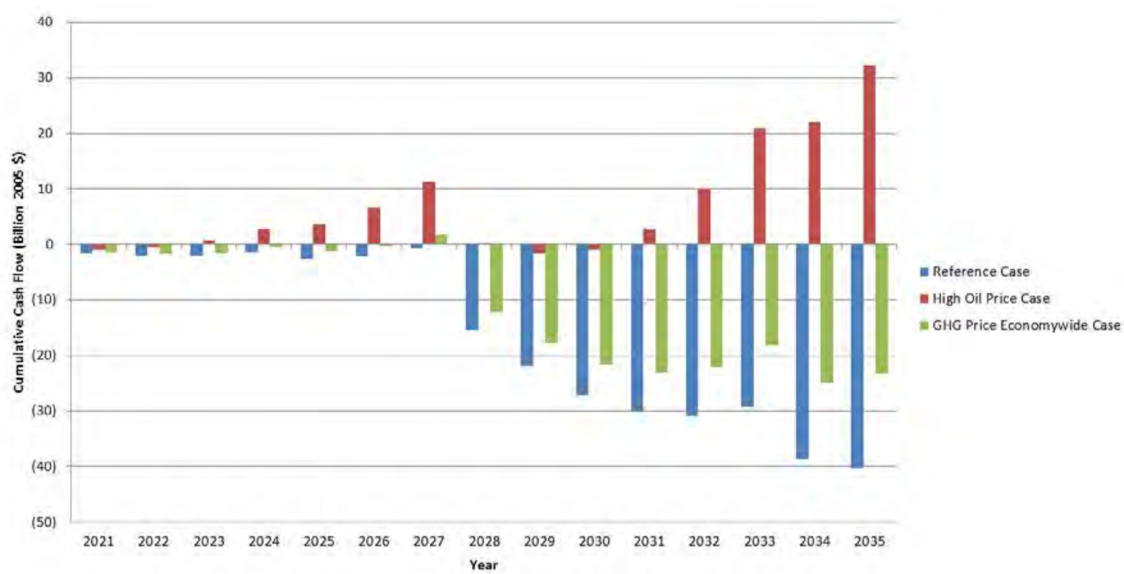

Figure 84: Cumulative cash flow in the H_2 Success scenario with centralized infrastructure delayed until tranche 3

In the GHG Price Economy-wide and References cases, delaying centralized infrastructure does not accelerate the time at which cumulative cash flow remains positive (Figure 85). Ultimately, the magnitude of the centralized infrastructure installed over the analysis period is the same whether centralized infrastructure is delayed or not. In fact, the cumulative capital investment is larger in most tranches as a result of the additional capital required for steam methane reformers in the first two tranches.

In the H_2 Partial Success scenario, centralized infrastructure is delayed for 13 years until the year 2038. The cumulative cash flow becomes positive within five years in the High Oil Price case and within the first eleven years in the GHG Price Economy-wide case (Figure 86). The High Oil Price case maintains strong profitability throughout the remainder of the analysis period. However, the introduction of centralized infrastructure results in negative cumulative cash flows for the other AEO price cases. In fact, delaying centralized infrastructure for two tranches increases the long-term costs and delays the year in which the cumulative cash flow remains positive in the Reference and GHG Price Economy-wide cases (Figure 87).

By delaying the large capital expenditures required for centralized infrastructure, supplying hydrogen with onsite production serves to reduce near-term hydrogen costs and improve the cumulative cash flow. However, the hydrogen price must be high (i.e., High Oil Price case) for the long-term profitability of supplying hydrogen to be improved. If hydrogen prices are not high, some type of subsidy will be required to make the business of supplying hydrogen economically viable.

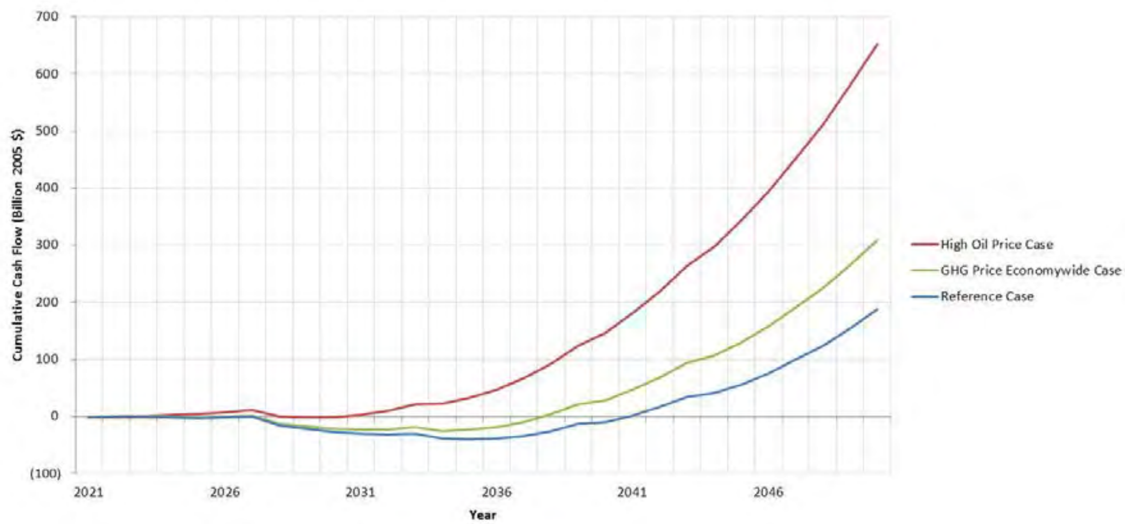

Figure 85: Cumulative cash flow over the entire study period for the H_2 Success scenario with centralized infrastructure delayed until tranche 3 (beyond 2035, hydrogen market price is the price projected in 2035)

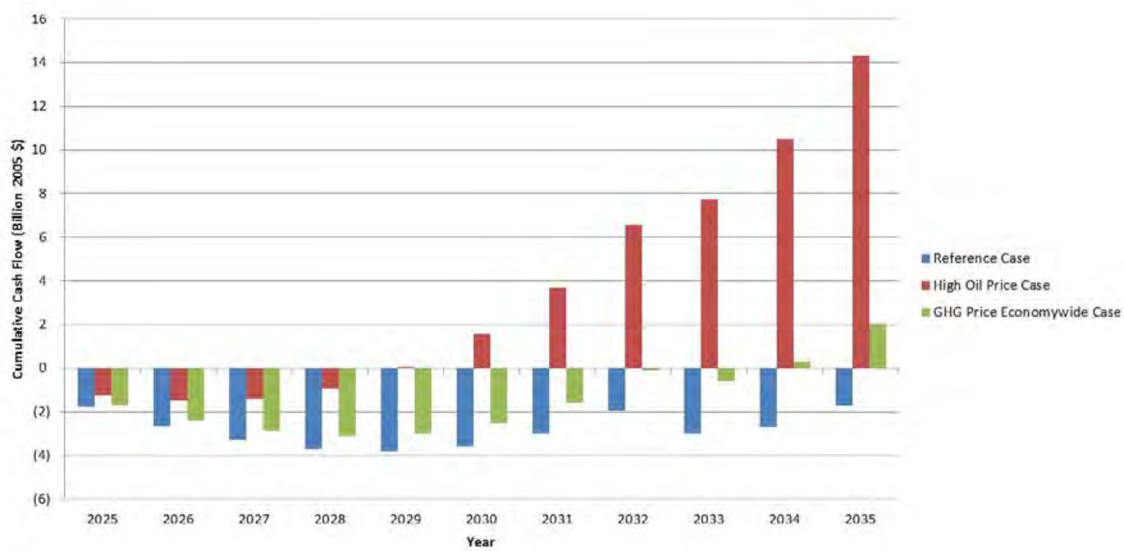

Figure 86: Cumulative cash flow in the H_2 Partial Success scenario with centralized infrastructure delayed until tranche 3

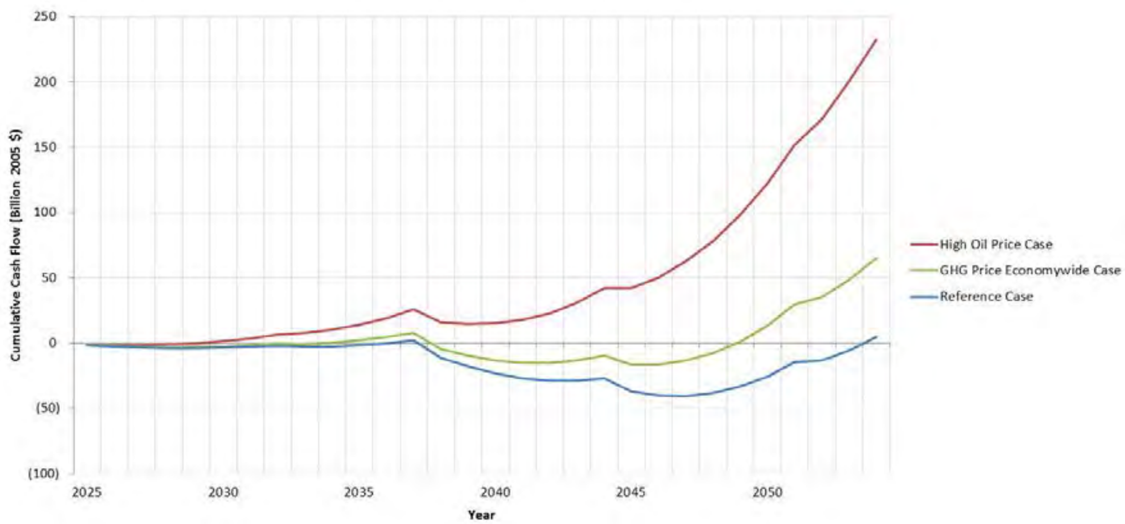

Figure 87: Cumulative cash flow over the entire study period for the H_2 Partial Success scenario with centralized infrastructure delayed until tranche 3 (beyond 2035, hydrogen market price is the price projected in 2035)

GHG Emissions

Because lower GHG emissions can be achieved through centralized coal-based hydrogen production with CCS, the delay of this infrastructure translates to larger GHG emissions from the HFCV fleet during the first two infrastructure tranches (Figure 88). However, the infrastructure in the first two tranches is designed to serve HFCVs representing less than 10% of the total LDV fleet. As a result, deployment of HFCVs under the H_2 Success scenario would reduce the annual GHG emissions of the national LDV fleet by only 0.8% from 2021 to 2027 if centralized infrastructure is delayed until tranche 3. In contrast, if centralized infrastructure with CCS is not delayed, the reduction would be 2.1%, a difference of about 1.3% in fleet-wide emissions. This analysis indicates that although centralized production with CCS could more than halve the GHG emissions associated with the HFCVs deployed in the first two tranches, the impact on the GHG emissions associated with the entire LDV fleet is relatively small in both cases. Thus, delaying centralized infrastructure does not appear to have a significant impact on the reduction of GHG emissions from the national LDV fleet.

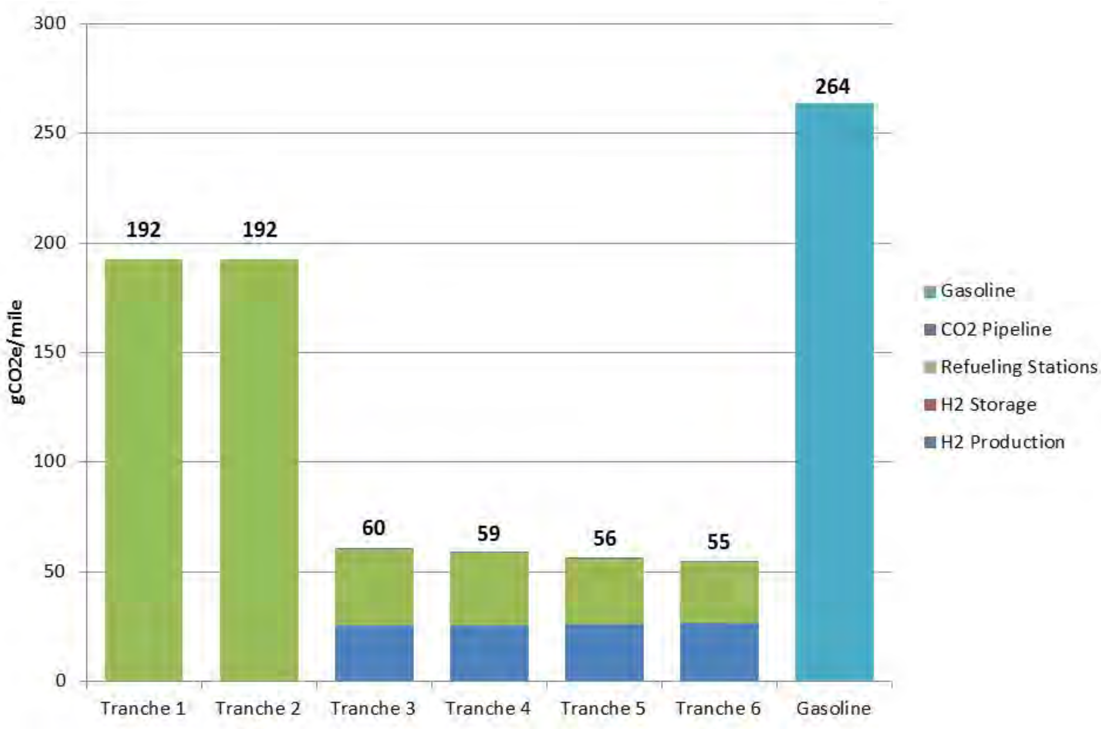

Figure 88: Average GHG intensity of the HFCV fleet in the H_2-CCS case when centralized infrastructure is delayed until tranche 3

4.1.4 Hydrogen Subsidy Cases

In sections 4.1.2 and 4.1.3, the model identifies large financial losses associated with the early deployment of hydrogen infrastructure. Consequently, in order to initiate the transition to a hydrogen-based transportation sector, policies will be required that incentivize the development of the requisite infrastructure. This section analyzes three policy cases for subsidizing infrastructure deployment.

- Accelerated Depreciation (MACRS-5): The schedule for depreciating capital is accelerated from the 15-year schedule (MACRS-15) used in the reference case to the MACRS-5 schedule. In this case, all capital expenditures within the 30-year analysis period can be depreciated within six years of installation according to the schedule in Table 54. Essentially, this policy provides very large and immediate tax benefits that help reduce the cost spikes associated with the installation of infrastructure in each tranche. This subsidy applies to all infrastructure tranches and, thus, provides a long-term subsidy for infrastructure investments.

- Production Tax Credit A (PTC-10): A production tax credit is provided for the first ten years of the analysis period that guarantees that a supplier will receive a price of \$10/kg H_2 regardless of the market price[17]. Consequently, the value of the annual tax credit will depend on the market price of hydrogen in each year, which is based on the three AEO oil price scenarios [70]. For example, if the market price is \$6/kg in year 1, the production tax credit will be \$4/kg so that the supplier essentially receives \$10 for each kilogram of hydrogen sold. The PTC generally declines with time as the market price of hydrogen increases. The total subsidy in each year is calculated by multiplying the PTC in each year by the quantity of hydrogen produced in each year. The net present value of the subsidy in each year is calculated using the cost of capital, which is 10.3% for production. These values are then summed over the ten-year period of the subsidy and the result is converted to 2005 US Dollars.

- Production Tax Credit B (PTC-5): A fixed \$5/kg H_2 production tax credit is provided for all hydrogen produced in the first ten years of the analysis period[18]. The tax credit is independent of the market price of hydrogen. The net present value of the subsidy is calculated using the same method as PTC-10.

Table 54: MACRS-5 depreciation schedule

Year	Fraction of asset depreciated
1	0.2000
2	0.3200
3	0.1920
4	0.1152
5	0.1152
6	0.0576

[17] The value of \$10/kg is selected as the guaranteed market price of hydrogen since earlier analysis indicates that the breakeven price of hydrogen during the first 10-year period is between \$9.18/kg and \$9.50/kg, depending on the HFCV deployment rate. Consequently, a guaranteed price of \$10/kg should allow suppliers to breakeven within the first ten years.

[18] The value of \$5/kg for the fixed PTC is selected since this is the value that when added to the market price of hydrogen will exceed the calculated breakeven cost of hydrogen during the first period. For example, in the case in which the market price of hydrogen is the smallest (i.e., Reference case), the price is \$4.91/kg to \$5.37/kg. Thus, when the PTC is added, the price received by the supplier will be \$9.91/kg to \$10.37/kg.

Two infrastructure deployment cases are examined, including the optimized infrastructure deployment described in section 4.1.2 in which centralized infrastructure is installed in tranche one and the onsite production case in which centralized infrastructure is delayed until tranche 2 (section 4.1.3.1). In addition, the two HFCV deployment scenarios are evaluated (i.e., H_2 Success and H_2 Partial Success). For all deployment and policy cases, the cumulative cash flow and the net present cost of the total subsidy are compared under the three AEO oil price cases, which are summarized in section 0. It should be noted that this analysis assumes that the entire infrastructure is built by a single entity. Thus, subsidies that are applied to hydrogen production (e.g., production tax credits) benefit the entity that operates the entire supply chain.

4.1.4.1 Reference Case

In the Reference case, the market price of hydrogen in each year is derived from the Reference AEO oil price projection to 2035[19]. Beyond 2035, the real price of oil is assumed to remain constant, which provides a conservative estimate of the future price of hydrogen. A comparison of the impacts of the various policy cases for each HFCV and infrastructure deployment case is provided in Table 55.

Given the H_2 Success HFCV deployment scenario and the infrastructure scenario in which centralized infrastructure is not delayed, the impact of the various policy cases on the cumulative cash flow are illustrated in Figure 89. As expected, all of the policy cases improve the economic outlook. Specifically, the year in which cumulative cash flow remains positive (i.e., the project becomes profitable) is earlier and the size of the maximum cumulative loss (i.e., buy-

---

[19] See section 0 for a detailed explanation. Essentially, it is assumed that the market price of hydrogen is determined by the oil price. The AEO oil prices are converted from 2009 to 2005 dollars and then the oil prices are converted to equivalent hydrogen prices by assuming that HFCVs are projected to have 63% better fuel economy than gasoline HEVs.

down cost) is smaller (Table 55). The year in which the maximum cumulative loss occurs does not necessarily mark the time at which the annual cash flow permanently becomes positive. Although the cumulative cash flow reaches its minimum, negative annual cash flow can still occur (e.g., when the PTCs expire and/or a new infrastructure tranche is installed).

The production tax credit (PTC) cases are more effective than the accelerated depreciation schedule (MACRS-5) case in incentivizing infrastructure deployment. Given the market prices of hydrogen under the reference case, the annual production tax credits are similar in both the PTC-5 and PTC-10 cases (e.g., $5/kg in PTC-5 and $5.09-$4.73/kg in PTC-10). As a result, the cumulative cash flow becomes positive in 2027 and the remaining buy-down cost for industry (after subsidies) is about $5 billion in both cases. For comparison, in the case without subsidies, the cumulative cash flow becomes positive in 2041 and the buy-down cost is almost $46 billion. The net present cost of the subsidy is about $35 billion in both the PTC-5 and PTC-10 cases with the cost slightly lower in the PTC-10 case since the tax credits are smaller in most years (e.g., the PTC is greater than $5/kg in the first two years when the quantity of hydrogen produced is small and less than $5/kg in the last eight years of the subsidy period).

In the H_2 Partial Success deployment scenario, the policies are unable to overcome the high costs and low utilization of infrastructure (Figure 90). With the production tax credits, the cumulative cash flow does become positive in 2032, but then descends back into negative territory as new infrastructure is built and the tax credits expire. Although the buy-down cost is reduced in all cases, the year in which infrastructure becomes profitable is still delayed until around 2050. The net present cost of the subsidies is smaller in the H_2 Partial Success scenario than the H_2 Success scenario since less hydrogen is produced in the first ten years and less infrastructure is built during the analysis period. In addition, the production tax credits in the PTC-10 case are slightly smaller since the first infrastructure is delayed until 2025 when the market price of hydrogen (i.e., oil price) is assumed to be larger. The total subsidy ranges from $16 billion for the MACRS-5 case to $18 billion for the PTC-5 case.

Table 55: Comparison of the impacts of the various policy cases for each HFCV and infrastructure deployment case (Reference oil price)

	H_2 Success				H_2 Partial Success			
	PTC-5	PTC-10	MACRS-5	No Policy	PTC-5	PTC-10	MACRS-5	No Policy
Centralized Infrastructure in Tranche 1								
Production Tax Credit ($/kg)	$5.00	$5.09-$4.73	N/A	N/A	$5.00	$4.87-$4.66	N/A	N/A
Positive Cum. Cash Flow (Yr.)	2027	2027	2038	2041	2050	2050	2048	2053
Buy-down Cost (Billion$)	4.9	4.9	20.5	45.6	11.9	13.4	16.9	39.8
Cost of Subsidy (Billion$ NPV)	35.5	34.1	26.4	0	17.8	16.8	15.9	0
Centralized Infrastructure Delayed to Tranche 2								
Production Tax Credit ($/kg)	$5.00	$5.09-$4.73	N/A	N/A	$5.00	$4.87-$4.66	N/A	N/A
Positive Cum. Cash Flow (Yr.)	2022	2022	2038	2042	2050	2051	2050	2054
Buy-down Cost (Billion$)	0.07	0.04	18.9	47.9	16.9	18.5	18.2	44.9
Cost of Subsidy (Billion$ NPV)	35.5	34.1	26.3	0	17.8	16.8	15.4	0

If centralized infrastructure is delayed for one tranche under the H_2 Success scenario, the introduction of production tax credits substantially improves the economics of early hydrogen infrastructure deployment (Figure 91). If onsite production is supported with the production tax credits in the PTC-5 or PTC-10 cases, profitability is achieved in year 2022 and the remaining buy-down cost is reduced to less than $100 million. The net present costs of the two PTC cases are similar at about $35 billion. The MACRS-5 case costs about $26 billion, but only accelerates the year at which cumulative cash flow becomes positive by a few years relative to the case without subsidies.

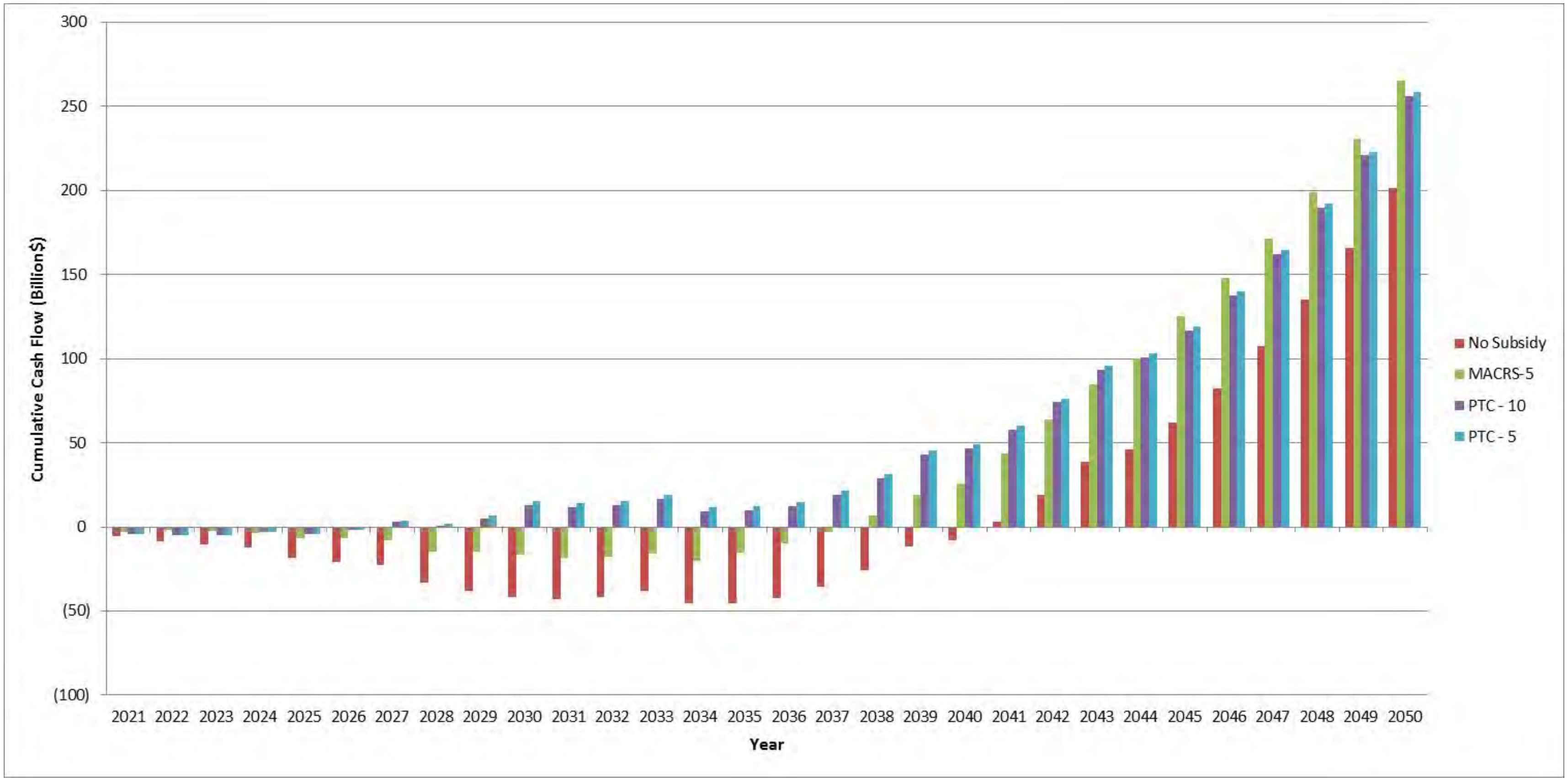

Figure 89: Cumulative cash flow given the different policy cases in the H_2 Success scenario with centralized infrastructure in tranche 1 (Reference oil price)

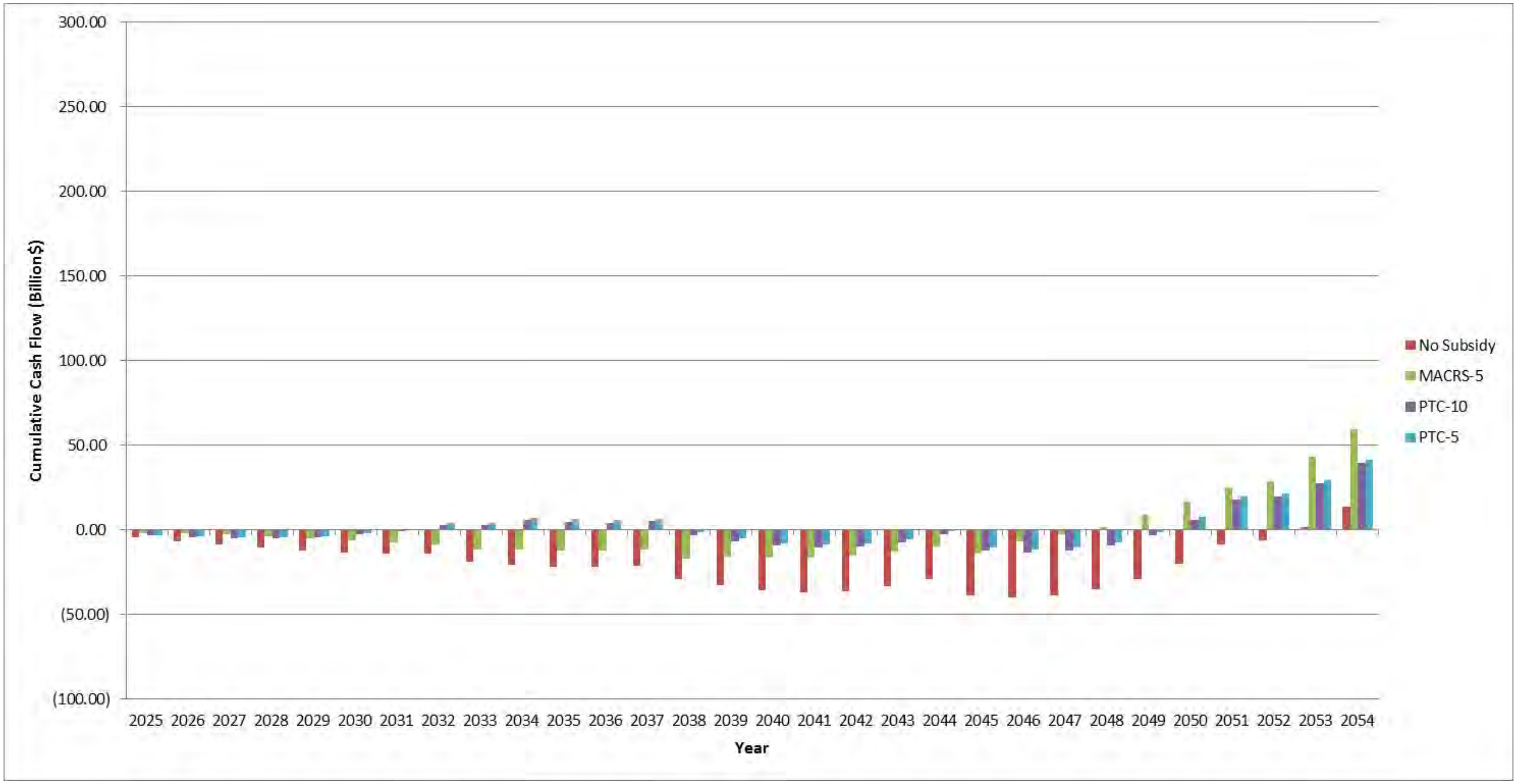

Figure 90: Cumulative cash flow given the different policy cases in the H_2 Partial Success scenario with centralized infrastructure in tranche 1 (Reference oil price)

In the H_2 Partial Success scenario, the two PTC cases lead to positive cumulative cash flow within a few years (Figure 92). However, the expiration of PTCs and introduction of centralized infrastructure results in annual losses that drive the cumulative cash flow back into negative territory by 2038. Positive cumulative cash flow does not return until around 2050 in both PTC cases. Consequently, given slow HFCV deployment, the delay of centralized infrastructure does not improve the long-term profitability of the project even though it does improve the near-term economics. The net present costs of the different subsidy cases range from $16 billion in the MACRS-5 case to $18 billion in the PTC-5 case.

4.1.4.2 High Oil Price Case

In the High Oil Price case, the market price of hydrogen in each year is derived from the oil price projection to 2035 from the AEO High Oil Price scenario. Beyond 2035, the real price of oil is assumed to remain constant. A comparison of the impacts of the various policy cases for each HFCV and infrastructure deployment case is provided in Table 56.

Given the H_2 Success HFCV deployment scenario and the case in which centralized infrastructure is installed in tranche 1, all policy cases lead to positive cumulative cash flow by year 2027 (Figure 93). In the High Oil Price case, the values of the PTCs in the PTC-5 and PTC-10 cases are substantially different since the market price of hydrogen is assumed to be larger. Specifically, the PTCs in the PTC-10 case range from $2.87/kg in year 1 to $2.38/kg in year 10. In contrast, the PTCs in the PTC-5 case are fixed at $5/kg for the first ten years. Since the PTCs in the PTC-5 case are larger, positive cumulative cash flow is achieved more quickly (by 2024), but at a much larger net present cost (~$36 billion). In the PTC-10 case, infrastructure deployment becomes profitable in 2027 at about half the net present cost (~$18 billion). The remaining buy-down costs in the PTC-5 and PTC-10 cases are $3.4 billion and $4.9 billion, respectively. The MACRS-5 case achieves the smallest buy-down cost at $2.3 billion, but costs about $26 billion and leads to profitability within six years.

Table 56: Comparison of the impacts of the various policy cases for each HFCV and infrastructure deployment case (High oil price)

	H_2 Success				H_2 Partial Success			
	PTC-5	PTC-10	MACRS-5	No Policy	PTC-5	PTC-10	MACRS-5	No Policy
Centralized Infrastructure in Tranche 1								
Production Tax Credit ($/kg)	$5.00	$2.87-$2.38	N/A	N/A	$5.00	$2.59-$2.25	N/A	N/A
Positive Cum. Cash Flow (Yr.)	2024	2027	2026	2033	2030	2032	2034	2040
Buy-down Cost (Billion$)	3.4	4.9	2.3	17.7	3.0	4.9	1.7	8.5
Cost of Subsidy (Billion$ NPV)	35.5	18.0	26.4	0	17.8	8.5	15.9	0
Centralized Infrastructure Delayed to Tranche 2								
Production Tax Credit ($/kg)	$5.00	$2.87-$2.38	N/A	N/A	$5.00	$2.59-$2.25	N/A	N/A
Positive Cum. Cash Flow (Yr.)	2021	2022	2022	2033	2026	2027	2026	2029
Buy-down Cost (Billion$)	0.00	0.04	0.12	13.5	0.14	0.68	0.48	1.5
Cost of Subsidy (Billion$ NPV)	35.5	18.0	26.3	0	17.8	8.5	15.4	0

In the H_2 Partial Success scenario, all subsidy cases achieve positive cumulative cash flow by 2034 under the High Oil Price case (Figure 94). As expected, profitability is achieved most quickly given the PTC-5 case (within six years in 2030), but at the largest cost (~$18 billion). The PTC-10 case leads to profitability within eight years in 2032 at a net present cost of only ~$9 billion. Without subsidies, positive cumulative cash flow is not achieved until 2040 and the buy-down cost is about $8.5 billion. The remaining buy-down costs in the PTC-5 and PTC-10 cases are $3 billion and $5 billion, respectively. In the MACRS-5 case, profitability is achieved by 2034 at a net present cost of about $16 billion. This analysis indicates that the PTC-10 case accelerates the profitability of hydrogen supply at the lowest cost to the government.

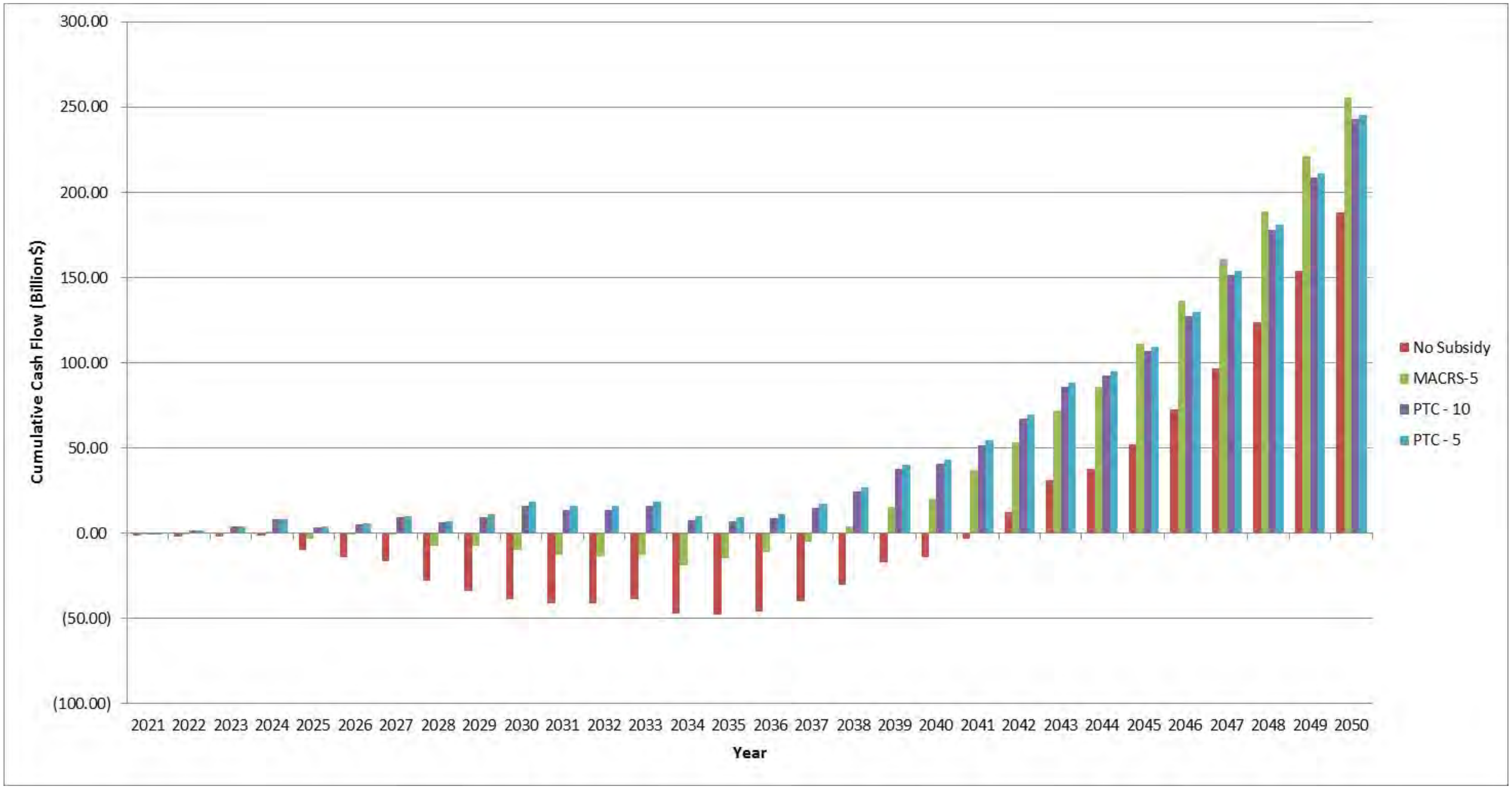

Figure 91: Cumulative cash flow given the different policy cases in the H_2 Success scenario with centralized infrastructure delayed until tranche 2 (Reference oil price)

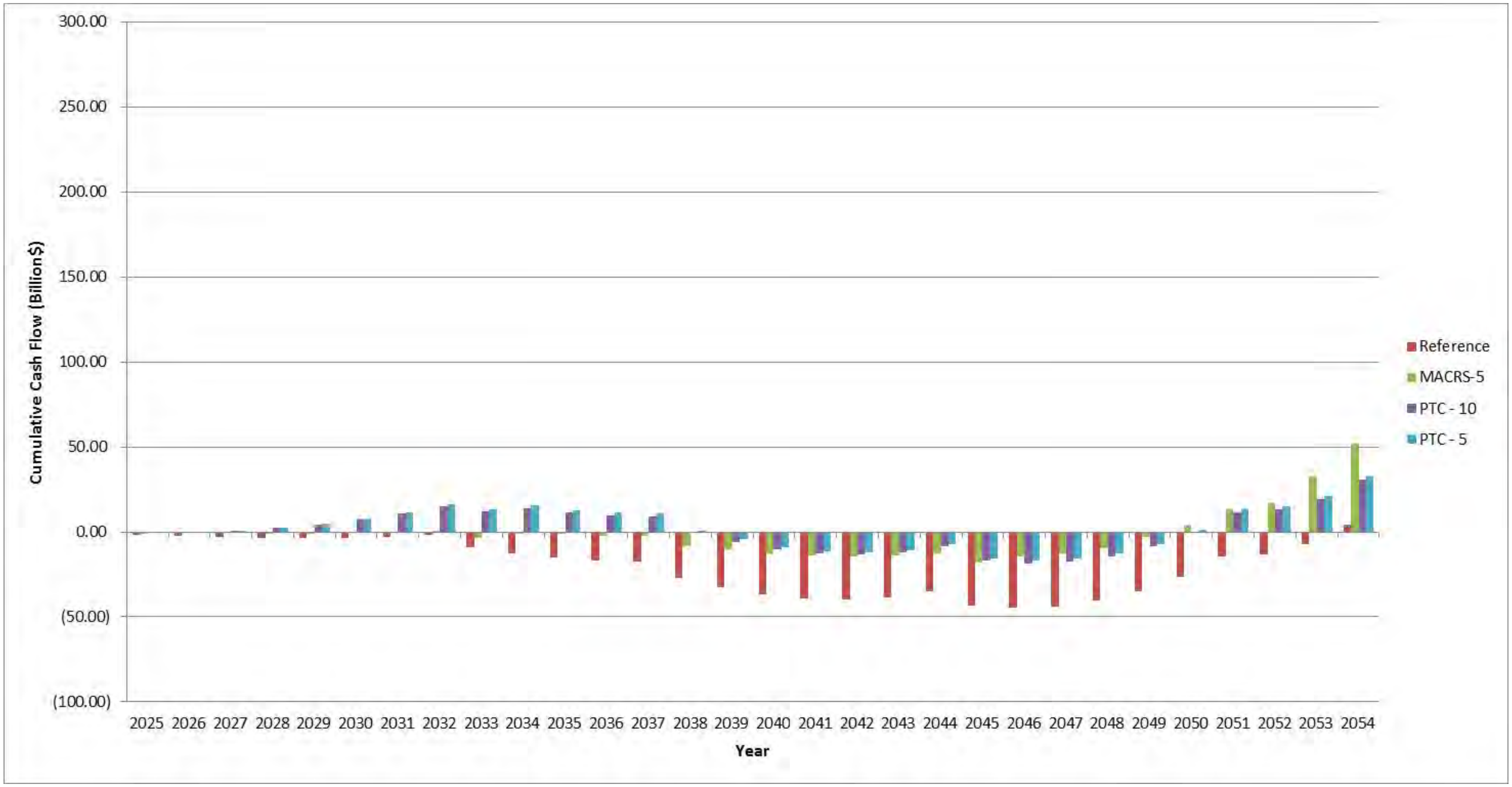

Figure 92: Cumulative cash flow given the different policy cases in the H_2 Partial Success scenario with centralized infrastructure delayed until tranche 2 (Reference oil price)

In the case in which HFCV deployment follows the H_2 Success scenario and centralized infrastructure is delayed until tranche 2, the PTC cases lead to profitability within the first two years (Figure 95). Specifically, PTC-5 leads to immediate profitability (i.e., zero buy-down cost) and PTC-10 achieves profitability in the second year (2022) with a buy-down cost of only ~$40 million. The net present costs of the subsidies in the PTC-5 and PTC-10 cases are $36 billion and $18 billion, respectively. The MACRS-5 case also achieves profitability in the second year at a net present cost of about $26 billion. In contrast, the case without subsides does not achieve positive cumulative cash flow until year 2033 and the buy-down cost is about $13 billion. By combining subsidies and onsite production, a favorable climate for investing in early hydrogen infrastructure is created in which profitability can be achieved within two years of operation.

In the H_2 Partial Success scenario where centralized infrastructure is delayed for one tranche, the economic climate for infrastructure deployment is favorable even in the absence of subsidies. Specifically, deployment becomes profitable by 2029 at a buy-down cost of only $1.5 billion. Although the subsidies do accelerate profitability, the cost of subsidies is excessive in comparison with the buy-down cost without subsidies (Table 56). The MACRS-5 and PTC-5 cases achieve profitability in 2026 at a net present cost of $15 billion and $18 billion, respectively (Figure 96). The PTC-10 case reaches positive cumulative cash flow in 2027 at a net present cost of $8.5 billion. It is notable that the economic outlook associated with the H_2 Partial Success HFCV deployment scenario is only favorable in the High Oil Price case where the projected market prices for hydrogen are largest.

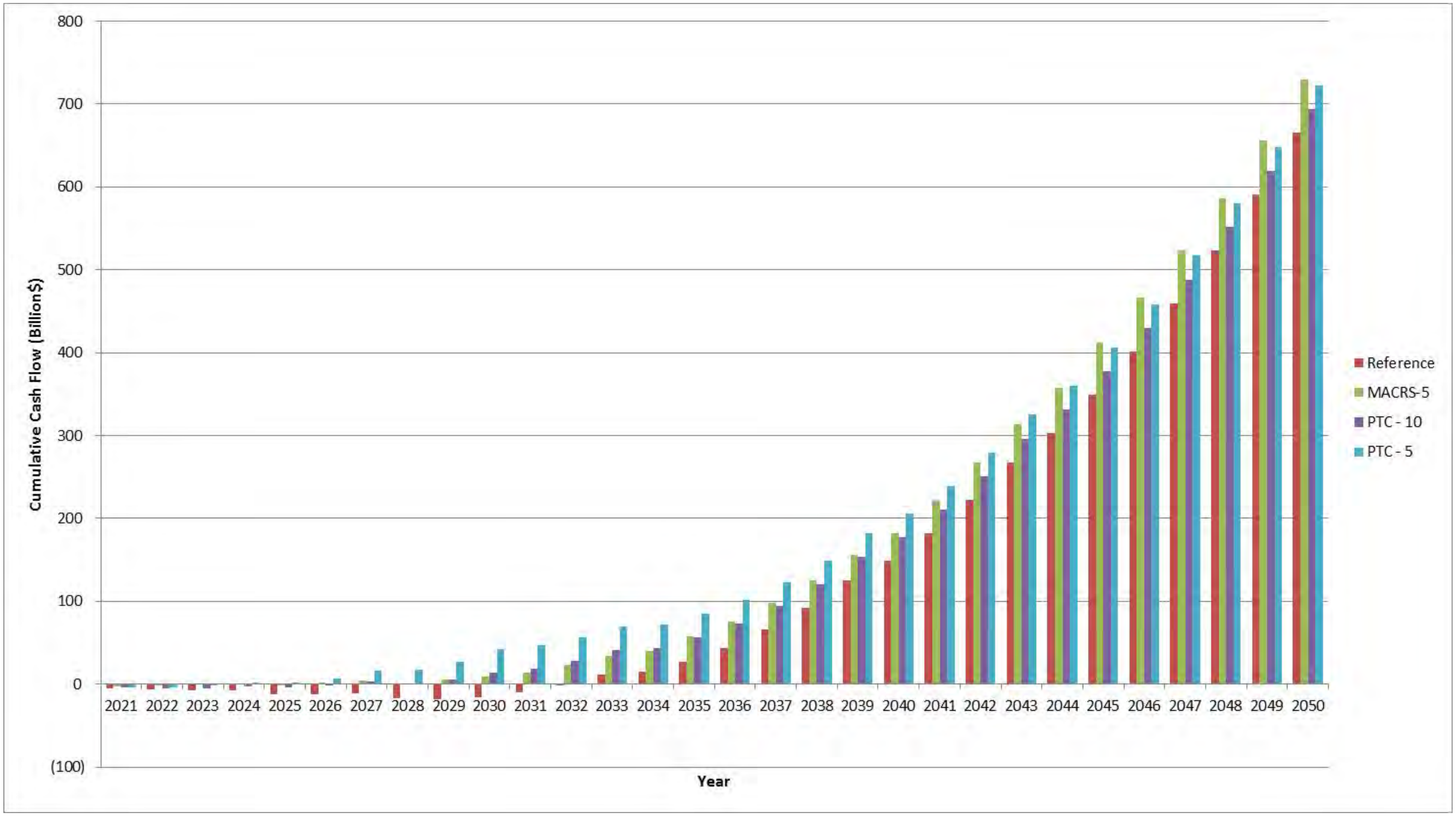

Figure 93: Cumulative cash flow given the different policy cases in the H_2 Success scenario with centralized infrastructure in tranche 1 (High oil price)

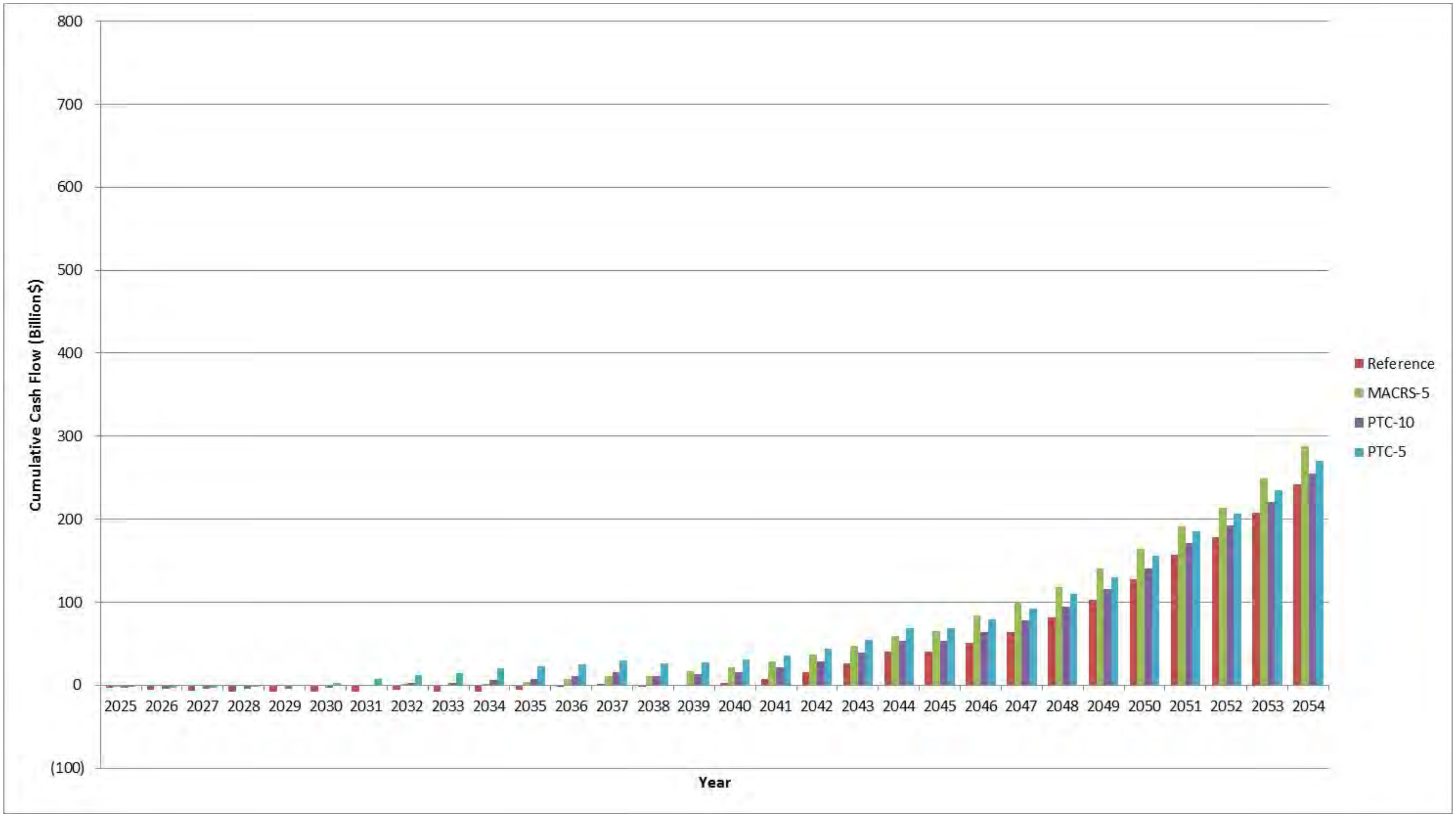

Figure 94: Cumulative cash flow given the different policy cases in the H_2 Partial Success scenario with centralized infrastructure in tranche 1 (High oil price)

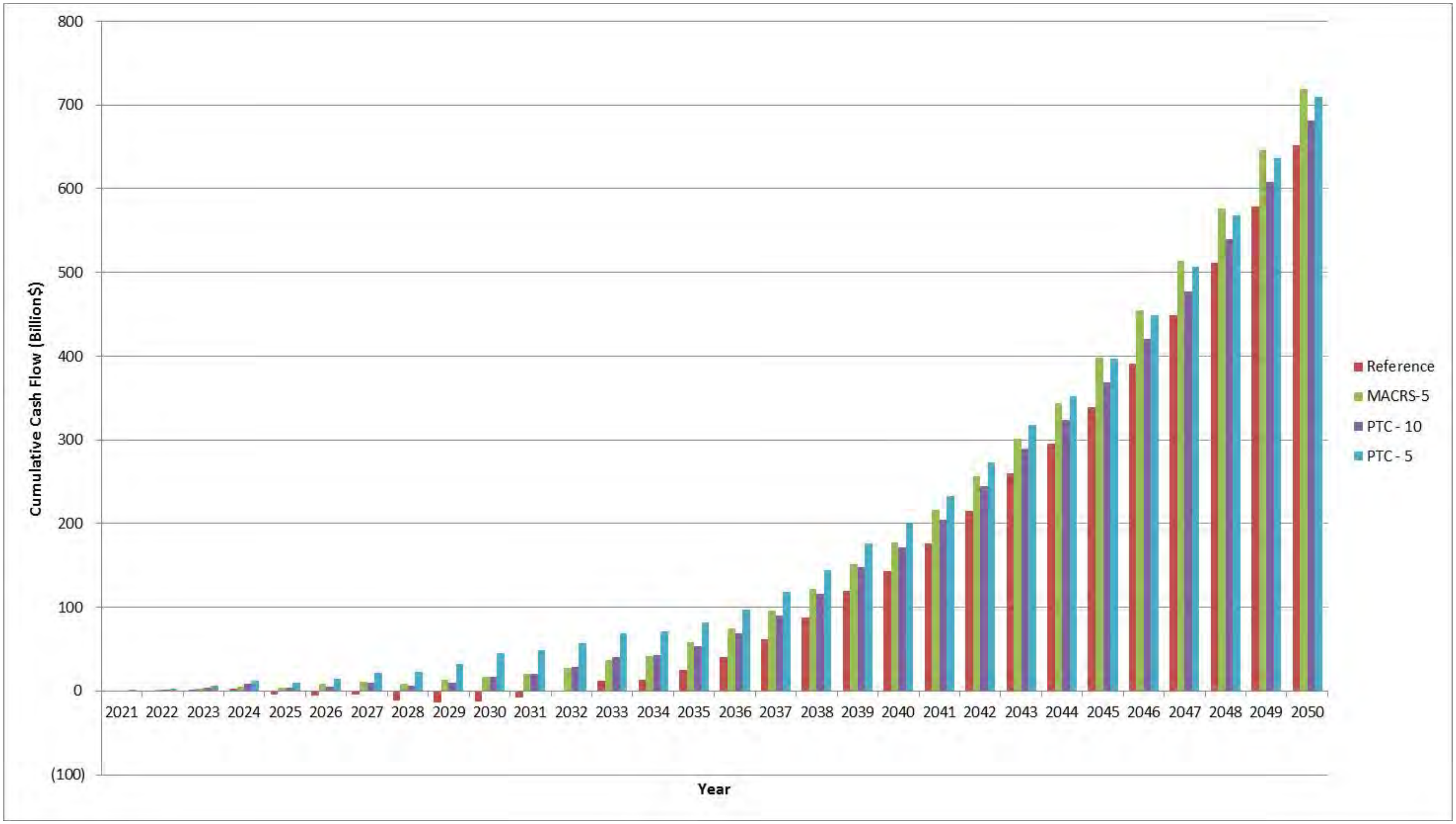

Figure 95: Cumulative cash flow given the different policy cases in the H_2 Success scenario with centralized infrastructure delayed until tranche 2 (High oil price)

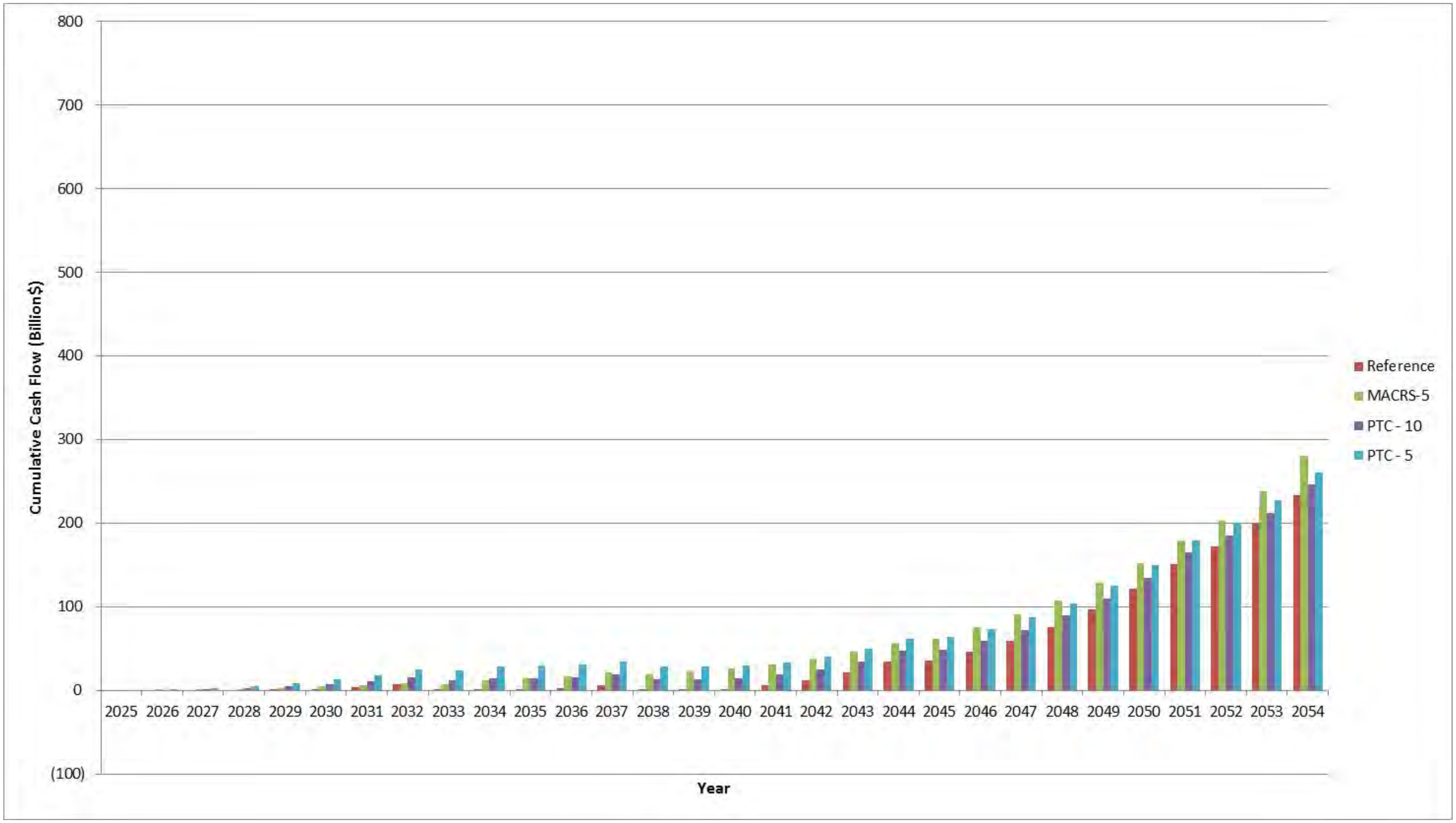

Figure 96: Cumulative cash flow given the different policy cases in the H_2 Partial Success scenario with centralized infrastructure delayed until tranche 2 (High oil price)

4.1.4.3 GHG Price Economy-wide Case

In the GHG Price Economy-wide case, the market price of hydrogen in each year is derived from the oil price projection to 2035 from the AEO GHG Price Economy-wide scenario. Beyond 2035, the real price of oil is assumed to remain constant. As a reminder, the GHG Price Economy-wide case represents a scenario in which the oil price reflects an economy-wide CO_2 price of $25/tonne starting in 2013 that increases to $75/tonne by 2035. In this case, the projected oil price is slightly larger than the Reference case, but smaller than the High Oil Price case (Figure 66). A comparison of the impacts of the various policy cases for each HFCV and infrastructure deployment case is provided in Table 57.

Given the H_2 Success scenario and the case in which centralized infrastructure is installed in tranche 1, the two PTC cases result in positive cumulative cash flow by 2027 (Figure 97). The production tax credits in the PTC-10 case range from $4.68/kg in year 1 to $4.21 in year 10. Consequently, they are only 6-16% smaller than the fixed $5/kg PTC in the PTC-5 case. Since the PTC-5 credits are slightly larger, this case achieves positive cumulative cash flow one year earlier than the PTC-10 case. However, the net present cost of the production tax credits is also slightly larger at $36 billion. The MACRS-5 case is less successful in promoting hydrogen infrastructure deployment as it does not achieve positive cumulative cash flow until 2035, which is only a few years earlier than the case without subsidies.

In the H_2 Partial Success scenario, the PTC-5 case achieves positive cumulative cash flow by 2031 (Figure 98). In contrast, positive cumulative cash flow occurs within the first eight years in the PTC-10 case, but then turns negative once the production tax credits expire. Permanent positive cumulative cash flow is not achieved until 2042 in the PTC-10 case. Similarly, the MACRS-5 case does not achieve positive cumulative cash flow until 2043. However, in all cases, *annual* cash flow is not consistently positive until 2045 and cumulative profit does not exceed $10 billion until 2046. Consequently, although the PTC-5 case does yield positive cumulative cash flow within the first ten years, annual cash flows indicate significant losses for decades, which suggests that the subsidies may not be sufficient to promote infrastructure deployment in this scenario.

Table 57: Comparison of the impacts of the various policy cases for each HFCV and infrastructure deployment case (GHG price)

	H_2 Success				H_2 Partial Success			
	PTC-5	PTC-10	MACRS-5	No Policy	PTC-5	PTC-10	MACRS-5	No Policy
Centralized Infrastructure in Tranche 1								
Production Tax Credit ($/kg)	$5.00	$4.68-$4.21	N/A	N/A	$5.00	$4.40-$4.05	N/A	N/A
Positive Cum. Cash Flow (Yr.)	2026	2027	2035	2038	2031	2042	2043	2049
Buy-down Cost (Billion$)	4.6	4.9	11.7	36.1	4.3	4.9	10.0	26.0
Cost of Subsidy (Billion$ NPV)	35.5	30.8	26.4	0	17.8	15.0	15.9	0
Centralized Infrastructure Delayed to Tranche 2								
Production Tax Credit ($/kg)	$5.00	$4.68-$4.21	N/A	N/A	$5.00	$4.40-$4.05	N/A	N/A
Positive Cum. Cash Flow (Yr.)	2021	2022	2035	2039	2026	2043	2043	2050
Buy-down Cost (Billion$)	0.00	0.04	6.0	34.1	0.55	4.4	2.7	27.7
Cost of Subsidy (Billion$ NPV)	35.5	30.8	26.3	0	17.8	15.0	15.4	0

Given the H_2 Success scenario and the case in which centralized infrastructure is delayed for one tranche, both PTC cases achieve positive cumulative cash flow by 2022 (Figure 99). In the PTC-5 case, there is zero remaining buy-down cost, but the net present cost of the subsidy is $36 billion. The remaining buy-down cost in the PTC-10 case is limited to $40 million and the net present cost of the subsidy is $31 billion. In the reference case without subsidies, the buy-down cost is about $34 billion and positive cumulative cash flow is delayed until 2039. Although the cost of the production tax credits is large, the PTC-10 and PTC-5 cases do accelerate the profitability of infrastructure deployment and, thus, would provide ample incentive for building refueling stations with onsite production.

In the H_2 Partial Success scenario, the PTC-5 case achieves positive cumulative cash flow in the second year (Figure 100). The cumulative cash flow remains positive throughout the study period despite significant annual losses for two decades. The other policy cases achieve positive cumulative cash flow, but decline back into negative territory once centralized infrastructure is introduced and tax credits expire. In all policy cases, it does not appear that significant profit can be made for at least two decades if HFCV deployment follows the H_2 Partial Success scenario.

4.1.4.4 General Insights

In evaluating the three policy cases, the policies that provide production tax credits are more effective than the MACRS-5 case at reducing the buy-down cost and accelerating the time at which cumulative cash flow remains positive. Although the PTC-5 case provides the largest subsidy, it is less flexible and provides excessive incentives in the case where the market price of hydrogen is large (i.e., High Oil Price case).

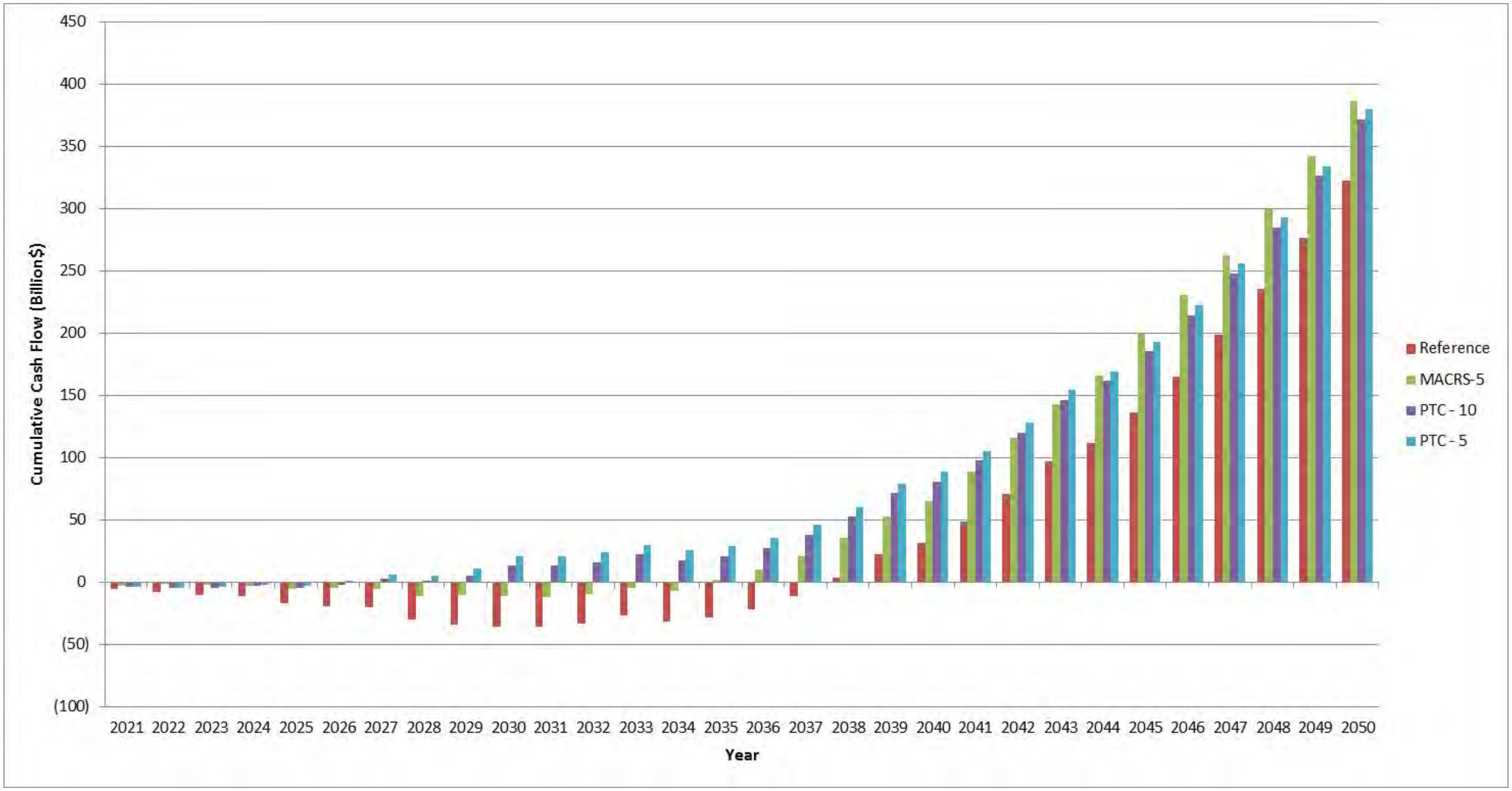

Figure 97: Cumulative cash flow given the different policy cases in the H_2 Success scenario with centralized infrastructure in tranche 1 (GHG price)

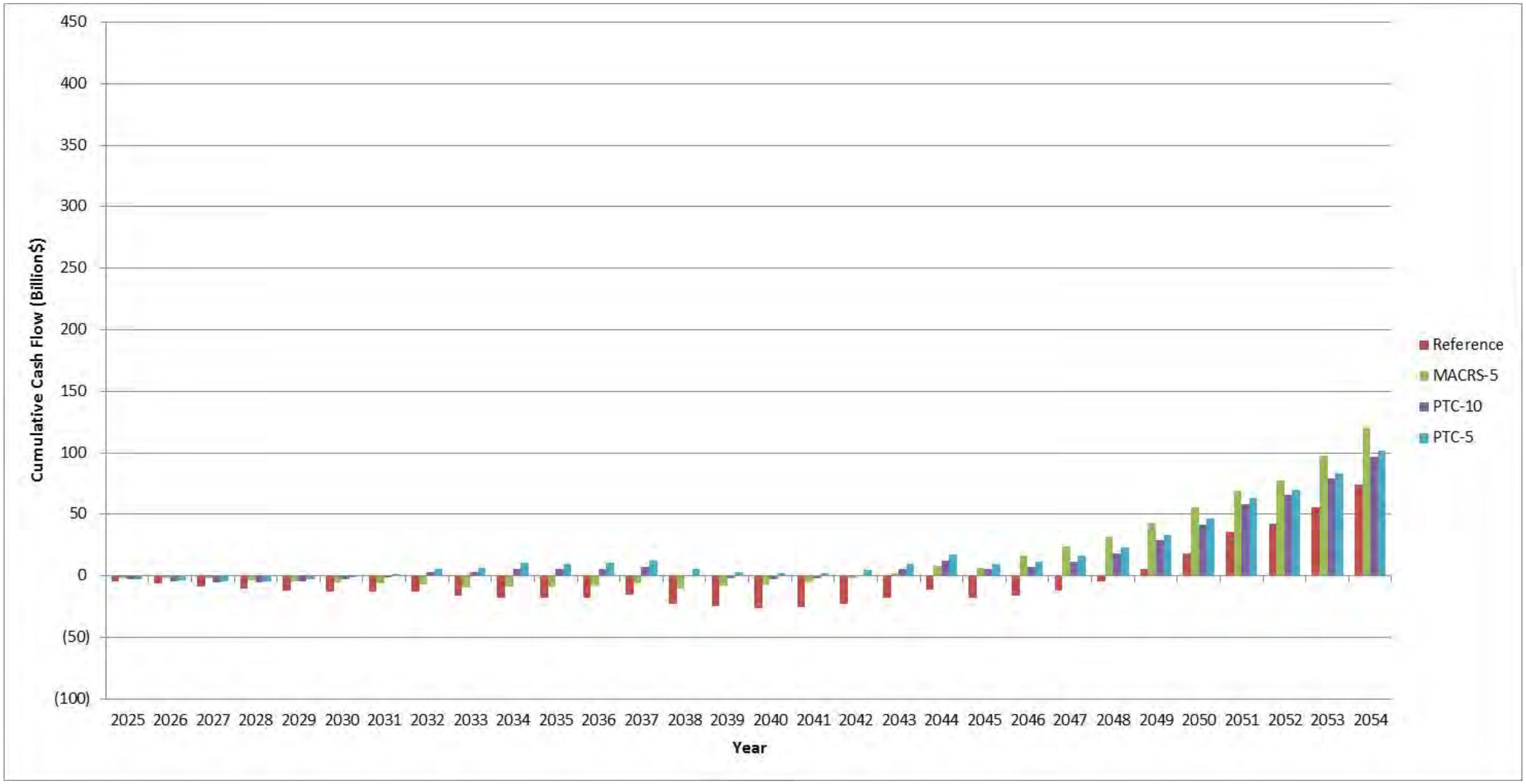

Figure 98: Cumulative cash flow given the different policy cases in the H_2 Partial Success scenario with centralized infrastructure in tranche 1 (GHG price)

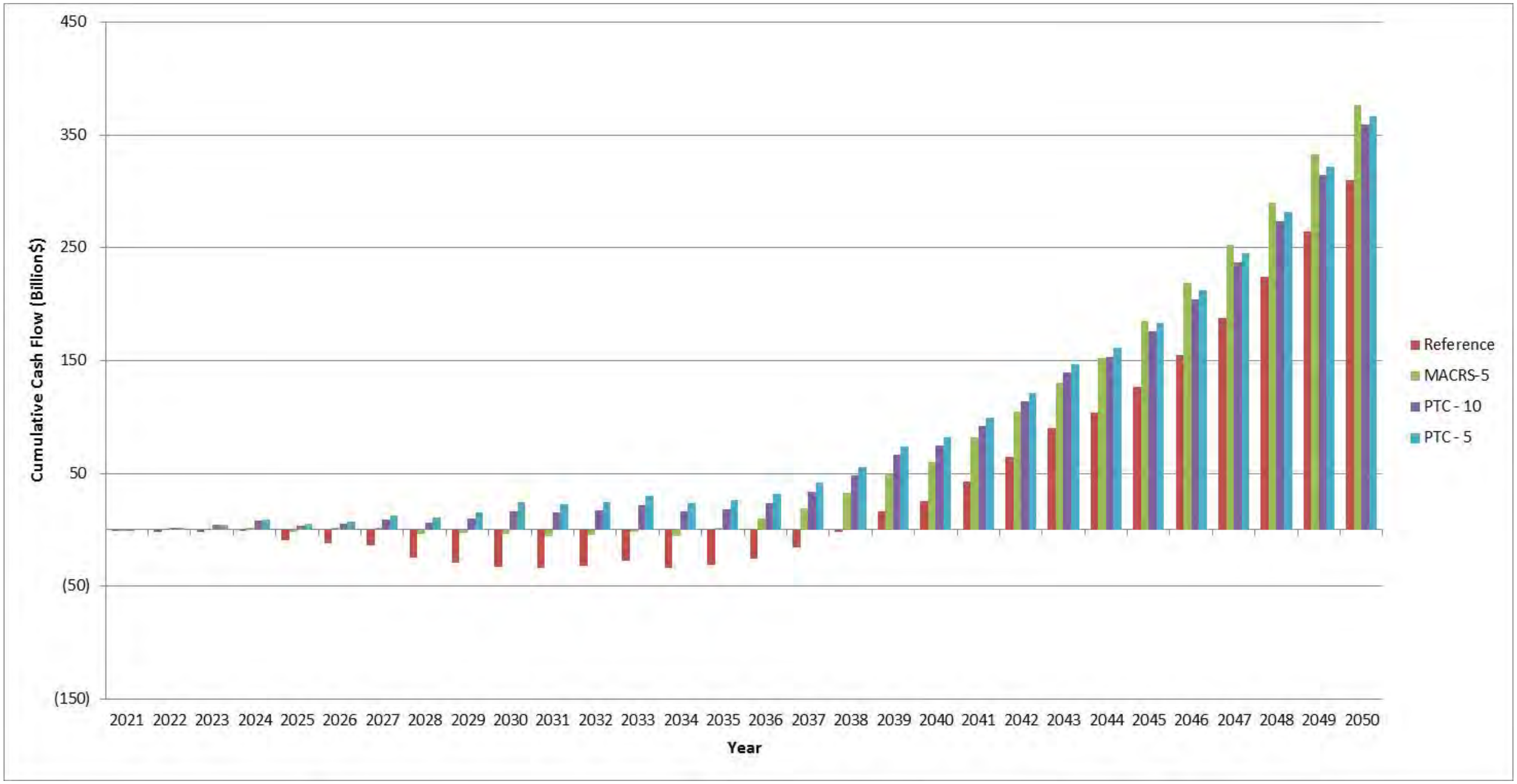

Figure 99: Cumulative cash flow given the different policy cases in the H_2 Success scenario with centralized infrastructure delayed until tranche 2 (GHG price)

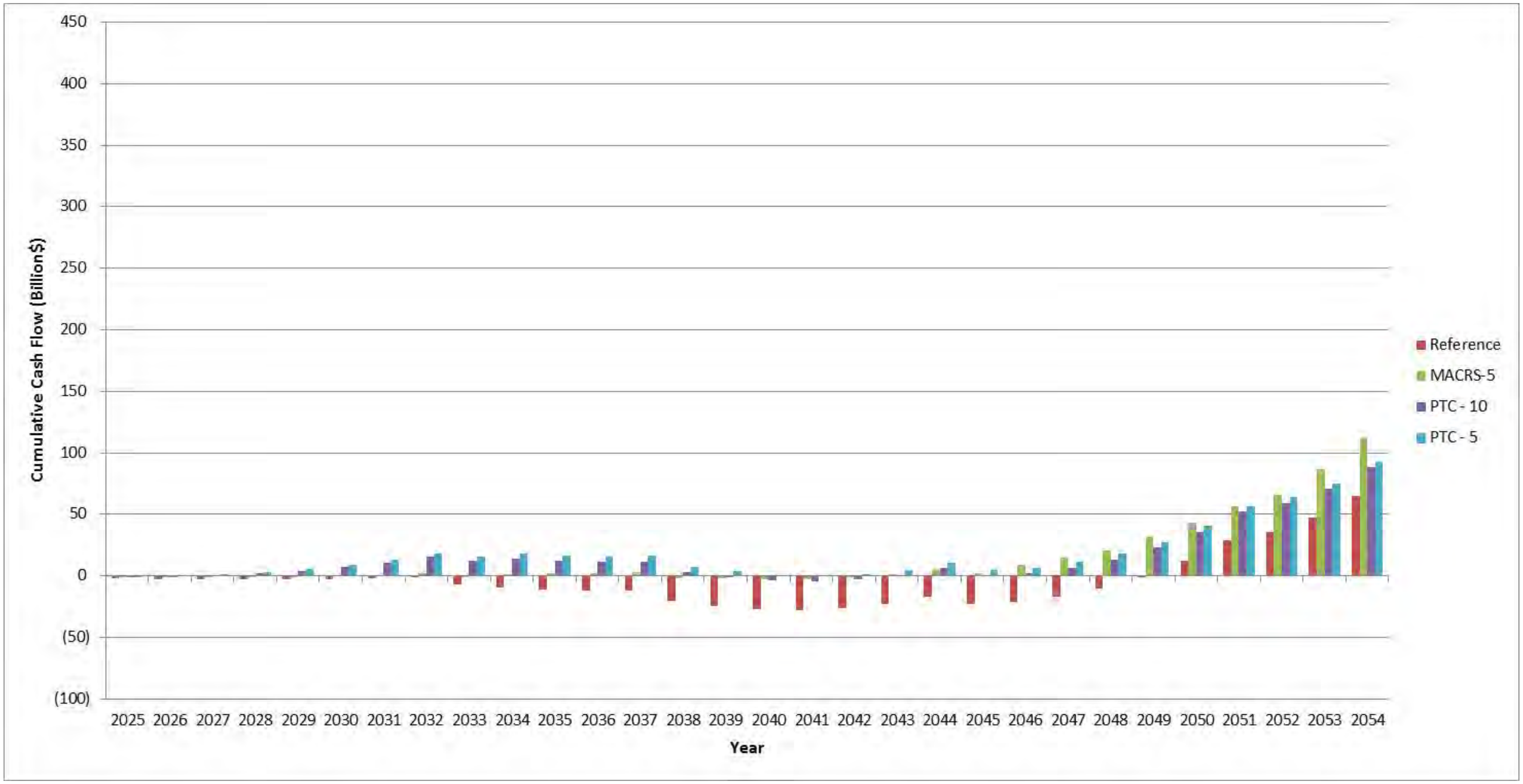

Figure 100: Cumulative cash flow given the different policy cases in the H_2 Partial Success scenario with centralized infrastructure delayed until tranche 2 (GHG price)

Rather than providing a fixed credit as in the PTC-5 case, the PTC-10 case effectively guarantees a hydrogen price to the supplier by providing the difference between the market price and the price target, which is $10/kg in this case. In this way, if the market price of hydrogen is large, as in the High Oil Price case, the required credit is reduced and the total cost of the subsidy is smaller. For example, the production tax credit in the PTC-10 case is, on average, $4.79/kg in the Reference case, but only $2.51/kg in the High Oil Price case. Thus, the PTC-10 case provides a more efficient mechanism for determining the value of the production tax credit, assuming that an appropriate guaranteed price level is identified.

In general, delaying centralized infrastructure for one tranche results in smaller buy-down costs and accelerated achievement of positive cumulative cash flow. The exception is the Reference case given the H_2 Partial Success HFCV deployment scenario. In this case, the low market price of hydrogen means that, even with subsidies, the profits made in the near-term are not sufficient to counteract the losses once centralized infrastructure is introduced. Moreover, the majority of production tax credits are consumed by onsite production and are no longer available to support centralized infrastructure. As a result, delaying centralized infrastructure reduces near-term costs, but increases the buy-down cost and delays the time at which permanent positive cumulative cash flow is achieved.

In the H_2 Partial Success HFCV deployment scenario, a favorable climate for hydrogen infrastructure investment is only realized if the market price for hydrogen is large (i.e., under the High Oil Price case). In other words, a combination of subsidies and high hydrogen prices is required for hydrogen infrastructure deployment to be successful in the case when HFCV deployment is slow. However, the net present cost of subsidies is also smallest in the case when

PTC-10 is applied in this scenario. Specifically, the net present cost of PTC-10 is only $8.5 billion if the price of hydrogen is high and HFCV deployment is slow.

Given the High Oil Price case, subsidies provide a favorable environment for hydrogen infrastructure investment in all cases. When centralized infrastructure is introduced in the first tranche, positive cumulative cash flow is achieved within seven years in both HFCV deployment scenarios, and when it is delayed for one tranche, positive cumulative cash flow is achieved within two years. Moreover, in the case in which centralized infrastructure is delayed and HFCV deployment is slow, subsidies are not required since the buy-down cost is only $1.5 billion without subsidies.

The net present cost of the subsidy is dependent on the policy chosen, the HFCV deployment scenario, and, in the PTC-10 case, the market price of hydrogen. The total subsidy cost is smallest when the market price is large, HFCV deployment is slow, and PTC-10 is used ($8.5 billion). It is largest when PTC-5 is used and HFCV deployment follows the H2 Success scenario ($35.5 billion).

Delaying centralized infrastructure for one tranche reduces the buy-down cost and accelerates the time at which cumulative cash flow remains positive. However, this model assumes that the profits incurred by suppliers of onsite production will be invested in the development of centralized infrastructure. In reality, there is a danger that suppliers of infrastructure for onsite production will be different from the suppliers of centralized infrastructure and, thus, the near-term profits made possible by production tax credits may not be invested in centralized infrastructure. Since centralized infrastructure requires larger and more risky investments, a mechanism needs to be included that guarantees that the profits from early subsidies are invested in the deployment of centralized infrastructure.

It is also important to note that this model assumes that a single entity builds and operates the entire hydrogen supply chain. Consequently, it is assumed that, regardless of where the subsidies are applied within the supply chain, the benefits can be applied to the components requiring the largest subsidies. For example, if the subsidy is applied to production (e.g., production tax credits), the profits accrued at the production site can be applied to subsidize hydrogen transmission and distribution. In reality, production facilities and pipeline networks may be built and operated by different entities. In this case, production tax credits may incentivize production, but do nothing to encourage investment in distribution networks and refueling stations. As a result, the development of more sophisticated policies will likely be required in order to ensure that all components of the supply chain are incentivized.

4.1.5 Comparison with National Research Council hydrogen transition study

In 2008, the National Research Council (NRC) released a report that evaluates the cost and infrastructure requirements for making a transition to hydrogen fuel cell vehicles in the light-duty vehicle sector within the United States [35]. To model infrastructure deployment, a steady-state model is used that quantifies the infrastructure requirements in each year from the present to 2050. In this model, infrastructure is designed in each year to meet only the current demand (i.e., no oversizing) and does not consider previously built infrastructure (i.e., designs are independent). As a result, the model assumes that infrastructure is fully utilized in every year. The model considers several production pathways, including onsite production via natural gas reforming and electrolysis and centralized production utilizing coal, natural gas, or biomass.

Although the report evaluates a national rollout, infrastructure modeling is conducted only at the city level. Specifically, independent infrastructure is designed for each city and the development of integrated regional supply networks is not considered. As a result, the type of production (e.g., onsite or centralized) in each city is determined by the magnitude of demand and regional feedstock cost. Moreover, in the case of centralized production, the model assumes that the facility is located within or on the edge of the city and, therefore, no transmission pipelines are needed. Regarding CCS infrastructure, the cost of CO_2 capture is included for coal-based hydrogen plants and it is assumed that each facility has a 160-km CO_2 pipeline that connects the facility to a CO_2 storage site. CO_2 storage costs are not modeled.

In contrast, the *Hydrogen Infrastructure Deployment Model* (HIDM) described in this document incorporates much more spatial and temporal detail, but considers fewer potential production pathways. Most importantly, the HIDM allows for the development of integrated regional supply networks and examines more realistic scenarios of how infrastructure might deploy over time. As a result, the model considers underutilization of infrastructure capacity during deployment, explicitly incorporates replacement costs, and expands upon previously-built infrastructure. In addition, the model includes corporate taxes and depreciation, which are not included in the NRC report.

As a result of the differences in the two models, a comparison of the outputs can provide insight into how the incorporation of more spatial and temporal detail affects hydrogen infrastructure cost and design at the regional or national level. Moreover, these models are well-suited for comparison since they share component-level cost assumptions [10], report in 2005 constant dollars, evaluate the same time period, and use the same HFCV deployment scenarios. This section compares the reported infrastructure requirements, capital costs, breakeven prices of hydrogen, and subsidy recommendations for the H_2 Success HFCV deployment scenario.

4.1.5.1 Infrastructure Design

The NRC report provides detailed inventories of infrastructure requirements for three years (2020, 2035, and 2050). Table 58 compares the infrastructure requirements and capital costs in these three years for the two reports. Since the analysis period in this document does not begin until 2021, the infrastructure inventory in this year will be compared with the one from 2020 for the NRC report. Moreover, it should be noted that the NRC report evaluates the entire United States whereas this document includes only the western United States. Consequently, for comparison, the western United States values are adjusted to reflect national values by assuming that infrastructure and capital costs scale with hydrogen demand (i.e., if hydrogen demand is two times larger nationally, capital costs associated with the HIDM are doubled to reflect the national equivalent). In reality, this assumption may not hold true since higher population density in the eastern United States could result in different infrastructure designs, which, for example, may have shorter transmission pipeline lengths per demand center.

In the 2020-21 timeframe, about 58% of projected national hydrogen demand is located within the western United States. In the HIDM, the infrastructure installed in 2021 is initially oversized and designed to supply about 3.9 million HFCVs, or about 2400 tonnes H_2 per day. Thus, it is operating at about 36% of capacity. In contrast the model used in the NRC report is designed to support only the projected number of vehicles in 2020, which is 1.8 million HFCVs. As a result, the infrastructure requirements and capital cost identified by the HIDM are much larger. However, this reflects the fact that large-scale centralized infrastructure would likely need to be installed in tranches and oversized to anticipate near-term demand. Consequently, the capital investment will be much larger than the value identified by a steady-state model that assumes infrastructure is built only for current demand.

Table 58: Comparison of infrastructure requirements in this report and the NRC report (adjusted values reported in brackets for HIDM)

	2020 NRC	2021 HIDM	2035 NRC	2035 HIDM	2050 NRC	2050 HIDM
No. of cars served (million)	1.8	1.4	61	22.7	219	74
Hydrogen demand (tonnes per day)	1,410	818	38,000	14,000	120,000	45,000
Infrastructure capital cost (Billion$)	2.6	29 (8.6*) [50 (15*)]	139	147 [399]	415	309 [824]
Total no. of stations	2,112 (100% onsite)	2,575 [4,429] (14% onsite)	56,000 (40% onsite)	15,000 [41,000] (3% onsite)	180,000 (44% onsite)	31,000 [84,000] (0% onsite)
No. of central plants	0	4 [7]	113	28 [76]	210	56 [151]
Distribution pipeline length (km)	0	10,000 [17,000]	63,000	43,000 [116,000]	129,000	67,000 [181,000]
Transmission pipeline length (km)	0	6,000 [10,000]	0	26,000 [70,000]	0	47,000 [127,000]
CO2 pipeline length (km)	0	800 [1,400]	3,200	5,500 [15,000]	12,600	8,300 [22,500]

*Number in parentheses is capital cost if 100% of hydrogen is supplied by onsite production at 2,575 stations.

The values are also larger in the HIDM since centralized infrastructure is introduced in 2021 whereas the NRC model assumes that all hydrogen is supplied via onsite production at this time. As a result, there are significant additional costs associated with production facilities and pipelines. The HIDM estimates the total capital cost in 2021 to be about $50 billion nationally, as opposed to the $2.6 billion estimated in the NRC report. This difference represents about a 20-fold increase in cost when oversizing and early adoption of centralized infrastructure is included.

A more direct comparison involves the case where centralized infrastructure is delayed for one tranche. In this case, all hydrogen is supplied via onsite production, which is similar to the NRC scenario. Given this scenario, the adjusted capital cost is $15 billion nationally, which is still about six times larger since the infrastructure is designed for projected demand in 2025. In the NRC report, the projected number of HFCVs in 2025 is 10 million. If the NRC value is adjusted to support this number of HFCVs, the projected capital cost is about $14 billion. Consequently, in the case where all hydrogen is supplied by onsite production, the estimated capital costs are similar when compared using the same assumptions. However, the steady-state model does not account for underutilization from initial oversizing of infrastructure and, thus, may substantially underestimate capital costs in specific years.

In 2035, about 37% of projected national hydrogen demand is located within the western United States. In the HIDM, the fourth tranche has been constructed and is designed to support about 36 million HFCVs. Consequently, in 2035, the infrastructure is operating at about 64% of capacity. It is projected to each full capacity in about 2039. In contrast, the NRC model is designed to support only the current demand in 2035, which is generated by 61 million HFCVs nationally.

The HIDM estimates the total adjusted infrastructure capital cost to be about $399 billion in 2035, which is approximately three times larger than the estimate in the NRC report. There are five primary reasons for the difference in estimates. First, the HIDM accounts for underutilization of infrastructure whereas the NRC model does not. Second, because the NRC model is city-based, it assumes that no hydrogen transmission pipelines are required. Based on the HIDM, approximately 70,000 km of transmission pipeline may be required nationally, which could add about $43 billion to the total cost. Third, the NRC model does not include the costs associated with CO_2 storage, which could add another $5 billion. Fourth, the NRC model assumes a fixed CO_2 pipeline length per coal-based production facility of 160 km, whereas the spatial analysis in the HIDM suggests that the value may be closer to 300 km in the western U.S. Thus, the total CO_2 pipeline length estimated by the NRC model is about 50% of the value estimated by the HIDM. Moreover, only a small fraction of the production facilities are coal-based in the NRC model so fewer facilities utilize CCS. Finally, since regional supply networks are not considered, the NRC model assumes that more cities are supplied by onsite production. As a result, the estimate of hydrogen distribution pipelines is also about 50% of the value estimated by the HIDM.

However, it is interesting to note that the numbers of refueling stations and production facilities estimated by the HIDM are smaller. Since the HIDM allows production facilities to serve multiple cities via regional pipeline networks, fewer though larger production facilities are required. In addition, the average size of refueling stations in the HIDM is slightly larger with a maximum capacity of 1,800 kg per day as opposed to 1,500 kg per day in the NRC model. Thus, fewer refueling stations are required in the HIDM.

In 2050, about 38% of projected national hydrogen demand is located within the western United States. In the HIDM, the infrastructure is fully utilized since the infrastructure installed in the sixth tranche is designed to support the number of HFCVs in 2050. Consequently, the infrastructure is fully utilized in both reports, allowing for a more direct comparison. The HIDM estimates the total infrastructure capital cost to be about $824 billion nationally in 2050, which is approximately double the estimate in the NRC report. The cost is much larger in the HIDM because H_2 transmission, CO_2 storage, and replacement costs for retired equipment are included in this model, but not included in the NRC model. In addition, it is assumed that no hydrogen is produced onsite in 2050 in the HIDM so the total length of distribution pipeline is about 40% larger. However, the construction of larger centralized production facilities that serve multiple cities translates to 30% fewer production facilities in the HIDM. Yet, the number of coal-based facilities estimated by the HIDM is double the value in the NRC model since hydrogen is produced exclusively by coal gasification with CCS in the HIDM. Consequently, the estimate of the total length of CO_2 pipeline is also approximately double in the HIDM. Finally, about 50% fewer refueling stations are required by the HIDM.

Without understanding the breakdown of costs in the NRC report, it is difficult to compare individual component costs between the models. However, the HIDM does indicate that the inclusion of replacement costs accounts for the largest portion of the difference in the total cumulative capital cost between the models (~$200 billion or 50% of the difference). The two other major components that constitute the additional cost are the inclusion of transmission pipelines and CO_2 storage (~25%) and the additional distribution pipelines required since all hydrogen is supplied from centralized facilities (~25%).

In summary, the NRC model underestimates the capital cost of infrastructure since it does not account for oversizing and does not consider several contributors to cost, including equipment replacement and some important infrastructure components (e.g., transmission pipelines). Moreover, because the NRC model does not allow integrated regional supply networks, it tends to overestimate the number of cities with onsite production and, thus, underestimates the length of distribution pipeline. The model also overestimates the required number of production facilities since each city with centralized production has its own plant. In contrast, the HIDM incorporates more spatial and temporal detail by allowing for explicit modeling of regional supply networks and accounting for underutilization over time. As a result, the HIDM provides a more realistic estimate of infrastructure requirements and cost.

4.1.5.2 Breakeven Price of Hydrogen

The breakeven prices of hydrogen estimated in this document are substantially larger than the levelized costs of hydrogen estimated in the NRC report. As discussed in the previous section, the differences are largely attributable to the fact that the HIDM incorporates a more realistic representation of infrastructure underutilization and allows for the development of regional supply networks. Figure 101 compares the average breakeven price of hydrogen over each ten-year analysis period for the two models. For the HIDM, it examines the case in which centralized infrastructure is built immediately (HIDM-Base) and the case in which it is delayed for one tranche (HIDM-Delayed Centralized).

This figure indicates that the discrepancy in the breakeven price is especially large in the first period when there is significant underutilization of capacity. Specifically, the HIDM-Base value is about 2.8 times larger than the NRC value. The inclusion of infrastructure components that are not modeled by the NRC model (i.e., H_2 transmission and CO_2 storage) accounts for about 25% of the cost difference. The remainder is partially explained by the difference in the proportion of cities served by onsite production, but primarily explained by lower utilization rates (i.e., effective capacity factors) (Table 59). The NRC model assumes fixed capacity factors for each component, regardless of year. In the first period, much smaller effective capacity factors are modeled in the HIDM, especially in relation to pipelines since the model has limited nominal pipe sizes and oversizes for projected flows over the lifetime of the pipeline. In the HIDM-Delayed Centralized case, centralized infrastructure is delayed for only four years so the breakeven price of hydrogen over the ten-year period is only slightly smaller than in the HIDM-Base case.

In the second period, the breakeven prices reported by both HIDM cases are only 50-55% larger than the value estimated by the NRC model. In this period, the effective capacity factors are more similar as infrastructure in the HIDM becomes better utilized over time. Therefore, more of the difference in price is explained by the additional components modeled in the HIDM (~37%) and less is explained by differences in utilization.

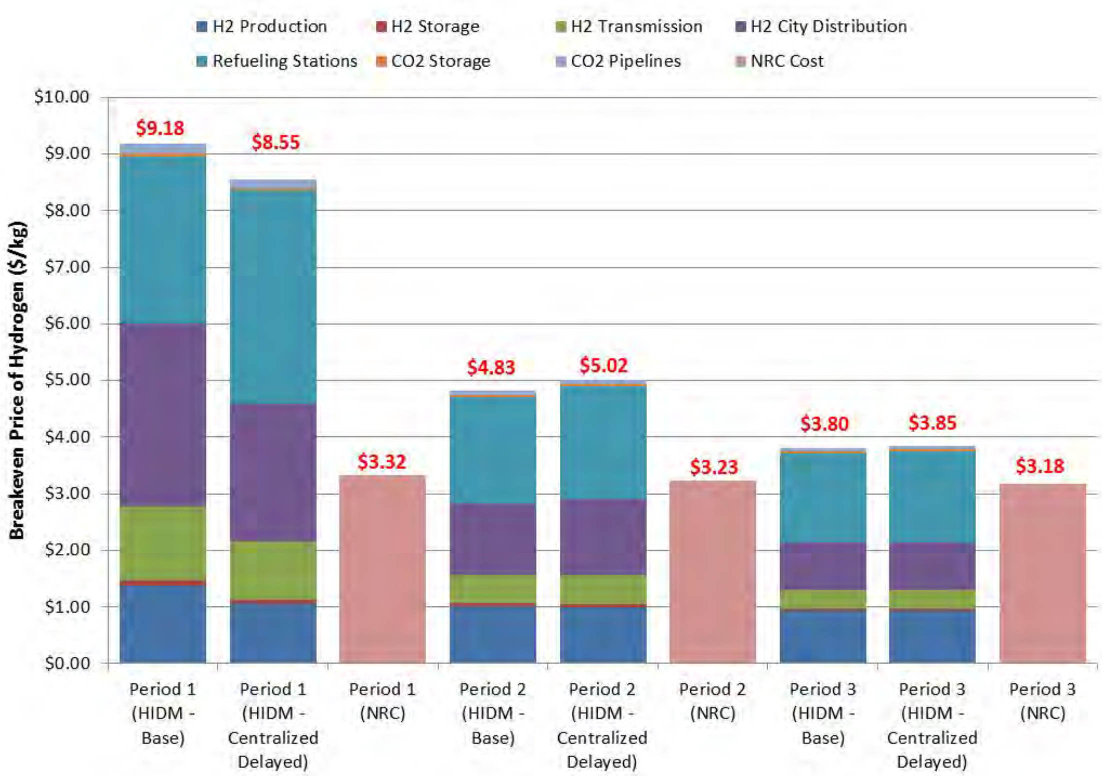

Figure 101: Breakeven price of hydrogen in each analysis period for the HIDM and NRC model (H_2 Success)

Table 59: Comparison of effective capacity factors used in the HIDM and NRC model for major infrastructure components

	Period 1		Period 2		Period 3	
	NRC	HIDM*	NRC	HIDM	NRC	HIDM
H_2 Production	90%	44%	90%	64%	90%	70%
H_2 Transmission	N/A	12%	N/A	30%	N/A	60%
H_2 Distribution	100%	13%	100%	37%	100%	60%
H_2 Refueling Stations	70%	49%	70%	67%	70%	74%
CO_2 Pipelines	N/A	26%	N/A	47%	N/A	60%

*Values provided for the HIDM-Base case. In the HIDM-Delayed Centralized case, the refueling station value would remain the same and the other values would be slightly larger since this infrastructure is not required in the first tranche when underutilization is largest. In all other periods, the values are identical in the two HIDM cases.

In the third period, the breakeven prices estimated by the two models begin to converge as the effective capacity factors become more similar. However, the breakeven prices are still about 20% larger in both HIDM cases and about 65% of the difference is explained by additional components. It should be noted that, even in the third period, the effective capacity factors are smaller in the HIDM for most components. In particular, the capacity factors for pipelines remain relatively small, which is the result of the limited number of nominal pipe sizes in the model. Given more potential pipeline sizes, pipeline diameters could be better matched with actual flows, which would increase the effective capacity factor and decrease the cost.

Since as much as 75% of the difference in the breakeven prices of the two models is explained by low utilization rates, any deployment strategy that can increase utilization will also decrease the cost of supplying hydrogen. In reality, infrastructure planners will have more flexibility in component sizing and the timing of construction than is allowed in the HIDM. This flexibility will likely allow for more efficient strategies for deploying infrastructure and, thus, better utilization and smaller infrastructure costs. Since component sizing and investment timing is constrained in the HIDM, the cost estimates represent high estimates of the cost of coal-based hydrogen infrastructure deployment. It is likely that the actual cost will be somewhere between the estimates provided by the HIDM and NRC model.

4.1.5.3 Subsidy Recommendations

The NRC report estimates the cost to the government of supporting (i.e., subsidizing) a transition to hydrogen-based light-duty vehicles assuming the H_2 Success HFCV deployment scenario. It includes both the cost of infrastructure and hydrogen fuel cell vehicles. Since the cost of fuel cell vehicles is not included in this document, a comparison will be made with the recommendations for infrastructure subsidies only. Assuming that oil prices are defined by the AEO High Oil Price case [70], the NRC report concludes that cumulative cash flow for infrastructure becomes positive in 2017, which is before the analysis in this study begins.

In contrast, given the H_2 Success deployment scenario and AEO High Oil Price case, the HIDM estimates larger infrastructure costs and, consequently, positive cumulative cash flow is delayed until 2033 (i.e., sixteen years later than the NRC estimate). Moreover, positive cumulative cash flow is achieved in 2033 whether centralized infrastructure is delayed or not (Table 56). In the case in which centralized infrastructure is introduced in the first tranche, the buy-down cost is approximately $18 billion for only the western United States. It decreases to about $14 billion if centralized infrastructure is delayed until the second tranche.

In terms of the recommended subsidy, the NRC report suggests that the government should pay for half of the total infrastructure cost until 2023, which is estimated as a subsidy of $8 billion. In this document, the introduction of a production tax credit that guarantees a hydrogen price of $10/kg (PTC-10) would accelerate the year in which cumulative cash flow becomes positive to 2027 in the case in which centralized infrastructure is installed in the first tranche and to 2022 in the case where centralized infrastructure is delayed until the second tranche. The cost of the production tax credits in both cases is $18 billion for only the western United States. Thus, the net present cost of this subsidy for the entire United States would likely be $35-50 billion, or 4 to 6 times the value estimated in the NRC report. It should also be noted that the NRC report only considers the best case scenario in which the oil price is high. As discussed in section 4.1.4, scenarios with lower oil prices will require larger subsidies and less favorable conditions for private investment.

4.2 Sub-regional Case Studies

The study area used for the regional case study of the western United States is divided into six sub-regions, which are defined by the optimal rollout strategy defined in the western U.S. study (Figure 102). Four independent hydrogen supply networks develop in tranche 2, which define the Northwest, Midwest, Southwest, and Pacific West regions. The Pacific West region is further divided into three sub-regions: Pacific, Intermountain, and Plains. The Pacific sub-region includes California, Nevada, Arizona, and part of New Mexico since the hydrogen production facilities in these states are largely developed to serve California demand. The Intermountain sub-region primarily includes the states within the central Rocky Mountains: Utah, Colorado, and parts of Idaho, Wyoming, and Nebraska. Several of the production facilities within this sub-region also serve California, but significant hydrogen demand also exists in the Denver and Salt Lake City metro areas. The Plains sub-region includes Montana, North Dakota, and parts of South Dakota and Wyoming. This sub-region is dominated by sparsely distributed small cities that are not served by centralized production until tranche 5.

The optimization model is not applied independently to each sub-region, but rather the sub-regional case studies are considered subsets of the optimized infrastructure design defined by the western U.S. case study. In each sub-region, the subset of infrastructure components that is required to serve the demand centers within the sub-region is quantified. In many cases, hydrogen is imported from other sub-regions (e.g., California ultimately imports hydrogen from the Plains, Intermountain, and Southwest sub-regions). As a result, although infrastructure may be outside a particular sub-region, the production facilities and associated transmission pipelines and CCS equipment are considered part of the infrastructure required to serve that sub-region. The costs of the individual components required to serve a sub-region are quantified based on the portion of the component's use that is allocated to the sub-region. This is conducted for each infrastructure component (e.g., 82% of the transmission pipeline segment from node 1570 to node 1555 in tranche 4 serves the Pacific sub-region and 18% serves the Intermountain sub-region).

The purpose of the sub-regional case studies is to compare the infrastructure requirements and costs between sub-regions with the objective of learning how the geographic characteristics of each sub-region and the region as a whole impact hydrogen cost. In this section, the infrastructure design and costs associated with each sub-region are briefly summarized and then various metrics are developed to compare the sub-regions.

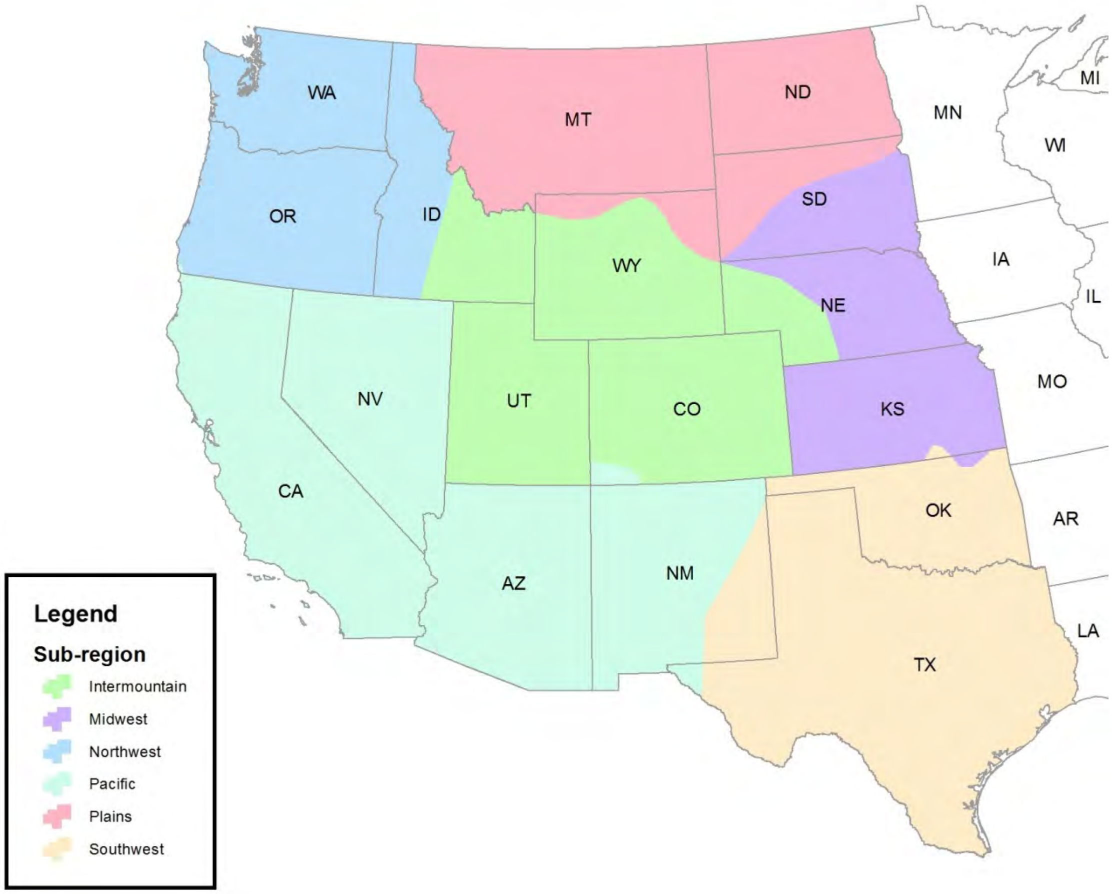

Figure 102: Boundary of sub-regions

4.2.1 Northwest

The Northwest sub-region includes Oregon, Washington, and part of Idaho (Figure 103). This sub-region has only two potential hydrogen production sites within its boundary (n256 and n480) and both sites have CO_2 storage sites in close proximity. The major cities within the study area are Seattle, Portland, and Boise (Figure 104).

4.2.1.1 Infrastructure Design

Several infrastructure design characteristics are unique to the Northwest sub-region. First, it shares very little of its supply network with other sub-regions. Until tranche 4, the supply network remains disconnected from the other sub-regions. At this point, hydrogen begins to be imported from production facilities in the Intermountain sub-region as a result of the limited number of potential production sites within the Northwest. However, despite this dependence on the Intermountain sub-region, greater than 85% of the transmission pipeline capacity serving the Northwest is allocated on average to the Northwest, which suggests that very little of the pipeline capacity is shared (Table 62).

Another characteristic is that the two major demand centers (Seattle and Portland) are located in the far western portion of the sub-region and are distant from other large metropolitan areas (Figure 104). As a result, early infrastructure is isolated to the corridor between these cities and outlying areas are initially served by onsite production (Table 61). In the first two tranches, approximately 50% of the demand centers are supplied by onsite production. The close proximity of demand centers served by centralized production also means that a relatively compact transmission pipeline network is required. As a result, the average transmission pipeline length per demand center remains well below 100 km (Table 62).

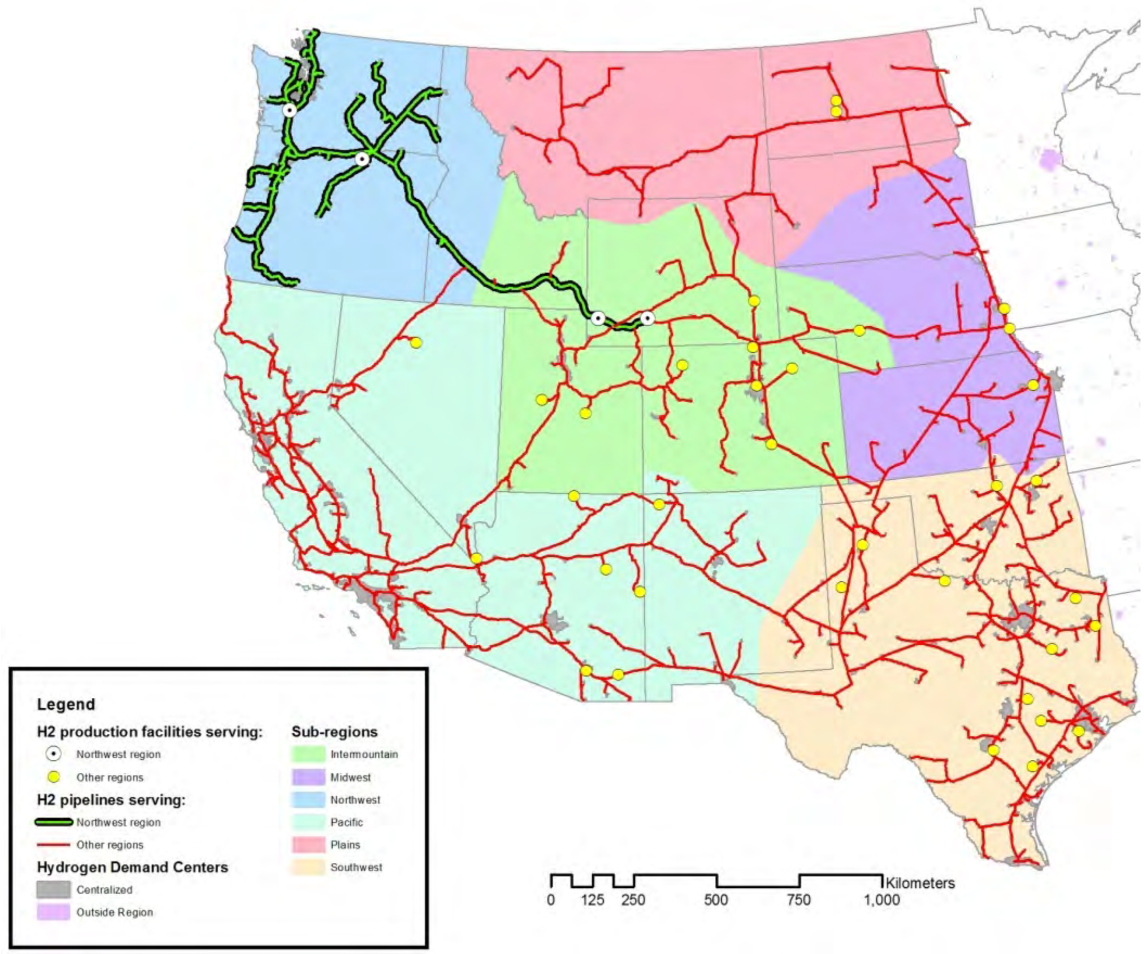

Figure 103: Subset of infrastructure required to serve the Northwest sub-region in all tranches

Although the isolated geography of the Northwest sub-region leads to a compact transmission pipeline network, it also limits the opportunity to aggregate H_2 production among many large demand centers. As a result, the minimum H_2 production facility size (300 t/day) is built at site n256 in each of the first two tranches for a total nameplate capacity of 600 tonnes per day (Table 60). Given that the total hydrogen demand projected to be served by centralized production is only ~150 tonnes per day and ~350 tonnes per day in tranches 1 and 2, respectively, even these small plants are significantly oversized. The combination of small underutilized plants and a relatively high delivered coal cost is expected to yield high production costs within the sub-region in the first few tranches.

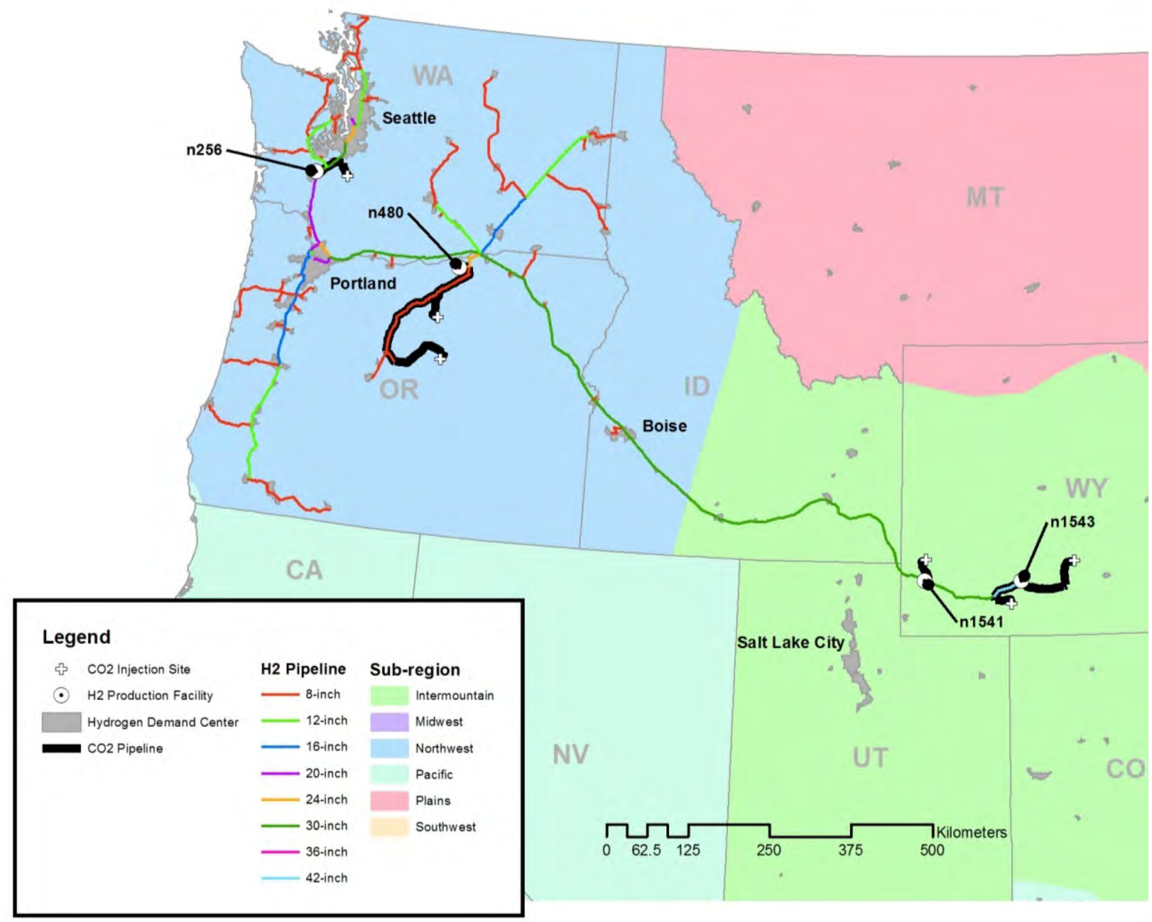

Figure 104: Infrastructure requirements within the Northwest sub-region in tranche 6

Regarding CCS infrastructure, the H_2 production site (n256), at which all facilities are built in the first three tranches, is located in close proximity to adequate CO_2 storage capacity (Figure 104). A 72-km CO_2 pipeline is built that connects the production site to a single CO_2 storage site. As a result, CO_2 transport and storage costs are expected to be low in the first three tranches. In the remaining tranches, four additional production facilities at sites n480, n1541, and n1543 are built and contribute hydrogen to the Northwest sub-region. Site n480 is located near an aquifer with low CO_2 storage density so a relatively long pipeline is required to connect the production site to two CO_2 storage sites. The average number of CO_2 storage sites per H_2 production site and the average length of CO_2 pipeline per H_2 production site can be used as proxies for the availability of local CO_2 storage capacity within a sub-region. In the Northwest, there are on average less than two CO_2 storage sites per H_2 production site and less than 200 km of CO_2 pipeline per H_2 production site (Table 62), which indicates adequate local CO_2 storage capacity.

Table 60: H_2 production facility requirements for the H_2 Success and H_2 Partial Success scenarios in the Northwest sub-region

	Tranche 1	Tranche 2		Tranche 3		Tranche 4		Tranche 5		Tranche 6	
Plant Nameplate Capacity (tonnes/day)	# of H_2 Plants	# of New H_2 Plants	Cumulative # of H_2 Plants	# of New H_2 Plants	Cumulative # of H_2 Plants	# of New H_2 Plants	Cumulative # of H_2 Plants	# of New H_2 Plants	Cumulative # of H_2 Plants	# of New H_2 Plants	Cumulative # of H_2 Plants
300	1	1	2	0	2	0	2	1	3	0	3
600	0	0	0	0	0	0	0	0	0	0	0
900	0	0	0	1	1	0	1	0	1	0	1
1200	0	0	0	0	0	1	1	0	1	0	1
1500	0	0	0	0	0	1	1	0	1	0	1
Total	1	1	2	1	3	1	5	1	6	0	6
Avg. Nameplate Capacity (tonnes/day)	300	300		500		840		750		750	
Total Nameplate Capacity (tonnes/day)	300	600		1,500		4,200		4,500		4,500	
Avg. fraction of production allocated to region	1.00	1.00		1.00		0.58		0.89		0.96	
Number of unique H_2 production sites	1	1		1		3		3		4	
Avg. delivered coal cost ($/GJ)	1.8	1.8		1.8		1.8		1.7		1.6	

Table 61: Number of demand centers served by centralized and onsite supply in the Northwest sub-region

	Tranche 1	Tranche 2	Tranche 3	Tranche 4	Tranche 5	Tranche 6
	# of demand centers	# of demand centers	# of demand centers	# of demand centers	# of demand centers	# of demand centers
Centralized Supply	4	10	33	49	75	79
Onsite Supply	5	9	9	6	4	0
Total	9	19	42	55	79	79
% Onsite Demand Centers	56%	47%	21%	11%	5%	0%
% Hydrogen Supplied Onsite	14%	19%	4%	2%	0.4%	0%
Total Hydrogen Demand (tonnes/day)	180	433	1107	2152	3230	4594

Table 62: H_2 and CO_2 pipeline requirements in the Northwest sub-region

	Tranche 1	Tranche 2		Tranche 3		Tranche 4		Tranche 5		Tranche 6	
	New Pipeline (km)	New Pipeline (km)	Cumulative Pipeline (km)	New Pipeline (km)	Cumulative Pipeline (km)	New Pipeline (km)	Cumulative Pipeline (km)	New Pipeline (km)	Cumulative Pipeline (km)	New Pipeline (km)	Cumulative Pipeline (km)
H_2 Transmission											
Total Length (km)	289	294	583	1979	2562	835	3397	951	4348	543	4890
Avg. pipeline length per demand center (km)	72	58		78		69		58		62	
Avg. fraction of pipeline use allocated to region	1.00	1.00		1.00		0.88		0.93		0.95	
H_2 Distribution											
Total Length (km)	844	663	1506	1789	3295	1691	4986	1789	6775	1291	8066
Avg. pipeline length per demand center (km)	211	151		100		102		90		102	
Avg. fraction of pipeline use allocated to region	1.00	1.00		1.00		1.00		1.00		1.00	
CO_2 Transport											
Total Length (km)	72	0	72	0	72	397	468	48	516	212	728
Avg. pipeline length per H_2 production site (km)	72	72		72		156		172		182	
Avg. fraction of pipeline use allocated to region	1.00	1.00		1.00		0.89		0.97		0.95	
# of demand centers (centralized supply)	4	10		33		49		75		79	

Table 63: CO_2 storage requirements in the Northwest sub-region

	Tranche 1	Tranche 2		Tranche 3		Tranche 4		Tranche 5		Tranche 6	
	New	New	Cumulative	New	Cumulative	New	Cumulative	New	Cumulative	New	Cumulative
# of storage sites	1	0	1	0	1	2	3	1	4	2	6
# of injection wells	2	2	4	7	11	22	33	4	37	13	50
Avg. number of storage sites per H_2 production site	1	1		1		1		1.3		1.5	

4.2.1.2 Cost

The cumulative capital investment in each tranche for the H_2 Success and H_2 Partial Success scenarios in the Northwest sub-region are given in Table 64. The cumulative capital investment in tranche 6 is approximately $30 billion, which is about 10% of the cumulative capital investment required for the entire western United States. Because pipelines are not as oversized in the H_2 Partial Success scenario, the capital investment is slightly lower in the first three tranches.

As a percentage of the cumulative capital investment, the H_2 production cost is larger in the first four tranches in the Northwest sub-region than in the western U.S. region since small underutilized facilities are built (Figure 105). The impact is even larger in the H_2 Partial Success scenario where the production cost represents greater than 25% of the total cumulative capital investment in the first two tranches since plants are underutilized for a longer period of time. The capital investment for transmission pipelines occupies a smaller percentage of the total investment in the first two tranches in the Northwest sub-region since the transmission pipeline network is limited to a small area.

Figure 106 compares the breakeven prices of hydrogen ($/kg) in the Northwest sub-region and the western U.S. case study given the H_2 Success scenario. During the first ten-year period, the levelized cost of H_2 production is about 38% higher in the Northwest case study as a result of the small underutilized production facilities and higher delivered cost of coal. In addition, the levelized cost of H_2 storage is more than double in the Northwest region since storage facilities are oversized for the projected production at the site. Thus, the storage facility is built for a 1500 t/day plant in tranche 1 even though the H_2 demand in the first two tranches reaches only about 350 t/day. The levelized costs of CO_2 storage and refueling stations are also about 15% larger in the first period while the cost associated with CO_2 pipelines is about 30% smaller since only one 72-km pipeline is built during this period. Refueling station costs are larger in the Northwest sub-region since more stations include onsite production. The levelized costs associated with H_2 transmission and distribution pipelines are virtually identical between the two case studies. In total, the breakeven price of hydrogen increases by about 10% in the first period relative to the western U.S. case study. This price increase is driven primarily by the larger costs associated with H_2 production and storage.

Table 64: Cumulative capital investment (Billion $) in the Northwest sub-region for each tranche

	Tranche 1	Tranche 2	Tranche 3	Tranche 4	Tranche 5	Tranche 6
H2 Success						
H_2 Production	0.5	1.0	2.1	3.5	4.8	5.9
H_2 Storage	0.1	0.1	0.1	0.3	0.3	0.3
H_2 Transmission	0.2	0.3	1.7	2.2	2.5	2.9
H_2 Distribution	1.0	1.7	3.1	4.5	5.9	8.2
Refueling Stations	0.5	1.0	2.4	4.4	7.6	11.6
CO_2 Transport	0.02	0.04	0.1	0.2	0.2	0.3
CO_2 Injection	0.1	0.1	0.1	0.4	0.4	0.5
Total Capital Investment (Billion 2005$)	2.3	4.3	9.5	15.4	21.7	29.6
H_2 Partial Success						
H_2 Production	0.5	1.0	2.1	3.5	4.8	N/A
H_2 Storage	0.1	0.1	0.1	0.3	0.3	N/A
H_2 Transmission	0.2	0.3	1.6	2.4	2.7	N/A
H_2 Distribution	0.5	1.2	2.6	5.2	6.5	N/A
Refueling Stations	0.5	1.0	2.4	4.9	7.6	N/A
CO_2 Transport	0.02	0.04	0.1	0.2	0.3	N/A
CO_2 Injection	0.1	0.1	0.1	0.5	0.5	N/A
Total Capital Investment (Billion 2005$)	1.8	3.6	8.9	16.9	22.7	N/A

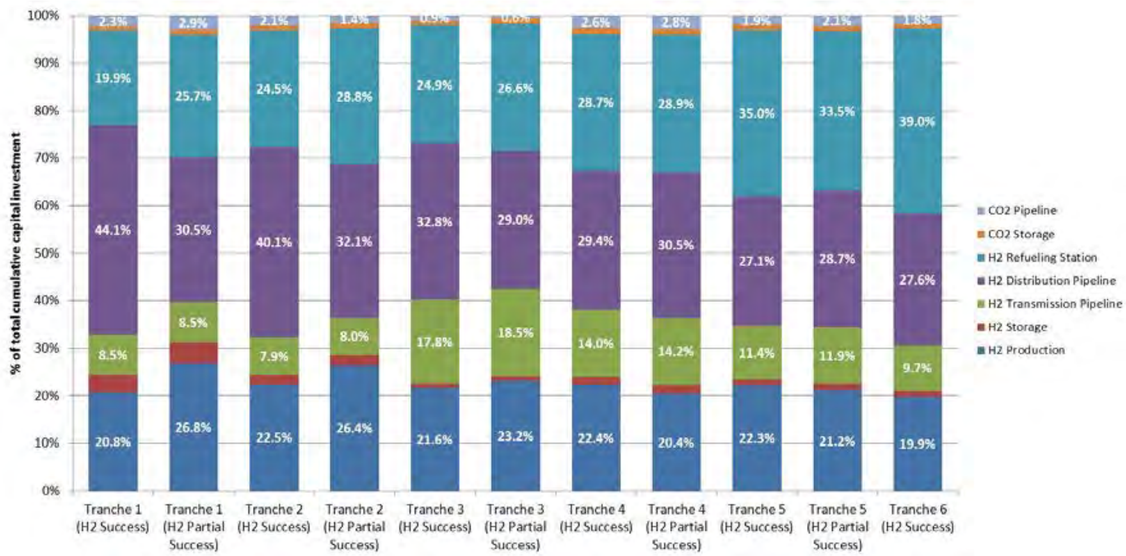

Figure 105: Percentage of total cumulative capital investment associated with each component in the Northwest sub-region

In the second period, the breakeven price of hydrogen is still about 4% larger in the Northwest sub-region. The increase is attributable to larger levelized costs of H_2 production and transmission pipelines. The larger levelized cost of H_2 transmission pipelines occurs even though the average pipeline length per demand center is smaller in the Northwest sub-region. The increase is the result of the smaller pipeline diameters required in the Northwest. Consequently, transmission pipelines in the Northwest do not achieve the economies-of-scale associated with the larger diameter pipelines used in other sub-regions.

In the third period, the breakeven price of hydrogen is smaller in the Northwest sub-region than the price calculated for the western U.S. The lower cost is attributable to better utilization of H_2 production facilities and distribution pipelines. Throughout most of the study period, the Northwest sub-region has a higher breakeven price of hydrogen since the isolated geography of the region leads to small underutilized production facilities, a greater percentage of demand centers served by onsite production, and smaller diameter transmission pipelines. Essentially, the Northwest sub-region does not achieve economies-of-scale or high utilization of capacity until tranche 6. With even lower utilization rates in the H_2 Partial Success scenario, the breakeven price of hydrogen is $12.25/kg in period 1, $6.44/kg in period 2, and $5.00/kg in period 3 (Figure 107).

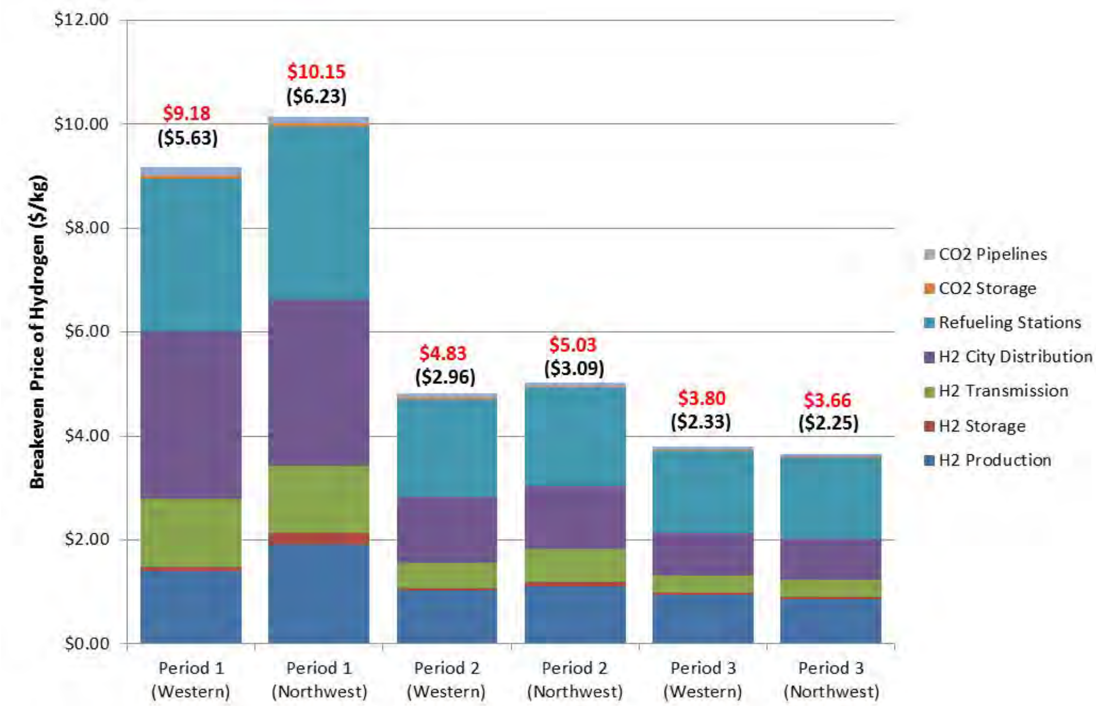

Figure 106: Comparison of the breakeven price of hydrogen under the H_2 Success scenario in the Northwest sub-region and western U.S. (number in parentheses is the $/gallon gasoline equivalent)

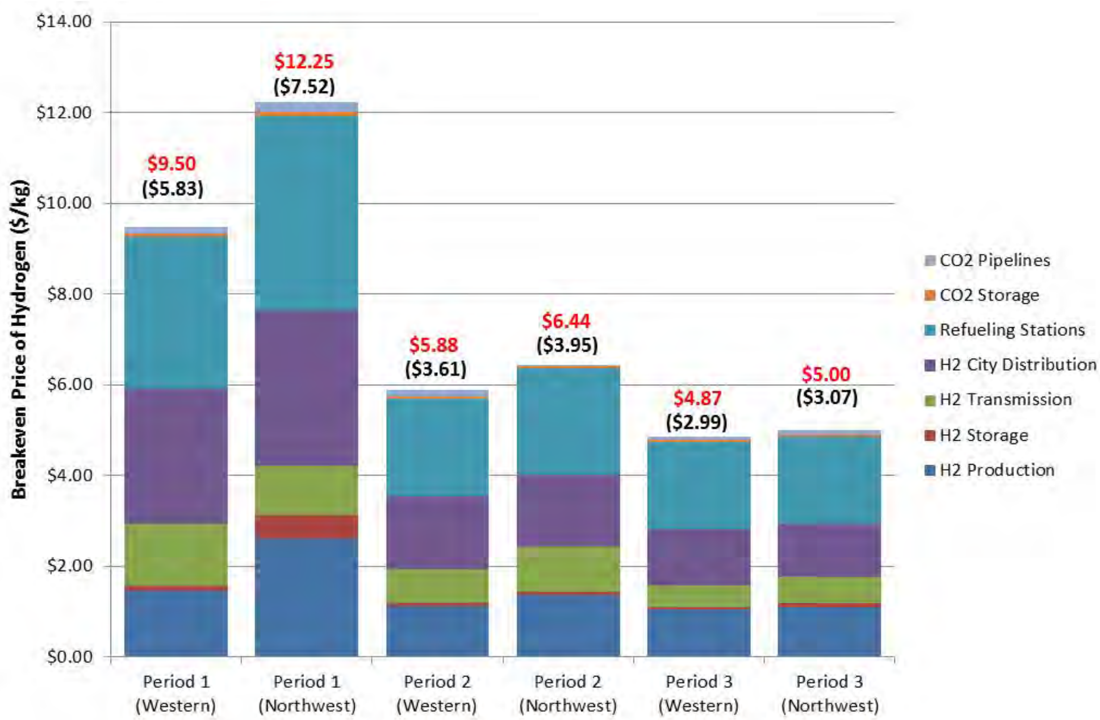

Figure 107: Comparison of the breakeven price of hydrogen under the H_2 Partial Success scenario in the Northwest sub-region and western U.S. (number in parentheses is the $/gallon gasoline equivalent)

4.2.2 Plains

The Plains sub-region includes the states of Montana and North Dakota and parts of South Dakota and Wyoming (Figure 108). This sub-region has very low population density and contains no cities with a population greater than 150,000 people. As a result, the regional hydrogen demand is extremely low in the first two tranches (Table 66). Two potential H_2 production sites are located within the sub-region and both are in close proximity to adequate CO_2 storage capacity.

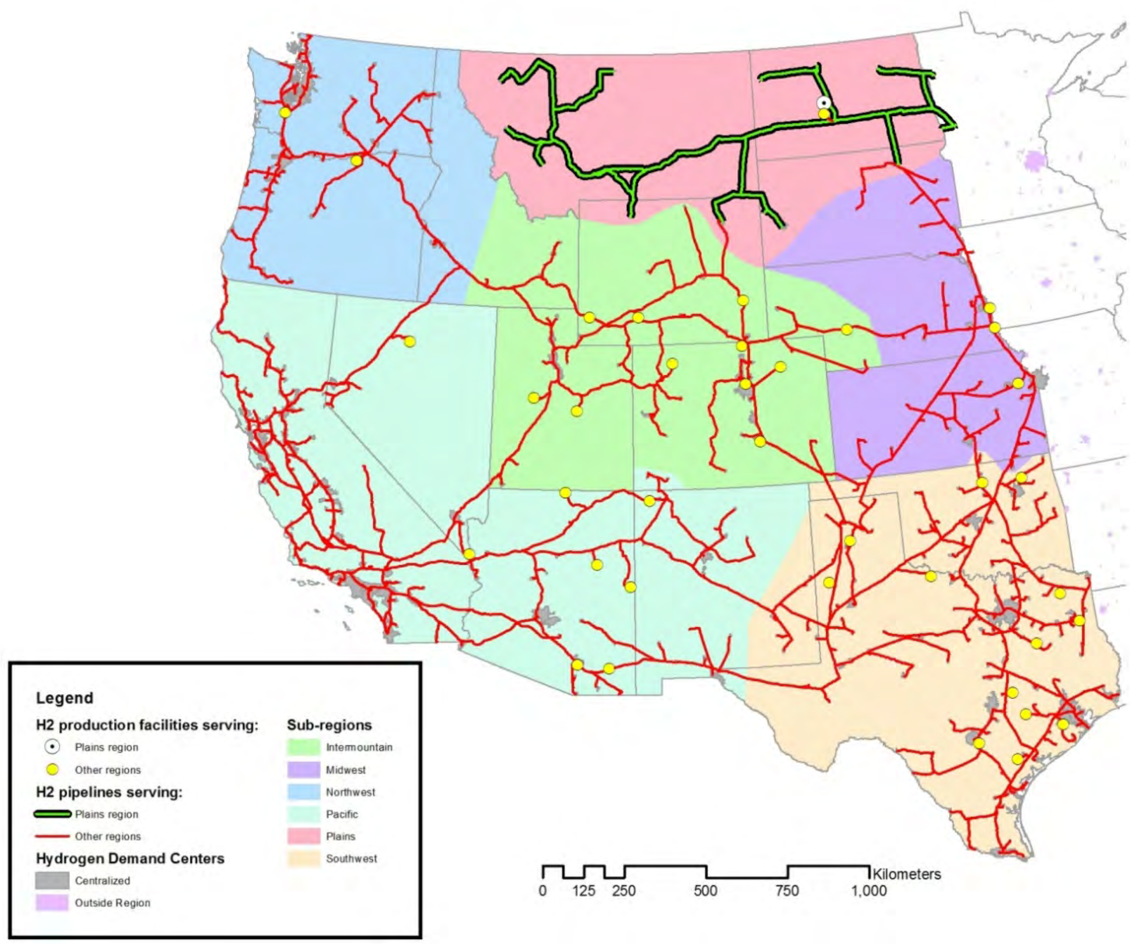

Figure 108: Subset of infrastructure required to serve the Plains sub-region in all tranches

4.2.2.1 Infrastructure Design

As a result of the low population density within the sub-region, centralized infrastructure is not viable until tranche 5. Prior to the introduction of centralized infrastructure, hydrogen is supplied exclusively by onsite production at individual refueling stations (Table 66). In tranche 5, the total hydrogen demand within the sub-region is only about 350 tonnes per day. However, centralized infrastructure becomes viable because the delivered coal cost is very low ($1.2/GJ) at the potential production sites and, consequently, centralized H_2 production facilities are built to export hydrogen to other sub-regions. These exports allow economies-of-scale to be achieved that would not be possible if hydrogen was produced only for sub-regional demand. In fact, less than 50% of the production at the H_2 plants is allocated to meet the demand within the sub-region (Table 65).

Because the Plains sub-region has very low population density, the average length of H_2 transmission pipeline per demand center is approximately 150 km, which is almost double the value identified in the western U.S. case study in tranche 6 (Table 67). In addition, the average pipeline diameter by length is also small at less than 15 inches in both tranches. As a result, it is expected that the cost of H_2 transmission will be relatively high in the Plains sub-region.

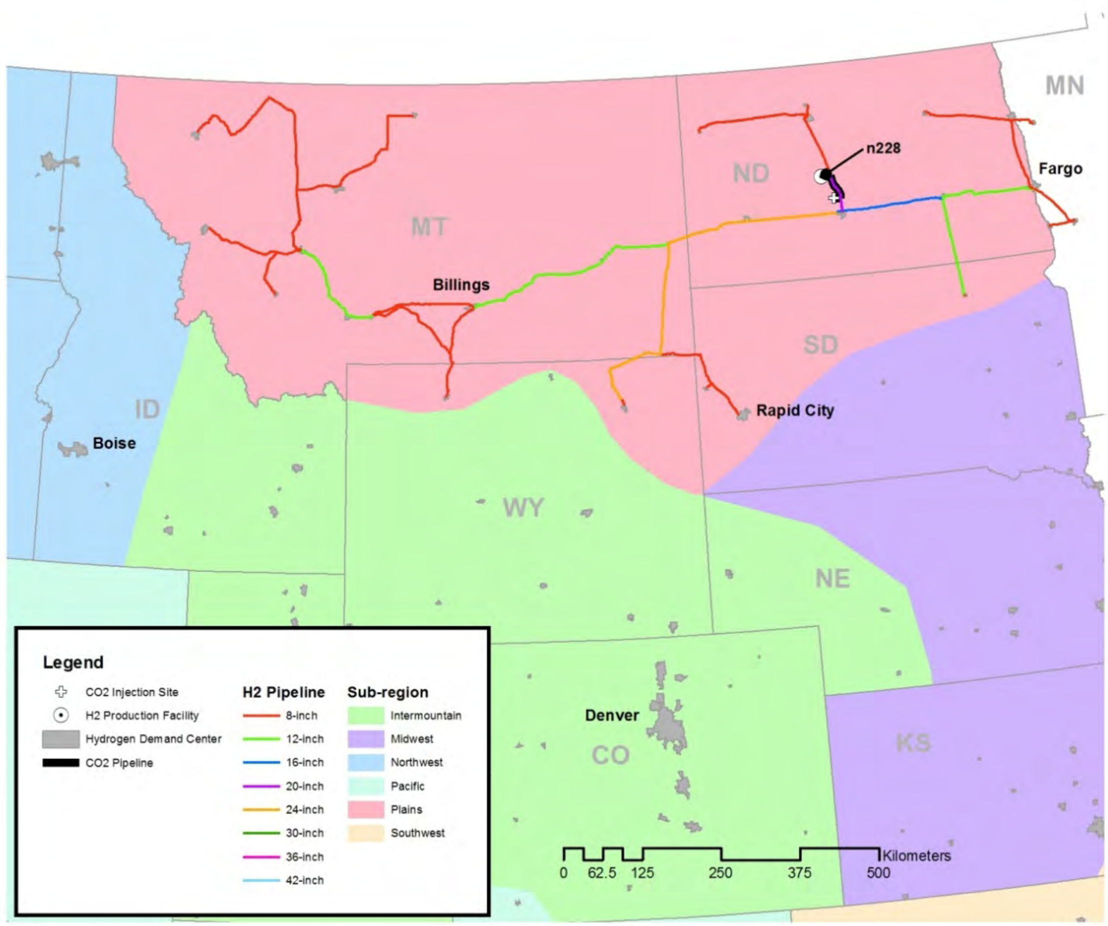

Figure 109: Infrastructure requirements within the Plains sub-region in tranche 6

Table 65: H_2 production facility requirements for the H_2 Success and H_2 Partial Success scenarios in the Plains sub-region

	Tranche 1	Tranche 2		Tranche 3		Tranche 4		Tranche 5		Tranche 6	
Plant Nameplate Capacity (tonnes/day)	# of H_2 Plants	# of New H_2 Plants	Cumulative # of H_2 Plants	# of New H_2 Plants	Cumulative # of H_2 Plants	# of New H_2 Plants	Cumulative # of H_2 Plants	# of New H_2 Plants	Cumulative # of H_2 Plants	# of New H_2 Plants	Cumulative # of H_2 Plants
300	0	0	0	0	0	0	0	0	0	0	0
600	0	0	0	0	0	0	0	0	0	1	1
900	0	0	0	0	0	0	0	1	1	0	1
1200	0	0	0	0	0	0	0	0	0	0	0
1500	0	0	0	0	0	0	0	0	0	0	0
Total	0	0	0	0	0	0	0	1	1	1	2
Avg. Nameplate Capacity (tonnes/day)	N/A	N/A		N/A		N/A		900		750	
Total Nameplate Capacity (tonnes/day)	N/A	N/A		N/A		N/A		900		1500	
Avg. fraction of production allocated to region	N/A	N/A		N/A		N/A		0.45		0.47	
Number of unique H_2 production sites	N/A	N/A		N/A		N/A		1		1	
Avg. delivered coal cost ($/GJ)	N/A	N/A		N/A		N/A		1.2		1.2	

Table 66: Number of demand centers served by centralized and onsite supply in the Plains sub-region

	Tranche 1	Tranche 2	Tranche 3	Tranche 4	Tranche 5	Tranche 6
	# of demand centers	# of demand centers	# of demand centers	# of demand centers	# of demand centers	# of demand centers
Centralized Supply	0	0	0	0	18	27
Onsite Supply	1	7	13	18	9	0
Total	1	7	13	18	27	27
% Onsite Demand Centers	100%	100%	100%	100%	33%	0%
% Hydrogen Supplied Onsite	100%	100%	100%	100%	12%	0%
Total Hydrogen Demand (tonnes/day)	5	38	108	229	364	517

Table 67: H_2 and CO_2 pipeline requirements in the Plains sub-region

	Tranche 1	Tranche 2		Tranche 3		Tranche 4		Tranche 5		Tranche 6	
	New Pipeline (km)	New Pipeline (km)	Cumulative Pipeline (km)	New Pipeline (km)	Cumulative Pipeline (km)	New Pipeline (km)	Cumulative Pipeline (km)	New Pipeline (km)	Cumulative Pipeline (km)	New Pipeline (km)	Cumulative Pipeline (km)
H_2 Transmission											
Total Length (km)	0	0	0	0	0	0	0	2732	2732	1383	4114
Avg. pipeline length per demand center (km)	N/A	N/A		N/A		N/A		152		152	
Avg. fraction of pipeline use allocated to region	N/A	N/A		N/A		N/A		0.78		0.79	
H_2 Distribution											
Total Length (km)	0	0	0	0	0	0	0	733	733	298	1031
Avg. pipeline length per demand center (km)	N/A	N/A		N/A		N/A		41		38	
Avg. fraction of pipeline use allocated to region	N/A	N/A		N/A		N/A		1.00		1.00	
CO_2 Transport											
Total Length (km)	0	0	0	0	0	0	0	65	65	0	65
Avg. pipeline length per H_2 production site (km)	N/A	N/A		N/A		N/A		65		65	
Avg. fraction of pipeline use allocated to region	N/A	N/A		N/A		N/A		0.41		0.43	
# of demand centers (centralized supply)	0	0		0		0		18		27	

Table 68: CO_2 storage requirements in the Plains sub-region

	Tranche 1	Tranche 2		Tranche 3		Tranche 4		Tranche 5		Tranche 6	
	New	New	Cumulative	New	Cumulative	New	Cumulative	New	Cumulative	New	Cumulative
# of storage sites	0	0	0	0	0	0	0	1	1	0	1
# of injection wells	0	0	0	0	0	0	0	20	20	4	24
Avg. number of storage sites per H_2 production site	N/A	N/A		N/A		N/A		1.0		1.0	

In contrast, the average pipeline length per demand center associated with H_2 distribution is about 40 km in tranches 5 and 6, which reflects the fact that the demand centers within the sub-region are small (Table 67). Consequently, the cost associated with distribution pipelines is expected to be small. Regarding CCS infrastructure, a single injection site is shared by two H_2 production sites, of which only one (n228) supplies the Plains sub-region (Figure 109). There is adequate CO_2 storage capacity in close proximity to the production site so only a short 65-km CO_2 pipeline is required (Table 67).

4.2.2.2 Cost

Given low regional hydrogen demand, the cumulative capital investment is very small in the Plains sub-region. In the first four tranches, hydrogen is supplied exclusively by onsite production and the cumulative capital investment ranges from $20 million in tranche 1 to $900 million in tranche 4 (Table 69). In tranche 6, the cumulative capital investment is $4.4 billion, which is about 1% of the investment required for the entire western U.S.

As expected, the cost of refueling stations represents 100% of the capital investment in the first four tranches (Figure 110). Once centralized infrastructure is introduced, the capital expenditure is dominated by the cost of refueling stations and H_2 transmission since demand centers have low demand and are widely dispersed. The percentage of capital attributed to H_2 distribution pipelines is only ~11%, compared to ~28% in the western U.S., since cities within the Plains sub-region are small.

In comparing the breakeven price of hydrogen for the Plains sub-region and western U.S., it is apparent that hydrogen is supplied by onsite production in the Plains sub-region for the majority of the first two 10-year periods in the H_2 Success scenario (Figure 111). As a result, the breakeven price is dominated by the cost of refueling stations. However, even though the regional demand is very low in the Plains sub-region, the use of onsite steam methane reformers results in a 25% smaller breakeven price since onsite production is not as impacted by underutilization as the infrastructure associated with centralized production.

Table 69: Cumulative capital investment (Billion $) in the Plains sub-region for each tranche

	Tranche 1	Tranche 2	Tranche 3	Tranche 4	Tranche 5	Tranche 6
H2 Success						
H_2 Production	0.0	0.0	0.0	0.0	0.5	0.9
H_2 Storage	0.0	0.0	0.0	0.0	0.04	0.04
H_2 Transmission	0.0	0.0	0.0	0.0	0.7	1.1
H_2 Distribution	0.0	0.0	0.0	0.0	0.3	0.4
Refueling Stations	0.02	0.1	0.4	0.9	1.3	1.8
CO_2 Transport	0.0	0.0	0.0	0.0	0.03	0.04
CO_2 Injection	0.0	0.0	0.0	0.0	0.02	0.02
Total Capital Investment (Billion 2005$)	0.02	0.1	0.4	0.9	2.8	4.4
H_2 Partial Success						
H_2 Production	0.0	0.0	0.0	0.0	0.5	N/A
H_2 Storage	0.0	0.0	0.0	0.0	0.04	N/A
H_2 Transmission	0.0	0.0	0.0	0.0	0.7	N/A
H_2 Distribution	0.0	0.0	0.0	0.0	0.3	N/A
Refueling Stations	0.02	0.1	0.4	0.9	1.3	N/A
CO_2 Transport	0.0	0.0	0.0	0.0	0.03	N/A
CO_2 Injection	0.0	0.0	0.0	0.0	0.02	N/A
Total Capital Investment (Billion 2005$)	0.02	0.1	0.4	0.9	2.8	N/A

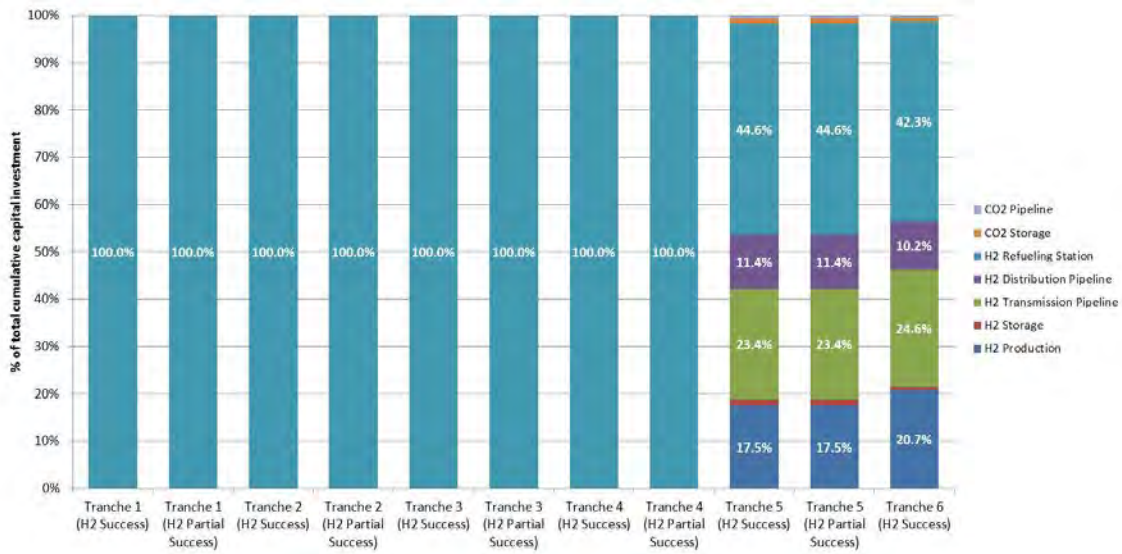

Figure 110: Percentage of total cumulative capital investment associated with each component in the Plains sub-region

Centralized infrastructure is introduced towards the end of the second period so the breakeven price is still dominated by the cost of onsite production. However, the investment in both onsite and centralized infrastructure results in higher costs and the breakeven price is slightly larger in the Plains sub-region. Once centralized infrastructure is fully deployed in the third period, much higher costs for H_2 transmission and refueling stations prevents the large decline in the breakeven price that is witnessed in the western U.S. In fact, the breakeven price of hydrogen remains about the same in the second and third periods.

In the H_2 Partial Success scenario, centralized infrastructure is not introduced until the last three years of the third period. Consequently, the breakeven price of hydrogen is dominated by the cost of refueling stations in all three periods. Given the slower deployment of HFCVs in this scenario, the use of onsite production achieves a smaller breakeven price of hydrogen in the first two periods. However, once centralized infrastructure is introduced in the third period, the price increases, suggesting that a lower price may be achieved in the Plains sub-region by employing only onsite production in all tranches. Essentially, the geography of this sub-region (i.e., small, dispersed cities) may result in prohibitive costs associated with centralized infrastructure and particularly H_2 transmission pipelines. As a result, onsite production may be the preferred method of supplying hydrogen in the Plains sub-region.

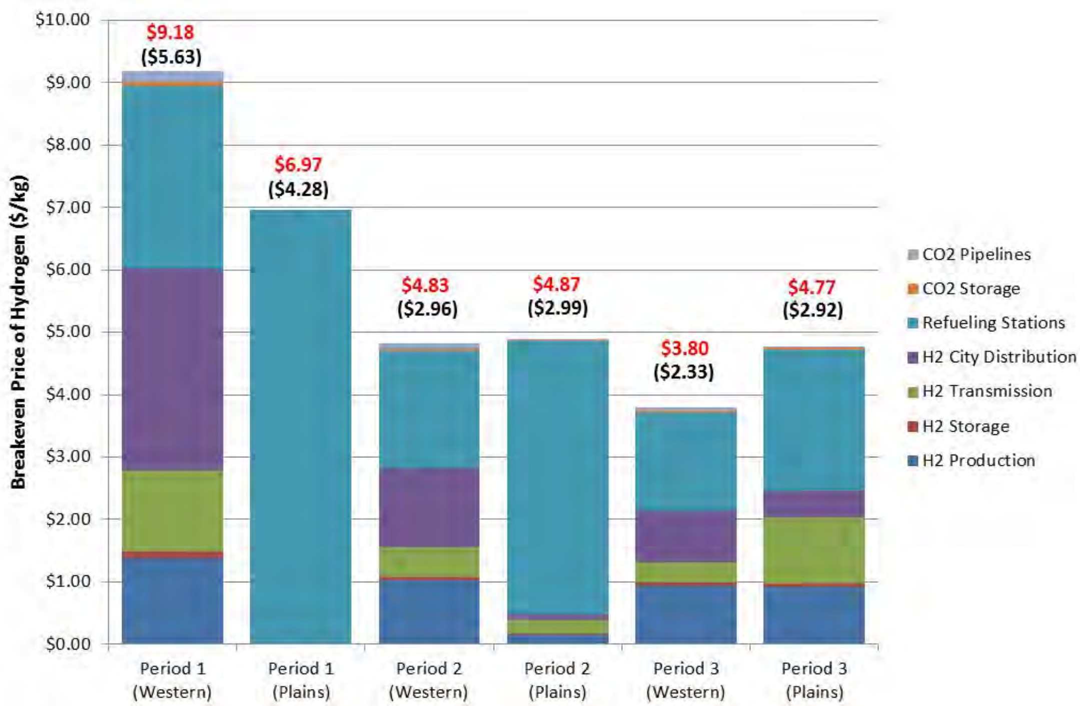

Figure 111: Comparison of the breakeven price of hydrogen under the H_2 Success scenario in the Plains sub-region and western U.S. (number in parentheses is the $/gallon gasoline equivalent)

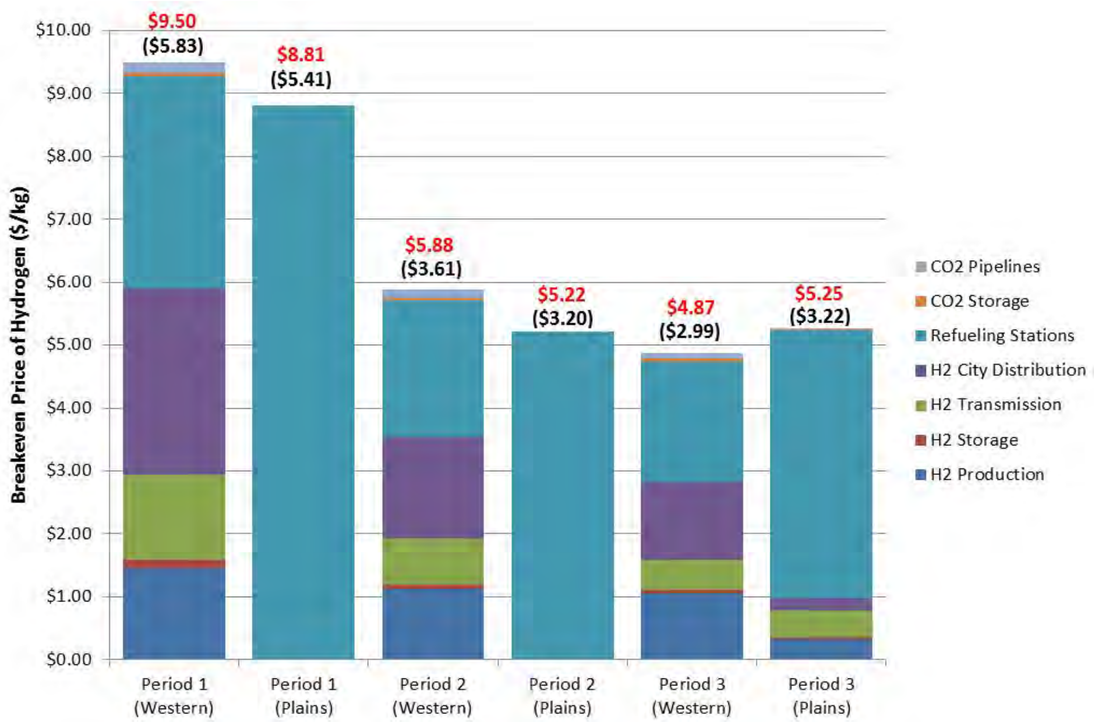

Figure 112: Comparison of the breakeven price of hydrogen under the H_2 Partial Success scenario in the Plains sub-region and western U.S. (number in parentheses is the $/gallon gasoline equivalent)

4.2.3 Pacific

The Pacific sub-region includes the states of California, Nevada, Arizona, and New Mexico (Figure 113). This sub-region contains over 50% of the hydrogen demand in the entire western U.S. The large metropolitan areas in California (e.g., San Francisco and Los Angeles) constitute the majority of demand, but no potential coal-based hydrogen production sites exist within the state. As a result, huge quantities of hydrogen are imported from production facilities in surrounding states. Arizona and New Mexico are included in the Pacific sub-region since the majority of hydrogen infrastructure built within these two states is used to supply demand in California.

4.2.3.1 Infrastructure Design

The design of hydrogen infrastructure within the Pacific sub-region is primarily influenced by the need to transport huge quantities of hydrogen into California. As a result, large trunk pipelines are developed from production facilities located in surrounding states. Because hydrogen demand is large within this sub-region, large production facilities can be built in early tranches (Table 70). For example, in tranche 1, 45 demand centers with a total demand of about 1500 tonnes per day are served by centralized production (Table 71). The average nameplate capacity of production facilities ranges from about 1000 tonnes per day in tranche 1 to about 1200 tonnes per day in tranche 6 (Table 70). The huge hydrogen demand within the sub-region eventually requires hydrogen to be imported from facilities in states as far as North Dakota and Oklahoma (Figure 113).

The large hydrogen demand and inadequate local production capacity within the Pacific sub-region result in the development of an extensive transmission pipeline network (Figure 114). In the first four tranches the average pipeline length per demand center varies from 80 to 100 km (Table 72). However, in tranche 5, the production capacity of the nearest sites is maximized and transmission pipelines must extend further to access new capacity. As a result, the average pipeline length per demand center increases to almost 120 km by tranche 6. The need for large trunk pipelines to transport hydrogen long distances is confirmed by the average diameter of transmission pipelines in each tranche, which varies between 21 and 25 inches. The average H_2 distribution pipeline length per demand center is also relatively large since there are many large metropolitan areas within this sub-region (Table 72).

Regarding CCS infrastructure, the Pacific sub-region includes very low CO_2 storage capacity within close proximity to potential production sites. This is particularly evident in Arizona and Nevada where extremely long CO_2 pipelines are required to access storage capacity (Figure 114). In fact, the average CO_2 pipeline length per H_2 production site is almost 500 km in tranche 2 and reaches a minimum of 224 km in tranche 6 (Table 72). Despite the need for long CO_2 pipelines, the accessed aquifers have sufficient storage capacity and, thus, the ratio of storage sites to H_2 production sites is generally about 1:1 (Table 73).

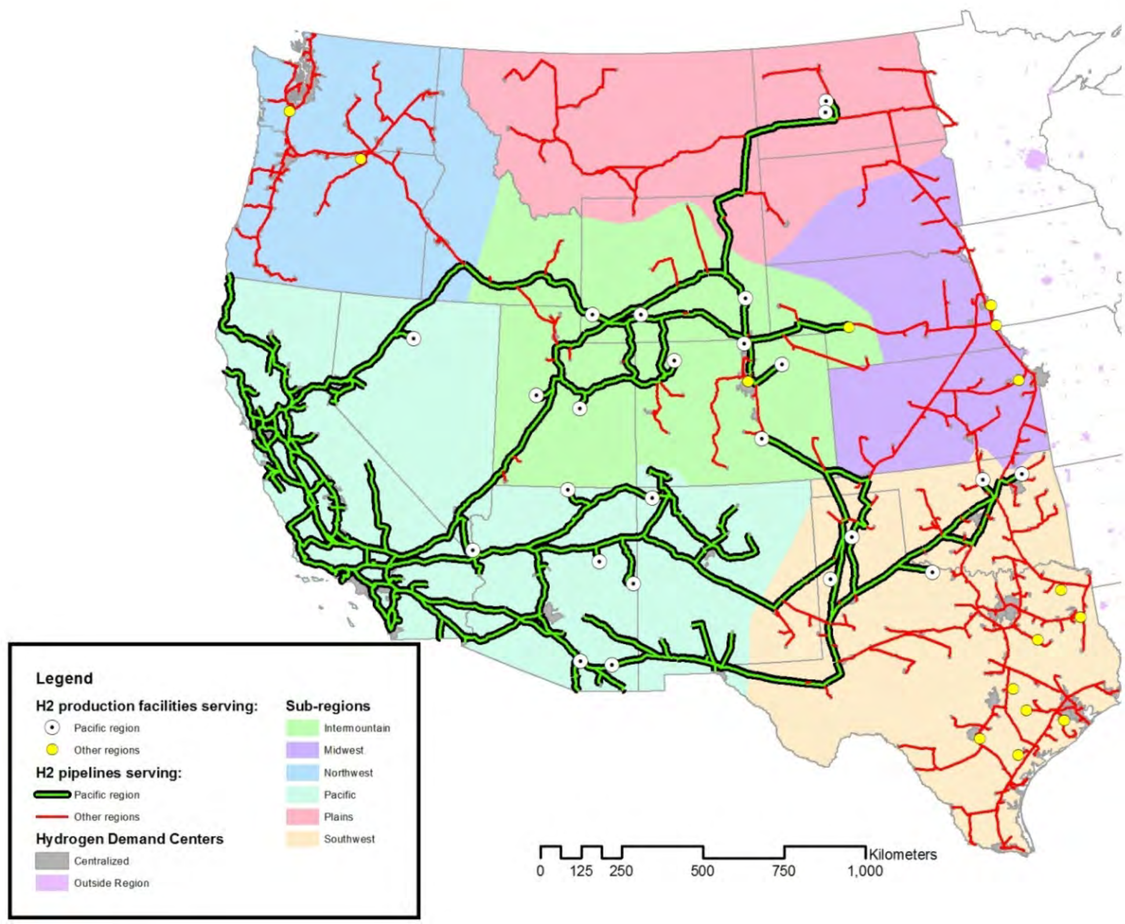

Figure 113: Subset of infrastructure required to serve the Pacific sub-region in all tranches

4.2.3.2 Cost

The Pacific sub-region is characterized by relatively large H_2 production facilities and long H_2 transmission and CO_2 transport pipelines. As a result, it is expected that the H_2 transmission and CO_2 transport costs will be relatively large and the H_2 production costs will be relatively small because of better economies-of-scale. In addition, several large cities reside within the sub-region and, consequently, the average H_2 demand per demand center is over 100 tonnes per day by tranche 6. Thus, relatively large diameter H_2 distribution pipelines are required.

Table 74 indicates that the cumulative capital investment is dominated by the cost of H_2 distribution pipelines since the model initially oversizes pipelines to meet the projected capacity requirements over the life of the pipeline. The distribution cost is particularly high in the H_2 Success scenario since rapid HFCV deployment translates to higher projected capacity requirements and thus more oversized pipelines. In tranche 6, the cumulative capital investment in the Pacific sub-region is ~$168 billion, which is about 54% of the investment required for the entire western U.S.

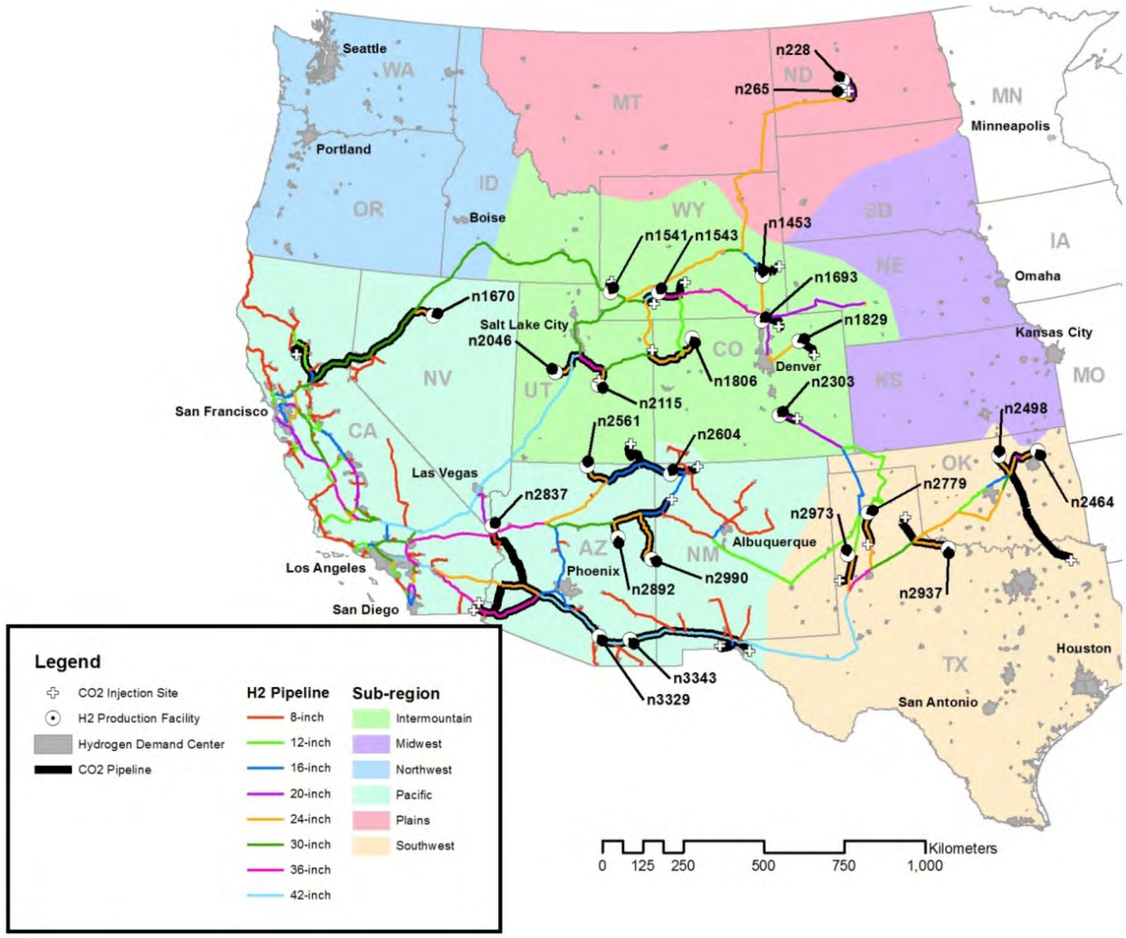

Figure 114: Infrastructure requirements within the Pacific sub-region in tranche 6

Table 70: H_2 production facility requirements for the H_2 Success and H_2 Partial Success scenarios in the Pacific sub-region

	Tranche 1	Tranche 2		Tranche 3		Tranche 4		Tranche 5		Tranche 6	
Plant Nameplate Capacity (tonnes/day)	# of H_2 Plants	# of New H_2 Plants	Cumulative # of H_2 Plants	# of New H_2 Plants	Cumulative # of H_2 Plants	# of New H_2 Plants	Cumulative # of H_2 Plants	# of New H_2 Plants	Cumulative # of H_2 Plants	# of New H_2 Plants	Cumulative # of H_2 Plants
300	0	1	1	0	1	1	2	0	2	0	2
600	1	0	1	2	3	0	3	1	4	1	5
900	0	0	0	0	0	0	0	2	2	1	3
1200	0	0	0	0	0	0	0	1	1	0	1
1500	1	1	2	2	4	5	9	3	12	7	19
Total	2	2	4	4	8	6	14	7	21	9	30
Avg. Nameplate Capacity (tonnes/day)	1,050	975		1,013		1,136		1,143		1,200	
Total Nameplate Capacity (tonnes/day)	2,100	3,900		8,100		15,900		24,000		36,000	
Avg. fraction of production allocated to region	0.90	0.88		0.93		0.89		0.85		0.82	
Number of unique H_2 production sites	2	3		6		12		17		24	
Avg. delivered coal cost ($/GJ)	1.6	1.8		1.9		1.8		1.8		1.9	

Table 71: Number of demand centers served by centralized and onsite supply in the Pacific sub-region

	Tranche 1	Tranche 2	Tranche 3	Tranche 4	Tranche 5	Tranche 6
	# of demand centers	# of demand centers	# of demand centers	# of demand centers	# of demand centers	# of demand centers
Centralized Supply	45	66	103	136	162	182
Onsite Supply	9	9	10	20	20	0
Total	54	75	113	156	182	182
% Onsite Demand Centers	17%	12%	9%	13%	11%	0%
% Hydrogen Supplied Onsite	5%	2%	1%	1%	1%	0%
Total Hydrogen Demand (tonnes/day)	1,487	2,673	6,003	11,378	16,460	23,410

Table 72: H_2 and CO_2 pipeline requirements in the Pacific sub-region

	Tranche 1	Tranche 2		Tranche 3		Tranche 4		Tranche 5		Tranche 6	
	New Pipeline (km)	New Pipeline (km)	Cumulative Pipeline (km)	New Pipeline (km)	Cumulative Pipeline (km)	New Pipeline (km)	Cumulative Pipeline (km)	New Pipeline (km)	Cumulative Pipeline (km)	New Pipeline (km)	Cumulative Pipeline (km)
H_2 Transmission											
Total Length (km)	3831	2900	6732	1517	8249	4411	12660	4612	17271	4056	21327
Avg. pipeline length per demand center (km)	85	102		80		93		107		117	
Avg. fraction of pipeline use allocated to region	1.00	0.99		0.99		0.95		0.91		0.93	
H_2 Distribution											
Total Length (km)	6565	2882	9448	5287	14734	6253	20987	4760	25747	5039	30786
Avg. pipeline length per demand center (km)	146	143		143		154		159		169	
Avg. fraction of pipeline use allocated to region	1.00	1.00		1.00		1.00		1.00		1.00	
CO_2 Transport											
Total Length (km)	568	876	1444	1028	2472	1461	3933	602	4535	849	5383
Avg. pipeline length per H_2 production site (km)	284	481		412		328		267		224	
Avg. fraction of pipeline use allocated to region	0.98	0.96		0.97		0.88		0.87		0.90	
# of demand centers (centralized supply)	45	66		103		136		162		182	

Table 73: CO_2 storage requirements in the Plains sub-region

	Tranche 1	Tranche 2		Tranche 3		Tranche 4		Tranche 5		Tranche 6	
	New	New	Cumulative	New	Cumulative	New	Cumulative	New	Cumulative	New	Cumulative
# of storage sites	2	3	5	3	8	4	12	4	16	6	22
# of injection wells	16	15	31	36	67	62	129	65	194	88	282
Avg. number of storage sites per H_2 production site	1.0	1.7		1.3		1.0		0.9		0.9	

Table 74: Cumulative capital investment (Billion $) in the Pacific sub-region for each tranche

	Tranche 1	Tranche 2	Tranche 3	Tranche 4	Tranche 5	Tranche 6
H2 Success						
H_2 Production	2.2	4.1	8.8	16.1	23.3	33.4
H_2 Storage	0.2	0.2	0.5	0.9	1.2	1.8
H_2 Transmission	3.2	6.0	7.2	9.6	12.7	18.3
H_2 Distribution	9.4	12.9	19.3	27.2	32.9	49.7
Refueling Stations	3.6	6.0	12.5	23.0	38.9	58.8
CO_2 Transport	0.1	0.3	0.6	1.1	1.6	2.5
CO_2 Injection	0.3	0.8	1.6	2.5	2.9	3.7
Total Capital Investment (Billion 2005$)	19.0	30.3	50.5	80.2	113.5	168.2
H_2 Partial Success						
H_2 Production	2.2	4.1	8.8	16.1	23.3	N/A
H_2 Storage	0.1	0.2	0.5	1.0	1.3	N/A
H_2 Transmission	2.3	4.4	5.5	12.1	15.2	N/A
H_2 Distribution	5.3	8.2	14.7	33.1	38.8	N/A
Refueling Stations	3.6	6.0	12.5	26.6	38.9	N/A
CO_2 Transport	0.1	0.3	0.6	1.2	1.8	N/A
CO_2 Injection	0.3	0.8	1.6	2.7	3.1	N/A
Total Capital Investment (Billion 2005$)	14.0	24.0	44.1	92.8	122.4	N/A

As a percentage of capital, the H_2 distribution cost represents almost 50% of the total investment in tranche 1 of the H_2 Success scenario (Figure 115). H_2 distribution represents a smaller percentage over time as distribution pipelines become better utilized. H_2 transmission represents a larger percentage of the cost in the Pacific sub-region than in the western U.S. since the region requires an extensive supply network to meet demand. As expected, the contribution of H_2 production is slightly smaller and the contribution of CO_2 pipelines is slightly larger.

Since the capital requirement for the Pacific sub-region represents over 50% of the capital investment for the entire western U.S., the breakeven price of hydrogen for the western U.S. is greatly influenced by the Pacific sub-region. Consequently, the difference in the breakeven prices of hydrogen in the two regions is about 1% in the H_2 Success scenario (Figure 116). However, in looking at individual components, a few differences are identified. The costs associated with refueling stations and H_2 production are smaller in the Pacific sub-region in the first period. The production cost is smaller because larger plants are built and the refueling station cost is smaller because a smaller fraction of hydrogen is supplied by onsite production in the Pacific sub-region (Table 71). These lower costs are largely offset by larger costs associated with CO_2 and H_2 distribution and transmission pipelines.

In the second period, the cost differences are sustained with the exception of production costs, which are approximately equal in the two regions. The CO_2 pipeline cost is about 18% larger in the Pacific sub-region since more production facilities are built in Arizona and Nevada in the second period. In the third period, H_2 and CO_2 pipeline costs are still slightly larger. In general, underutilization of oversized and relatively long pipelines causes the breakeven price of hydrogen to be slightly larger in the Pacific sub-region.

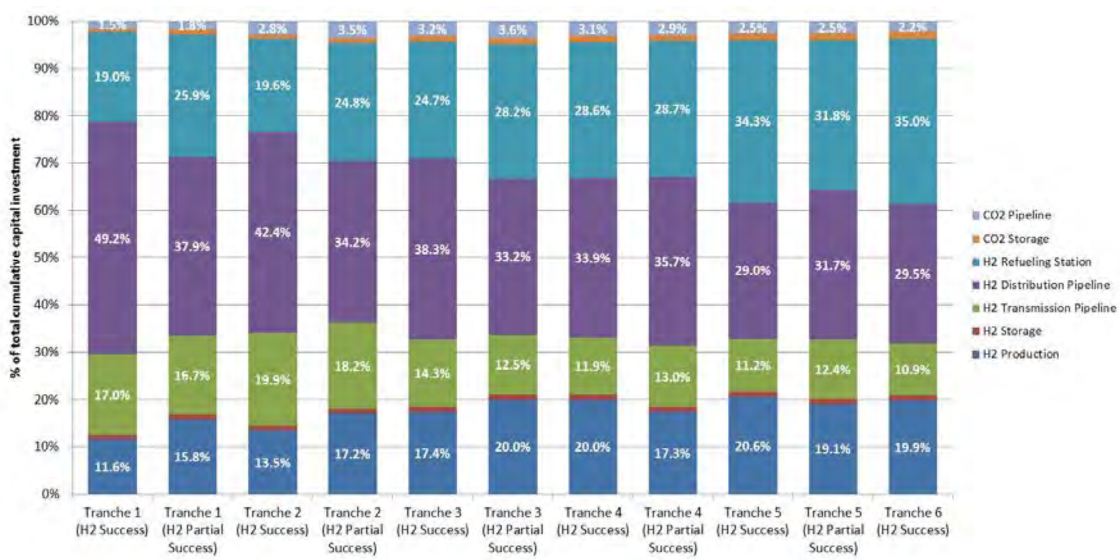

Figure 115: Percentage of total cumulative capital investment associated with each component in the Pacific sub-region

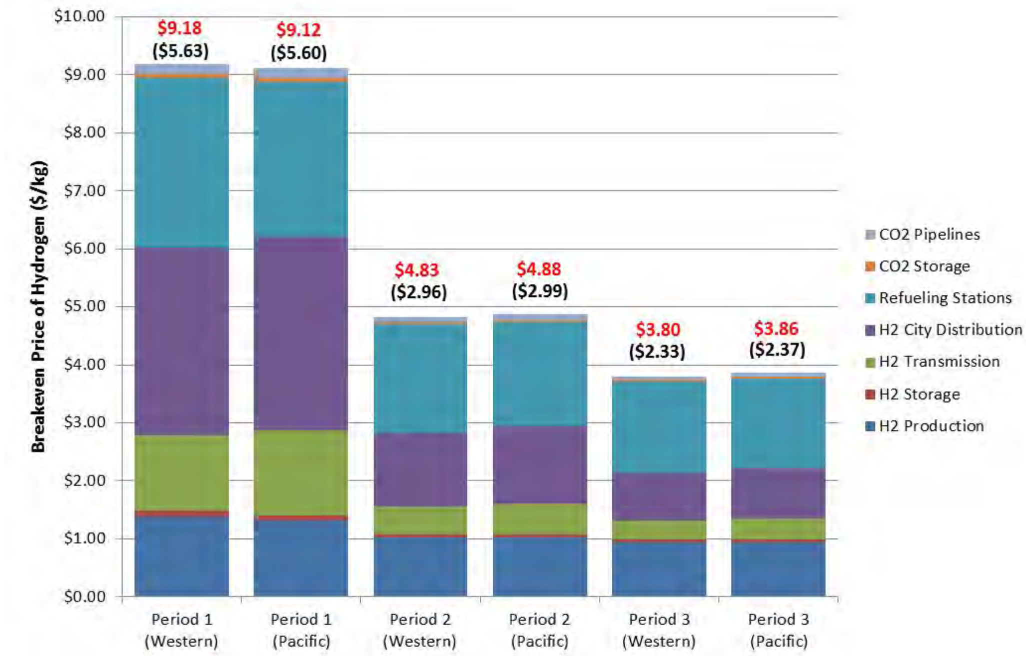

Figure 116: Comparison of the breakeven price of hydrogen under the H_2 Success scenario in the Pacific sub-region and western U.S. (number in parentheses is the $/gallon gasoline equivalent)

In the H_2 Partial Success scenario, the breakeven price of hydrogen is about 6% smaller in the first period since H_2 and CO_2 pipelines are not as oversized in this case (Figure 117). By reducing the initial size of pipelines, the utilization improves and the levelized cost is reduced. Less oversizing also contributes to a smaller breakeven price in the second period. However, by the third period, the benefit of smaller diameter pipelines disappears since increasing pipeline flows require that the original pipelines are replaced with larger diameter pipelines. Since the average pipeline length per demand center is larger in the Pacific sub-region, larger transmission costs translate to a higher breakeven price of hydrogen. Essentially, this sub-region illustrates the significant cost penalty associated with oversizing pipelines for projected capacity requirements in 20 years.

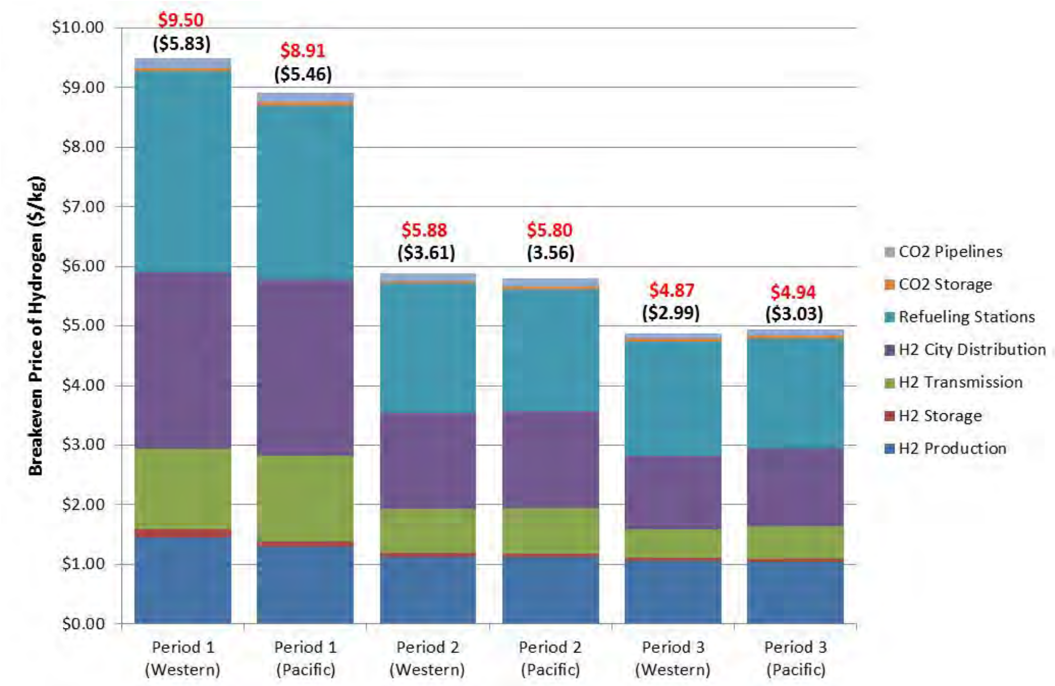

Figure 117: Comparison of the breakeven price of hydrogen under the H_2 Partial Success scenario in the Pacific sub-region and western U.S. (number in parentheses is the $/gallon gasoline equivalent)

4.2.4 Intermountain

The Intermountain sub-region includes Utah and Colorado and parts of Idaho, Wyoming, and Nebraska (Figure 118). The geography is characterized by mountainous terrain with relatively dispersed small cities. However, two large metropolitan areas (Denver and Salt Lake City) exist within this sub-region. There are eleven potential centralized hydrogen production sites so the sub-region has adequate capacity to meet regional demand. In addition, the sub-region is characterized by low delivered coal costs as a result of its proximity to major coal mines.

4.2.4.1 Infrastructure Design

The infrastructure design in the Intermountain sub-region is greatly influenced by its proximity to the large H_2 demand concentrated in the neighboring Pacific sub-region. Essentially, the transmission pipeline network and production facilities within the Intermountain sub-region are primarily designed to export hydrogen to the Pacific sub-region. This is evident from the large trunk pipeline corridors that pass through this sub-region (Figure 119). In addition, since much of the regional production capacity is used to supply the Pacific sub-region, the Intermountain sub-region must eventually import hydrogen from the Plains sub-region.

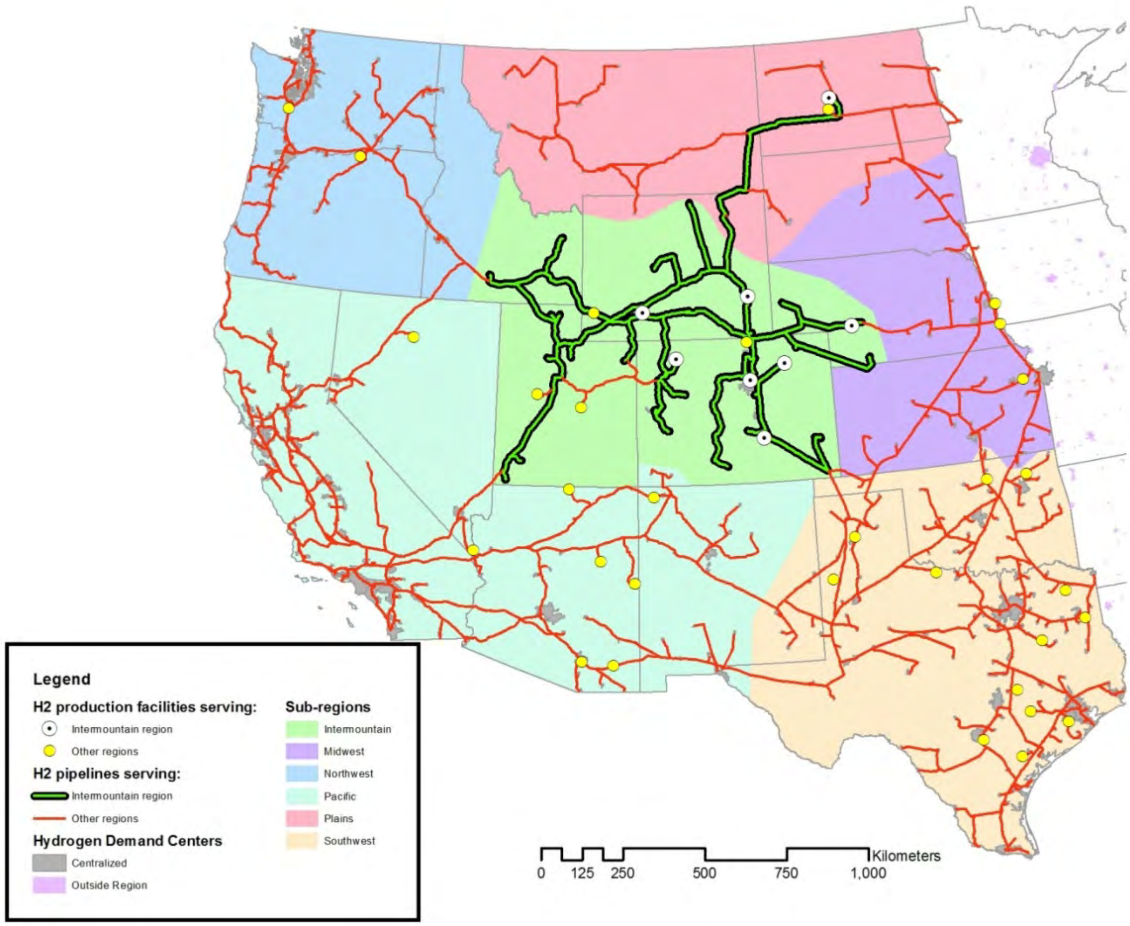

Figure 118: Subset of infrastructure required to serve the Intermountain sub-region in all tranches

Because the infrastructure is designed to meet the aggregated demand of two sub-regions, economies-of-scale are achieved much more quickly than if the infrastructure were designed only to supply the relatively low demand in the Intermountain sub-region (Table 76). For example, the regional hydrogen demand is only 165 tonnes per day in tranche 1, but this demand is supplied by a 1500 t/day production facility that also serves the Pacific sub-region. In fact, only 13% of the facility's production is allocated to the Intermountain sub-region (Table 75). Low allocation rates are also identified for H_2 transmission and CO_2 pipelines since the majority of pipeline capacity is attributed to the Pacific sub-region (Table 77).

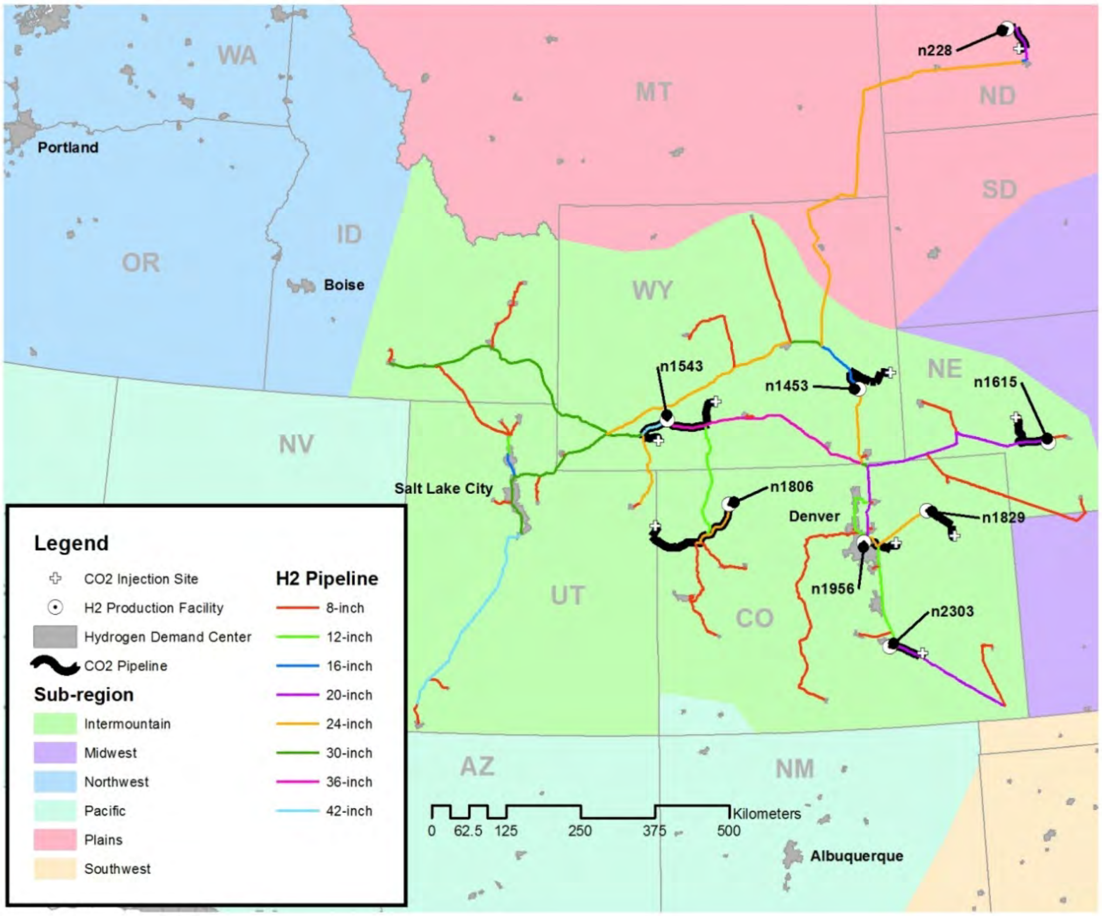

Figure 119: Infrastructure requirements within the Intermountain sub-region in tranche 6

Because demand centers are widely dispersed in this sub-region, the average transmission pipeline length per demand center is greater than 100 km in all tranches (Table 77). However, on average, only about 50% of pipeline use (and thus cost) is attributed to the Intermountain sub-region in the last three tranches. The average distribution pipeline length per demand center is relatively small since most cities within the sub-region are relatively small.

Regarding CCS infrastructure, most H_2 production sites within the sub-region are located in close proximity to adequate CO_2 storage capacity (Figure 119). As a result, the average CO_2 pipeline length per H_2 production site is less than 200 km in all tranches and there is approximately one storage site for each production site in most tranches (Table 78).

Table 75: H_2 production facility requirements for the H_2 Success and H_2 Partial Success scenarios in the Intermountain sub-region

	Tranche 1	Tranche 2		Tranche 3		Tranche 4		Tranche 5		Tranche 6	
Plant Nameplate Capacity (tonnes/day)	# of H_2 Plants	# of New H_2 Plants	Cumulative # of H_2 Plants	# of New H_2 Plants	Cumulative # of H_2 Plants	# of New H_2 Plants	Cumulative # of H_2 Plants	# of New H_2 Plants	Cumulative # of H_2 Plants	# of New H_2 Plants	Cumulative # of H_2 Plants
300	0	0	0	1	1	0	1	0	1	0	1
600	0	0	0	0	0	0	0	1	1	3	4
900	0	0	0	0	0	0	0	1	1	1	2
1200	0	0	0	0	0	1	1	0	1	0	1
1500	1	0	1	0	1	1	2	1	3	0	3
Total	1	0	1	1	2	2	4	3	7	4	11
Avg. Nameplate Capacity (tonnes/day)	1,500	1,500		900		1,125		1,071		927	
Total Nameplate Capacity (tonnes/day)	1,500	1,500		1,800		4,500		7,500		10,200	
Avg. fraction of production allocated to region	0.13	0.29		0.53		0.43		0.39		0.41	
Number of unique H_2 production sites	1	1		2		3		6		7	
Avg. delivered coal cost ($/GJ)	1.4	1.4		1.5		1.6		1.6		1.6	

Table 76: Number of demand centers served by centralized and onsite supply in the Intermountain sub-region

	Tranche 1	Tranche 2	Tranche 3	Tranche 4	Tranche 5	Tranche 6
	# of demand centers	# of demand centers	# of demand centers	# of demand centers	# of demand centers	# of demand centers
Centralized Supply	8	12	17	26	37	50
Onsite Supply	2	4	8	7	13	0
Total	10	16	25	33	50	50
% Onsite Demand Centers	20%	25%	32%	21%	26%	0%
% Hydrogen Supplied Onsite	5%	5%	7%	4%	2%	0%
Total Hydrogen Demand (tonnes/day)	165	362	835	1,611	2,386	3,394

Table 77: H_2 and CO_2 pipeline requirements in the Intermountain sub-region

	Tranche 1	Tranche 2		Tranche 3		Tranche 4		Tranche 5		Tranche 6	
	New Pipeline (km)	New Pipeline (km)	Cumulative Pipeline (km)	New Pipeline (km)	Cumulative Pipeline (km)	New Pipeline (km)	Cumulative Pipeline (km)	New Pipeline (km)	Cumulative Pipeline (km)	New Pipeline (km)	Cumulative Pipeline (km)
H_2 Transmission											
Total Length (km)	1072	216	1288	680	1968	935	2903	2185	5088	1770	6857
Avg. pipeline length per demand center (km)	134	107		116		112		138		137	
Avg. fraction of pipeline use allocated to region	0.65	0.73		0.69		0.51		0.53		0.51	
H_2 Distribution											
Total Length (km)	841	609	1451	775	2224	1195	3419	1081	4499	995	5496
Avg. pipeline length per demand center (km)	105	121		131		131		122		110	
Avg. fraction of pipeline use allocated to region	1.00	1.00		1.00		1.00		1.00		1.00	
CO_2 Transport											
Total Length (km)	91	121	212	69	282	121	403	386	788	(76)	712
Avg. pipeline length per H_2 production site (km)	91	212		141		134		131		102	
Avg. fraction of pipeline use allocated to region	0.13	0.29		0.58		0.32		0.30		0.33	
# of demand centers (centralized supply)	8	12		17		26		37		50	

Table 78: CO_2 storage requirements in the Intermountain sub-region

	Tranche 1	Tranche 2		Tranche 3		Tranche 4		Tranche 5		Tranche 6	
	New	New	Cumulative	New	Cumulative	New	Cumulative	New	Cumulative	New	Cumulative
# of storage sites	1	1	2	1	3	1	4	4	8	1	9
# of injection wells	12	1	13	3	16	21	37	45	82	27	109
Avg. number of storage sites per H_2 production site	1.0	2.0		1.5		1.3		1.3		1.3	

4.2.4.2 Cost

Since the majority of infrastructure in the Intermountain sub-region is built to supply the large hydrogen demand in the Pacific sub-region, the supply network achieves better economies-of-scale than would be expected given the regional hydrogen demand. As a result, the levelized costs within the region are similar to those of a region with greater demand. The cumulative capital investment in tranche 6 is ~$23 billion, which is about 7% of the investment required for the entire western U.S. (Table 79).

Table 79: Cumulative capital investment (Billion $) in the Intermountain sub-region for each tranche

	Tranche 1	Tranche 2	Tranche 3	Tranche 4	Tranche 5	Tranche 6
H2 Success						
H_2 Production	0.2	0.4	1.1	2.3	3.6	5.4
H_2 Storage	0.01	0.01	0.1	0.1	0.2	0.3
H_2 Transmission	0.4	0.4	0.5	0.6	0.9	1.9
H_2 Distribution	0.9	1.5	2.3	3.4	4.2	6.2
Refueling Stations	0.4	0.8	1.8	3.3	5.7	8.6
CO_2 Transport	0.01	0.02	0.05	0.1	0.2	0.4
CO_2 Injection	0.01	0.01	0.06	0.1	0.2	0.2
Total Capital Investment (Billion 2005$)	1.9	3.2	5.9	9.9	15.1	22.9
H_2 Partial Success						
H_2 Production	0.2	0.4	1.1	2.3	3.6	N/A
H_2 Storage	0.04	0.04	0.1	0.2	0.3	N/A
H_2 Transmission	0.3	0.4	0.4	1.0	1.3	N/A
H_2 Distribution	0.5	1.0	1.8	4.0	4.9	N/A
Refueling Stations	0.4	0.8	1.8	3.7	5.7	N/A
CO_2 Transport	0.01	0.02	0.05	0.2	0.2	N/A
CO_2 Injection	0.03	0.03	0.08	0.1	0.2	N/A
Total Capital Investment (Billion 2005$)	1.5	2.7	5.3	11.4	16.1	N/A

Several large diameter transmission pipeline corridors are constructed within this sub-region in order to export hydrogen to California. As a result, early transmission pipelines are oversized and underutilized, resulting in relatively high costs of transmission in the first tranche. However, as these large pipelines become better utilized, the percentage of the total capital investment that is attributed to transmission declines until it is only about 8% of total costs in tranche 6 (Figure 120). The percentage of total capital associated with CO_2 pipelines is relatively small in this region since H_2 production sites are located in close proximity to CO_2 storage sites.

In the H_2 Success scenario, the breakeven price of hydrogen is 3-8% smaller in the Intermountain sub-region relative to the western U.S. throughout the study period (Figure 121). The price difference is largely attributable to better economies-of-scale associated with H_2 production and transmission and shorter H_2 distribution and CO_2 pipelines. In the H_2 Partial Success scenario, the breakeven price is 6% larger in the first period as a result of poor utilization of oversized H_2 transmission and distribution pipelines (Figure 122). However, as these pipelines become better utilized, the breakeven price declines and is 9% and 6% smaller in the second and third periods, respectively. Essentially, the economies-of-scale gained by producing hydrogen for California lead to relatively low hydrogen prices within the sub-region.

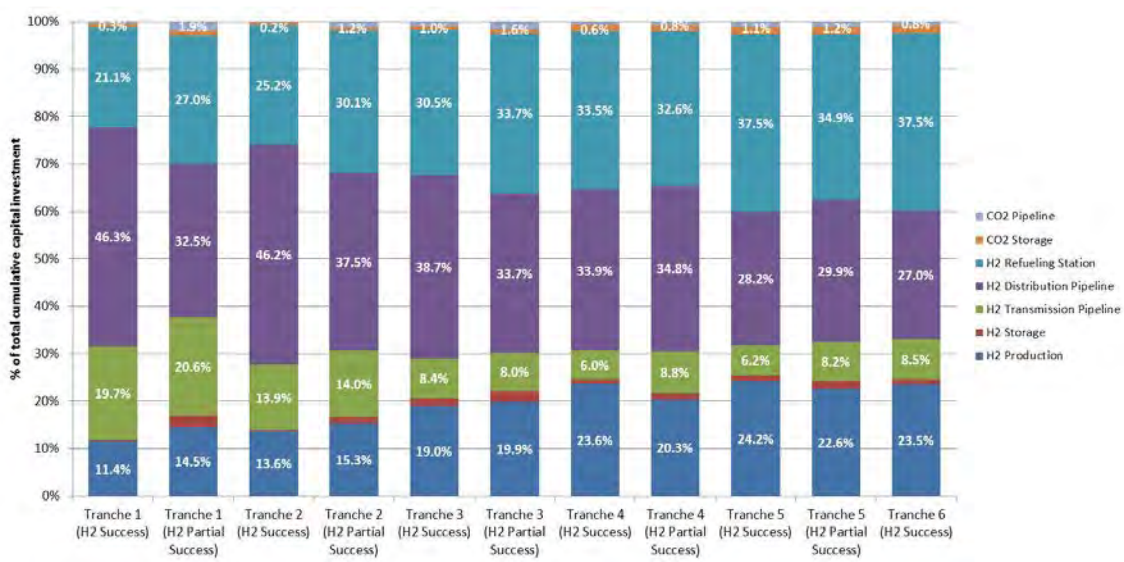

Figure 120: Percentage of total cumulative capital investment associated with each component in the Intermountain sub-region

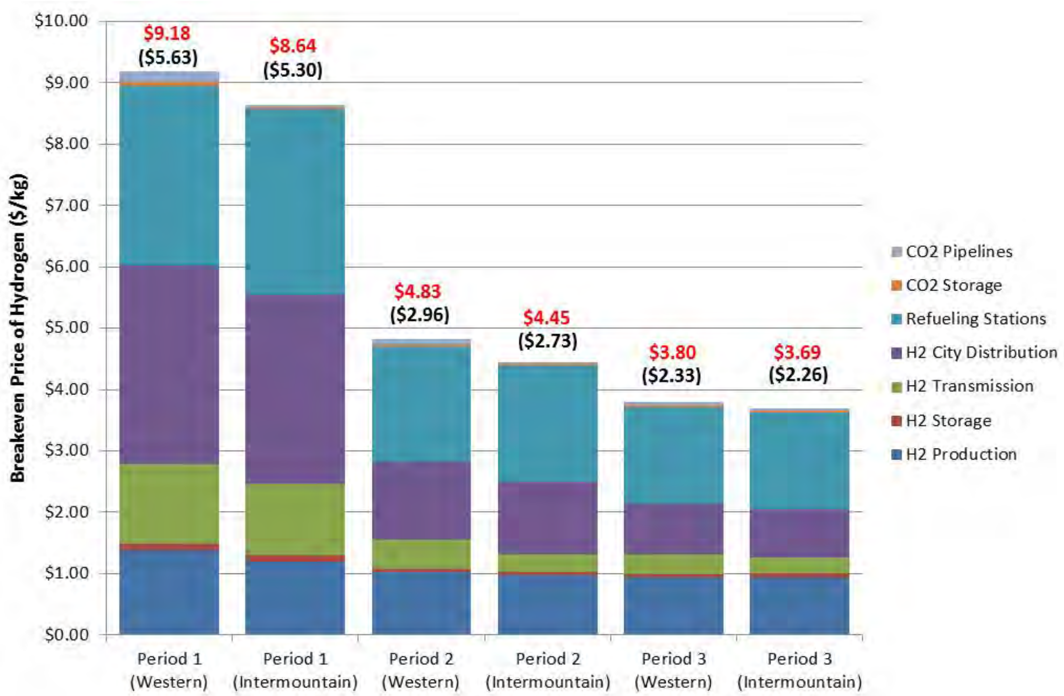

Figure 121: Comparison of the breakeven price of hydrogen under the H_2 Success scenario in the Intermountain sub-region and western U.S. (number in parentheses is the $/gallon gasoline equivalent)

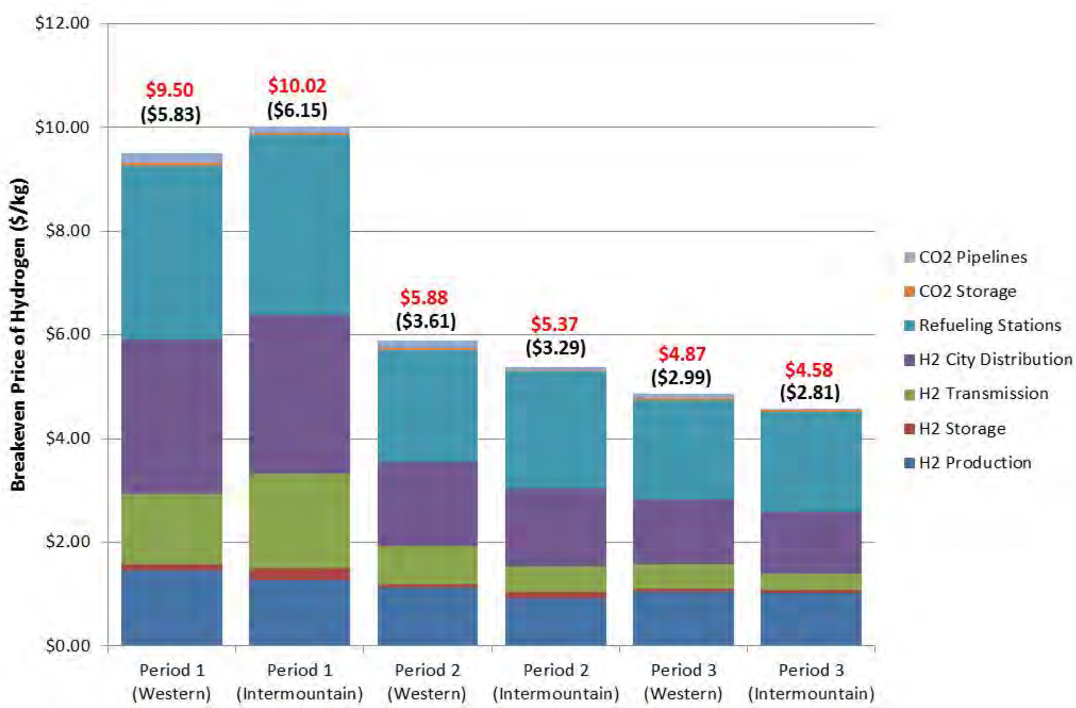

Figure 122: Comparison of the breakeven price of hydrogen under the H_2 Partial Success scenario in the Intermountain sub-region and western U.S. (number in parentheses is the $/gallon gasoline equivalent)

4.2.5 Midwest

The Midwest sub-region includes parts of South Dakota, Nebraska, Kansas, and Oklahoma (Figure 123). The three largest metropolitan areas each have a population less than 500,000 and include Kansas City, Wichita, and Omaha (Figure 124). As a result, this sub-region is characterized by low regional hydrogen demand and does not support centralized production in the first tranche (Table 81). The hydrogen production potential within the sub-region exceeds regional demand and benefits from low delivered coal costs (Table 80). Consequently, regional production facilities export hydrogen to the Southwest sub-region.

4.2.5.1 Infrastructure Design

The Midwest sub-region is characterized by low regional hydrogen demand and low delivered coal prices. In the first tranche, there is insufficient demand to warrant investment in centralized infrastructure. Consequently, hydrogen is supplied to the seven demand centers using onsite production at refueling stations. In the second tranche, an independent supply network develops that includes a small 300 t/day production facility (n1491) connected to six demand centers. The remaining three demand centers, which represent about 33% of regional H_2 demand, continue to be supplied by onsite production. This small production facility is connected to a single CO_2 storage site by a 389 km pipeline (Table 82).

In the third tranche, the Midwest supply network connects to the Southwest sub-region and a second larger production facility is built at site n1491 with most of the production exported to the Southwest. To store the CO_2 from these facilities, several storage sites are required since the nearest aquifer has low CO_2 storage density (Table 83). Figure 124 indicates that these storage sites are connected by an extensive CO_2 pipeline network. Consequently, the cost of CO_2 storage and transport is expected to be large in this sub-region

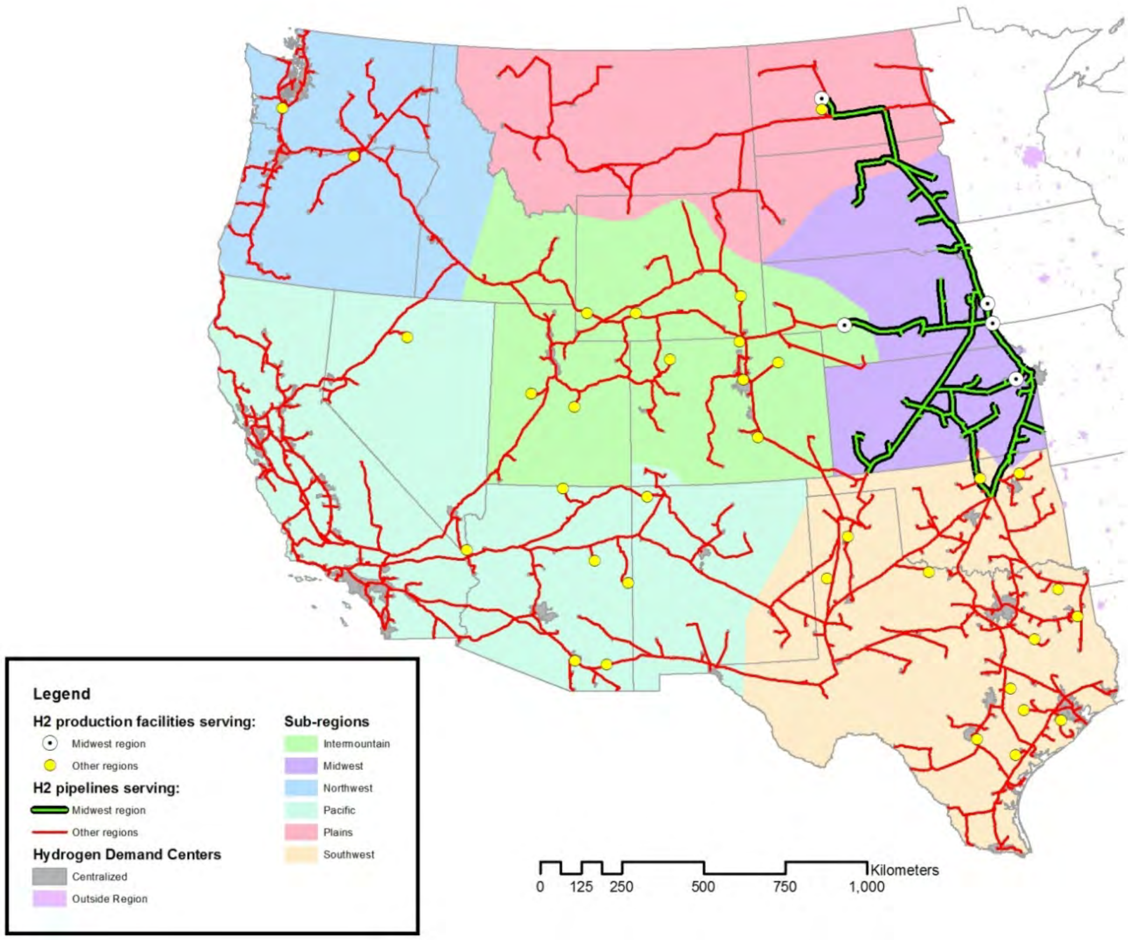

Figure 123: Subset of infrastructure required to serve the Midwest sub-region in all tranches

Throughout the study period, the average nameplate capacity of H_2 production facilities remains relatively small and over 50% of regional production capacity is exported in tranches 5 and 6 (Table 80). It is interesting that in tranche 6, hydrogen is imported into the Midwest sub-region from facilities in the Plains and Pacific sub-regions (n228 and n1615) while hydrogen produced in the Midwest is exported back to the Pacific sub-region via larger, pre-existing pipelines. The average transmission pipeline length per demand center is approximately 100 km with 75-80% of pipeline capacity allocated to the Midwest sub-region (Table 82). The relatively small average length of distribution pipelines per demand center suggests that most cities are small in the sub-region.

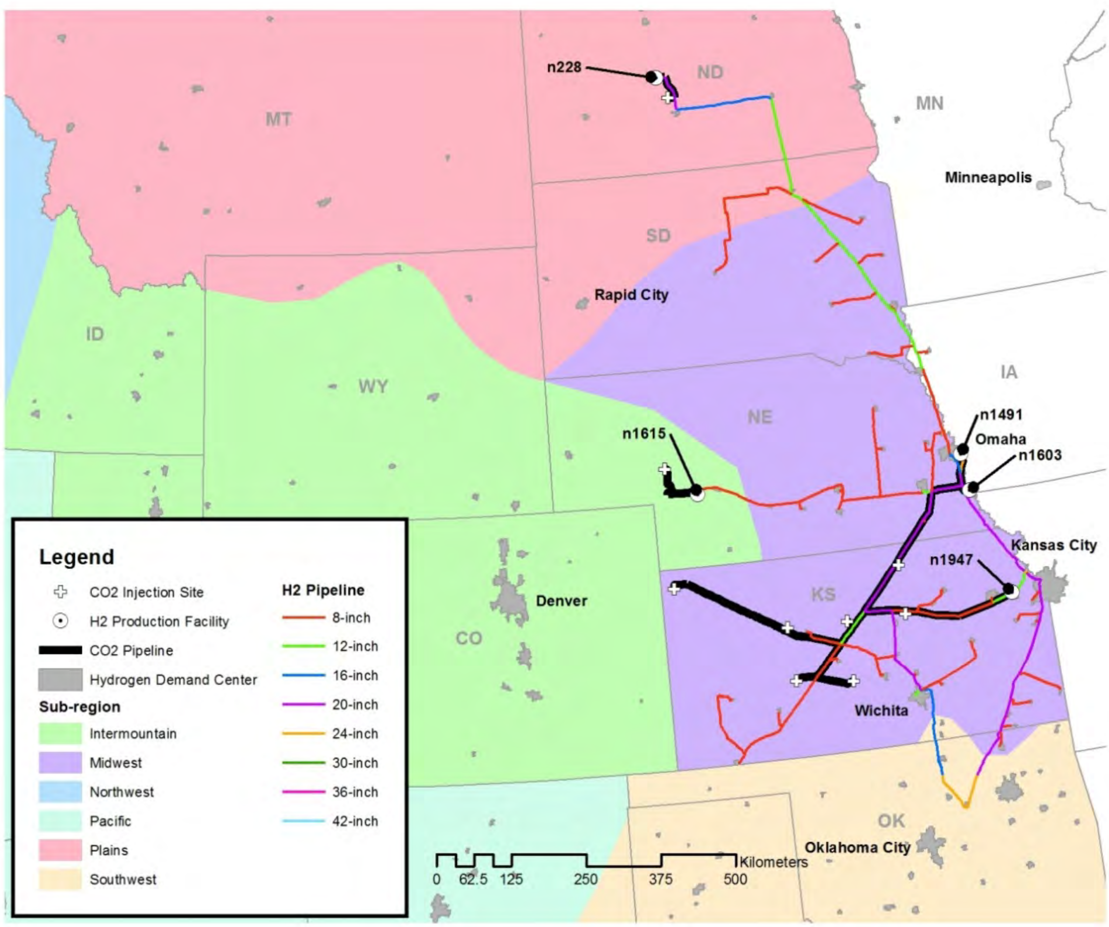

Figure 124: Infrastructure requirements within the Midwest sub-region in tranche 6

Table 80: H_2 production facility requirements for the H_2 Success and H_2 Partial Success scenarios in the Midwest sub-region

	Tranche 1	Tranche 2		Tranche 3		Tranche 4		Tranche 5		Tranche 6	
Plant Nameplate Capacity (tonnes/day)	# of H_2 Plants	# of New H_2 Plants	Cumulative # of H_2 Plants	# of New H_2 Plants	Cumulative # of H_2 Plants	# of New H_2 Plants	Cumulative # of H_2 Plants	# of New H_2 Plants	Cumulative # of H_2 Plants	# of New H_2 Plants	Cumulative # of H_2 Plants
300	0	1	1	0	1	0	1	0	1	1	2
600	0	0	0	0	0	0	0	0	0	2	2
900	0	0	0	0	0	0	0	2	2	0	2
1200	0	0	0	1	1	0	1	0	1	0	1
1500	0	0	0	0	0	0	0	1	1	0	1
Total	0	1	1	1	2	0	2	3	5	3	8
Avg. Nameplate Capacity (tonnes/day)	N/A	300		750		750		960		788	
Total Nameplate Capacity (tonnes/day)	N/A	300		1,500		1,500		4,800		6,300	
Avg. fraction of production allocated to region	N/A	1.00		0.44		0.78		0.41		0.46	
Number of unique H_2 production sites	0	1		1		1		4		5	
Avg. delivered coal cost ($/GJ)	N/A	1.4		1.4		1.4		1.4		1.4	

Table 81: Number of demand centers served by centralized and onsite supply in the Midwest sub-region

	Tranche 1	Tranche 2	Tranche 3	Tranche 4	Tranche 5	Tranche 6
	# of demand centers	# of demand centers	# of demand centers	# of demand centers	# of demand centers	# of demand centers
Centralized Supply	0	6	16	23	42	48
Onsite Supply	7	3	6	11	6	0
Total	7	9	22	34	48	48
% Onsite Demand Centers	100%	33%	27%	32%	13%	0%
% Hydrogen Supplied Onsite	100%	19%	4%	5%	2%	0%
Total Hydrogen Demand (tonnes/day)	80	211	553	1,080	1,606	2,284

Table 82: H_2 and CO_2 pipeline requirements in the Midwest sub-region

	Tranche 1	Tranche 2		Tranche 3		Tranche 4		Tranche 5		Tranche 6	
	New Pipeline (km)	New Pipeline (km)	Cumulative Pipeline (km)	New Pipeline (km)	Cumulative Pipeline (km)	New Pipeline (km)	Cumulative Pipeline (km)	New Pipeline (km)	Cumulative Pipeline (km)	New Pipeline (km)	Cumulative Pipeline (km)
H_2 Transmission											
Total Length (km)	0	656	656	1045	1701	930	2631	887	3518	1445	4963
Avg. pipeline length per demand center (km)	N/A	109		106		114		84		103	
Avg. fraction of pipeline use allocated to region	N/A	1.00		0.74		0.83		0.82		0.82	
H_2 Distribution											
Total Length (km)	0	749	749	1018	1767	738	2504	812	3316	707	4023
Avg. pipeline length per demand center (km)	N/A	125		110		109		79		84	
Avg. fraction of pipeline use allocated to region	N/A	1.00		1.00		1.00		1.00		1.00	
CO_2 Transport											
Total Length (km)	0	389	389	385	774	0	774	232	1006	363	1369
Avg. pipeline length per H_2 production site (km)	N/A	389		774		774		252		274	
Avg. fraction of pipeline use allocated to region	N/A	1.00		0.44		0.78		0.66		0.68	
# of demand centers (centralized supply)	0	6		16		23		42		48	

Table 83: CO_2 storage requirements in the Midwest sub-region

	Tranche 1	Tranche 2		Tranche 3		Tranche 4		Tranche 5		Tranche 6	
	New	New	Cumulative	New	Cumulative	New	Cumulative	New	Cumulative	New	Cumulative
# of storage sites	0	1	1	5	6	0	6	3	9	0	9
# of injection wells	0	2	2	12	14	0	14	40	54	11	65
Avg. number of storage sites per H_2 production site	N/A	1.0		6.0		6.0		2.3		1.8	

4.2.5.2 Cost

In the first tranche, hydrogen is supplied exclusively by onsite production and, thus, the total capital investment of $300 million is incurred by refueling stations. In subsequent tranches, centralized infrastructure is installed, but the cumulative capital investment remains relatively small. In tranche 6, the investment is $15 billion, which represents about 5% of the capital investment required for the entire western U.S. (Table 84).

Table 84: Cumulative capital investment (Billion $) in the Midwest sub-region for each tranche

	Tranche 1	Tranche 2	Tranche 3	Tranche 4	Tranche 5	Tranche 6
H2 Success						
H_2 Production	0.0	0.5	0.8	1.4	2.3	3.5
H_2 Storage	0.0	0.04	0.04	0.04	0.1	0.2
H_2 Transmission	0.0	0.3	0.5	0.6	1.1	1.4
H_2 Distribution	0.0	0.8	1.7	2.3	2.9	3.5
Refueling Stations	0.3	0.5	1.2	2.3	3.9	5.9
CO_2 Transport	0.0	0.02	0.1	0.1	0.1	0.2
CO_2 Injection	0.0	0.2	0.4	0.4	0.5	0.6
Total Capital Investment (Billion 2005$)	0.3	2.4	4.8	7.2	11.1	15.3
H_2 Partial Success						
H_2 Production	0.0	0.5	0.8	1.4	2.3	N/A
H_2 Storage	0.0	0.05	0.05	0.05	0.2	N/A
H_2 Transmission	0.0	0.2	0.5	0.6	1.1	N/A
H_2 Distribution	0.0	0.7	1.5	2.2	2.8	N/A
Refueling Stations	0.3	0.5	1.2	2.6	3.9	N/A
CO_2 Transport	0.0	0.02	0.1	0.1	0.1	N/A
CO_2 Injection	0.0	0.2	0.4	0.4	0.5	N/A
Total Capital Investment (Billion 2005$)	0.3	2.2	4.6	7.2	10.9	N/A

A relatively large percentage of capital is associated with H_2 production in tranche 2 since the initial production facility has a nameplate capacity of only 300 tonnes per day (Figure 125). However, this number declines as the region builds larger production facilities that are used to export hydrogen to the Southwest sub-region. The percentage of capital associated with hydrogen distribution and transmission pipelines is small relative to the western U.S. case study since the average demand center size is smaller and the pipelines are not as oversized in early tranches.

In contrast, the percentage of capital associated with CO_2 pipelines and storage is extremely large in the Midwest since the sub-region has low CO_2 storage capacity. Approximately 10% of capital is associated with CO_2 transport and storage as opposed to about 3% in the western U.S. (Figure 125).

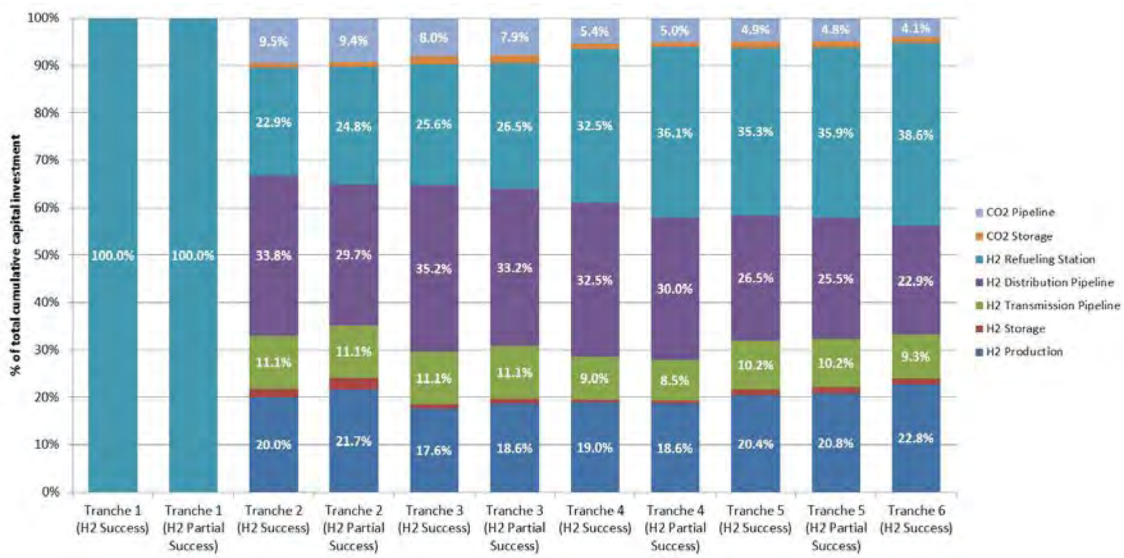

Figure 125: Percentage of total cumulative capital investment associated with each component in the Midwest sub-region

Figure 126: Comparison of the breakeven price of hydrogen under the H_2 Success scenario in the Midwest sub-region and western U.S. (number in parentheses is the $/gallon gasoline equivalent)

In both the H_2 Success and H_2 Partial Success scenarios, the breakeven price of hydrogen is 5% larger in the Midwest sub-region relative to the western U.S. in the first period (Figure 126 and Figure 127). The difference is primarily attributed to increases in the costs of CO_2 pipelines and refueling stations. The refueling station cost is larger because a greater fraction of hydrogen is supplied by onsite production during this period. In the H_2 Success scenario, the breakeven prices of hydrogen are similar in the two case studies during the second and third periods. By exporting hydrogen to the Southwest region, better economies-of-scale are achieved in H_2 production and transmission and the lower costs of these components offset the higher costs associated with CO_2 pipelines and refueling stations.

In the H_2 Partial Success scenario, slower HFCV deployment leads to low utilization of infrastructure, which results in higher costs associated with production and H_2 pipelines. In combination with the higher costs associated with CO_2 transport and refueling stations, the breakeven price is 16% larger in the Midwest region in the second period (Figure 127). In the third period, better utilization of infrastructure leads to a 3% smaller breakeven price in the Midwest. However, in general, this sub-region has higher breakeven prices of hydrogen than the western U.S. as a result of poor access to CO_2 storage capacity and low regional hydrogen demand. However, this sub-region resides on the border of the study area. If the neighboring states in the eastern United States were included in the study region, this sub-region may achieve lower costs by connecting to large metropolitan areas in these states (e.g., Minneapolis).

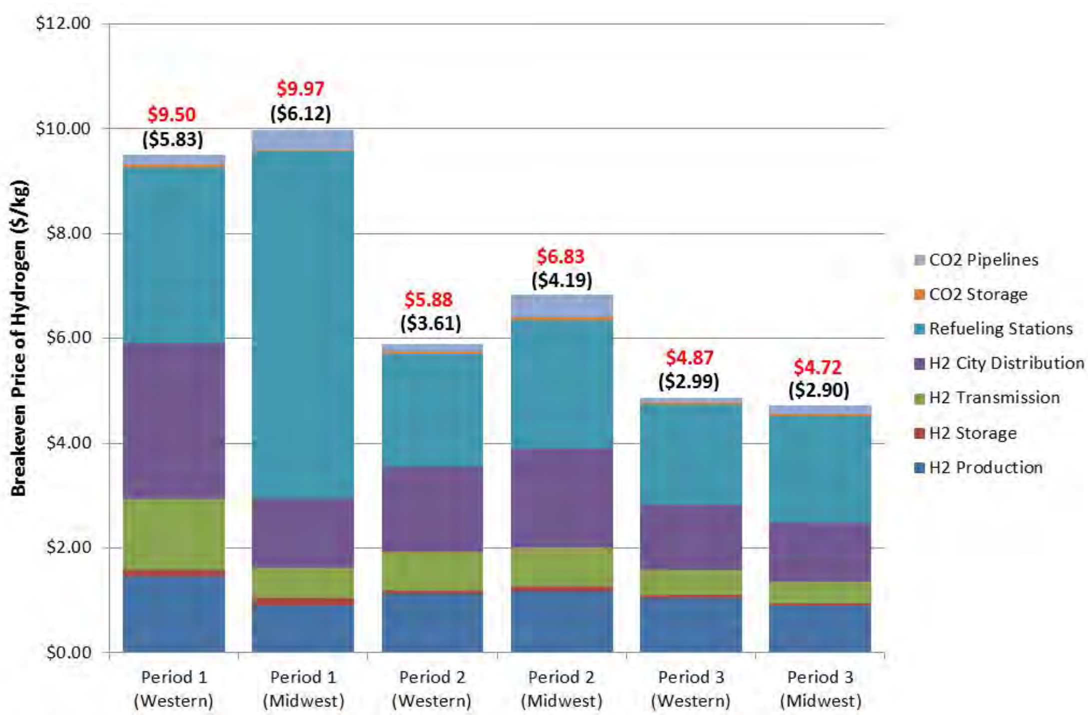

Figure 127: Comparison of the breakeven price of hydrogen under the H_2 Partial Success scenario in the Midwest sub-region and western U.S. (number in parentheses is the $/gallon gasoline equivalent)

4.2.6 Southwest

The Southwest sub-region includes Texas, Oklahoma, and part of New Mexico (Figure 128). The majority of the hydrogen demand occurs in the eastern portion of the sub-region, including the metropolitan areas of Houston, Dallas, San Antonio, Austin, and Oklahoma City (Figure 129). In contrast, the western portion of the study area is arid with relatively small, dispersed demand centers. Approximately 20% of the total hydrogen demand within the western U.S. resides in the Southwest sub-region. The region also includes abundant coal-based H_2 production potential and CO_2 storage capacity.

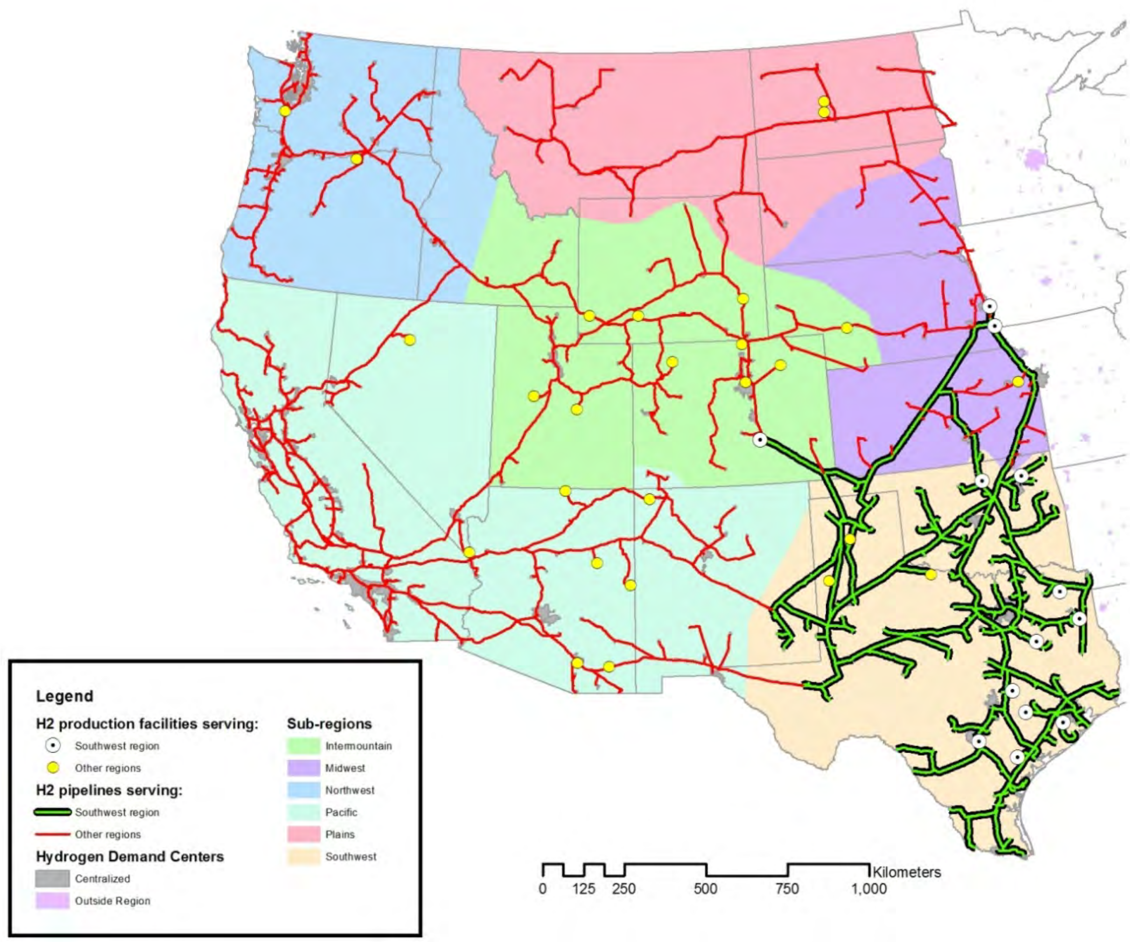

Figure 128: Subset of infrastructure required to serve the Southwest sub-region in all tranches

4.2.6.1 Infrastructure Design

In the first tranche, a compact centralized supply network develops that links a single production facility (n3438) to the four largest cities in central Texas. The remaining demand centers in the south, west, and north of the sub-region are supplied by onsite production and represent 18% of total demand. In the second tranche, the transmission pipeline network extends into Oklahoma and southern Texas, but still remains relatively compact and independent from other sub-regions. In the third tranche, the Southwest and Midwest sub-regions are linked and the Southwest begins to import hydrogen from the Midwest. A small 8-inch pipeline extends along the I-20 corridor into western Texas, but the majority of the area continues to be supplied by onsite production. In the fourth tranche, a large trunk pipeline extends from Oklahoma into north Texas and New Mexico and links the Southwest sub-region to the Pacific sub-region. This pipeline allows hydrogen to be exported to the Pacific sub-region. In the fifth tranche, the trunk pipeline links to the Intermountain sub-region and an additional link is added to the Pacific sub-region. At this point, large quantities of hydrogen are exported from production facilities in Oklahoma and western Texas into the Pacific sub-region.

Despite relatively large demand in this sub-region, the average nameplate capacity of production facilities is small throughout the study period (Table 85). Coupled with high delivered coal costs, the cost of production is expected to be large. The average transmission pipeline length per demand center ranges from 80 to 120 km and > 80% of the use and cost of these pipelines is attributed to the Southwest sub-region (Table 87). The average distribution pipeline length per demand center is large in the first few tranches since large cities are served during this period.

The average CO_2 pipeline length per hydrogen production site is very large in this sub-region since it receives some of its supply from the Midwest sub-region, which requires very long pipelines to access CO_2 storage capacity (Table 87). However, it is also important to note that very little of the use of the pipelines in the Midwest is allocated to the Southwest sub-region since 70-80% of the associated hydrogen production is utilized within the Midwest. Most H_2 facilities within the Southwest sub-region have good access to CO_2 storage capacity with the exception of the facilities in Oklahoma (Figure 129). The ratio of CO_2 storage sites to H_2 production sites also reflects the poor access to CO_2 storage capacity in the Midwest sub-region (Table 88).

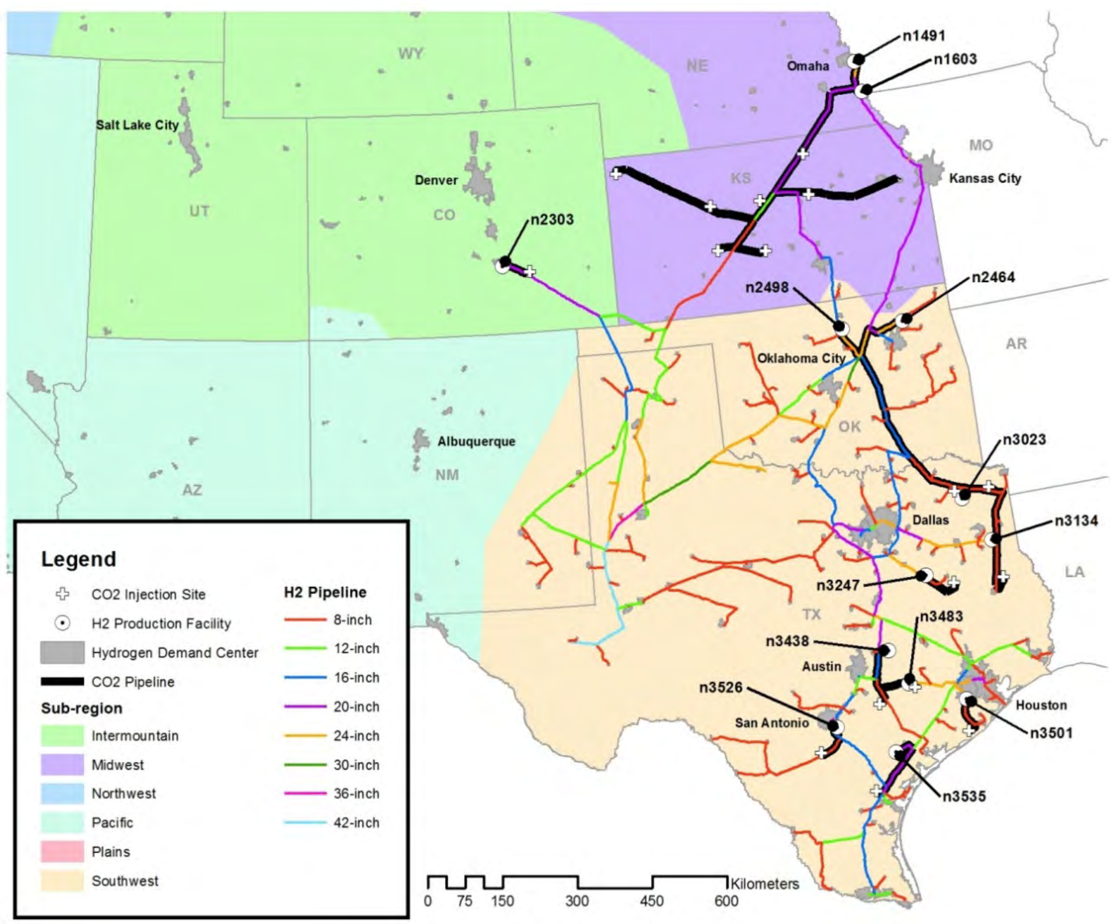

Figure 129: Infrastructure requirements within the Southwest sub-region in tranche 6

Table 85: H_2 production facility requirements for the H_2 Success and H_2 Partial Success scenarios in the Southwest sub-region

	Tranche 1	Tranche 2		Tranche 3		Tranche 4		Tranche 5		Tranche 6	
Plant Nameplate Capacity (tonnes/day)	# of H_2 Plants	# of New H_2 Plants	Cumulative # of H_2 Plants	# of New H_2 Plants	Cumulative # of H_2 Plants	# of New H_2 Plants	Cumulative # of H_2 Plants	# of New H_2 Plants	Cumulative # of H_2 Plants	# of New H_2 Plants	Cumulative # of H_2 Plants
300	0	0	0	2	2	0	2	0	2	2	4
600	1	1	2	1	3	0	3	2	5	0	5
900	0	0	0	0	0	1	1	0	1	2	3
1200	0	0	0	1	1	0	1	1	2	1	3
1500	0	0	0	0	0	2	2	1	3	2	5
Total	1	1	2	3	6	3	9	4	13	7	20
Avg. Nameplate Capacity (tonnes/day)	600	600		600		833		878		900	
Total Nameplate Capacity (tonnes/day)	600	1,200		3,600		7,500		11,400		18,000	
Avg. fraction of production allocated to region	1.00	1.00		0.81		0.82		0.79		0.72	
Number of unique H_2 production sites	1	1		3		5		9		13	
Avg. delivered coal cost ($/GJ)	1.9	1.9		1.8		1.8		1.8		1.9	

Table 86: Number of demand centers served by centralized and onsite supply in the Southwest sub-region

	Tranche 1	Tranche 2	Tranche 3	Tranche 4	Tranche 5	Tranche 6
	# of demand centers	# of demand centers	# of demand centers	# of demand centers	# of demand centers	# of demand centers
Centralized Supply	9	22	53	102	136	158
Onsite Supply	9	14	21	25	22	0
Total	18	36	74	127	158	158
% Onsite Demand Centers	50%	39%	28%	20%	14%	0%
% Hydrogen Supplied Onsite	18%	10%	7%	3%	2%	0%
Total Hydrogen Demand (tonnes/day)	456	1,015	2,489	4,925	7,265	10,332

Table 87: H_2 and CO_2 pipeline requirements in the Southwest sub-region

	Tranche 1	Tranche 2		Tranche 3		Tranche 4		Tranche 5		Tranche 6	
	New Pipeline (km)	New Pipeline (km)	Cumulative Pipeline (km)	New Pipeline (km)	Cumulative Pipeline (km)	New Pipeline (km)	Cumulative Pipeline (km)	New Pipeline (km)	Cumulative Pipeline (km)	New Pipeline (km)	Cumulative Pipeline (km)
H_2 Transmission											
Total Length (km)	945	1653	2598	2903	5502	2783	8284	3099	11383	2685	14069
Avg. pipeline length per demand center (km)	105	118		104		81		84		89	
Avg. fraction of pipeline use allocated to region	1.00	1.00		0.98		0.94		0.90		0.82	
H_2 Distribution											
Total Length (km)	2050	1850	3900	3198	7100	4068	11167	3312	14480	3050	17530
Avg. pipeline length per demand center (km)	228	177		134		109		106		111	
Avg. fraction of pipeline use allocated to region	1.00	1.00		1.00		1.00		1.00		1.00	
CO_2 Transport											
Total Length (km)	147	0	147	855	1002	575	1577	463	2040	642	2682
Avg. pipeline length per H_2 production site (km)	147	147		334		315		227		206	
Avg. fraction of pipeline use allocated to region	1.00	1.00		0.66		0.57		0.65		0.60	
# of demand centers (centralized supply)	9	22		53		102		136		158	

Table 88: CO_2 storage requirements in the Southwest sub-region

	Tranche 1	Tranche 2		Tranche 3		Tranche 4		Tranche 5		Tranche 6	
	New	New	Cumulative	New	Cumulative	New	Cumulative	New	Cumulative	New	Cumulative
# of storage sites	1	0	1	7	8	2	10	4	14	3	17
# of injection wells	4	6	10	21	31	31	62	32	94	57	151
Avg. number of storage sites per H_2 production site	1.0	1.0		2.7		2.0		1.6		1.3	

4.2.6.2 Cost

The cumulative capital investment in the Southwest sub-region in tranche 6 is approximately $69 billion, which represents about 22% of the capital required for the western U.S. (Table 89). Approximately 18% of the hydrogen demand is met by onsite production in the first tranche and the percentage of hydrogen supplied onsite remains relatively large through tranche 3. As a result, the relative contribution of refueling stations to the cumulative capital investment is slightly higher than the value identified for the western U.S. (Figure 130).

Table 89: Cumulative capital investment (Billion $) in the Southwest sub-region for each tranche

	Tranche 1	Tranche 2	Tranche 3	Tranche 4	Tranche 5	Tranche 6
H2 Success						
H_2 Production	0.8	1.6	3.9	7.5	10.8	15.9
H_2 Storage	0.1	0.1	0.2	0.3	0.5	0.7
H_2 Transmission	0.5	1.3	2.4	3.3	3.9	5.2
H_2 Distribution	2.4	4.4	7.3	10.8	13.7	19.0
Refueling Stations	1.2	2.4	5.3	10.1	17.1	26.1
CO_2 Transport	0.04	0.1	0.2	0.5	0.7	1.2
CO_2 Injection	0.1	0.2	0.4	0.6	0.8	1.3
Total Capital Investment (Billion 2005$)	5.2	10.1	19.8	33.2	47.5	69.2
H_2 Partial Success						
H_2 Production	0.8	1.6	3.9	7.5	10.8	N/A
H_2 Storage	0.1	0.1	0.2	0.4	0.6	N/A
H_2 Transmission	0.4	1.3	2.4	3.9	4.5	N/A
H_2 Distribution	1.2	2.8	5.8	11.9	14.8	N/A
Refueling Stations	1.2	2.4	5.3	11.3	17.1	N/A
CO_2 Transport	0.04	0.1	0.2	0.5	0.7	N/A
CO_2 Injection	0.1	0.2	0.3	0.7	0.9	N/A
Total Capital Investment (Billion 2005$)	3.9	8.5	18.2	36.3	49.4	N/A

The percentage of capital associated with production is relatively large in this sub-region since the average nameplate capacity is small (Figure 130). However, the contributions of H_2 transmission and CO_2 transport pipelines are relatively small. The transmission costs are small because the pipeline networks developed in early tranches are compact and link cities with relatively large demand, which allows the construction of large diameter trunk pipelines. Although the average CO_2 pipeline length is large, the cost is relatively small because very little of the cost associated with the longest pipelines is allocated to the Southwest region. Specifically, only 20-30% of the cost of CO_2 pipelines associated with facilities in the Midwest is allocated to the Southwest and the percentage of the cost that is associated with Oklahoma facilities and allocated to the Southwest drops to 44% by tranche 6 since 56% of the H_2 production is exported to the Pacific sub-region. Consequently, the CO_2 transport costs are much smaller than expected given the average pipeline length per production site.

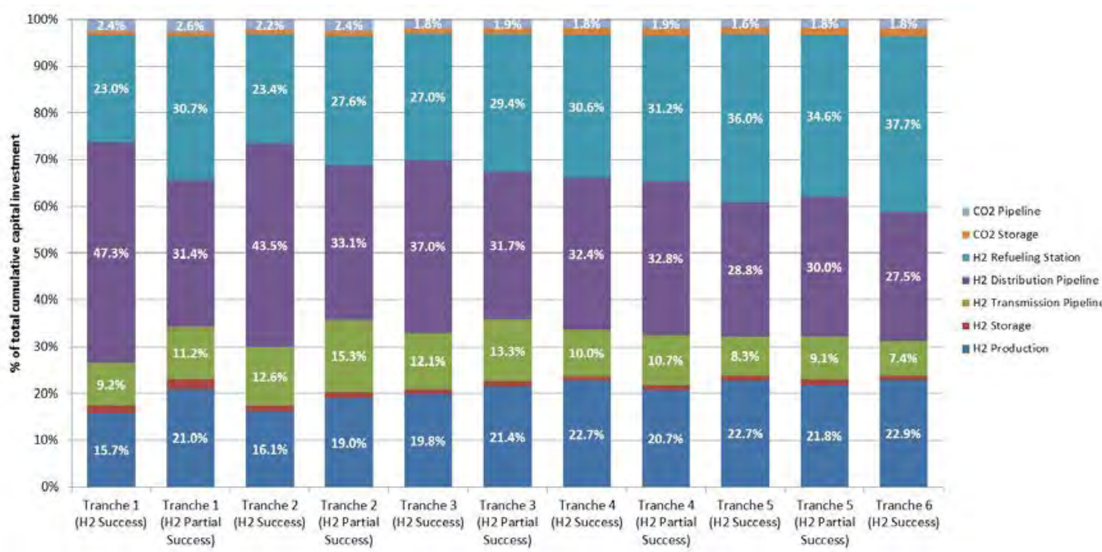

Figure 130: Percentage of total cumulative capital investment associated with each component in the Southwest sub-region

In the H_2 Success scenario, the breakeven price of hydrogen in each period is similar to the value identified for the western U.S. (Figure 131). The breakeven price is less than 1% larger in the first period because of higher production and refueling stations costs. The higher production costs are partially the result of high average delivered coal costs in the sub-region. However, these larger costs are mostly offset by lower costs of H_2 and CO_2 pipeline transport. In the second and third periods, the breakeven price in the Southwest sub-region is about 1% smaller as a result of lower H_2 transmission pipeline costs.

In the H_2 Partial Success scenario, the breakeven price of hydrogen is almost 10% larger in the Southwest sub-region than the western U.S. (Figure 132). With slower HFCV deployment, underutilization of infrastructure exacerbates the difference in H_2 production and refueling stations costs in the two regions. In the second period, the breakeven price continues to be about 1% larger in the Southwest sub-region. However, smaller H_2 pipeline costs result in a lower breakeven price in the third period.

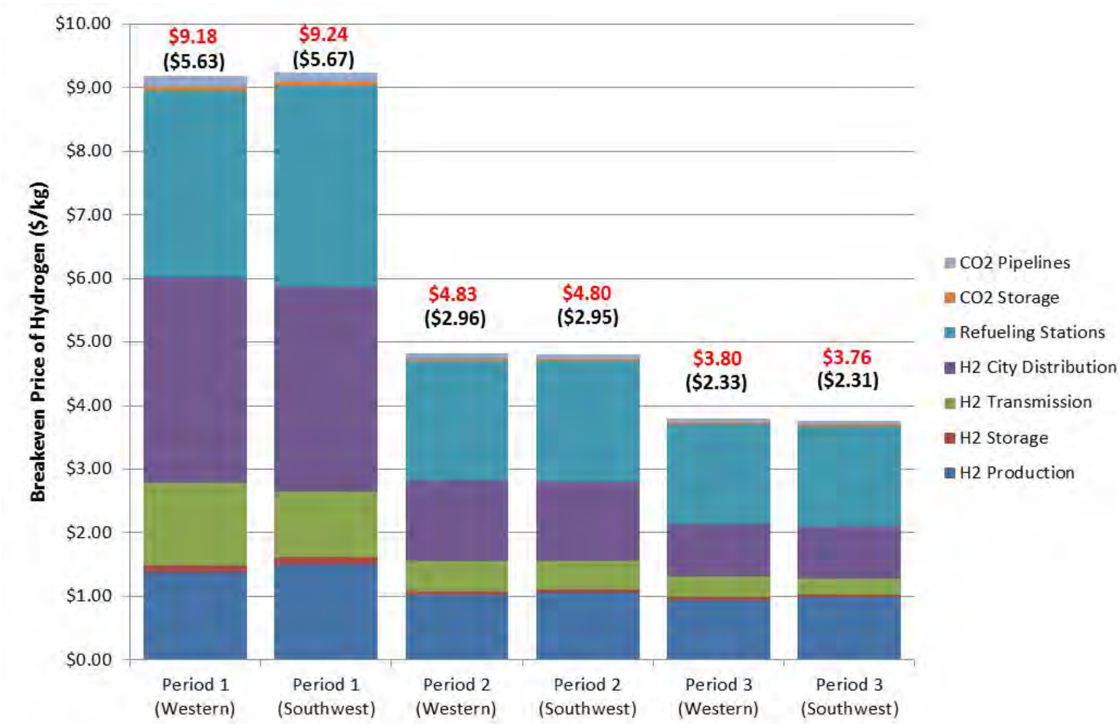

Figure 131: Comparison of the breakeven price of hydrogen under the H_2 Success scenario in the Southwest sub-region and western U.S. (number in parentheses is the $/gallon gasoline equivalent)

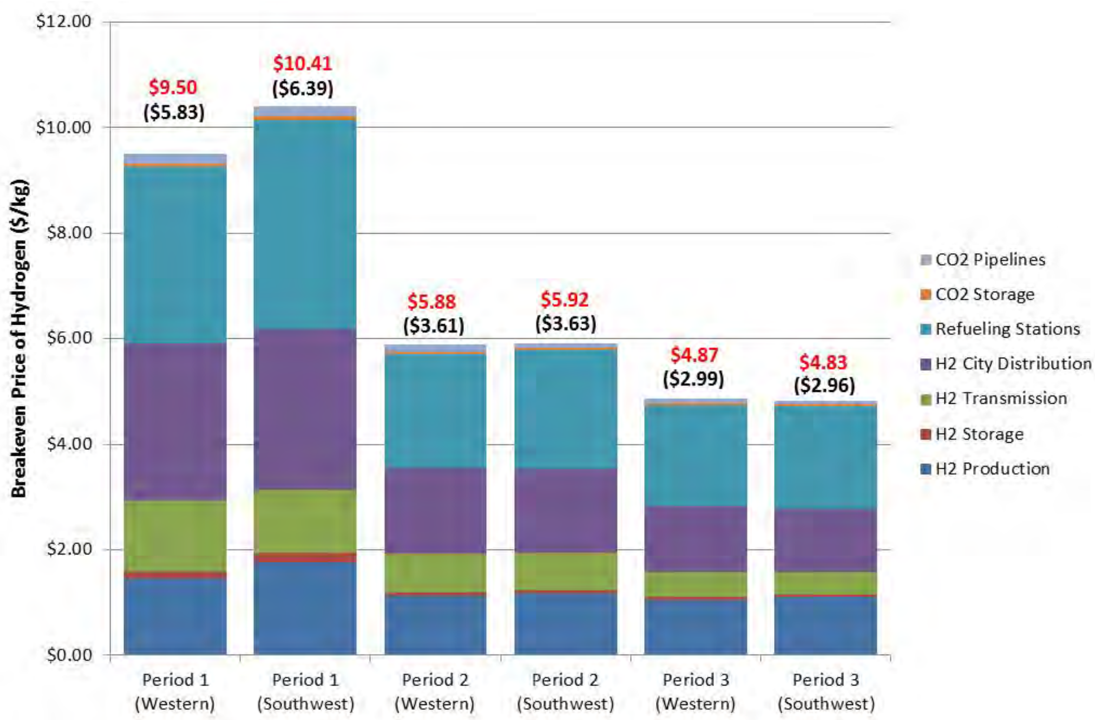

Figure 132: Comparison of the breakeven price of hydrogen under the H_2 Partial Success scenario in the Southwest sub-region and western U.S. (number in parentheses is the $/gallon gasoline equivalent)

4.2.7 Sub-regional Comparison

This section compares the levelized costs associated with each infrastructure component in the six sub-regions. The comparison is limited to the components that are the largest contributors to cost, including H_2 production, H_2 transmission, H_2 distribution, H_2 refueling stations, and CO_2 transport. For each component, various metrics are provided that help describe the differences in cost. Where possible, these metrics are used to develop equations that can be used in steady-state models to identify more realistic costs that account for underutilization, infrastructure sharing, and more realistic pipeline lengths. The comparison is provided for the H_2 Success scenario only.

4.2.7.1 H_2 Production

The cost of centralized H_2 production via coal gasification with CCS is determined by several metrics, which are compared for each sub-region in Table 90. The average nameplate capacity represents the average size of production facilities that serve the sub-region. A larger value suggests better economies-of-scale and a lower levelized cost of production is expected. The median average nameplate capacity in each analysis period increases from 600 tonnes/day in period 1 to 893 tonnes/day in period 3. The fraction of capacity allocated to a sub-region is an indicator of the fraction of production capacity that is utilized within a sub-region. A larger value represents less export to other sub-regions with 100% meaning that a sub-region uses all of its production capacity. A small value suggests that, in the absence of exports, the sub-region would be served by smaller production facilities and, thus, would have larger production costs than realized with exports. In general, sharing of production capacity through exports increases over time as sub-regions become increasingly interconnected. The median value of this metric declines from 90% in period 1 to 74% in period 3.

The effective capacity factor is the average capacity factor during the ten-year analysis period and accounts for underutilization as a result of oversizing and the rate of vehicle deployment. The effective capacity factor increases over time as infrastructure becomes better utilized. The median value increases from 43% in period 1 to 70% in period 3. The levelized cost generally declines as the effective capacity factor increases.

The average delivered coal cost indicates the feedstock cost within each sub-region and higher coal costs translate to higher costs of production. Finally, H_2 supplied by centralized supply indicates the percentage of hydrogen that is supplied by centralized production facilities. This value is generally larger than 90% except in sub-regions where implementation of centralized supply is delayed for one or more tranches (e.g., Plains and Midwest). In these cases, the levelized cost of production during the ten-year period will be lower than expected since the cost of onsite production is not included and, thus, the levelized cost of production will be zero for years in which hydrogen is supplied onsite.

In general, levelized costs of production are large when the delivered coal cost is large and the average nameplate capacity and effective capacity factor are small (Table 90). In comparing costs among sub-regions, the Northwest sub-region has the highest levelized cost of production in the first period since the sub-region is characterized by large delivered coal costs and a very small effective capacity factor and average nameplate capacity (Figure 133). Interestingly, the three sub-regions with the largest production costs are those that remain unconnected to other sub-regions for the majority of the first period. In contrast, the Pacific and Intermountain sub-regions are interconnected and the sharing of production capacity and large hydrogen demand in the Pacific sub-region allows large production facilities to be built. As a result, the levelized cost of production is relatively small in these sub-regions despite the high delivered coal costs associated with facilities serving the Pacific sub-region.

Table 90: Comparison of H_2 production metrics for each sub-region given the H_2 Success scenario

	Period 1	Period 2	Period 3
Northwest			
Levelized Cost of Production ($/kg H_2)	1.91	1.11	0.86
Average Nameplate Capacity (tonnes/day)	360	729	750
Fraction of Capacity Allocated to Region	100%	74%	94%
Effective Capacity Factor (%)	36%	62%	70%
Average Delivered Coal Cost ($/kg H_2)	0.35	0.35	0.32
H_2 Supplied by Centralized Supply (%)	90.2%	97.6%	99.9%
Plains			
Levelized Cost of Production ($/kg H_2)	N/A	0.16	0.91
Average Nameplate Capacity (tonnes/day)	N/A	900	795
Fraction of Capacity Allocated to Region	N/A	45%	46%
Effective Capacity Factor (%)	N/A	56%	65%
Average Delivered Coal Cost ($/kg H_2)	N/A	0.25	0.25
H_2 Supplied by Centralized Supply (%)	0.0%	14.4%	97.3%
Pacific			
Levelized Cost of Production ($/kg H_2)	1.31	1.02	0.94
Average Nameplate Capacity (tonnes/day)	1016	1100	1183
Fraction of Capacity Allocated to Region	90%	90%	83%
Effective Capacity Factor (%)	47%	64%	71%
Average Delivered Coal Cost ($/kg H_2)	0.35	0.36	0.37
H_2 Supplied by Centralized Supply (%)	97.9%	99.1%	99.8%
Intermountain			
Levelized Cost of Production ($/kg H_2)	1.20	0.97	0.94
Average Nameplate Capacity (tonnes/day)	1320	1052	970
Fraction of Capacity Allocated to Region	30%	46%	40%
Effective Capacity Factor (%)	45%	64%	70%
Average Delivered Coal Cost ($/kg H_2)	0.29	0.31	0.31
H_2 Supplied by Centralized Supply (%)	94.0%	95.9%	99.5%
Midwest			
Levelized Cost of Production ($/kg H_2)	1.37	0.88	0.88
Average Nameplate Capacity (tonnes/day)	525	771	840
Fraction of Capacity Allocated to Region	72%	64%	45%
Effective Capacity Factor (%)	38%	64%	69%
Average Delivered Coal Cost ($/kg H_2)	0.28	0.28	0.29
H_2 Supplied by Centralized Supply (%)	82.1%	95.6%	99.5%
Southwest			
Levelized Cost of Production ($/kg H_2)	1.51	1.06	0.98
Average Nameplate Capacity (tonnes/day)	600	768	893
Fraction of Capacity Allocated to Region	94%	81%	74%
Effective Capacity Factor (%)	43%	64%	70%
Average Delivered Coal Cost ($/kg H_2)	0.36	0.36	0.36
H_2 Supplied by Centralized Supply (%)	90.7%	96.5%	99.6%

In the second period, the relationship of production costs in the sub-regions remains similar to the first period except the cost in the Midwest sub-region is now lower than the costs in the Pacific and Intermountain sub-regions. The decline in the production cost in the Midwest sub-region results from the combination of low delivered coal costs and capacity sharing with the

Southwest sub-region, which increases the average nameplate capacity. The levelized cost of production associated with the Plains sub-region is extremely low since hydrogen is supplied by onsite production until the last year of the second period (i.e., centralized production only occurs in one year of the ten-year period). Consequently, the levelized cost of centralized production is small since only 9% of hydrogen is supplied by centralized production during this period. In the third period, the cost of production is similar in all sub-regions as the effective capacity factor converges to about 70%.

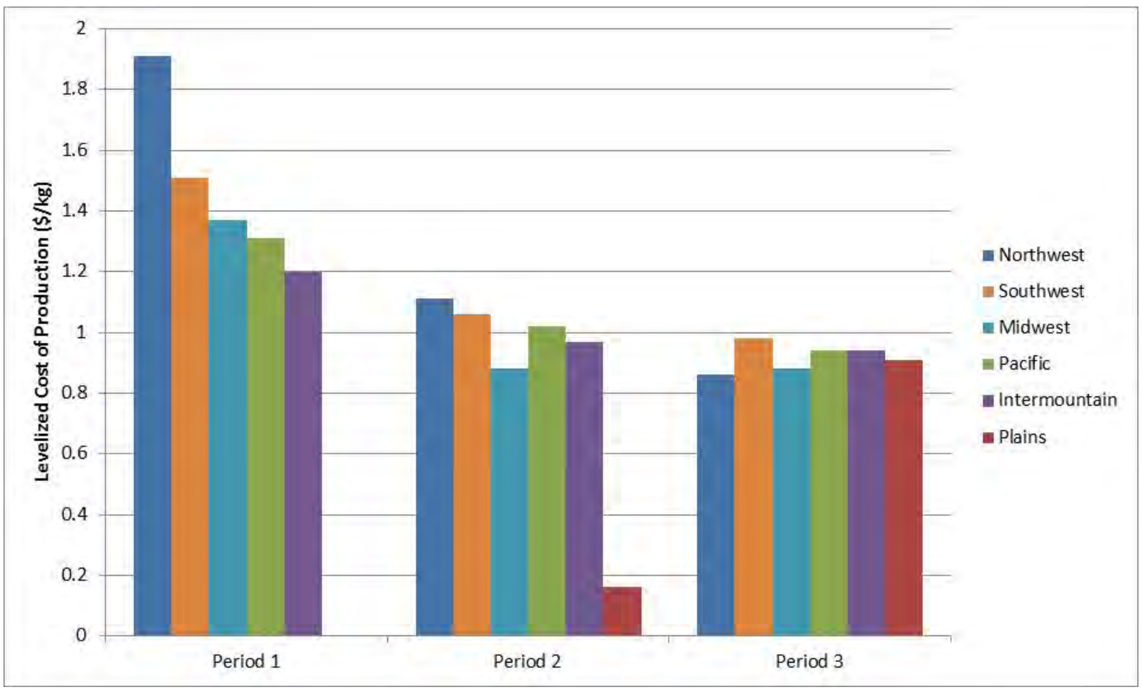

Figure 133: Levelized Cost of Production ($/kg) for each sub-region given the H_2 Success scenario

If the feedstock cost, which is specific to each sub-region, is removed, the non-fuel levelized cost of production, which includes capital and fixed O&M, is primarily determined by the effective capacity factor. Figure 134 illustrates the relationship between the non-fuel levelized cost of production (lc_{prod}^{nf}) and the effective capacity factor (*cf*) and is represented by equation 90. The observations for the Plains sub-region in period 2 and the Midwest sub-region in period 1 have been omitted since the centralized production costs are strongly influenced by the fact that much of the hydrogen is not supplied by centralized facilities during these periods. In the Plains sub-region in period 2, 91% of hydrogen is produced onsite and, in the Midwest sub-region in period 1, 47% of hydrogen is produced onsite.

$$lc_{prod}^{nf} = 0.3661cf^{-1.328} \tag{90}$$

Equation 90 indicates the importance of accounting for underutilization of infrastructure during HFCV deployment and highlights why steady-state models of hydrogen infrastructure, which assume a fixed capacity factor between 80% and 90% for production facilities, tend to underestimate levelized costs. Figure 134 suggests that in the early phases of deployment when the effective capacity factor is small, a steady-state model can underestimate the non-fuel levelized cost of production by more than 50%. The total levelized cost of production is the sum of the non-fuel levelized cost and the levelized cost of the coal feedstock.

One simple method for developing more realistic capacity factors for steady-state models could be to assume that infrastructure can only be installed at fixed intervals (e.g., every five years). In contrast to most steady-state models that assume that infrastructure is optimized in each year, oversizing infrastructure for a fixed period would allow a capacity factor to be developed based on the projected HFCV deployment rate. However, the capacity factor will decrease as the interval between installations is extended. Consequently, it is important to identify a realistic period for which infrastructure is oversized for anticipated demand.

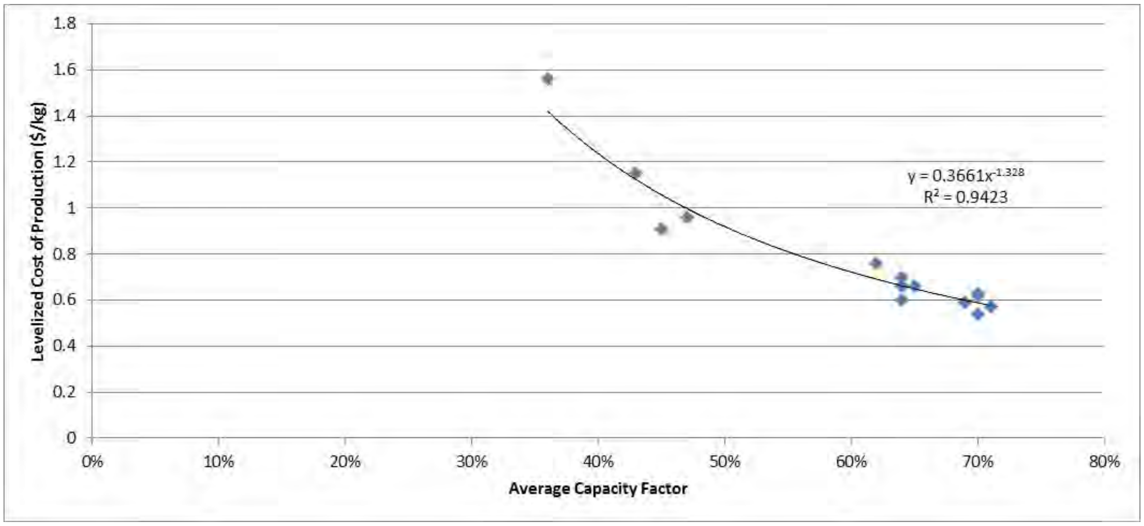

Figure 134: Non-fuel levelized cost of production as a function of effective capacity factor

4.2.7.2 H_2 Transmission

The factors that influence the cost of H_2 transmission are listed for each sub-region in Table 91. The average pipeline length per demand center is the total pipeline length divided by the number of demand centers served by centralized production. It is expected that the levelized cost of production will increase as the average pipeline length increases. The median value for each time period ranges between 100 and 108 km, which supports the common assumption in steady-state models that the transmission pipeline length between a city and production facility is 100 km.

The adjusted average pipeline length per demand center accounts for sharing of pipeline capacity between sub-regions. It is the average pipeline length multiplied by the average fraction of pipeline capacity allocated to the sub-region. For example, if the average pipeline length is 100 km and the average fraction of pipeline capacity allocated to the sub-region is 50%, the adjusted pipeline length will be 50 km per demand center. Essentially, the model only charges the sub-region for 50% of the cost of the pipeline since the other 50% is being used by other sub-regions and, thus, from an accounting perspective, the average pipeline length per demand center is only 50 km. The median value for the adjusted pipeline length per demand center ranges from 88 km in period 1 to 77 km in period 3, which indicates that the benefit from pipeline sharing increases as networks become more interconnected over time.

The effective capacity factor is the average percentage of pipeline capacity utilized in each time period and represents the extent to which pipelines are underutilized. The values associated with H_2 transmission are very small with the median value ranging from 15% in the first period to 58% in the third period. Significant underutilization is experienced in H_2 transmission since the model oversizes pipelines to meet the projected flow requirements over the entirety of the 20-year lifetime. As a result, in the best case, these pipelines will not become fully utilized for at least twenty years. However, since the model is limited to only eight nominal pipe sizes from 8 to 42 inches, pipeline capacity is often not perfectly matched to pipeline flow and pipelines can be oversized because the optimal pipe size resides between two available sizes. Consequently, even in the third period, the median effective capacity factor is only 58%.

The average pipeline diameter is expected to be larger in regions with high hydrogen demand. Generally, larger pipeline diameters suggest better economies-of-scale and, thus, lower levelized costs. However, since early pipelines are oversized for future flows, the need for large diameter pipelines can also lead to small effective capacity factors and, thus, higher levelized costs in early periods. For example, as a result of oversizing for large future hydrogen flows, the average pipeline diameter in the Pacific sub-region is 24 inches in the first two periods. The large pipelines are highly underutilized with an effective capacity factor of only 13% and the highest levelized cost of transmission in the first period.

In general, the levelized cost of transmission is largest when the effective capacity factor is small and the adjusted average pipeline length per demand center is large. In comparing the levelized costs among sub-regions, the Pacific sub-region has the highest cost in the first period since the pipeline network is extensive and consists of large underutilized pipelines (Figure 135). The transmission cost in the Northwest sub-region is also large in the first period since the sub-region has the smallest effective capacity factor. However, the relatively compact network and smaller diameter pipelines allows the cost to be lower than the value in the Pacific sub-region. The sub-regions with the lowest transmission costs are the Southwest and Midwest, which have smaller average pipeline diameters and slightly larger effective capacity factors.

In the second period, the Pacific and Northwest sub-regions continue to have the largest transmission costs since they have low effective capacity factors. The transmission cost in the Intermountain sub-region decreases substantially as a result of good utilization and a small adjusted average pipeline length per demand center. The small adjusted pipeline length is achieved through sharing of infrastructure with the Pacific sub-region. The low transmission cost associated with the Plains region occurs because centralized infrastructure is implemented in only the last year of the period.

In the third period, the transmission costs are similar in all sub-regions except the Plains. The cost is unusually large in the Plains sub-region despite a relatively large effective capacity factor since the adjusted average pipeline length per demand center is very large and the average pipeline diameter is very small. Essentially, small quantities of hydrogen are being transported long distances, which results in poor economies-of-scale and large levelized costs of transmission.

Table 91: Comparison of H_2 transmission metrics for each sub-region given the H_2 Success scenario

	Period 1	Period 2	Period 3
Northwest			
Levelized Cost of Transmission ($/kg H_2)	1.31	0.66	0.34
Average Pipeline Length per Demand Center (km)	70	71	62
Adjusted Average Pipeline Length per Demand Center (km)	70	65	57
Effective Capacity Factor (%)	6%	26%	59%
Average Pipeline Diameter (inch)	17.9	18.8	16.7
Mean Nearest Neighbor Distance (km)	31	31	27
Plains			
Levelized Cost of Transmission ($/kg H_2)	N/A	0.21	1.06
Average Pipeline Length per Demand Center (km)	N/A	152	152
Adjusted Average Pipeline Length per Demand Center (km)	N/A	119	120
Effective Capacity Factor (%)	N/A	41%	56%
Average Pipeline Diameter (inch)	N/A	13.9	12.5
Mean Nearest Neighbor Distance (km)	N/A	120	107
Pacific			
Levelized Cost of Transmission ($/kg H_2)	1.47	0.54	0.36
Average Pipeline Length per Demand Center (km)	89	91	114
Adjusted Average Pipeline Length per Demand Center (km)	88	87	105
Effective Capacity Factor (%)	13%	33%	64%
Average Pipeline Diameter (inch)	24.2	23.8	22.1
Mean Nearest Neighbor Distance (km)	39	29	30
Intermountain			
Levelized Cost of Transmission ($/kg H_2)	1.16	0.29	0.26
Average Pipeline Length per Demand Center (km)	121	116	137
Adjusted Average Pipeline Length per Demand Center (km)	82	66	71
Effective Capacity Factor (%)	17%	40%	66%
Average Pipeline Diameter (inch)	20.2	22.0	20.3
Mean Nearest Neighbor Distance (km)	47	61	67
Midwest			
Levelized Cost of Transmission ($/kg H_2)	0.97	0.45	0.36
Average Pipeline Length per Demand Center (km)	108	109	97
Adjusted Average Pipeline Length per Demand Center (km)	94	87	80
Effective Capacity Factor (%)	20%	35%	52%
Average Pipeline Diameter (inch)	14.9	13.6	11.8
Mean Nearest Neighbor Distance (km)	67	61	49
Southwest			
Levelized Cost of Transmission ($/kg H_2)	1.02	0.44	0.26
Average Pipeline Length per Demand Center (km)	109	88	88
Adjusted Average Pipeline Length per Demand Center (km)	108	84	74
Effective Capacity Factor (%)	15%	30%	53%
Average Pipeline Diameter (inch)	15.4	14.7	14.3
Mean Nearest Neighbor Distance (km)	54	40	39

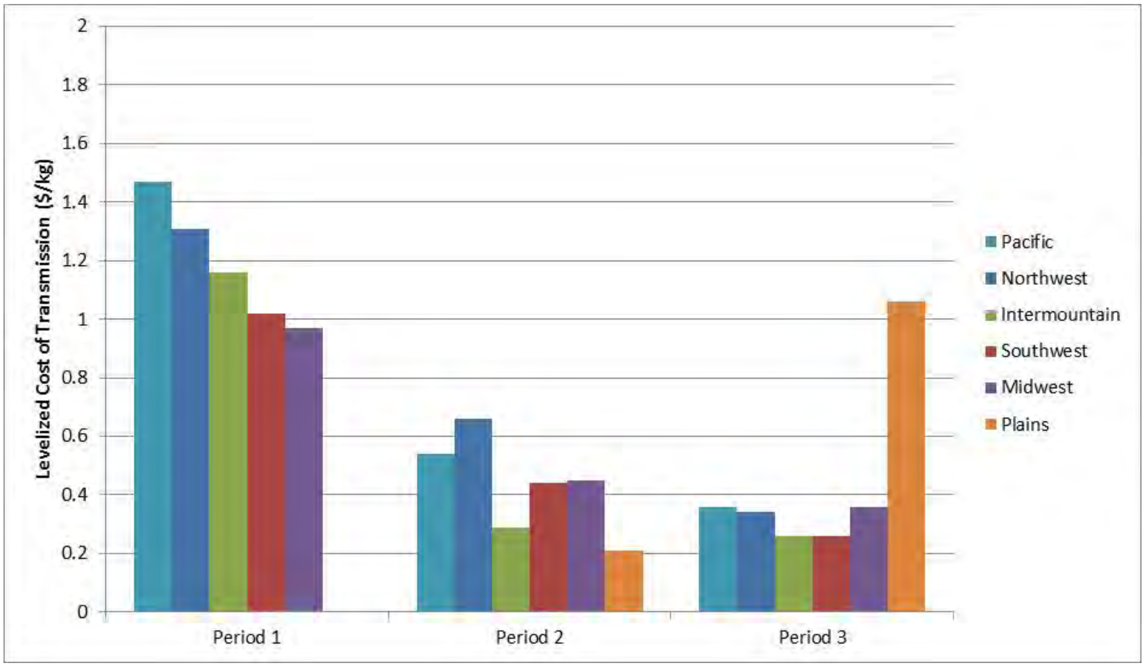

Figure 135: Levelized cost of transmission ($/kg) for each sub-region given the H_2 Success scenario

Steady-state models of hydrogen infrastructure have some inherent problems that prevent the calculation of accurate transmission costs. First, most models are spatially simplified by assuming that a single pipeline connects a single city to a single production facility. As a result, they are incapable of accounting for the benefits achieved by the sharing of interconnected regional pipeline networks. Moreover, the transmission pipeline is assumed to be a generic distance (e.g., 100 km), which means that these models do not account for regional variation in pipeline distances based on the spatial distribution of demand. Finally, the models assume that infrastructure is fully utilized upon completion and, thus, do not consider underutilization resulting from slow development of hydrogen demand or from the oversizing of early pipelines. Consequently, the design and economics of a transmission pipeline network is much more complex than represented by generic steady-state models.

Fortunately, the insights gained from the sub-regional case studies can generate rules-of-thumb that can help improve the cost estimates provided by steady-state models. First, it is desirable to identify a spatial metric that can estimate the average pipeline length per demand center without requiring a time-consuming optimization model. The "mean nearest neighbor distance" identifies the mean distance between neighboring demand centers within a sub-region. This metric is calculated in a geographic information system (GIS) using only the centroid locations of the regional demand centers. Figure 136 shows that about 75% of the variability in the average pipeline length per demand center (L_{ave}^{p}) can be described by a logarithmic function of the mean nearest neighbor distance (*NND*) (equation 91).

$$L_{ave}^{p} = 52.043 ln(NND) - 97.095 \tag{91}$$

This equation provides a simple method for estimating the average pipeline length per demand center in a specific geographic region. Replacing the generic pipeline distance with this value may provide an improved estimate that accounts for the spatial distribution of demand within a region.

Although equation 91 does account for the sharing of pipeline capacity by multiple demand centers within a region, it does not account for sharing between regions. Therefore, if the study region is expected to be connected with other regions, the average pipeline length per demand center must be adjusted. The magnitude of the adjustment is highly dependent on the extent of sharing between regions. For example, the Southwest sub-region shares much of its pipeline network with other sub-regions and, thus, the adjusted pipeline length per demand center is 32 to 48% lower than the unadjusted length in the three analysis periods. The median values for all sub-regions indicate a 1% reduction in period 1, a 14% reduction in period 2 and a 17%

reduction in period 3. The adjustment increases over time as sub-regions become more interconnected.

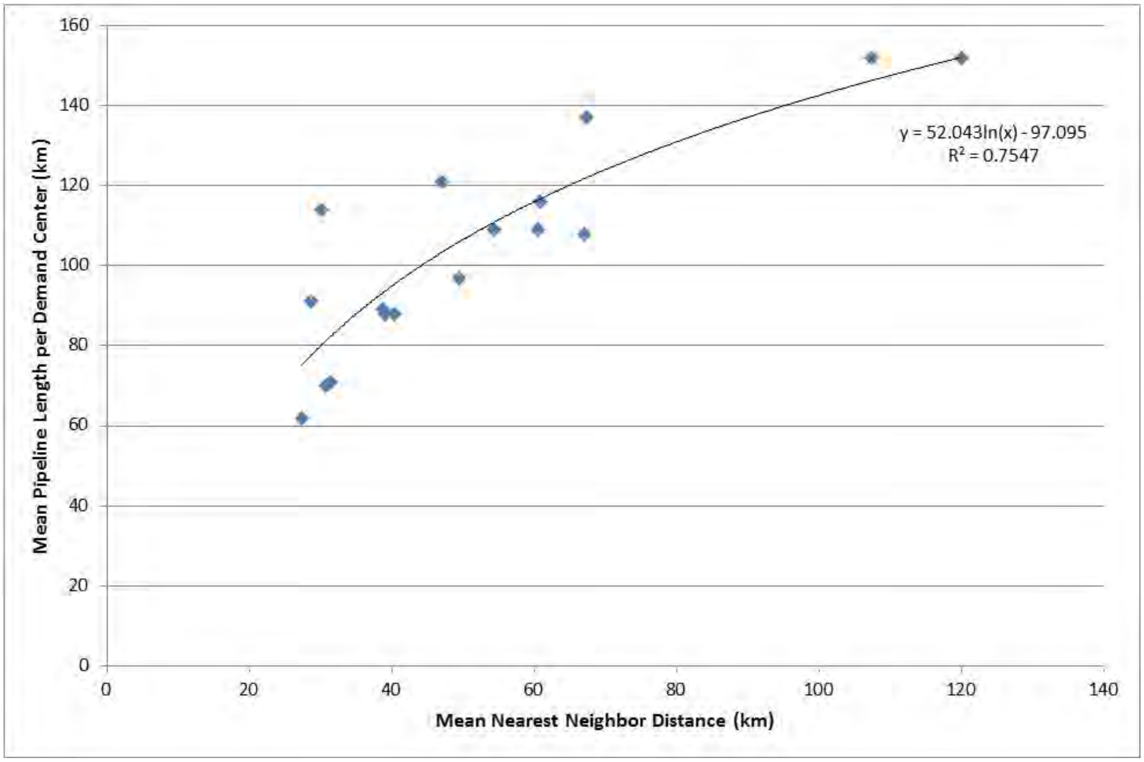

Figure 136: Relationship between the mean nearest neighbor distance and the mean pipeline length per demand center

To better incorporate underutilization into steady-state models, an effective average capacity factor should be calculated based on the projected HFCV deployment rate during the analysis period and the assumption about pipeline oversizing (e.g., based on a 20-year projection of hydrogen flow). The generic capacity factor, which assumes full utilization, can be replaced in the steady-state model by the effective capacity factor in order to provide a better estimate of the levelized cost of transmission. Alternatively, Figure 137 suggests that the effective capacity factor (*cf*) can be used to directly estimate the levelized cost of transmission (lc_{trans}) (equation 92).

92 $$lc_{trans} = 0.246cf^{-0.714}$$

The data show one major outlier, which is the observation for the Plains sub-region in period 3. As described earlier, the cost is unusually large in this case since long, small diameter pipelines are required to transport hydrogen between very distributed demand centers with relatively low demand. Thus, the effective capacity factor describes only about 63% of the variability in the levelized cost of transmission with the majority of the remainder described by the average pipeline length and diameter. This finding reiterates the importance of improving the estimates of the adjusted average pipeline length and the effective capacity factor in steady-state models. Again, an improved capacity factor could be estimated by assuming a fixed interval for infrastructure installations and using the HFCV deployment rate to determine average capacity factors over each interval.

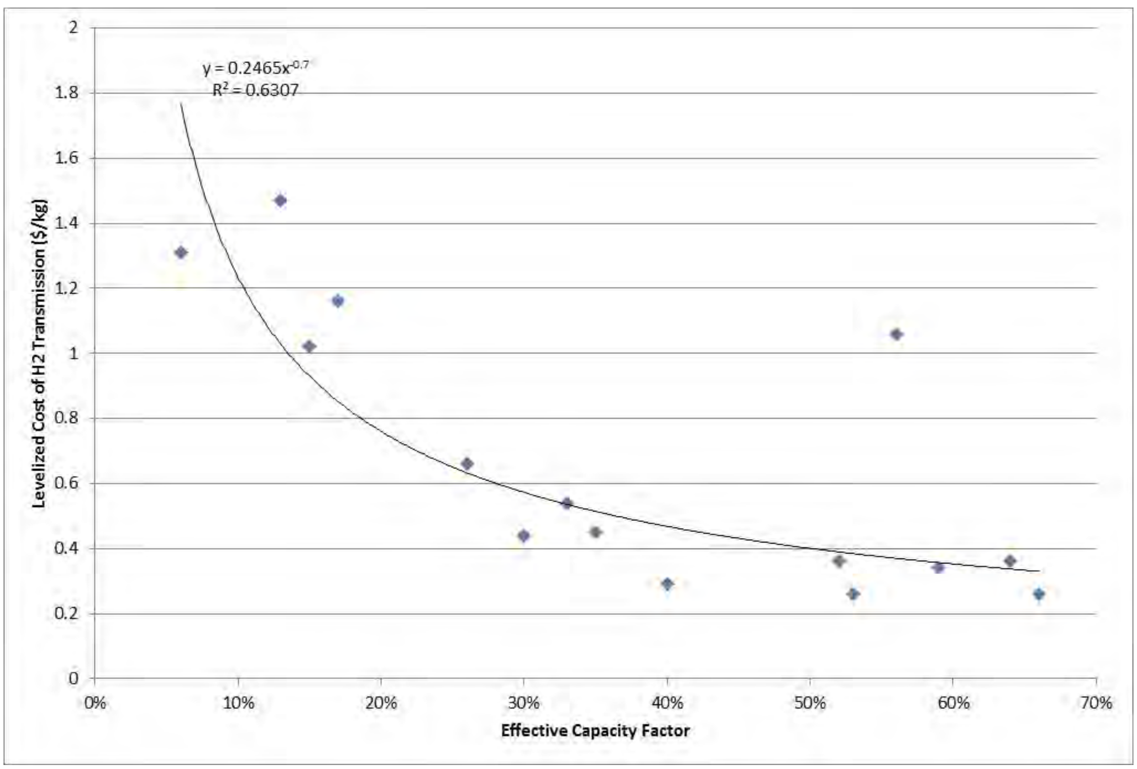

Figure 137: Levelized cost of H_2 transmission as a function of effective capacity factor

4.2.7.3 H_2 Distribution

Distribution pipelines transport hydrogen from demand center centroids (i.e., distribution centers) to individual refueling stations within each demand center. The summary metrics that determine the cost of distribution pipelines are listed for each sub-region in Table 92. The design of the distribution network is determined using the Idealized City Model described in section 2.2.4. In this model, the length of distribution pipelines in a demand center is a function of the city radius and the number of refueling stations. The average city radius indicates the area of a demand center. This value decreases over time as hydrogen infrastructure is extended to smaller cities.

As the average city radius decreases, the average pipeline length per demand center also generally declines. However, the Pacific sub-region is an exception since it includes many large cities with a high density of hydrogen demand, as indicated by the average city H_2 demand metric. In these cities, the radius does not increase substantially over time, but the density of refueling stations and the pipelines that supply them do increase. As a result, the average city radius declines with time, but the average pipeline length per demand center increases. Assuming that the effective capacity factor is held constant, it is expected that the levelized cost of distribution will decrease as the average pipeline length per demand center decreases. The median value of the average pipeline length per demand center ranges from 144 km in the first period to 105 km in the third period.

The effective capacity factor is the average percentage of pipeline capacity utilized in each time period and represents the extent to which pipelines are underutilized. Similar to H_2 transmission pipelines, the values associated with H_2 distribution are very small with the median value ranging from 12% in the first period to 56% in the third period. The reasons for the low effective capacity factor are identical to those described for H_2 transmission pipelines, including oversizing for projected flows in 20 years and a limited selection of nominal pipe diameters.

The average pipeline diameter is expected to be larger in regions where the average H_2 demand per city is large. In general, larger pipeline diameters suggest better economies-of-scale and, thus, lower levelized costs. However, since the diameters of early pipelines are oversized for future flows, the need for large diameter pipelines can also lead to small effective capacity factors and, thus, higher levelized costs in early periods.

The three major determinants of the levelized cost of H_2 distribution is the average pipeline length per demand center, the average diameter, and the effective capacity factor. In the first period, there is little variation in the effective capacity factor between sub-regions (Figure 138). As a result, there is less variation in distribution costs among sub-regions than identified for transmission and production costs. The sub-regions with the highest distribution costs are also those with the largest average pipeline length per demand center. The cost in the Midwest sub-region is small since only 53% of the hydrogen consumed during the first period is supplied by centralized infrastructure.

In the second and third periods, there is even less variation in distribution costs between sub-regions. The distribution cost for the Plains sub-region in period 2 is very small since only 9% of the hydrogen consumed during this period is supplied by centralized infrastructure. In the third period, the distribution cost remains low in the Plains sub-region since it is characterized by small cities and thus benefits from an average pipeline length per demand center of only 39 km.

Between the first and second periods, there is a large decline in the levelized cost of distribution as oversized pipelines become better utilized.

Table 92: Comparison of H_2 distribution metrics for each sub-region given the H_2 Success scenario

	Period 1	Period 2	Period 3
Northwest			
Levelized Cost of Distribution (\$/kg H_2)	3.20	1.19	0.79
Average Pipeline Length per Demand Center (km)	160	100	99
Average Pipeline Diameter (inch)	7.5	6.6	6.4
Effective Capacity Factor (%)	11%	31%	53%
Average City Radius (km)	10.6	6.8	5.7
Average City H_2 Demand (tonnes/day)	36	40	54
Plains			
Levelized Cost of Distribution (\$/kg H_2)	N/A	0.10	0.43
Average Pipeline Length per Demand Center (km)	N/A	41	39
Average Pipeline Diameter (inch)	N/A	4.5	4.4
Effective Capacity Factor (%)	N/A	41%	56%
Average City Radius (km)	N/A	4.5	4.2
Average City H_2 Demand (tonnes/day)	N/A	18	19
Pacific			
Levelized Cost of Distribution (\$/kg H_2)	3.34	1.32	0.86
Average Pipeline Length per Demand Center (km)	144	151	166
Average Pipeline Diameter (inch)	8.8	8.4	8.3
Effective Capacity Factor (%)	13%	39%	67%
Average City Radius (km)	9.0	7.4	6.5
Average City H_2 Demand (tonnes/day)	42	77	120
Intermountain			
Levelized Cost of Distribution (\$/kg H_2)	3.08	1.17	0.79
Average Pipeline Length per Demand Center (km)	118	130	113
Average Pipeline Diameter (inch)	7.2	7.0	6.7
Effective Capacity Factor (%)	13%	40%	60%
Average City Radius (km)	8.5	7.4	5.8
Average City H_2 Demand (tonnes/day)	30	56	66
Midwest			
Levelized Cost of Distribution (\$/kg H_2)	2.60	1.26	0.79
Average Pipeline Length per Demand Center (km)	118	106	82
Average Pipeline Diameter (inch)	7.2	6.7	6.5
Effective Capacity Factor (%)	11%	29%	48%
Average City Radius (km)	8.8	6.7	4.7
Average City H_2 Demand (tonnes/day)	31	40	45
Southwest			
Levelized Cost of Distribution (\$/kg H_2)	3.22	1.24	0.81
Average Pipeline Length per Demand Center (km)	185	117	110
Average Pipeline Diameter (inch)	7.6	7.0	6.7
Effective Capacity Factor (%)	12%	33%	55%
Average City Radius (km)	11.4	7.0	5.6
Average City H_2 Demand (tonnes/day)	42	46	62

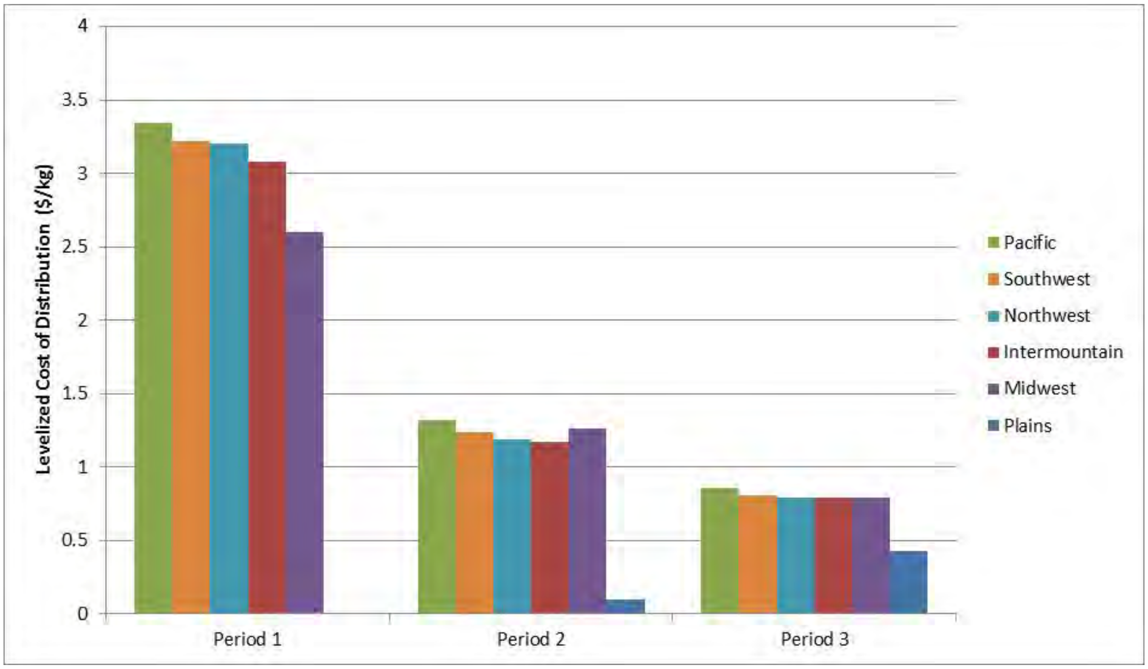

Figure 138: Levelized cost of distribution ($/kg) for each sub-region given the H_2 Success scenario

Figure 139 suggests that the effective capacity factor is the most important determinant of the levelized cost of distribution, explaining more than 90% of the variability in cost. Thus, equation 93 can be used to estimate the levelized cost of distribution (lc_{dist}) as a function of the capacity factor (*cf*).

93 $$lc_{dist} = 0.4375cf^{-0.94}$$

This equation suggests that models that use a fixed capacity factor of 80-90% can underestimate the cost of distribution by more than 60% during early deployment when the effective capacity factor is small.

4.2.7.4 H_2 Refueling Stations

The summary metrics that impact the cost of H_2 refueling station costs are listed for each sub-region in Table 93. The average number of refueling stations per city is generally a function of the average hydrogen demand per city. This metric is provided to quantify the magnitude of refueling station infrastructure that is required in each analysis period. Although an increase in the number of stations translates to a larger capital investment, it has little impact on the levelized cost of stations since it is correlated with additional demand. In contrast, the average quantity of H_2 dispensed daily at each station indicates the average size of refueling stations. It is expected that larger stations will achieve better economies-of-scale and, thus, lower levelized costs.

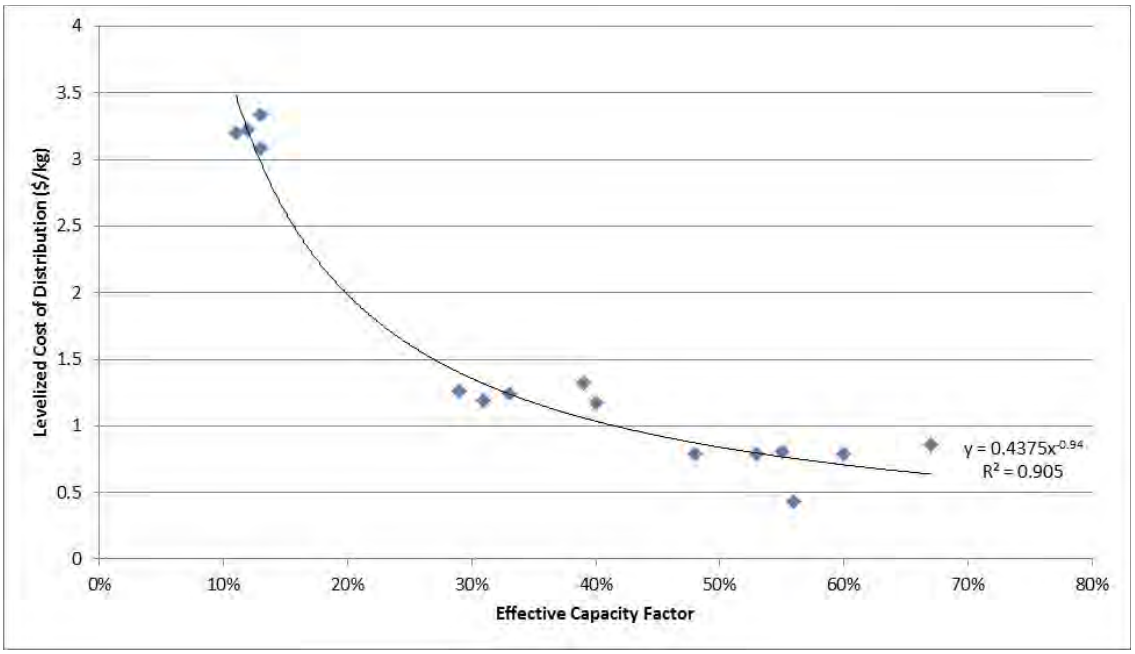

Figure 139: Levelized cost of H_2 distribution as a function of effective capacity factor

The effective capacity factor is the average percentage of refueling station capacity that is utilized during an analysis period. Since refueling stations are available in relatively small capacities, the model does not oversize stations for long-term demand projections. Rather, stations are designed to meet only the projected demand in each tranche and additional stations are added in subsequent tranches to meet demand growth. As a result, much higher effective capacity factors are achieved by refueling stations in each analysis period. The median value of the effective capacity factor is 47% in the first period and 74% in the third period.

The percentage of H_2 supplied onsite indicates the percentage of hydrogen that is produced at refueling stations using onsite steam methane reformation. This value is generally below 15%, but is much higher in two sub-regions. In the Plains sub-region, centralized infrastructure is not introduced until the last year of the second period. As a result, all of the hydrogen in the first period and 91% of the hydrogen in the second period is produced onsite. In the Midwest sub-region, centralized infrastructure is introduced in the fifth year of the first period so about 50% of the hydrogen is produced onsite during this period. Since stations with onsite production require steam methane reformers, the levelized cost of refueling stations is much higher in sub-regions with significant onsite production.

This is extremely clear when comparing the levelized cost of refueling stations between sub-regions (Figure 140). The Plains sub-region has substantially larger station costs in all periods as a result of the investment in onsite production. Although only 4% of hydrogen is produced onsite in the third period, the residual capital expenditure on onsite production in previous periods keeps the station costs large. In reality, the incorporation of a salvage value for steam methane reformers may mitigate some of this cost. In the Midwest sub-region, the refueling station cost is large in the first period since 50% of the hydrogen is produced onsite. The costs associated with the remaining sub-regions in the first period also reflect the percentage of hydrogen produced onsite. The costs descend from the Northwest sub-region, in which 13% of hydrogen is produced onsite, to the Pacific sub-region where only 3% of hydrogen is produced onsite.

Table 93: Comparison of H_2 refueling station metrics for each sub-region given the H_2 Success scenario

	Period 1	Period 2	Period 3
Northwest			
Levelized Cost of Refueling Stations ($/kg H_2)	3.32	1.89	1.57
Average # of Refueling Stations per City	20	26	37
Average H_2 Dispensed Daily per Station (kg/day)	1128	1387	1427
Effective Capacity Factor (%)	46%	67%	74%
Percentage H_2 Supplied Onsite (%)	13%	2%	0%
Plains			
Levelized Cost of Refueling Stations ($/kg H_2)	6.97	4.38	2.26
Average # of Refueling Stations per City	6	9	13
Average H_2 Dispensed Daily per Station (kg/day)	1131	1328	1342
Effective Capacity Factor (%)	43%	67%	73%
Percentage H_2 Supplied Onsite (%)	100%	91%	4%
Pacific			
Levelized Cost of Refueling Stations ($/kg H_2)	2.67	1.80	1.54
Average # of Refueling Stations per City	34	51	82
Average H_2 Dispensed Daily per Station (kg/day)	1084	1347	1420
Effective Capacity Factor (%)	50%	67%	74%
Percentage H_2 Supplied Onsite (%)	3%	1%	0%
Intermountain			
Levelized Cost of Refueling Stations ($/kg H_2)	3.03	1.90	1.58
Average # of Refueling Stations per City	21	32	44
Average H_2 Dispensed Daily per Station (kg/day)	1106	1365	1421
Effective Capacity Factor (%)	47%	67%	74%
Percentage H_2 Supplied Onsite (%)	6%	5%	1%
Midwest			
Levelized Cost of Refueling Stations ($/kg H_2)	3.92	1.99	1.62
Average # of Refueling Stations per City	16	22	30
Average H_2 Dispensed Daily per Station (kg/day)	1153	1393	1424
Effective Capacity Factor (%)	45%	67%	74%
Percentage H_2 Supplied Onsite (%)	47%	4%	1%
Southwest			
Levelized Cost of Refueling Stations ($/kg H_2)	3.17	1.90	1.58
Average # of Refueling Stations per City	26	28	42
Average H_2 Dispensed Daily per Station (kg/day)	1111	1370	1421
Effective Capacity Factor (%)	47%	67%	74%
Percentage H_2 Supplied Onsite (%)	12%	4%	1%

In the second and third periods, the average station size, percentage of H_2 supplied onsite, and effective capacity factor are very similar in all sub-regions except the Plains sub-region. As a result, there is little variability in the levelized cost of refueling stations between these sub-regions. Since the average station size does not vary much between sub-regions within each period, the major determinants of cost are the effective capacity factor and the percentage of hydrogen produced onsite.

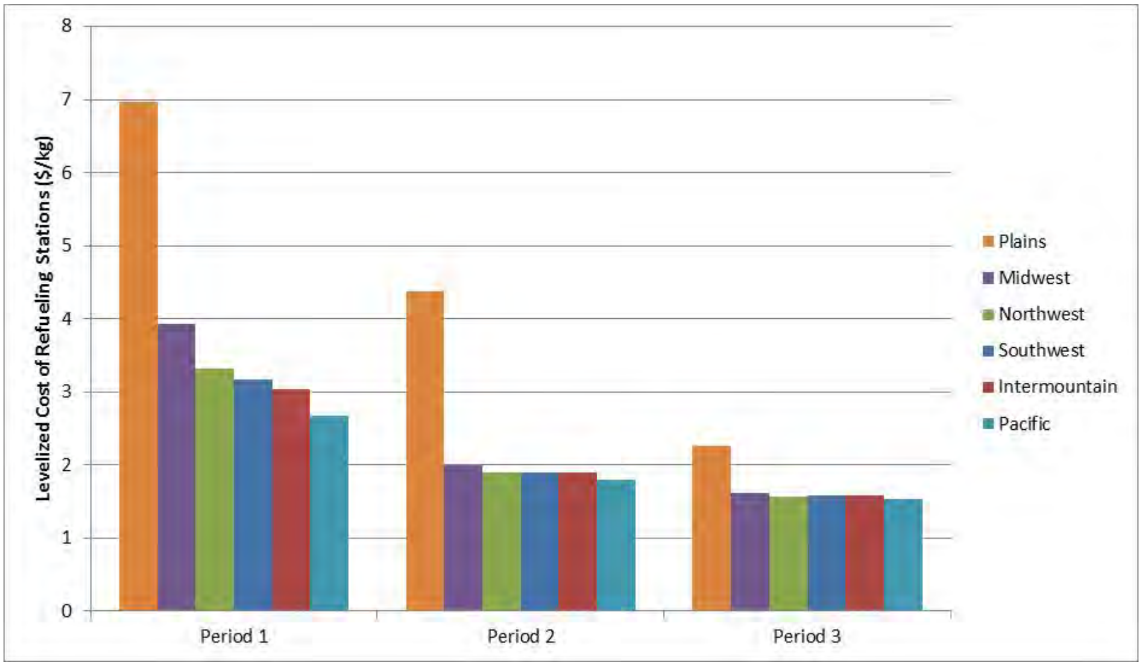

Figure 140: Levelized cost of refueling stations ($/kg) for each sub-region given the H_2 Success scenario

Figure 141 shows the relationship between the effective capacity factor and the levelized cost of refueling stations when all observations are included. The red circles highlight the four observations that are influenced by substantial onsite production. These observations include all periods associated with the Plains sub-region and the first period in the Midwest sub-region. It is clear that the costs associated with these observations are substantially larger for a given capacity factor since refueling stations that include onsite production are more expensive. As a result, the refueling station costs associated with sub-regions in which there is a large percentage of hydrogen supplied by onsite production cannot be predicted with the same model that predicts refueling station costs in sub-regions with low percentages of onsite production.

Upon removing the observations that are impacted by substantial onsite production, the remaining data represents observations in which less than 15% of the hydrogen is produced onsite. Given these observations, the effective capacity factor can explain about 98% of the variability in the levelized cost of refueling stations (Figure 142). The power function given in equation 94 estimates the levelized cost of refueling stations ($lc_{station}$) based on the effective capacity factor (*cf*).

$$lc_{station} = 1.0324cf^{-1.46} \tag{94}$$

This equation is yet another reminder of the importance of accurately estimating the effective capacity factor when performing infrastructure modeling. Figure 142 suggests that a steady-state model that uses a fixed capacity factor greater than 75% may underestimate the levelized cost of refueling stations by as much as 50% during early deployment when the effective capacity factor is small.

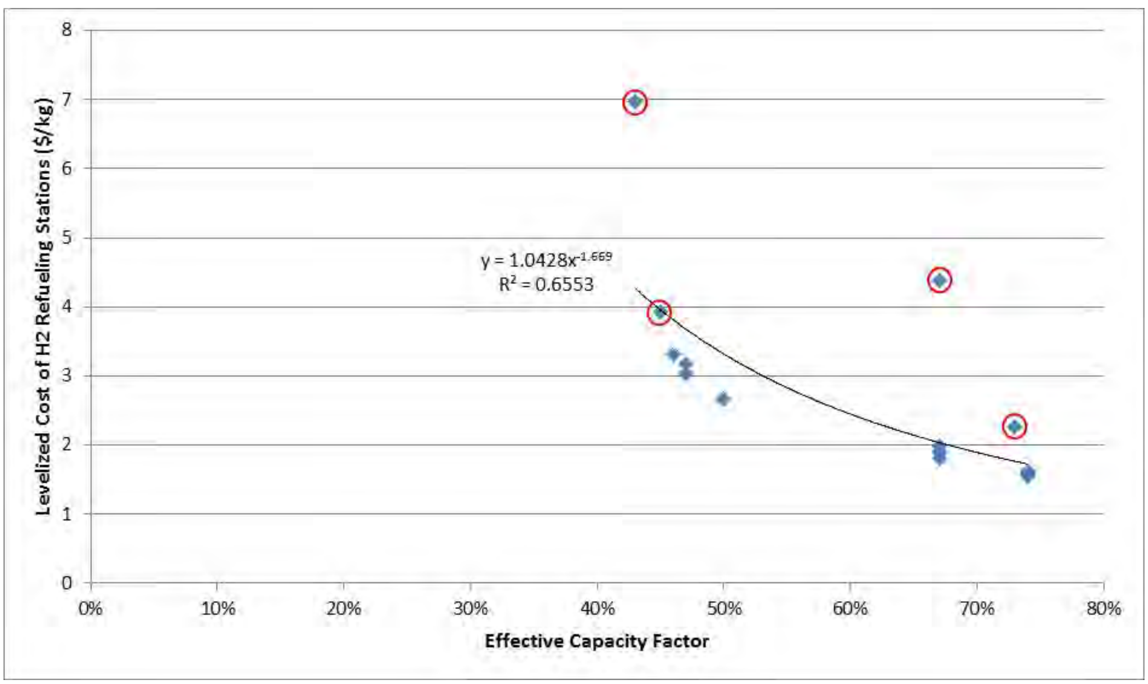

Figure 141: Levelized cost of H_2 refueling stations as a function of effective capacity factor (observations that are influenced by substantial onsite production are circled in red)

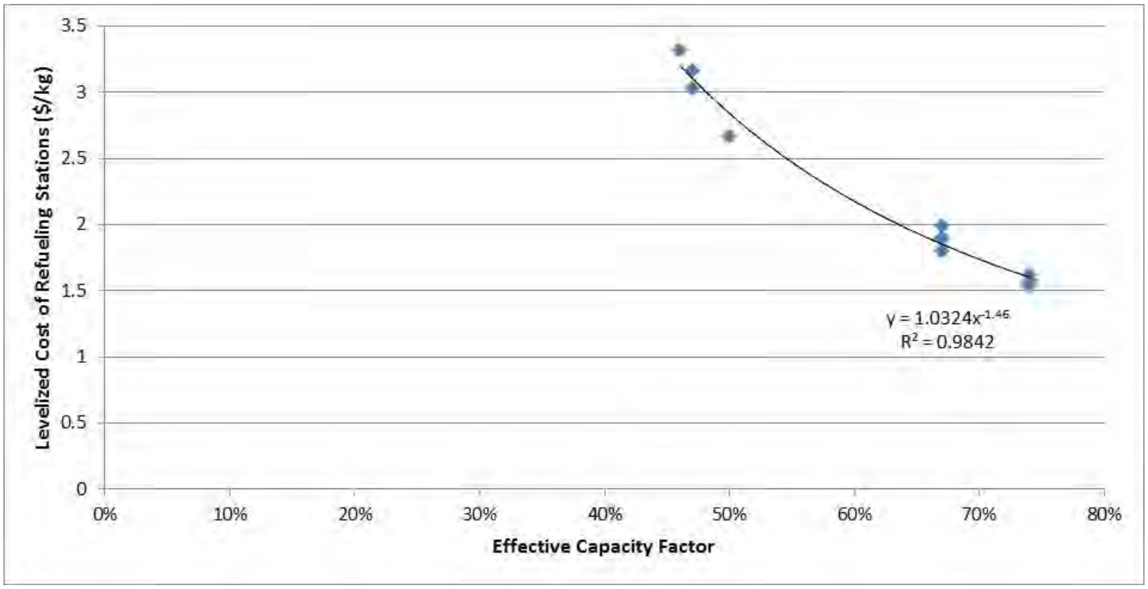

Figure 142: Levelized cost of H_2 refueling stations as a function of effective capacity factor, including only observations in which less than 15% of hydrogen is supplied by onsite production

4.2.7.5 CO_2 Transport

The summary metrics that influence the levelized cost of CO_2 transport are listed in Table 94. The average pipeline length per H_2 production site indicates the proximity of production sites to CO_2 storage sites. The metric varies widely between sub-regions depending upon the proximity and capacity of CO_2 storage sites. In the Pacific sub-region, the value is large since production sites in Arizona and Nevada are distant from potential CO_2 storage sites. However, in the Midwest sub-region, there are storage sites in close proximity, but the capacity of these sites is small and thus long pipelines are required to access multiple storage sites. In general, as the average pipeline length increases, the levelized cost of CO_2 transport also increases.

The adjusted average pipeline length per demand center accounts for sharing of CO_2 pipeline capacity between sub-regions. It is the average pipeline length multiplied by the average fraction of pipeline capacity allocated to the sub-region. This metric essentially identifies the average length of pipeline that contributes to cost within a sub-region. In the Intermountain sub-region, extensive sharing of CO_2 pipelines with other sub-regions decreases the average pipeline length by 60-68%. On average, inter-regional pipeline sharing decreases the average pipeline length assigned to a sub-region by 17% in the first period and 35% in the third period. The adjusted average pipeline length per production site varies from 25 to 500 km depending upon the conditions in each sub-region. However, the median value for all sub-regions is approximately 170 km in the first period and about 150 km in the third period.

Although the model does oversize CO_2 pipelines based on the projected flow over the 20-year lifetime, many of the pipelines serve a single production site and are thus sized for near-term flows. This is supported by the fact that the average number of CO_2 storage sites per production site is usually greater than one. Since very few CO_2 pipeline networks connect multiple production facilities, fewer large trunk pipelines are developed. As a result, CO_2 pipelines tend to be less oversized than H_2 pipelines and, consequently, the effective capacity factor is generally larger in the first period. In fact, the lowest effective capacity factors are identified in the sub-regions with the largest average pipeline diameters, which suggests that the pipelines in these sub-regions are the most oversized. The median value for the effective capacity factor is 33% in the first period and 60% in the third period.

In comparing the levelized cost of CO_2 transport between sub-regions, the cost in the Midwest sub-region is much larger in all periods since the CO_2 storage reservoir in the region has very low storage density (Figure 143). Consequently, very long pipelines are required to access multiple storage sites. This observation is supported by the large values for the adjusted average pipeline length per production site. The costs for the remaining sub-regions follow the same trend as the adjusted average pipeline length with the sub-regions with the lowest costs also having the shortest average pipeline lengths.

In the second period, the CO_2 transport cost in the Southwest sub-region drops below the cost in the Northwest sub-region even though the effective capacity factor is smaller and the adjusted average pipeline length and average pipeline diameter are larger. The reason for the decline is the fact that about 40% of the pipeline capacity, on average, is allocated to other sub-regions during this period. If the average pipeline diameter is adjusted to include sharing, it drops to about 17 inches from 27 inches, which suggests that the majority of the capacity of the largest diameter pipelines is allocated to other sub-regions. As a result, the average pipeline diameter of pipelines allocated to this sub-region is actually quite low and, thus, a low cost of CO_2 transport is achieved.

In the third period, the levelized cost of CO_2 transport remains large in the Midwest region, but is between 2 and 7 cents per kg of hydrogen in the other sub-regions. The costs are especially low in the Intermountain and Plains sub-regions since the adjusted average pipeline lengths per production site are so small.

Table 94: Comparison of CO_2 transport metrics for each sub-region given the H_2 Success scenario

	Period 1	Period 2	Period 3
Northwest			
Levelized Cost of CO_2 Transport ($/kg H_2)	0.13	0.08	0.05
Average Pipeline Length per Production Site (km)	72	132	179
Adjusted Average Pipeline Length per Production Site (km)	72	122	171
Effective Capacity Factor (%)	34%	54%	60%
Average # of CO_2 storage sites per production site	1.0	1.0	1.4
Average Pipeline Diameter (inch)	21.3	22.0	22.5
Plains			
Levelized Cost of CO_2 Transport ($/kg H_2)	N/A	0.01	0.02
Average Pipeline Length per Production Site (km)	N/A	65	65
Adjusted Average Pipeline Length per Production Site (km)	N/A	27	28
Effective Capacity Factor (%)	N/A	49%	77%
Average # of CO_2 storage sites per production site	N/A	1.0	1.0
Average Pipeline Diameter (inch)	N/A	25.0	25.0
Pacific			
Levelized Cost of CO_2 Transport ($/kg H_2)	0.18	0.11	0.07
Average Pipeline Length per Production Site (km)	382	347	237
Adjusted Average Pipeline Length per Production Site (km)	370	316	211
Effective Capacity Factor (%)	38%	52%	65%
Average # of CO_2 storage sites per production site	1.3	1.1	0.9
Average Pipeline Diameter (inch)	20.9	24.0	24.6
Intermountain			
Levelized Cost of CO_2 Transport ($/kg H_2)	0.04	0.02	0.03
Average Pipeline Length per Production Site (km)	142	136	111
Adjusted Average Pipeline Length per Production Site (km)	48	54	35
Effective Capacity Factor (%)	33%	48%	60%
Average # of CO_2 storage sites per production site	1.5	1.4	1.3
Average Pipeline Diameter (inch)	20.8	21.7	24.1
Midwest			
Levelized Cost of CO_2 Transport ($/kg H_2)	0.57	0.20	0.13
Average Pipeline Length per Production Site (km)	582	722	267
Adjusted Average Pipeline Length per Production Site (km)	365	481	180
Effective Capacity Factor (%)	15%	35%	57%
Average # of CO_2 storage sites per production site	3.5	5.6	2.0
Average Pipeline Diameter (inch)	27.1	25.0	25.3
Southwest			
Levelized Cost of CO_2 Transport ($/kg H_2)	0.15	0.06	0.05
Average Pipeline Length per Production Site (km)	203	312	212
Adjusted Average Pipeline Length per Production Site (km)	169	189	131
Effective Capacity Factor (%)	20%	36%	54%
Average # of CO_2 storage sites per production site	1.5	2.2	1.4
Average Pipeline Diameter (inch)	28.7	27.0	26.5

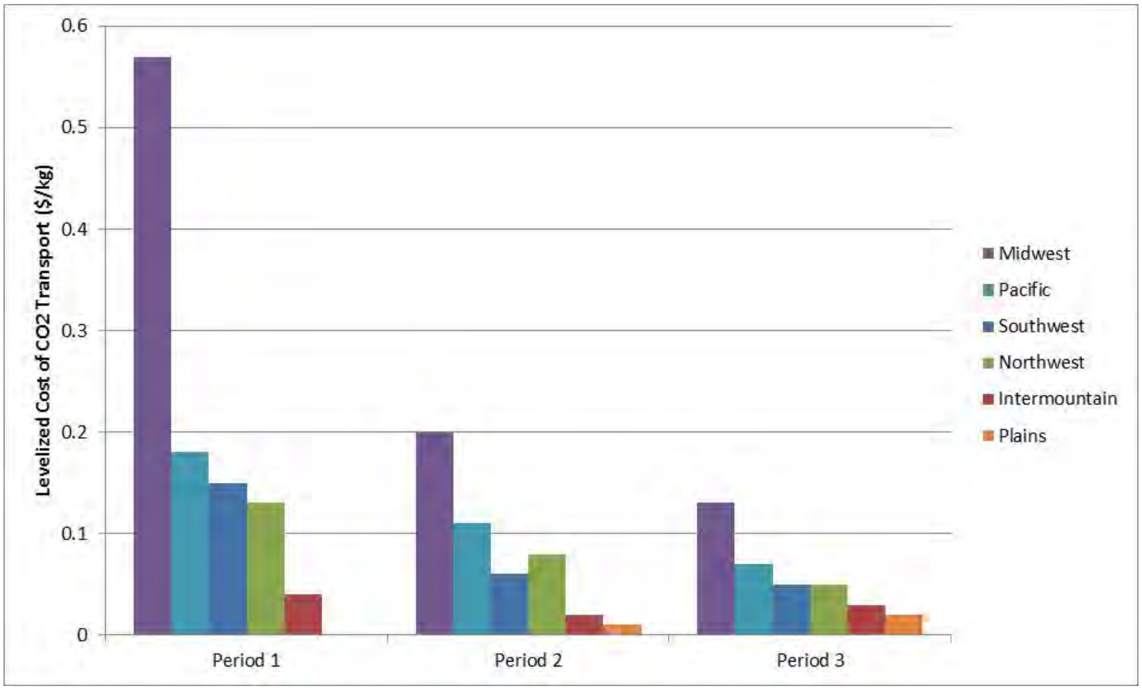

Figure 143: Levelized cost of CO_2 transport ($/kg) for each sub-region given the H_2 Success scenario

The modeling suggests that the effective capacity factor, adjusted average pipeline length per production site, and average pipeline diameter are the most important determinants of the CO_2 transport cost. However, this analysis indicates that the average pipeline diameter should be adjusted to account for the diameter of pipelines that are shared between sub-regions. The variable that explains the most variability in cost is the adjusted average pipeline length per production site (Figure 144). However, it only explains about 64% of the variability and several outliers indicate the importance of the effective capacity factor as an explanatory variable. The largest outlier is the observation associated with the first period in the Midwest sub-region in which a large average pipeline length is combined with an effective capacity factor of 15%. Consequently, a more accurate regression model would account for both the adjusted average pipeline length and the effective capacity factor

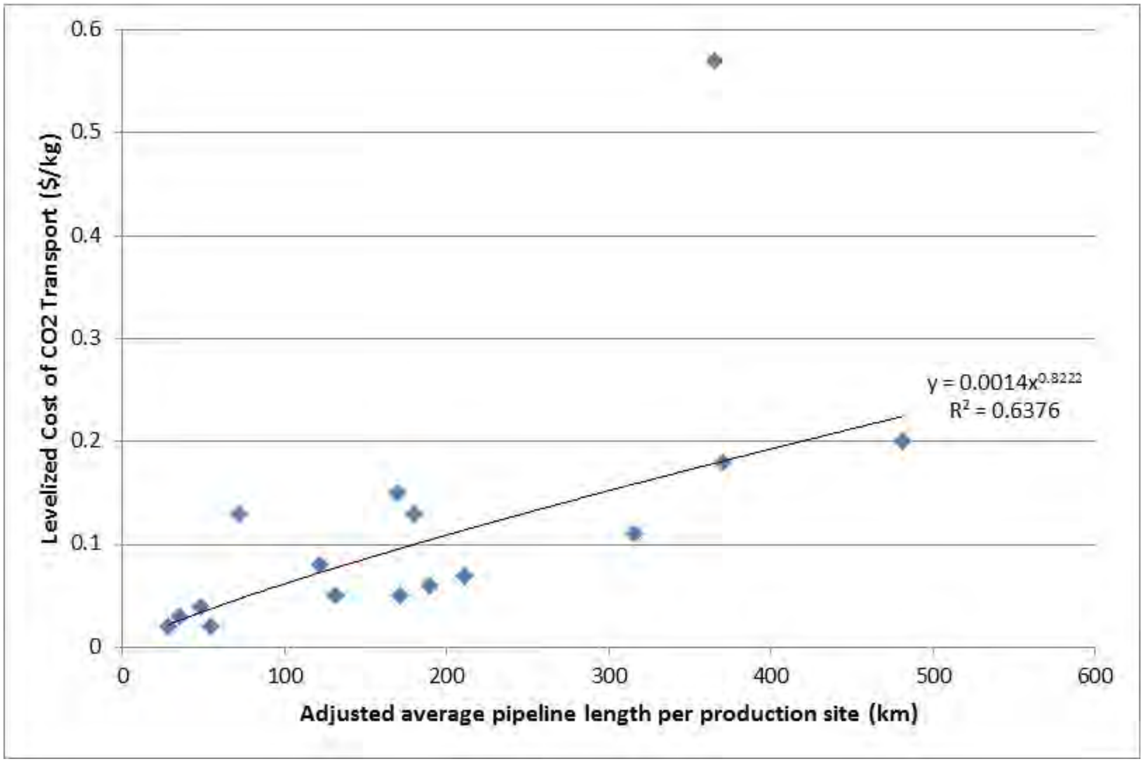

Figure 144: Levelized cost of CO_2 transport as a function of the adjusted average pipeline length per production site

4.2.7.6 Total Cost

In this section, the total levelized cost of hydrogen is compared between sub-regions for both the H_2 Success and H_2 Partial Success scenarios. In the H_2 Success scenario, the total levelized cost is extremely large in the first few years of infrastructure deployment since infrastructure is very underutilized. The annual levelized costs in the first year tend to be the largest in sub-regions that are geographically isolated and have relatively low demand (Figure 145). However, costs decline quickly in sub-regions that are supplied exclusively by onsite production (e.g., Plains and Midwest) since this infrastructure can be installed in small increments that experience less underutilization. In fact, as the refueling stations with onsite production become better utilized, the levelized cost drops below \$5/kg within the first five years. Early levelized costs are especially high in the Northwest sub-region as a result of high production costs that stem from a combination of high delivered coal costs and small, underutilized production facilities (Figure 146).

In the second tranche, centralized infrastructure is introduced to the Midwest sub-region. However, approximately 20% of the hydrogen continues to be supplied by onsite production, resulting in high refueling station costs. In combination with high CO_2 transport costs due to poor local storage capacity, the Midwest sub-region has the highest hydrogen cost through tranche 2. The Plains sub-region continues to be supplied by onsite production and achieves the lowest cost through the first decade.

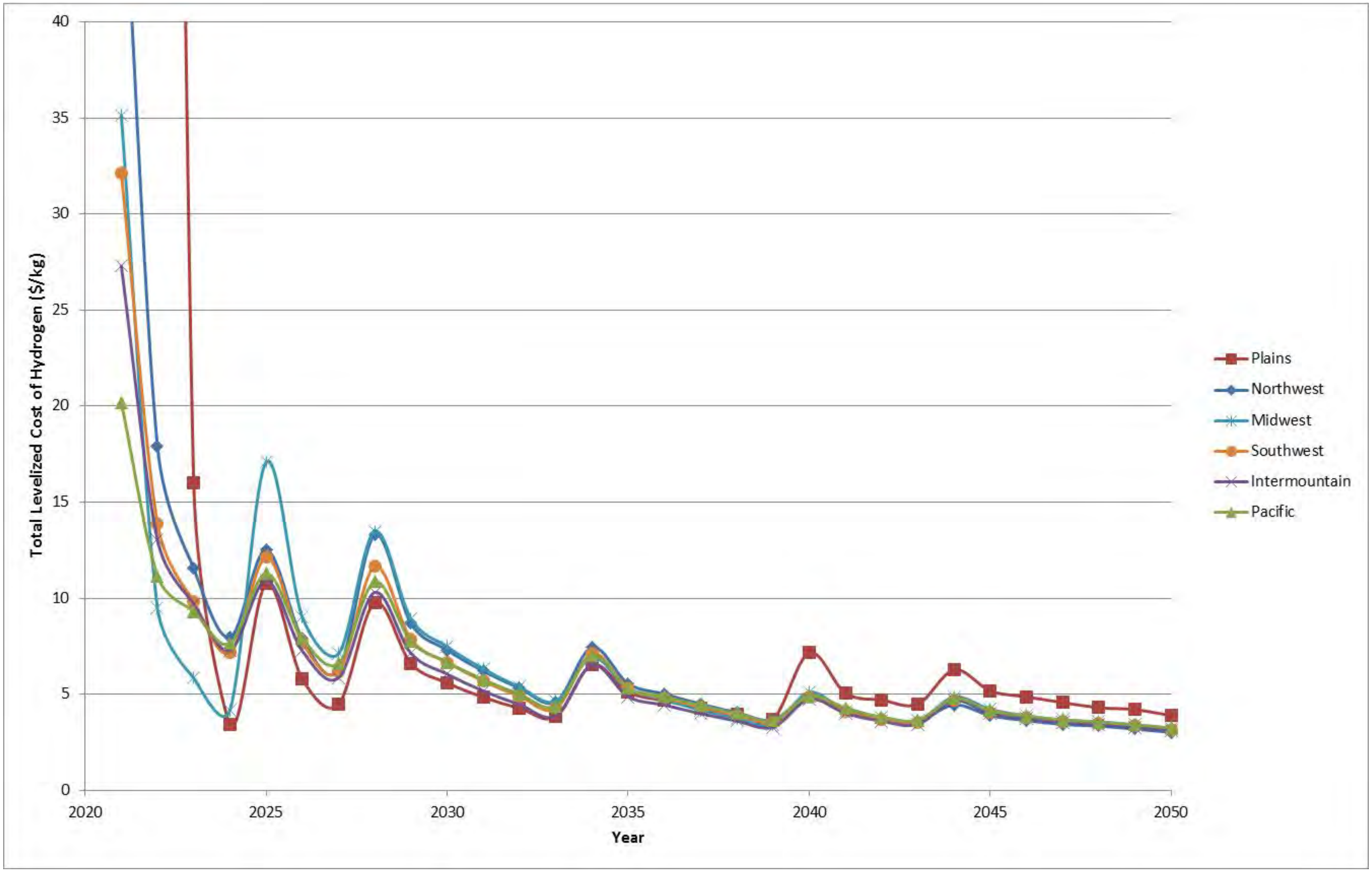

Figure 145: Annual levelized cost of hydrogen over the 30-year study period for each sub-region given the H_2 Success scenario

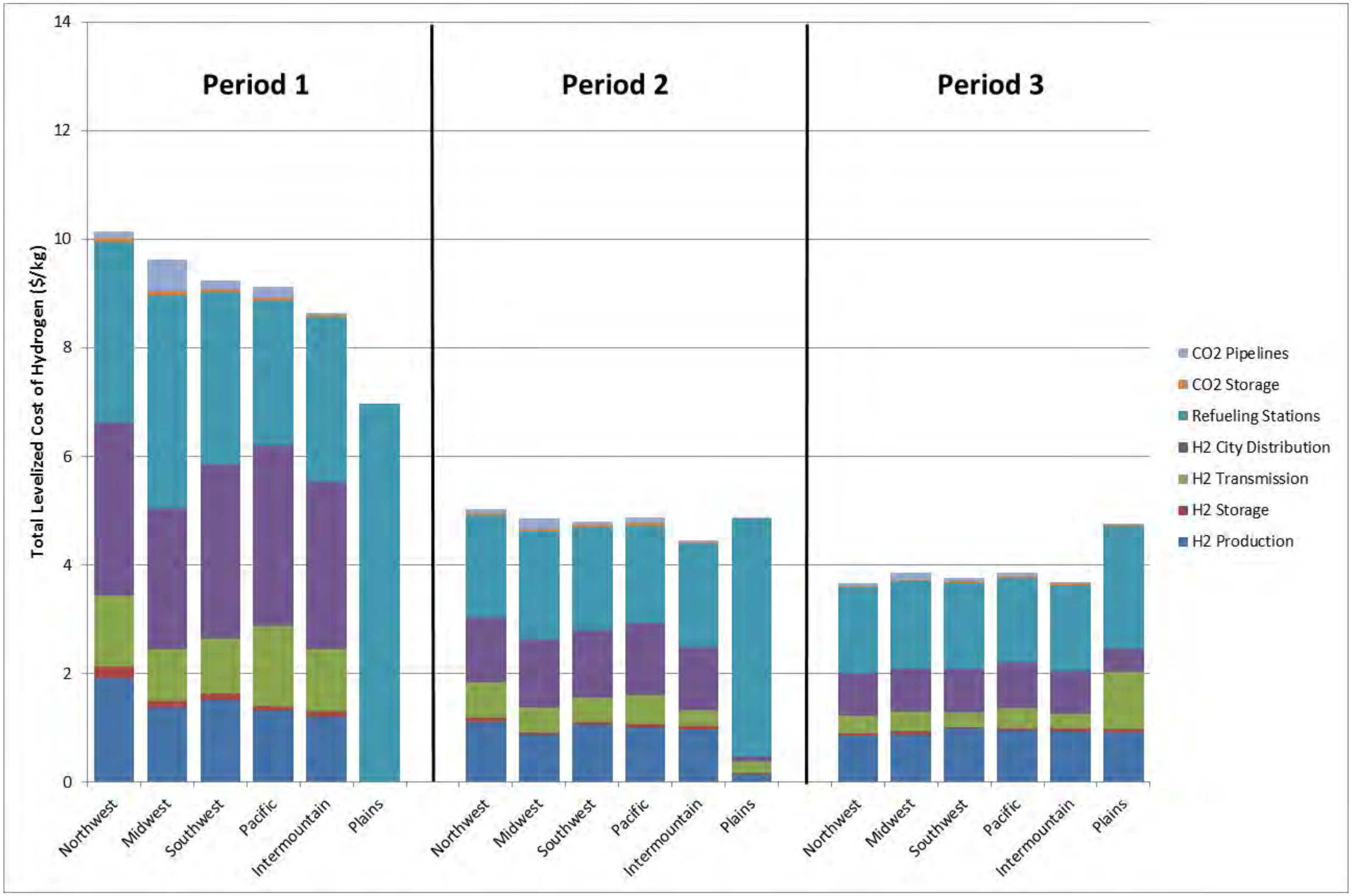

Figure 146: Levelized cost of hydrogen for each infrastructure component, 10-year analysis period, and sub-region given the H_2 Success scenario

In comparing the annual levelized costs, a pattern emerges in which more isolated sub-regions tend to have higher costs. Specifically, the Southwest, Midwest, and Northwest sub-regions have the highest costs in the first 15 years. During this time, which includes the first three tranches, these sub-regions maintain isolated supply networks with minimal interconnection with other sub-regions occurring only in the third tranche. In contrast, the Intermountain sub-region achieves the smallest annual costs since it benefits from interconnection with the large demand in the Pacific sub-region. In the fourth tranche, all of the sub-regions become interconnected and the costs for all sub-regions begin to converge. This finding suggests that there is a real benefit associated with interconnecting sub-regions since it allows for better economies-of-scale and improved utilization.

In the first twenty years, the Plains sub-region represents the cost of onsite production and the other sub-regions represent the cost of centralized infrastructure. During this period, the cost of centralized and onsite infrastructure converge after about 13 years, which suggests that onsite infrastructure may be the lower cost strategy in all sub-regions in the first three tranches.

In the final ten years, all sub-regions are interconnected and supplied primarily by centralized infrastructure. During this period, the levelized costs are similar in all sub-regions except the Plains. In the Plains, the introduction of centralized infrastructure in tranche 5 results in larger levelized costs since the sub-region has very dispersed small cities that are not particularly suited to centralized infrastructure. As a result, it may be preferable to maintain onsite production in this sub-region throughout the study period.

At the end of the 30-year study period, the levelized cost in the Plains sub-region is ~$4/kg while the costs converge to about $3/kg in the other sub-regions. The levelized costs for the ten-year analysis periods also show the convergence of costs in the third period (Figure 146). Specifically, the levelized costs for all sub-regions except the Plains converge at about $4/kg, while the cost in the Plains sub-region is approximately $5/kg.

In the H_2 Partial Success scenario, lower utilization rates associated with slower HFCV deployment generally result in higher levelized costs of hydrogen (Figure 147). However, in the first 10-year period, the slower ramp-up benefits the Plains and Pacific sub-regions (Figure 148). The Plains sub-region benefits because onsite production tends to be lower cost during early deployment. In the Pacific sub-region, costs decline because the projected 20-year pipeline flows are smaller and, thus, the CO_2 and H_2 pipelines are less oversized. Since the sub-region suffers from significant oversizing in the H_2 Success scenario as a result of very high projected demand, slower HFCV deployment results in a substantial decline in the diameter of pipelines installed in the first tranche in the H_2 Partial Success scenario. The reduced oversizing translates to much lower costs associated with H_2 and CO_2 pipelines during the first period. In the second and third periods, lower utilization rates result in larger levelized costs in all sub-regions in the H_2 Partial Success scenario.

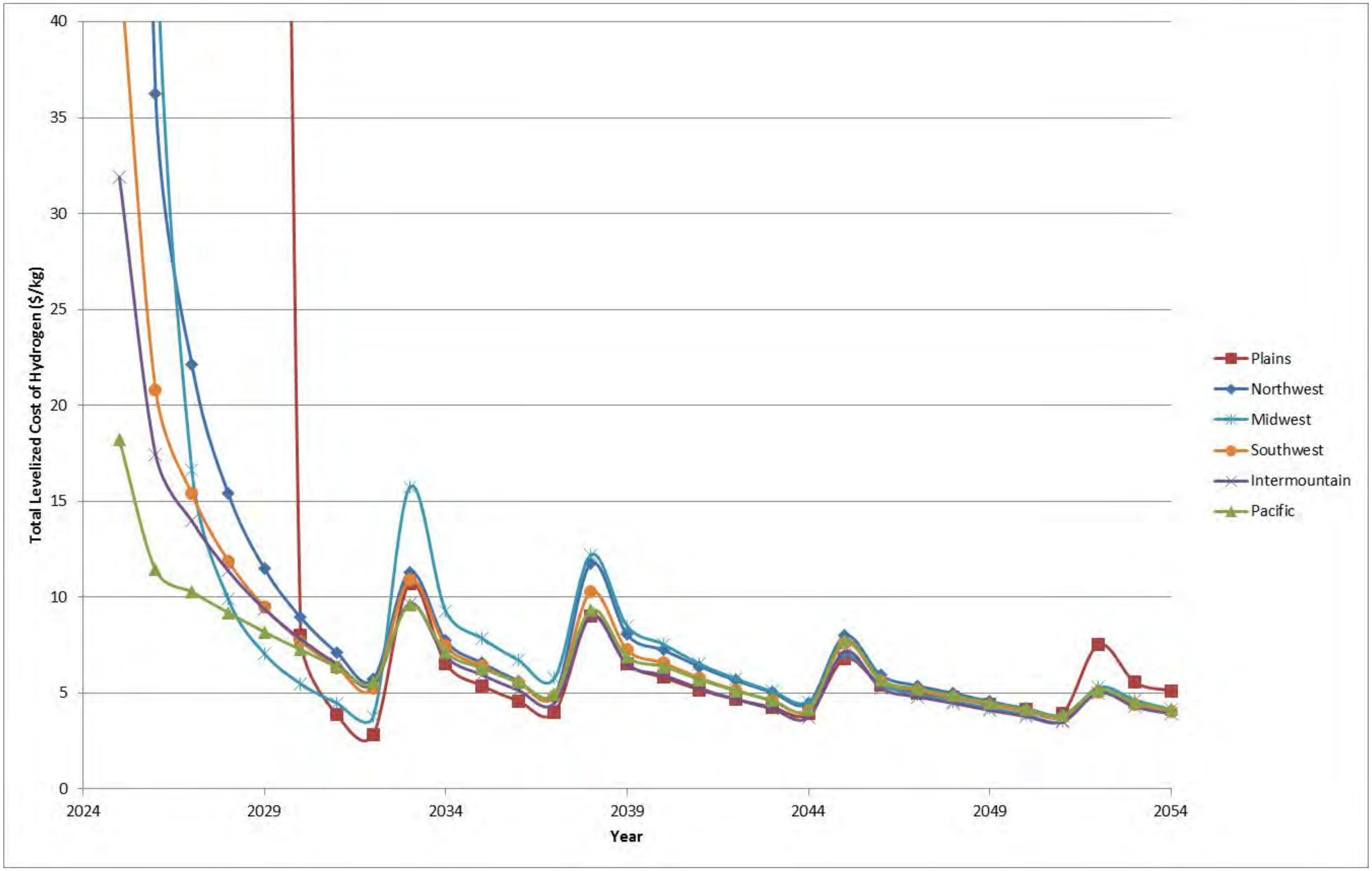

Figure 147: Annual levelized cost of hydrogen over the 30-year study period for each sub-region given the H_2 Partial Success scenario

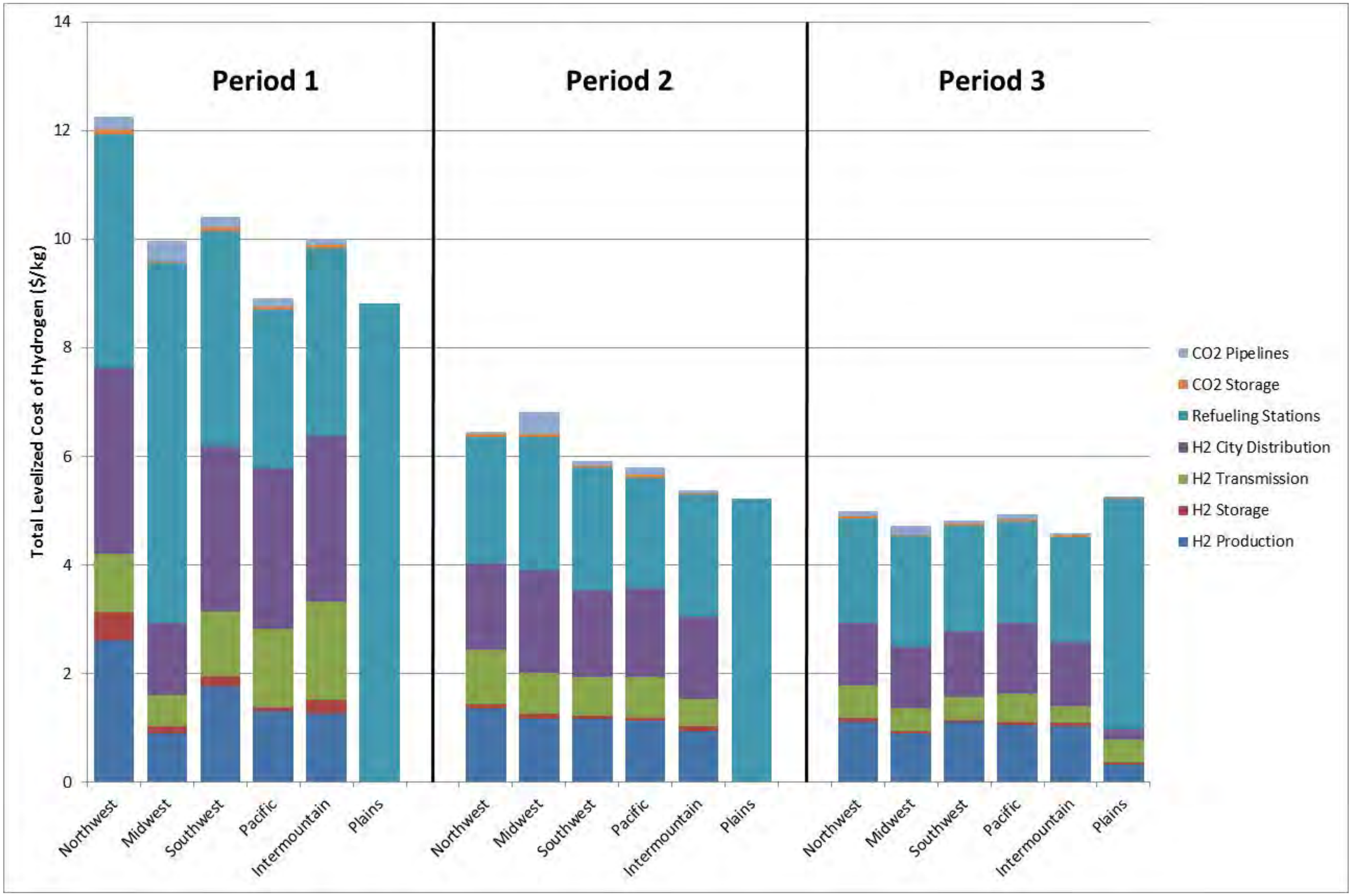

Figure 148: Levelized cost of hydrogen for each infrastructure component, 10-year analysis period, and sub-region given the H_2 Partial Success scenario

Despite lower utilization rates in the H_2 Partial Success scenario, two general trends are similar to those identified in the H_2 Success scenario. First, levelized costs tend to be larger in more isolated sub-regions and the costs only converge when the supply networks in all sub-regions become interconnected in tranche 4. Second, onsite production costs, as represented by the Plains sub-region, converge with costs associated with centralized infrastructure after about the same number of years as identified in the H_2 Success scenario. Consequently, the analysis suggests that the optimum number of years for delaying centralized infrastructure is about thirteen and it appears to be independent of the HFCV deployment rate. This finding is supported by the analysis in section 4.1.3.2, in which the impacts of delaying centralized infrastructure until tranche 3 are explored. In this analysis, the only scenario that quickly achieves permanent positive cumulative cash flow is the H_2 Partial Success scenario in which centralized infrastructure is delayed for 13 years.

In the H_2 Partial Success scenario, the annual levelized costs converge at about $4/kg at the end of the study period (Figure 147). Again, the cost in the Plains sub-region is larger at $5/kg since centralized infrastructure is introduced in tranche 5. The levelized cost calculated over the final ten-year period ranges from about $4.60/kg in the Intermountain sub-region to $5.30/kg in the Plains sub-region (Figure 148).

4.2.7.7 General Insights

The comparison of infrastructure design and cost in the six sub-regions provides several insights into the drivers of infrastructure cost. First, the average percentage of infrastructure capacity utilized over an analysis period is a major determinant of the cost of hydrogen. This metric can be incorporated into infrastructure models as an effective capacity factor and must account for underutilization resulting from the rate of HFCV deployment and oversizing of infrastructure. Since the extent of oversizing varies by component, an effective capacity factor should be derived for each component. The effective capacity factor generally increases over time as infrastructure becomes better utilized and tends to be smallest for pipelines since this model oversizes pipelines for the projected flow over their 20-year lifetimes. The effective capacity factor is largest for refueling stations, which are only oversized for near-term demand. However, even in this case, the median effective capacity factor is only 47% in the first period and 74% in the third period given the H_2 Success scenario.

Second, the length of pipelines is an important determinant of CO_2 transport and H_2 transmission and distribution costs. Ideally, the length of H_2 transmission and CO_2 transport pipelines will be adjusted in infrastructure models to account for sharing of pipeline capacity between sub-regions. Pipeline supply networks tend to become more interconnected over time and this model suggests that, on average, sharing can be represented as a decrease in the average pipeline length per demand center for transmission pipelines of 1% in the first period and 17% in the third period. Sharing is more significant for CO_2 pipelines, resulting in a 17% decline in the average pipeline length per production site in the first period and a 35% decline in the third period.

Sharing of infrastructure capacity is also an important determinant of cost for other infrastructure components. In examining the total levelized cost in each sub-region, a trend emerges that suggests that more isolated (i.e., less connected) sub-regions tend to have larger levelized costs. As sub-regions become more connected over time, the total levelized costs in all sub-regions tend to converge, which suggests that interconnection improves utilization and economies-of-scale.

It is important to note that steady-state infrastructure models generally do not incorporate underutilization, regionally-specific metrics like pipeline length, and regional sharing of infrastructure. Since this study indicates that all of these factors are important determinants of cost, they need to be better incorporated into steady-state models to improve cost estimates. This section provides some equations and average values that can improve the inputs provided to steady-state models.

5.0 Conclusions

To better understand the costs associated with hydrogen and CCS infrastructure deployment, models are needed that provide detailed inventories of the infrastructure components required in real geographic regions and that consider the timing of infrastructure installations and the impact of timing on infrastructure utilization. In Section 2, a hydrogen infrastructure deployment model is described that optimizes the design of coal-based hydrogen supply networks with CCS at discrete market penetration levels. The model is unique because it can incorporate high resolution spatial data, track infrastructure investments over time, and model integrated regional supply networks that link multiple production facilities, hydrogen demand centers, and CO_2 injection sites. In Section 3, the *CCS Deployment Model* is described, which optimizes the roll-out of CCS infrastructure for pre-specified CO_2 reduction targets. This model is applied to a case study in the southwestern U.S. to explore how the bonus allowances and CO_2 prices described in the American Power Act (APA) impact CCS deployment. In Section 4, the *Hydrogen Infrastructure Deployment Model* is applied to a case study in the western United States and the model is also demonstrated in several sub-regions in order to explore how hydrogen infrastructure design and cost differ among regions. The major insights provided by the analyses in each section are explained in the following sections.

5.1 Model Development

In Sections 2 and 3, the *Hydrogen Infrastructure Deployment Model* (HIDM) and *CCS Deployment Model* are described. The HIDM includes several modules that model the spatial distribution of regional hydrogen demand, the deployment of regional hydrogen supply networks and CO_2 storage networks, the design and cost of individual infrastructure components, and the timing of infrastructure investments. The model has several attributes that are unique among existing hydrogen infrastructure models.

First, whereas existing models of regional infrastructure deployment use simplified spatial representations of the locations of supply and demand, this model is capable of incorporating, if known, the exact locations of potential production sites, pipeline routes, city distribution centers, and CO_2 injection sites. Moreover, given these data, the model can identify integrated regional H_2 and CO_2 pipeline networks for linking multiple production facilities to cities and CO_2 storage sites. The optimization tools track the flow of hydrogen along each segment of pipeline and allow for the aggregation of supply into trunk pipelines. As a result, unlike other models, this model can explore the potential benefits of integrated regional supply networks in which multiple cities share supply infrastructure. Because the model utilizes detailed spatial inputs, it also provides spatially-detailed outputs (e.g., the optimal design for the H_2 transmission pipeline network in a specific region).

By tracking infrastructure investments over time and constraining future installments based on previously built infrastructure, the model also incorporates a more realistic infrastructure deployment scenario. Specifically, the model assumes that infrastructure is deployed in stages based upon projected near-term demand and future decisions are constrained by previous investments. This approach is quite different from a steady-state approach that examines independent “snapshots” in time or dynamic approaches that either assume perfect foresight or incorporate uncertainty in future hydrogen demand. Unlike steady-state models, the tracking of installed capacity over time allows the model to account for the underutilization of infrastructure that occurs as a result of oversizing infrastructure in anticipation of future demand. As is discussed in the next two sections, underutilization of capacity has a profound impact on the levelized cost of hydrogen.

Although an improvement over existing hydrogen infrastructure models, the hydrogen optimization tools developed in this document could be improved. In particular, the current tools are deterministic models that optimize infrastructure design at static HFCV market penetration levels (e.g., 10 million HFCVs). Thus, the timing of infrastructure investments is fixed and depends only on the HFCV deployment rate that is specified as an input (e.g., H_2 Success or H_2 Partial Success). Moreover, although the tools do incorporate previously built infrastructure, they do not consider future infrastructure requirements or uncertainty in future hydrogen demand. As a result, these tools are not useful for determining the optimal timing or sizing of infrastructure investments contingent on long-term demand projections. These weaknesses could be addressed through the development of dynamic modeling tools with annual time steps that could identify more temporally dispersed deployment strategies that may improve system-wide utilization. In particular, a stochastic model that considers uncertainty in hydrogen demand would be useful since the actual rate of growth in hydrogen demand will have a large impact on infrastructure utilization and the levelized cost of hydrogen.

The *CCS Deployment Model* shares many of the traits and benefits of the hydrogen optimization tools, but is designed specifically to identify optimal CCS deployment strategies for meeting CO_2 reduction targets proposed by policy. This trait allows the model to be used to examine the effectiveness of policy in promoting CCS deployment. The model is also unique in its spatially-explicit representation of CO_2 capture costs. Rather than assuming a fixed capture cost for each plant type (e.g., IGCC with CCS) regardless of location, the model uses information about existing plants to identify a unique avoided cost of CO_2 capture for each location. This approach yields a large range of capture costs for each plant type, which depends on the size, capacity factor, efficiency, and CO_2 emission rate of the existing plant. In some cases where inefficient and/or underutilized plants are replaced, very low avoided costs of capture are possible in the power sector.

5.2 CCS Case Study in the Southwestern United States

With widely distributed potential CO_2 injection sites in the southwestern U.S., large regional networks are not common in early stages of CCS deployment. However, as CCS adoption increases and local storage capacity is consumed, integrated regional disposal networks develop in some areas to access additional storage capacity. In the “Low Capacity” scenario, in which CO_2 storage capacity is considered more limited, longer and more integrated networks develop throughout the study area. The deployment strategies identified by this model suggest that storage capacity constraints are the primary cause for the development of integrated regional disposal networks.

CCS abatement costs for individual CO_2 sources indicate that ~300 Mt CO_2 per year can be avoided via CCS for a cost below ~\$50/tCO_2 avoided. In order to achieve a 360 Mt CO_2 per year reduction (~75% of regional emissions) via CCS, the cost increases to \$105/tCO_2 avoided since CCS must be installed on industrial and power plants with higher capture costs. However, this value still falls below the EPA projected CO_2 price in 2050, which is \$114/tCO_2 avoided. In exploring the levelized benefit of installing CCS rather than paying a CO_2 price for emissions, it appears that the CCS bonus allowances proposed by the American Power Act are sufficient to drive investment in Phases 1 and 2 even if the CO_2 price remains at the clearing price. However, after these subsidies expire, CCS investment will only continue if the CO_2 price remains above the clearing price.

The “Low Capacity” scenario suggests that longer and more integrated disposal networks develop when capacity is more limited. As a result, the total average abatement cost increases by 3-10%. However, since capture costs constitute the majority of the abatement cost, this will likely have little impact on the viability of CCS deployment. In exploring the trade-offs between oversizing pipelines for 2050 flow requirements versus organically expanding pipelines to meet incremental flow increases, it appears that the latter (i.e., organic) approach is more cost-effective.

5.3 Hydrogen Case Study in the Western United States

In a large geographic region, such as the western United States, independent regional centralized hydrogen supply networks initially develop in several sub-regions. Within these sub-regions, the minimum demand that supports centralized infrastructure is approximately 150 tonnes per day. In all sub-regions, the supply network connects at least four demand centers (i.e., no individual demand center has a dedicated production facility). As hydrogen demand increases, the regional supply networks become increasingly connected and a completely integrated network develops by 2050. The average transmission pipeline length per demand center ranges between 80 and 100 km during the 30-year study period.

In contrast, the CO_2 transport and storage network consists primarily of pipelines that connect individual production facilities to dedicated storage sites. The exception is in areas in which local CO_2 storage capacity is inadequate (e.g., Arizona and the Midwest). In these areas, long trunk pipelines are shared by multiple facilities. The total length of CO_2 pipelines is only about 7% of the total length of H_2 distribution and transmission pipelines. The CO_2 captured during the lifetime operation of all H_2 production facilities built in the six tranches would require less than 10% of the available CO_2 storage capacity within the region. Only one storage basin, which is located in the Midwest, experiences capacity constraints during the study period.

The cumulative capital investment given the H_2 Success scenario is approximately $310 billion for the full HFCV deployment to 2050. This infrastructure serves about 94 million cumulative HFCVs, which translates to a cost of $3,300 per HFCV in 2050. However, this number decreases over time from $7,300 at the end of the first tranche in 2024[20]. In the first tranche, approximately 65% of the cumulative capital investment is associated with H_2 and CO_2 pipeline transport since the pipelines are oversized for the projected flow over their lifetimes. In the sixth tranche, the three largest contributors to the capital cost are pipeline transport (40%), refueling stations (35%), and centralized production (21%). The cost of CO_2 transport and storage infrastructure represents only 4% of the total capital investment.

When each infrastructure tranche is installed, the design capacity exceeds the demand for several years until demand finally matches capacity and the infrastructure becomes fully utilized. During this period, the infrastructure is underutilized. In the case of pipelines, which are oversized for their projected flows in 20 years, the average capacity factor during the first ten-year analysis period is only 12-25% in the H_2 Success scenario. The average capacity factor

[20] This study only looks at coal-based hydrogen production with pipeline delivery. It is possible that hydrogen costs could be reduced using alternative feedstocks or onsite production; particularly during early deployment.

for refueling stations, which are very flexible and modular in their design, is still only 50% in the first period. By the third period, the average capacity factor for all components increases to 60-75%. However, this range is still lower than the capacity factors generally assumed in most steady-state models for various infrastructure components (80-100%).

As a result of the low utilization of capacity in the first period, the breakeven price of hydrogen is approximately $9/kg in the H_2 Success scenario (~$6/gallon gasoline equivalent accounting for the higher fuel economy of a hydrogen FCV compared to an efficient gasoline vehicle). In the second and third periods, the price declines to ~$5/kg and ~$4/kg, respectively, but is still larger than predicted in most steady-state models since this model accounts for underutilization, whereas steady-state models do not. In the H_2 Partial Success scenario when HFCV deployment is slower, the breakeven prices of hydrogen are significantly larger since underutilization is greater and infrastructure components achieve economies-of-scale more slowly.

Given assumptions about the market price of hydrogen, the analysis of cumulative cash flow suggests that, even in the high price scenario, more than a decade will be required before cumulative cash flow becomes positive. Thus, it is unlikely that private corporations will invest in centralized hydrogen infrastructure without subsidies or other incentives. However, if centralized infrastructure is delayed for one tranche, the buy-down cost is reduced but the year in which cumulative cash flow remains positive does not improve unless the market price of hydrogen is high and HFCV deployment is slow, which further delays centralized infrastructure. Thus, even if early hydrogen demand is supplied by onsite production, subsidies will be required to incentivize early infrastructure deployment.

The best environment for hydrogen infrastructure investment is created when centralized infrastructure is delayed one tranche, the market price for hydrogen is high, and a production tax credit guarantees that suppliers receive $10/kg for all hydrogen supplied in the first ten years of the study period (i.e., subsidy case PTC-10). In this environment, the cumulative cash flow becomes positive within the first two years of infrastructure installation in both HFCV deployment scenarios. However, if the H_2 price is not high, subsidies are only effective if HFCV deployment is relatively fast (i.e., under the H_2 Success scenario). The total net present cost of the production tax credits ranges from $8 billion to $34 billion depending on the market price of hydrogen and the HFCV deployment rate.

5.4 Sub-regional Hydrogen Case Studies

The comparison of infrastructure design and cost in the six sub-regions provides several insights into the drivers of infrastructure cost. First, the average percentage of infrastructure capacity utilized over an analysis period is a major determinant of the cost of hydrogen. This metric can be incorporated into infrastructure models as an effective capacity factor for each component and must account for underutilization resulting from the rate of HFCV deployment and oversizing of infrastructure. The effective capacity factor generally increases over time as infrastructure becomes better utilized and tends to be smallest for pipelines since this model oversizes pipelines for the projected flow over their 20-year lifetimes. The effective capacity factor is largest for refueling stations, which are only oversized for near-term demand. However, even for refueling stations, the median effective capacity factor is only 47% in the first period and 74% in the third period given the H_2 Success scenario.

Second, the length of pipelines is an important determinant of CO_2 transport and H_2 transmission and distribution costs. Ideally, the length of H_2 transmission and CO_2 transport pipelines will be adjusted in infrastructure models to account for sharing of pipeline capacity between sub-regions. Pipeline supply networks tend to become more interconnected over time and this model suggests that, on average, sharing can be represented as a decrease in the average pipeline length per demand center for transmission pipelines of 1% in the first period and 17% in the third period. Sharing is more significant for CO_2 pipelines, resulting in a 17% decline in the average pipeline length per production site in the first period and a 35% decline in the third period.

Sharing of infrastructure capacity is also an important determinant of cost for other infrastructure components. In examining the total levelized cost in each sub-region, a trend emerges that suggests that more isolated (i.e., less connected) sub-regions tend to have larger levelized costs. As sub-regions become more connected over time, the total levelized costs in all sub-regions tend to converge, which suggests that interconnection improves utilization and economies-of-scale.

It is important to note that steady-state infrastructure models generally do not incorporate underutilization, regionally-specific metrics like pipeline length, and regional sharing of infrastructure. Since this study indicates that all of these factors are important determinants of cost, they need to be better incorporated into steady-state models to improve cost estimates.

5.5 Final Comments

This document describes models for examining how centralized hydrogen and CCS infrastructure with pipeline distribution might deploy in real geographic regions. They are an improvement over existing hydrogen and CCS infrastructure models since they can incorporate high resolution spatial data, model the development of integrated regional supply networks, and account for the underutilization of infrastructure over time. Although the models examine coal-based hydrogen production in the western United States and CCS deployment in the southwestern United States, they can be modified to examine other feedstocks and geographic regions.

One of the major insights provided by the hydrogen model is the importance of the capacity factor in determining the levelized cost of hydrogen associated with each component. Consequently, any deployment or infrastructure design strategies that can increase infrastructure utilization can lead to substantial reductions in cost. In reality, infrastructure planners will have more flexibility in the timing of investments and the location and sizing of components than is represented in this model. This added flexibility will inevitably lead to improved capacity factors and, thus, it is likely that the results of this model represent a conservative (i.e., high) estimate of hydrogen costs. Consequently, it is suggested that these costs are considered an upper bound with the cost estimates from steady-state models representing the lower bound.

Future work is needed to develop dynamic models that consider infrastructure deployment under hydrogen and electricity demand uncertainty while still incorporating high resolution spatial detail. Such a model would allow more flexibility in the timing of infrastructure investments and would yield valuable insights into the optimal timing of investments and the range of potential costs given uncertainty in demand.

References

[1] IEA Greenhouse Gas R&D Programme (IEA GHG), 2007. Co-production of hydrogen and electricity by coal gasification with CO2 capture. prepared by Foster Wheeler Italiana, report number 2007/13, Milan, Italy.

[2] National Research Council (NRC), 2004. The Hydrogen Economy: Opportunities, Costs, Barriers, and R&D Needs. Committee on Alternatives and Strategies for Future Hydrogen Production and Use, Washington, DC.

[3] Kreutz, T., Williams, R., Consonni, S., Chiesa, P., 2005. Co-production of hydrogen, electricity and CO2 from coal with commercially ready technology. Part B: Economic analysis. International Journal of Hydrogen Energy 30, 769-784.

[4] Ogden, J., Yang, C., Johnson, N., Ni, J., Johnson, J., 2004. Conceptual Design of Optimized Fossil Energy Systems with Capture and Sequestration of Carbon Dioxide. Final report for USDOE Award Number DE-FC26-02NT41623, report no. 41623R04.

[5] Parsons Infrastructure and Technology Group Inc., 2002. Hydrogen production facilities - plant performances and cost comparisons: final report. to U.S. Department of Energy.

[6] Gray, D., Tomlinson, G., 2002. Hydrogen from Coal. Mitretek Systems.

[7] U.S. Department of Energy, 2008. H2A Current Central Hydrogen Production from Coal with CO2 Sequestration version 2.1.1. National Renewable Energy Laboratory, Golden, CO.

[8] U.S. Energy Information Administration, 2011. Average Cost of Coal Delivered for Electricity Generation by State, March 2011 and 2010, Electric Power Monthly, June 2011, Washington, DC.

[9] Hong, B., Slatick, E., 1994. Carbon Dioxide Emission Factors for Coal. EIA Quarterly Coal Report, January-April 1994 DOE/EIA-0121(94/Q1), 1-8.

[10] U.S. Department of Energy, 2008. H2A Delivery Scenario Analysis Model Version 2.2. Argonne National Laboratory, Center for Transportation Research, Chicago, IL.

[11] Nicholas, M., Handy, S., Sperling, D., 2004. Hydrogen Refueling Network Analysis Using Geographic Information Systems, National Hydrogen Association, Long Beach, CA.

[12] U.S. Department of Energy, 2008. H2A Current Forecourt Hydrogen Production from Natural Gas (1500 kg/day), Version 2.1.2. Directed Technologies Inc., Arlington, VA.

[13] Ogden, J., Johnson, N., 2010. Techno-economic analysis and modeling of carbon dioxide capture and storage technologies, in: Maroto-Valer, M. (Ed.), Developments and innovation in carbon dioxide capture and storage technology: Carbon dioxide capture, transport and industrial applications (Volume 1). Woodhead Publishing Ltd, Cambridge, UK, pp. 27-63.

[14] Zhang, Z.X., Wang, G.X., Massarotto, P., Rudolph, V., 2006. Optimization of pipeline transport for CO2 sequestration. Energy Conversion and Management 47, 702-715.

[15] Gale, J., Davison, J., 2004. Transmission of CO2--safety and economic considerations. Energy 29, 1319-1328.

[16] Svensson, R., Odenberger, M., Johnsson, F., Strömberg, L., 2004. Transportation systems for CO2--application to carbon capture and storage. Energy Conversion and Management 45, 2343-2353.

[17] Doctor, R., Palmer, A., Coleman, D., Davison, J., Hendriks, C., Kaarstad, O., Ozaki, M., 2005. Transport of CO2, in: Metz, B., Davidson, O., de Coninck, H., Loos, M., Meyer, L. (Eds.), IPCC Special Report on Carbon Dioxide Capture and Storage. Cambridge University Press, Cambridge, UK.

[18] Hendriks, C., Wildenborg, T., Feron, P., Graus, W., Brandsma, R., 2003. EC-Case Carbon Dioxide Sequestration. Ecofys report number M70066.

[19] Woodhill Engineering Consultants, 2002. Transmission of CO2 and energy. IEA Greenhouse Gas R&D Programme report number PH4/6, Cheltenham, UK.

[20] McCoy, S.T., Rubin, E.S., 2008. An engineering-economic model of pipeline transport of CO2 with application to carbon capture and storage. International Journal of Greenhouse Gas Control 2, 219-229.

[21] Bock, B., Rhudy, R., Herzog, H.J., Klett, M., Davison, J., De La Torre Ugarte, D.G., Simbeck, D.R., 2003. Economic Evaluation of CO2 Storage and Sink Enhancement Options. TVA Public Power Institute, Muscle Shoals, AL.

[22] Vandeginste, V., Piessens, K., 2008. Pipeline design for a least-cost router application for CO2 transport in the CO2 sequestration cycle. International Journal of Greenhouse Gas Control 2, 571-581.

[23] Skovholt, O., 1993. CO2 transportation system. Energy Conversion and Management 34, 1095-1103.

[24] Parker, N., 2004. Using Natural Gas Transmission Pipeline Costs to Estimate Hydrogen Pipeline Costs. UC Davis Institute of Transportation Studies, Davis, CA.

[25] Ahmed, T., 2006. Reservoir Engineering Handbook, Third Edition ed. Elsevier, Burlington, MA.

[26] McCoy, S.T., 2008. The Economics of CO2 Transport by Pipeline and Storage in Saline Aquifers and Oil Reservoirs, Engineering and Public Policy. Carnegie Mellon University, Pittsburgh, PA, p. 267.

[27] Hendriks, C., 1994. Carbon Dioxide Removal from Coal-fired Power Plants, Department of Science, Technology, and Society. Utrecht University, Utrecht, The Netherlands.

[28] Nordbotten, J.M., Celia, M.A., Bachu, S., 2005. Injection and storage of CO2 in deep saline aquifers: analytical solution for CO2 plume evolution during injection. Transport in Porous Media 58, 339-360.

[29] Stauffer, P.H., Viswanathan, H.S., Pawar, R.J., Guthrie, G.D., 2009. A System Model for Geologic Sequestration of Carbon Dioxide. Environmental Science & Technology 43, 565-570.

[30] Bank, G.C., Kuuskraa, V.A., 2006. The Economics of Powder River Basin Coalbed Methane Development. Advanced Resources International, Inc., prepared for U.S. Department of Energy.

[31] Eccles, J.K., Pratson, L., Newell, R.G., Jackson, R.B., 2009. Physical and Economic Potential of Geological CO2 Storage in Saline Aquifers. Environmental Science & Technology 43, 1962-1969.

[32] API, 2007. 2004 Joint Association Survey (JAS) on drilling costs. American Petroleum Institute, Washington, DC.

[33] EIA, 2007. Costs and indices for oil and gas field equipment and production operations - 1988 through 2006. Energy Information Administration - Office of Oil and Gas, Washington, DC.

[34] U.S. Department of Energy, 2005. Carbon Capture and Sequestration Systems Analysis Guidelines. National Energy Technology Laboratory, Pittsburgh, PA.

[35] National Research Council (NRC), 2008. Transitions to Alternative Transportation Technologies - A Focus on Hydrogen. Committee on Assessment of Resource Needs for Fuel Cell and Hydrogen Technologies, Washington, DC.

[36] Ni, J., Johnson, N., Ogden, J.M., Yang, C., Johnson, J., 2005. Estimating hydrogen demand distribution using geographic information systems (GIS), National Hydrogen Association, Washington, DC.

[37] Johnson, N., Ogden, J., 2012. A spatially-explicit optimization model for long-term hydrogen pipeline planning. International Journal of Hydrogen Energy 37, 5421-5433.

[38] GAMS Development Corporation, 2010. General Algebraic Modeling System, 23.3.3 ed, Washington, DC.

[39] U.S. Environmental Protection Agency, 2007. eGRID database ver. 1.1, Washington, DC.

[40] U.S. Department of Transportation, 2010. National Pipeline Mapping System. Pipeline and Hazardous Materials Safety Administration.

[41] U.S. Census Bureau, 2000. Urbanized Areas. U.S. Department of Commerce, Washington, DC.

[42] U.S. Geological Survey, 1999. National Elevation Dataset (NED) 1 arc-second. EROS Data Center, Sioux Falls, SD.

[43] Chiesa, P., Consonni, S., Kreutz, T., Robert, W., 2005. Co-production of hydrogen, electricity and CO2 from coal with commercially ready technology. Part A: Performance and emissions. International Journal of Hydrogen Energy 30, 747-767.

[44] U.S. Department of Energy, 2011. National Carbon Sequestration Database and Geographic Information System (NATCARB), v. 1104, in: National Energy Technology Laboratory (Ed.), Pittsburgh, PA.

[45] Yang, C., Ogden, J., 2007. Determining the lowest-cost hydrogen delivery mode. International Journal of Hydrogen Energy 32, 268-286.

[46] Johnson, N., Yang, C., Ogden, J., 2008. A GIS-based assessment of coal-based hydrogen infrastructure deployment in the state of Ohio. International Journal of Hydrogen Energy 33, 5287-5303.

[47] Berkenpas, M., Rubin, E.S., Zaremsky, C.J., 2010. Integrated Environmental Control Model (IECM), in: 6.2.4, v. (Ed.), 6.2.4 ed. Carnegie Mellon University, Center for Energy and Environmental Studies, Pittsburgh, PA.

[48] Rubin, E.S., Yeh, S., Antes, M., Berkenpas, M., Davison, J., 2007. Use of experience curves to estimate the future cost of power plants with CO2 capture. International Journal of Greenhouse Gas Control 1, 188-197.

[49] Metz, B., Davidson, O., de Coninck, H., Loos, M., Meyer, L., 2005. IPCC Special Report on Carbon Dioxide Capture and Storage. Cambridge University Press, New York.

[50] van Straelen, J., Geuzebroek, F., Goodchild, N., Protopapas, G., Mahony, L., CO2 capture for refineries, a practical approach. International Journal of Greenhouse Gas Control 4, 316-320.

[51] Simmonds, M., Hurst, P., Wilkinson, M., Watt, C., Roberts, C., 2002. A study of very large scale post combustion CO2 capture at a refining and petrochemical complex, Sixth International Conference on Greenhouse Gas Control Technologies, Kyoto, Japan.

[52] Barker, D.J., Turner, S.A., Napier-Moore, P.A., Clark, M., Davison, J.E., 2009. CO2 Capture in the Cement Industry. Energy Procedia 1, 87-94.

[53] IEA Greenhouse Gas R&D Programme (IEA GHG), 2008. CO2 Capture in the Cement Industry. prepared by Mott MacDonald Ltd, report number 2008/3.

[54] McCollum, D., Ogden, J., 2006. Techno-Economic Models for Carbon Dioxide Compression, Transport, and Storage & Correlations for Estimating Carbon Dioxide Density and Viscosity. UC Davis Institute of Transportation Studies, Davis, CA.

[55] IPCC, 2005. IPCC Special Report on Carbon Dioxide Capture and Storage. Cambridge University Press, Cambridge, UK.

[56] U.S. Environmental Protection Agency, 2010. EPA Analysis of the American Power Act in the 111th Congress. Office of Atmospheric Programs, Washington, DC.

[57] Spencer, L., Bradshaw, J., Bradshaw, B., Lahtinen, A.-L., Chirinos, A., 2011. Regional storage capacity estimates: prospectivity not statistics. Energy Procedia 4, p. 4857-4864.

[58] U.S. Energy Information Administration, 2011. U.S. refineries operable capacity (2011 data), www.eia.gov/energyexplained/index.cfm?page=oil_refining#tab4, Washington, DC.

[59] Advanced Resources International, 2006. Basin oriented strategies for CO2 enhanced oil recovery: East and Central Texas. Prepared for U.S. Department of Energy, Office of Fossil Energy - Office of Oil and Natural Gas.

[60] Advanced Resources International, 2006. Basin oriented strategies for CO2 enhanced oil recovery: Permian Basin. Prepared for U.S. Department of Energy, Office of Fossil Energy - Office of Oil and Natural Gas.

[61] Advanced Resources International, 2006. Basin oriented strategies for CO2 enhanced oil recovery: Rocky Mountain Region. Prepared for U.S. Department of Energy, Office of Fossil Energy - Office of Oil and Natural Gas.

[62] INGAA Foundation, 2009. Developing a Pipeline Infrastructure for CO2 Capture and Storage: Issues and Challenges. prepared by ICF International.

[63] Jaramillo, P., Griffin, W.M., McCoy, S.T., 2009. Life cycle inventory of CO_2 in an enhanced oil recovery system. Environmental Science & Technology 43, p. 8027-8032.

[64] Reeves, S.R., Taillefert, A., Pekot, L., 2003. The Allison Unit CO2-ECBM pilot: a reservoir modeling study. Advanced Resources International, Inc., prepared for U.S. Department of Energy.

[65] CONCAWE, 2007. Well-to-wheels Analysis of Future Automotive Fuels and Powertrains in the European Context, Report Version 2c (March). Conservation of Clean Air and Water in Europe (CONCAWE), Brussels, Belgium.

[66] Bandivadekar, A., Bodek, K., Cheah, L., Evans, C., Groode, T., Heywood, J., Kasseris, E., Kromer, M., Weiss, M., 2008. On the Road in 2035: Reducing Transportation's Petroleum Consumption and GHG Emissions. Laboratory for Energy and the Environment, Massachusetts Institute of Technology, Cambridge, MA.

[67] Wang, M., Huo, H., Johnson, L., He, D., 2006. Projection of Chinese Motor Vehicle Growth, Oil Demand, and CO2 Emissions through 2050, Report ANL/ESD/06-6. Argonne National Laboratory, Energy Systems Division, Argonne, IL.

[68] International Energy Agency (IEA), 2009. Transport, Energy, and CO2 - Moving Towards Sustainability. International Energy Agency, Paris, France.

[69] Plotkin, S., Singh, M., 2009. Multi-Path Transportation Futures Study: Vehicle Characterization and Scenario Analyses. Report ANL/ESD/09-5. Argonne National Laboratory, Argonne, IL.

[70] U.S. Energy Information Administration, 2011. Annual Energy Outlook 2011. U.S. Department of Energy, Office of Integrated and International Energy Analysis, Washington, DC.

[71] Koornneef, J., van Keulen, T., Faaij, A., Turkenburg, W., 2008. Life cycle assessment of a pulverized coal power plant with post-combustion capture, transport and storage of CO2. International Journal of Greenhouse Gas Control 2, 448-467.

[72] U.S. Energy Information Administration, 2008. Energy Market and Economic Impacts of S.2191, the Lieberman-Warner Climate Security Act of 2007, in: Office of Integrated Analysis and Forecasting (Ed.). U.S. Department of Energy, Washington, DC.

[73] U.S. Energy Information Administration, 2011. Annual Coal Report, Table 26: U.S. Coal Consumption by End Use Sector, by Census Division and State, 2010. U.S. Department of Energy, Washington, DC.